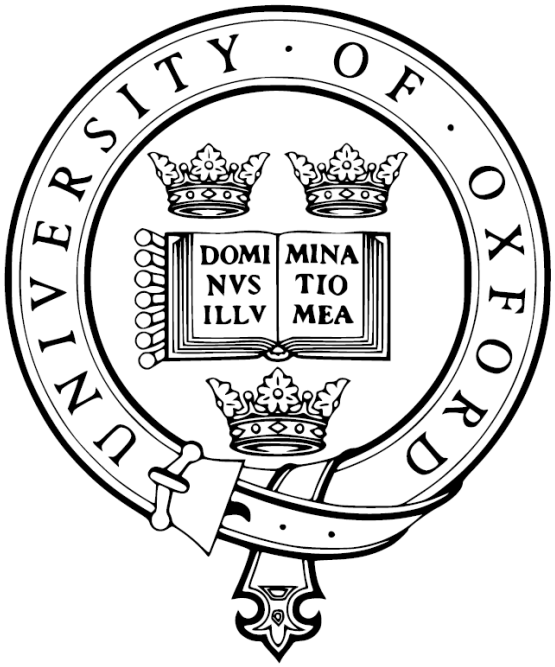
Evolved P450 Mutants as General Oxidation Catalysts



A thesis submitted to the

Board of the Faculty of the Physical Sciences

in partial fulfilment of the requirements for the degree of

Doctor of Philosophy of the University of Oxford

Lucy Allison Harwood

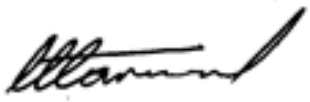
Wadham College

University of Oxford

Trinity Term 2021

Declaration

The work described in this thesis was carried out in the Chemistry Research Laboratory and the Inorganic Chemistry Laboratory, University of Oxford, from February 2017 until September 2021, under the supervision of Professor Jeremy Robertson and Professor Luet L. Wong. All of the work is my own unless otherwise stated and has not been submitted previously for any other degree at this or any other university



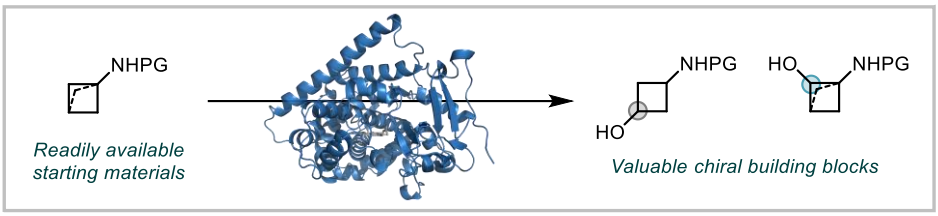
Lucy A. Harwood

September 2021

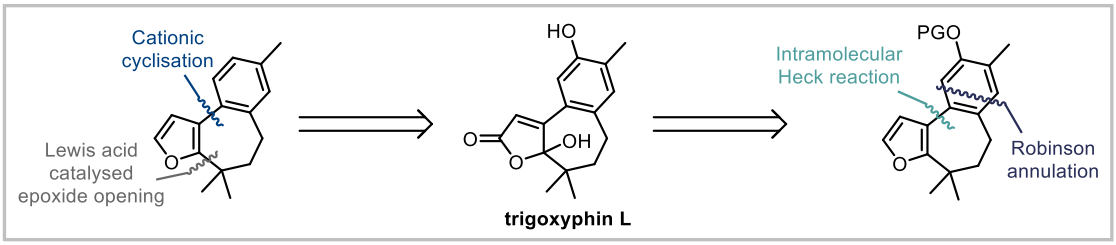
Abstract

Chapter 1 introduces chemical methods for oxidation and noteworthy examples applied to total synthesis. Subsequently, a brief history of biocatalysis and enzymes as oxidation catalysts will be discussed, and cytochrome P450 monooxygenases and their applications will be introduced.

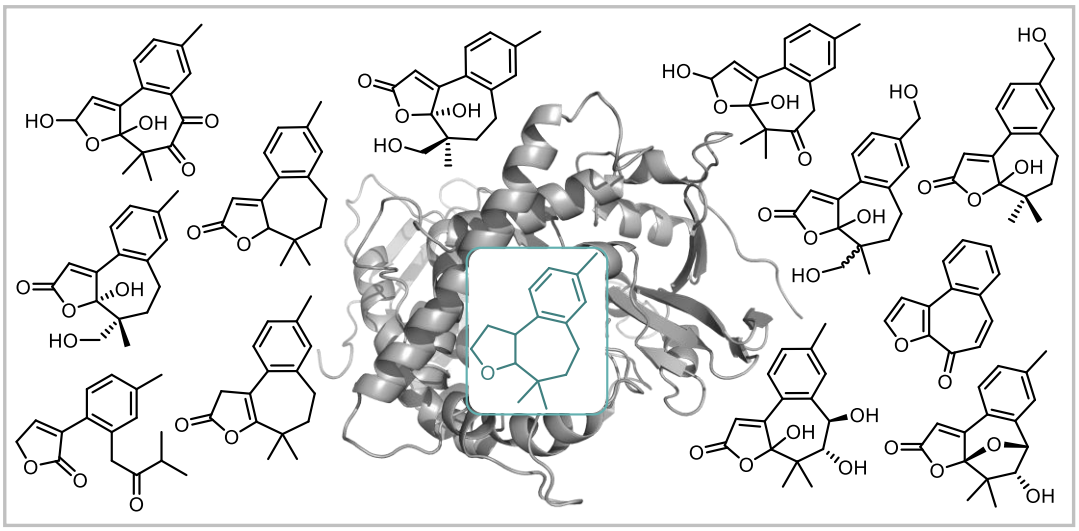
Chapter 2 describes the application of cytochrome P450 mutants as catalysts to affect the regio-, diastereo- and enantioselective hydroxylation of *N*-protected cycloalkylamines, cycloalkylcarboxamides and BCPAs. The derivatisation of these key building blocks into medicinally relevant structures will also be discussed. Furthermore, a first proof-of-principle of the kinetic resolution of sulfoxides will be reported.



Chapter 3 explores the synthetic efforts towards the natural product trigoxyphin L. Improvements to a previous synthetic route, two routes based on a C(sp^2)–C(sp^2) bond disconnection and a final route constructing the aryl ring *via* Robinson annulation will be discussed. New methodologies including an intramolecular Heck cross-coupling and a Lewis acid catalysed coupling of furfuryl alcohols with silyl enol ethers will be presented.



Chapter 4 focuses on the late-stage functionalisation of trigoxyphin-type core structures, yielding a range of natural product analogues from our library of $P450_{BM3}$ mutants. This work describes an enzymatic platform for the diversity-oriented C–H hydroxylation of complex chemical scaffolds.



Acknowledgments

Firstly, thank you to both my supervisors Jeremy Robertson and Luet Wong, I could not imagine doing my DPhil with anyone else. Jeremy, your encyclopedic knowledge of organic chemistry and your supportive attitude towards all your students allowed me to develop and grow as a scientist in ways I could not have imagined. I will owe all my future academic successes from the great foundation I received under your mentorship. I am eternally grateful.

Thank you to Jon Burton for supervising me during my first rotation. You are incredibly kind and supportive, and your passion and enthusiasm for chemistry is infectious.

Thank you to everyone who made my time at Syngenta so enjoyable and productive, but especially to Mell who has been an incredible industrial mentor over the years.

Thanks also to all the facilities and analytical service staff of the CRL, without who this work wouldn't have been possible. Particularly to the crystallography team, Kirsten and Amber, who solved all the single crystal X-ray structures described in this work.

Thank you to all my fellow SBMers who made my move to Oxford easier and my first few months so enjoyable, but especially to Jonny for the many good pub trips and to Jess, in whom I have a lifelong friend.

Thanks to all past and present members of both research groups, who provided a great working environment (although not the tidiest at times!). To Victoria, the first person I knew in the group, thank you for everything over the years and I hope you find happiness back up North. To Wenyu, thank you for taking me under your wing when I first started, and with immense patience teaching me all things P450-related. To Matt, thank you for all your help with the (many, many) technological problems I have, and to distract me from work with a good gossip and a good coffee. To Yuan, thank you for all your help over the years, you are one of the kindest people I know and an incredibly talented scientist. To my lab bench-mate Alice, thank you for always keeping me laughing and brightening my day.

To Jonny, without you in the lab I would have gone insane long ago. Thank you for being such a great friend over the years, who's always up for a pub trip to enjoy a shot in a pint and a thorough discussion about the Pauson-Khand mechanism.

To Vicky, you are like a sister to me. Thank you for looking after me so well while I was writing and making my final year one to remember (or not remember, depending on how much gin we've had...).

Thank you to my incredible mum, who has always supported me through all my endeavors. I'm extremely proud to be your daughter, and if I can achieve a fraction of the things you have, then I'll count myself very fortunate.

Finally thank you to Mix, I am so lucky to have you in my life and I could not have done this without you. Your love and support pulled me up through the tough times and you always put a smile on my face. You inspire me to be a better scientist and a better person, and I cannot wait to see what we achieve in life together.

Abbreviations

δ	NMR chemical shift
ν_{max}	Infrared absorption maximum
Ac	Acetyl
AIBN	Azobisisobutyronitrile
APCI	Atmospheric pressure chemical ionization
Ar	Aryl
Bn	Benzyl
Boc	*tert*-Butoxycarbonyl
BCP	Bicyclo[1.1.1]pentane
BCPA	Bicyclo[1.1.1]pentylamine
BINAP	2,2'-Bis(diphenylphosphino)-1,1'-binaphthyl
BQ	Benzoquinone
br	Broad
cat	Catalyst
Cbz	Carboxybenzyl
COSY	COrrelation SpectroscopY
Cy	Cyclohexyl
CYP	Cytochromes P450
d	Doublet
DAST	Diethylaminosulfur trifluoride
DCC	*N*,*N*'-Dicyclohexylcarbodiimide
DCE	Dichloroethane
DHF	Dihydrofuran

DIAD	Diisopropyl azodicarboxylate
DIBAL	Diisobutylaluminum hydride
DIPA	Diisopropylamine
DIPEA	*N*,*N*-Diisopropylethylamine (Hünig's base)
DMA	*N*,*N*-Dimethylacetamide
DMAP	4-Dimethylaminopyridine
DME	Dimethoxyethane
DMF	Dimethylformamide
DMP	Dess–Martin periodinane
DMSO	Dimethylsulfoxide
DNA	Deoxyribonucleic acid
DPPA	Diphenylphosphoryl azide
ee	Enantiomeric excess
EI	Electron ionisation
ESI	Electrospray ioisation
eq.	equivalents
et al.	*et alia*
FID	Flame ionization detector
FT	Fourier transform
GC	Gas chromatography
GDH	Glucose dehydrogenase
HATU	1-[Bis(dimethylamino)methylene]-1H-1,2,3-triazolo[4,5-b]pyridinium 3-oxide hexafluorophosphate
HFIP	1,1,1,3,3,3-Hexafluoro-2-propanol
HPLC	High-performance liquid chromatography
HRMS	High resolution mass spectrometry
IPTG	isopropylthio-β-galactoside

IR	Infrared
IUPAC	International Union of Pure and Applied Chemistry
J	Coupling cnonstant
LCMS	Liquid chromatography-mass spectrometry
LDA	Lithium diisopropylamide
LSF	Late-stage functionalisation
m	Multiplet
M	Molar
m-CPBA	*meta*-Chloroperoxybenzoic acid
MD	Molecular dynamics
MOM	Methoxymethyl
MP	Melting point
Ms	Methanesulfonyl
$NADP^+$	Nicotinamide adenine dinucleotide phosphate
NBS	N-Bromosuccinimide
NMR	Nuclear Magnetic Resonance
o	Ortho
p	Para
PDB	Protein data bank
PDE	Phosphodiesterase
PTSA	*p*-Toluenesulfonic acid
R	Unspecified organic group
RCM	Ring-closing metathesis
R_f	Retention factor
rt	Room temperature
S_NAr	Nucleophilic aromatic substitution

TEA	Triethylamine
Tf	Trifluoromethanesulfonyl
TFA	Trifluoroacetic acid
THF	Tetrahydrofuran
TON	Turnover number
TLC	Thin layer chromatography
TMS	Trimethylsilyl
TMSCl	Chlorotrimethylsilane
TPSH	2,4,6-Triisopropylbezenesulfonylhydrazide
TTN	Total turnover number
UV	Ultraviolet
WT	Wild type

Amino acid codes

Amino acid	Three letter code	One letter code
alanine	Ala	A
arginine	Arg	R
asparagine	Asn	N
aspartic acid	Asp	D
cysteine	Cys	C
glutamic acid	Glu	E
glutamine	Gln	Q
glycine	Gly	G
histidine	His	H
isoleucine	Ile	I
leucine	Leu	L
lysine	Lys	K
methionine	Met	M
phenylalanine	Phe	F
proline	Pro	P
serine	Ser	S
threonine	Thr	T
tryptophan	Trp	W
tyrosine	Tyr	Y
valine	Val	V

Table of Contents

Abstract i

Acknowledgments iii

Abbreviations v

Amino acid codes ix

Table of Contents x

Chapter 1 : Introduction

1.1. Total Synthesis..... 1

1.1.1. On the importance of natural product total synthesis 1

1.1.2. Oxidations in total synthesis 1

1.1.2.1. Oxidations of Activated C–H bonds 3

1.1.2.2. Oxidations of Unactivated C–H bonds 5

1.2. Biocatalysis 12

1.2.1. History of biocatalysis 12

1.2.2. Biocatalytic total synthesis 16

1.2.3. Chemo-enzymatic total synthesis 18

1.2.3.1. Enzymatic hydroxylation 19

1.2.4. Cytochrome P450 monooxygenases 21

1.2.4.1. $P450_{BM3}$ (CYP102A1) 23

1.2.5. $P450_{BM3}$ in synthesis 24

1.2.5.1. Substrate Engineering 24

1.2.5.2. Protein Engineering 27

1.3. Aims and proposed work 29

1.4. References for Chapter 1 30

Chapter 2 : Enantioselective $P450_{BM3}$ Hydroxylation of Aminocycloalkanes

2.1. Introduction..... 36

2.1.1. Bioisosteres in medicinal chemistry..... 36

2.1.2. Use of bicyclo[1.1.1]pentanes as bioisosteres..... 39

2.1.3. Synthesis of bicyclo[1.1.1]pentanes 40

2.1.4. Importance of small ring hydroxy-amino-cycloalkanes 46

2.1.5. Aims of this project 48

2.2. Synthesis of amine substrates..... 49

2.3. Synthesis of 1,2-hydroxy-aminocyclobutanes..... 49

2.3.1. Access to *trans* 1,2-hydroxy-aminocyclobutanes 49
2.3.2. Access to *cis* 1,2-hydroxy-aminocyclobutanes..... 56
2.4. Synthesis of 1,3-hydroxy-aminocyclobutanes..... 59
2.5. Synthesis of C2-hydroxylated amino-bicyclo[1.1.1]pentanes 64
2.6. Derivatisation of hydroxylated building blocks 75
2.7. Other reactivity 78
2.7.1. Substrates not tolerated 78
2.7.2. Carboxamides 79
2.7.3. Sulfoxides 82
2.8. Conclusions 85
2.9. References for Chapter 2 85

Chapter 3 : Synthetic Efforts Towards Trigoxyphin Natural Products

3.1. Introduction 90
3.1.1. Trigoxyphin 90
3.1.2. Aims of this project 92
3.2. First-generation synthetic route to *deoxy*-trigoxyphin **3.11**..... 93
3.2.1. Previous work within the group 93
3.2.2. Improvements to route 94
3.3. Second-generation synthetic route *via* cationic cyclisation..... 95
3.3.1. Retrosynthesis 95
3.3.2. Lewis acid mediated coupling of tolyl substrate **3.26** 95
3.3.3. Attempted cationic cyclisation of **3.32**..... 98
3.3.4. Alternative substrates for Lewis acid mediated coupling 99
3.3.5. Intramolecular Heck coupling of **3.52** 100
3.3.5.1. Retrosynthesis and literature precedent 100
3.3.5.2. Previous work in the group 102
3.3.5.3. Towards *deoxy*-trigoxyphin L **3.11**..... 103
3.4. Third-generation synthetic route *via* Heck-type cross-coupling 105
3.4.1. Synthesis and Heck reaction of model substrates 105
3.4.2. Synthesis of Heck substrate **3.74** towards trigoxyphin L synthesis 107
3.4.3. Screening of Pd-catalysed Heck conditions 112
3.5. Fourth-generation synthetic route *via* Robinson annulation 114
3.6. Conclusions and future work..... 118
3.7. References for Chapter 3 118

Chapter 4 : Late-Stage Functionalisation of Trigoxyphin Scaffolds

4.1. Introduction 121
4.1.1. Late-stage functionalisation in synthesis 121
4.1.1.1. Chemo- vs bio- catalysis 121
4.1.2. Aromatic hydroxylation 123
4.1.3. Aims of this project 127
4.2. Screening of trigoxyphin model systems with $P450_{BM3}$ 127
4.3. Screening of trigoxyphin intermediates with $P450_{BM3}$ 129
4.3.1. Diol **3.21** 129
4.3.2. Ketone **3.22** 130
4.3.3. Furan **3.12** 131
4.3.4. Hydroxy-butenolide **3.11** 132
4.4. Chemical late-stage functionalisation 137
4.5. Conclusions and future work 137
4.6. References for Chapter 4 138

Chapter 5 : Appendices

5.1. Appendices for Chapter 2 141
5.1.1. Screening data tables for substrate **2.68** 141
5.1.1.1. Initial screening data 141
5.1.1.2. Screening of RL/YF/HL/IG- and RP/HL/IG-based mutants for **2.75** 143
5.1.1.3. Screening of GV/A184I-based mutants for **2.78** 144
5.1.2. Screening data tables for substrate **2.71** 145
5.1.2.1. Initial screening data 145
5.1.2.2. Further screening for **2.82** 147
5.1.3. Screening data tables for substrate **2.70** 148
5.1.3.1. Initial screening data 148
5.1.4. Screening data tables for substrate **2.73** 150
5.1.4.1. Initial screening data 150
5.1.4.2. Screening of GV/A184I/I263G-based mutants for **2.84** 152
5.1.4.3. Screening of A330P-based mutants for **2.85** 152
5.1.4.4. Screening of R19/F87I-based mutants for **2.86** 153
5.1.5. Screening data tables for substrate **2.74** 154
5.1.5.1. Initial screening data 154
5.1.6. Screening data tables for substrate **2.72** 156
5.1.6.1. Initial screening data 156
5.1.7. Screening data tables for substrate **2.108** 157

5.1.7.1. Initial screening data 157
5.2. Appendices for Chapter 3 159
5.2.1. Conditions screened for Lewis acid coupling of **3.27** with **3.25** 159
5.2.2. Conditions screened for cationic cyclisation of **3.32** and **3.39** 160
5.2.3. Heck conditions screened by Syngenta for substrate **3.52** 161
5.2.4. Heck conditions screened by Syngenta for substrate **3.62** 162
5.3. Appendices for Chapter 4 163
5.3.1. Screening data tables for substrate **4.37** 163
5.3.2. Screening data tables for substrate **3.63** 164
5.3.3. Screening data tables for substrate **3.21** 166
5.3.4. Screening data tables for substrate **3.22** 167
5.3.5. Screening data tables for substrate **3.12** 169
5.3.6. Screening data tables for substrate **3.11** 170
5.3.6.1. 2017 initial screening data 170
5.3.6.2. 2021 initial screening data 172
5.3.6.3. Further screening of RP/H171L/I263G-based mutants 174
5.4. Tables of mutations 175
5.4.1. Initial screening plates 175
5.4.2. Focused second generation libraries 185
5.5. References for Chapter 5 188

Chapter 6 : Experimental Details

6.1.Materials and Methods 189
6.1.1. General considerations 189
6.1.2. Gas chromatography analysis 190
6.1.3. Enzymes and molecular biology 190
6.2. Experimental procedures for Chapter 2 191
6.2.1. $P450_{BM3}$ screening conditions 191
6.2.2. Synthesis of starting materials 192
6.2.3. Preparative scale $P450_{BM3}$ reactions 201
6.2.3.1. General procedure I (GP-I) 201
6.2.3.2. Isolation of amine metabolites 202
6.2.3.3. Isolation of carboxamide metabolites 213
6.2.4. Moshers ester analysis for determination of absolute configuration of **2.70A** ...216
6.2.5. Derivatisation of metabolites 217
6.2.6. Single crystal X-ray data for compounds in Chapter 2 222
6.2.6.1. Crystal data and structure refinement for **2.75** 222

6.2.6.2. Crystal data and structure refinement for **2.82** 223
6.2.6.3. Crystal data and structure refinement for **2.80** 224
6.2.6.4. Crystal data and structure refinement for **2.84** 225
6.2.6.5. Crystal data and structure refinement for **2.86** 226
6.2.6.6. Crystal data and structure refinement for **2.93** 227
6.3. Experimental procedures for Chapter 3 228
6.3.1. General procedures (GP-II and GP-III) 228
6.3.2. Experimental details for first-generation route to trigoxyphin 229
6.3.3. Experimental details for second-generation route to trigoxyphin 237
6.3.4. Experimental details for third-generation route to trigoxyphin 249
6.3.5. Experimental details for fourth-generation route to trigoxyphin 262
6.3.6. Miscellaneous compounds 267
6.4. Experimental procedures for Chapter 4 281
6.4.1. Screening conditions 281
6.4.2. Preparative scale $P450_{BM3}$ reactions and isolation of metabolites 282
6.4.3. Single crystal X-ray data for compounds in Chapter 4 291
6.4.3.1. Crystal data and structure refinement for **4.41** 291
6.4.3.2. Crystal data and structure refinement for **4.50b** 292
6.4.4. Experimental details for chemical LSF 293
6.5. References for Chapter 6 296

Chapter 1 : Introduction

1.1. Total Synthesis

1.1.1. On the importance of natural product total synthesis

The golden age of organic chemistry, *i.e.* the second half of the 20th century, saw huge advances in the field of organic synthesis. E. J. Corey introduced a new way of thinking about total synthesis with the concept of retrosynthetic analysis,[1] where focus on making bonds in the most creative way led to highly efficient syntheses.[2] Today, the total synthesis of complex natural products is still one of the most exciting areas of research.[3] Synthetic organic chemists can use total synthesis as a true field-test of new methodologies to work on advanced scaffolds, or when requiring exquisite selectivity, and conversely new chemistries are often developed out of a need for new chemistry to work on specific targets in route development. Furthermore, unexpected discoveries can often arise and creative solutions to these problems push the field of organic chemistry forward into new directions.[4]

Achieving new and efficient routes to complex bioactive molecules is important for scientific innovation and can provide adequate material for biological testing where isolation from natural sources is insufficient. These developments in academic research can provide tools for industry to simplify and shorten syntheses of pharmaceutical candidates, thereby reducing waste and overall cost,[5] and many productive collaborations between academia and industry[6] demonstrate what can be achieved with a joint goal of achieving the 'ideal synthesis'.[7]

1.1.2. Oxidations in total synthesis

The goal of modern total synthesis is to access complex chemical targets in the most redox efficient and atom economical way. With this goal in mind, the ability to selectively functionalise a single C–H bond was described by Bergman in 1995 as the 'Holy Grail'[8] of synthetic chemistry and, since then, C–H functionalisation has risen from a curiosity to becoming one the most prominent fields in modern organic chemistry.[9] Many elegant methods have been developed using directing groups, either pre-installed in the substrate or transient,[10] or without any functional group to direct to a specific C–H bond (*Figure 1*).[11]

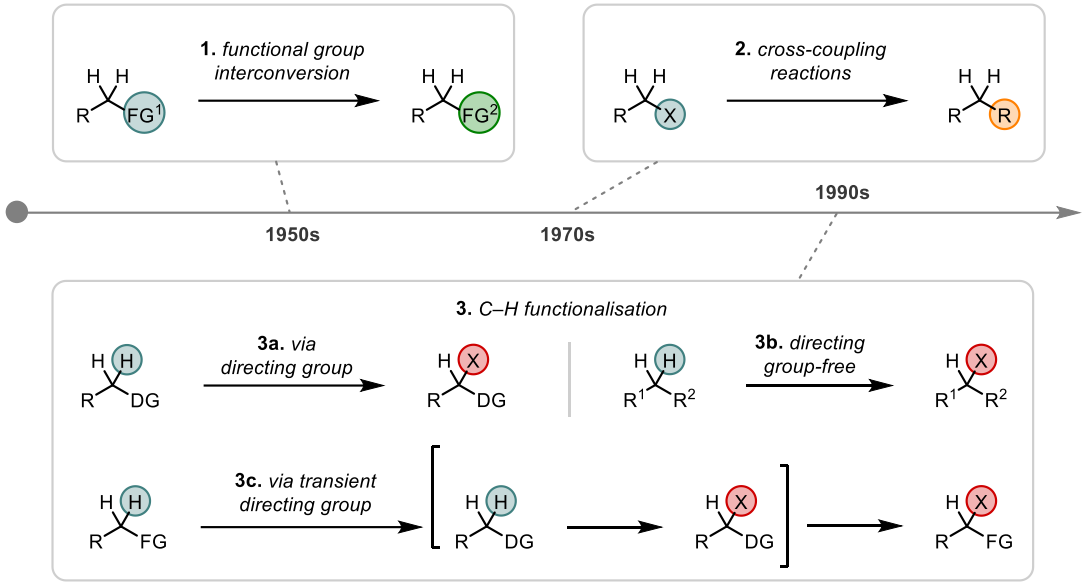


Figure 1 – Chemical approaches to the installation of new functionality within a molecule.

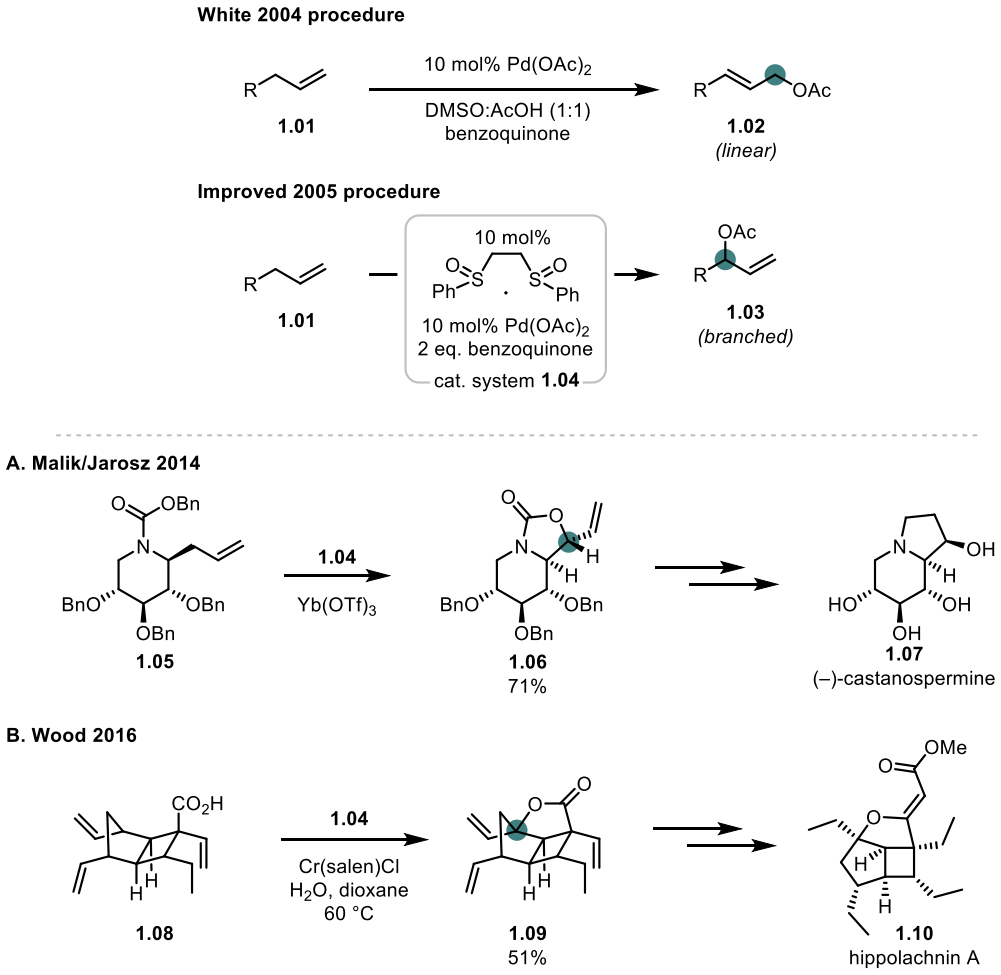
C–H oxidation can generally be defined as the direct conversion of an inert C–H bond to a higher oxidation state C–X bond, potentially in the presence of other more reactive functionalities.[12] Unlike traditional chemical oxidations, which require sometimes tedious and wasteful functional group interconversions and extensive protecting group strategies, C–H oxidation can install a hydroxyl group at a late stage in the synthesis, bypassing these issues.[13] Nature has taken advantage of this strategy using enzymes as catalysts (*Section 2.2*); however, this discussion will highlight key examples using synthetic organic chemistry.

C–H bonds are the most inert and common functionality found in organic compounds; however, they can be distinguished by their differing electronic and steric environments. Carbons which are adjacent to a heteroatom or unsaturation, such as C–C double or triple bonds, are described as 'activated', whereas positions which are only surrounded by other C–H bonds, for example in alkanes, are classified as 'unactivated'.

1.1.2.1. Oxidations of Activated C–H bonds

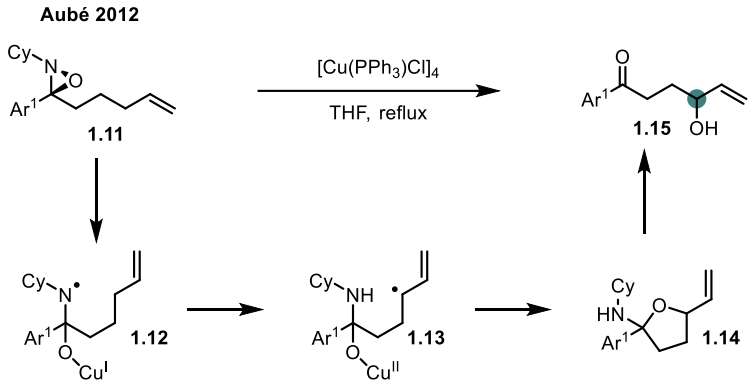
Traditionally, harsh conditions and strong metal oxidants, such as Mn(VII), Cr(VI) and Se(IV), are required for oxidation at activated positions.[14] Tolerance of other functional groups and over-oxidation can often be an issue; however, many recent reports using milder conditions bypass these limitations.

White demonstrated that a Pd(II)/bis-sulfoxide catalytic system,[15] inspired by earlier work on the beneficial effect of DMSO as an additive,[16] could achieve a range of C–H functionalisation chemistries[17] including allylic oxidation (*Scheme 1*).[18] This methodology was successfully applied by Malik and Jarosz in the synthesis of (–)-castanospermine[19] **1.07** (*Scheme 1.A*), and for the carboxylic acid directed C–H oxidation in the Wood synthesis of hippolachnin A **1.10** (*Scheme 1.B*).[20]



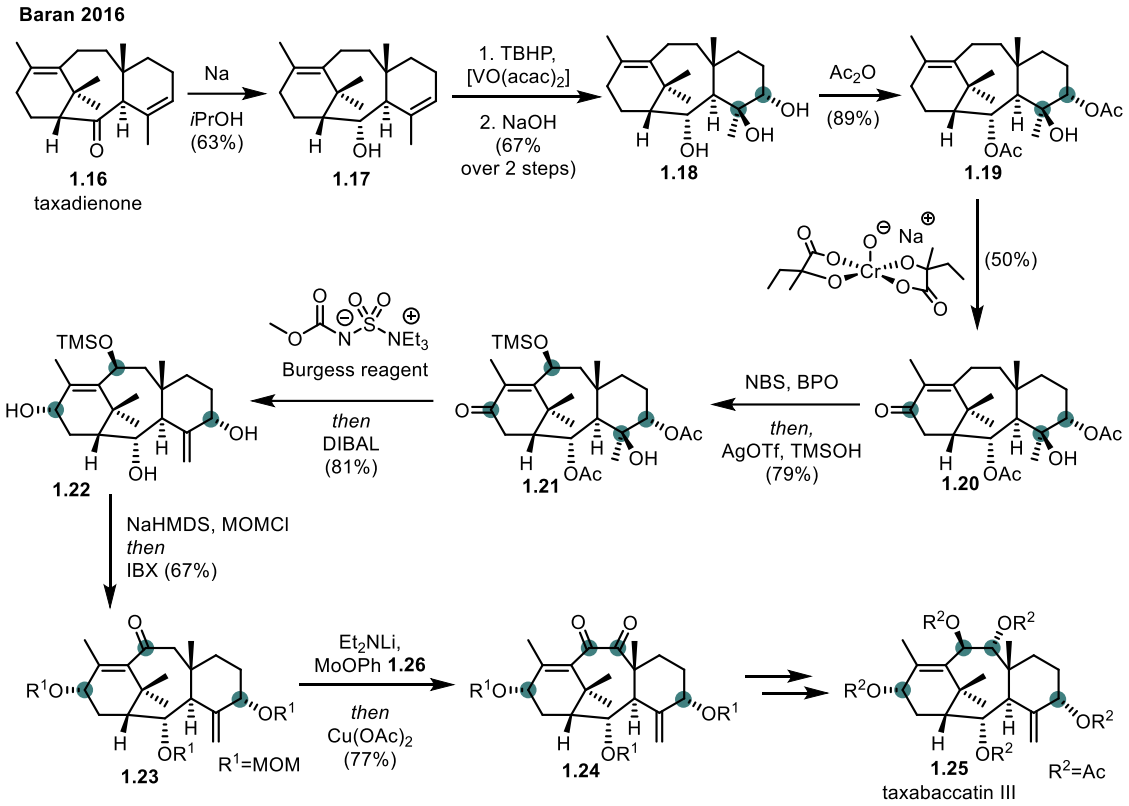
Scheme 1 – Pd(II)/bis-sulfoxide/benzoquinone conditions for C–H oxidations.

Aubé demonstrated that oxaziridine **1.11** could undergo intramolecular oxidation of activated C–H bonds using Cu(I) catalysis to form allylic and benzylic alcohols (*Scheme 2*).[21] In this reaction, Cu(I) promotes the hydrolysis of **1.11**, to form *N*-centred radical **1.12** which could undergo 1,5-hydrogen abstraction forming allylic radical **1.13**. This then undergoes radical recombination to form cyclic intermediate **1.14**, which is hydrolysed to form product **1.15**. Although highly chemo-selective, this process is limited only to this specific class of substrates and, unlike other Cu-catalysed radical allylic oxidations (*i.e.*, Kharasch–Sosnovsky reaction), no stereoselective variant has been reported.[22]



Scheme 2 – Copper catalysed intramolecular allylic C–H oxidation.

Baran's strategic use of oxidations of activated C–H bonds, towards the synthesis of taxanes, highlights how this effective strategy can streamline complex natural product synthesis.[23] His two-phase approach, inspired by terpene biosynthesis, includes a 'cyclase phase', which forms the core structure, and an 'oxidase phase' which selectively installs C–O bonds through the use of C–H activation chemistry. These C–O bonds are installed late-stage at either an allylic position, in **1.20** and **1.21**, or α to a ketone in **1.24** (*Scheme 3*). Despite these advances, Baran's route still requires many redox inefficient steps and functional groups interconversions. For example, TMS protected alcohol introduced in **1.21** is oxidised to **1.23** and then reduced again in the final compound **1.25**; similarly, hydroxy functionality installed using Vedejs' reagent **1.26** (MoOPh) is immediately oxidised to **1.24**, and then is also reduced in taxabaccatin III **1.25**. This synthesis also requires a wasteful protecting group strategy. These limitations are avoided in taxol biosynthesis, where P450s can selectively oxidise the desired C–H bond in the presence of similar C–H bonds and other unprotected alcohols. There are still selectivity issues even in biocatalysis, where numerous oxidised side-products are found in the Pacific yew tree (*Taxus brevifolia*) creating the diversity found in the taxane family.



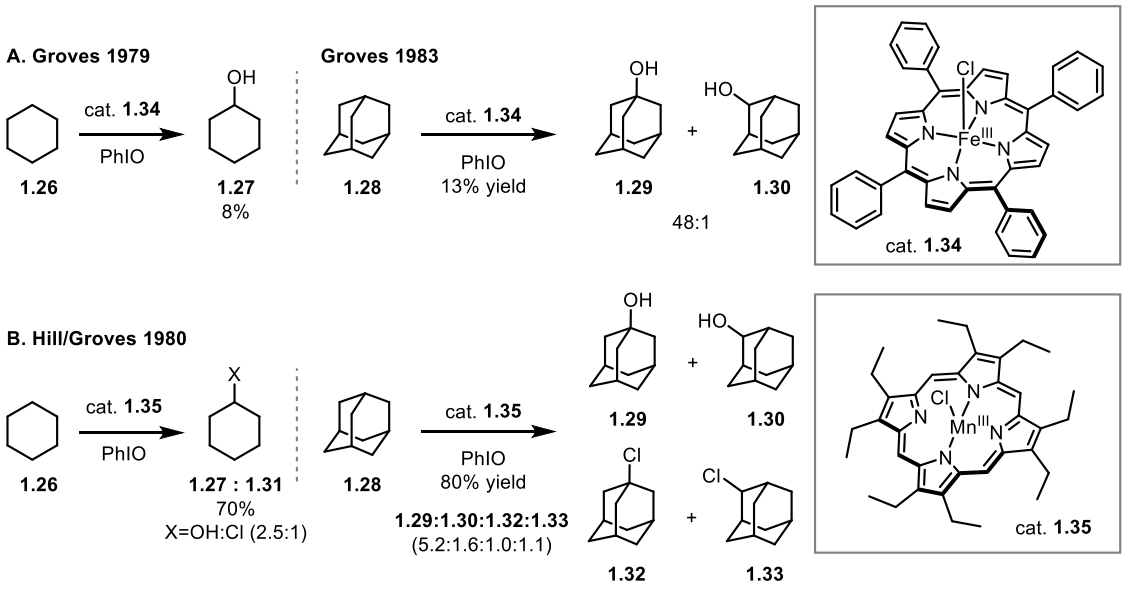
Scheme 3 – Baran's synthesis of taxabaccatin III, see ref [23] for full reaction conditions.

Although oxidation at activated positions can provide extremely high chemoselectivities and conversions, reactivity is inherently limited by the substrate structure.

1.1.2.2. Oxidations of Unactivated C–H bonds

Synthetic chemistry has taken inspiration from Nature's ability to conduct highly selective catalysis on unactivated C–H bonds, with considerable effort over the last few decades on the development of new chemical catalysts that imitate oxidative enzymes. These can be generally categorised into metal-based catalysts, often using coordinating ligands to fine-tune the redox potential of the metal, or metal-free reagents. These catalysts are designed based on the method of catalysis, including: directed- or chelation controlled, where functionality in the substrate forms a metallocycle with the catalyst to direct to a neighbouring C–H bond; remote functionalisation, where C–H bond activation is far from the site of catalyst interaction; and innate functionalisation, where reactivity is dictated by the steric or electronic bias of the substrate only.

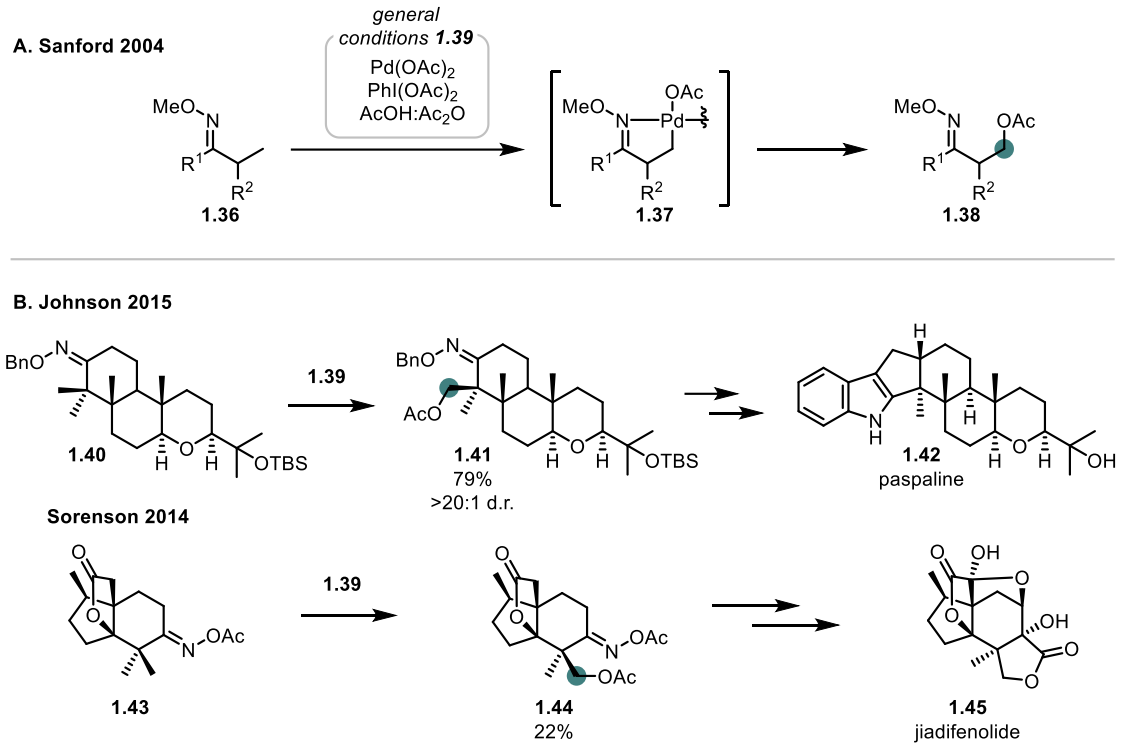
The heme-iron group of P450 enzymes was the original inspiration for metalloporphyrin-based catalysts, with pioneering work by Breslow describing an 'artificial enzyme' consisting of a catalytic metal ion surrounded by a hydrophobic binding cavity (cyclohexylamylose),[24] which was further developed into an artificial P450 capable of regioselective steroid hydroxylation.[25] After completing his doctoral studies with Breslow, Groves independently reported a catalytic iron-porphyrin system (cat. **1.34**) to achieve the hydroxylation of cyclohexane **1.26**, with minimal over-oxidation of cyclohexanol **1.27**, and adamantane **1.28** (*Scheme 4.A*).[26] In back-to-back publications, Hill and Groves reported manganese-based catalysts, such as cat. **1.35**, that drastically improved the conversion of these substrates, although chlorinated side-products (**1.31 – 1.33**) were then observed (*Scheme 4.B*).[27] More advanced iron and manganese, and even cobalt, osmium and ruthenium porphyrin based catalytic systems have since been developed.[28]



Scheme 4 – Early examples of metalloporphyrins as C–H oxidation catalysts.

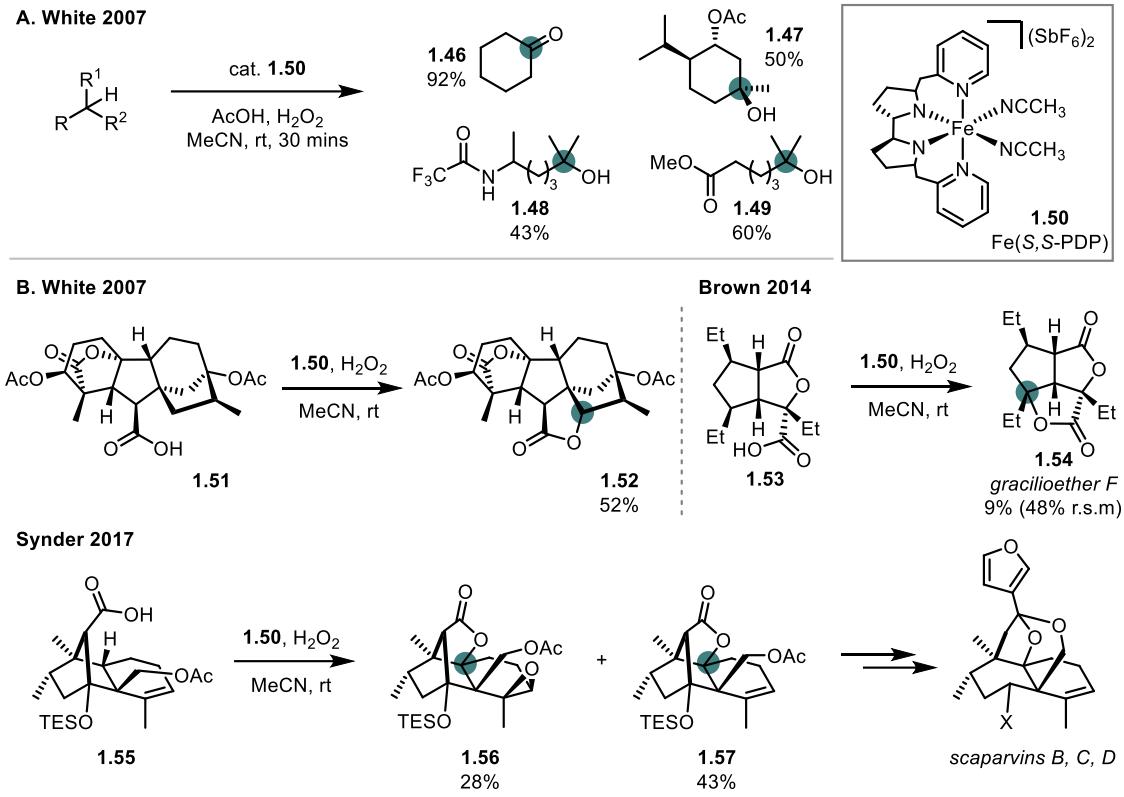
Porphyrin based metal catalysts often show poor regio- and chemo-selectivity, an issue circumvented when using non-porphyrin catalysts, in part due to the extra tunability that can be achieved by careful design of the coordinating ligands. Many recent natural product syntheses feature metal-catalysed C–H functionalisation reactions, often using directing-groups strategies to improve regioselectivity and frequently using expensive gold,[29] iridium, rhodium, or palladium catalysts.[30]

Sanford developed a Pd(II)-catalysed directed oxygenation of inert C–H bonds, using methoxy imine **1.36** as the directing group and $PhI(OAc)_2$ as the terminal oxidant (conditions **1.39**, *Scheme 5.A*).[31] This has been effectively used in the total synthesis of paspaline[32] **1.42** and jiadifenolide[33] **1.45** to differentiate geminal methyl groups (*Scheme 5.B*).



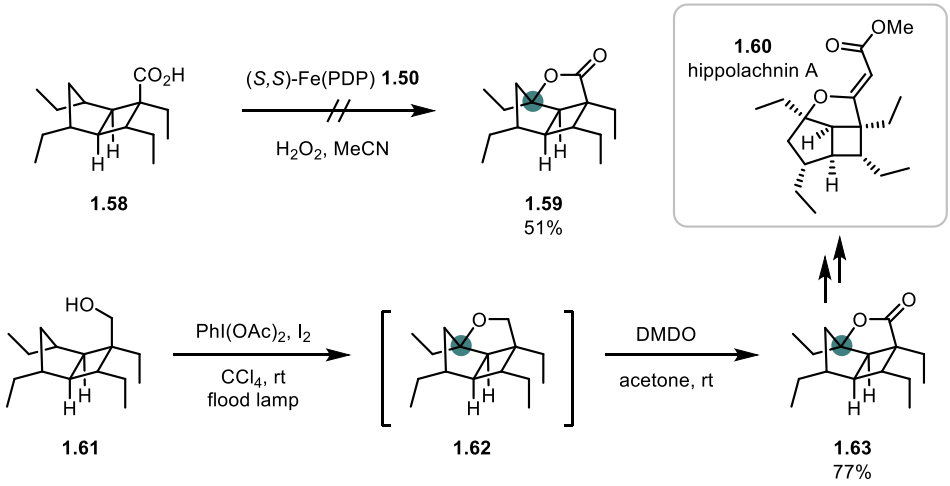
Scheme 5 –Pd-catalysed directed C–H acetoxylations.

One of the most important developments in this field was the pioneering work of White, who with graduate student Chen, developed an Fe(PDP) catalyst **1.50** capable of predictable, selective hydroxylations of inert C(sp^3)–H bonds (*Scheme 6.A*).[34] This reagent system is tolerant of a range of functionalities, as can be seen in selected examples **1.46 – 1.49** which were produced in good yields. This catalyst system has been used in the synthesis of multiple complex natural products in which the formation of lactone rings proceeds *via* late-stage carboxylate directed C–H oxidation, as can be seen in **1.52**, **1.54**[35] and **1.57**[36] (S*cheme 6.B*).



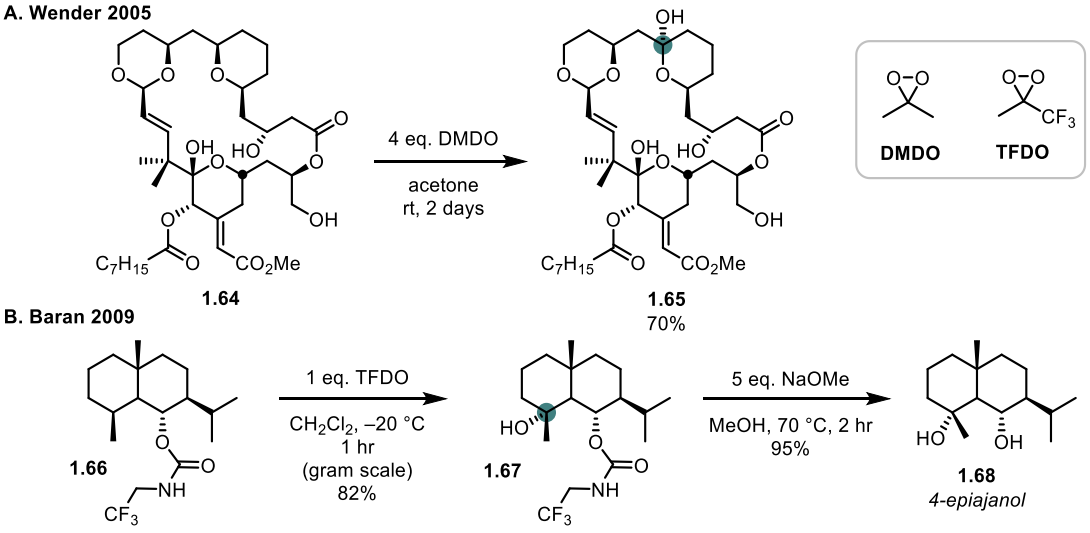
Scheme 6 – Use of the White–Chen catalyst **1.50** for (A) the innate functionalisation of sp^3 C–H bonds, and (B) the formation of lactones in natural product synthesis *via* directed functionalisation.

Brown attempted to use the Fe(PDP) catalyst **1.50** for the directed C–H oxidation of **1.58**; however, only over-oxidation products were observed, and a route redesign was required.[37] A new synthesis proceeded through tetrahydrofuran intermediate **1.62**, from alcohol **1.61**, then oxidation using dimethyl dioxirane (DMDO) to furnish lactone **1.63**, and further elaboration to hippolachnin A **1.60** (*Scheme 7*).[38]



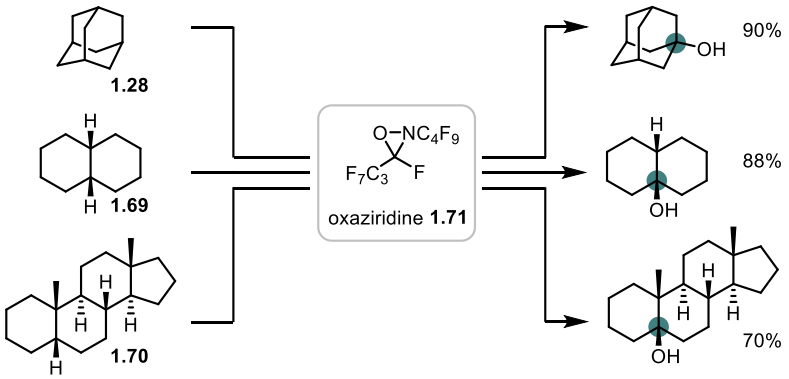
Scheme 7 – C–H oxidation chemistry in Brown's synthesis of hippolachnin A **1.60**.

Dioxiranes are commonly employed for C–H oxidation as they can exhibit excellent levels of selectivity and reactivity; however, super-stoichiometric equivalents are often required.[39] Although dioxiranes are often used for epoxidations, the direct hydroxylation of unactivated C–H bonds is also possible. A highly selective hydroxylation of bryostatin analogue **1.64** at C9 to **1.65** was reported by Wender (*Scheme 8.A*), using DMDO.[40] Baran used stoichiometric amounts of the more reactive 3-methyl(trifluoromethyl)dioxirane (TFDO) in the synthesis of a range of eudesmane terpenes including 4-epiajanol **1.68** (*Scheme 8.B*),[41] achieving excellent regioselectivity for the oxidation of a single tertiary C–H bond in **1.66**.[42]



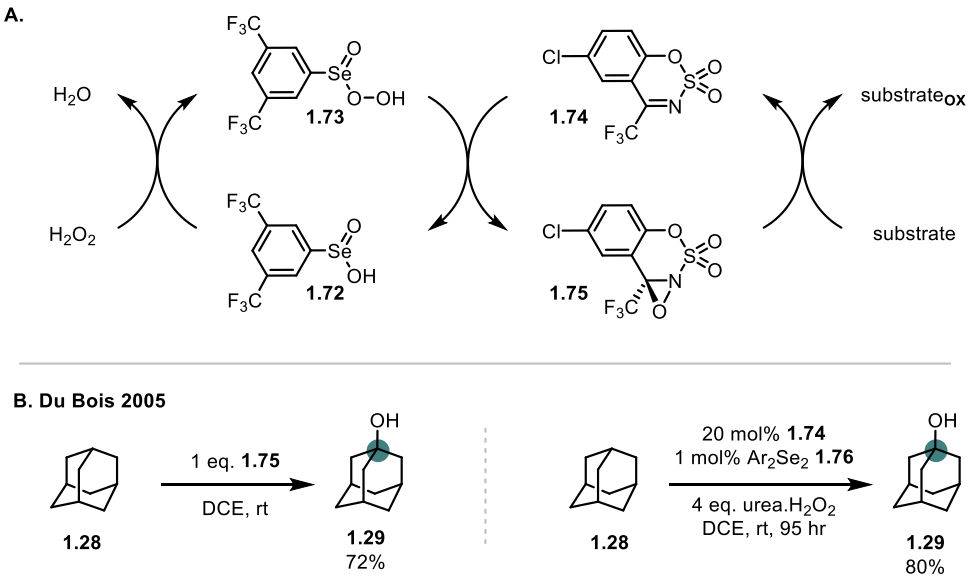
Scheme 8 – Examples of dioxirane catalysed C–H oxidation in natural product synthesis.

Oxaziridines offer similar reactivity to dioxiranes; however, they are remarkably stable and therefore considerably safer and easier to synthesise.[43] Resnati first reported the use of perfluorinated oxaziridine **1.71** for direct hydroxylation of hydrocarbons, favouring oxidation of tertiary C–H bonds in a range of simple aliphatic substrates including **1.28**, **1.69**, and steroid **1.70** (*Scheme 9*).[44]



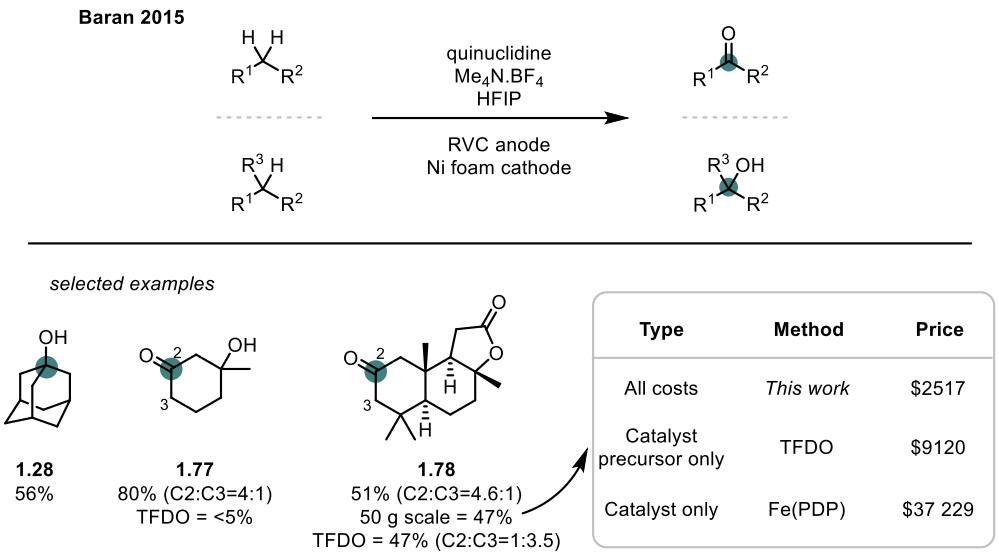
Scheme 9 - Perfluorinated oxaziridines for selective hydroxylation of hydrocarbons **1.28**, **1.69** and **1.70**.

A catalytic version of this reaction was developed by Du Bois, using benzoxathiazine oxaziridine **1.75** and hydrogen peroxide with co-catalyst diselenide **1.76**.[45] The oxidation of substrate regenerates the catalyst imine **1.74**, which in turn is oxidised by perseleninic acid **1.73** to reform the active oxaziridine catalyst **1.75** (*Scheme 10.A*). This elegant catalysis could effect C–H bond hydroxylation, Baeyer–Villiger oxidation and epoxidation with good yields, and displayed an increased yield compared to stoichiometric conditions (*Scheme 10.B*). A further improvement was seen using Oxone® as the terminal oxidant, where reaction times could be shortened to 24 hr.[46]



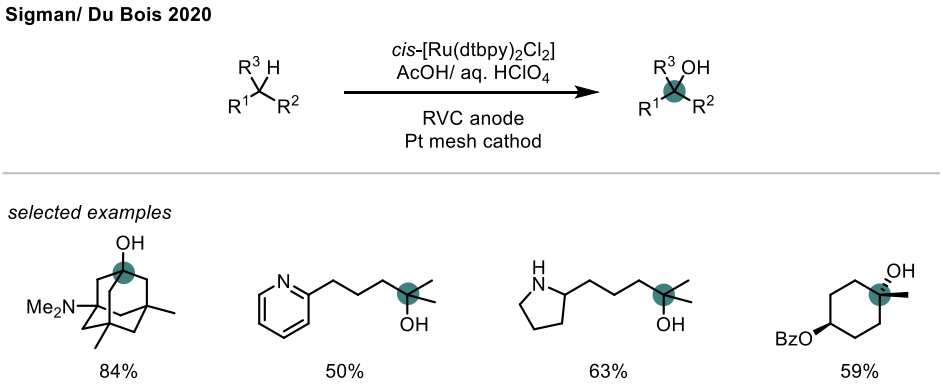
Scheme 10 – Benzothiazine oxaziridine catalysis for C–H bond hydroxylation.

Examples of scalable C–H oxidation are rare, in part due to the often-complicated procedures for the preparation of reagents such as dioxiranes, and the high cost associated with many metal-based catalysts. Baran recently reported a quinuclidine-mediated electrochemical process that bypasses these issues, and oxidation of unactivated secondary and tertiary C–H bonds was achieved on large scale in high yields (*Scheme 11*).[47] Conversions were generally comparable with TFDO, or improved in some examples such as cyclohexanol **1.77**, and were easily achieved in up to 50 g scale (sclareolide **1.78**). The comparative costs associated with performing similar reactions on this scale highlight the practicality of this method.



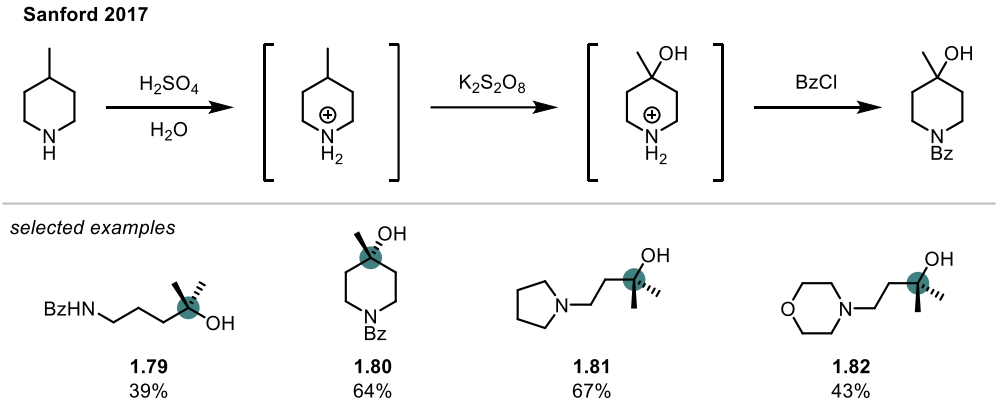
Scheme 11 – Selected examples from Baran's report of electrochemical oxidation (RVC = Reticulated vitreous carbon).

Previous methods describe oxidation of only C- and O- containing substrates; however, Sigman and Du Bois were able to extend this electrochemical approach to include amine-derived substrates, using ruthenium catalysis (*Scheme 12*).[48] By replacing super-stoichiometric amounts of chemical oxidants with an electric current as the terminal oxidant, these methods reduce waste and provide significantly milder conditions.



Scheme 12 – Sigman and Du Bois Ru-catalysed electrochemical C–H oxidation.

Similarly, Sanford used protonated amines in her report of C(sp^3)–H oxidation, in order to prevent *N*-oxidation and to deactivate proximal C–H bonds, achieving remote hydroxylation of a range of aliphatic amines with $K_2S_2O_8$.[49] Cyclic amines **1.80** and **1.81** were produced in good yields, whereas linear chain **1.79** and morpholine **1.82** achieved modest, but still synthetically useful, yields.



Scheme 13 – Sanford oxidation of tertiary C(sp^3)–H bonds of amines.

Despite many recent advances in the area of C–H oxidation, chemical catalysts often still suffer from low selectivity and forcing conditions (super-stoichiometric reagents, prolonged reaction times, etc.). Selectivity is frequently controlled by the electronic and steric parameters of the substrate, with oxidation usually limited to tertiary C–H bonds, and discrimination between similar C–H bonds remains challenging. Biocatalysts can offer complementary reactivity to the known chemical methods for C–H functionalisation, with enzymes able to selectively discriminate between unactivated C–H bonds in a variety of substrates.

1.2. Biocatalysis

1.2.1. History of biocatalysis

Biocatalysis is a key part of the modern organic chemist's toolbox; however, enzymes were in use long before the field of biocatalysis was conceptualised, with examples dating as far back as 7000 BC for the fermentation of sugars into alcohol.[50] It was originally thought that a 'life-force' was necessary for this transformation, as Pasteur identified that fermentation was possible without the presence of oxygen but could not isolate a specific enzyme which catalysed it.[51] Leibig conversely claimed that a purely chemical reagent was carrying out this process, and in 1897 Buchner's ground-breaking discovery that a dead yeast extract could successfully catalyse the same fermentation process put this argument to rest, and earned him the 1907 Nobel Prize in Chemistry.[52]

Although the first enzyme was identified in 1833,[53] and the idea that they are catalysts was introduced soon after in 1836,[54] the first model to try to explain how they work was not described

until much later when Fischer proposed the 'lock-and-key' model in 1894 (*Figure 2*).[55] This idea, that enzymes have specific active sites which accommodate only specific substrates, is drastically over-simplified considering our modern understanding of enzymatic systems; however, it still provides a conceptually straightforward introduction for beginners to the field. Furthermore, Pauling stated that enzymes stabilise the transition state and not the substrate,[56] a theory which was further extended by Koshland in his report of the induced fit model (*Figure 2*).[57]

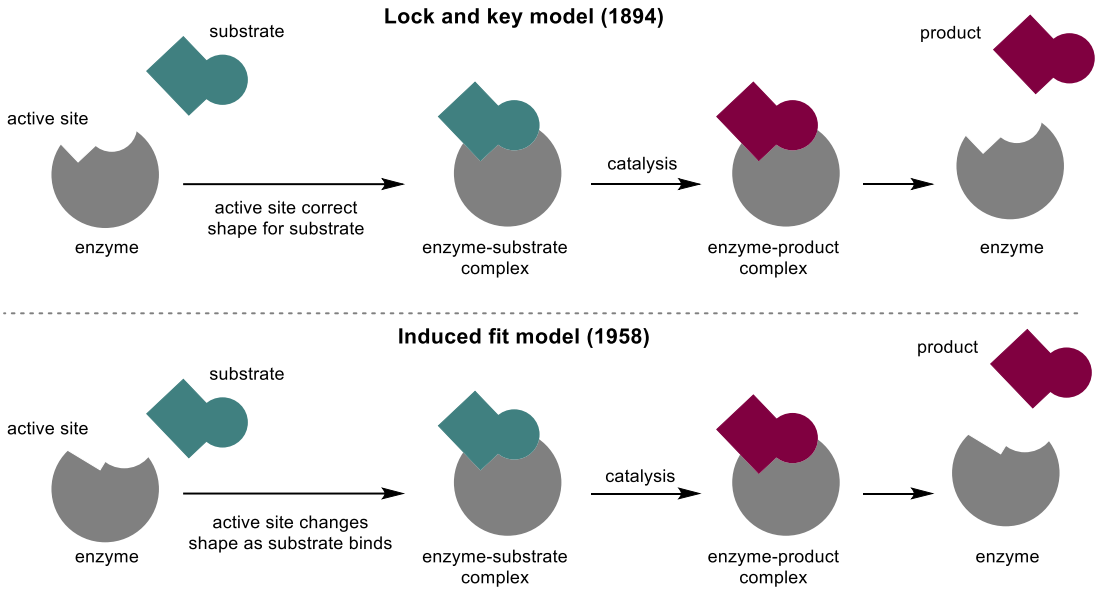


Figure 2 – Graphical representations of the lock and key model, and the induced fit model of enzymes.

By 1913, academics were starting to propose ideas of how enzymes generally worked, with the publication of the Michaelis–Menten model of kinetics (S*cheme 14*) describing that an enzyme should bind to the enzyme (forming the enzyme-substrate complex) before catalysis can occur. However, any detail on the mechanism of such catalysis was still largely unknown.

$$E + S \rightleftharpoons ES \longrightarrow E + P$$

Scheme 14 – The Michaelis–Menten model of enzyme kinetics. Terms defined as E = enzyme, S = substrate, ES= enzyme-substrate complex, P = product.

Two further breakthroughs in the field came in 1951, when Frederick Sanger determined the amino acid sequence of insulin, *i.e.* its primary structure (which won him his first Nobel Prize in Chemistry in 1958),[58] and Pauling proposed how secondary structures may be composed of regular features such as α-helices and β-sheets,[59] based on his exceptional understanding of the chemical bond, for which he was awarded the Nobel Prize in 1954.

Although X-ray diffraction evidence to support Pauling's proposed secondary structures was published in 1951,[60] a protein structure was not solved until Kendrew and Perutz's report in 1958 described the tertiary structure of the globular protein myoglobin,[61] for which they shared the Nobel Prize in 1962. This ground-breaking work paved the way for an entire field of protein crystallography, with researchers inspired to understand how the structure of proteins and enzymes can affect the function.[62]

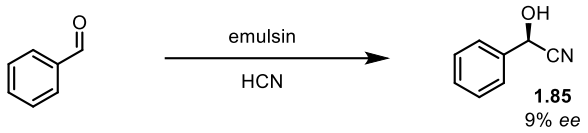
Many protein structures were solved in the following decades; when the Protein Data Bank (PDB) was founded in 1971 it contained just seven structures[63] but by 1986 there were over 200 structures and by the end of 2020 there were nearly 173,000.[64] Improvements in technology mean there are alternative methods for determining protein structures, such as cryo-electron microscopy[65] (cryo-EM) and DeepMind's AlphaFold.[66]

New technological advances in physical chemistry techniques allowed for a greater mechanistic understanding of how enzymes worked;[67] however, as they could still not be produced in large quantities their use was mainly confined to academic laboratories with minimal use in industry. A key development was the discovery that enzymes could be immobilised[68] and therefore recycled easily, and in the 1950s several groups achieved this immobilisation on solid supports,[69] with biotranformations being a key technology in the pharmaceutical and food industries ever since.[70] A notable early example was developed by Bayer in 1972 and is still in use to this day, in which an immobilised penicillin acylase is used to produce 6-aminopenicillic acid **1.84** *via* hydrolysis of penicillin G **1.83** (*Scheme 15*).[71]



Scheme 15 – Bayer process for the enzymatic hydrolysis of pencillin G to form 6-aminopenicillic acid.

Although issues with production of enzymes in large quantities existed, there were several significant biocatalytic process reported throughout the first half of the 20th century; using either whole cell, partially purified enzymes, or cell extracts. The earliest enantioselective synthesis was reported in 1908 by Rosenthaler,[72] describing the reaction to form (*R*)-mandelonitrile **1.85** using emulsin (enzymes including oxynitrilase extracted as a mixture from bitter almonds).[73]



Scheme 16 – First enantioselective synthesis, reported by Rosenthaler.

Around the mid-20th century, Prelog reported his seminal work on the stereoselective reduction of ketones using microbial strains of alcohol dehydrogenases (ADHs).[74] Based on this work, ADHs were isolated and characterised, and a selection of Prelog and anti-Prelog ADHs are commercially available today.

Advances in mechanistic understanding and practical techniques for the isolation and purification of enzymes continued throughout the middle of the 20th century but synthetic reports using enzymes remained infrequent and were largely ignored by organic chemists. One of the biggest limitations of this technology at that time was that enzymes needed to be isolated from natural sources, often a challenging process which yielded little material. Two breakthroughs in the field came in the 1970s with Sanger developing a method for the sequencing of DNA strands[75] (1980 Nobel Prize in Chemistry shared with Walter Gilbert), and the first example of recombinant DNA methodology by Paul Berg (1980 Nobel Prize in Chemistry) which made it possible to introduce DNA from any organism into a host organism such as *Escherichia coli* or *Bacillus subtilis*.[76] Furthermore, in 1983 an important report by Kary Mullis described the polymerase chain reaction (PCR, 1993 Nobel Prize) and all these new technologies allowed the field of biocatalysis to flourish (*Figure 3*).[77] Several excellent reviews summarise the history of biocatalysis in organic chemistry.[78]

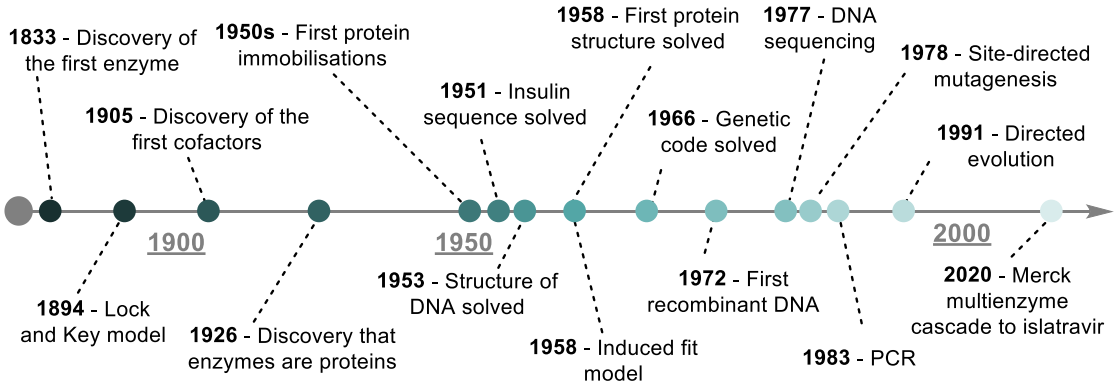
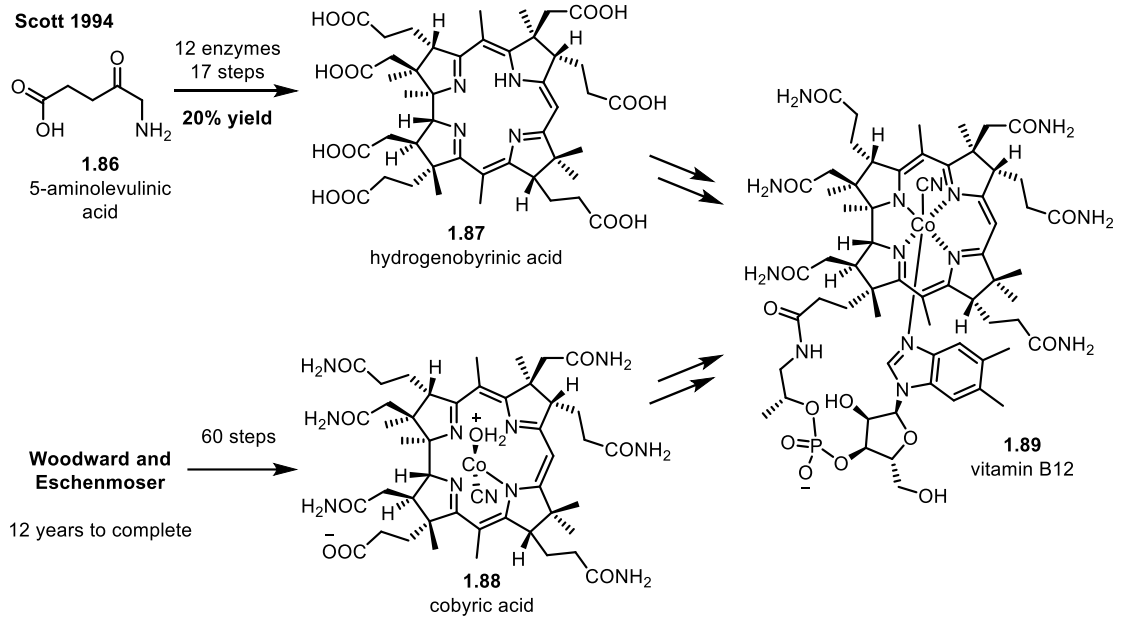


Figure 3 – Timeline of breakthrough research in biochemistry.

The field has seen significant advancements in protein engineering (such as directed evolution), screening analytics (such as high throughput screening and microfluidics), and computational techniques. These have all provided more efficient methods for the development of highly evolved enzymes and have been extensively reviewed.[79]

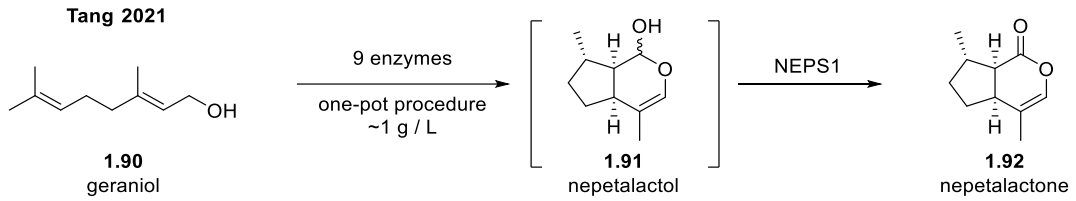
1.2.2. Biocatalytic total synthesis

Using enzymes from biosynthetic pathways clearly has many advantages when attempting the synthesis of a known natural product. Many impressive reports use multienzyme cascades; for example, Scott *et al.* (*Scheme 17.A*) described the synthesis of vitamin B12 precursor hydrogenobyrinic acid **1.87** in one pot from 5-aminolevulinic acid **1.86**, using 12 enzymes with an overall yield of 20%.[80] In comparison, the entirely nonbiological synthesis of vitamin B12 by Woodward and Eschenmoser consisted of 60 synthetic steps, taking over 100 students 12 years to complete.[81] This is widely accepted as one of the most impressive total syntheses ever achieved, and a direct comparison of the two approaches is futile as both syntheses have different goals. However, this example highlights what can be achieved from either strategy, as both are exemplary syntheses of an iconic complex natural product.



Scheme 17 – Biocatalytic synthesis of vitamin B12 precursor **1.87**, and the famous Woodward–Eschenmoser total synthesis of vitamin B12 **1.89** *via* intermediate cobyric acid **1.88**.

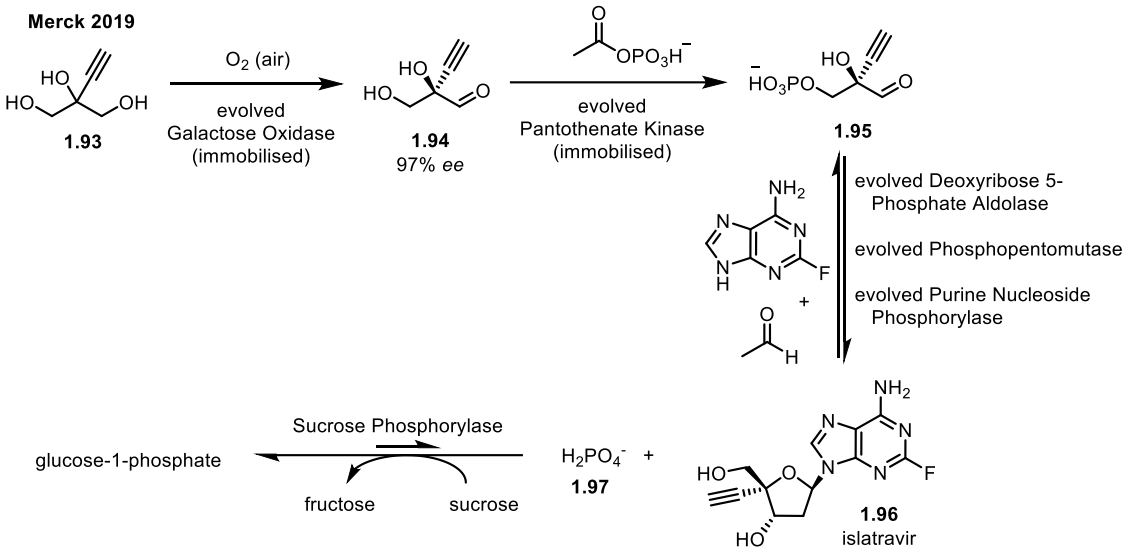
A recent example from Tang and co-workers describes a one-pot procedure using four biosynthetic enzymes and five accessory and cofactor regeneration enzymes for the synthesis of nepetalactone **1.92** (*Scheme 18*).[82] Taking advantage of an orthogonal cofactor regeneration system allowed a low ratio of $NADP^+$:NADPH and a high ratio of NAD^+:NADH to be maintained, which led to ideal conditions achieving ~1 g/L of nepetalactol **1.91** production from geraniol **1.90**. With the addition of the nepetalactol-related short-chain reductase/dehydrogenase (NEPS1) complete conversion to nepetalactone **1.92** could be achieved in 8.5 hr without the need for any further co-factors.



1.90 geraniol **1.91** nepetalactol **1.92** nepetalactone

Scheme 18 – One-pot enzymatic sequence involving 10 enzymes to produce nepetalactone **1.92** from geraniol **1.90**.

These examples employ enzymes from the biosynthetic pathway of the target compound, which clearly streamlines the synthesis as the enzymes have naturally-evolved substrate specificity. However, scientists from Merck showed that it was possible to use five enzymes engineered by directed evolution, with four auxiliary enzymes to produce islatravir **1.96** from 2-ethynylglycerol **1.93** in a three-step *in vitro* cascade with an overall yield of 51%.[83] In this revolutionary new process route no intermediates were isolated, meaning waste was reduced, and thermodynamically unfavourable reactions could be linked together so that any inhibitory intermediates could be consumed. The key to pushing the final equilibrium toward formation of product **1.96** was capture of the inorganic phosphate **1.97**, which inhibits these enzymes. Previous chemical syntheses of islatravir report between twelve – eighteen steps, require protecting group strategies and express difficulty in controlling the anomeric stereochemistry of nucleosides.[84]



Scheme 19 – Biocatalytic cascade for the synthesis of islatravir **1.96** by scientists at Merck.

1.2.3. Chemo-enzymatic total synthesis

Although total synthesis solely using enzymes for every transformation is impressive, biocatalysis is more often used for only one or two steps in a synthetic route. This combines the best of both disciplines, organic chemistry and biocatalysis, and expands the toolbox available to synthetic chemists in their route planning.[85] Due to the high substrate specificity achievable with enzymatic transformations, incorporation into syntheses at either an early-stage or late-stage is possible (*Figure 4*).

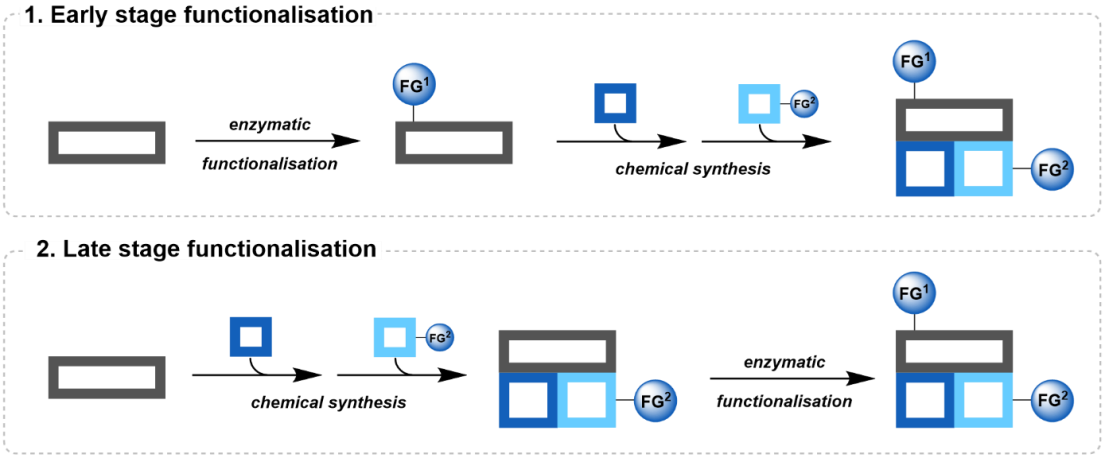
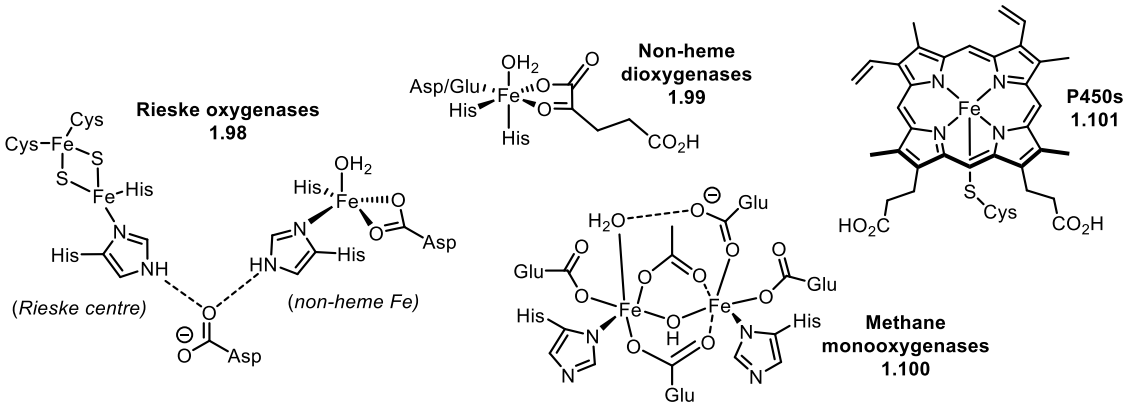


Figure 4 – Conceptual approaches to enzymatic functionalisation in synthesis route development.

1.2.3.1. Enzymatic hydroxylation

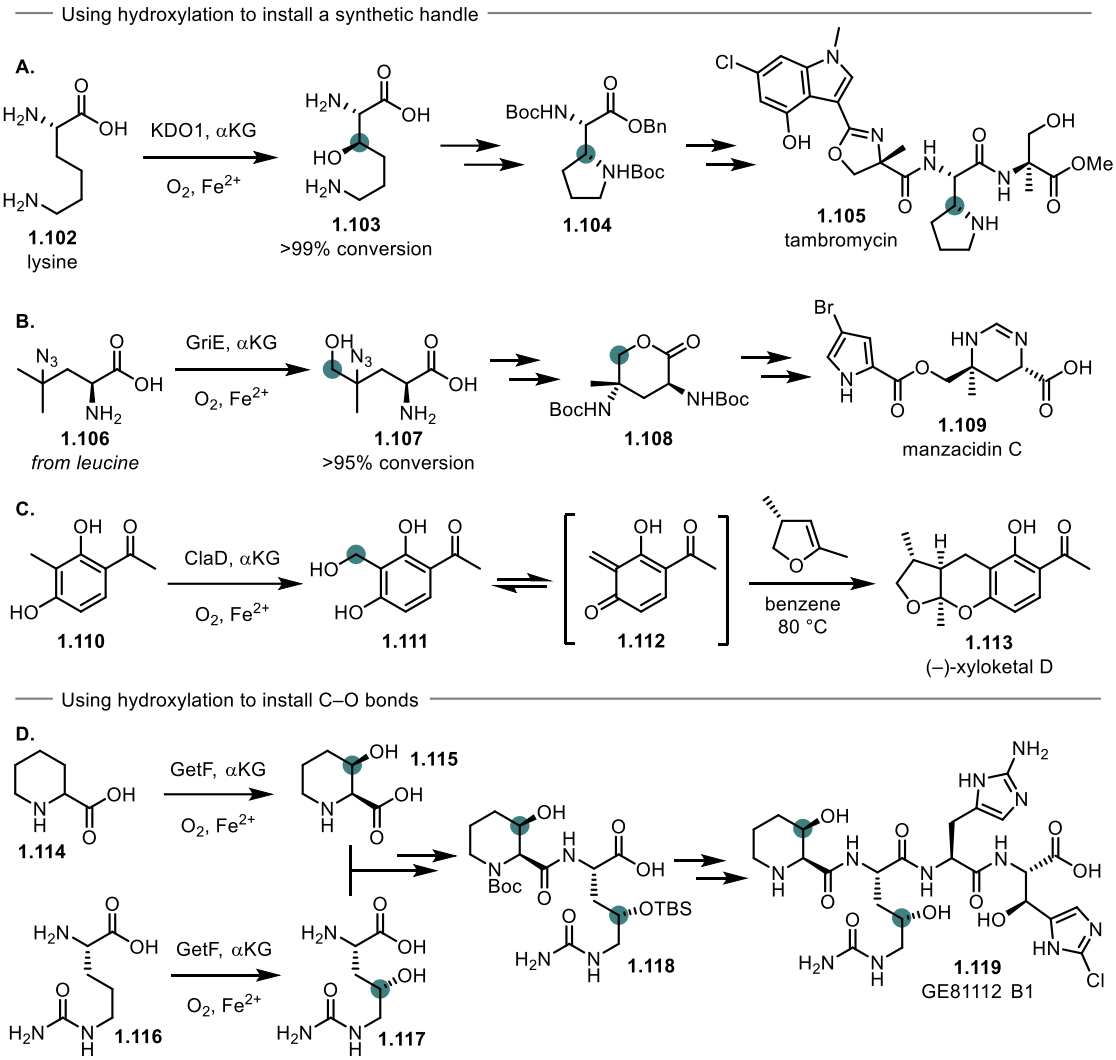
Nature has supplied a wide variety of enzymes which are capable of hydroxylating both activated and inert C–H bonds, including Cu-, Mo- or Fe-based and even metal-free enzymes.[86] Iron based enzymes are by far the most used for the oxyfunctionalisation of aliphatic substrates, including: Rieske oxygenases **1.98**, non-heme dioxygenases **1.99**, methane monooxygenases **1.100**, P450s **1.101**, and unspecified peroxygenases (with functionally similar to P450 but not requiring co-factors or redox partners).[87]



Scheme 20 – Fe-dependent hydroxylation enzymes.

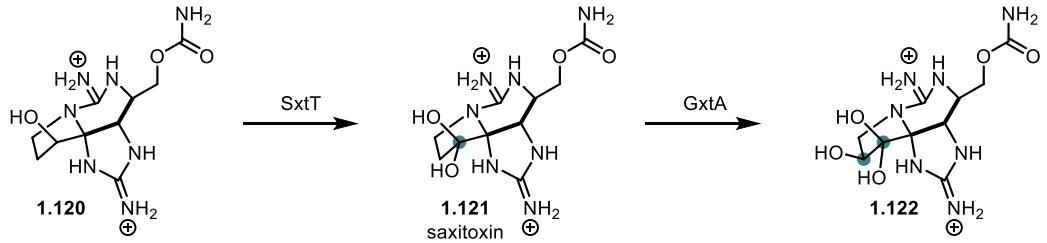
Although many early reports describe enzymatic hydroxylation to form synthetic building blocks, the following discussion focuses on recent examples that highlight the high level of selectivity which can be achieved using Fe-dependent oxygenases. Renata used iron- and α-ketoglutarate-dependent dioxygenases (Fe/αKGs), to form noncanonical amino acids (ncAAs) as key building blocks for a range of natural product syntheses (*Scheme 21*).[88] These alcohol moieties did not appear in the target compounds **1.105** and **1.109** but created a synthetic handle in **1.103** and **1.107** for further transformations (*Scheme 21.A,B*). The chiral pool approach was also used in Renata's synthesis of GE81112 B1 **1.119**, where enzymatic hydroxylation was used to install stereodefined C–O bonds (*Scheme21.D*).[89]

Narayan also used this class of oxygenases to achieve benzylic hydroxylation of **1.110** to form **1.111**, which, upon elimination, formed *ortho*-quinone methide **1.112**. Subsequent Diels–Alder reaction with the relevant dienophile afforded (–)-xyloketal D **1.113** in 64% overall yield (*Scheme 21.C*).[90]



Scheme 21 - α-Ketoglutarate-dependent dioxygenases in synthesis.

These selected examples show how oxygenases can be used to form key building blocks; however, there are also many reports where enzymes are used at a later stage in the synthetic route. Narayan used Rieske oxygenases SxtT and GxtA in the synthesis of saxitoxin **1.121** and analogues including 11-β-hydroxy-STX **1.122** from **1.120** (*Scheme 22*), achieving exquisite selectivity.[91]

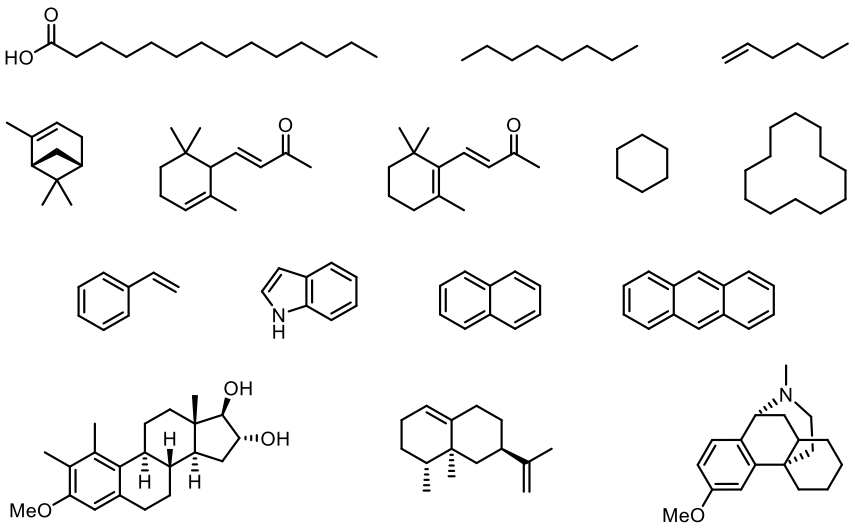


Scheme 22 – Rieske oxygenases in bioinspired synthesis of saxitoxin.

Although these reports demonstrate a variety of oxygenases used in natural product total synthesis, the P450 monooxygenases are the most widely used subclass for C–H hydroxylation.

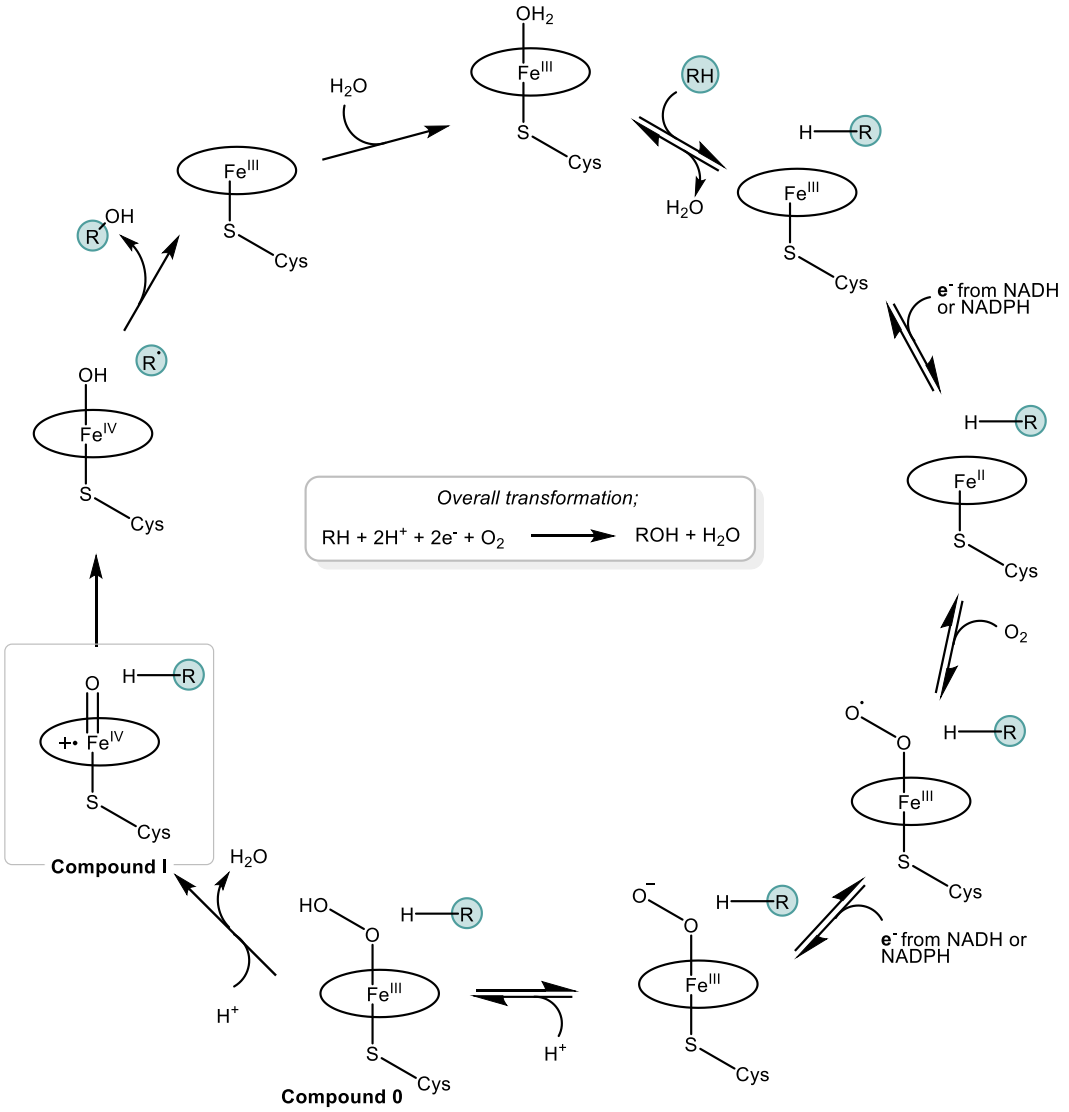
1.2.4. Cytochrome P450 monooxygenases

P450 enzymes have emerged as one of the most promising classes of biocatalysts for use in synthesis due to the wide scope of tolerated substrates (*Scheme 23*), the high level of selectivity which can be achieved between functionalisation of similar C – H bonds, and the mutability and ease of protein engineering allowing for rapid catalyst development.[92]



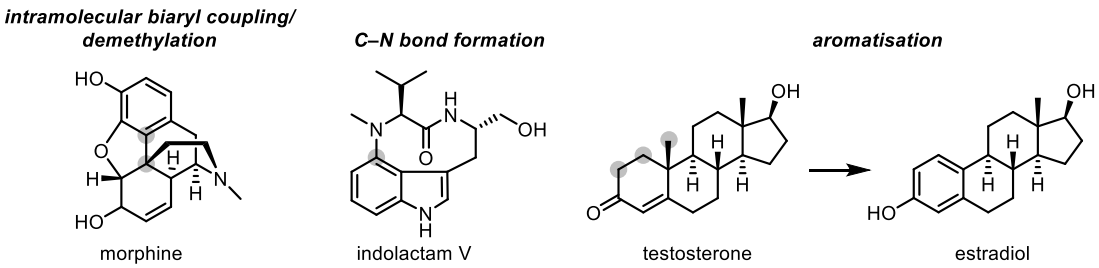
Scheme 23 – Selected examples of tolerated substrates.

The P450 cytochrome superfamily (CYP) consists of haem *b*-dependent monooxygenases, whose name arises from the characteristic 450 nm absorption band of the CO-bound ferrous state.[93] They are best known for their ability to insert an oxygen atom, from molecular oxygen, into a wide range of C–H bonds; however, other reactivities such as epoxidation, C–C bond formation, and even reduction have been reported.[94] The radical rebound mechanism of P450-catalysed reactions is well-established (*Scheme 24*),[95] and is not discussed in detail here. Importantly, the catalytically active species is named 'Compound I' and is formed through protonation and loss of water, *via* heterolytic O–O bond cleavage, of 'Compound 0'.



Scheme 24 – The P450 catalytic cycle.

P450s are found in the biosynthetic pathways of many natural products, within which they catalyse a variety of chemistries aside from hydroxylation, including, biaryl coupling and demethylation,[96] C–N bond formation,[97] and aromatisation (*Scheme 25*).[98]



Scheme 25 – Selected reactions catalysed by P450s in biosynthetic pathways.

1.2.4.1. $P450_{BM3}$ (CYP102A1)

CYP102A1 is more commonly known as $P450_{BM3}$, named as it was the third P450 isolated from *Bacillus megaterium* by Fulco in the 1970s.[99] The newly discovered enzyme was found to catalyse the hydroxylation (and epoxidation with olefinic substrates) of a range of fatty acids using only NADPH and oxygen. After full characterisation it was found that the P450 'haem' domain was fused to a 'reductase' domain and therefore was catalytically self-sufficient, making it an ideal candidate for academic research.

Many crystal structures have been solved of $P450_{BM3}$, either with or without mutations, allowing visualisation of key residues in the active site and access channels, and aiding mutagenesis studies (*Figure 5*). The importance of access channel mutations Arg47 and Tyr51 has long been explored, Fulco originally suggesting that this hydrophilic region binds the carboxylic acid of the native substrate (long-chain fatty acids) enabling effective catalysis. In almost all published crystal structures Ala264 is hydrogen bonded to the water molecule nearest the haem, showing a clear involvement in the protein's conformational movement upon substrate binding. Another residue suggested to be involved in active site reorganisation is Phe87, lying perpendicular to the porphyrin and then rotating 90° to orient closer to the iron centre, thereby displacing the axial water molecule. These mutations, and many others, have been extensively studied through protein engineering, either through rational design of mutagenesis or directed evolution approaches.

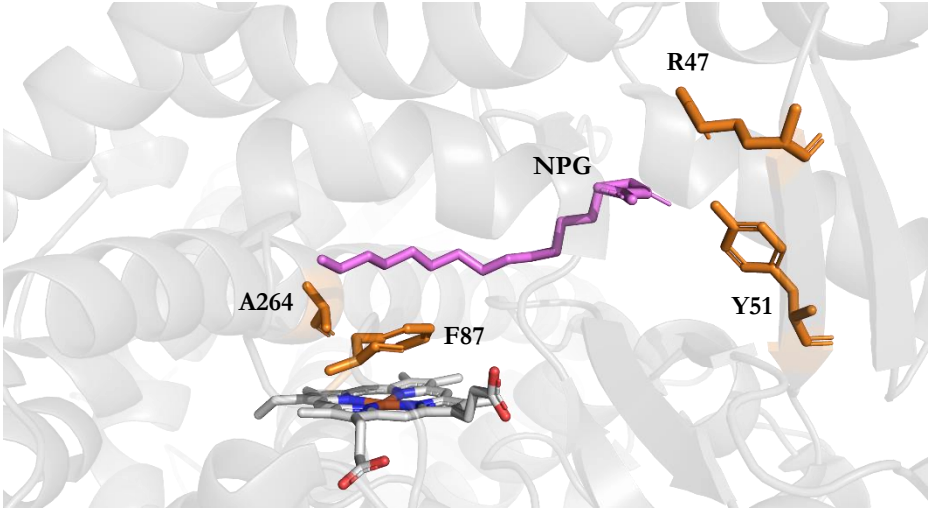


Figure 5 – *N*-Palmitoylglycine (NPG) bound $P450_{BM3}$ crystal structure (PDB ID: 1JPZ), showing residues R47, Y51, F87 and A264 in orange.

Despite such structural insights, it remains difficult to predict which residues and mutations will have beneficial effects on selectivity or reactivity. The area of P450 research continues to grow, with many disciplines including microbiology, computational biology, physical chemistry, chemical biology, and synthetic organic chemistry contributing valuable perspectives on this field.

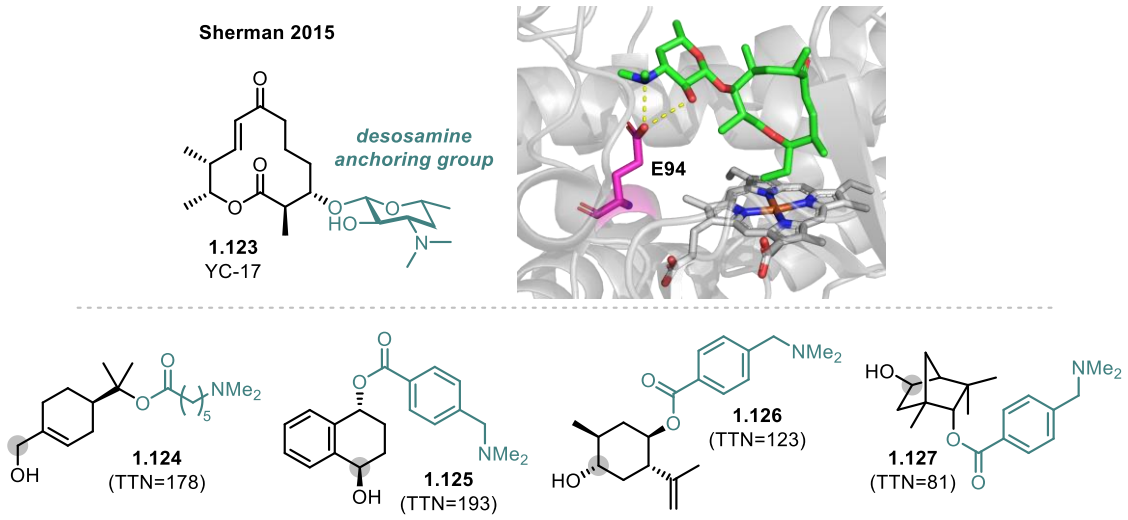
1.2.5. $P450_{BM3}$ in synthesis

The vast engineering potential and substrate tolerance of P450s have created the opportunity for many groups to achieve impressive syntheses incorporating biocatalysis using $P450_{BM3}$. Two approaches are generally undertaken to improve the catalytic potential: engineering of substrates (or using additives such as decoy molecules) or protein engineering.

1.2.5.1. Substrate Engineering

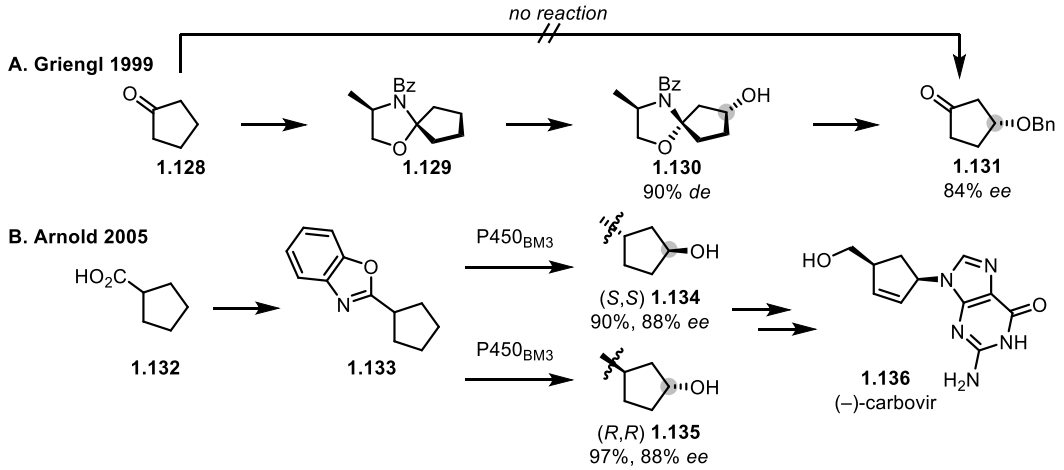
The idea of a substrate engineering strategy for P450 catalysis was first proposed by Griengl and co-workers, who introduced docking and protecting (d/p) groups to non-native substrates to facilitate reactivity.[100] Similarly to common practice in organic synthesis, the protection of certain functional groups prevents unwanted reactivity, but within an enzyme active site the 'protecting group' can also provide a docking site to improve substrate recognition.[101]

Nature uses this strategy in the P450 oxidation of many native substrates; for example, the natural desosamine anchor in YC-17 **1.123** provides a salt-bridge interaction between the protonated amine and the Glu94 carboxylate within the PikC P450 active site as shown in the co-crystal structure (*Scheme 26*). Based on this, Sherman then used synthetic dimethylamine anchors to afford a range of PikC mono-hydroxylation metabolites **1.124 – 1.127**.[102]



Scheme 26 – PikC P450 (CYP107L1) co-crystal with ligand YC-17 (PDB ID: 2C6H), and selected products of PikC P450 hydroxylation using synthetic anchoring groups reported by Sherman.

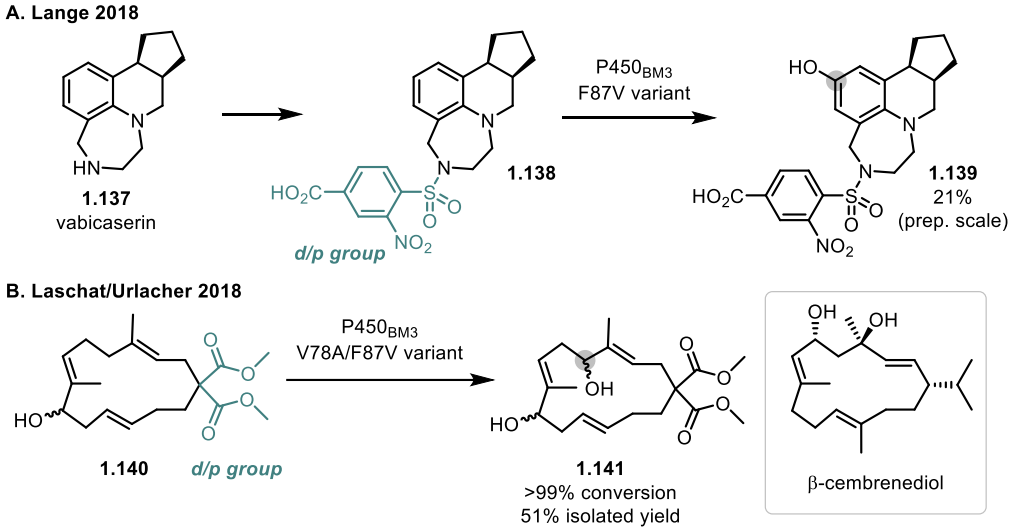
Griengl's initial 1999 report used the fungus *Beauveria bassiana* ATCC 7159 to demonstrate that unreactive cyclopentanone **1.128** could be effectively hydroxylated after the ketone moiety was masked as a spirooxazolidine **1.129**, to produce **1.130** with high enantiomeric excess (*Scheme 27.A*). Arnold used this strategy in the $P450_{BM3}$ hydroxylation of **1.133**, to render carboxylic acid **1.132** reactive, during the synthesis of an intermediates (**1.134** and **1.135)** towards carbovir **1.136** (*Scheme 27.B*).[103]



Scheme 27 – d/p approach in the bio-hydroxylation of non-native substrates.

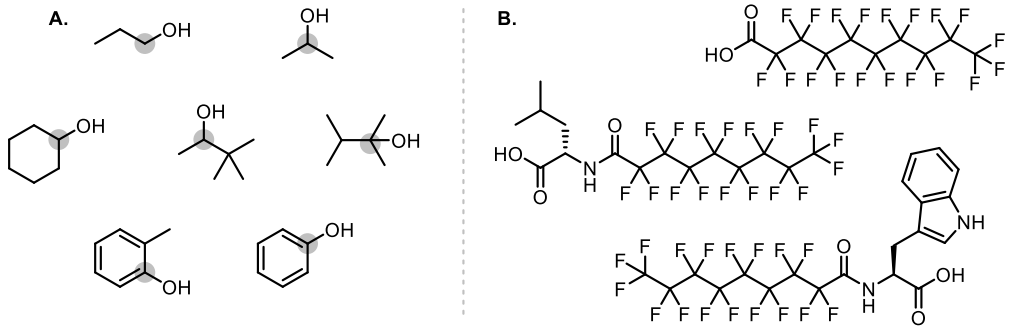
A combination of substrate and protein engineering was used to effect the mono-hydroxylation of vabicaserin **1.137**, using modified nosyl protecting groups chosen, in part, due to the results of molecular dynamics (MD) simulations that reveal potential docking interactions with active site residues (*Scheme 28.A*).[104] Laschat and Urlacher found that increasing the size and polarity

of the exocyclic substituents in cembranoids, for example incorporation of dimethyl diester functionality in **1.140**, improved the regioselectivity of $P450_{BM3}$ hydroxylation to give **1.141** in high conversion (*Scheme 28.B*).[105]



Scheme 28 – Examples of d/p groups for P450 hydroxylation.

A different substrate-controlled approach was reported by Watanabe and Reetz, in which decoy molecules control the reactivity rather than relying on manipulating the substrate. Decoy molecules, such as perfluorocarboxylic acids (PFCs), are recognised by the enzyme as substrates and induce active site reconfiguration and the formation of the active species Compound I. However, with no oxidisable C–H bonds, these compounds merely occupy space in the active site, allowing smaller substrates, such as methane[106] or ethane,[107] cycloalkanes,[108] and benzene,[109] to be effectively oxidised (*Scheme 29*).

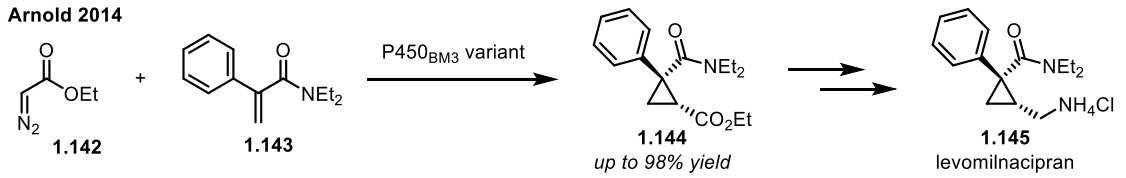


Scheme 29 – A) Selected examples of small substrates catalysed by $P450_{BM3}$ with the addition of decoy molecules, and B) examples of decoy molecules used.

1.2.5.2. Protein Engineering

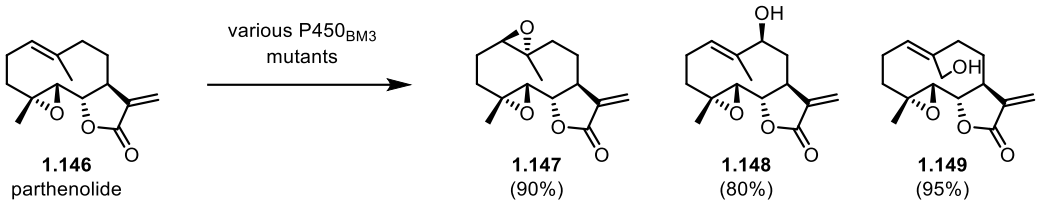
A range of modern protein engineering techniques are used by researchers in the field; these include rational engineering, site-saturation mutagenesis (where influential residues are mutated to every single amino acid) and directed evolution.[110] Rational engineering and site-saturation mutagenesis rely on prior knowledge of the protein structure and which residues influence protein stability, potentially affecting substrate selectivity and reactivity. However, the effects of individual point mutations are often hard to predict. Using directed evolution methods, the generation of large enzyme libraries with randomly generated mutations, paired with an effective analytical technique, can produce highly evolved catalysts over several rounds of mutagenesis.[111]

These engineering techniques are capable of enhancing the existing reactivity of P450s and creating new enzymes which are able to catalyse non-native chemistries.[112] For example, alkene cyclopropanation by carbene transfer is a well-established chemical transformation; however, this had not been previously reported to be catalysed by enzymes. Arnold reported that histidine-ligated $P450_{BM3}$ was able to catalyse a highly enantioselective cyclopropanation, and this was applied to the formal synthesis of levomilnacipran **1.145**, where **1.144** is produced in excellent yield from **1.142** and **1.143** (*Scheme 30*).[113] Further research into the tunability of the axially ligated residue led to the development of a 'P411' enzyme (replacement the Cys ligand with Ser) which has since been used to catalyse a range of carbenoid and nitrenoid reactions.[114]



Scheme 30 – Arnold's synthesis of levomilnacipran using a $P450_{BM3}$-catalysed carbenoid cyclopropanation.

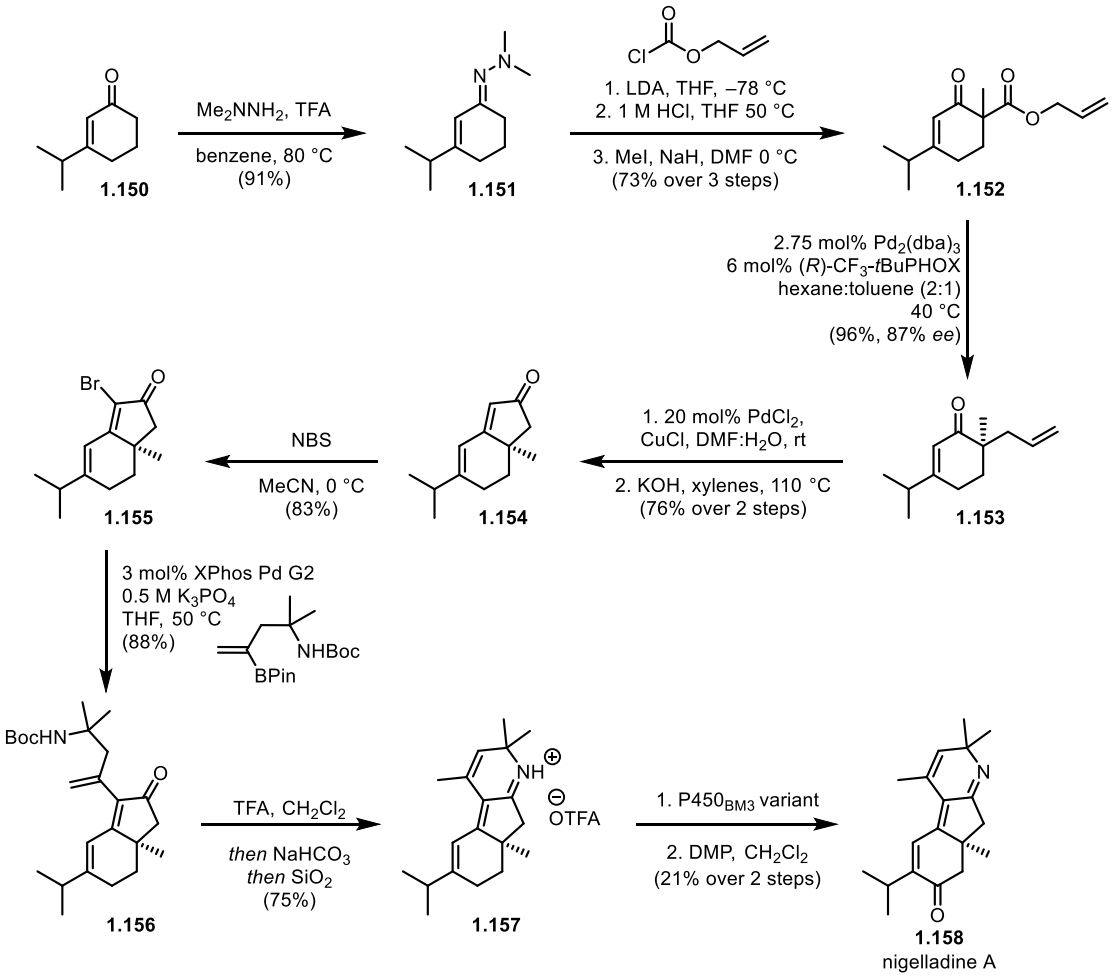
Fasan used directed evolution, aided by computational tools, to develop $P450_{BM3}$ enzymes capable of oxidising the sesquiterpene lactone parthenolide **1.146** (*Scheme 31*).[115] A previously reported P450 capable of oxidising a range of bulky terpene compounds, containing 16 mutations, was further evolved through multiple rounds of mutagenesis to yield products **1.147 – 1.149** with high levels of selectivity.



Scheme 31 – Engineered $P450_{BM3}$-catalysed oxidations of parthenolide analogues.

The strategy of using enzymes already evolved to accept known substrates as a starting point for further mutagenesis can save time and expedite catalyst optimisation. Arnold used a focused library of $P450_{BM3}$ mutants, known to tolerate large substrates, in a collaborative effort with the Stoltz lab leading to the total synthesis of nigelladine A **1.158** (*Scheme 32*).[116] Attempts to directly α-acylate enone **1.150** failed due to self-aldol additions, so transformation to hydrazone **1.151** was required before acylation, hydrolysis and methylation to form **1.152**. Asymmetric allylic alkylation yielded **1.153** in high yield and enantioselectivity, then Tsuji–Wacker oxidation and aldol condensation gave **1.154**. Bromination provided **1.155**, Pd-catalysed cross-coupling with the relevant boronic acid gave triene **1.156**, and cyclisation with TFA afforded compound **1.157**.

All attempts to oxidise tricyclic compound **1.157** with chemical reagents gave low yielding regioisomeric mixtures of oxygenated products. Screening of a small library of engineered $P450_{BM3}$ mutants resulted in the identification of enzymes yielding the desired regioselectivity, yielding an alcohol which was oxidised chemically to yield nigelladine A **1.158**.



Scheme 32 – Arnold/ Stoltz total synthesis of nigelladine A **1.158**.

These selected examples illustrate how P450 enzymes can be effectively incorporated into the chemoenzymatic total synthesis of complex natural products. Complementary selectivity to chemical methodology can be achieved, thereby adding to the current toolbox available to synthetic organic chemists.

1.3. Aims and proposed work

This thesis aims to show evidence of how biocatalysis can be incorporated into a range of synthetic routes; specifically, how $P450_{BM3}$ can be applied to the synthesis of key building blocks or as a tool for a late-stage approach in a total synthesis. Additionally, challenging our current P450 library with new substrates will allow us to gain further understanding of the enzyme's capabilities.

1.4. References for Chapter 1

(1) E. J. Corey, *Angew. Chem. Int. Ed. Engl.*, **1991**, *30*, p455-465.

(2) T. Newhouse, P. S. Baran and R. W. Hoffman, *Chem. Soc. Rev.*, **2009**, *39*, p3010-3021.

(3) S. E.Reisman and T. J. Maimone, *Acc. Chem. Res.,* **2021**, *54(8)*, p1815-1816.

(4) a) K. C. Nicolaou and S. Rigol, *Nat. Prod. Rep.*, **2020**, *37*, p1404-1435; b) Z.-C. Wu and D. L. Boger, *Nat. Prod. Rep.*, **2020**, *37*, p1511-1531.

(5) Y. Hayashi, *Acc. Chem. Res.,* **2021**, *54(6)*, p1385-1398.

(6) Q. Michaudel, Y. Ishihara and P. S.Baran, *Acc. Chem. Res.*, **2015**, *48*, p712-721.

(7) a) D. S. Peters, C. R. Pitts, K. S. McClymont, T. P. Stratton, C. Bi, P. S. Baran, *Acc. Chem. Res.*, **2021**, *54*, p605-617; b) T. Gaich and P. S. Baran, *J. Org. Chem.*, **2010**, *75*, p4657-4673; N. Z. Burns, P. S. Baran, R. W. Hoffman, *Angew. Chem. Int. Ed.*, **2009**, *48*, p2854-2867.

(8) B. A. Arndtsen, R. G. Bergman, T. A. Mobley ad T. H. Peterson, *Acc. Chem. Res.*, **1995**, *28*, p154-162.

(9) Selected examples include; a) H. M. L. Davies and D. Morton, *J. Org. Chem.,* **2016**, *81*, *2*, p343-350; b) D. J. Abrams, P. A. Provencher, E. J. Sorensen, *Chem. Soc. Rev.*, **2018**, *47*, p8925-8967; c) H. M. L. Davies and D. Morton, *ACS Cent. Sci.,* **2017**, *3(9)*, p936-943; c)E. J. E. Caro-Diaz, M. Urbano, D. J. Buzard and R. M Jones, *Bioorg. Med. Chem. Lett.*, **2016**, *26*, p5378-5383.

(10) T. W. Lyons and M. S. Sanford, *Chem. Rev.*, **2010**, *110(2)*, p1147-1169.

(11) T. Rogge, N. Kaplaneris, N. Chatani, J. Kim, S. Chang, B. Punji, L. L. Schafer, D. G. Musaev, J. Wencel-Delord, C. A. Roberts, R. Sarpong, Z. E. Wilson, M. A. Brimble, M. J. Johansson and L. Ackermann, *Nat. Rev. Meth. Primers*, **2021**, *1*, article 43.

(12) Y. Qiu and S. Gao, *Nat. Prod. Rep.*, **2016**, *33*, p562-581.

(13) M. C White, *Science*, **2012**, *335*, p807-809.

(14) W. J. Mijs and C. R. H. I. de Jonge, Organic syntheses by oxidation with metal compounds, Springer Science & Business Media, 2013.

(15) M. S. Chen, N. Prabagaran, N. A. Labenz and M. C. White, *J. Am. Chem. Soc.*, **2005**, *127*, p6970-6971.

(16) M. S. Chen and M. C. White, *J. Am. Chem. Soc.*, 2004, 126, 1346-1347.

(17) a) E. M. Stang and M. C. White, *Angew. Chem. Int. Ed.*, **2011**, *50*, p2094-2097; b) E. M. Stang and M. C. White, *J. Am. Chem. Soc.*, **2011**, *133*, p14892-14895; c) G. T. Rice and M. C. White, *J. Am. Chem. Soc.,* **2009**, *131(33)*, p11707–11711; d) A. J. Young and M. C. White, *J. Am. Chem. Soc.,* **2008**, *130(43)*, p14090-14091.

(18) D. J. Covell and M. C. White, *Angew. Chem. Int. Ed.*, **2008**, *47*, p6448-6451.

(19) M. Malik, G. Witkowski and S. Jarosz, *Org. Lett.,* **2014**, *16(14)*, p3816-3819.

(20) M. E. McCallum, C. M. Rasik, J. L Wood and M. K. Brown, *J. Am. Chem. Soc.*, **2016**, *138(7)*, p2437-2442.

(21) H. F. Motiwala, B. Gülgeze and J. Aubé, *J. Org. Chem.*, **2012**, *77*, p7005-7022.

(22) G. Sekar, A. DattaGupta and V. K. Singh, *J. Org. Chem.* **1998**, *63(9)*, p2961-2967.

(23) C. Yuan, Y. Jin, N. C. Wilde and P. S. Baran, *Angew. Chem. Int. Ed.*, **2016**, *55*, p8280-8284.

(24) R. Breslow and L. E. Overmann, *J. Am. Chem. Soc.*, **1970**, *94(2)*, p1075-1077.

(25) R. Breslow, X. Zhang and Y. Huang, *J. Am. Chem. Soc.*, **1997**, *119(19)*, p4535-4536.

(26) a) J. T. Groves, T. E. Nemo and R. S. Myers, *J. Am. Chem. Soc.*, **1979**, *101*, p1032-1033; b) J.T. Groves and T. E. Nemo, *J. Am. Chem. Soc.*, **1983**, *105*(20), p6243-6248.

(27) a) C. L. Hill and B. C. Schardt, *J. Am. Chem. Soc.*, **1980**, *102(20)*, p6374-6375; b) J. T. Groves, W. J. Kruper Jr. and R. C. Haushalter, *J. Am. Chem. Soc.,* **1980**, *102(20)*, p6375-6377; c) P. Battioni, J. P. Renaud, J. F. Bartoli, M. Reina-Artiles, M. Fort and D. Mansuy, *J. Am. Chem. Soc.*, **1988**, *110(25)*, p8462-8470.

(28) a) C.-M. Che, V. Kar-Yan Lo, C.-Y. Zhou and J.-S. Huang, *Chem. Soc. Rev.*, **2011**, *40*, p1950-1975; b) H. Lu and X. P. Zhang, *Chem. Soc. Rev.*, **2011,** *40*, p1899-1909.

(29) T. C. Boorman and I. Larrosa, *Chem. Soc. Rev.*, **2011**, *40*, p1910-1925.

(30) L. McMurray, F. O'Hara and M. J. Gaunt, *Chem. Soc. Rev.*, **2011**, *40*, p1885-1898.

(31) L. V. Desai, K. L. Hull and M. S. Sanford, *J. Am. Chem. Soc.,* **2004**, *126*, p9542-9543.

(32) R. J. Sharpe and J. S. Johnson, *J. Org. Chem.*, **2015**, *80*, p9740-9766.

(33) D. A. Siler, J. D. Mighion and E. J. Sorensen, *Angew. Chem. Int. Ed.*, **2014**, *53*, p5332-5335.

(34) a) M. S. Chen, M. C. White, *Science*, **2007**, *318*, p.783-787; b) new 'slow addition' procedure: N. A. Vermeulen, M. S. Chen and M. C. White, *Tetrahedron*, **2009**, *65*, p3078-3084; c) next generation catalyst: P. E. Gormisky and M. C. White, *J. Am. Chem. Soc.*, **2013**, *135*, p14052-14055.

(35) C. M. Rasik and M. K. Brown, *Angew. Chem. Int. Ed.*, **2014**, *53*, p14522-14526.

(36) Q. Ye, P. Qu and S. A. Synder, *J. Am. Chem. Soc.,* **2017**, *139(51)*, p18428-18431.

(37) M. E. McCallum, C. M. Rasik, J. L. Wood, and M. K. Brown, *J. Am. Chem. Soc.*, **2016**, *138*, p2437-2442.

(38) D. J. Abrams, P. A. Provencher and E. J. Sorensen, *Chem. Soc. Rev.*, **2018**, *47*, p8925-8967.

(39) R. Curci and L. D'Accolti, *Acc. Chem. Res.*, **2006**, *39*, p1-9.

(40) P. A. Wender, M. K. Hilinski and A. V. W. Mayweg, *Org. Lett.,* **2005**, *7(1)*, p79-82.

(41) K. Chen and P. S. Baran, *Nature*, **2009**, *459*, p824-828.

(42) L. Zou, R. S. Paton, A. Eschenmoser, T. R. Newhouse, P. S. Baran and K. N. Houk, *J. Org. Chem.*, **2013**, *78*, p4037-4048.

(43) K. S. Williamson, D. J. Michaelis and T. P. Yoon, *Chem. Rev.*, **2014**, *114*, p8016-8036.

(44) a) D. D. DesMarteau, A. Donadelli, V. Montanari, V. A. Petrov and G. Resnati, *J. Am. Chem. Soc.*, **1993**, *115*, p4897-1898; b) A. Arnone, M. Cavicchioli, V. Montanari and G. Resnati, *J. Org. Chem.*, **1994**, *59(19)*, p5511-5513.

(45) a) B. H. Brodsky and J. Du Bois, *J. Am. Chem. Soc.,* **2005**, *127*, p15391-15393; b) N. D. Litvinas, B. H. Brodsky and J. Du Bois, *Angew. Chem. Int. Ed.*, **2009**, *48*, p4513-4516.

(46) A. M. Adams and J. Du Bois, *Chem. Sci.*, **2014**, *5*, p656-659.

(47) Y. Kawamata, M. Yan, Z. Liu, D.-H. Bao, J. Chen, J. T. Starr and P. S. Baran, *J. Am. Chem. Soc.*, **2017**, *139*, p7448-7451.

(48) S. G. Robinson, J. B. C. Mack, S. N. Alektiar, J. Du Bois and M. S. Sigman, *Org. Lett.*, **2020**, *22*, p7060-7063.

(49) M. Lee and M. S. Sanford, *Org. Lett.*, **2017**, *19*, p572-575.

(50) P. E. McGovern, J. Zhang, J. Tang, Z. Zhang, G. R. Hall, R. A. Moreau, A.Nuñez, E. D. Butrym, M. P. Richards, C. S. Wang, G. Cheng, Z. Zhao, C.Wang, *Proc. Natl. Acad. Sci. USA*, **2004**, *101*, p17593-17598.

(51) R. Kohler, *J. Hist. Biol.* **1971**, *4*, 35-61.

(52) https://www.nobelprize.org/prizes/chemistry/1907/buchner/lecture.

(53) E. F. Armstrong, *Nature* **1933**, *131*, p535-537.

(54) A. J. B. Robertson, *Platinum Met. Rev.,* **1975**, *19*, p64-69.

(55) E. Fischer, *Ber. Dtsch. Chem. Ges.*, **1894**, *27*, p2985-2993.

(56) L. Pauling, *Nature,* **1948**, *167*, p707.

(57) D. E. Koshland, *Proc. Natl. Acad. Sci. USA*, **1958**, *44*, p98-104.

(58) a) F. Sanger, H. Tuppy, *Biochem. J.* **1951**, *49*, p463-481; b) F. Sanger, H. Tuppy, *Biochem. J.*, **1951**, *49*, p481-490.

(59) a) L. Pauling, R. B. Corey, *J. Am. Chem. Soc.,* **1950**, *72*, p5349; b) L. Pauling, R. B. Corey, *Proc. Natl. Acad. Sci. USA*, **1951**, *37*, p729-740.

(60) M. F. Perutz, *Nature*, **1951**, *167*, p1053-1054.

(61) a) J. C. Kendrew, G. Bodo, H. M. Dintzis, R. G. Parrish, H. Wyckoff, D. C.Phillips, *Nature*, **1958**, *181*, p662-666; b) J. C. Kendrew, R. E. Dickerson, B. E. Strandberg, R. G. Hart, D. R. Davies, D. C. Phillips, V. C. Shore, *Nature*, **1960**, *185*, p422-427.

(62) S. de Chadarevian, *Protein Sci.*, **2018**, *27*, p1136-1143.

(63) a) *Nature New Biology,* **1971**, *233*, p223; b) *Structure*, **2012**, *20*, p391-396.

(64) https://www.rcsb.org/stats/growth/growth-releasedstructures.

(65) E. Callaway, *Nature*, **2020**, *578(7794)*, p201.

(66) E. Callaway, *Nature*, **2021**, *595(7869)*, p635.

(67) T. D. H. Bugg, *Nat. Prod. Reports*, **2001**, *18*, p465-493.

(68) U. T. Bornscheuer, K. Buchholz, *Eng. Life Sci.*, **2005**, *5*, p309-323.

(69) a) N. Grubhofer, L. Schleith, *Naturwissenschaften*, **1953**, *40*, p508; b) G. Manecke, K. E. Gillert, *Naturwissenschaften*, **1955**, *42*, p212; c) F. Micheel, J. Ewers, *Makromol. Chem.*, **1949**, *3*, p200.

(70) M. P. Thompson, I. Peñafiel, S. C. Cosgrove and N. J. Turner, *Org. Process Res. Dev.*, **2019**, *23*, p9-18.

(71) K. Buchholz, *Appl. Microbiol. Biotechnol.* **2016**, *100*, p3825-3839.

(72) H. B. Kagan and K. Gopalaiah, *New J. Chem.*, **2011**, *35*, p1933-1937.

(73) L. Rosenthaler, *Biochem. Z.*, **1908**, *14*, p238.

(74) V. Prelog, *Pure Appl. Chem.*, **1964**, *9*, p119.

(75) F. Sanger, S. Nicklen, A. R. Coulson, *Proc. Natl. Acad. Sci. USA,* **1977**, *74*, p5463-5467.

(76) B. R. Glick, J. J. Pasternak, C. L. Patten, Molecular Biotechnology: Principles and Applications of Recombinant DNA; ASM Press: Washington, DC, **2010**.

(77) K. B. Mullis, *Angew. Chem., Int. Ed. Engl.*, **1994**, *33*, p1209.

(78) M. T. Reetz, *J. Am. Chem. Soc.*, **2013**, *135(34)*, p12480-12496; b) R. A. Sheldon, D. Brady and M. L. Bode, *Chem. Sci.*, **2020**, *11*, p2587-2605; c) C. M. Heckmann and F. Paradisi, *ChemCatChem*, **2020**, *12*, p6082-6102.

(79) a) D. Yi, T. Bayer, C. P. S. Badenhorst, S. Wu, M. Doerr, M. Höhne and U. T. Bornscheuer, *Chem. Soc. Rev.*, **2021**, *50*, p8003-8049; b) J. B. Pyser, S. Chakrabarty, E. O. Romero and A. R. H. Narayan, *ACS Cent. Sci.*, **2021**, *7*, p1105-1116; c) P. N. Devine, R. M. Howard, R. Kumar, M. P. Thompson, M. D. Truppo and N. J. Turner, *Nat. Rev. Chem.*, **2018**, *2*, p409-421.

(80) C. A. Roessner, J. B. Spencer, N. J. Stolowich, J. Wang, G. P. Nayar, P. J. Santander, C. Pichon, C. Min, M. T. Holderman, A. I. Scott, *Chem. Biol.*, **1994**, *1*, p119.

(81) G. W. Craig, *J. Porphyrins Phthalocyanines*, **2015,** *19*, p1-20.

(82) U. Bat-Erdene, J. M. Billingsley, W. C. Turner, B. R. Lichman, F. M. Ippoliti, N. K. Garg, Sarah E. O'Connor and Y. Tang, *ACS Catal.*, **2021**, *11*, p9898-9903.

(83) M. A. Huffman, A. Fryszkowska, O. Alvizo, M. Borra-Garske, K. R. Campos, K. A. Canada, P. N. Devine, D. Duan, J. H. Forstater, S. T. Grosser, H. M. Halsey, G. J. Hughes, J. Jo, L. A. Joyce, J. N. Kolev, J. Liang, K. M. Maloney, B. F. Mann, N. M. Marshall, M. McLaughlin, J. C. Moore, G. S. Murphy, C. C. Nawrat, J. Nazor, S. Novick, N. R. Patel, A. Rodriguez-Granillo, S. A. Robaire, E. C. Sherer, M. D. Truppo, A. M. Whittaker, D. Verma, L. Xiao, Y. Xu, H. Yang, *Science*, **2019**, *366*, p1255-1259.

(84) a) M. Kageyama, T. Nagasawa, M. Yoshida, H. Ohrui, S. Kuwahara, *Org. Lett.*, **2011**, *13*, p5264-5266; b) M. Kageyama, T. Miyagi, M. Yoshida, T. Nagasawa, H. Ohrui and S. Kuwahara, *Biosci. Biotechnol. Biochem.*, **2012**, 76(6), p1219-1225; c) K. Fukuyama, H. Ohrui and S. Kuwahara, *Org. Lett.*, **2015**, *17*, p828-831; d) M. McLaughlin, J. Kong, K. M. Belyk, B. Chen, A. W. Gibson, S. P. Keen, D. R. Lieberman, E. M. Milczek, J. C. Moore, D. Murray, p926-929.

(85) a) J. C. Lewis, P. S. Coelhob and F. H. Arnold, *Chem. Soc. Rev.*, **2011**, *40*, p2003-2021; b) W. Wang, D. F. Taber and H. Renata, *Chem. Eur. J.*, **2021**, DOI:10.1002/chem.202101232

(86) J. Münch, P. Püllmann, W. Zhang and M. J. Weissenborn, *ACS Catal.*, **2021**, *11*, p9168-9203.

(87) C. Aranda, J. Carro, A. González-Benjumea, E. D. Babota, A. Olmedo, D. Linde, A. T. Martínez and A. Gutiérrez, DOI: 10.1016/j.biotechadv.2021.107703.

(88) a) X. Zhang, E. King-Smith, and H. Renata, *Angew. Chem. Int. Ed.,* **2018**, *57*, p5037-5041; B) C. R. Zwick III and H. Renata, *J. Am. Chem. Soc.,* **2018**, *140(3)*, p1165-1169.

(89) C. R. Zwick III, M. B. Sosa and H. Renata, *J. Am. Chem. Soc.,* **2021**, *143(3)*, p1673-1679.

(90) T. J. Doyon, J. C. Perkins, S. A. Baker Dockrey, E. O. Romero, K. C. Skinner, P. M. Zimmerman and A. R. H. Narayan, *J. Am. Chem. Soc.,* **2019**, *141(51)*, p20269-20277.

(91) A. L. Lukowski, D. C. Ellinwood, M. E. Hinze, R. J. DeLuca, J. Du Bois, S. Hall and A. R. H. Narayan, *J. Am. Chem. Soc.*, **2018**, *140(37)*, p11863-11869.

(92) R. Fasan, *ACS Catal.*, **2012**, *2*, p647-666.

(93) C. J. C. Whitehouse, S. G. Bell and L.-L. Wong, *Chem. Soc. Rev.*, **2012**, *41*, p1218-1260.

(94) a) P. R. Ortiz de Montellano and J. J. De Voss, in Cytochrome P450: Structure, Mechanism and Biochemistry, ed. P. R. Ortiz de Montellano, Plenum Publishers, New York, 3rd edn, 2005, pp. 183-246; b) J. B. Y. H. Behrendorff, *Front. Mirobiol.*, **2021**, *12*, article 649273.

(95) F. P. Guengerich, *ACS Catal.*, **2018**, *8*, p10964-10976.

(96) N. Grobe, B. Zhang, U. Fisinger, T. M. Kutchan, M. H. Zenk and F. P. Guengerich, *J. Biol. Chem.*, **2009**, *284(36)*, p24425-24431.

(97) F. He, T. Mori, I. Morita, H. Nakamura, M. Alblova, S. Hoshino, T. Awakawa and I. Abe, *Nat. Chem. Bio.*, **2019**, *15*, p1206-1213.

(98) D. Ghosh, J. Griswold, M. Erman and W. Pangborn, *J. Steroid Biochem. Mol. Biol.*, **2010**, *118*, p197-202.

(99) Y. Miura and A. J. Fulco, *J. Biol. Chem.*, **1974**, *249*, p1880-1888.

(100) G. Braunegg, A. de Raadt, S. Feichtenhofer, H. Griengl, I. Kopper, A. Lehmann, H. Weber, *Angew. Chem. Int. Ed.*, **1999**, *38*, p2763-2766.

(101) J. Xu, C. Wang and Z. Cong, *Chem. Eur. J.*, **2019**, *25*, p6853-6863.

(102) a) A. R. H. Narayan, G. Jiménez-Osés, P. Liu, S. Negretti, W. Zhao, M. M. Gilbert, R. O. Ramabhadran, Y. Yang, L. R. Furan, Z. Li, L. M. Podust, J. Montgomery, K. N. Houk and D. H. Sherman, *Nat. Chem.*, **2015**, *7*, p653-660; b) S. Li, M. R. Chaulagain, A. R. Knauff, L. M. Podust, J. Montgomery and D. H. Sherman, *Proc. Natl. Acad. Sci. USA*, **2009**, *106*, p18463-18468; c) S. Negretti, A. R. Narayan, K. C. Chiou, P. M. Kells, J. L. Stachowski, D. A. Hansen, L. M. Podust, J. Montgomery and D. H. Sherman, *J. Am. Chem. Soc.*, **2014**, *136*, p4901-4904.

(103) D. F. Münzer, P. Meinhold, M. W. Peters, S. Feichtenhofer, H. Griengl, F. H. Arnold, A. Glieder and A. de Raadt, *Chem. Commun.*, **2005**, p2597-2599.

(104) C. Vickers, G. Backfisch, F. Oellien, I. Piel and U. E. W. Lange, *Chem. Eur. J.*, **2018**, *24*, p17936-17947.

(105) P. Le-Huu, D. Rekow, C. Krüger, A. Bokel, T. Heidt, S. Schaubach, B. Claasen, S. Hölzel, W. Frey, S. Laschat and V. B. Urlacher, *Chem. Eur. J.*, **2018**, *24*, p12010-12021.

(106) a) N. Kawakami, O. Shoji, Y. Watanabe, *Angew. Chem. Int. Ed.*, **2011**, *50*, p5315-5318; b) F. E. Zilly, J. P. Acevedo, W. Augustyniak, A. Deege, U. W. Häusig and M. T. Reetz, *Angew. Chem. Int. Ed.*, **2011**, *50*, p2720-2724.

(107) Z. Cong, O. Shoji, C. Kasai, N. Kawakami, H. Sugimoto, Y. Shiro and Y. Watanabe, *ACS Catal.*, **2015**, *5(1)*, p150-156.

(108) S. D. Munday, O. Shoji, Y. Watanabe, L. L. Wong, S. G. Bell, *Chem. Commun.*, **2016**, *52* , p1036-1039.

(109) a) O. Shoji, T. Kunimatsu, N. Kawakami and Y. Watanabe, *Angew. Chem. Int. Ed.*, **2013**, *52*, p6606-6610; b) O. Shoji, S. Yanagisawa, J. K. Stanfield, K. Suzuki, Z. Cong, H. Sugimoto, Y. Shiro and Y. Watanabe, *Angew. Chem. Int. Ed.*, **2017**, *56*, p10324-10329; c) M. Karasawa, J. K. Stanfield, S. Yanagisawa, O. Shoji and Y. Watanabe, *Angew. Chem. Int. Ed.*, **2018**, *57*, p12264-12269.

(110) Z. Li, Y. Jiang, F. P. Guengerich, L. Ma, S. Li and W. Zhang, *J. Biol. Chem.*, **2020,** *295(3)*, p833-849.

(111) J. B. Y. H. Behrendorff, W. Huang and E. M. J. Gillam, *Biochem. J.*, **2015**, *467*, p1-15.

(112) S. C. Hammer, A. M. Knight and F. H. Arnold, *Curr. Opin. Green Sustain. Chem.*, **2017**, *7*, p23-30.

(113) Z. J. Wang, H. Renata, N. E. Peck, C. C. Farwell, P. S. Coelho and F. H. Arnold, *Angew. Chem. Int. Ed.*, **2014**, *53*, p6810-6813.

(114) a) N. P. Dunham and F. H. Arnold, *ACS Catal.*, **2020**, *10*, p12239-12255; b) R. K. Zhang, K. Chen, X. Huang, L. Wohlschlager, H. Renata and F. H. Arnold, *Nature*, **2019**, *565*, p67-72.

(115) J. N. Kolve, K. M. O'Dwyer, C. T. Jordan and R. Fasan, *ACS Chem. Biol.*, **2014**, *9*, p164-173.

(116) S. A. Loskot, D. K. Romney, F. H. Arnold and B. M. Stoltz, *J. Am. Chem. Soc.*, **2017**, *139*, p10196-10199.

Chapter 2 : Enantioselective $P450_{BM3}$ Hydroxylation of Aminocycloalkanes

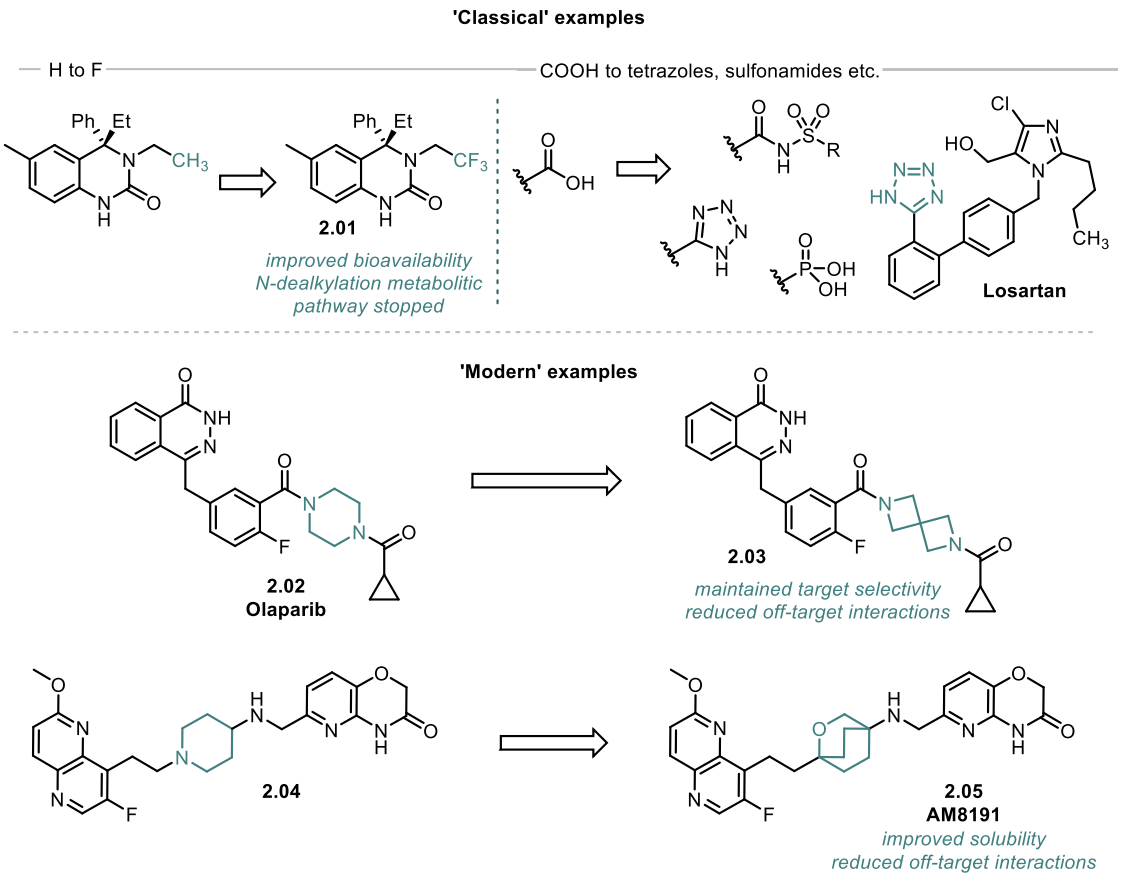
2.1. Introduction

2.1.1. Bioisosteres in medicinal chemistry

Bioisosterism is an established concept to replace chemical substituents or groups to improve the absorption, distribution, metabolism, excretion and toxicity (ADMET) properties of a drug candidate without changing the geometry of the compound. Classical examples of bioisosteres include the replacement of a methyl group for a trifluoromethyl group, which was shown to improve the bioavailability of compound **2.01** by blocking a particular undesired metabolic pathway;[1] and the carboxylic acid functional group which has many potential bioisosteres including tetrazole,[2] which has been shown to be particularly effective in the drug Losartan (*Scheme 1*).

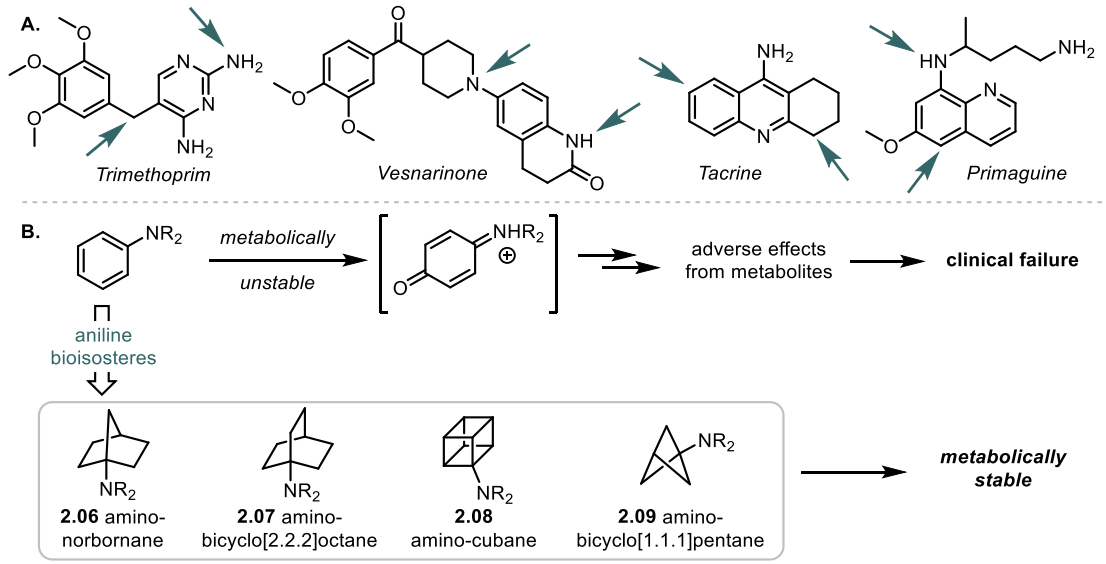
Through manipulation of specific motifs it is possible to enhance potency and selectivity, reduce toxicity, improve bioavailability (by reducing unwanted metabolic side-reactions) and move into new IP-free chemical space. The influential 'escape from flatland' publication in 2009 described the movement of the chemical industry to include more sp^3-rich scaffolds vs the predominant sp^2, to improve on key pharmacokinetic properties and ultimately reduce the failure rate of drug candidates.[3] During the last decade there has been a surge in the publication of synthetic methodologies towards more intricate ring systems, and more complex sp^3-rich scaffolds are increasingly found in the patent literature of potential small molecule treatments.

Makvandi and Mach showed that cell cytotoxicity and off-target interactions could be reduced by simply replacing the piperazine moiety of Olaparib **2.02** with its diazaspirocyclic bioisostere **2.03** (*Scheme 1*).[4] A similar effect was reported during the development of novel broad spectrum antibacterial agents by Merck, WuXi AppTec and Kyorin Pharmaceuticals.[5] X-ray crystallography was used to show that the binding of the oxabicyclooctane-linked analogue AM8191 **2.05** was comparable to that of the original piperidine-linked structure **2.04**, while exhibiting improved physical properties such as solubility and decreased off-target interactions.



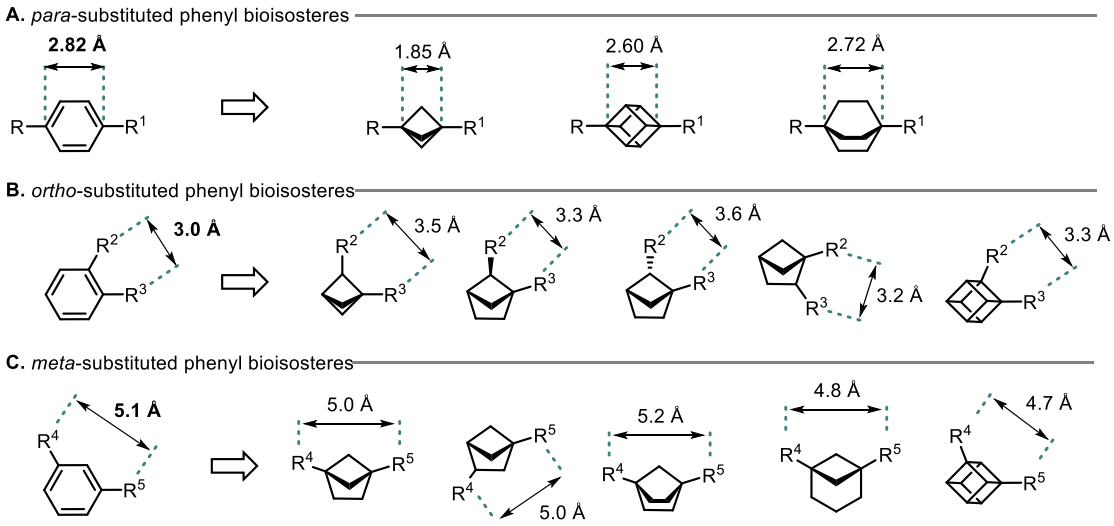
Scheme 1 – Classical vs. modern bioisosteres in medicinal chemistry.

The development of robust and reliable C–N bond forming chemistry (such as S_NAr, Buchwald–Hartwig and Chan–Lam cross couplings) mean that anilines are now a very common motif in drug discovery (around 14% marketed drugs in 2009 contained aromatic amines).[6] Despite its widespread use, this has proven to be a problematic substructure as anilines can undergo metabolic oxidation by CYP450 (*Scheme 2.A*) to create highly reactive intermediates such as quinone-imines and quinone-methides, and this bioactivation pathway can cause serious adverse drug interactions.[7] As a solution to this issue several aniline bioisosteres have been developed including amino-norbornane **2.06**, amino-bicyclo[2.2.2]octane **2.07**, amino-cubane **2.08** and amino-bicyclo[1.1.1]pentane (BCPA) **2.09** (*Scheme 2.B*).[8]



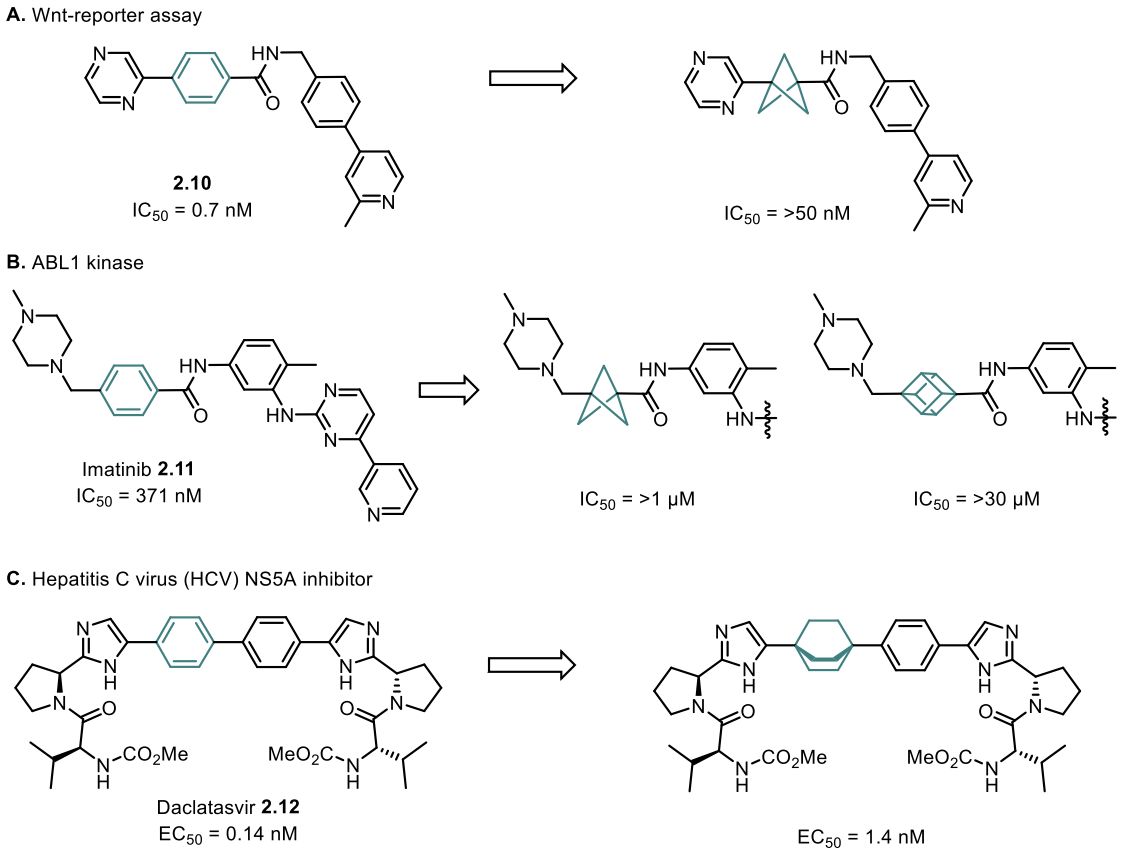
Scheme 2 – (A) Drugs containing metabolically labile functionality which can form quinone reactive intermediates, the site of bioactivation shown with blue arrows, (B) Reactive metabolites formed from anilines, and sp^3-rich ring systems currently reported as bioisosteres for aryl amines.

When choosing to replace an aryl ring in a bioactive compound, beyond the advantages that a saturated bioisostere could provide such as improved metabolic stability or water solubility, other factors should be considered. It is hard to predict the exact influence such a replacement could have on activity; however, if its main role is as a linker of defined length, then maintaining binding activity is achieved by holding substituents in a similar orientation in the protein receptor as the phenyl counterpart. In this case, both the size of the molecule and the angle of the substituents are most important (comparisons can be seen in *Scheme 3* data from Mykhailiuk[9]).



Scheme 3 – Comparison of the sterics of *ortho-*, *meta-* and *para-* substituted benzene isosteres.

However, in some cases specific aryl-protein interactions are the key to strong binding to the target receptor, whereby the phenyl ring exhibits π-interactions with other functionalities in the receptor such as the aromatic amino acids, the protonated amino groups of arginine or lysine residues, or other weak dipole interactions.[10] In these cases, replacing the phenyl ring is detrimental to the activity of the compound, as shown in *Scheme 4* with compound **2.10** (A)[11], imatinib **2.11** (B)[12] and daclatasvir **2.12** (C).[13]

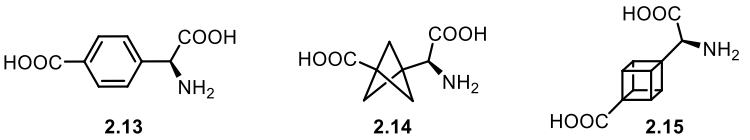


Scheme 4 – Drug candidates with decreased potency due to replacement of aryl group with saturated bioisostere.

2.1.2. Use of bicyclo[1.1.1]pentanes as bioisosteres

The earliest report of the effect of using BCP as a phenyl replacement was in 1996, by Pellicciari and co-workers (*Scheme 5*), who found the saturated analogue **2.14** of **2.13**, a known selective antagonist of the metabolic glutamate receptor of group 1 (mGlu1a), was found to be three times

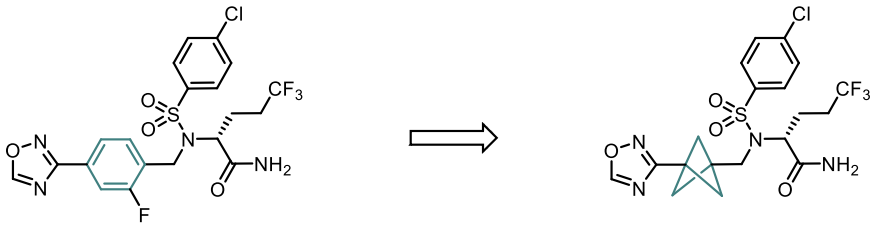
more potent.[14] Interestingly, cubane analogue **2.15** was an order of magnitude less active,[15] despite also traditionally being used as a benzene isostere.[16]



mGlu1a IC_{50}	65±5 μM	25±6 μM	232±55 μM

Scheme 5 – mGlu1a selective antagonist **2.13** and the saturated bioisosteric analogues **2.14** and **2.15**.

Scientists from Pfizer reported that the replacement of the fluorophenyl moiety for a BCP unit in γ-secretase inhibitor **2.16** resulted in drastically improved ADMET properties and increased potency in **2.17** (*Scheme 6*).[17]



BMS-708,163 **2.16**
IC_{50} = 0.225 nM
ElogD = 4.70
kinetic solubility = 0.6 μM
thermodynamic solubility = 0.90 μM

2.17
IC_{50} = 0.178 nM
ElogD = 3.80
kinetic solubility = 216 μM
thermodynamic solubility = 29.4 μM

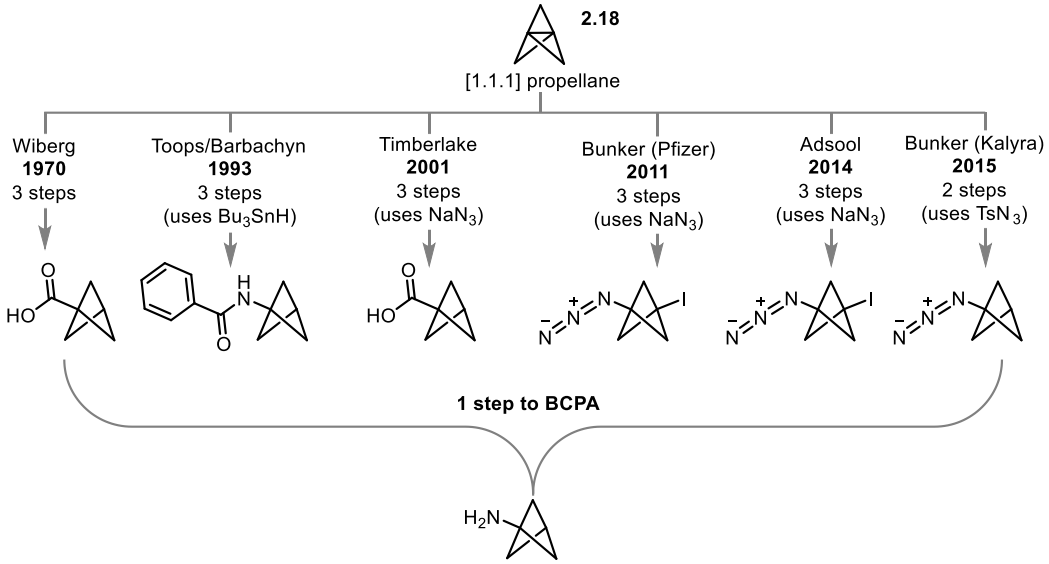
Scheme 6 – Improved physiochemical properties on the substitution of the fluorophenyl motif in **2.16** for bicyclo[1.1.1]pentane.

Since synthetic methods for BCP cores have predominantly focused on 1,3-functionalised systems, these structures are the most commonly found in medical chemistry campaigns; however, with the increasing number of publications on both chiral BCP and BCPs with C2-functionalisation, it is expected that these will find their way into many pharmaceutical compound libraries in the future.

2.1.3. Synthesis of bicyclo[1.1.1]pentanes

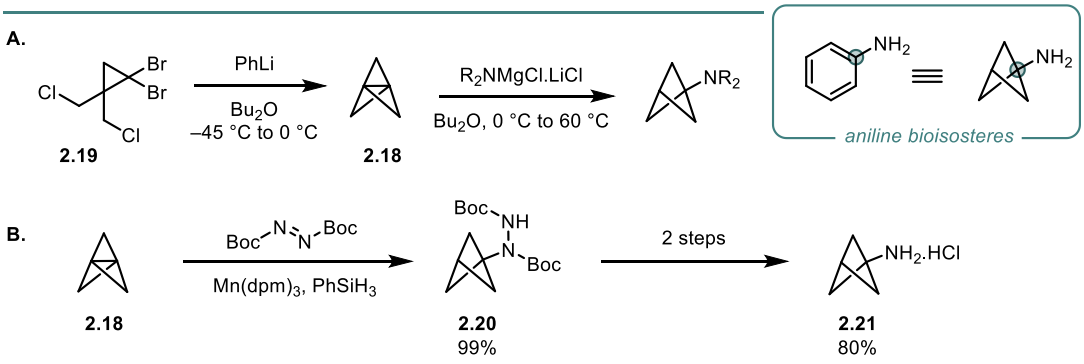
The first synthesis of the unfunctionalised bicyclo[1.1.1]pentane core was reported in 1964 by Wiberg,[18] with the same group developing a synthesis of [1.1.1]propellane **2.18** in 1982. This work inspired the development by Szeimies,[19] of a new synthesis of [1.1.1]propellane using 1,1-dibromo-2,2-bis(chloromethyl)cyclopropane **2.19** via nucleophilic displacement, which has allowed this field to flourish and is still used to access compound **2.18**.

Many groups have developed routes to bicyclo[1.1.1]pentyl amines (BCPAs) from [1.1.1]propellane, mostly requiring multi-step syntheses using toxic and hazardous reagents such as Bu_3SnH or azides (*Scheme 7*);[20] clearly, an improved protocol involving milder conditions was required.



Scheme 7 – Early methods for the synthesis of BCPA.

A breakthrough in the field came in 2015 when the Baran group, in collaboration with Pfizer Inc., described conditions for a one-pot, scalable synthesis of BCPAs using a pioneering strain-release amination approach,[21] achieving rapid access to an entire class of BCP amines by taking advantage of the innate reactivity of the strained central C–C bond of [1.1.1]propellane **2.18** (*Scheme 8.A*). A 2011 report by scientists at Pfizer demonstrated the use of a radical hydrohydrazination reaction to prepare 1-bicyclo[1.1.1]pentylhydrazine which could be reduced to give BCPA **2.21** (*Scheme 8.B*).[22] Both of these early reports were limited to mono-substituted BCPAs.

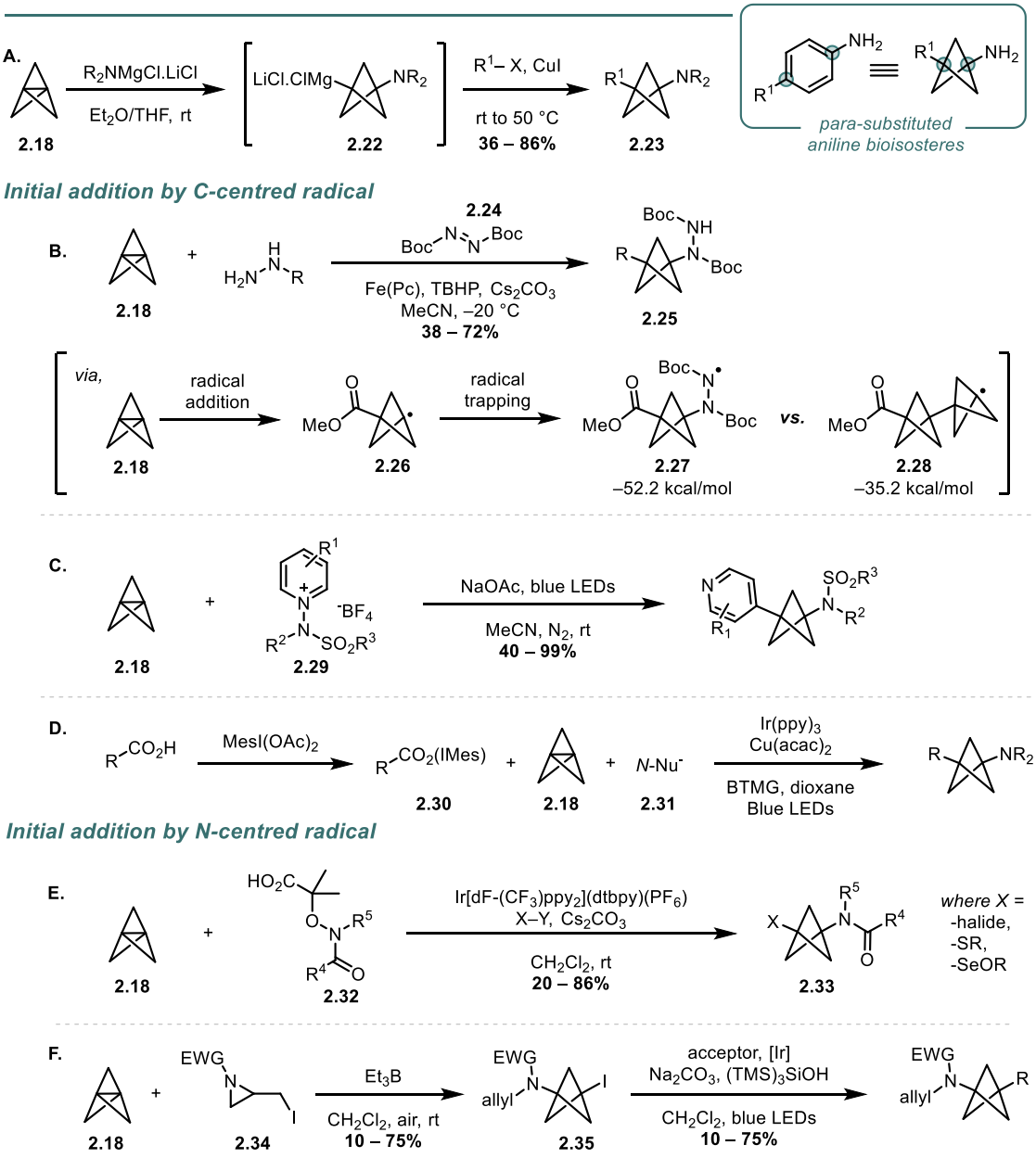


Scheme 8 – Methods towards mono-substituted aniline bioisosteres.

A lack of methodology to directly functionalise at the C3 position of BCPAs led multiple groups to develop syntheses of 1,3-functionalised BCPAs from [1.1.1] propellane **2.18**. Gleason further developed Baran's original methodology, to incorporate an *in-situ* trapping of metalated intermediate **2.22** with electrophiles, to generate a range of highly functionalised BCPAs **2.23** (*Scheme 9.A*).[23]

Methodologies proceeding by the radical ring-opening of [1.1.1] propellane to form BCPAs can be generally categorised by whether the first step involves either *C*- or *N*-centered radicals. One problem that can arise with radical reactions involving **2.18** is polymerisation; however, Uchiyama's carboamination strategy bypasses this problem by using di-*tert*-butyl azodicarboxylate **2.24** as a radical acceptor to react with **2.18**, giving a more stable radical intermediate **2.27** compared to **2.28** (*Scheme 9.B*).[24] A recent report using this radical approach describes a visible-light catalysed aminopyridylation procedure using **2.29** which requires no external photocatalyst (*Scheme 9.C*).[25] MacMillan showed that photoredox-genearated alkyl radicals from **2.30,** on reaction with [1.1.1] propellane **2.18,** could produce a radical intermediate which could then be coupled with a range of nitrogen nucleophiles **2.31** using copper catalysis (*Scheme 9.D*).[26]

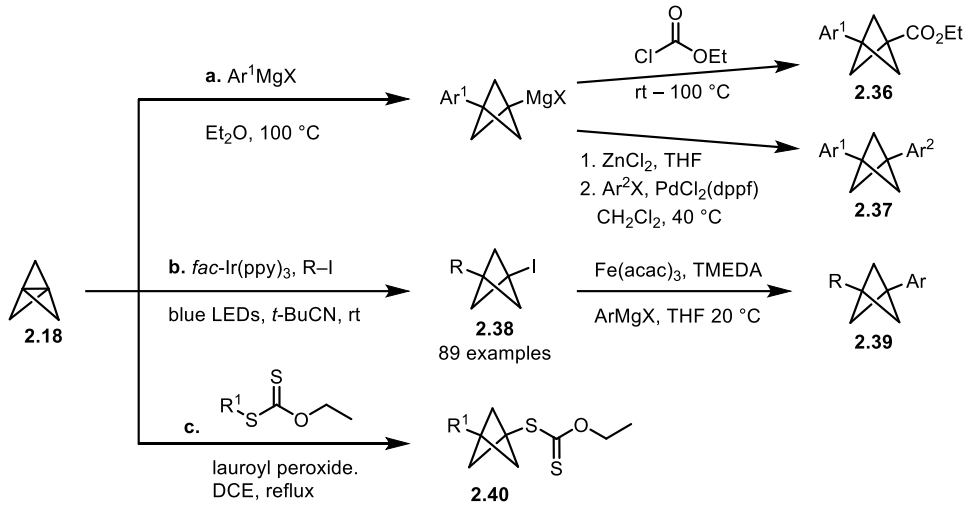
Leonori reported the use of amidyl radicals from **2.32** for the ring opening reaction of **2.18**, and subsequent trapping of the C3 radical with a range of radicophiles to yield BCPAs with functional groups **2.33** previously inaccessible by existing methods (*Scheme 9.E*).[27] Very recently Anderson has developed a similar approach to Leonori, using *N*-centred radicals generated from α-iodoaziridines **2.34** as suitable acceptors in an atom transfer radical addition to form BCPA iodides **2.35** (*Scheme 9.F*).[28] These useful building blocks could be further derivatised at the bridgehead C–I bond using Giese-type methodology, where the use of silanols could generate radicals from simple alkyl halides using photoredox catalysis.



Scheme 9 – Modern syntheses of 1,3-functionalised BCPAs.

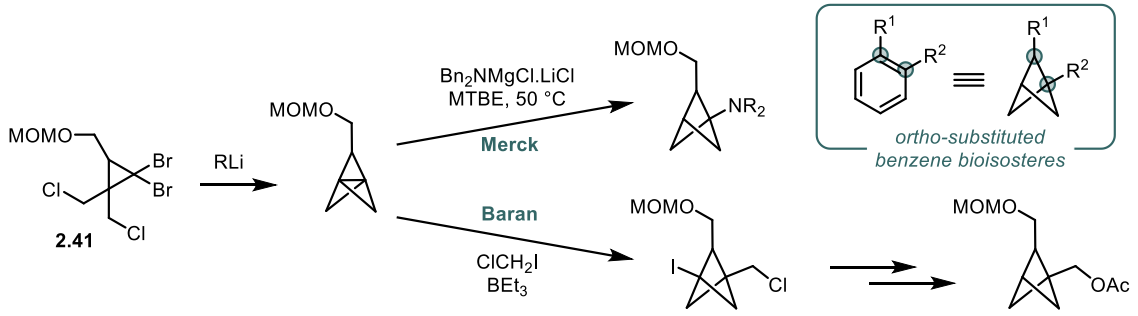
There are many elegant methodologies reported for the synthesis of 1,3-difunctionalised BCPs, bearing a variety of carbon-based functionalities, as valuable bioisosteres of *para*-substituted phenyl rings. Traditional methods rely on functional group manipulation of bicyclo[1.1.1]pentane-1,3-dicarboxylic acid,[29] as the synthesis of its precursor bisacetyl-BCP is well-established and can be performed on kilogram scale.[30] However many modern approaches are based around the ring-opening of [1.1.1] propellane with organometallic reagents or radicals, similar to syntheses of BCPAs shown previously, forming functionalised intermediates containing synthetic handles for further derivatisation.

Knochel reported that the products of ring opening of [1.1.1] propellane **2.18** with Grignard reagents could undergo either a) quenching with ethylchloroformate to product the corresponding ethyl esters **2.36**, or b) transmetalation with $ZnCl_2$ and subsequent Negishi cross-coupling to afford bisarylated BCPs **2.37** (*Scheme 10.a*).[31] Anderson used photoredox catalysis to generate a wide variety of BCP-iodides **2.38**,[32] which could be transformed into a range of difunctionalised BCPs **2.39** by iron-catalysed Kumada coupling (*Scheme 10.b*).[33] Furthermore, the Riant group developed a simple, one-pot procedure for the synthesis of BCP xanthates **2.40** (*Scheme 10.c*).[34]



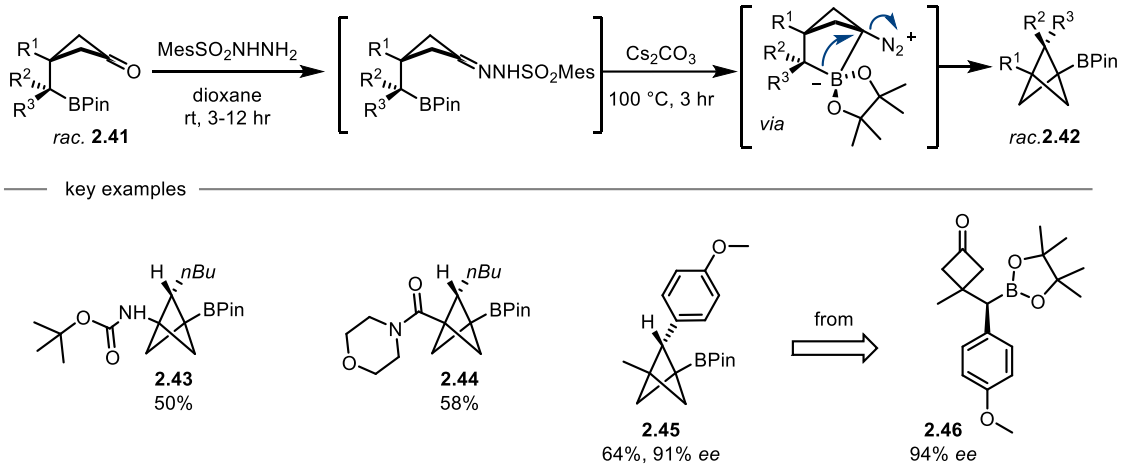
Scheme 10 – Selected reports and approaches towards the synthesis of 1,3-difunctionalised BCPs.

Baran's strain-release amination methodology was extended both within the same group[35] and by Merck[36] (*Scheme 11)*, to include functionalisation at the C2 position by using MOM-protected alcohol starting material **2.41**. This approach suffers from the constraint of a substrate requiring a protecting group, and incorporation of C2 functionality was only achieved racemically. Consequently, were industry to adopt this methodology it would require costly chromatographic separation of enantiomers for testing.



Scheme 11 – Extension of the strain-release amination methodology to include C2-functionalised BCPAs.

Most of the methodologies previously discussed are based on the strain-release of [1.1.1]propellane, however Qin and co-workers developed a novel method for forming C2-functionalised BCPs via cyclisation (*Scheme 12*).[37] The use of mesitylsulfonyl hydrazide was key for effective hydrazone condensation of cyclobutanone **2.41,** and generation of diazo intermediate *in situ* set the stage for cyclisation to racemic **2.42**. A high tolerance of a wide variety of functional groups was achieved, a broad substrate scope includes BCPA **2.43** and amide **2.44,** and the BPin group can be further functionalised to provide a modular platform for the construction of highly-substituted BCPs. The chiral BCP **2.45** was included in the scope; however, this simply originates from enantioenriched starting material **2.46**.



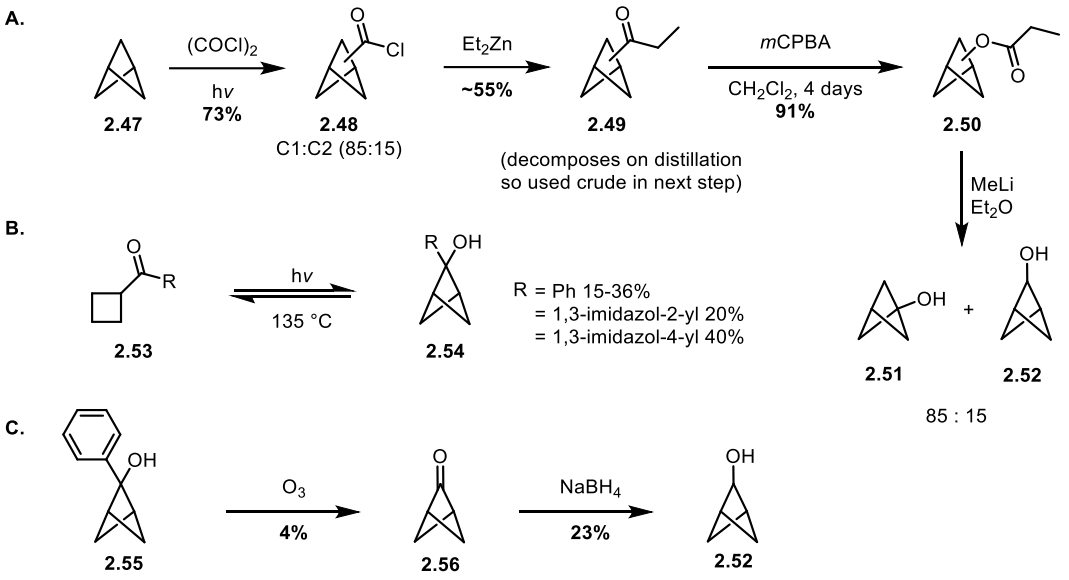
Scheme 12 – Qin's methodology for the synthesis of C2-functionalised BCPs via intramolecular cyclisation, with relevant scope examples including carbamate **2.43**, amide **2.44** and chiral BCP **2.45**.

There are many impressive syntheses of chiral-BCPs bearing an adjacent stereocentre;[38] however, there are currently no enantioselective C–H functionalisations to form 'chiral-at-BCP' ring systems.

An excellent minireview by Poole discusses all the existing methodologies toward C2-functionalised BCPs, that reveals the lack of direct methods. Methods available for the preparation of BCP-2-ol compounds are described as 'rare' and 'extremely inefficient' and are predominantly from the 1970s or earlier with no modern examples.

Scheme 13.A shows how BCP-2-ol **2.52** can be accessed through a telescoped synthesis from a mixture of acyl chlorides **2.48**, via Baeyer–Villiger oxidation of mixed ketones **2.49** and hydrolysis

of the resulting esters **2.50**.[39] No isolated yields are reported for the final step, however the 85:15 ratio of regioisomers carried through the synthesis is not in favour of the C2-alcohol **2.52** meaning that a maximum overall yield of ~5% is possible from BCP **2.47**. Norrish–Yang cyclisation of a range of cyclobutyl aryl ketones **2.53** achieved the formation of C2-disubstituted BCPs of type **2.54** in poor yields (*Scheme 13.B*).[40] In a separate report these were shown to undergo ozonolysis in extremely poor yield (4%) to produce ketone **2.56**, which could then be reduced to yield BCP-2-ol **2.52** in low yield (*Scheme 13.C*).[41]



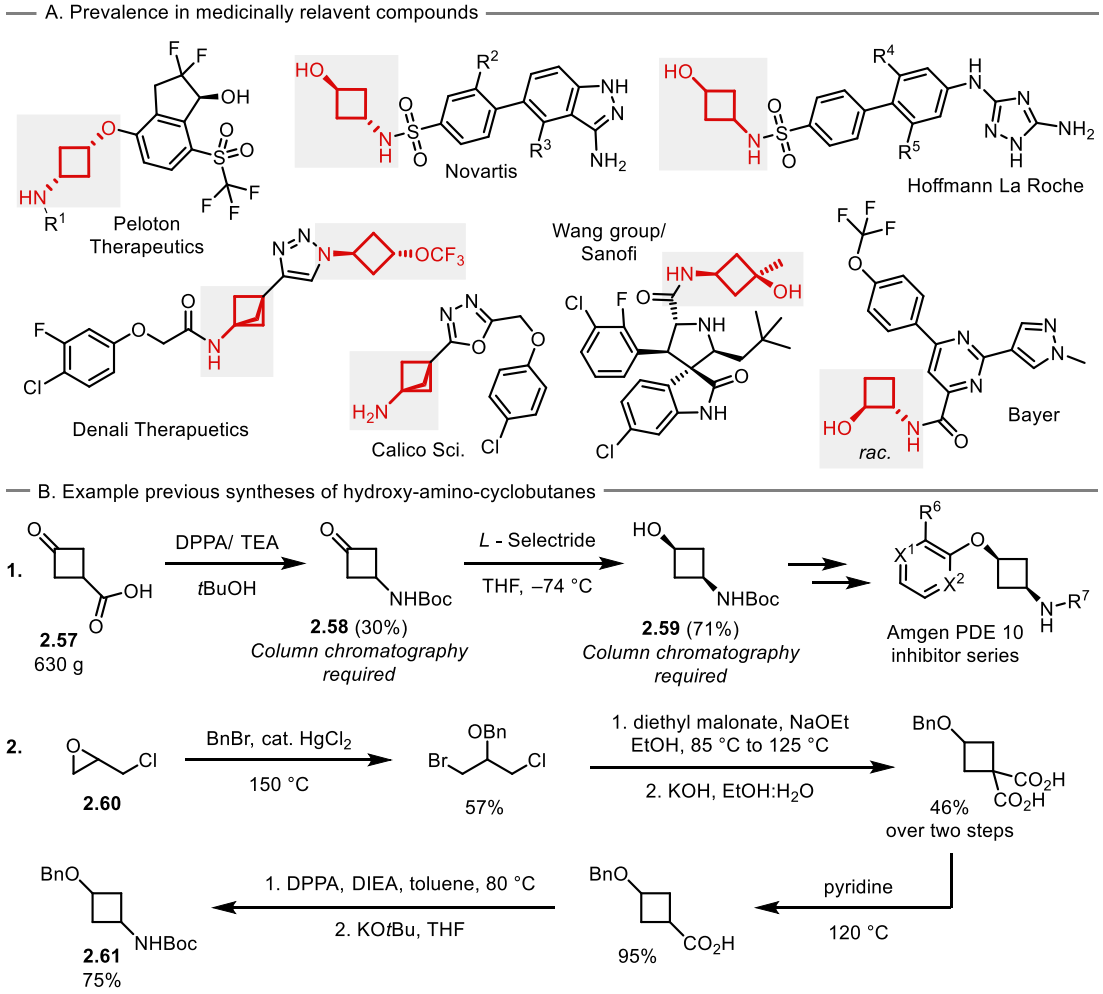
Scheme 13 – Existing methods for the synthesis of bicyclo[1.1.1]pentan-2-ol **2.52**.

The development of an enantioselective synthesis of chiral BCP alcohols via direct C2-functionalisation of the parent BCP would clearly be highly valuable, bringing this field of research into the 21st century.

2.1.4. Importance of small-ring hydroxy-amino-cycloalkanes

It has been shown that BCPs are increasingly common substructures in medicinal chemistry; however, the popularity of aliphatic small rings more broadly has long been established and this area has been extensively reviewed by scientists at AstraZeneca.[42] Hydroxy-amino-cyclobutanes specifically are privileged motifs in synthesis and, as such, are found in a plethora of pharmaceutical candidates (*Scheme 14.A*). These motifs can be used as additions to biologically active structures in order to explore chemical space in QSAR studies or can even constitute the series core structure.

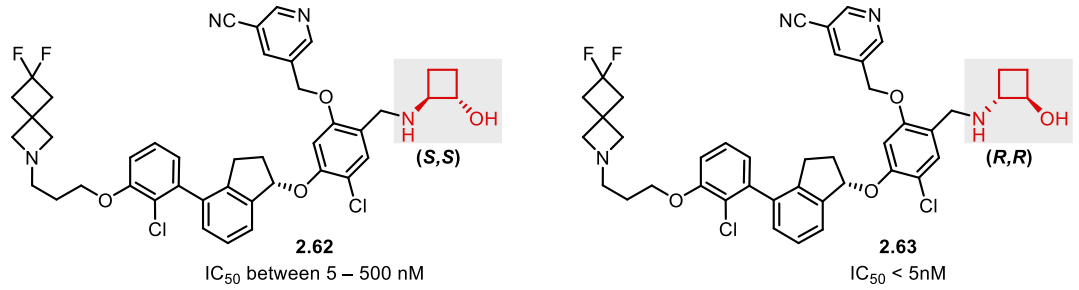
Each regioisomer requires a bespoke synthesis, as there is currently no methodology to access all isomers from a single starting material. Some reported syntheses are shown in *Scheme 14*, highlighting the use of the Curtius rearrangement to access 1,3-regioisomer **2.59**. Amgen process chemists used this chemistry on large scale to install the Boc-protected amine in compound **2.58**, followed by a reduction of the ketone using L-Selectride to form 1,3-*cis* compound **2.59,** en route to a series of PDE 10 inhibitors. This route used the expensive starting material cyclobutanone carboxylic acid **2.57**, required the use of large amounts of toxic and potentially explosive DPPA, and both steps require column chromatography. Scientists at GSK reported a similar synthesis using this rearrangement, starting instead from epichlorohydrin **2.60** with additional steps to form the cyclobutane ring and resulting in benzyl protected fragment **2.61**.



Scheme 14 – (A) Examples of hydroxy-amino-cycloalkanes from Peleton Therapeutics,[43] Novartis,[44] Roche,[45] Sanofi and Wang,[46] Bayer,[47] Denali Therapeutics,[48] GSK,[49] Calico Sciences;[50] and (*B*) approaches to 3-hydroxy-1-aminocyclobutanes using a Curtius rearrangement by (1) Amgen[51] and (2) GSK[52].

A well-established medicinal chemistry principle is that different enantiomers exhibit different biological activities, and relevant examples of this phenomena can be seen in a series of small molecules developed as potential anti-cancer treatments by Chemocentryx, Inc.[53] They showed that the (*R,R*) enantiomer **2.63** displayed much higher levels of potency, with significantly lower IC_{50} values compared to the (*S,S*) analogue **2.62** (*Scheme 15*).

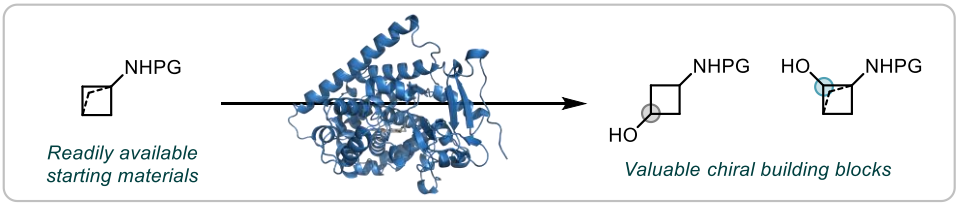
When only small quantities of material are required, scientists in discovery chemistry teams can rely on chromatographic separation techniques such as chiral-phase preparative HPLC, rather than developing enantioselective syntheses. Although chromatography can be achieved on kilogram scale, if a scalable enantioselective method towards the synthesis of these motifs were developed it would be highly advantageous and could result in a considerable cost and waste reduction.



Scheme 15 – Two specific *trans*-2-hydroxy-1-aminocyclobutane examples by Chemocentryx, Inc. for the treatment of cancer using small molecule PD-L1 inhibitors.

2.1.5. Aims of this project

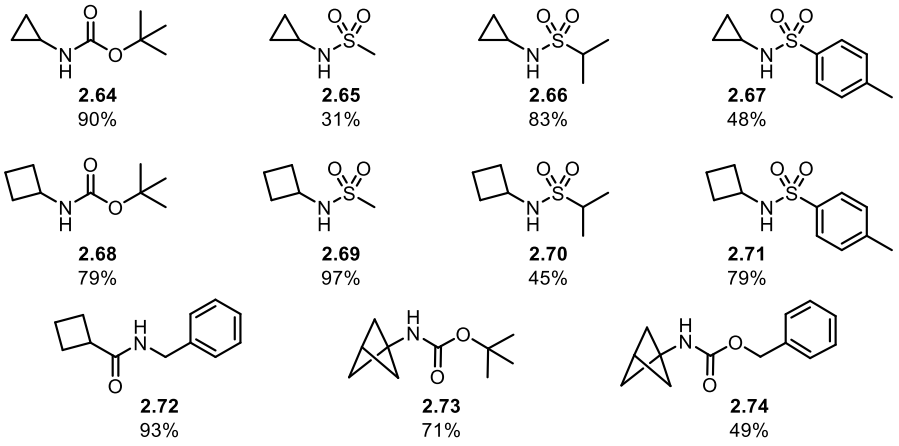
In this project we set out to identify cytochrome P450 mutants, containing combinations of residue mutations, which can effect the conversion and selectivity of the enzymatic oxidation of *N*-protected cycloalkylamines, cycloalkylcarboxamides and BCPAs (*Scheme 16*). By varying the amine protecting group, we aim to alter the substrate binding orientation in the active site and therefore fine-tune regio-, diastero- and enantioselectivity.



Scheme 16 – Substrates for *m*P450 oxidation which will be discussed in this chapter.

2.2. Synthesis of amine substrates

Procedures for the preparation of all starting materials **2.64** – **2.74** can be found in the *Chapter 6: Experimental Details* and are unoptimised (S*cheme 17*). The four main protecting groups in this study (Boc-, Ms-, Ips- and Ts-) were chosen to provide a variety of steric and electronic effects for any potential interactions within the P450 active site, and in part due to previous group success using these moieties.



Scheme 17 – Isolated yields of all the substrates screened in this project.

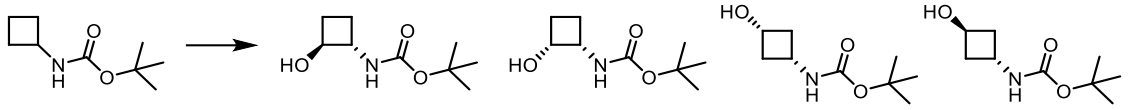
2.3. Synthesis of 1,2-hydroxy-aminocyclobutanes

Reports of the synthesis of 1,2-hydroxy-aminocyclobutanes are generally less common than for the 1,3-analogues, in part due to the chemical strategies used to access them. As they are inherently chiral, they also require an extra level of stereochemical control and so methodology to directly synthesise these regioisomers from the parent amine, with high levels of diastero- and enantioselectivity, would be highly valuable.

2.3.1. Access to *trans*-1,2-hydroxy-aminocyclobutanes

Initial efforts began using *tert*-butyloxycarbonyl (Boc)-protected cyclobutylamine **2.68** as previous work within our group had shown this protecting group to be well tolerated with our library of $P450_{BM3}$ mutants. A select library of 48 enzymes was chosen for initial screening, containing mutants which had previously shown varied metabolite profiles, and which could allow rapid access to high levels of selectivity without the need for extensive screening and multiple rounds of

mutagenesis.[54] Wild type $P450_{BM3}$ showed no conversion; however, across the entire 48-enzyme panel this was a well-accepted substrate with the top 10 mutants achieving >90% conversion (*Chapter 5: Appendices* for full screening data). *Table 1* shows the top 10 mutants for the formation of 1,2-*trans* compound **2.75**, achieving high overall conversions at the substrate:enzyme ratio of 500:1.



2.68 **2.75** **2.76** **2.77** **2.78**

Entry	Mutant	Conversion /%	2.75 /%	2.76 /%	2.77 /%	2.78 /%	Other /%	TTN
1	KT2/L188G/I263G	97	79	1	4	12	1	485
2	RK/A328G	71	71	-	-	-	-	355
3	RP/H171L/I263G	99	70	2	4	20	3	495
4	RP/H171L/I263G/A184I	100	68	-	4	20	8	500
5	R47L/Y51F/KSK19	90	63	-	-	13	14	450
6	KU3/S72W /A330P	98	61	28	1	5	3	490
7	R19/F87I/L437LV	96	54	1	5	26	10	480
8	R19/F87I	81	45	9	2	23	2	405
9	KSK19/I263G	83	42	2	5	28	6	415
10	RT2/S72G/A330W	69	41	11	1	2	14	345

Table 1 – Top 10 mutants for the conversion of **2.68** into metabolite **2.75**, measured by GC integration. Scheme represents relative configuration. TTN rounded to nearest 5.

From *Table 1*, mutation I263G appears important for high conversion to product **2.75** (*Entries 1,3,4 and 9*), and A328G was influential for high selectivity (*Entry 2*). When glycine was swapped to leucine at 328 (*Table 2*, *Entry 2*) both conversion and selectivity decreased, and now favouring *cis*-metabolite **2.76** (discussed in *Section2.3.2*). The addition of other glycine mutations did not affect selectivity, but overall conversion was significantly diminished (*Entries 3 and 4*).

Entry	Mutant	Conversion /%	2.75 /%	2.76 /%	2.77 /%	2.78 /%	Other /%	TTN
1	RK/**A328G**	71	71	-	-	-	-	355
2	RK/**A328L**	50	8	22	2	10	8	250
3	RK/**A328G**/P329G/A330G	43	37	1	-	2	3	215
4	RK/**A328G**/A264G	8	5	1	-	-	2	40

Table 2 – Selected screening results highlighting the importance of Ala328, measured by GC integration.

From original screening data (*Table 1*), full conversion and high selectivity was achieved with base mutant RP/H171L/I263G (*Entries 3 and 4*) and so was chosen for further optimisation. Preparative scale reaction using RP/H171L/I263G/A184I was performed on 0.6 mmol scale, comparing the use of two organic co-solvents to solubilise the substrate (EtOH and DMSO), monitoring over the course of three days (*Figure 1*) . Although DMSO allowed a higher conversion after 72 hr, both reactions gave 35% isolated yield with a 98% *ee*, which could be raised to enantiopurity (>99.9%) by recrystallisation by liquid-liquid diffusion (DCM/heptane). In the example using DMSO, more non-productive conversion is observed as isolated yields are identical.

Previously, the presence of a heavy atom was required for determination of absolute stereochemistry using X-ray through the Flack parameter – a measure reflecting dispersion effects.[55] Light atoms usually show a small anomalous dispersion effect, which leads to an impossible Flack parameter with no meaning. However, with the advancement of technology absolute stereochemical assignments can now be made on structures containing only C, H, N and O atoms. The absolute configuration of **2.75** was thus determined by single crystal X-ray crystallography.

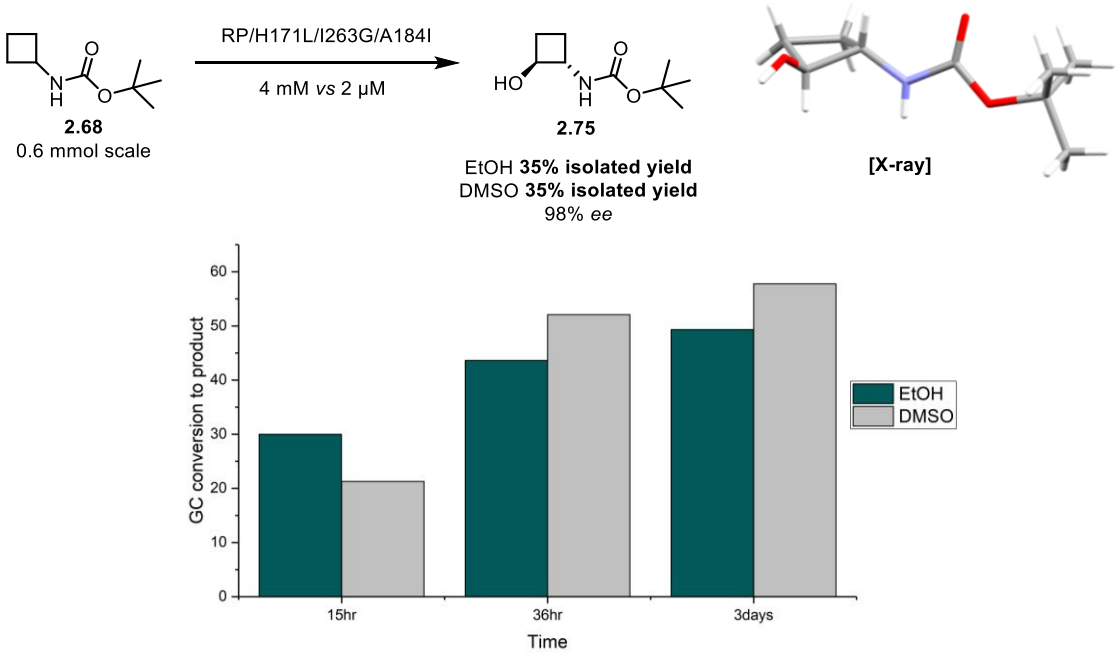


Figure 1 – Comparison of organic solvents used for substrate stock solution in reaction of RP/H171L/I263G/A184I with Boc **2.68**.

With proof that this reaction remained successful on a synthetically useful scale, efforts turned to a search for mutants with improved conversion and regioselectivity. This class of small-sized rings clearly benefits from a decreased active site space, and so mutants containing active site mutations to bulkier residues, thereby truncating the substrate pocket for increased selectivity, were explored.

Recently, colleagues at Nankai University, Tianjin, China provided a crystal structure of the $P450_{BM3}$ mutant RP/F87V/E267V/L437LV, whereby it was possible to see a shift in orientation of the L437 side-chain to now point downwards towards the active site, caused by the inserted valine at 438.

With this new understanding, substrate **2.68** was then screened against a selection of mutants from our library which contained this L437LV insertion mutation, and the results are presented in *Table 3*. As expected, RP/H171L/I263G/L437LV (*Table 3, entry 5*) was an excellent mutant, with full conversion and high regioselectivity to **2.75**. Comparison with *entries 4b* and *5b* highlight the significant improvement which can be achieved on addition of this mutation.

Entry	Mutant	Conversion /%	2.75 /%
1	RP/F87V/E267V/L437LV	81	30
2	RP/V78F /F87V/E267V /L437LV	95	25
3	RP/F87G /H171L/I263G /L437LV	21	14
4a	R19/F87I/L437LV	96	56
4b	*R19/F87I*	*81*	*45*
5a	**RP/H171L/I263G/L437LV**	**>99**	**82**
5b	*RP/H171L/I263G*	*99*	*70*

Table 3 – Selected mutants containing L437LV screened against Boc **2.68,** measured by GC integration.

In order to rationalise the effect of the addition of the L437LV mutation, the active sites of the MD simulated protein structures were analysed with mesh view, allowing visualisation of the available space above the heme (*Figure 2*). In RP/H171L/I263G, residue Leu437 does not exert much influence with the substrate pocket remaining relatively large; however, after insertion of valine at 438 it can be seen that the new orientation of Leu437 causes significant truncation of the active site and thus explains the increase in selectivity observed.

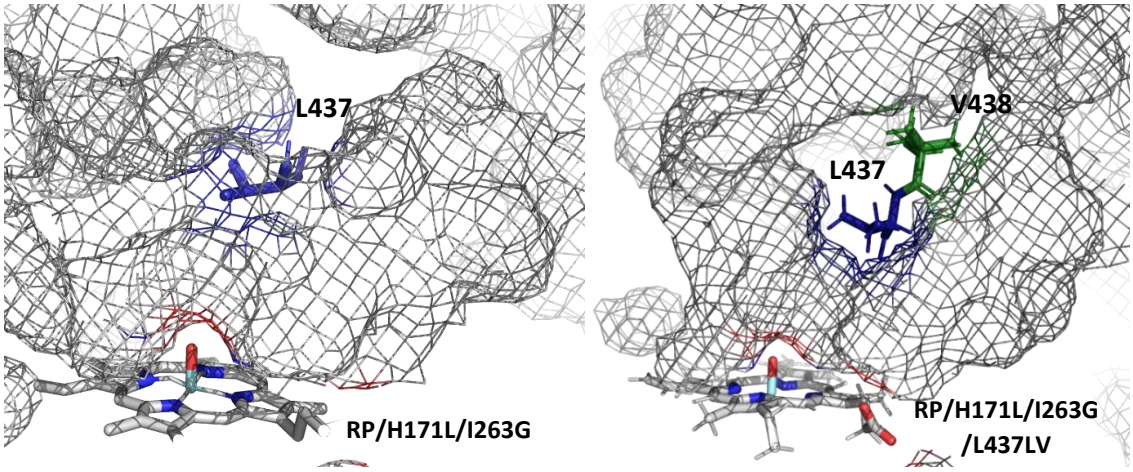


Figure 2 – MD simulated protein structure of RP/H171L/I263G (from PDB ID: 1JPZ) and RP/H171L/I263G/L437LV (from crystal structure of RP/F87V/E267V/L437LV), with mesh shown indicating free space, and residues L437 (blue) and V438 (green) highlighted.

A titre test screen using this mutant showed that an excellent turnover was possible (TTN = 11950) with a substrate concentration as high as 10 mM and an enzyme concentration of 0.25 μM (*Figure 3.A*), equating to a catalyst loading of only 25 ppm. Using this enzyme concentration, a preparative scale reaction was performed using 2 mM substrate concentration and addition of the substrate from stock solution in small aliquots, as opposed to in one portion, was found to be the key to achieving high conversion (*Figure 3.B*).

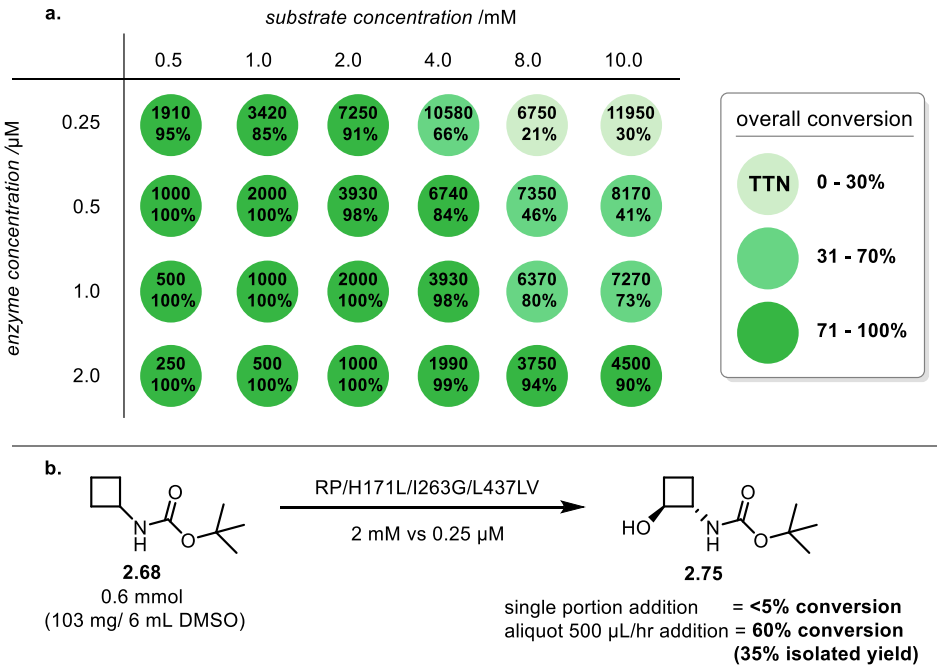


Figure 3 - a) Titre test of substrate **2.68** with RP/H171L/I263G/L437LV; b) preparative scale reactions on 0.6 mmol scale. TTN rounded to nearest 10, measured by GC integration.

The 'RP' base mutant consists of the mutations R47L/Y51F/I401P. Ile401 is neighbour to the heme cysteine proximal ligand (Cys400) and mutation to proline has a known 'accelerator' effect, with this increase in reactivity attributed to a weakening of the heme iron-water ligand interaction, rendering the water easier to displace by an incoming substrate to initiate the catalytic cycle.[56] Despite this improvement in reactivity towards unnatural substrates, previous work within the group by Li[57] discovered that reverting I401P back to isoleucine dramatically increased protein expression, a key factor to performing these reactions on large scale. Comparing the screening results of both RP/H171L/I263G/L437LV and R47L/Y51F/H171L/I263G/L437LV revealed an identical reactivity profile; however, a repeat of the titre test showed a lower overall TTN (*Figure 4*).

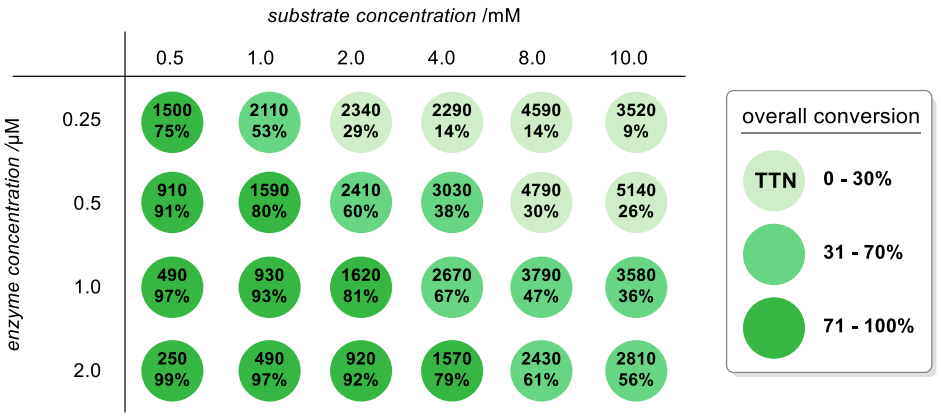


Figure 4 – Titre test screen using R47L/Y51F/H171L/I263G/L437LV with substrate **2.68**. TTN rounded to nearest 10, measured by GC integration.

A screen using 27 similar mutants based on the H171/I263G (HL/IG) combination did not reveal any significant improvements in reactivity or selectivity, and so efforts were directed towards optimising the reaction conditions using R47L/Y51F/H171L/I263G/L437LV.

From *Figure 4* it was determined that 10 mM *vs* 2.0 μM was a suitable substrate:enzyme ratio, providing >50% conversion with high concentrations which would allow a decrease of the reaction volume to improve the practical setup. To further improve the conversion, the effect of aeration of the reaction medium was investigated across the first 12 hours of a 1.0 mmol (171 mg) scale reaction (*Figure 5*). Firstly, oxygen was bubbled through the phosphate buffer prior to the reaction but then no further bubbling during the reaction, which resulted in a slight increase in conversion but still <10% at 12 hr. A significant improvement was achieved when either air or oxygen was directly bubbled into the reaction throughout the reaction. Although using oxygen was superior in terms of

conversion, there are added safety issues to consider. Furthermore, the increased rate of turnover of the catalytic cycle can cause the reaction medium to become acidic (from a build-up of gluconic acid from the GDH/glucose regeneration cycle), which requires neutralisation with aqueous hydroxide (NaOH or KOH is suitable).

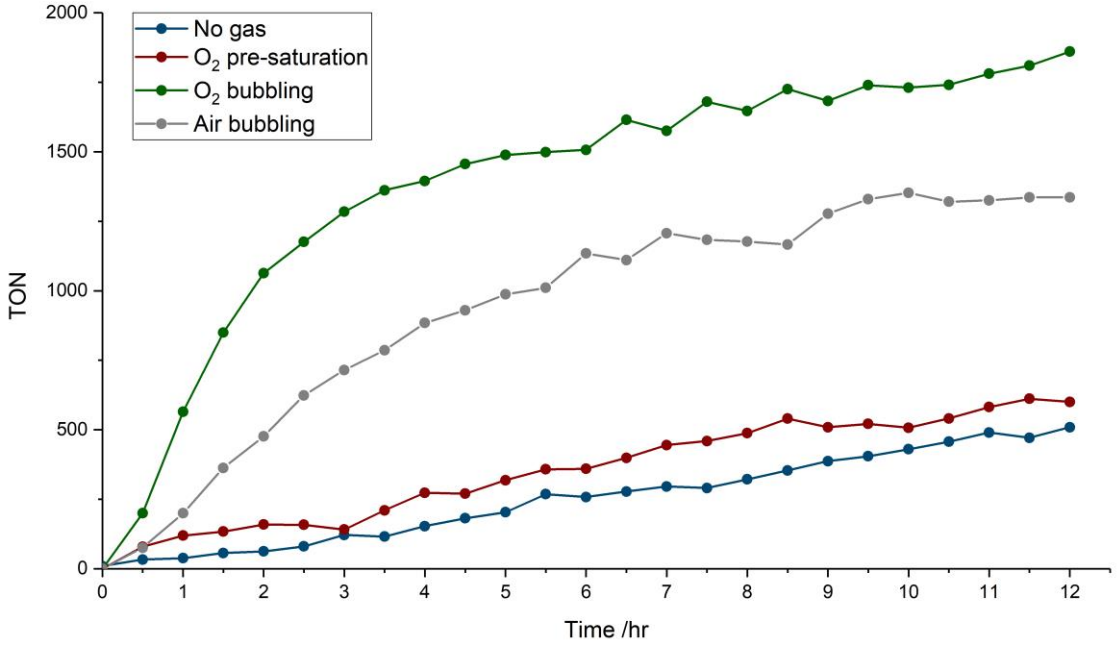
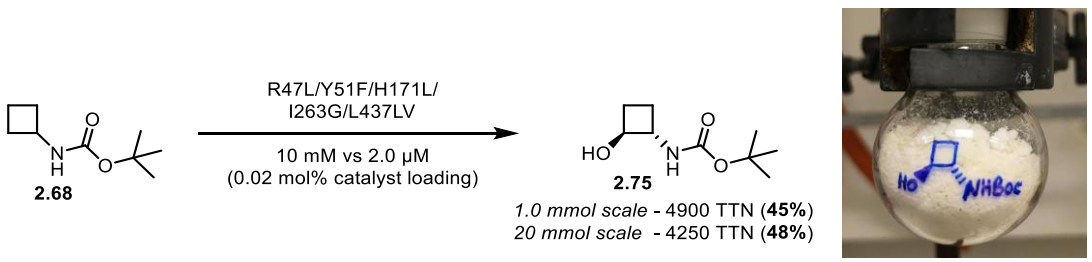


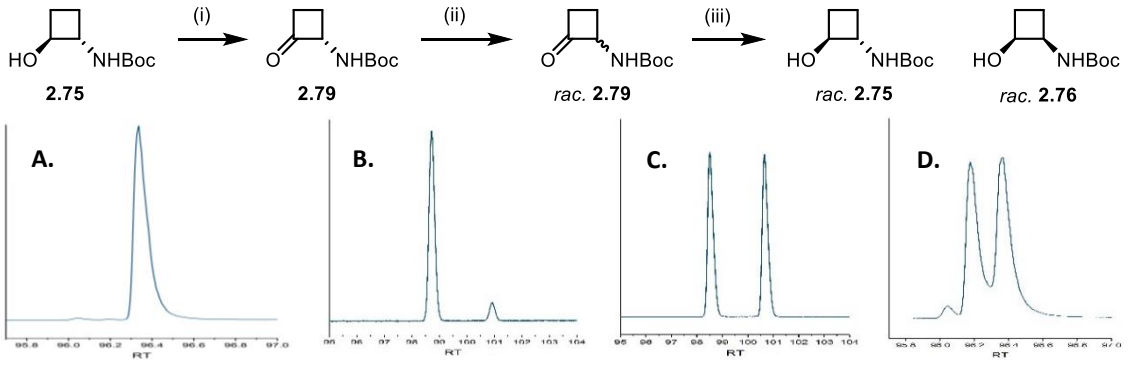
Figure 5 – Effect of aeration of reaction using R47L/Y51F/H171L/I263G/L437LV at 2.0 μM with substrate **2.68** at 10 mM on 1 mmol scale.

Using these reaction conditions, a reaction using 1.0 mmol substrate over 3 days gave 98% conversion with a 45% isolated yield. A similar result was found on gram-scale, using 20 mmol of **2.68** (3.42 g) which achieved an 85% conversion but a 48% isolated yield, providing access to grams of valuable enantiopure building block **2.75** (*Scheme 18*). A specific cause of the lower isolated yield could not be determined but is possibly due to α-hydroxylation of the starting material which leads to decomposition to products undetectable by GC analysis.



Scheme 18 – Large scale reactions of R47L/Y51F/H171L/I263G/L437LV with substrate **2.68**, including isolated compound from 20 mmol (3.42 g) gram-scale reaction. Isolated yield shown in parentheses.

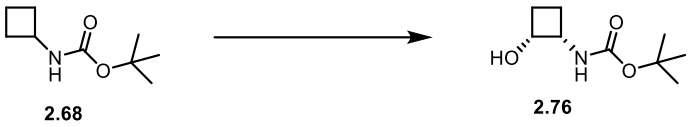
In order to validate chiral GC analysis, attempts to synthesise racemic standards were made; however, these compounds are difficult and expensive to make using traditional chemical methods. As an alternative to designing an entirely new chemical route, transformation of enantioenriched metabolite **2.75** into the racemic analogue was proposed by means of (i) oxidation, (ii) racemisation and (iii) reduction as shown in S*cheme 19*. Oxidation using DMP proceeded smoothly in 81% yield. Chiral GC traces A and B show enantioenriched alcohol **2.75** and ketone **2.79**. Racemisation was achieved by stirring overnight with Cs_2CO_3 in ethanol; however, considerable material was lost during this step to unknown side products, and so the crude mixture was directly carried forward for the next step. Chiral GC trace C shows racemic ketone **2.79**. Traditional reduction conditions using $NaBH_4$ formed a mixture of *cis* and *trans* alcohols **2.75** and **2.76**. Chiral GC trace D shows the crude mixture of diastereomers formed after the reduction; however, these compound peaks overlap using all GC methods tested, where the central peak represents an enantiomer of each diastereomer.



Scheme 19 – Synthesis of racemic material from enantioenriched compound **2.75** including chiral GC traces for each intermediate. (i) Dess–Martin periodinane, CH_2Cl_2; (ii) Cs_2CO_3, EtOH; (iii) $NaBH_4$, MeOH.

2.3.2. Access to *cis*-1,2-hydroxy-aminocyclobutanes

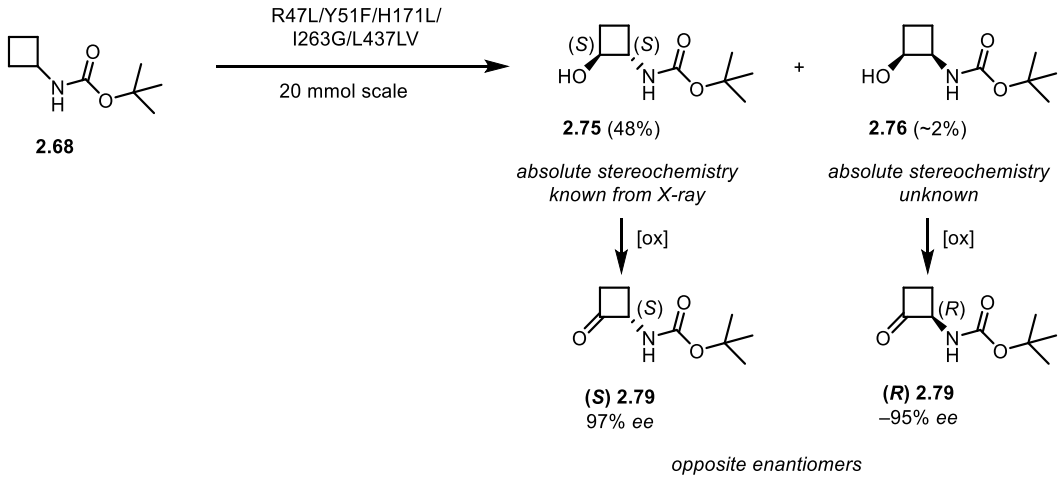
Functionalisation at the C2-position with *cis* stereochemistry proved considerably more challenging than for the *trans* analogue. As shown from the initial screening data (*Chapter 5: Appendices*), only three mutants gave *cis*-metabolite **2.76** with a TON>100 (*Table 4*). Mutant KU3/S72W/A330P gave excellent conversion but poor selectivity (29%), whereas *entries 2* and *3* show that the mutation A328L was the key to improving selectivity. As discussed in *Section 2.3.1.* changing from A328G to A328L provided a switch in selectivity from *trans* to *cis*-1,2 metabolites.



Entry	Mutant	Conversion /%	2.76 /%	TTN	Selectivity /%	TON
1	KU3/ S72W/A330P	98	28	490	29	140
2	GV/A184I/**A328L**	51	27	253	55	140
3	RK/**A328L**	50	22	250	44	110

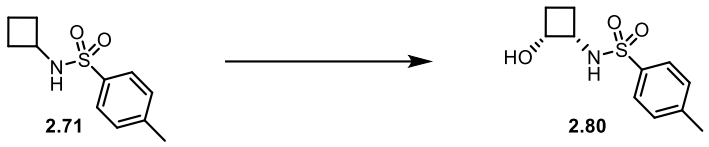
Table 4 – Selected mutants for the formation of *cis* **2.76**, ordered by overall conversion, measured by GC integration. Scheme shows relative configuration only. Selectivity determined as the conversion of this regioisomer/ all metabolites produced.

The absolute stereochemistry of *cis*-1,2-Boc-metabolite **2.76** was determined by comparison of oxidised *trans*-metabolite **2.75** with known absolute stereochemistry using material from previous large-scale reaction from *Section 2.3.1.* (*Scheme 18*). After oxidation of both metabolites from the reaction with R47L/Y51F/H171L/I263G/L437LV, and comparison of the subsequent chiral GC traces, it was found that the cyclobutanones **2.79** were opposite enantiomers and so *cis*-alcohol was assigned as (*1R*,*2S*).



Scheme 20 – Determination of absolute stereochemistry of *cis*-metabolite **2.76**.

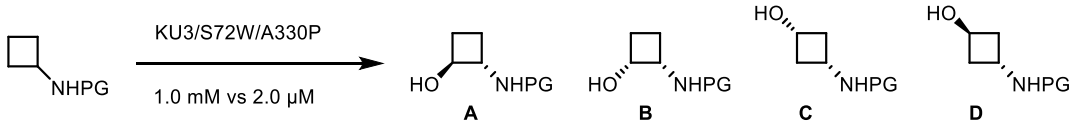
Exchanging the Boc protecting group for tosyl improved the ratio of C2:C3 regioisomers to 1:1 with KU3/S72W/A330P, with a TTN=310 but a selectivity for the *cis* C2 compound **2.80** of only 19% (*Table 5, entry 1*). The selectivity was nearly doubled to 35% using related mutant KU3/A330S/L437LA which yielded a TON=240 (*entry 2*).



Entry	Mutant	Conversion/%	2.80 /%	TTN	Selectivity /%	TON
1	KU3/S72W /A330P	62	12	310	19	60
2	KU3/A330S/L437LA	68	24	680	35	240

Table 5 – Top KU3-based mutants for the formation of *cis* **2.80**, measured by GC integration. TTN rounded to nearest 10.

A switch to the isopropylsulfonyl (ipsyl) protected cyclobutylamine **2.70** with mutant KU3/S72W/A330P gave high conversion and also some selectivity toward the 2-hydroxylated product; however, a stronger preference for the *cis* regioisomer **2.70.B** was now observed (*Table 6*).



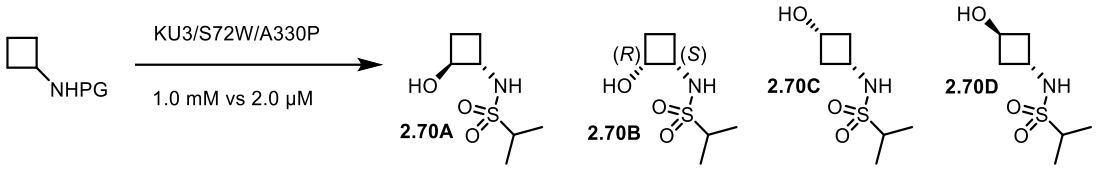
Entry	*N*-protecting group	A /%	B /%	C /%	D /%
1	Boc-	61	28	1	5
2	Tosyl-	-	12	-	12
3	Ipsyl-	27	53	11 (mix of C and D)	

Table 6 – Overall product distribution for mutant KU3/S72W/A330P with Boc **2.68**, tosyl **2.71** and ipsyl **2.70** substrates, measured by GC integration. Scheme shows relative configuration only.

As KU3/S72W/A330P was the only mutant to give conversion for ipsyl-protected substrate **2.70**, efforts turned toward improving the reaction conditions rather than exploring other mutations. Low mass recovery can sometimes be problematic in biocatalytic reactions due to the formation of a gelatinous layer of protein debris during reaction workup and extraction using organic solvents such as ethyl acetate. Addition of a protease and heating at 50 °C for 1 hr prior to extraction was tested; however, this was not found to increase the crude mass obtained.

The choice of organic co-solvent can dramatically affect reaction conversion, as the tolerance of P450s for different solvents is varied. Using an ethanol substrate stock, a 30% conversion of **2.70** (measured by GC) was observed after 40 hr on a 0.1 mmol scale reaction, which was improved to 45% with a switch to DMSO (*Table 7*). These solvents can also be reactive substrates in their own right (see *Section 2.7.3*) and, if possible, avoiding the use of organic co-solvents altogether would be ideal. These amine substrates were soluble in phosphate buffer, thereby allowing the solid starting

material to be added directly to the reaction medium resulting in an increase in conversion to 83%. Moshers ester analysis was used to assign absolute stereochemistry of 2.70A (*Chapter 6: Section 6.2.4.*)

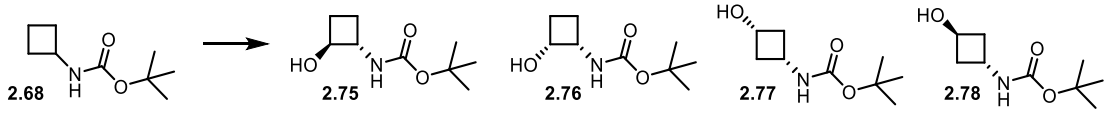


Entry	Solvent Used for Substrate Stock	GC Conversion
1	EtOH	30%
2	DMSO	45%
3	Neat (no solvent)	83%

Table 7– Comparison of organic co-solvents for the reaction of KU3/S72W/A330P with **2.70** after 40 hr.

2.4. Synthesis of 1,3-hydroxy-aminocyclobutanes

As access to the 1,2-hydroxy-aminocyclobutanes had been established, attention turned to functionalisation at the C3 position of the cyclobutane ring. From initial screening, multiple mutants were found to convert Boc-aminocyclobutane **2.68** into 1,3-*trans*-metabolite **2.78** with high selectivity (*Table 8*). F87V is extremely important for selectivity, as a significant increase is observed from 54% selectivity with GQ/I263G/A328L (*Entry 5*), to 77% with GVQ/I263G/A328L (*Entry 3*).



Entry	Mutant	Conversion /%	2.75 /%	2.76 /%	2.77 /%	2.78 /%	Other /%	TTN
1	GV/A184I	99	9	6	3	71	10	495
2	K19/F87V/Q403P	97	16	1	4	62	14	485
3	GVQ/I263G/A328L	78	2	0	6	60	10	390
4	VQ/S72G/A330W	93	26	7	5	51	4	465
5	GQ/I263G/A328L	91	3	2	33	49	4	455
6	K19/F87V/E267V	98	33	5	4	47	9	490
7	K19/F87V/I263G	89	31	1	4	45	8	445
8	GVQ/A330W	86	22	4	5	43	12	430
9	RP/A82M/I263A	64	5	8	8	42	1	320
10	GVQ	78	24	3	3	39	9	390

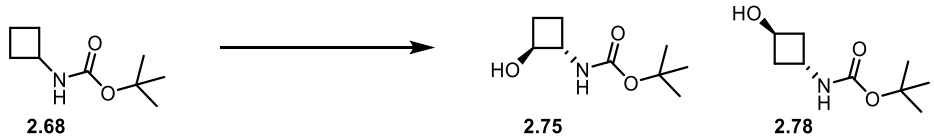
Table 8 – Top 10 mutants for the conversion of **2.68** into metabolite **2.78**, measured by GC integration, reported to 2 sig. fig. Scheme represents relative configuration.

As GV/A184I was found to be the highest converting mutant for product **2.78**, a focused library using this base mutant was created to explore reactivity (*Table 9*). Mutations at Val26 (*Entry 2 and 6*) and Ala330 (*Entry 4 and 11*) gave the best selectivity, whereas mutations at Leu188 were key for high conversion (*Entries 1,3 and 5*).

Entry	Mutant	Conversion /%	2.75 /%	2.76 /%	2.77 /%	2.78 /%	Selectivity /%	TON
1	GV/A184I/H171L/L188Q	97	6	5	3	81	83	410
2	GV/A184I/V26M	94	4	8	3	78	84	390
3	GV/A184I/L188Q	92	6	5	3	77	83	380
4	GV/A184I/A330W	95	6	7	4	76	80	380
5	GV/A184I/L188M	94	5	11	3	74	79	370
6	GV/A184I/V26F	87	4	7	2	72	84	360
7	GV/A184I/L437M	95	6	10	4	72	75	360
8	GV/A184M	94	11	2	5	72	76	360
9	GV/A184I	86	4	12	2	67	78	330
10	GV/A184I/V26L	88	4	14	2	66	75	330
11	GV/A184I/A330I	79	3	8	3	64	81	320
12	GV/A184I/L437F	86	11	7	6	60	70	300

Table 9 – Top 12 mutants from GV/A184I library for the synthesis of **2.78**, ordered by TON, measured by GC integration with TON rounded to nearest 10. Scheme represents relative configuration.

Interestingly, there is a switch in reactivity found when changing from a regular substitution mutation at Leu437, to the insertion mutation (*Table 10*). Both favour the *trans*- metabolites; however, L437F and L437M favour hydroxylation at C3 (*Entries 1 and 2*), and L437LF and L437LM favour C2 (*Entries 3 and 4*).



2.68 **2.75** **2.78**

Entry	Mutant	Conversion /%	TTN	2.75 /%	2.78 /%
1	GV/A184I/**L437F**	86	430	11	60
2	GV/A184I/**L437M**	95	480	6	72
3	GV/A184I/**L437LF**	98	490	65	13
4	GV/A184I/**L437LM**	95	470	44	39

Table 10 – Switch in selectivity of substitution *vs.* insertion mutation at Leu437, measured by GC integration.

TTN rounded to nearest 10

During this second-generation library screening, a change in selectivity depending on the substrate: enzyme ratio was observed. A time course of the reaction of **2.68** with GV/A184I at differing ratios gave conversion data as expected, where a low ratio of 250:1 (*i.e.*, 0.4 mol% catalyst loading) gives near quantitative conversion within 5 hours, and a high ratio of 2000:1 (*i.e.*, 0.05 mol% catalyst loading) is significantly slower only reaching 50% conversion over the initial 12 hours (*Figure 6.A*). *Figure 6.B* shows that every time the substrate concentration is doubled, an approximate 4% loss in selectivity to **2.78** is observed.

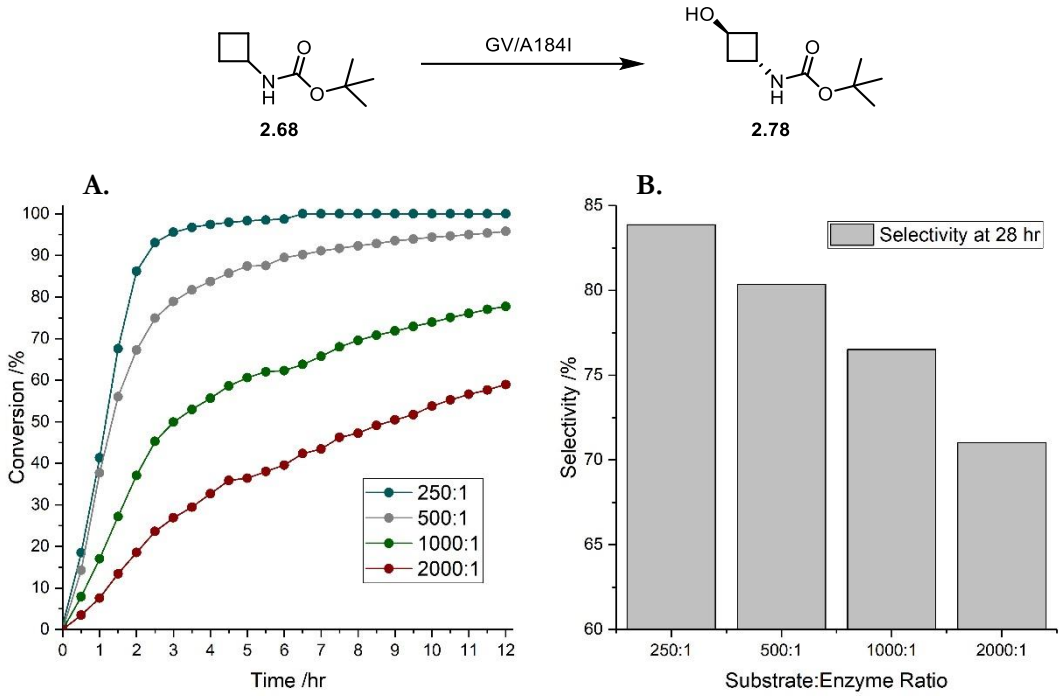
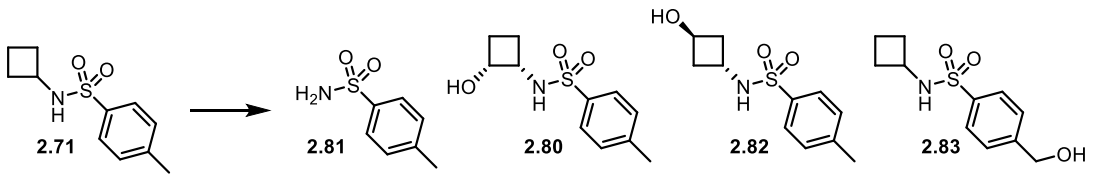


Figure 6 – A) Conversion from 0 – 12 hr of Boc **2.68** with GV/A184I at different substrate : enzyme ratios; B) change in selectivity of product **2.78** at different substrate : enzyme ratios at 28 hr.

Continuing with the approach of varying the amine protecting group, initial screening of 48 mutants with toluenesulfonyl (tosyl, Ts-) protected aminocyclobutane **2.71** showed *trans*-3-hydroxy aminocyclobutane **2.82** to be the major metabolite produced throughout, albeit with the production of significant amounts of side-products **2.81** and **2.83** (*Table 11*). The I263G mutation appears important for the conversion to unwanted product **2.83** (*Entries 1,2,5,6 and 7*), whereas tosylamine **2.81** is assumed to arise from the decomposition of the unstable α-hydroxylation product.



Entry	Mutant	Conversion /%	**2.81** /%	**2.80** /%	**2.82** /%	**2.83** /%
1	K19/F87V/I263G	100	3	-	40	31
2	RP/H171L/I263G/A184I	100	-	-	57	31
3	VQ/S72G/A330W	100	9	2	75	7
4	GV/A184I	>99	28	-	50	-
5	KT2/L188G/I263G	99	-	-	47	39
6	RP/H171L/I263G	99	-	-	37	51
7	GVQ/I263G	98	2	-	54	19
8	GVQ/A330W	98	7	-	68	11
9	K19/F87V/Q403P	97	11	5	52	2
10	GVQ	86	5	4	61	7

Table 11 – Top 10 mutants ordered by conversion, measured by GC integration, showing product distribution for tosyl- aminocyclobutane **2.71**. Full data table in *Chapter 5: Appendices*.

As can be seen from *Table 11* above, a variety of base mutants gave good conversion and mutations at residues Ser72, Phe87 and Ala330 appear important. A further plate of 22 mutants was screened with similar mutations to further optimise the formation of **2.82**. Mutations to larger amino acid residues such as tryptophan (W) appear advantageous due to both sterics and possible π-interactions with the aromatic tosyl group.

Comparison of the selectivity data from the two sets of screens indicates that adding bulky substituents at A328 to F87V-based mutants lowered selectivity, but the opposite is true for F87A/I263A (*Table 12, Entry 2*). A330W increases C3 oxidation only when combined with F87V and not F87I (*Entry 7*), and S72W lowers selectivity (*Entry 4*) whereas S72G increases it. The high selectivity of RT2/F81W (*Entry 1*) is unexpected, especially since there are no active site substitutions in the RT2 precursor variant (R47L/Y51F/A191T/N239H/I259V/A276T/L353I). This data suggests new combinations such as RT2/F81W/A330W, perhaps with S72G also present, could further improve selectivity in future work.

Entry	Mutant	Conversion /%	2.82 /%	TTN	Selectivity /%	TON
1	RT2/F81W	95	83	950	88	830
2	K19/F87A/A328I/I263A	99	79	990	79	790
3	RT2/A330W	82	67	820	81	670
4	GVQ/S72W	61	36	610	60	36
5	R19/A330W	30	21	300	72	2140
6	K19/F87V/A328L	54	17	540	32	170
7	R19/F87I/A330W	46	16	460	36	170
8	RT2/A330P/V78I	16	10	160	62	100
9	RT2/A330P/A82M	16	9	160	58	90
10	R19/F87I/A330P	12	4	120	32	40

Table 12 – Selected mutants screened for the synthesis of *trans* **2.82**, ordered by TON, measured by GC integration. Full data table in *Chapter 5: Appendices*. TTN/TON rounded to nearest 10.

In order to optimise the potential titre of the system, the mutant which yielded the highest TON (RT2/F81W) was selected and a screen was performed which gave some insight into the ideal concentrations for both substrate and enzyme (*Figure 7*). It is evident that in order to keep conversion >70% a ratio of approximately 2000:1 or lower is optimal.

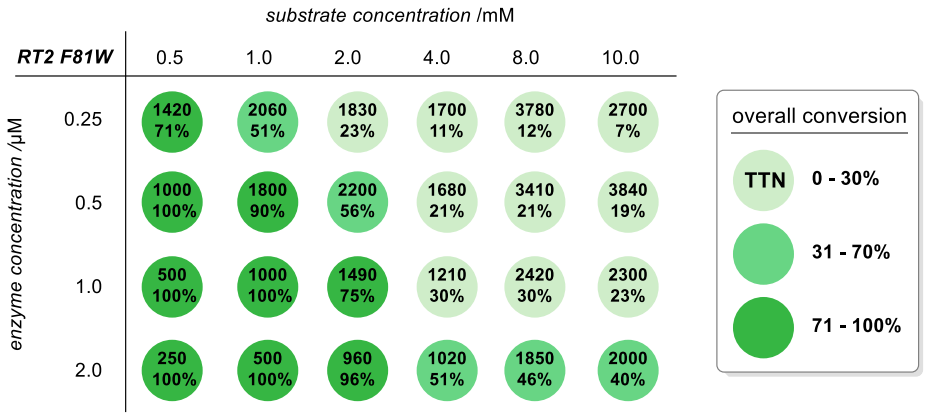
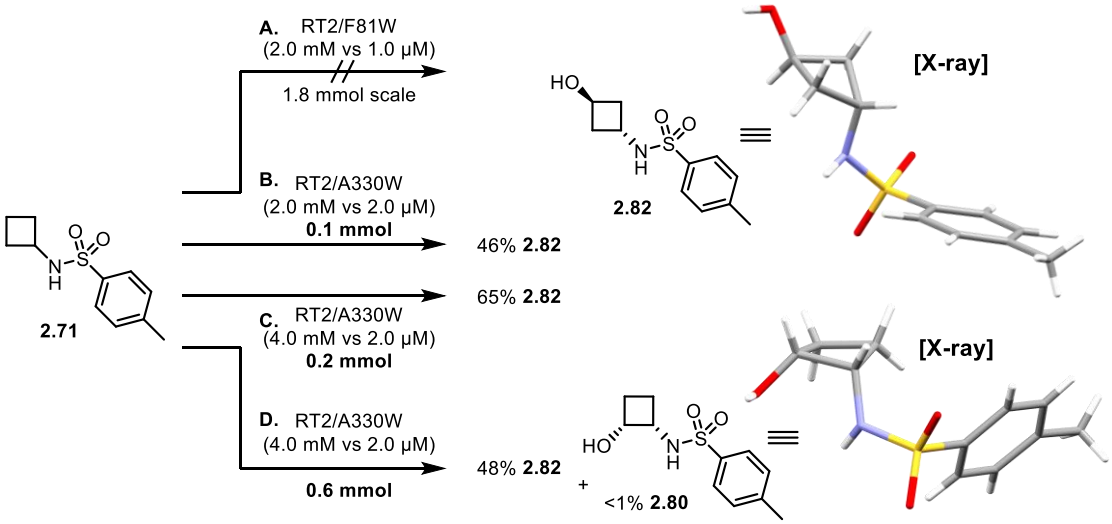


Figure 7 – Titre test for mutant RT2/F81W with substrate tosyl **2.71**, showing both TTN and % conversion. TTN rounded to nearest 10, measured by GC integration.

Although this reaction performed well on analytical scale, when scaled up to 1.8 mmol (400 mg) the reaction saw minimal conversion (*Scheme 21.A*). The failure of this reaction could be attributed to the large amount of toxic organic solvent (18 mL DMSO substrate stock) added in one portion. To improve the scalability of this reaction, a different mutant (RT2/A330W) was tested on

smaller preparative scale of 0.1 mmol (*Scheme 21.B*). A ratio of 1000:1 (2.0 mM vs 2.0 µM) achieved a 46% isolated yield, and the substrate concentration could be further increased to 4.0 mM with an improved isolated yield of 65% to allow for a more practical reaction volume (*Scheme 21.C*). Crystallisation was achieved using liquid-liquid diffusion (CH_2Cl_2/heptane) and the structure of metabolite **2.82** was confirmed using single crystal X-ray crystallography.

At this increased concentration the reaction was performed on synthetically useful scale (0.6 mmol) and 69 mg of metabolite **2.82** was obtained with 48% isolated yield. From this reaction a small amount of metabolite **2.80** (<1% isolated yield) was also obtained, a crystal was grown using vapour diffusion (CH_2Cl_2/hexane) from which the absolute stereochemistry was determined using single crystal X-ray crystallography (*Scheme 21*).



Scheme 21 – Preparative scale reactions of tosyl **2.71**, and X-ray crystal structures of **2.80** and **2.82**.

2.5. Synthesis of C2-hydroxylated amino-bicyclo[1.1.1]pentanes

Introduction of a bridgehead -CH_2- into the cyclobutane ring system creates the 3D analogue bicyclo[1.1.1]pentane and it was expected that this class of compounds would be well-tolerated substrates for the panel of P450 mutants.

As can be seen from *Figure 8*, GV/A184I showed the highest overall conversion of **2.73** (64%) with a conversion to the C2-functionalised chiral metabolite **2.84** of >30%. Boc-oxidation products **2.85** and **2.86** were also produced in varying amounts throughout the screen.

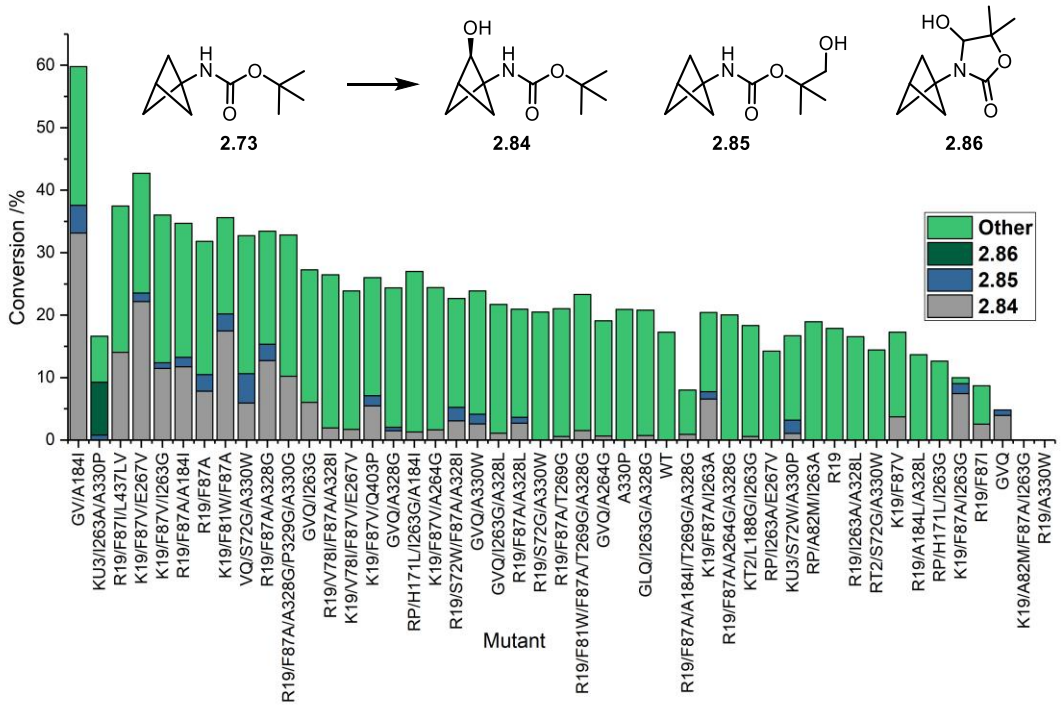


Figure 8 – Screening data from the panel of 48 P450 mutants after 24 hr, ordered by % GC conversion.

To provide insight into enzyme-substrate interactions and potentially some guidance for mutagenesis, Boc-BCP substrate **2.73** was docked into the active site of GV/A184I to visualise which key residues could influence conversion and selectivity. Interestingly the generated poses highlight that the bicyclo[1.1.1]pentane core is very similar to a *t*-butyl group, as the docked poses show very well matched but opposite orientations between the Boc and BCP groups (*Figure 9*).

Using docking methodology developed within the group,[58] an MD simulated protein structure, in the ferryl state, is separated into four replicas and further grouped into three clusters per replica. Using AutoDock Vina, the ligand is then docked into each of the 12 clusters to generate nine poses per cluster, based on a grid box size of either 20 or 30 Å. These poses are then individually analysed and are deemed 'productive' if they meet the following three criteria: 1) the closest C within 4 Å of the ferryl oxygen, 2) the Fe–O–H angle within the range of 115° – 145° and 3) the O–H–C angle within 135° – 165°. If the pose does not meet these criteria, it is considered unproductive.

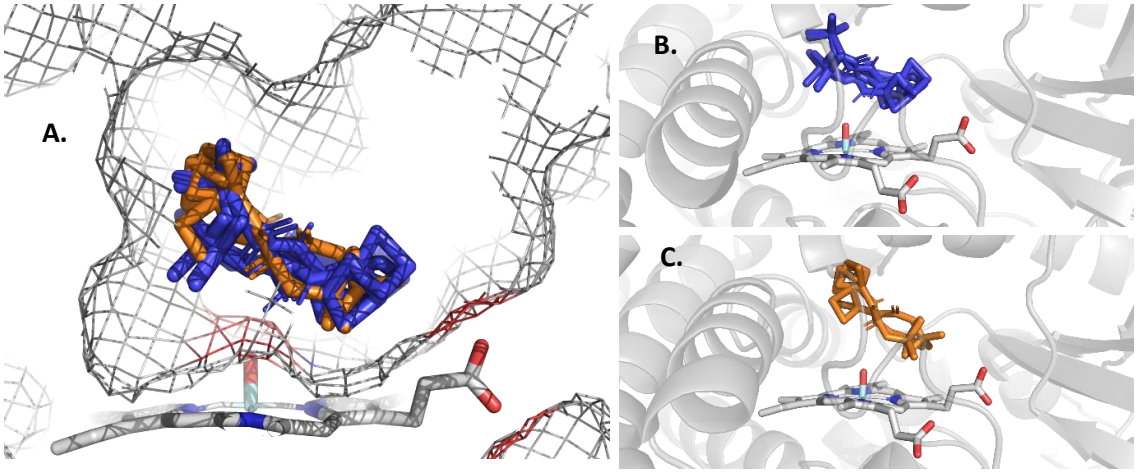


Figure 9 – a) All poses from replica 1/cluster 1 (R1/C1) overlaid with mesh shown to highlight active site substrate pocket; b,c) Poses of each orientation shown.

As can be seen from the above images all R1/C1 poses were classified as unproductive and poses generated throughout all four replicas showed similar results; therefore, docking-guided mutagenesis was not an option and, instead, mutants containing a variety of active site mutations, which have been shown to be influential with similar substrates, were proposed. Some mutations, such as S72 (*Figure 10.b*), A330 (*Figure 10.a/c*) and L437 (*Figure 10.a*), were chosen to disrupt potential hydrogen bonds with unfavourable poses. It should be noted that the $P450_{BM3}$ substrate pocket is dominated by hydrophobic residues, with only a few side-chains, *i.e.* S72, capable of H-bonding.

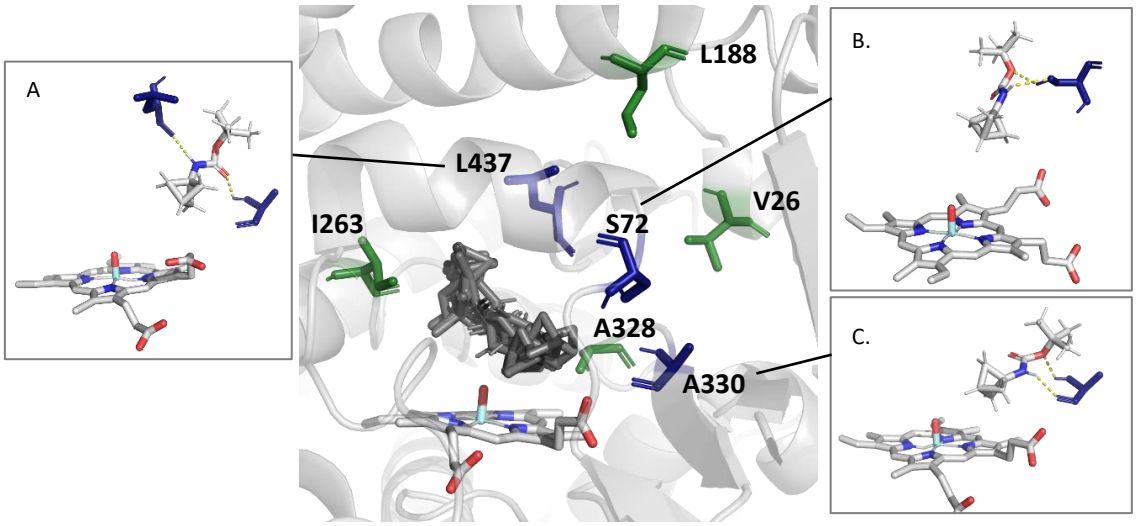
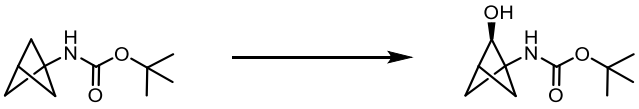


Figure 10 – Residues targeted for mutagenesis. Residues in blue were proposed due to unproductive poses in docking, with bonding (mutations shown in grey boxes), and residues in green were selected on the basis of previous improvement in conversion with similar substrates within the group.

All the mutants tested resulted in a significant decrease in conversion to metabolite **2.84** after 24 hr; however, base mutant GV/A184I exhibited a higher conversion than the initial screening result (*Table 12*). Notably, mutations at both V26 and A330 did not affect enantioselectivity but decreased the overall conversion (E*ntries 2 – 4* and *11 – 12*), and insertion mutations at L437 (*Entries 15 – 17*) had a considerably more detrimental effect than standard substitution mutations (*Entries 13* and *14*) on conversion and % *ee*.



2.73 **2.84**

Entry	Mutant	Conversion /%	2.84 /%	*ee* /%
1	**GV/A184I (base mutant)**	76	68	66
2	/V26L	59	50	70
3	/V26M	47	34	66
4	/V26F	47	21	63
5	/S72W (-A74G)	43	17	48
6	/S72M	28	5	57
7	/L188M	49	42	68
8	/L188Q	29	40	71
9	/I263W	29	<1	29
10	/A328L	1	1	-12
11	/A330I	35	27	62
12	/A330W	40	31	67
13	/L437M	42	32	64
14	/L437F	46	31	67
15	/L437LF	30	30	24
16	/L437LM	12	12	5
17	/L437LH	14	14	24

Table 13 – Library using GV/A184I base mutant. Each entry shows the mutation made at the specified residue showing % GC conversion and % yield as measured by normal phase GC, and % *ee* was measured by chiral phase GC.

The GV/A184I variant consists of mutations A74G/F87V/A184I (*Table 14, entry 1*) and, to explore which residues were most important, each constituent residue was mutated. The removal of A74G had previously been investigated (shown in *Table 13*, *entry 5*). Mutations at residue A184 to

either phenylalanine or methionine decreased conversion but did not affect enantioselectivity (*entries 2 – 3*), whereas substituting F87V with leucine or glycine abolished activity (*entries 4 – 5*).

Entry	**Mutations**			**Conv. /%**	**2.84 /%**	***ee /%***
1	**A74G**	**F87V**	**A184I**	76	68	66
2	AG	FV	A184**F**	5	5	63
3	AG	FV	A184**M**	33	24	69
4	AG	F87**L**	AI	<1	<1	45
5	AG	F87**G**	AI	0	0	-

Table 14 – Mutations explored in GV/A184I for the conversion of Boc-BCP substrate **2.73**. % GC conversion and % yield was measured by normal phase GC, and % *ee* was measured by chiral phase GC.

The switch of F87V to F87A was thought to play an important role in the enantioselectivity of this reaction. While analysing the mutants that give highest % *ee* for both enantiomers from the initial screening data, it was clear which residues are most influential (*Figure 11*). Access channel mutations R47L/Y51F do not likely play a role in the enantioselectivity; however, it was clear that exchanging F87A to F87V led to opposite enantiomers being accessed (with two exceptions GV/A184I and R19/F87I/L437LV). In comparison to chemo-catalysis, where the opposite enantiomer of the catalyst should provide the opposite enantiomer of the product, it is much more challenging for biotransformations to switch the product enantiomer and, it is important to have a clear distinction of which mutations can achieve this.

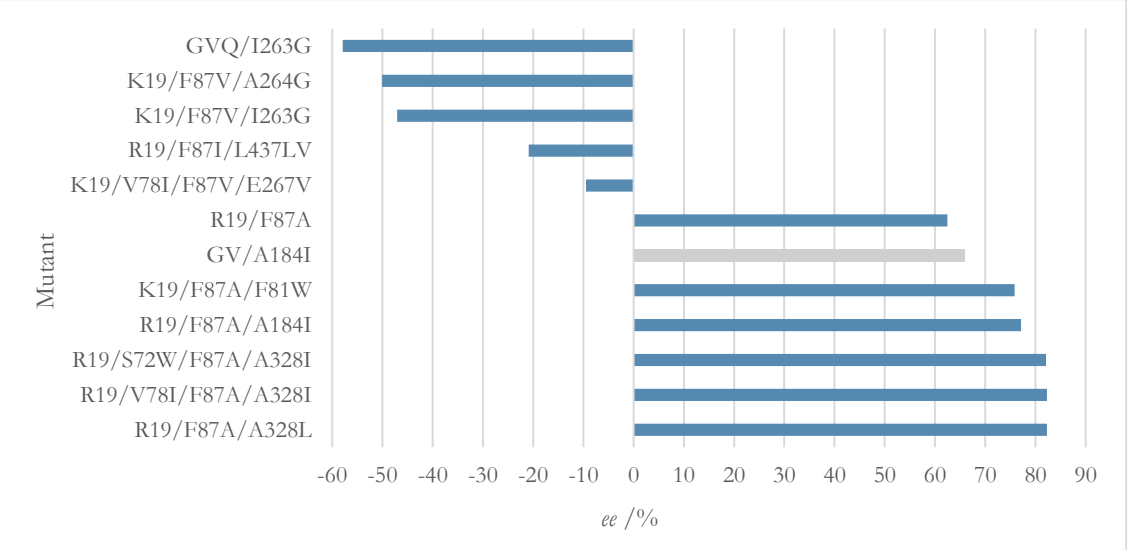


Figure 11 – Mutants which yield the highest enantioselectivity. Base mutant GV/A184I which is the focus of much of this study is highlighted in grey.

Mutations H171L and L188Q seemed to play a key role; however, no improvement was seen when these additions were made to GV/A184I (*Table 15, entries 2 – 3*). The introduction of F87A lead to a significant improvement in enantioselectivity; however, the conversion significantly decreased to only 10%.

Entry	Mutations			+	Conv. /%	2.84 /%	*ee /%*
1	**A74G**	**F87V**	**A184I**	**-**	76	68	66
2	AG	FV	AI	L188Q	29	40	71
3	AG	FV	AI	H171L/L188Q	14	14	59
4	AG	F87**A**	AI	-	10	9	80

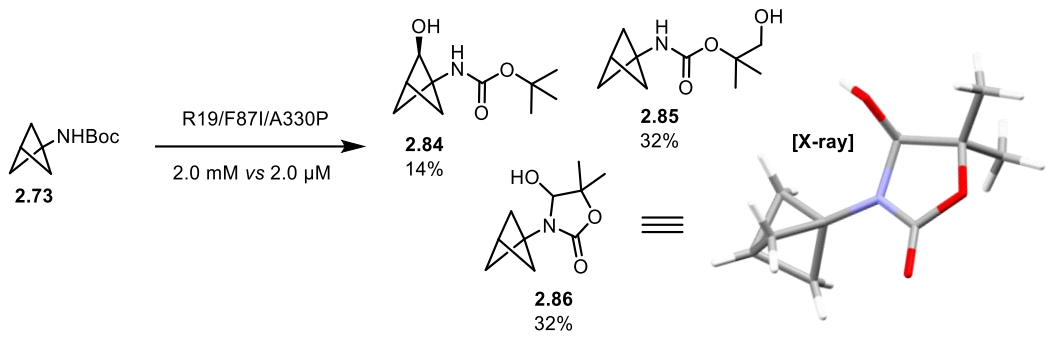
Table 15 – Mutations introduced based on pattern analysis of key residues from the initial screening data, measured by GC integration.

Introducing glycine residues at positions I263 and A328 to base mutant GV/A184I provided access to the alternative enantiomer. Mutants already within the library[59] were screened and all provided good enantioselectivity but poor conversion, and were not pursued any further. Selected results shown in *Table 16* below, and full screening data in *Chapter 5: Appendices*.

Entry	Mutant	Conv. /%	2.84 /%	*ee /%*
1	GL/A184I/I263G/A328G	22	1	-74
2	GI/A184I/I263G/A328G	18	3	-43
3	GV/A184I/I263G/A328G	17	5	-56

Table 16 – Screening data of selected GV/A184I/I263G/A328G based mutants, ordered by conversion and measured by GC integration.

As shown in *Scheme 22,* hydroxylation of the *N*-Boc protecting group was also observed. Although protecting group oxidation is not a desired outcome, mutant R19/F87I/A330P produced this as the major metabolite along with an interesting, cyclised product **2.86**, produced from further oxidation of **2.85**. The structure of **2.86** was confirmed by single crystal X-ray crystallography (*Scheme 22*). Crystallisation was achieved using liquid-liquid diffusion (CH_2Cl_2/heptane) and material crystalised as a racemate.



Scheme 22 – Reaction of Boc-BCP **2.73** with R19/F87I/A330P, conversion measured by GC integration, including X-ray crystal structure of metabolite **2.86**.

Mutant KU3/S72W/A330P also exhibited this switch in selectivity to *N*-Boc oxidation (although <10% conversion) and, since base mutant R19/F87I (without A330P) showed a very low conversion of <5%, it was proposed that A330P plays a pivotal role in producing metabolite **2.86**. 24 mutants containing the base mutant R19/F87I[60] and a variety of 20 mutants containing A330P were screened, with selected results shown in *Table 17*.

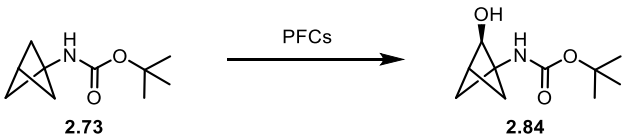
All mutations at the A330 residue, except phenylalanine (*entries 2 – 5*), decreased the overall conversion, as did the A330P mutation alone (*entry 6*) in which no conversion to **2.84** or **2.85** was observed.

Entry	Mutant	Conversion /%	2.84 /%	2.85 /%
1	R19/F87I/A330P	79	14	32
2	R19/F87I/A330I	4	3	1
3	R19/F87I/A330V	6	4	2
4	R19/F87I/A330F	7	6	2
5	R19/F87I/A330W	8	7	1
6	A330P	19	-	-

Table 17 – Table of selected mutants containing either R19/F87I or A330P; data measured using normal phase GC.

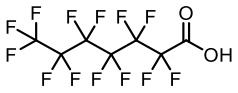
Since no variants which demonstrated any major improvements to the conversion of Boc-BCP **2.84** were found during mutagenesis or screening of the current library, the strategy was changed to try to optimise the reaction conditions using base mutant GV/A184I. Multiple reaction parameters were explored including the use of additives such as decoy molecules and cyclodextrin.

Perfluorocarboxylic acids (PFCs) can act as effective decoy molecules to improve the reactivity of more challenging substrates by filling space in the active site with a non-oxidisable substrate and creating the catalytically active ferryl oxygen species known as compound I.[61] PFCs with varying chain lengths were tested, over two concentrations, and a negative correlation was found; on increasing carbon chain length, a strong decrease in conversion and a slight degradation of % *ee* was observed (*Table 18*).

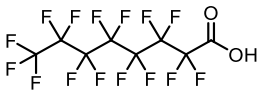


where-

PFC7 =



PFC8 =



etc.

		2 mM			4 mM		
Entry	**PFC**	**Conversion /%**	**2.84 /%**	***ee* /%**	**Conversion /%**	**2.84 /%**	***ee* /%**
1	PFC7	29	27	60	20	19	57
2	PFC8	12	12	58	1	0	54
3	PFC9	13	12	59	9	9	55
4	PFC10	10	10	55	18	9	53
5	PFC11	18	17	56	9	9	55
6	PFC12	14	14	-58	7	7	52
7	PFC13	5	5	53	5	5	52
8	PFC14	6	6	56	5	5	51
9	PFC18	9	8	57	6	8	51

Table 18 – The effect of PFCs on the conversion of **2.73** and enantioselectivity to metabolite **2.84** with GV/A184I. % GC conversion and % yield was measured by normal phase GC, and % *ee* was measured by chiral phase GC.

As shown in *Figure 12,* when the reaction was performed without the addition of methyl-β-cyclodextrin (*m*CD), an excellent conversion of 91% was achieved over prolonged reaction times (3 days), whereas, upon addition of *m*CD, the reaction is significantly inhibited.

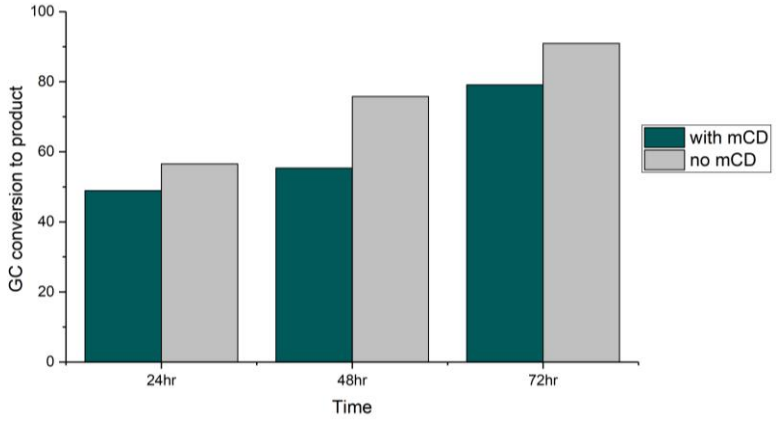
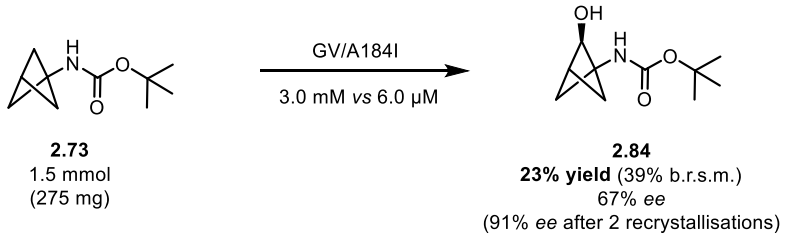


Figure 12 – Graph to show the effect of the addition of *m*-β-cyclodextrin on the reaction of BCP **2.73** with mutant GV/A184I over three days.

Using these conditions, the reaction was performed on a 1.5 mmol scale (275 mg) which, although low yielding, proved the value of the reaction on a synthetically useful scale, and 74 mg of product was isolated (*Scheme 23*). Using this material, multiple successive recrystallisations were performed, using liquid-liquid diffusion (DCM/heptane), improving the enantiomeric excess to 91%.



2.73
1.5 mmol
(275 mg)

2.84
23% yield (39% b.r.s.m.)
67% *ee*
(91% *ee* after 2 recrystallisations)

Scheme 23 – Large scale reaction (1.5 mmol) of Boc-BCP **2.73** with GV/A184I.

Since no improvement was observed during screening, it was decided that changing the BCPA protecting group might be effective. As described earlier, the *N*-Boc protecting group is very similar to the BCP core and it was proposed that the benzyloxycarbonyl (Cbz) would be a distinctive aromatic alternative. As seen in *Figure 13*, Cbz-BCP **2.74** was a considerably more tolerated substrate than Boc-BCP **2.73** with seven mutants showing full conversion. As expected, the product profile showed a greater number of metabolites than with Boc, as an increased number of potential oxidation sites exist. As the only chiral mono-hydroxylation metabolite is the C2-alcohol **2.87**, the data analysis was focused on this with all other compounds grouped together. Oxidation of the Cbz-protecting group led to phenolic products which were undetected by the GC analysis.

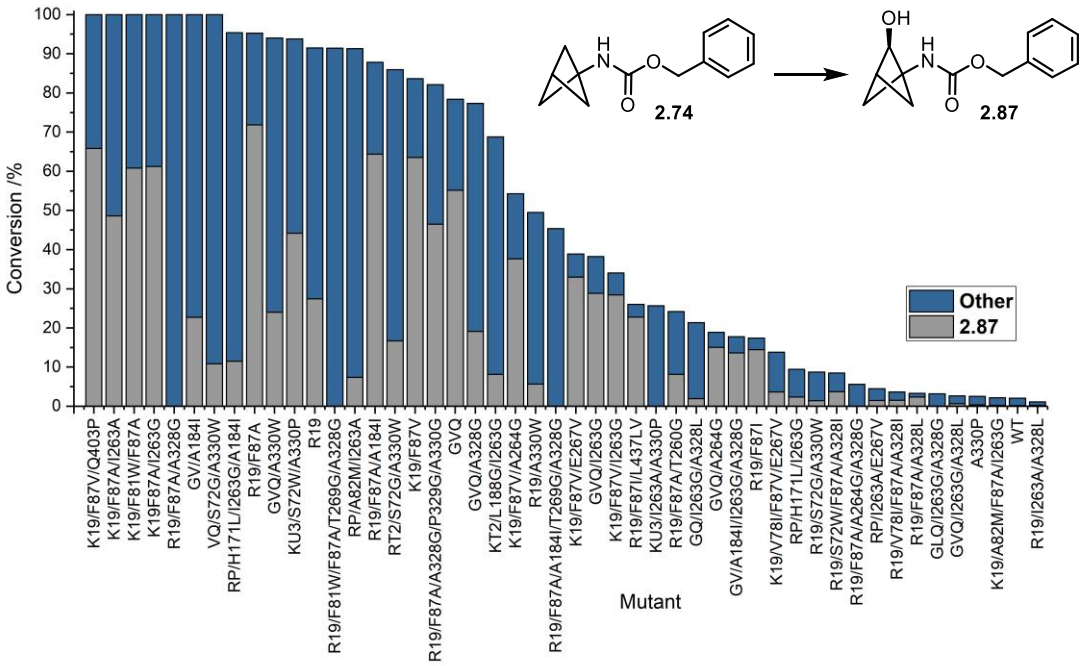


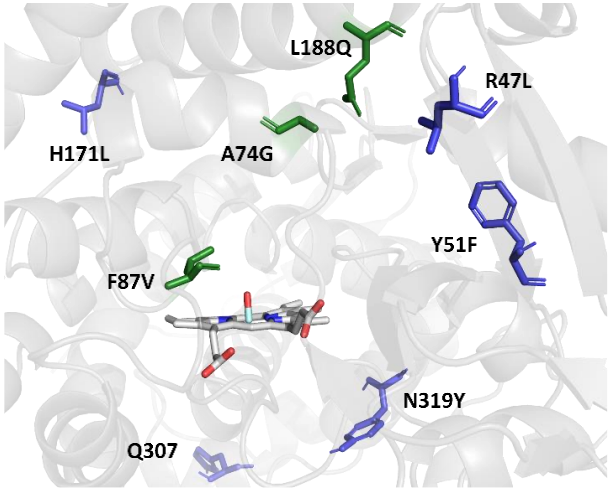
Figure 13 – Initial screening data for Cbz BCP **2.74**, ordered by overall conversion.

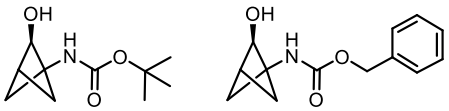
Analysis of the top mutants for conversion of **2.74**, reveals predominantly K19 or R19 (R47L/Y51F/K19) based mutants, and all containing substitutions at F87 to either alanine or valine (*Table 19*). Furthermore, higher enantioselectivities are seen with F87V rather than F87A (*Entries 2,4, and 7*).

Entry	Mutant	Conversion /%	2.87 /%	Other /%	TON	2.87 *ee* /%
1	R19/F87A	95	72	23	360	83
2	K19/F87V/Q403P	100	66	34	330	93
3	R19/F87A/A184I	88	64	23	320	51
4	K19/F87V	84	64	20	320	96
5	K19/F87A/I263G	100	61	39	310	12
6	K19/F87A/F81W	100	61	39	300	43
7	GVQ	78	55	23	280	95
8	K19/F87A/I263A	100	49	51	240	49
9	R19/F87A/A328G/P329G/A330G	82	47	36	230	69

Table 19 – Top nine mutants for the conversion of **2.74** to **2.87**, ordered by TON and measured by GC integration. TON rounded to nearest 10.

The strong preference for R19, or K19, based mutants is surprising given no active site mutations are involved, except for the addition of F87A or F87V in these cases. The R19 mutant contains R47L/Y51F/H171L/Q307H/N319Y mutations, and these can be seen in *Figure 14*. Furthermore, R19-based mutants generally matched the reactivity across the Boc- and Cbz-protected BCPAs (*Figure 14 , entries 1 – 4*), whereas the GVQ-based mutants react differently between these two substrates (*Entries 5 – 8*). The R19 substrate pocket is suitable for both BCPA substrates **2.84** and **2.87**, whereas GVQ is more substrate specific.

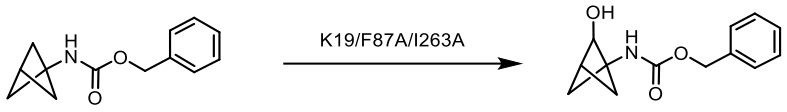




	Mutant	TON 2.84	TON 2.87
1	R19/F87I	31	72
2	K19/F87V/E267V	267	165
3	R19/F87A/F81W	204	304
4	K19/F87V/I263G	144	142
5	GVQ	40	276
6	GV/A184I	397	114
7	GVQ/A330W	33	120
8	GVQ/A328G	19	96

Figure 14 – MD simulated protein structure of GVQ (grey) from PDB ID:1JPZ, with mutated residues highlighted in green, and MD simulated protein stucture of R19 (protein cartoon hidden) from PDB ID:1JPZ, with mutated residues highlighted in blue. Table shows the different TON for both BCPA substrates **2.84** and **2.87**, for both R19- and GVQ- based mutants.

Both R19/F87A/A328G and R19/F87A/F81W/T269G/A328G gave high conversion, but a low GC peak area implies other products are produced and not detected using this analytical method. Although mutant K19/F87A/I263A did not achieve the highest selectivity, it was chosen for the scale-up reaction because very high protein production in *E. coli* can be achieved. A reaction on 0.05 mmol scale was low yielding, but sufficient for the purification and structural elucidation of chiral metabolite **2.87**, and assignment of the peaks representing the two enantiomers on chiral GC (*Scheme 25.B*).

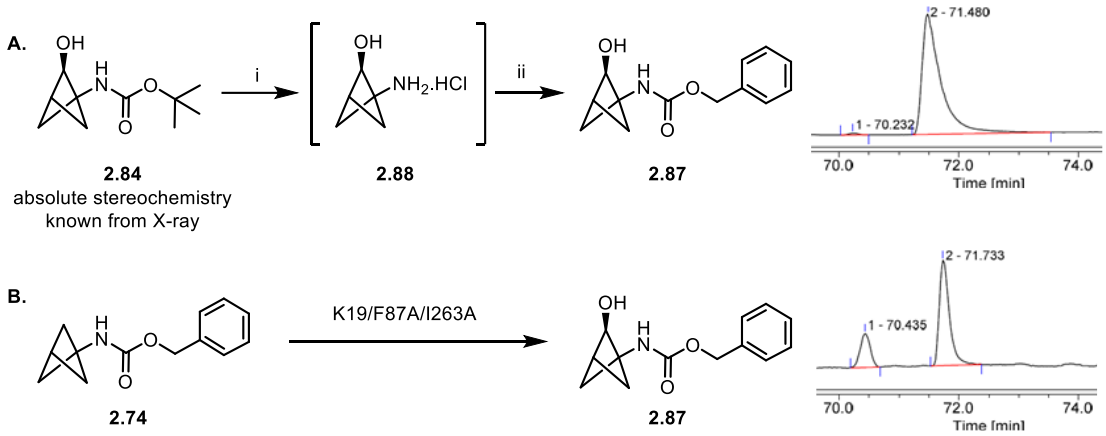


2.74
0.05 mmol (9 mg)

2.87
1.9 mg (**16%, 49% *ee***)

Scheme 24 – Semi-preparative scale reaction of Cbz-BCP **2.74** using mutant K19/F87A/I263A.

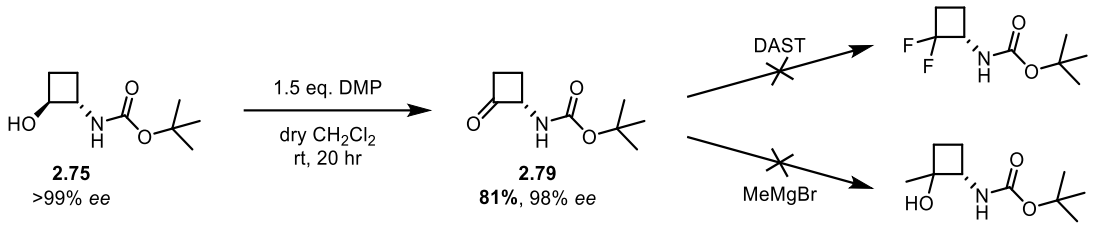
Attempts to grow crystals for determination of absolute configuration by X-ray crystallography were unsuccessful. However, deprotection of Boc-BCP alcohol **2.84** (obtained previously from the preparative scale reaction described in *Scheme 23*), followed by protection of the resulting amine hydrochloride salt **2.88** using CbzCl yielded Cbz-protected compound **2.87** with known absolute stereochemistry at C2 (*Scheme 25.A*). By comparison of the peaks on chiral-phase GC, it was possible to determine the major enantiomer of the Cbz-BCP metabolite **2.87** was the same as the major enantiomer produced using Boc protected material whose absolute stereochemistry had been determined by X-ray crystallography.



Scheme 25 – i) HCl, MeOH, 2 hr; ii) CbzCl, TEA, CH_2Cl_2, 17 hr, 27% over two steps.

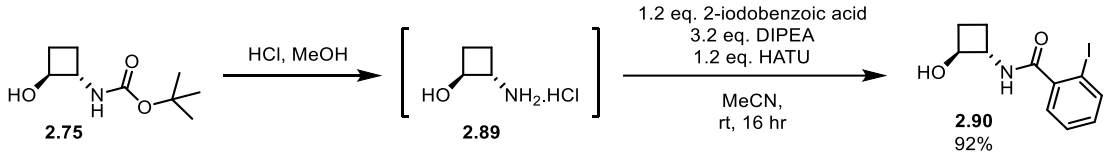
2.6. Derivatisation of hydroxylated metabolites

In order to demonstrate potential applications of these hydroxylated building blocks for synthesis, a selection of product derivatisations was conducted. As described in *Section 2.3.1.*, for the synthesis of racemic standards, oxidation of amino alcohol **2.75** using Dess–Martin periodinane was achieved in 81% yield without major degradation of enantiomeric excess (*Scheme 26*). Attempts to further functionalise this building block were unsuccessful on this scale (0.05 mmol).



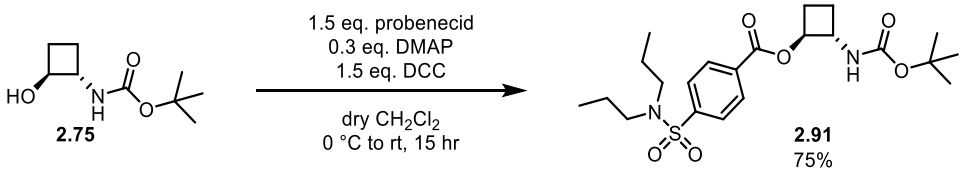
Scheme 26 – Oxidation of amino alcohol **2.75**, and unsuccessful attempts of Grignard addition and difluorination of carbonyl **2.79**.

Boc-deprotection and subsequent amide bond formation were achieved in excellent yield (92%), yielding aryl iodide **2.90** bearing a useful synthetic handle for further functionalisation in cross-coupling reactions (*Scheme 27*).



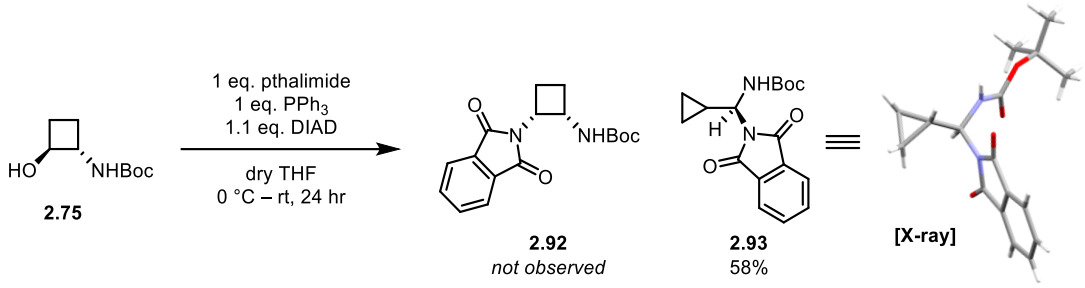
Scheme 27 – Boc-deprotection and amide bond formation to yield aryl iodide **2.90**.

Esterification of drug compound probenecid produced ester **2.91** in good yield (*Scheme 28*), illustrating the potential of these compounds to be used in QSAR studies, due to the ease of functionalisation of the alcohol moiety.



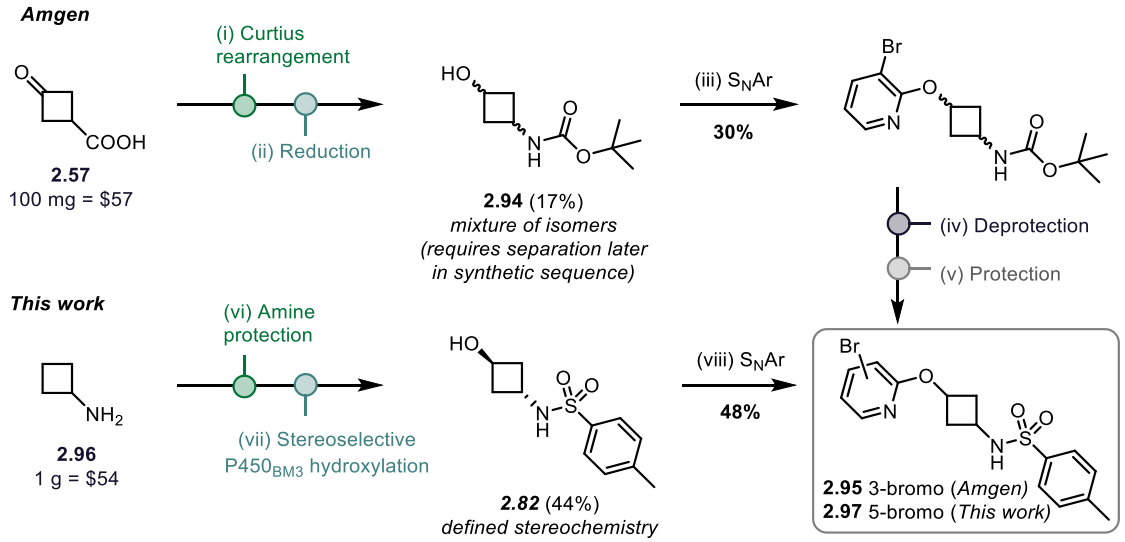
Scheme 28 – Functionalisation of drug Probenecid with amino alcohol **2.75**.

An attempt to prepare the orthogonally protected diamine **2.92** using standard Mitsunobu conditions failed and, instead, clean formation of cyclopropane **2.93** was observed, confirmed by single crystal X-ray crystallography (*Scheme 29*). Crystals were obtained as a single enantiomer, and were formed using the vapour diffusion method (CH_2Cl_2/hexane).



Scheme 29 – Observed rearrangement product **2.93** under Mitsunobu conditions.

To further validate the effectiveness of this methodology the synthesis of a key pharmaceutical candidate intermediate was achieved (*Scheme 30*). The route described by Amgen[62] consists of five steps with an overall yield of 4% to aryl ether **2.95**, from the expensive starting material 3-oxocyclobutanecarboxylic acid **2.57**. This route requires a protecting group switch which costs an additional two steps after the key S_NAr and a further reduction in yield. Starting from the more readily available cyclobutylamine **2.96**, in three steps and 26% overall yield a single diastereomer of drug intermediate **2.97** was produced.

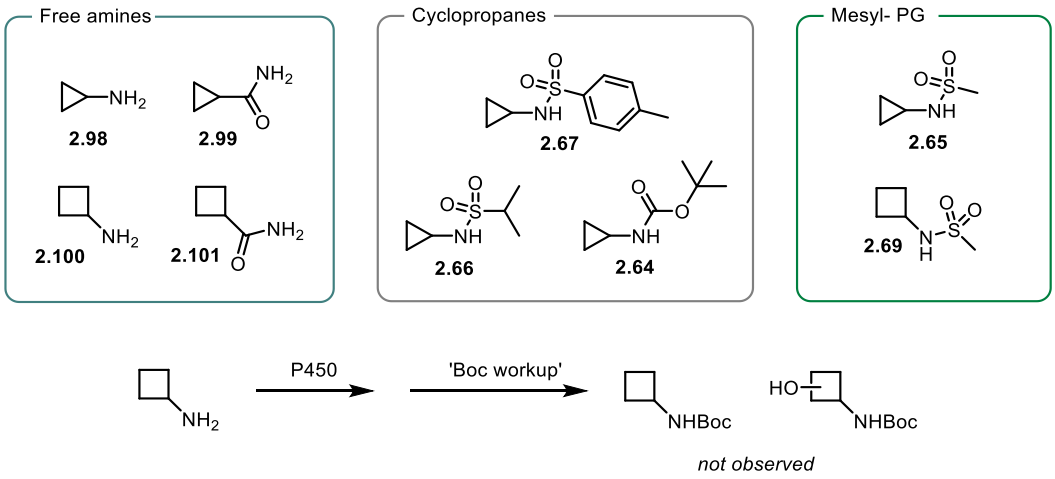


Scheme 30 – Price of starting materials quoted from MilliporeSigma US correct as of 1/7/2021. *Reagent and conditions;* (i) TEA, DPPA, toluene, 10 °C – rt, overnight *then* *t*BuOH, reflux, overnight, 30%; (ii) $NaBH_4$, EtOH, 10 °C – rt, 2 hr, 58%; (iii) NaH, DMF, 10 min *then* 3-bromo-2-fluoro-pyridine, 1 hr, 30%; (iv) 4.0 M HCl in MeOH, 2 hr, 95%; (v) *p*-TsCl, TEA, dry CH_2Cl_2, overnight, 80%; (vi) *p*TsCl, TEA, dry CH_2Cl_2, 16 hr, 84%; (vii) $P450_{BM3}$ mutant RT2/A330W, GDH, $NADP^+$, glucose, phosphate buffer, 48 hr, 65%; (viii) NaH, DMF, 10 min *then* 5-bromo-2-fluoro-pyridine, 1 hr, 48%.

2.7. Other reactivity

2.7.1. Substrates not tolerated

Aside from the protected amines described above, the free amines of both cyclobutylamine **2.100** and cyclopropylamine **2.98** were screened along with unprotected cyclopropyl- **2.99** and cyclobutylcarboxamide **2.101**, and all were found to show no conversion. GC analysis was inconclusive and so, in order to explore whether the issue was with reactivity or analysis, the screen was repeated with an additional Boc-protection workup procedure. This did not result in the appearance of either Boc-protected substrate or product (*Scheme 31*), showing that the free amine was either irreversibly binding with the P450 enzyme, undergoing degradation, or *N*-oxidation was preventing turnover.[63]



Scheme 31 – Substrates not tolerated including unprotected amines and carboxamides, cyclopropanes and mesyl protected compounds.

Conversion of cyclopropane substrates was not observed, probably due to the unusually high bond strength in this strained ring system (*Figure 15*). These C–H bonds are approximately 9 kcal/mol stronger than in cyclobutane (*entries 1 – 2*) so it is likely that C–H abstraction from cyclopropyl substrates is not possible with $P450_{BM3}$ enzymes. This may also explain why C3 functionalisation of BCP cores is not observed, as this C–H bond is similar in strength (*entry 5*).

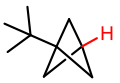
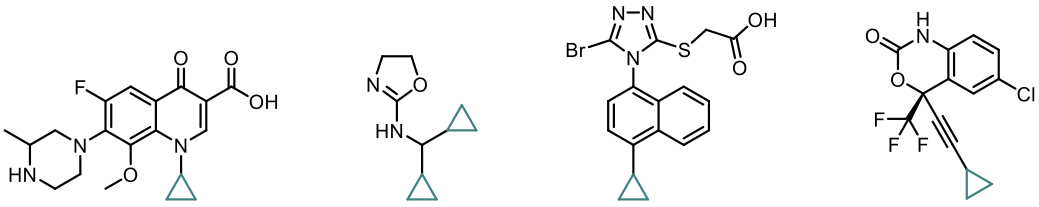
Entry	Structure	C–H BDE / kcal/mol
1		109.3
2		100.5
3		96.4
4		100
5		109.7 7 ±3.3

Figure 15 – Bond dissociation energies of small and medium sized ring systems.[64]

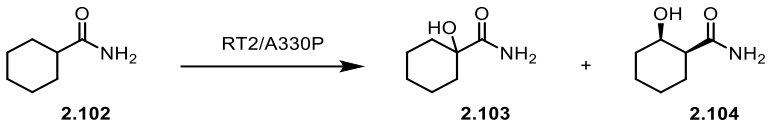
The inertness of the cyclopropyl group towards CYP enzymes forms the basis of a strategy used widely by medicinal chemists to improve the metabolic stability of potential drug candidates (selected examples shown in *Scheme 32*).[65] This realisation has inspired current projects within our group to adopt cyclopropyl carbamate as an effective protecting group to avoid unwanted oxidations at that position, and to push reactivity towards more desirable positions within the substrate.



Scheme 32 – Selected approved drugs containing the cyclopropyl motif.

2.7.2. Carboxamides

Previous work within the group, by Ren,[66] demonstrated that C–H hydroxylation of unprotected cyclohexylcarboxamide **2.102** was possible. RT2/A330P provided 100% conversion, with a roughly 1:1 ratio of metabolites **2.103** and **2.104** (*Scheme 33*).



Scheme 33 – Reaction of RT2/A330P with unprotected cyclohexylcarboxamide **2.102**.

As a continuation of this work, unprotected cyclobutylcarboxamide **2.101** was screened but was found to be unreactive. However, *N*-benzyl protected cyclobutylcarboxamide **2.72** was a well-tolerated substrate, giving a range of products with good conversion (*Figure 16*).

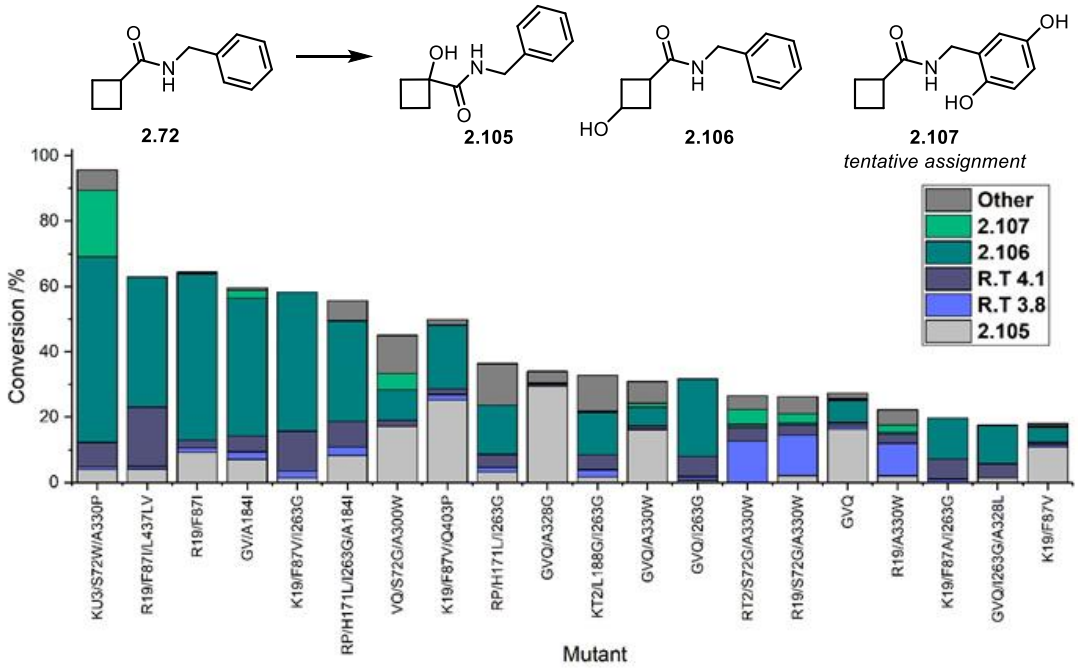


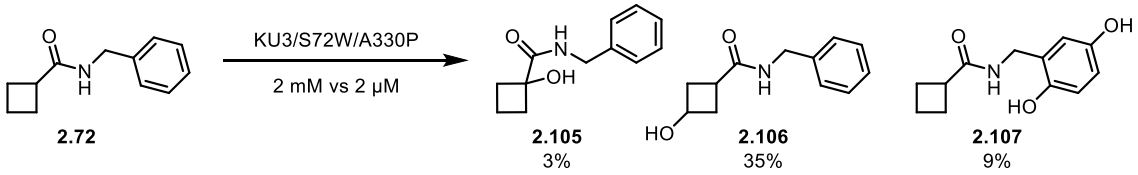
Figure 16 – Top 20 mutants for the conversion of *N*-benzyl protected cyclobutylcarboxamide **2.72**.

Analogous to the cyclohexyl- series, a major metabolite produced is α-hydroxy compound **2.105**. Good conversion and high selectivity can be achieved with mutant GVQ/A328G (*Table 20*, *Entry1*), with F87V, A330W and especially A328G important mutations for selectivity. For example, a switch from RK/A328G (*Entry 6*) to RK/A328L (*Entry 7*) destroys all activity, as does the introduction of any further glycine substitutions to RK/A328G (*Entries 8* and *9*).

Entry	Mutant	Conversion /%	2.105 /%	Selectivity /%	TON
1	GVQ/A328G	35	29	86	310
2	K19/F87V/Q403P	51	25	51	260
3	VQ/S72G/A330W	52	17	38	200
4	GVQ	28	16	59	170
5	GVQ/A330W	34	16	52	180
6	RK/A328G	15	12	82	130
7	RK/A328L	1	0	0	0
8	RK/A264G/A328G	1	0	0	0
9	RK/A328G/P329G/A330G	2	1	82	10

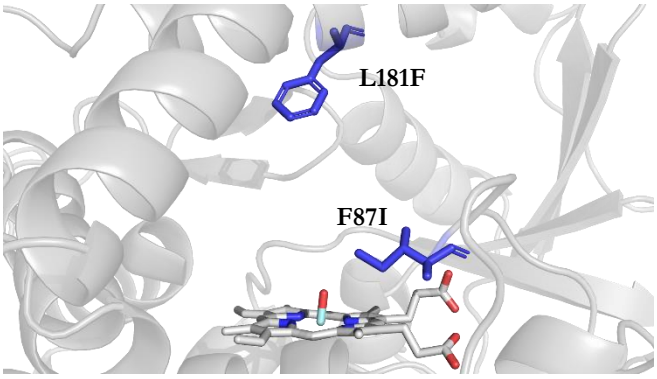
Table 20 – Top mutants for the conversion to metabolite **2.105**, and comparison of RK/A328G mutants, measured by GC integration. TON rounded to nearest 10.

Mutant KU3/S72W/A300P gave the highest overall conversion, achieving a TTN=970, and so preparative scale reaction on 0.16 mmol was conducted (*Scheme 34*). 3-Hydroxy metabolite **2.106** was isolated in moderate yield (35%), along with α-hydroxy **2.105** and tentatively assigned diol **2.107**.



Scheme 34 – Isolated yields of metabolites from preparative scale reaction of carboxamide **2.72**.

As R19/F87I seemed highly selective towards metabolite **2.106**, a further 40 R19/F87I-based mutants from our existing library[67] were tested (see *Chapter 5: Appendices* for full screening data). Mutation A184I proved very important for high conversion and selectivity to 3-hydroxy metabolite **2.106**. The highest conversion was observed with either L181F (*Figure 17*, *Entry 2*) or F81W (*Entry 3*), possibly due to beneficial π-interactions of the benzyl group in substrate **2.72** and these aromatic residues. The MD simulated protein structure of the mutant giving highest TON (R19/F87I/L181F *Entry 2*) is shown to highlight this potential effect of these active site mutations.



Entry	R19/F87I/	Conversion /%	2.106 /%	Selectivity /%	TON
1	-	38	30	78	300
2	+ L181F (shown in image)	100	96	96	960
3	+ F81W	100	92	92	920
4	+ A184I/V26L	96	89	93	890
5	+ A184I	92	84	92	840
6	+ A184I/L437F	87	80	91	800
7	+ A184I/S72L	86	56	65	560
8	+ A184I/L437M	82	75	92	750

Figure 17 – Top seven R19/F87I based mutants compared to R19/F87I for conversion of **2.72**, measured by GC integration. TON rounded to nearest 10.

For comparison, other mutations such as phenylalanine (*Table 21*, *Entry 2*) and methionine (*Entry 3*) at Ala184 showed lower conversion but maintained high selectivity.

Entry	Mutant	Conversion /%	2.106 /%	Selectivity /%	TON
1	R19/F87I/**A184I**	92	84	92	840
2	R19/F87I/**A184F**	19	17	85	170
3	R19/F87I/**A184M**	41	33	82	340

Table 21 – Comparison of substitution at A184, measured by GC integration. TON rounded to nearest 10.

Interestingly, the addition of A184I has a significant effect on overall conversion when added to other mutations. Addition to V26L (*Table 22*, *Entry 1* and *2*) resulted in an increased TON from 310 to 890; however, when added to V26M (*Entries 3* and *4*) a tenfold decrease was observed from TON=260 to 20. A dramatic increase in turnover and also selectivity was achieved from R19/F87I/L437M (*Entry 5*), with the addition of A184I (*Entry 6*).

Entry	Mutant	Conversion /%	2.106 /%	Selectivity /%	TON
1	R19/F87I/**V26L**	38	31	81	310
2	R19/F87I/**A184I/V26L**	96	89	93	890
3	R19/F87I/**V26M**	35	26	75	260
4	R19/F87I/**A184I/V26M**	3	2	75	20
5	R19/F87I/**L437M**	11	8	78	90
6	R19/F87I/**A184I/L437M**	82	75	92	750

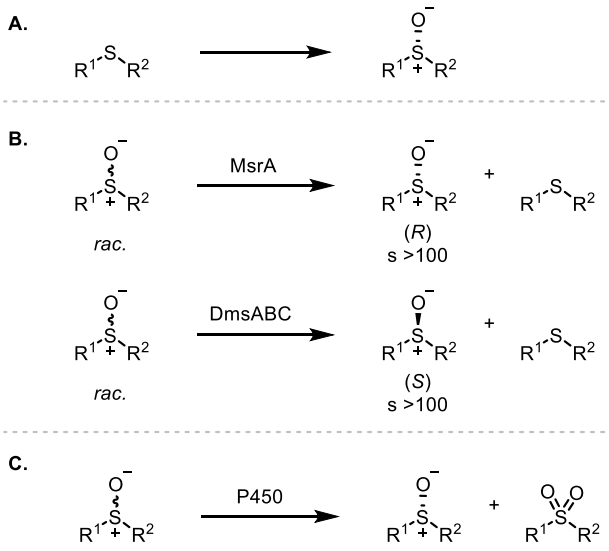
Table 22 – Comparison of mutants with/without A184I substitution, measured by GC integration. TON rounded to nearest 10.

Further work is ongoing within the group to continue the exploration of carboxamides as substrates for $P450_{BM3}$ oxidation and use of these building blocks for further synthesis.

2.7.3. Sulfoxides

During the course of this study an impurity was produced which co-eluted with certain metabolites during column chromatography purification, appearing as a singlet at 2.98 ppm in the ^{1}H NMR spectrum. This metabolite was identified as dimethylsulfone, resulting from oxidation of the organic co-solvent DMSO used in these biotransformations.

P450 oxidation at sulfur is an established field, and there are many reports of the asymmetric hydroxylation of sulfides to form enantioenriched sulfoxides as a complementary approach to traditional chemical methods (*Scheme 35.A*).[68] Furthermore, there have been reports of the synthesis of chiral sulfoxides *via* kinetic resolution, as described in our recent review on the topic;[69] either using oxidising enzymes such as Baeyer–Villiger monooxygenases[70] or taking advantage of the reverse process using reductases to reduce one enantiomer of a racemic sulfoxide to the relevant sulfide, leaving enantioenriched starting material (*Scheme 35.B*).[71] To the best of our knowledge there have been no reports using $P450_{BM3}$ to achieve kinetic resolution by means of oxidation of racemic sulfoxides to sulfones, and this led to an exploration of this possibility (*Scheme 35.C*) using methyl phenyl sulfoxide as a model substrate for this transformation.



Scheme 35 – Biocatalytic approaches to chiral sulfoxides.

Methyl phenyl sulfoxide proved to be a well-tolerated substrate (*Figure 18*). In an ideal kinetic resolution the transformation of one enantiomer of sulfoxide **2.108** would reach full conversion without oxidation of the other enantiomer, leaving enantiopure starting material with a maximum yield of 50%. As can be seen from *Figure 18*, the rate of oxidation is extremely fast, with 12 mutants showing over-oxidation (>50% conversion) in 6 hr, increasing to 18 mutants at 28 hr. More importantly, most mutants oxidise both enantiomers at a similar rate thereby leaving sulfoxide **2.108** racemic (or <10% *ee*); however, some mutants do exhibit enantiodiscrimination, with eight mutants showing a >10% ee at 6 hr and 13 mutants at 28 hr.

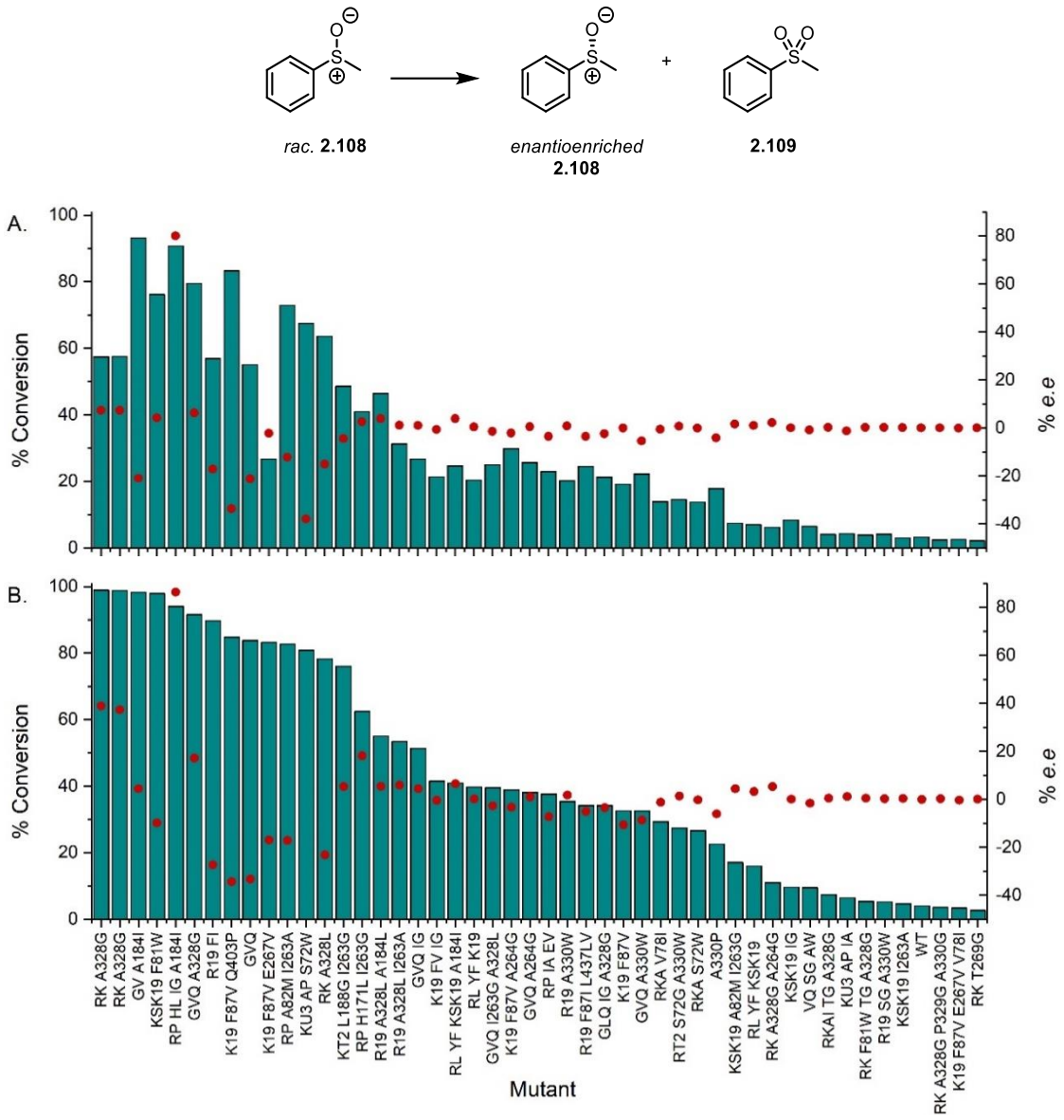
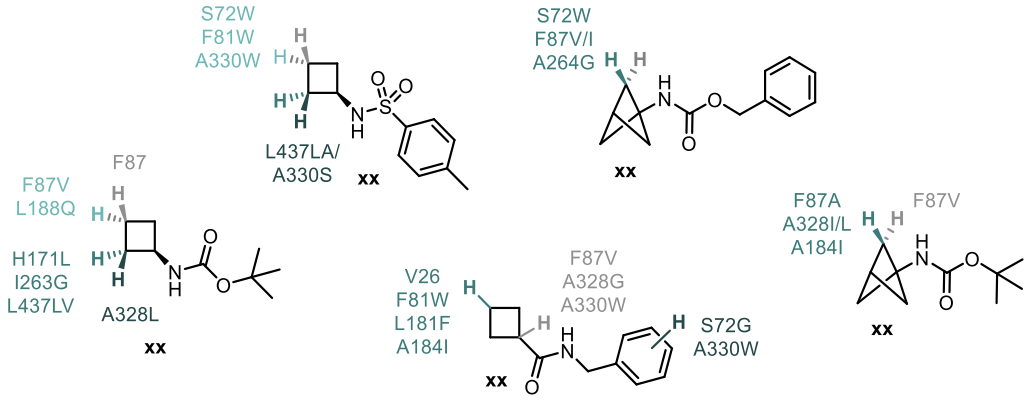


Figure 18 – Screening data for sulfoxide **2.108**, ordered by conversion to sulfone showing both % conversion (blue bar) and % *ee* (red dot). (A) Data after 6 hr, (B) data after 28 hr. Absolute stereochemistry not determined.

The above chart shows a clear outlier with mutant RP/H171L/I263G/A184I which, although showing conversion >95% to sulfone **2.109** (therefore only <5% conversion to desired sulfoxide **2.108**), is highly enantioselective. These initial results show proof-of-concept for the synthesis of enantioenriched sulfoxides *via* P450 kinetic resolution.

2.8. Conclusions

Enzymatic hydroxylation of a range of cyclic amines can be affected with excellent regio-, diastereo- and enantioselectivity, yielding a plethora of privileged ring structures for synthesis. Furthermore, this work describes the first direct enantioselective synthesis of BCPA's, unlocking new synthetic routes to chiral bioisosteres for medicinal chemistry. Based on the analysis of important mutations for the conversion of these substrates (*Scheme 36*), work is ongoing within our group into the enzymatic synthesis of related molecules.



Scheme 36 – Important mutations for selective hydroxylation of small-ring amines.

With the increasing diversity of chemistry possible with enzymes, biocatalysis is becoming a key approach not only in process chemistry but in discovery chemistry and fragment generation projects.[72] The process, and compounds, described within this work could find many applications in both academic and industrial syntheses.

2.9. References for Chapter 2

(1) J. C. Barrow, K. E. Rittle, T. S. Reger, Z.-Q. Yang, P. Bondiskey, G. B. McGaughey, M. G. Bock, G. D. Hartman, C. Tang, J. Ballard, Y. Kuo, T. Prueksaritanont, C. E. Nuss, S. M. Doran, S. V. Fox, S. L. Garson, R. L. Kraus, Y. Li, M. J. Marino, V. Kuzmick Graufelds, V. N. Uebele, and J. J. Renger, *ACS Med. Chem. Lett.,* **2010**, *1(2)*, p75-79.

(2) Y. Zou, L. Liu, G. Liu and G. Liu, *Future Med. Chem.*, **2020**, *12(2)*, p91-93.

(3) F. Lovering, J. Bikker, C. Humblet, *J. Med. Chem.* 2009, 52, 21, p6752-6756. Follow – up report: F. Lovering, Med. *Chem. Commun.*, **2013**, *4*, p515-519.

(4) S. W. Reilly, L. N. Puentes, K. Wilson, C.-J. Hsieh, C.-C. Weng, M. Makvandi and R. H. Mach, *J. Med. Chem.,* **2018**, *61*, p5367-5379.

(5) S.B. Singh, D. E. Kaelin, J. Wu, L. Miesel, C. M. Tan, P. T. Meinke, D. Olsen, A. Lagrutta, P. Bradley, J. Lu, S. Patel, K. W. Rickert, R. F. Smith, S. Soisson, C. Wei, H. Fukuda, R. Kishii, M. Takei and Y, Fukuda, *ACS Med. Chem. Lett.*, **2014**, *5(5)*, p609-614.

(6) A. Mirza, R. Desai, and J. Reynisson, J., *Eur. J. Med. Chem.,* **2009**, *44,* p5006-5011.

(7) J. S. Walsh and G. T. Miwa, *Annu. Rev. Pharmacol. Toxicol.,* **2011***, 51*, p145-167.

(8) T. M. Sodano, L. A. Combee and C. R. J. Stephenson, *ACS Med. Chem. Lett.*, **2020**, *11*, p1785-1788.

(9) P. K. Mykhailiuk, *Org. Biomol. Chem.*, **2019**, *17*, p2839-2849.

(10) R. F. de Freitas and M. Schapira, *MedChemComm*, **2017**, *8*, p1970-1981.

(11) N. T. Thirumoorthi and V. A. Adsool, *Org. Biomol. Chem.*, **2016**, *14*, p9485-9489.

(12) K. C. Nicolaou, D. Vourloumis, S. Totokotsopoulos, A. Papakyriakou, H. Karsunky, H. Fernando, J. Gavrilyuk, D. Webb and A. F. Stepan, *ChemMedChem*, **2016**, *11*, p31-37.

(13) M. Zhong, E. Peng, N. Huang, Q. Huang, A. Huq, M. Lau, R. Colonno and L. Li, *Bioorg. Med. Chem. Lett.*, **2014**, *24*, p5731-5737.

(14) R. Pellicciari, M. Raimondo, M. Marinozzi, B. Natalini, G. Costantino and C. Thomsen, *J. Med. Chem.*, **1996**, *39*, p2874-2876.

(15) R. Pellicciari, G. Costantino, E. Giovagnoni, L. Mattoli, I. Brabet and J.-P. Pin, *Bioorg. Med. Chem. Lett.*, **1998**, *8*, p1569-1574.

(16) B. A. Chalmers, H. Xing, S. Houston, C. Clark, S. Ghassabian, A. Kuo, B. Cao, A. Reitsma, C.-E. P. Murray, J. E. Stok, G. M. Boyle, C. J. Pierce, S. W. Littler, D. A. Winkler, P. V. Bernhardt, C. Pasay, J. J. De Voss, J. McCarthy, P. G. Parsons, G. H. Walter, M. T. Smith, H. M. Cooper, S. K. Nilsson, J. Tsanaktsidis, G. P. Savage, C. M. Williams, *Angew. Chem. Int. Ed.*, **2016**, *55*, p3580-3585.

(17) A. F. Stepan, C. Subramanyam, I. V. Efremov, J. K. Dutra, T. J. O'Sullivan, K. J. DiRico, W. S. McDonald, A. Won, P. H. Dorff, C. E. Nolan, S. L. Becker, L. R. Pustilnik, D. R. Riddell, G. W. Kauffman, B. L. Kormos, L. Zhang, Y. Lu, S. H. Capetta, M. E. Green, K. Karki, E. Sibley, K. P. Atchison, A. J. Hallgren, C. E. Oborski, A. E. Robshaw, B. Sneed and C. J. O'Donnell, *J. Med. Chem.*, **2012**, *55*, p3414-3424.

(18) K. B. Wiberg, D. S. Connor and G. M. Lampman, *Tetrahedron Lett.*, **1964**, *5(10)*, p531-534.

(19) K. Semmler, G. Szeimies and J. Belzner, *J. Am. Chem. Soc.*, **1985**, *107*, p6410-6411.

(20) M. D. Levin, P. Kaszynski and J. Michl, *Chem. Rev.,* **2000**, *100(1)*, p169-234.

(21) R. Gianatassio, J. M. Lopchuk, J. Wang, C.-M. Pan, L. R. Malins, L. Prieto, T. A. Brandt, M. R. Collins, G. M. Gallego, N. W. Sach, J. E. Spangler, H. Zhu, J. Zhu and P. S. Baran, *Science*, **2016**, *351 (6270)*, p241-246.

(22) K. D. Bunker, N. W. Sach, Q. Huang, P.F. Richardson, *Org. Lett.*, **2011**, *13*, p4746-4748.

(23) J. M. E. Hughes, D. A. Scarlata, A. C.-Y. Chen, J. D. Burch, J. L. Gleason, *Org. Lett.*, **2019**, *21*, p6800-6804.

(24) J. Kanazawa, K. Maeda, M. Uchiyama, *J. Am. Chem. Soc.,* **2017**,*139*, p17791-17794.

(25) S. Shin, S. Lee, W. Choi, N. Kim, S. Hong, *Angew. Chem. Int. Ed.* **2021**, *60*, 7873.

(26) X. Zhang, R. T. Smith, C. Le, S. J. McCarver, B. T. Shireman, N. I. Carruthers and D. W. C. MacMillan, *Nature*, **2020**, *580*, p220-226. For a similar approach using 2-component coupling see: Y. Liang, X. Zhang and D. W. C. MacMillan, *Nature*, **2018**, *559*, p83-88.

(27) J. H. Kim, A. Ruffoni, Y. S. S. Al-Faiyz, N. S. Sheikh, D. Leonori, *Angew. Chem. Int. Ed.*, **2020**, *59*, p8225-8231.

(28) H. D. Pickford, J. Nugent, B. Owen, J. J. Mousseau, R. C. Smooth and E. A. Andesron, *J. Am. Chem. Soc.*, **2021**, *143*, 9729−9736.

(29) J. Kanazawa and M. Uchiyama, *Synlett,* **2019**, *30*, 1–11.

(30) V. Ripenko, D. Vysochyn, I. Klymov, S. Zhersh and P. K. Mykhailiuk, DOI: 10.1021/acs.joc.1c00977.

(31) I. S. Makarov, C. E. Brocklehurst, K. Karaghiosoff, G. Koch, P. Knochel, *Angew. Chem. Int. Ed.,* **2017**, *56*, p12774-12777.

(32) J. Nugent, C. Arroniz, B. R. Shire, A. J. Sterling, H. D. Pickford, M. L. J. Wong, S. J. Mansfield, D. F. J. Caputo, B. Owen, J. J. Mousseau, F. Duarte and E. A. Anderson, *ACS Catal.*, **2019**, *9*, p9568-9574.

(33) J. Nugent, B. R. Shire, D. F. J. Caputo, H. D. Pickford, F. Nightingale, I. T. T. Houlsby, J. J. Mousseau and E. A. Anderson, *Angew. Chem. Int. Ed.* **2020**, *59*, p11866-11870.

(34) S. K. Rout, G. Marghem, J. Lan, T. Leyssens and O. Riant, *Chem. Commun.*, **2019**, *55*, p14976-14979.

(35) J.-X. Zhao, Y.-X. Chang, C. He, B. J. Burke, M. R. Collins, M. Del Bel, J. Elleraas, G. M. Gallego, T. P. Montgomery, J. J. Mousseau, S. K. Nair, M. A. Perry, J. E. Spangler, J. Vantourout and P. S. Baran, *PNAS*, **2021**, *118(28)*, p1-5.

(36) X. Ma, Y. Han and D. Bennett, *Org. Lett.,* **2020**, *22(22)*, p9133-9138.

(37) Y. Yang, J. Tsien, J. Hughes, B. Peters, R. Merchant and T. Qin, DOI: 10.26434/chemrxiv.13724827.v1.

(38) Selected recent examples; a) Z. J. Garlets, J. N. Sanders, H. Malik, C. Gampe, K. N. Houk and H. M. L. Davies, *Nat. Catal.,* **2020**, *3*, p351–357; b) M. L. J. Wong, A. J. Sterling, J. J. Mosseau, F. Duarte and E. A. Anderson, *Nat. Commun.*, **2021**, *12*, p1-9.

(39) K. B. Wiberg, V. Z. Williams, *J. Org. Chem.,* **1970**, *35*, p369-373.

(40) a) A. Padwa, E. Alexander, *J. Am. Chem. Soc.*, **1967**, *89*, 6376-6377; b) A. Padwa, E. Alexander, *J. Am. Chem. Soc.*, **1968**, *90*, 6871-6873.

(41) M. B. Sponsler, D. A. Dougherty, *J. Org. Chem.,* **1984**, *49*, p4978-4984.

(42) M. R. Bauer, P. Di Fruscia, S. C. C. Lucas, I. N. Michaelides, J. E. Nelson, R. I. Storer and B. C. Whitehurst, *RSC Med. Chem.*, **2021**, *12*, p448-471.

(43) WO2019191227A1

(44) WO2018/55550 A1

(45) WO2014/135495

(46) a) Y. Zhao, L. Liu, W. Sun, J. Lu, D. McEachern, X. Li, S. Yu, D. Bernard, P. Ochsenbein, V. Ferey, J.-C. Carry, J. R. Deschamps, D. Sun and S. Wang, *J. Am. Chem. Soc.*, **2013**, *135*, p7223-7234; b) Y. Zhao, S. Yu, W. Sun, L. Liu, J. Lu, D. McEachern, S. Shargary, D. Bernard, X. Li, T. Zhao, P. Zou, D. Sun and S. Wang, *J. Med. Chem.*, **2013**, *56*, p5553-5561.

(47) WO2019/101641

(48) WO2019/032743

(49) WO2017/202742

(50) WO2017/193030

(51) WO2011143366A1

(52) WO2007062333A2

(53) WO2020047035A1

(54) a) J. A. O'Hanlon, X. Ren, M. Morris, L. L. Wong and J. Robertson, *Org. Biomol. Chem.*, **2017**, *15*, p8780-8787; b) Y. Li and L. L. Wong, *Angew. Chem. Int. Ed.*, **2019**, *58*, p9551-9555.

(55) H. D. Flack, *Acta Cryst.*, **1983**, *A39*, p876-881.

(56) C. J. C. Whitehouse, W. Yen, J. A. Yorke, B. C. Rowlatt, A. J. F. Strong, C. F. Blanford, S. G. Bell, M. Bartlam, L.-L. Wong and Z. Rao, *ChemBioChem*, **2010**, *11*, p2549-2556.

(57) Y. Li, DPhil thesis, University of Oxford, 2020.

(58) Developed by DPhil student M. Fisher.

(59) Developed by DPhil student Y. Zhang.

(60) Developed by DPhil student X. Wong.

(61) a) C. Li and S. Shaik, *RSC Adv.*, **2013**,*3*, p2995-3005; b) Auclair K., Polic V. (2015) Use of Chemical Auxiliaries to Control P450 Enzymes for Predictable Oxidations at Unactivated C-H Bonds of Substrates. In: Hrycay E., Bandiera S. (eds) Monooxygenase, Peroxidase and Peroxygenase Properties and Mechanisms of Cytochrome P450. Advances in Experimental Medicine and Biology, vol 851. Springer, Cham.

(62) J. Allen, M. Frohn, P. Harrington, A. Pickrell, R. Rzasa, K. Sham, E. Hu (Amgen Inc.), WO2011/143366A1, **2011**.

(63) S. T. Seger, P. Rydberg and L. Olsen, *Chem. Res. Toxicol.,* **2015**, *28(4)*, p597-603.

(64) a) A. Fattahi, L. Lis, Z. A. Tehrani, S. S. Marimanikkuppam and S. R. Kass, *J. Org. Chem.*, **2012**, *77*, p1909-1914; b) D. R. Reed, S. R. Kass, K. R. Mondanero and W. P. Dailey, *J. Am. Chem. Soc.,* **2002**, *124*, 11, p2790-2795; c) Z. Tian, A. Fattahi, L. Lis and S. R. Kass, *J. Am. Chem. Soc.*, **2006**, *128 (11)*, p17087-17092.

(65) T. T. Talele, *J. Med. Chem.,* **2016**, *59*, p8712-8756.

(66) X. Ren, DPhil thesis, University of Oxford, 2020.

(67) Developed by DPhil student X. Wong.

(68) W. Mączka, K. Wińska, M. Grabarczyk, *Catalysts*, **2018**, *8*, p624.

(69) L. A. Harwood, L. L. Wong, J. Robertson, *Angew. Chem. Int. Ed.*, **2021**, 60, p4434-4447.

(70) A. Rioz-Martinez, G. de Gonzalo, D. E. Torres PazmiÇo, M.W. Fraaije, V. Gotor, *Eur. J. Org. Chem.*, **2010**, p6409-6416.

(71) (a) V. Nosek and J. Misek, *Angew. Chem., Int. Ed.*, **2018**, *57*, p9849; (b) V. Nosek and J. Misek, *Chem. Commun.*, **2019**, *55*, p10480-10483.

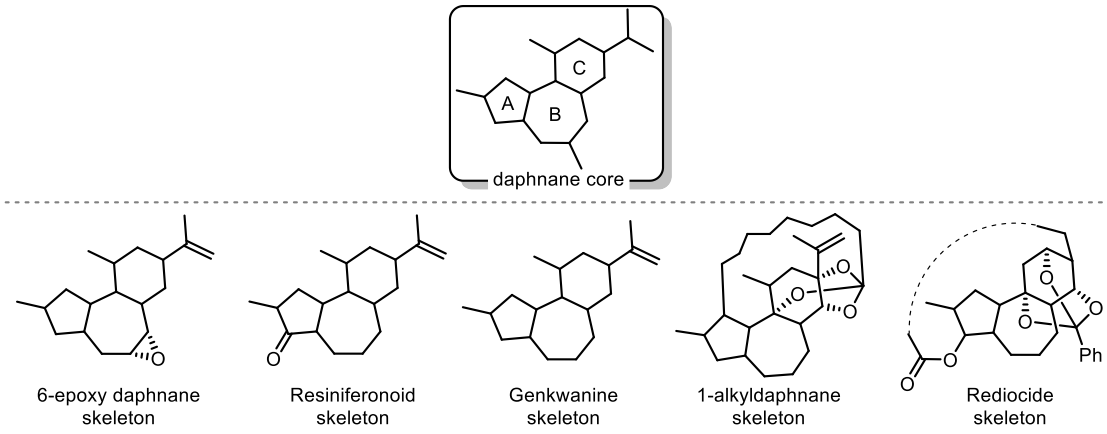
(72) J. I. Ramsden, S. C. Cosgrove and N. J. Turner, *Chem. Sci.*, **2020**, *11*, p11104-11112.

Chapter 3 : Synthetic Efforts Towards Trigoxyphin Natural Products

3.1 Introduction

3.1.1. Trigoxyphin

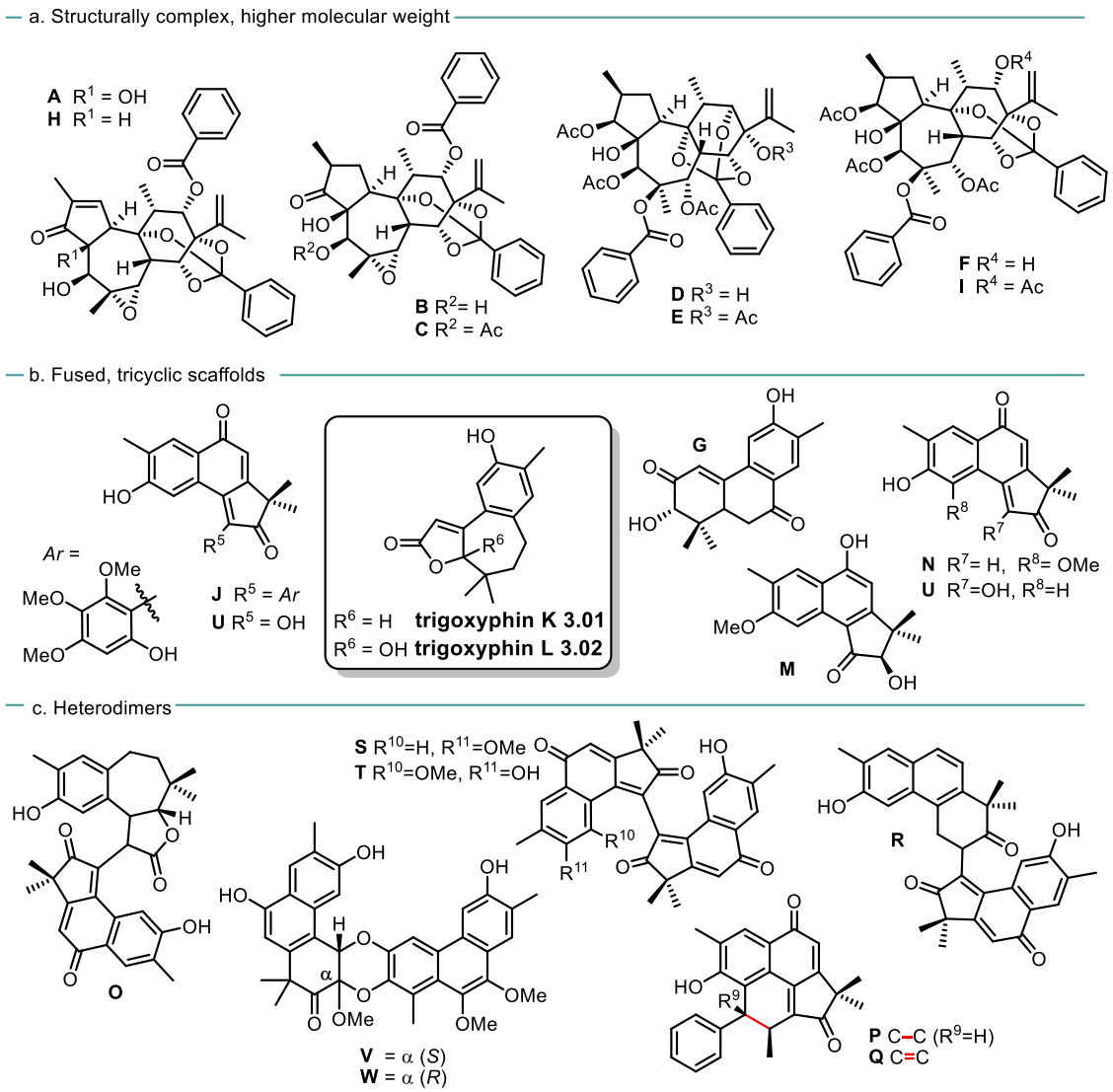
There are around 200 natural products classed as daphnane diterpenoids, many of which exhibit significant biological activities, including anti-HIV, anti-cancer and insecticidal. Their defining structural characteristic is a fused 5,7,6-ring system, possessing varying levels of oxidation, and they can generally be categorised into five subgroups (*Scheme 1*).



Scheme 1 – Five classes of daphnane diterpenoids.

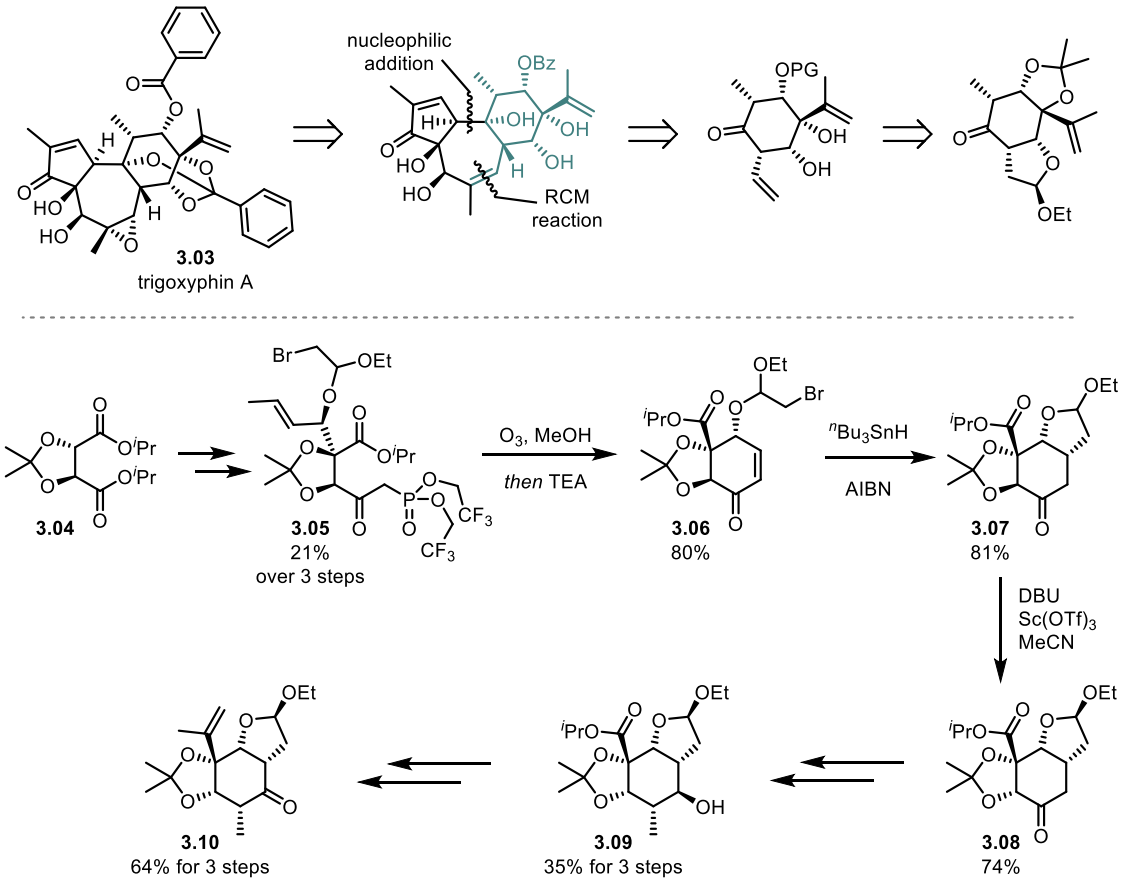
A prolific source of daphnane diterpeniods is the genus *Trigonostemon*, which contains approximately 50 plant species found mainly in tropical and subtropical regions of Asia and has produced a wide variety of natural products.[1] Isolated from the twigs of *Trigonostemon xyphophylloides* is the trigoxyphin natural product family of diterpenoids (trigoxyphin A – G,[2] H – I,[3] J – N,[4] O – T[5] and U – W[6]), which range in size and complexity as shown in S*cheme 2*.

Efforts in the group focus on the synthesis of trigoxyphin K **3.01** and L **3.02**, containing the stereotypical-5,7,6 ring system consistent with the other daphnane-type deterpenoids. Trigoxyphin K is reported to be a promising medicinal compound for treatment of immune inflammation, due to its ability to raise platelet and erythrocyte counts and induce vasodilation.[7] Trigoxyphin L differs only from K in that it contains a hydroxy-butenolide moiety, rather than a simple butenolide. Our group is interested in these compounds as ideal targets for late-stage aromatic C–H oxidations using our library of P450 mutants, and to explore new methodologies towards these core ring structures.



Scheme 2 – Family of trigoxyphin natural products, containing a variety of structural complexity.

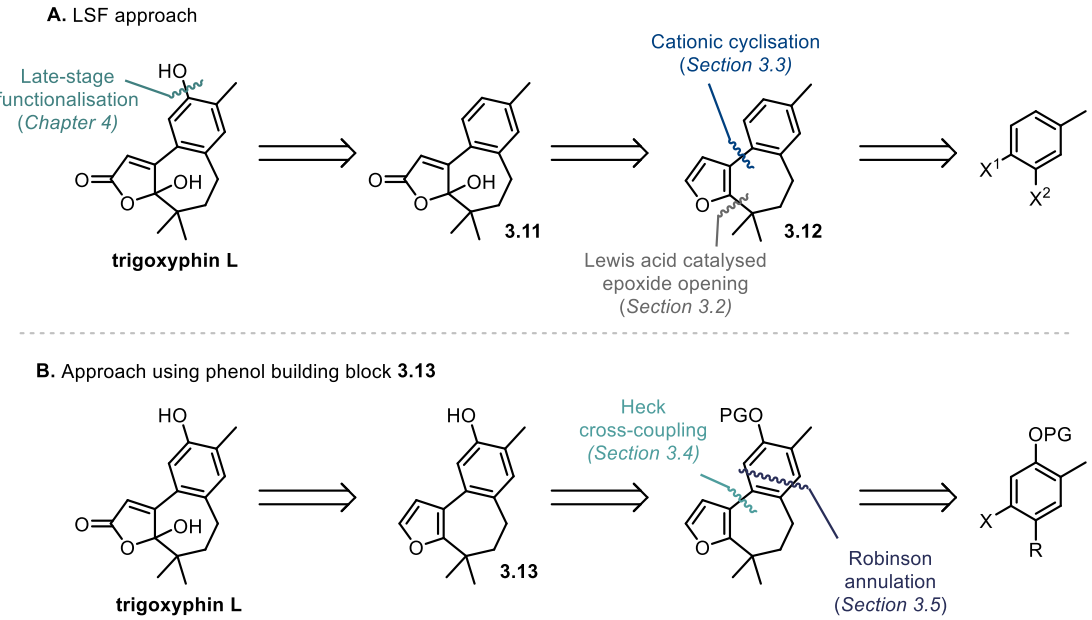
The only synthesis, or partial synthesis, reported of any compound belonging to the trigoxyphin natural product family is by the Lui group, who described the asymmetric synthesis of the six-membered ring of trigoxyphin A **3.03** (*Scheme 3*).[8] Analogous to trigoxyphin K **3.01** and L **3.02**, the core structure of trigoxyphin A contains a 5,7,6 fused ring system; however, the six-membered ring is aliphatic and contains many stereochemical features which are the focus of the Liu group publication. In three steps, phosphonate ester **3.05** was prepared from known compound **3.04**, which then underwent tandem ozonolysis and intramolecular Horner–Wadsworth–Emmons reaction with TEA to afford cyclohexanone **3.06** in 80% yield. Stereochemical inversion yielded the thermodynamically more stable acetal **3.08**, ready for the final six-step synthetic sequence to yield final cyclohexanone **3.10** in 12 steps and ~2% overall yield.



Scheme 3 – Lui group approach to trigoxyphin A, and synthesis of the six-membered ring fragment.

3.1.2. Aims of this project

This chapter will discuss the multiple routes to trigoxyphin **3.02** and its deoxygenated precursor **3.11**. Access to both compounds would provide analytical standards which would aid GC analysis during P450 screening, and to speed up product elucidation and reaction optimisation. Routes based on four different disconnections are discussed (*Scheme 4*): functionalising the C2 position of furan (*Section 3.2*), or the C3 position (*Section 3.3)* en route to *deoxy*-trigoxyphin L **3.11** for P450 catalysed aromatic hydroxylation, or towards trigoxyphin L **3.02** using a Heck disconnection (*Section 3.4*), or Robinson annulation (*Section 3.5*) as key steps.



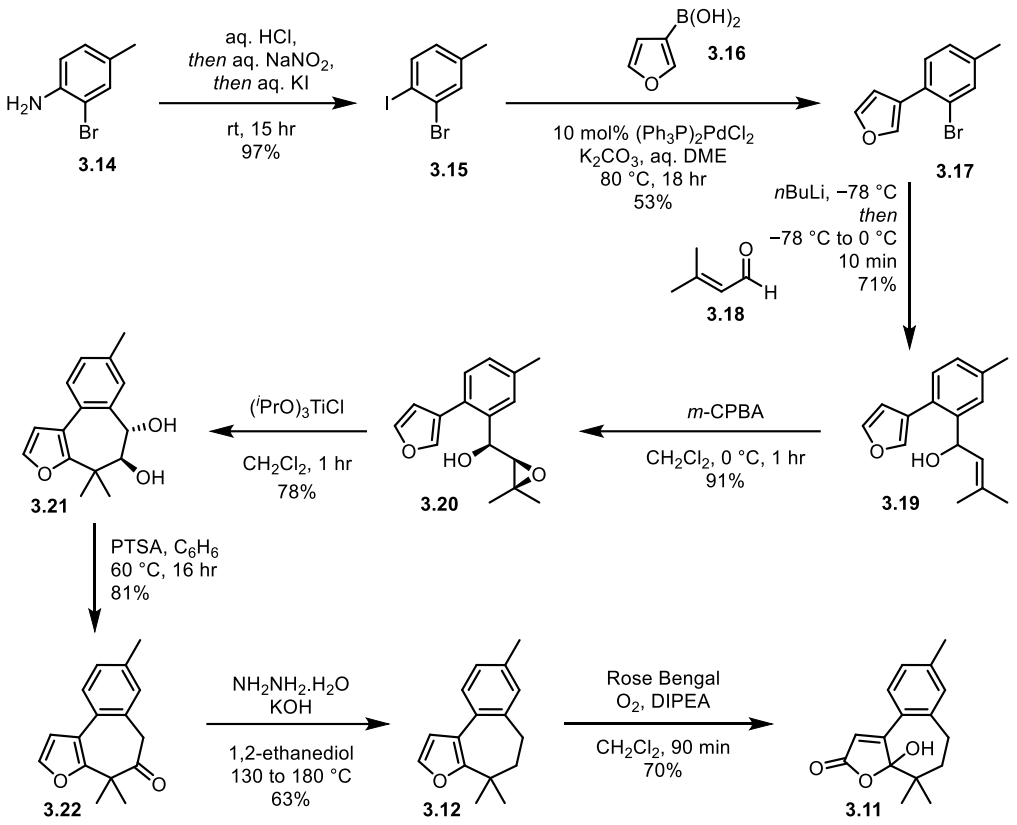
Scheme 4 – Approaches to trigoxyphin.

3.2. First-generation synthetic route to *deoxy*-trigoxyphin 3.11

3.2.1. Previous work within the group

The first-generation route developed within the group, by DPhil student O'Hanlon and improved by part II student Pickford,[9] provided a reliable and scalable route toward the trigoxyphin precursor **3.11** (*Scheme 5*).

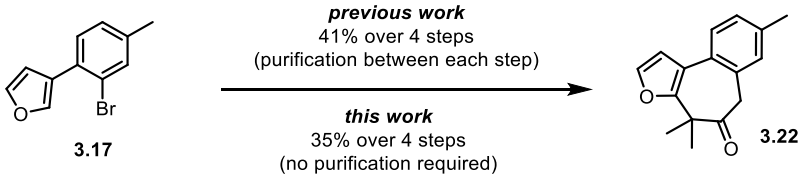
Aryl iodide **3.15** was produced *via* Sandmeyer reaction of aniline **3.14** in near quantitative yield, then elaborated by Suzuki coupling with boronic acid **3.16** in 53% yield. Lithium-halogen exchange of aryl bromide **3.17** and subsequent reaction with prenal **3.18** yielded allylic alcohol **3.19**; epoxidation to **3.20** and intramolecular Lewis acid catalysed epoxide opening formed the core seven-membered ring structure **3.21** in 50% yield over three steps. Diol **3.21** was transformed into ketone **3.22** using PTSA in 81% yield, then Wolff–Kishner reduction yielded structure **3.12** which was oxidised to produce final hydroxy-butenolide **3.11**.



Scheme 5 – First generation synthesis to trigoxyphin L precursor **3.11**.

3.2.2. Improvements to route

Previously this synthesis had been conducted with isolation of every intermediate using flash column chromatography; however, during this work it was discovered that crude material could be used through the four steps from **3.17** through to **3.22**, in 35% overall yield (*Scheme 6*). This resulted in a reduction of waste and time taken to complete the synthesis, with no purification or isolation of intermediates required. The synthesis could then be conducted on gram-scale yielding hydroxy-butenolide **3.11** in eight steps with 9.3% overall yield, starting from 5 g of aniline **3.14** yielding sufficient material (>300 mg) of the final four compounds **3.21**, **3.22**, **3.12**, and **3.11** in the synthetic sequence for P450 screening (*Chapter 4*).



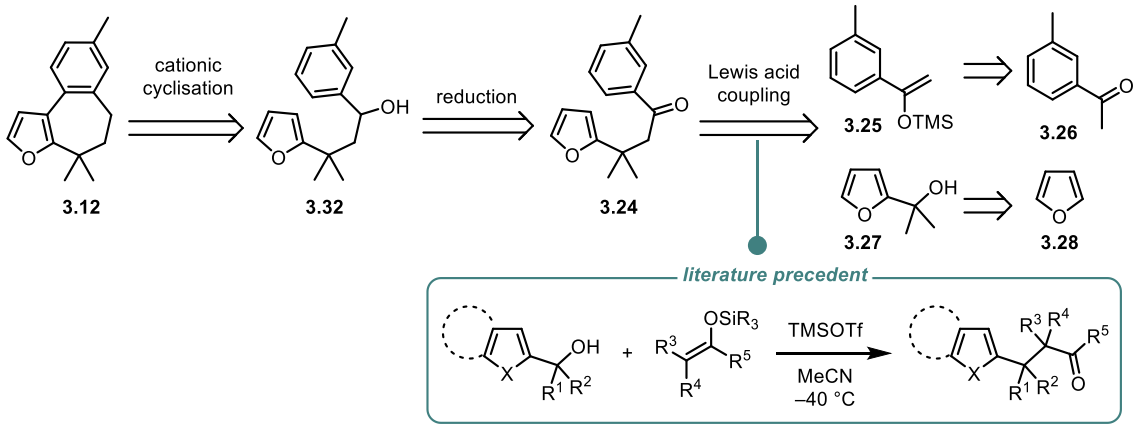
Scheme 6 – Synthesis of ketone **3.22** in 35% overall yield.

3.3. Second-generation synthetic route *via* cationic cyclisation

3.3.1. Retrosynthesis

The first-generation route provided reliable access to compound **3.11**; however, starting boronic acid was expensive (£56.20/g)[10] and so development of a potentially large-scale synthesis avoiding this intermediate was sought. Furthermore, this would provide an opportunity to develop new chemical methodology while exploring new strategies to trigoxyphin type cores.

In this approach we envisaged intermediate **3.12** would be formed *via* Lewis acid mediated cationic cyclisation, through activation of alcohol **3.32** (*Scheme 7*). Alcohol **3.32** would be the product of the reduction of ketone **3.24** which could be, in turn, obtained from silyl enol ether **3.25** and furfuryl alcohol **3.27**. This key disconnection was inspired by work reported by Martin, who developed a Lewis acid catalysed coupling of π-nucleophiles to heterocyclic alcohols.[11] Furfuryl alcohol **3.27** and enol ether **3.25** could easily be obtained in one step from furan **3.28** and 3-methylacetophenone **3.26**, respectively (see *Chapter 6* for full experimental details).

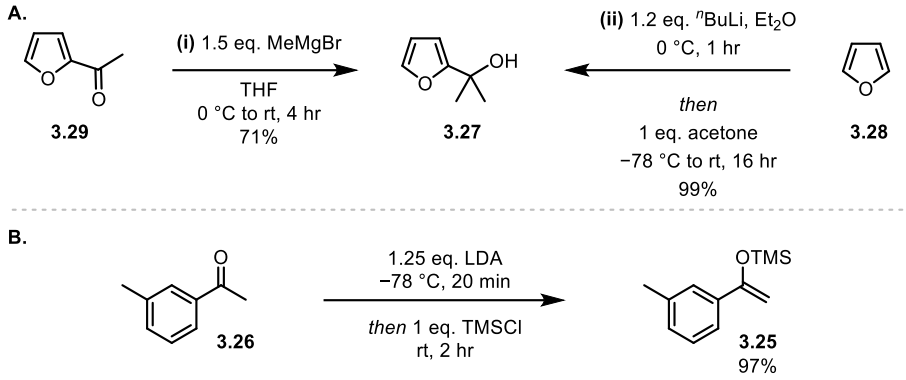


Scheme 7 – Second generation route retrosynthesis.

3.3.2. Lewis acid mediated coupling of tolyl substrate 3.26

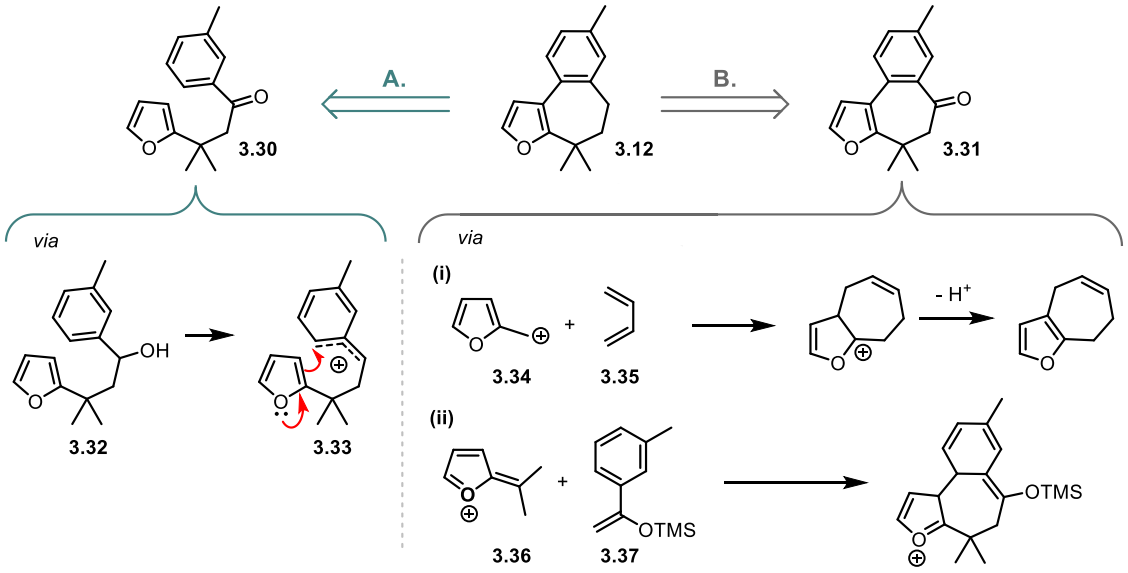
Substrates required for the Lewis acid mediated coupling, as described in *Scheme 7*, could be easily obtained in one step from cheap starting materials. Furfuryl alcohol **3.27** was obtained *via* two different methods: (a) Grignard addition into acetyl furan **3.29**, or (b) through the reaction of acetone with furyllithium (*Scheme 8.A*). Both reactions were high yielding; however, method (b) proceeded to

full conversion and did not require any chromatography. Silyl enol ether **3.25** was formed in quantitative yield by treatment of **3.26** with LDA and subsequent trapping using TMSCl (*Scheme 8.B*).



Scheme 8 – Syntheses of starting materials **3.27** and **3.25**.

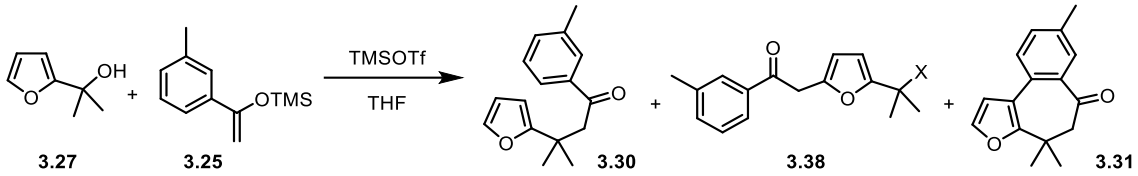
Coupling of silyl enol ether **3.25** with alcohol **3.27** was predicted to yield ketone **3.30**, based on literature precedent as described in *Scheme 7*. Formation of the seven-membered ring could then proceed through trapping of delocalised cation **3.33** *via* activation of alcohol **3.32** with a suitable Lewis acid or similar reagent (*Scheme 9.A*). Alternatively, it could be formed in an intermolecular manner directly from activated furyl cation **3.34** or **3.38** through (4+3) cycloadditions (formally [4+2] with diene **3.35** (*Scheme 9.B.i*).[12] Although enol ether **3.37** is electronically different to diene **3.35** (*Scheme 9.B.ii*), this reactivity may be catalysed by Lewis acids reagents used in this study and so this pathway cannot be ruled out.



Scheme 9 – Proposed mechanistic pathways for the formation of seven-membered ring **3.12**.

When conditions used by Martin were tested on these substrates a very poor yield of product **3.30** was observed (*Table 1 Entry 1*), predominantly returning starting materials **3.27** and **3.25**, and yielding regioisomer **3.38**. A range of catalysts were tested (*Chapter 5: Appendices*), leading to either complete decomposition or returned starting material. Trimethylsilyl trifluoromethanesulfonate (TMSOTf) was the only Lewis acid which produced desired compound **3.30** and so other parameters, such as time and temperature, were explored (*Table 1*).

Longer reaction times led to a higher proportion of regioisomer **3.38** (*Entry 1*), and raising the temperature resulted in a lower overall conversion (*Entries 2 – 5).* Even at lower temperatures desired product **3.30** appeared to decompose under the reaction conditions; consequently, short reaction times were key to achieving consistent yields of 57 – 61% of **3.30** (*Entries 6 – 8*). Subsequent repeats of this reaction consistently yielded between 60 – 74% isolated yield. Lowering the reaction temperature further to –92 °C did not lead to any further improvement in yield (*Entry 9*).

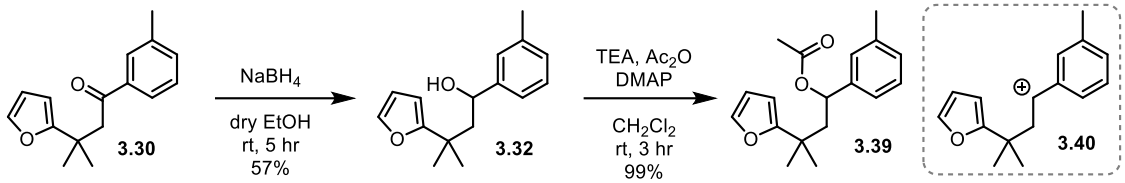


Entry	Temp /°C	Time /min	3.30 /%	3.38 /%	3.31 /%
1	–40	900	<10	26	-
2	–78	90	36	15	-
3	0	90	5	11	-
4	RT	90	*trace*	-	-
5	reflux	90	*trace*	-	-
6	–78	35	38	<5	-
7	**–78**	**10**	**61**	**<10**	-
8	–78	5	59	*trace*	-
9	–92	5	57	*trace*	-

Table 1 – Optimisation of Lewis acid mediated coupling of **3.27** and **3.25**. Figures quoted are isolated yield. X = unknown, regioisomeric structure determined by ^{1}H NMR.

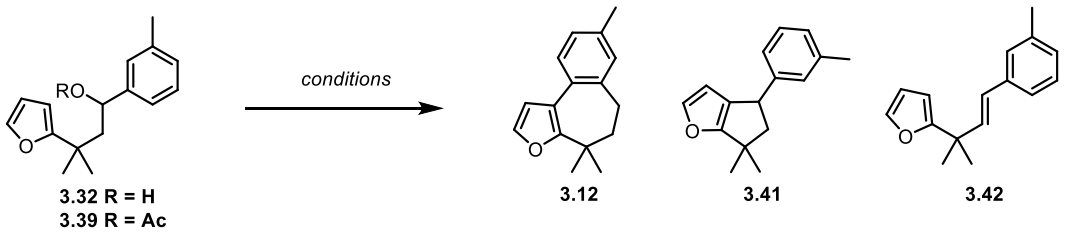
3.3.3. Attempted cationic cyclisation of 3.32

As no cyclised product was observed during screening of the coupling step (*Table 1*), efforts continued toward effecting the cyclisation *via* benzylic cation **3.40**. Substrates required for this cyclisation study were obtained through reduction of ketone **3.30** with $NaBH_4$ to form alcohol **3.32,** and then acetylation with Ac_2O/ DMAP to form **3.39** (*Scheme 10*).



Scheme 10 – Synthesis of alcohol **3.32** and acetyl protected alcohol **3.39**.

Selected literature conditions that were tested are shown in *Table 2* (full table in *Chapter 5: Appendices*). Most conditions produced either a complex mixture of inseparable products or complete decomposition of starting material. In only two of the reaction conditions tested (out of 15) were trace amounts of 5,5-cyclised product **3.41** and eliminated compound **3.42** detected (*Entries 7 and 8*).



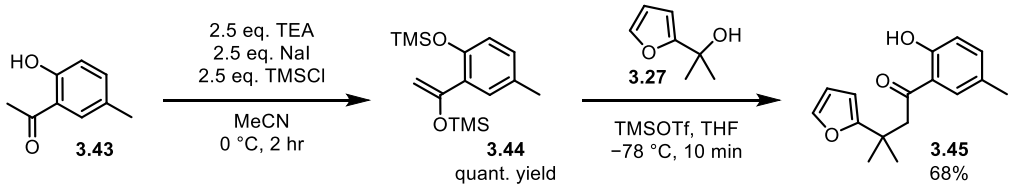
Entry	R =	Conditions (based on 1 eq. starting material)	Outcome
1	H	0.3 eq. $PTSA.H_2O$, C_6H_6 [0.15]	a
2	H	1.05 eq. $BF_3.OEt_2$, CH_2Cl_2 [0.1], 1 hr	a
3	H	5 mol% $AlCl_3$, 5 mol% PPh_3, MeCN, 80 °C[13]	a
4	H	10 mol% I_2, $MeNO_2$ [0.25] 80 °C, 30 min[14]	b
5	H	4 eq. $TiCl_4$, CH_2Cl_2 [0.1], −78 °C, 3 min[15]	b
6	H	TFA [0.1][16]	b
7	Ac	10 mol% $AuCl_3$, MeCN [0.5], 18 hr[17]	trace **3.41** and **3.42**
8	Ac	10 mol% $Yb(OTf)_3.H_2O$, $MeNO_2$ [0.25], 18 hr[18]	trace **3.41**

Table 2 – Conditions tested based on precedent of cyclisations from benzylic cation. Outcomes: (a) complex mixture of inseparable products, (b) decomposition, (c) no reaction. Values in [ ] are substrate concentration (M) in respective solvent. Temperature = rt, unless otherwise specified.

Although formation of products **3.41** and **3.42** show that the stabilised benzylic cation can form and be trapped by furan, or eliminate, desired product **3.12** was not observed. As this approach using cationic cyclisation was not productive, an alternative strategy was required.

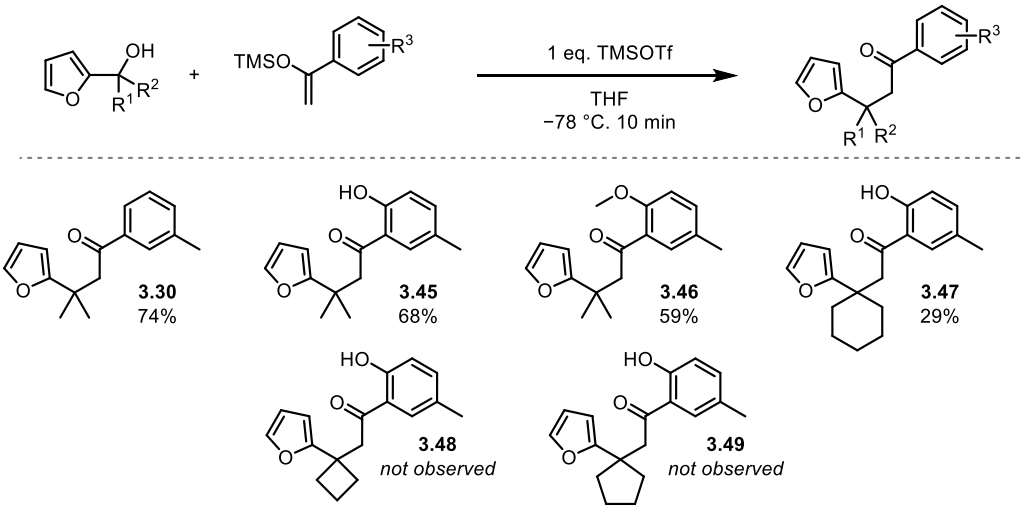
3.3.4. Alternative substrates for Lewis acid mediated coupling

As the Lewis acid catalysed reaction with substrate **3.25** had proceeded with very good yield (60 – 74% yield), other suitable substrates were explored. Conditions previously used for the formation of enol ether proved capricious when applied to the synthesis of di-silylated product **3.44**. Milder conditions (as described in *Scheme 11*) improved the reliability of this reaction such that **3.44** could be produced consistently in quantitative yield from **3.43**, and subsequent coupling yielded phenol **3.45** in 68% isolated yield.



Scheme 11 – Synthesis of phenol **3.45**.

Furthermore, synthesis of methoxy product **3.46** was achieved in good yield (59%); however, cyclohexyl product **3.47** was produced in significantly lower yield (29%), and cyclobutyl- and cyclopentyl- structures **3.48** and **3.49** were not observed (*Scheme 12*).



Scheme 12 – Substrates tested for TMSOTf-catalysed coupling. Yield stated denoted isolated yield.

When testing methoxy substrate **3.50**, the reaction outcome was found to be unreliable, and so different Lewis acids were investigated as potential catalysts. Indium (III) chloride was unreactive at −78 °C and only yielded trace product at rt (*Table 3*, *Entries 1 – 2*), along with $AlCl_3$ and $AlMe_3$ which only returned starting material **3.27**, **3.50** or hydrolysed **3.50** (*Entries 3 – 4*). Triflates were found to be more effective catalysts with both $Sc(OTf)_3$ and $Zn(OTf)_2$, at varied temperatures, yielding desired product **3.51** in good yield (*Entries 5 – 7*).



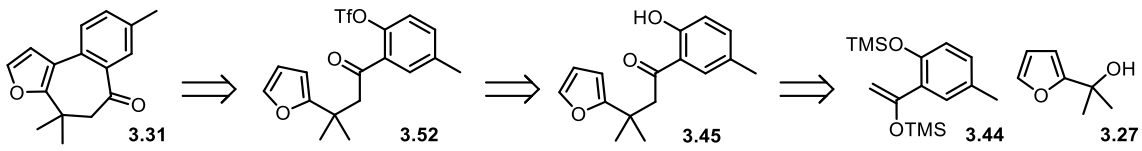
Entry	Temp /°C	Catalyst	3.27 /%	3.50 /%	3.51 /%
1	−78	$InCl_3$	42	N/A	Trace
2	RT	$InCl_3$	2	5	<14%
3	RT	$AlCl_3$	-	-	Trace
4	RT	$AlMe_3$	26	13	-
5	RT	$Zn(OTf)_2$	2	7	42
6	70	$Zn(OTf)_2$	-	-	53
7	RT	$Sc(OTf)_3$	-	-	24

Table 3 – Catalyst screening for coupling of methoxy substrate **3.50** with furfuryl alcohol **3.27**.

3.3.5. Intramolecular Heck coupling of 3.52

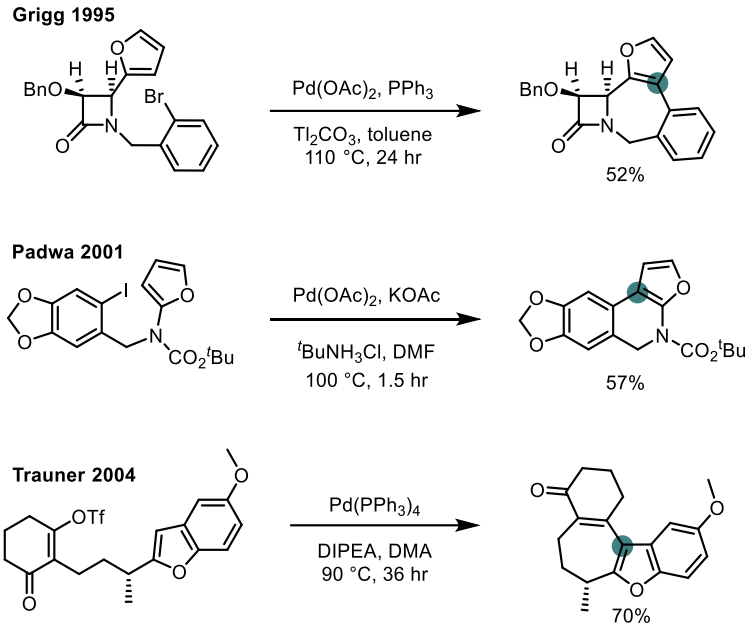
3.3.5.1. Retrosynthesis and literature precedent

As the cyclisation with unfunctionalised aromatic **3.32** had not been successful, aryl triflate **3.52** was envisaged as a suitable cross-coupling partner to afford the desired fused ring system *via* intramolecular Pd-catalysed Heck coupling or an equivalent process (*Scheme 13*). Compound **3.52** could arise from triflation of phenol **3.45**, which is a product of the Lewis acid mediated coupling discussed in *Section 3.3.4*.



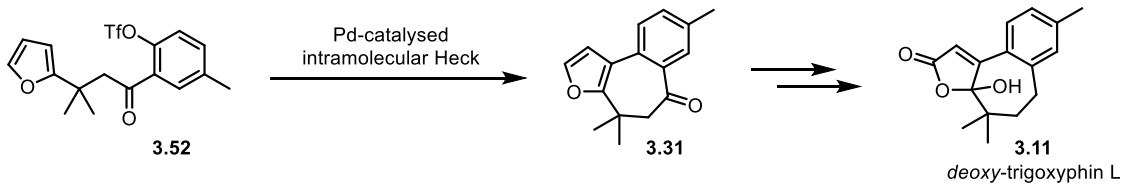
Scheme 13 – Modified approach from di-silylated **3.44** as starting material.

Heck cross-couplings constitute a common disconnection found in total synthesis routes;[19] however, there are just a few reported examples that achieve intramolecular arylation at the C3 position of furans (*Scheme 14*).[20]



Scheme 14 – Pd-catalysed intramolecular Heck couplings to C3 (benzo)furans.

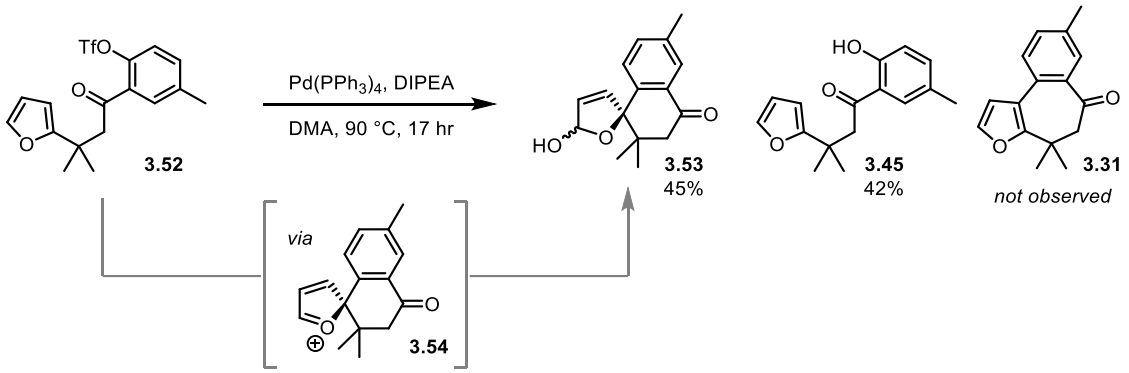
The transformation of substrate **3.52**, required for the synthesis of *deoxy*-trigoxyphin L **3.11** (*Scheme 15*), is challenged with the regioselectivity problem that furan functionalisation favours the more reactive C2 position. Furthermore, there is no directing group[21] or other influencing functional group to steer selectivity to the desired position. Investigating this route would provide the opportunity to develop new methodology towards intramolecular Heck couplings and establish a more direct route towards the synthesis of trigoxyphin-type core structures.



Scheme 15 – Proposed Heck reaction for the synthesis of *deoxy*-trigoxyphin L.

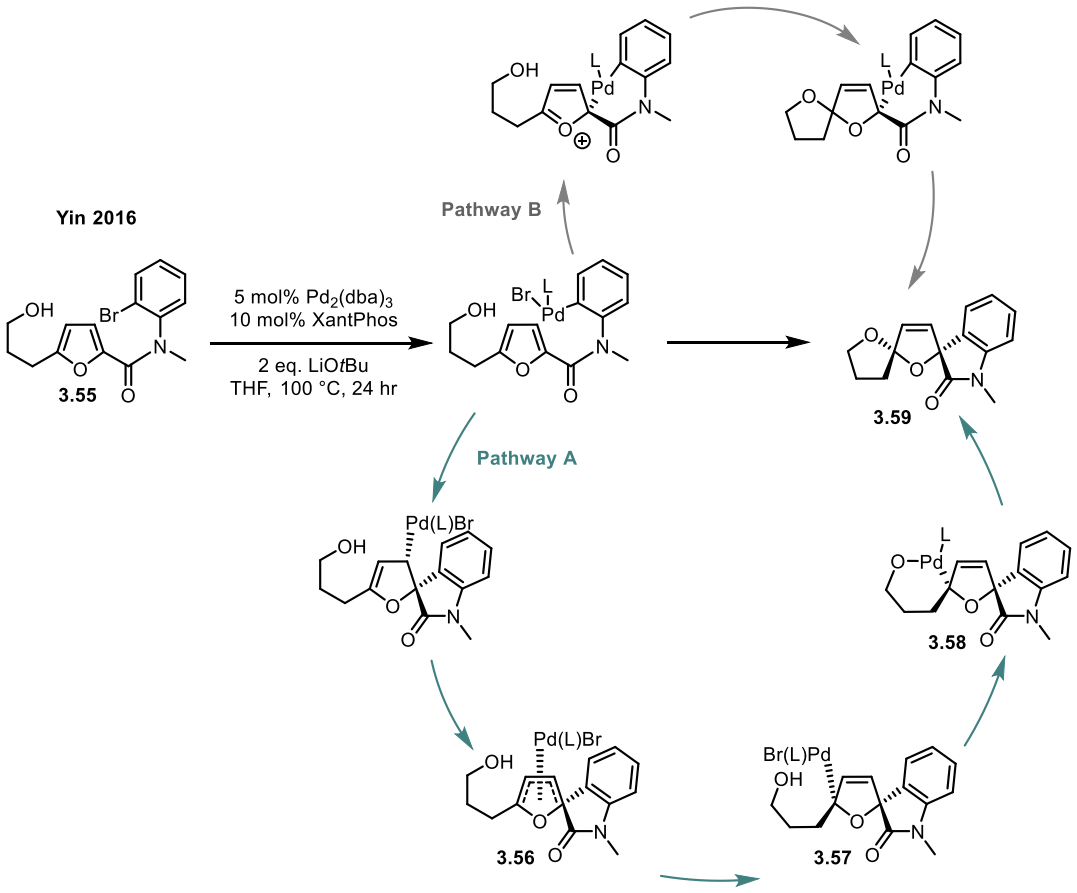
3.3.5.2. Previous work in the group

Substrate **3.52** was subjected to known Heck conditions;[22] however, C3-arylation was not observed, and only spirocycle **3.53** and phenol **3.45** were isolated by previous part II student Pickford (*Scheme 16*).[23] Spirocycle **3.53** is proposed to be formed through Pd-insertion at C2 and elimination to form oxonium **3.54**, which is then trapped by residual H_2O in the reaction (or, trapped by -OTf and subsequent hydrolysis during work-up). Phenol **3.45** could arise through Pd-insertion into the Ar-OTf bond, formation of the Ar-Pd-OH and reductive elimination, or through simple hydrolysis.



Scheme 16 – Isolated yields of spirocycle **3.53** and phenol **3.45** products of Heck coupling of **3.52**.

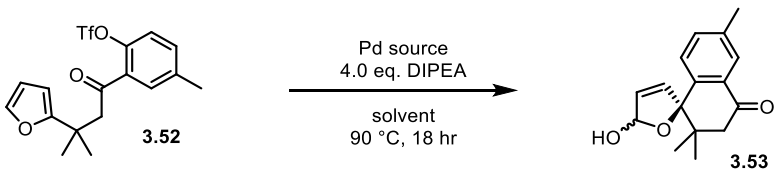
No attempts to observe oxonium intermediate **3.54** were made; however, Yin proposed a similar possible intermediate in a report describing the Pd-catalysed 2,5-alkoxyarylation of furans to access spirooxindoles (*Scheme 17*).[24] Discussion of alternative mechanisms included C2-arylation of furan **3.55** producing a palladium allyl complex **3.56**, followed by β-hydride elimination to **3.57** and acetalisation *via* a further nucleophilic addition into Pd to form **3.58** (*Pathway A*). The latter was proposed to be the prevailing mechanism as no other diastereomers were observed; however, our system resulted in a mixture of diastereomers meaning a mechanism similar to *Pathway B* is more likely.



Scheme 17 – Mechanistic pathways for the C2-arylation of furan substrate **3.55** and subsequent intramolecular nucleophilic trapping to form spirooxindole **3.59**.

3.3.5.3. Towards *deoxy*-trigoxyphin L 3.11

Building on the previous work by student Pickford (*Section 3.4.2.*) we anticipated the formation of spirocycle **3.53** from substrate **3.52** which, after exposure to literature conditions, afforded product in 24% isolated yield. The addition of either 1 eq. or 10% (v/v) of H_2O did not dramatically affect the yield of **3.53** (*Table* 4, Entry *2* – *3*); however, increasing the catalyst loading to 20 mol% (*Entry 4*) or 1 equivalent (*Entry 5*) significantly increased the yield to 77%.

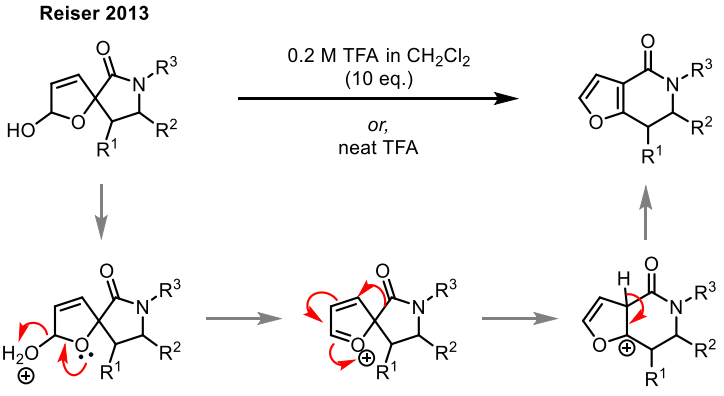


Entry	Pd Source	Solvent	Additives	3.53 /%
1	10mol% $Pd(PPh_3)_4$	DMA	-	24
2	10mol% $Pd(PPh_3)_4$	DMA	1 eq. H_2O	20
3	10mol% $Pd(PPh_3)_4$	aq. DMA	-	29
4	20mol% $Pd(PPh_3)_4$	aq. DMA	-	**77**
5	1 eq. $Pd(PPh_3)_4$	aq. DMA	-	**77**
6	10mol% $Pd(OAc)_2$	aq. DMA	-	18
7	10mol% $Pd(OAc)_2$	aq. DMA	20mol% PPh_3	15

Table 4 – Initial catalyst optimisation, yield represents % isolated yield. Aq. DMA indicates 9:1 ratio DMA:H_2O.

Screening conducted by Syngenta using a range of phosphine ligands, Pd catalysts and additives yielded only trace amounts of desired product **3.31** (<10%), and no spirocyclic product **3.53** was observed (*Chapter 5, Section 5.2.3.*).

As spirocycle **3.53** could be produced in good yield, attempts were made to transform this compound into the desired fused ring structure **3.31**. There is precent for 1,2-acyl shifts in related systems; however, no desired product was observed when the conditions shown in *Scheme 18* were tested with substrate **3.53**.[25]

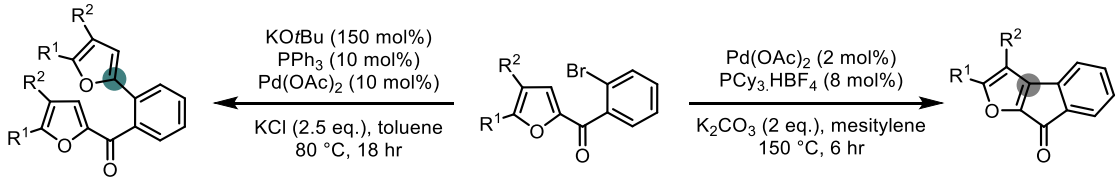


Scheme 18 – Rearrangement of spirocycle using TFA.

Although the desired C3 selectivity to produce **3.31** could not be achieved, good substrate conversion was seen using Pd-catalysed cross-couplings of these substrates and so a new route was designed based on this Heck disconnection.

3.4. Third-generation synthetic route *via* Heck-type cross-coupling

Only trace amounts of **3.31** had been observed throughout screening, and high yields were only achieved for functionalisation at the C2 position of furan. Rather than varying the electronic properties of the phosphine, we decided to test a range of substrates with varied functional groups to explore the general reactivity and selectivity trends of this transformation. As a basis for the design of our test substrate scope, we took inspiration from a report by Lin, describing the C2 and C3 direct arylation of furans using palladium catalysed cross-coupling (*Scheme 19*).[26]

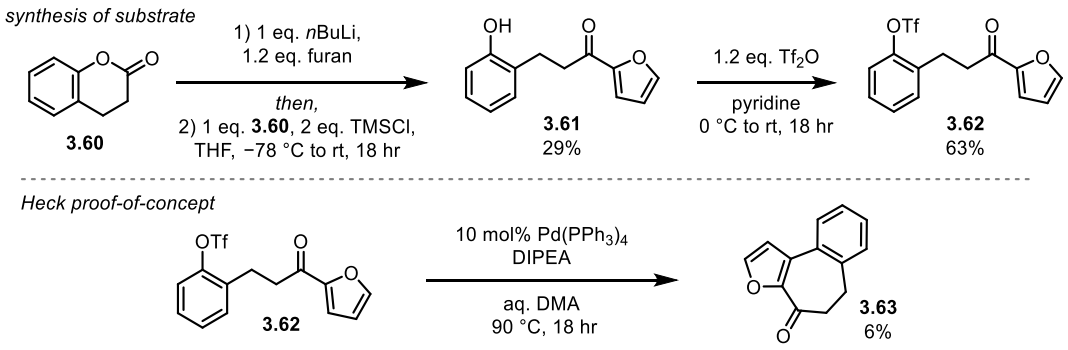


Scheme 19 – Yin report of α- and β-arylation of furans.

Furthermore, this new route would not contain the additional ketone contained in **3.52**, a consequence of the Lewis acid catalysed coupling, resulting in a more streamlined synthesis.

3.4.1. Synthesis and Heck reactions of model substrates

Analogous to Lin's report, we proposed replacing the gem-dimethyl functionality in **3.52** to a carbonyl adjacent to the furan ring. Under my supervision, previous part ii student Balfour developed a synthesis of model compound **3.62** which was achieved in 18% overall yield (*Scheme 20*).[27] Firstly, addition of furyllithium into **3.60** yielded phenol **3.61** in 29% yield, followed by triflation to **3.62** in 63% yield. Using previous conditions, a trace amount of desired fused compound **3.62** was isolated by Balfour which although low yielding, proves the desired reactivity can be achieved.



Scheme 20 – Previous work by group member Balfour.

Building on the successful proof-of-concept achieved by part II student Balfour, this work describes further optimisation of these conditions. Varied reaction concentrations were tested, and 0.02 M was found to be ideal, achieving a 27% isolated yield (*Table 5*, *Entry 2*). Notably, intermolecular coupling products and spirocyclic C2-arylation products were not observed with this substrate. Unlike previous reactivity, production of only one regioisomer **3.63** supports the occurrence of direct C3-functionalisation, rather than formation of a spirocycle and then [1,2] acyl- or aryl- shift.



Entry	Concentration /M	3.62 /%	3.64 /%	3.63 /%
1	0.01	19	18	20
2	0.02	29	14	27
3	0.05	31	14	14
4	0.1	38	10	12
5	0.15	13	11	16
6	0.2	53	8	11
7	0.5	23	21	14

Table 5 – Concentration screen of substrate **3.62** under standard Heck conditions.

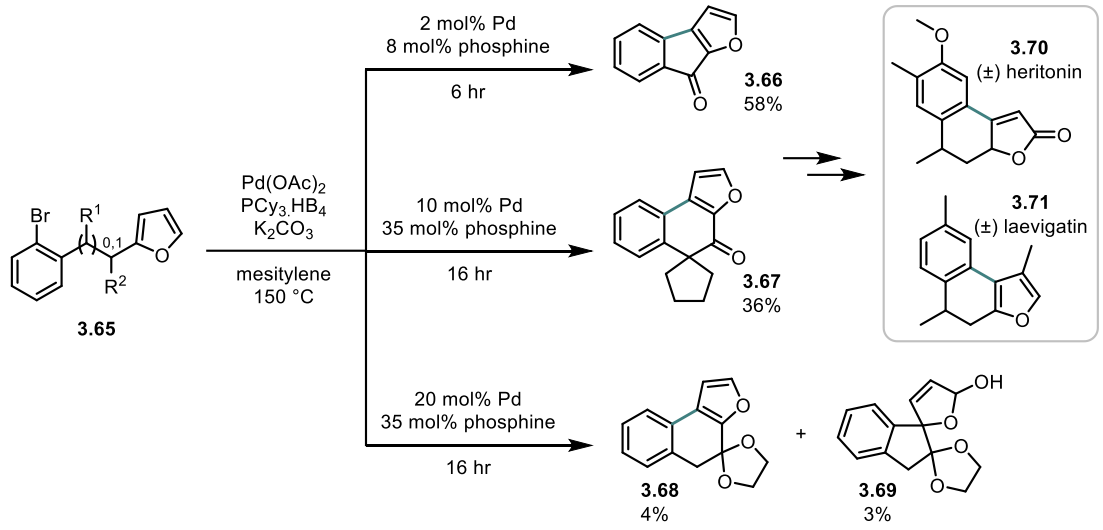
In collaboration with scientists at Syngenta, Jealott's Hill, screening of a range of palladium catalysts and bases revealed that substrate **3.62** was potentially not tolerant of inorganic bases (*Chapter 5*, *Section 5.2.4.*), and so for further optimisation DIPEA was used. The only improvement in yield was seen when active catalyst was generated *in situ* using $Pd(OAc)_2/PPh_3$, which provided 49% yield based on recovered starting material (*Scheme 21*).



Scheme 21 – Best conditions for the synthesis of tricyclic compound **3.63**.

Under my supervision, former part ii student Schrecker synthesised a range of aryl bromides **3.65** to test the generality of the conditions reported by Lin for C2-arylation on a range of substrates

more pertinent to our goal (*Scheme 22*).[28] Although ketal products **3.68** and **3.69** were only observed in trace amounts, both five- and six-membered rings **3.66** and **3.67** could be formed in good yields (58% and 36% respectively). A range of natural products, including heritonin **3.70** and laevigatin **3.71**, could potentially be accessed using this methodology to form the key C(sp^2)–C(sp^2) bond.

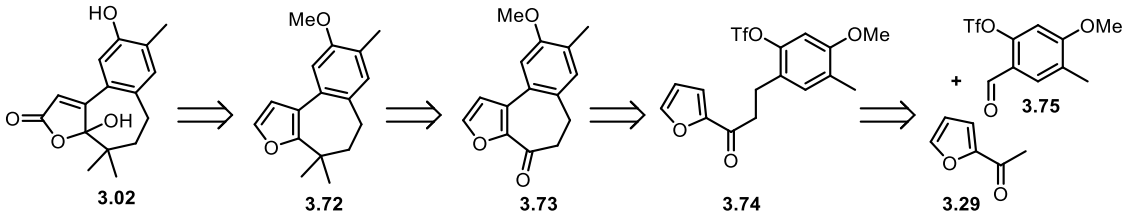


Scheme 22 – Synthesis of multi-ring structures using Lin reaction conditions.

Since these reaction conditions were consistently giving the desired fused ring structures with multiple substrates, a synthesis of the intermediate required for trigoxyphin (differing only by an additional methoxy- and methyl- group on the aryl ring) was developed.

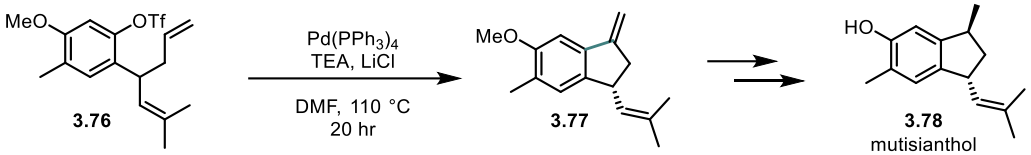
3.4.2. Synthesis of Heck substrate 3.74 towards trigoxyphin L synthesis

This route towards the synthesis of *deoxy*- or trigoxyphin L, with rapid assembly of the tricyclic core through an intramolecular Heck-type cross-coupling (*Scheme 23*), requires an extra step for functional group interconversion of the carbonyl in **3.73**, thought to favour the desired Heck selectivity, into the *gem*-dimethyl group found in the natural product **3.02**. The phenol functionality is latent in starting material **3.75** and carried through the synthesis, providing a complementary approach for comparison to late-stage functionalisation to form this C(sp^2)–O bond.



Scheme 23 – Retrosynthesis of Trigoxyphin L.

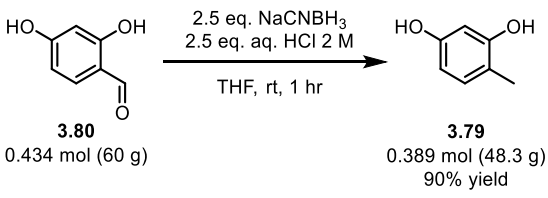
Known compound **3.76**, used by Shinde in the total synthesis of mutisianthol **3.78**, contains a similar aryl component to our required starting material **3.75** (*Scheme 24*).[29] This synthesis demonstrates that aryl triflate **3.76** can readily participate in intramolecular Heck couplings.



Scheme 24 – Shinde synthesis of mutisianthol **3.78** *via* intramolecular Heck reaction.

In order for a sufficient quantity of **3.74** to be produced for screening of Pd conditions at a later stage, the synthesis was initiated on large-scale. Starting material 4-methylresorcinol **3.79** is commercially available; however, is it prohibitively expensive at £266/gram[30] and so a reported procedure from 2,4-dihydroxybenzaldehyde **3.80** (£1.68/gram)[31] was conducted on 60 g scale (*Scheme 25*) with assistance from the process team at Syngenta.[32]

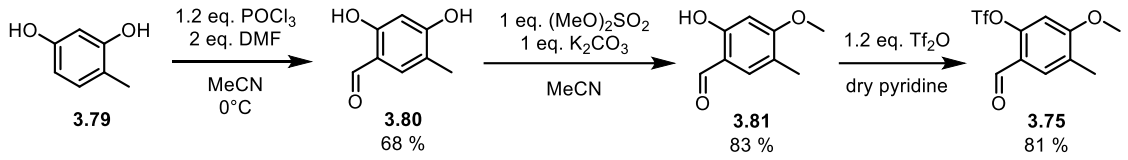
$NaBH(OAc)_3$ was tested as a safer alternative to $NaBH_3CN$; however, no conversion was observed even after prolonged reaction times (24 hr). Under optimised conditions for this reduction using 1.0 mol of $NaBH_3CN$, full conversion was achieved after 3 hours with 90% isolated yield of **3.79**, and no further purification required (*Scheme 25*).





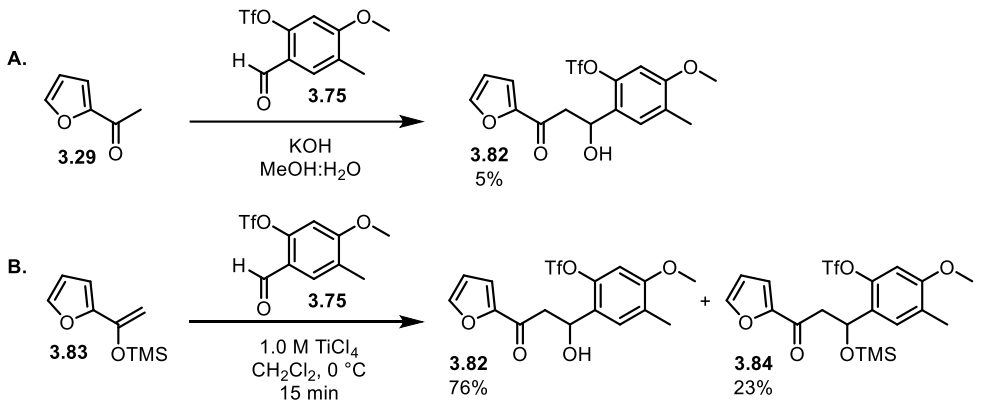
Scheme 25 – Multi-gram scale reduction of **3.80**.

Vilsmeier formylation of substrate **3.79** was achieved in only 40% yield using acetonitrile as the solvent, as reported by Shinde.[33] Increasing the reaction temperature, longer reaction times and pre-forming the Vilsmeier reagent were all unsuccessful in improving the yield. Precipitation of product **3.80** from the reaction and recrystallisation was found to be the key to achieving an increased, consistent yield of 68%. Both the regioselective methylation to form **3.81** and triflation to key intermediate **3.75** were achieved in very good yields (*Scheme 26*).



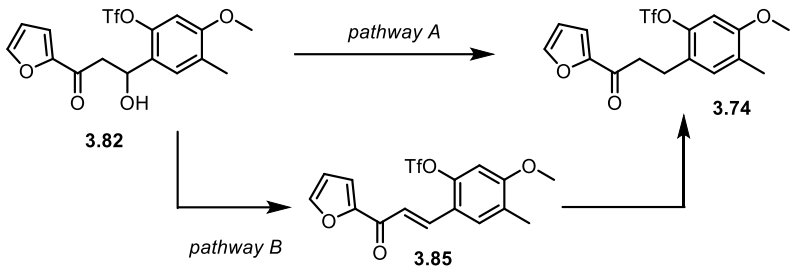
Scheme 26 – Synthesis of functionalised intermediate **3.75**.

When substrate **3.75** was subjected to base-catalysed aldol conditions only 5% isolated yield of alcohol **3.82** was obtained (*Scheme 27.A*). To improve the reactivity of the system, Mukaiyama–aldol conditions were employed using silyl enol ether **3.83** which produced both desired alcohol **3.82** and its TMS-protected analogue **3.84** (*Scheme 27.B*). Even with short reaction times, very good yields of alcohol **3.82** were possible.



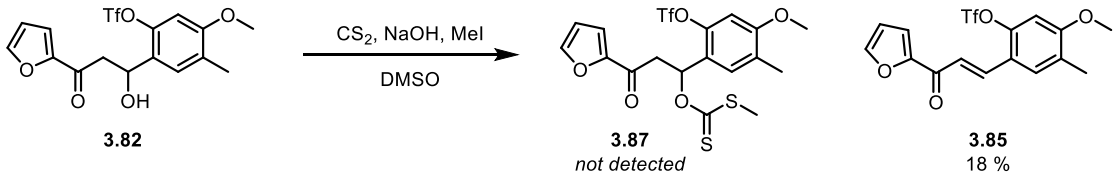
Scheme 27 – Aldol and Mukaiyama–aldol conditions for substrate **3.75**.

Removal of the hydroxyl group could in principle be achieved *via* multiple pathways: either through direct removal of the hydroxyl group (*Scheme 28.A*), or through an intermediate eliminated product **3.85** and hydrogenation (*Scheme 28.B*).



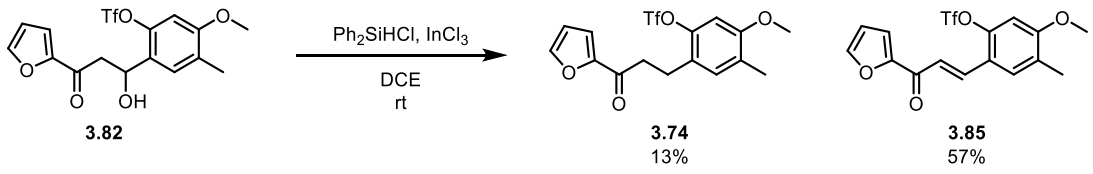
Scheme 28 – Methods of deoxygenation of **3.82**.

Barton–McCombie deoxygenation occurs through the radical reaction of a thiocarbonyl derivative with Bu_3SnH, driven by the formation of strong S–Sn bonds. Xanthates are commonly employed in this transformation; however, conditions described in *Scheme 29* proved unsuccessful for the formation xanthate **3.87** from alcohol **3.82**, and only eliminated product **3.85** was observed in low yield.



Scheme 29 – Failed attempt at forming xanthate **3.87**.

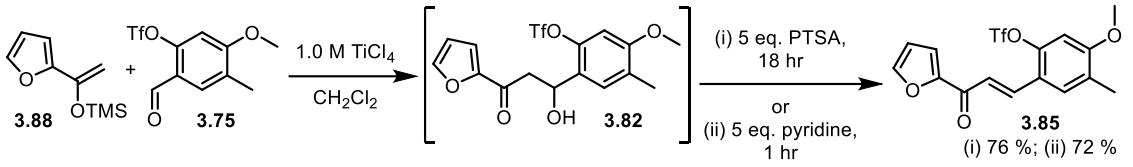
The Baba group reported a mild method for the reduction of secondary and tertiary alcohols using Ph_2SiClH with catalytic $InCl_3$.[34] One of the main advantages of this method is high chemoselectivity and tolerance of other sensitive functional groups, which would prove beneficial for this substrate, with desired product **3.74** produced in 13% yield (*Scheme 30*) .



Scheme 30 – Successful formation of substrate **3.74**.

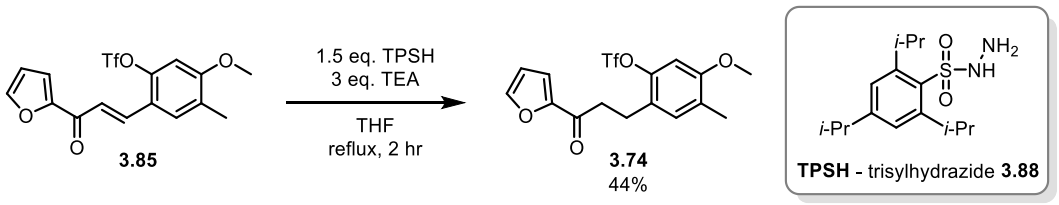
In practice, a drawback with this method was the formation of an inseparable silane by-product, which could not be removed through chromatography. This was potentially a significant problem as the silane should not be carried through to the next step, due to incompatibility with metal catalysis involving palladium.

The major product when attempting any manipulation of substrate **3.82** was found to be olefin **3.85**. To align efforts with the inherent reactivity of the system, methods were explored to achieve pathway b (*Scheme 28*) by proceeding through eliminated intermediate **3.85**. Similar yields were achieved by addition of either acid or base to the crude reaction mixture; however, the rate of reaction was considerably higher on addition of pyridine (*Scheme 31*).



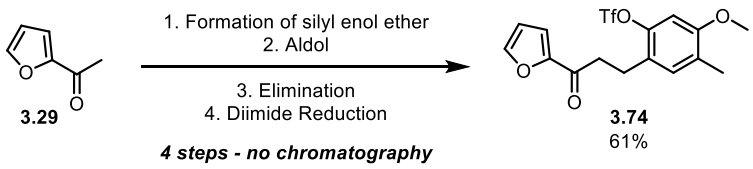
Scheme 31 – Formation of **3.85** by either base- or acid- catalysed elimination.

With compound **3.85** in hand methods were sought to reduce the C=C bond to produce ketone **3.74**. Milder methods, such as conjugate reduction with Stryker's reagent or a diimide reduction, were deemed more suitable than hydrogenations involving Pd/C since the latter may be incompatible with the aryl triflate and furan in this substrate. Diimide reduction was tested using trisyl hydrazide **3.88** and achieved a moderate yield of 44%. Starting material **3.85** and product **3.74** had the same R_f and so reaction monitoring by LCMS was required to ensure full conversion was reached (*Scheme 32*).



Scheme 32 – Diimide reduction of α,β-unsaturated compound **3.85**.

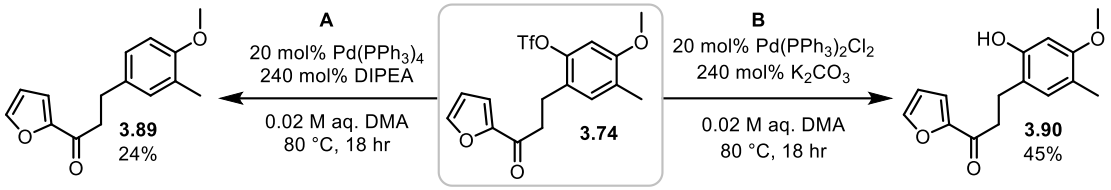
It was possible to perform this reduction on the unpurified aldol-elimination product **3.85**. This allowed for the synthetic sequence from starting material acetyl furan **3.29** through to aryl triflate **3.74** to be performed with no chromatography, with an overall improved yield of 61% (*Scheme 33*).



Scheme 33 – Reaction sequence performed without chromatography.

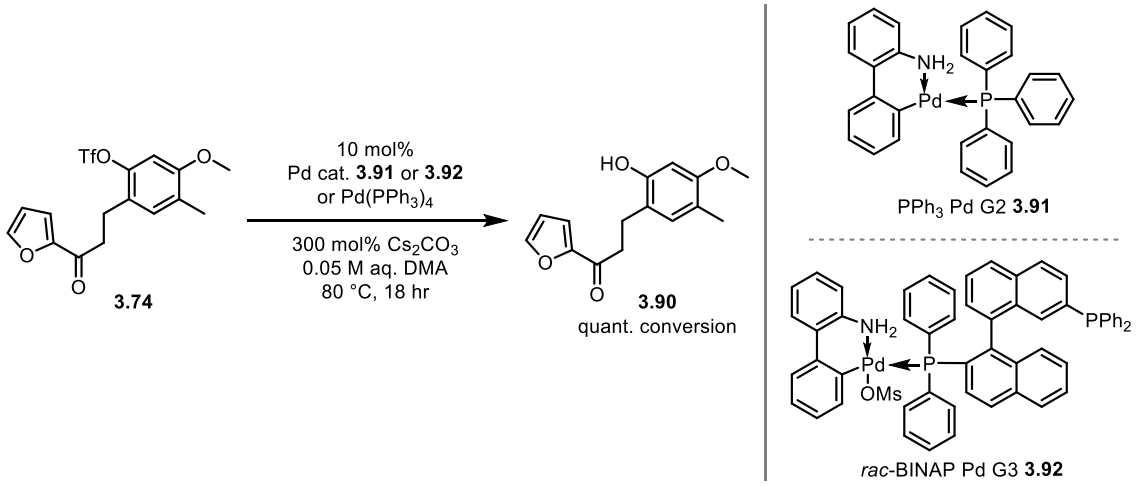
3.4.3. Screening of Pd-catalysed Heck conditions

Conditions A, which had previously yielded desired model system product **3.63**, were tested on substrate **3.74**; however, no desired product was observed, with a small amount of proto-detriflated product **3.89** isolated (*Scheme 34*). It had previously been shown that inorganic bases caused decomposition of starting material **3.62**, which was not observed with substrate **3.74** and only phenol **3.90** was isolated, either from triflate hydrolysis or insertion of Pd and addition of water (*Scheme 34.B*). Conditions which previously were able to affect the intramolecular Heck reaction of aryl bromides ($Pd(OAc)_2$/$Cy_3P{\cdot}HBF_4$/DIPEA/mesitylene), were also unsuccessful.



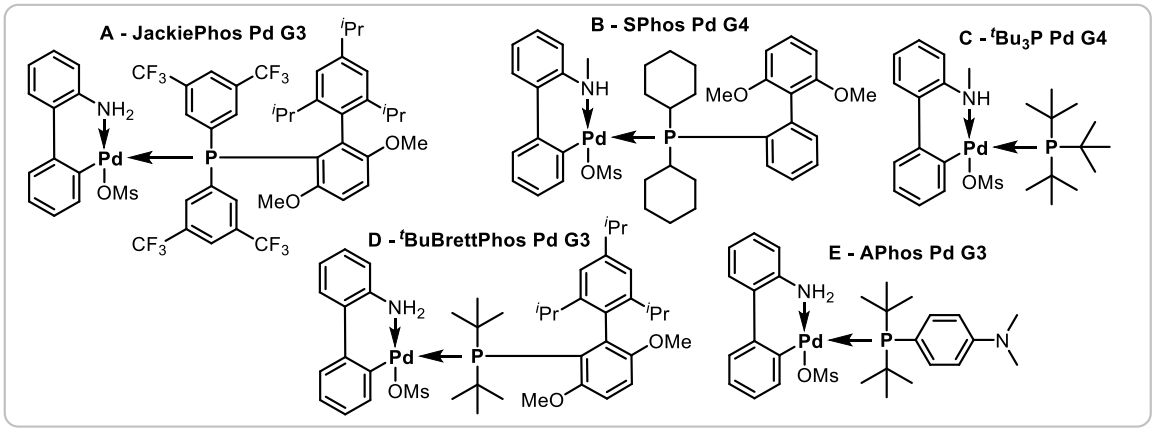
Scheme 34 – Comparison of products produced when using previously used Heck conditions.

Medium-throughput screening was conducted at Syngenta to systematically test reaction conditions including palladium catalyst, solvent, base and temperature. An initial 24-reaction screen involved two different bases (DIPEA and Cs_2CO_3), four different solvents (dioxane and DMA, with and without addition of water) and three different Pd sources ($Pd(PPh_3)_4$, PPh_3 Pd G2 **3.91** and *rac*-BINAP Pd G3 **3.92**); however, no product was observed throughout. All reactions except three gave no conversion; when using Cs_2CO_3 and aq. DMA, complete conversion to phenol **3.90** was observed (*Scheme 35*).



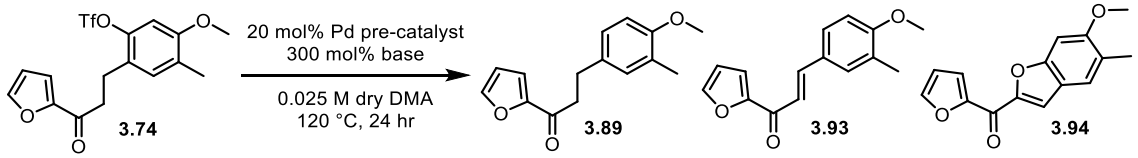
Scheme 35 – Three reaction conditions giving full conversion of substrate **3.74**.

Korenaga demonstrated that novel Buchwald-type ligands bearing electron-poor aryl groups could improve the reactivity in Pd-catalysed direct arylations,[35] and so ligands containing a range of steric and electronic environments were selected for screening with **3.74** (shown in *Scheme 36*), in dry DMA with either DIPEA or Cs_2CO_3.



Scheme 36 – Pd pre-catalysts screened in this study.

LCMS traces proved inaccurate and so reactions were purified individually to obtain isolated yields, with unproductive reactions omitted from *Table 6*. Although conversion appeared high, no desired product **3.73** was obtained; however, proto-detriflation product **3.89** was detected throughout, and isolated in small quantities (*Entries 2,4 and 5*). Notably, selectivity between products **3.93** and **3.94** switches with a change of base from DIPEA, which yields solely α,β-unsaturated ketone **3.93** which could arise from Pd-insertion in the neighbouring C–H bond and elimination, to Cs_2CO_3 which yields unexpected benzofuran **3.94**, albeit in low isolated yields.



Entry	Pd pre-cat.	Base	Conv. /%	3.89 /%	3.93 /%	3.94 /%
1	**a**	DIPEA	91	-	41	-
2	**b**	"	100	11	2	-
3	**a**	Cs_2CO_3	100	-	-	26
4	**b**	"	27	6	-	20
5	**c**	"	100	5	-	17
6	**d**	"	100	-	-	3

Table 6 – Selected results from catalyst screen with **3.74**, not including reactions with no conversion.

Previously (*Scheme 20*) we had shown that addition of water was beneficial for yielding desired tricyclic product **3.63**, and so the screen was repeated using aq. DMA. To expedite product isolation, samples were combined and purified together, and isolated compounds were resubmitted to LCMS to determine retention times. One reaction yielded a new compound with correct mass on LCMS, which is speculated to be desired compound **3.73** due to characteristic disubstituted furan doublet peaks on ^{1}H NMR (*Figure 1*). The reaction using JackiePhos Pd G3 and Cs_2CO_3 achieved 6% yield; however, on a larger scale this reactivity could not be reproduced.

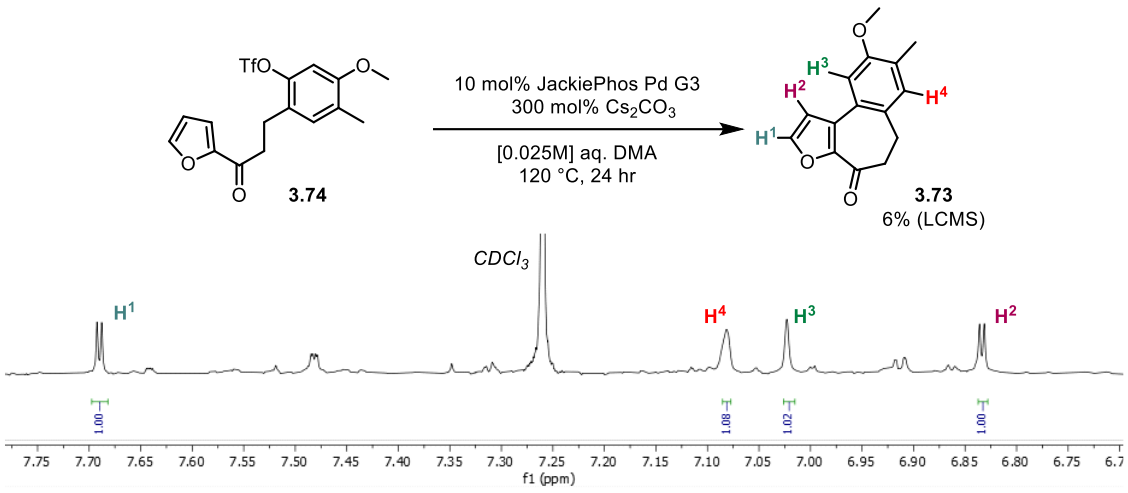


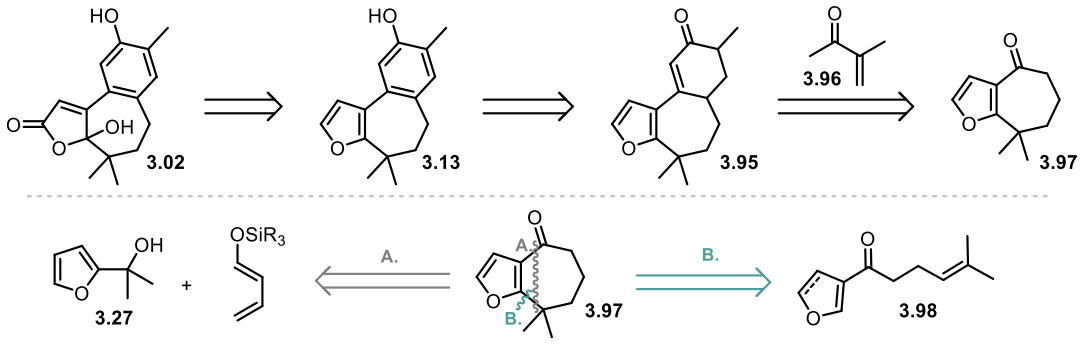
Figure 1 – Reaction yielding trace amount of **3.73**, and ^{1}H NMR spectrum of an impure sample showing peaks characteristic of a disubstituted furan.

Although there was now suggestion that this reaction works, only a trace amount of product was observed throughout all screening with no obvious reactivity patterns to guide further optimisation; accordingly, this route was discontinued, and focus turned to an alternative trigoxyphin disconnection.

3.5. Fourth-generation synthetic route *via* Robinson annulation

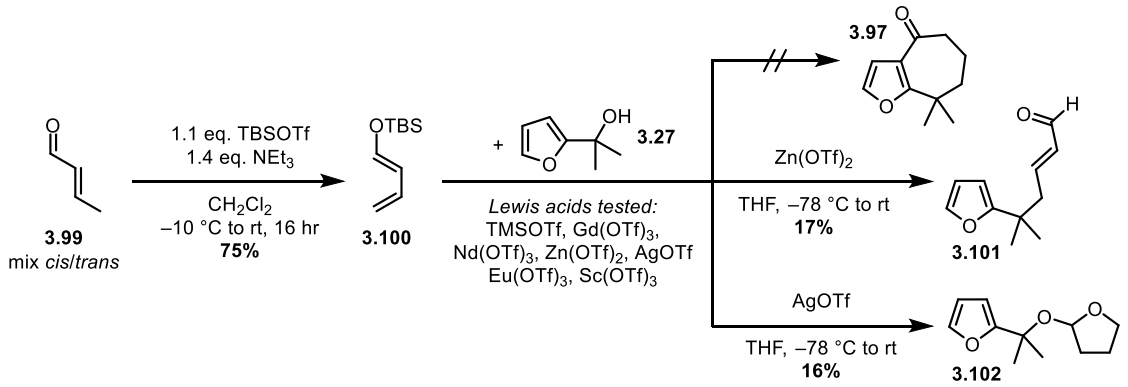
Challenges concerning the efficient formation of the aryl-furan C–C bond *via* Pd-catalysed cross-coupling could not be overcome; therefore, a different retrosynthetic analysis was explored (*Scheme 37*). Phenol **3.13** could arise from oxidation and aromatisation of enone **3.95**, which could be formed *via* Robinson annulation of cycloheptanone **3.97** with 3-methylbut-3-en-2-one **3.96**.

Cycloheptanone **3.97** could, in turn, be formed in one-step from a formal cycloaddition with a diene and furfuryl alcohol **3.27** (*Scheme 37.A*), for which there is precedent for similar processes.[36] If the one-step approach proved unsuccessful then disconnecting the furan C2 bond (*Scheme 37.B*), leads to **3.98** from either furan or 2,3-dihydrofuran (DHF), the forward syntheses of which are discussed below.



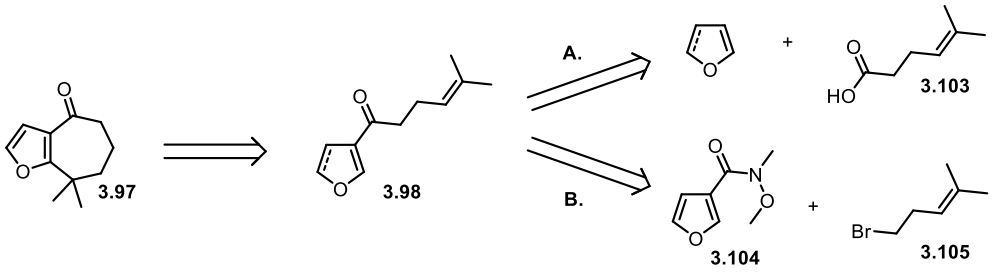
Scheme 37 – Retrosynthetic analysis with the Robinson annulation as the key disconnection.

Pathway A is potentially the shortest route to seven-membered ring **3.97**; starting from crotonaldehyde **3.99**, diene **3.100** was formed cleanly in 75% isolated yield (*Scheme 38*). Multiple Lewis acid catalysts were tested in dry THF; however, no desired cycloheptanone **3.97** was observed. Aldehyde **3.101** was produced in varying amounts with all catalysts, and the highest yield (17% yield) was achieved using $Zn(OTf)_2$. This showed that furfuryl alcohol **3.27** successfully forms a cation under these conditions, which can react with the correct regioselectivity with diene **3.100**. Using AgOTf, this compound was produced in trace amounts (~1% yield) along with new product **3.102** (16% yield) as a result of reaction with THF. To avoid this unwanted product different solvents were tested in combination with TMSOTf ($MeNO_2$ and HFIP); however, immediate decomposition was observed.



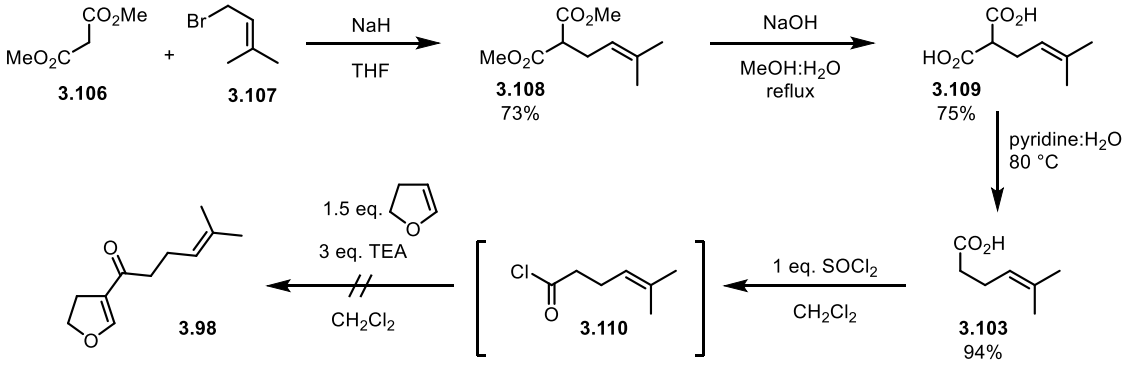
Scheme 38 – Formation of diene **3.100**, and triflate-catalysed cycloaddition tests with alcohol **3.27**.

As the cycloheptanone ring could not be formed directly in one step, consideration turned to compound **3.98** as a suitable precursor (*Scheme 39*) that could potentially be formed either through direct C3-acylation of DHF with acid **3.103** (or acyl chloride derivative), or from addition of alkyl bromide **3.105** after halogen exchange into Weinreb amide **3.104**.



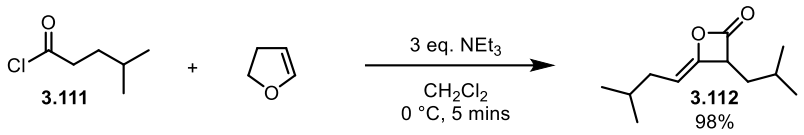
Scheme 39 – Alternative retrosynthesis of cycloheptanone **3.97**.

Synthesis of acid **3.103** was achieved through a reported sequence (*Scheme 40*), starting from malonate **3.106** and prenyl bromide **3.107** to yield diester **3.108** in 73 % isolated yield. Transformation into diacid **3.109** and decarboxylation to desired acid **3.103** was achieved in 71% yield over two steps. Acyl chloride **3.110** was generated *in situ*; however, reaction with DHF yielded a complex mixture of products. Although excess base was used, residual HCl from the previous steps to form acid chloride **3.110** might have caused this reaction to fail by protonation and potential polymerisation of DHF.



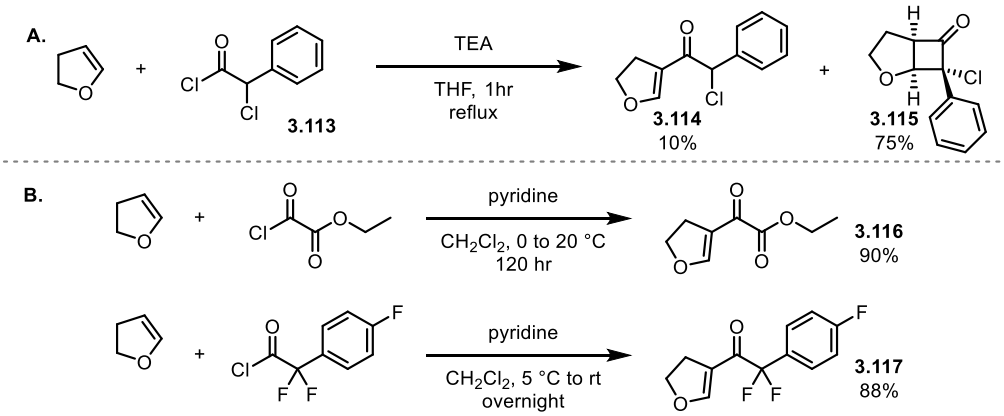
Scheme 40 – Synthetic sequence for **3.98**.

In order to test if acylation of DHF could work in the absence of HCl, commercially available acid chloride **3.111** was used in this reaction (*Scheme 41*); however, near quantitative isolated yield of lactone **3.112** was observed, formed through dimerisation of the ketene formed from acid chloride **3.111**. Further cooling of the reaction and slow addition, or high dilution conditions may supress formation of this unwanted product.



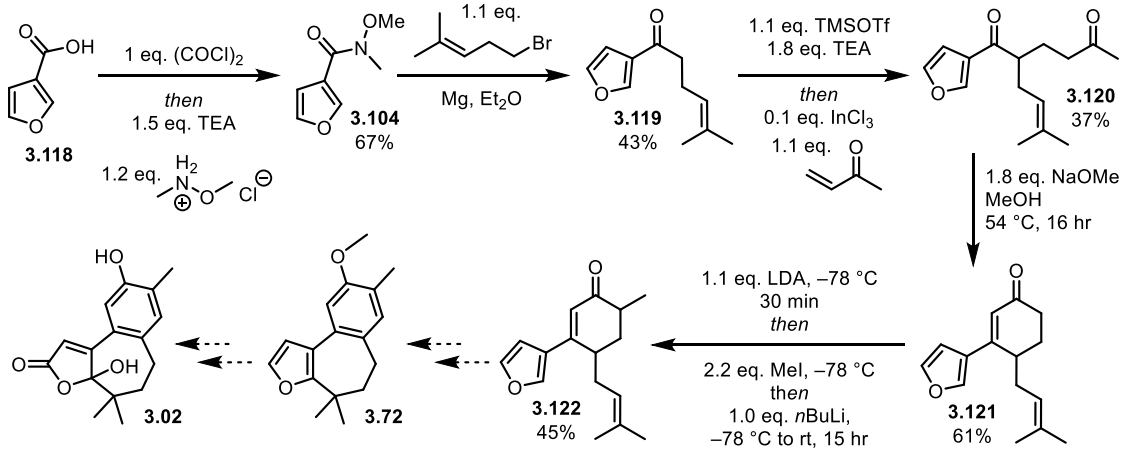
Scheme 41 – Test reaction of acyl chloride **3.111** with 2,3-dihydrofuran.

There is precedent for similar heterodimer cycloadditions (*Scheme 42.A*), where the ketene formed from **3.113** reacts with DHF to form **3.115** in 75% yield.[37] This unwanted pathway can be prevented by using an acyl chloride which is unable to form a ketene, thus yielding the direct acylation products **3.116** and **3.117** (*Scheme 42.B*).[38]



Scheme 42 – Reported acylations of DHF with various acyl chlorides.

Work on this project was continued by current group member Li, starting from 3-furoic acid **3.118** in five steps and 3% overall yield to enone **3.122** (*Scheme 43*). Aromatisation and formation of seven-membered ring would yield intermediate **3.72**, followed by methyl deprotection and furan oxidation to provide trigoxyphin L **3.02**.



Scheme 43 – New synthetic route to trigoxyphin by current DPhil student Li. Solid arrows indicate successful reactions, dotted arrows show future work.

3.6. Conclusions and future work

Through the process of pursuing the total synthesis of the daphnane diterpenoids trigoxyphin L and K, new synthetic methodologies have been explored and developed. The Lewis acid mediated coupling of furfuryl alcohols with silyl enol ethers, yields a variety of furan structures in moderate to very good yields (*Section 3.3.*). Furthermore, extensive screening of Pd-catalysed Heck cross-coupling conditions enhanced our understanding of the reactivity of these substrates, leading to the formation of both complex spirocyclic and fused ring systems (*Section 3.4.*). Work is ongoing within the group towards the final synthetic route of trigoxyphin L, with the first total synthesis of these structures hopefully to be completed in the near future.

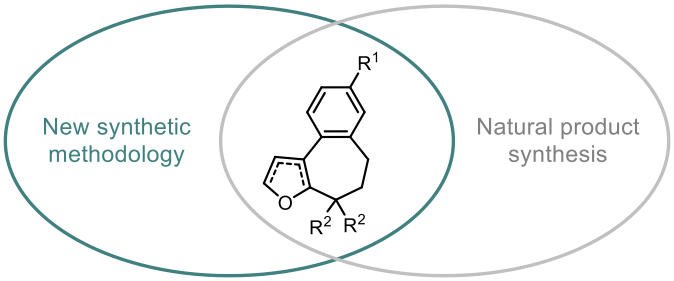


Figure 2 – The intersection of total synthesis and methodology allows for the exploration of chemical space surrounding trigoxyphin-type structures.

3.7. References for Chapter 3

(1) Y.-X. Jin, L.-L. Shi, D.-P. Zhang, H.-Y. Wei, Y. Si, G.-X. Ma and J. Zhang, *Molecules*, **2019**, *24*, p1842-1855.

(2) B.-D. Lin, M.-L. Han, Y.-C. Ji, H.-D. Chen, S.-P. Yang, S. Zhang, M.-Y.Geng and J.-M. Yue, *J. Nat. Prod.,* **2010**, *73(7)*, p1301–1305.

(3) B. Yang, G.-Y. Chen, X.-P. Song, L.-Q. Yang, C.-R. Han, X.-Y. Wu, X.-M. Li and B. Y. Zou, *Inoorg. Med. Chem. Lett.*, **2012**, *22(11),* p3828-3830.

(4) B. Yang, G.-Y. Chen, X.-P. Song, L.-Q. Yang, X.-Y. Wu, C.-R. Han, W.-H. Chen, B.-Y. Zou and X.-M. Li, *Bioorg. Med. Chem. Lett.*, **2013**, *23*, p5748-5751.

(5) B. Yang, G.-Y. Chen, X.-P. Song, L.-Q. Yang, C.-R. Han, X.-Y. Wu, C.-J. Zheng, X. Ran and R.-F. Tang, *Tetrahedron Lett.*, **2013**, *54*, p6434-6438.

(6) S.-F. Li, H.-P. He and X.-J. Hao, *Nat. Prod. Res.*, **2015**, 29:19, p1845-1849.

(7) (i) T. Lihua, CN 103751170 A 20140430. (ii) T. Lihua, CN 103751176 A 20140430. (iii) T. Lihua, CN 103751178 A 20140430. (iv) T. Lihua, CN 103720686 A 20140416. (v) T. Lihua, CN 103751177 A 20140430.

(8) J. Feng, T. Yu, Z. Zhang, J. Li, S. Fu, J. Chen and B. Liu, *Chem. Commun.*, **2018**, *54*, p7665-7668.

(9) J. O'Hanlon, DPhil Thesis, University of Oxford, 2016.

(10) Correct at time of writing – 16/09/2021 (sigmaalrich.com).

(11) T-H. Fu, A. Bonaparte and S. F. Martin, *Tetrahedron Lett.,* **2009**, *50*, p3253-3257.

(12) (i) M. J. Palframan and G. Pattenden, *Tetrahedron Lett.*, **2013**, *54*, p324-328. (ii) G. Pattenden and J. M. Winne, *Tetrahedron Lett.,* **2009**, *50*, p7310-7313. (iii)K-S. Cao, H-X Bian, W-H. Zheng, *Org. Biomol. Chem.,* **2015***, 13*, p6449-6452. (iv) J. Hullaert, D. R. Laplace and J. Winne, *Eur. J. Org. Chem.,* **2014**, p3097-3100. (v) D. R. Laplace, B. Verbraeken, K. V. Hecke and J. Winne, *Chem. Eur. J.,* **2014**, 253 – 262. (vi) D. R. Laplace and J. M. Winne, *Synlett,* **2015**, *26*, p467-470. (vii) Y. Liu, Z. Sun, S. Li, K. Xiang, Y. Zhang and Y. Li, *RSC Adv.,* **2016**, *6*, p26965-26958. (viii) J. M. Winne, S. Catak, M. Waroquier and V. V. Speybroeck, *Angew. Chem. Int. Ed.,* **2011**, *50*, p11990-11993. (ix) J. Zhang, L. Li, Y. Wang, W. Wang, J. Xue and Y. Li, *Org. Lett.,* **2012**, *14*, p4528-4230.

(13) C. Liu, B. Pan and Y. Gu, *Chinese Journal of Catalysis*, **2016**, *37*, p979-986.

(14) Z. Li, Z. Duan, H. Wang, R. Tian, Q. Zhu and Y. Wu, *Synlett,* **2008,** *16*, p2535-2539.

(15) S. R. Angle and M. S. Louie, *Tet. Lett.,* **1989**, *30(42)*, p5741-5744.

(16) C. S. Schneider and K. H. Pook, *J. Chem. Soc. Perkin Trans. I,* **1986**, p877-883.

(17) K. Mertins, I. Iovel, J. Kischel, A. Zapf and M. Beller, *Adv. Synth. Catal.,* **2006**, *348*, p691-695.

(18) M. Noji, T. Ohno, K. Fuji, N. Futaba, H. Tajima and K. Ishii, *J. Org. Chem.,* **2003**, *68*, p9340-9347.

(19) a) D. Paul, S. Das, S. Saha, H. Sharma, R. Kumar Goswami, *Eur. J. Org. Chem.*, 10.1002/ejoc.202100071; b) K. C. Nicolaou, P. G. Bulger and D. Sarlah, *Angew. Chem. Int. Ed.*, **2005**, *44*, p4442-4489.

(20) a) M. Burwood, B. Davies, I. Diaz, R. Grigg, P. Molina, V. Sridharan, M Hughes, *Tetrahedron Lett.*, **1995**, *36*, p9053-9056; b) A. Padwa, M. A. Brodney, S. M. Lynch, *J. Org. Chem.*, **2001**, *66*, p1716-1724.

(21) B. Štefane, U. Grošelj, J. Svete, F. Požgan, D. Kočar, H. B. Žugelj, *Eur. J. Org. Chem.*, **2019**, *2-3*, p432-441.

(22) C. Hughes and D. Trauner. *Tetrahedron.* **2004**, 60, 9675-9686.

(23) H. Pickford, Part II Thesis, University of Oxford, 2017.

(24) J. Liu, X. Xu, J. Li, B. Liu, H. Jiang and B. Yin, *Chem. Commun.*, **2016**, *52*, p9550-9553.

(25) G. Kachkovskyi, C. Faderl and O. Reiser, *Adv. Synth. Catal.,* **2013**, 355, p2240-2248.

(26) X. Zhang, J. Liu, Y. Yang, F. Wang, H. Jiang and B. Yin, *Org. Chem. Front.*, **2016**, *3*, p1105-1110.

(27) R. Balfour, Part II Thesis, University of Oxford, 2018.

(28) L. Schrenker , Part II Thesis, University of Oxford, 2019.

(29) S. B. Bhorkade, K. B. Gavhane and V. S. Shinde, *Tetrahedron*, **2016**, *72*, p1954-1959.

(30) Correct at time of writing – 18/08/2021 (sigmaalrich.com).

(31) Correct at time of writing – 18/08/2021 (sigmaalrich.com).

(32) The reaction concentration was doubled to allow for safe and practical handling of large volumes of solvent. A jacketed reaction vessel was used to allow for careful monitoring and cooling of the reaction due to the large exotherm produced, both during the reduction and on addition of the 2N aq. HCl. The most dangerous issue which had to be addressed before the reaction was carried out was the containment and disposal of the 1 mole of HCN gas that could possibly be produced on addition of a strong acid to the sodium cyanoborohydride. Although it is unlikely that such a large volume of gas would be evolved due to the partially aqueous reaction mixture and the high solubility of HCN in water, the reaction is very acidic (pH X) and so maximum yield of HCN must be assumed. A large gas scrubber was attached to the vessel in which and gas evolved was bubbled through 1M NaOH, and on workup all aqueous waste was tested for cyanide and bleached before disposal.

(33) S. B. Bhorkade, K. B. Gavhane and V. S. Shinde, *Tetrahedron*, **2016**, *72*, p1954-1959.

(34) M. Yasuda, Y. Onishi, M. Ueba, T. Miyai and A. Baba, *J. Org. Chem.*, **2001**, *66*, p7741-7744.

(35) T. Korenaga, R. Sasaki and K. Shimada, *Dalton Trans.*, **2015**, *44*, p19642-19650.

(36) J. M. Winne, S. Catak, M. Waroquier, V. Van Speybroeck, *Angew. Chem. Int. Ed.*, **2011**, *50*, p11990-11993.

(37) S. Naidorf-Meir and A. Hassner, *J. Org. Chem.*, **1992**, *57(19)*, p5102-5105.

(38) a) O. O. Stepaniuk, V. O. Matvienko, I. S. Kondratov, O. V. Shishkin, D. M. Volochnyuk, P. K. Mykhailiuk, A. A. Tolmacheva, *SYNTHESIS*, **2012**, *44*, p895-902; b) M. Ya. Bugera, K. V. Tarasenko, I. S. Kondratov, I. I. Gerus, B. V. Vashchenko, V. E. Ivasyshyn and O. O. Grygorenko, *Eur. J. Org. Chem.*, **2020**, p1069-1077.

Chapter 4 : Late-Stage Functionalisation of Trigoxyphin Scaffolds

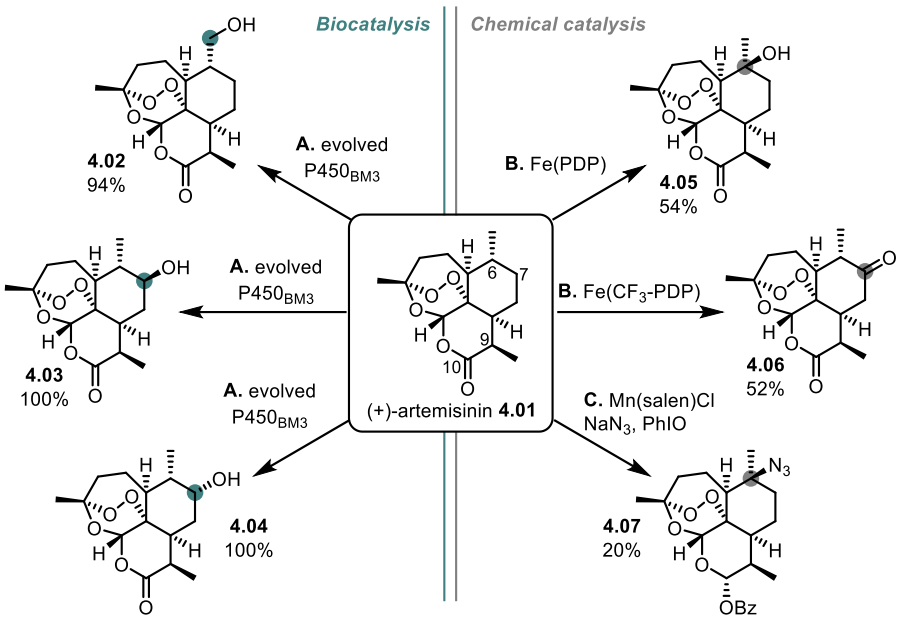
4.1. Introduction

4.1.1. Late-stage functionalisation in synthesis

Through major advancements in organic synthesis, the late-stage functionalisation (LSF) of complex scaffolds *via* C–H activation has become an integral tool in both academia and industry. With the development of highly chemo-selective methodologies, with high functional group tolerance and without the requirement for pre-installation of specific functionalities, LSF approaches can offer a rapid way to generate analogues of compounds of interest. Excellent reviews on this topic cover how effective LSF strategies can be applied to the industrial syntheses of drug-like compounds.[1]

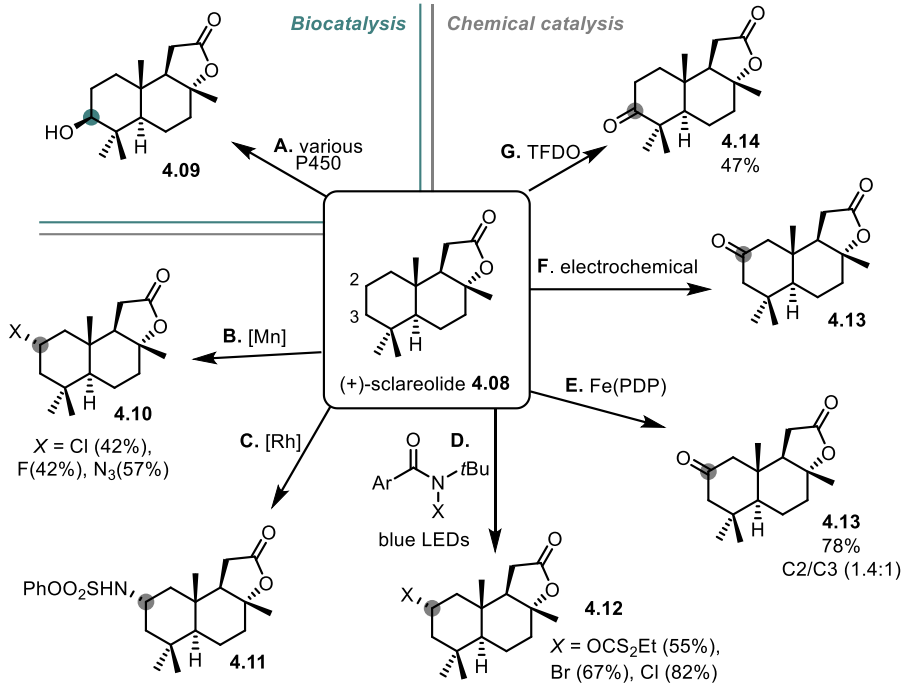
4.1.1.1. Chemo- *vs* bio- catalysis for late-stage functionalisation

Examples of such LSF strategies, using either chemical or biological approaches, have been implemented in the functionalisation of two important compounds: artemisinin and sclareolide. Artemisinin **4.01** is a sesquiterpene lactone used in the treatment of human malaria and has been the aim of considerable synthetic efforts to modify its structure in the search for improved anti-malarial agents.[2] Focus has traditionally revolved around modification at the C9/C10 positions of the lactone ring as these are readily accessible by chemical methods; however, recently there have been reports of functionalisation of the cyclohexane ring. Accessing other positions would be highly valuable to explore further chemical space. Fasan employed engineered $P450_{BM3}$ to obtain previously inaccessible C7 alcohols (*R*) **4.03** and (*S*) **4.04** in 100% yield, and hydroxymethyl metabolite **4.02** in 94% using highly evolved enzymes containing up to seventeen mutations.[3] Using the White Fe(PDP) catalyst (discussed in *Chapter 1*), regioselective hydroxylation at C6 was achieved giving **4.05** in 54% yield,[4] and using the more sterically hindered CF_3 modified catalyst yielded ketone **4.06** in a similar 52% yield (*Scheme 1.B*).[5] Groves showed that a manganese-catalysed functionalisation at C6 produced azide **4.07**, albeit in low yield (S*cheme 1.C*).[6]



Scheme 1 – Selected examples for the comparison of bio- and chemo- catalytic methods for the late-stage functionalisation of artemisinin. A) Biocatalytic reactions were performed on 0.4 g scale achieving isolated yields of >90% of **4.02**, **4.03** and **4.04**.

The sesquiterpene lactone sclareolide **4.08** is often used a model substrate for C–H functionalisation reactions due to the electronically and sterically varied range of C–H bonds, albeit not containing any C(sp^2)–H bonds. In separate reports Bell and Renata reported the biocatalytic hydroxylation at C3 using engineered P450s (*Scheme 2.A*).[7] Similarly to the previous example with artemisinin, Groves' Mn-porphyrin catalysed C–H functionalisation was used to perform a C2 selective halogenation and azidation (*Scheme 2.B*). Both Baran and Du Bois reported on the use of a rhodium catalyst which could achieve nitrene insertion selectively at C2, giving **4.11** in 98% and 60% yields, respectively (*Scheme 2.C*).[8] Work by the Alexanian group described the visible light mediated chlorination,[9] bromination[10] and xanthylation[11] of sclareolide using *N*-centered radicals (*Scheme 2.D*): this allowed the introduction of a range of functionalities in moderate to very good yields (55 – 82%) with high selectivity. C2 ketone **4.13** could be formed either using the classic Fe(PDP) catalyst for sp^3 C–H functionalisation,[12] or by electrochemical oxidation,[13] and selectivity for the C3 ketone **4.14** could be achieved using methyl(trifluoromethyl)dioxirane[13] (*Scheme 2.G*).



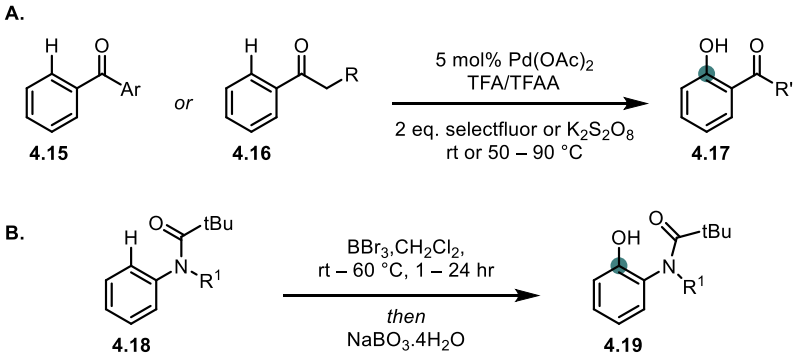
Scheme 2 - Selected examples comparing bio- and chemo- catalytic methods for the late-stage functionalisation of sclareolide **4.08**.

These examples highlight how complementary bio- and chemo-catalytic approaches can be employed to access different C–H bonds in complex natural products. Depending on the desired outcome it is possible to achieve high selectivity for specific substrates using highly evolved enzymes; or a variety of chemical reagents capable of functionalising a range of compounds.

4.1.2. Aromatic hydroxylation

Many elegant methods now exist for the direct functionalisation of C(sp^3)–H bonds; however, for the purposes of this project, and the synthesis of trigoxyphin, we are more interested in aromatic hydroxylation. The direct hydroxylation of arenes, especially in complex molecules containing diverse functionality, is one of the most challenging transformations in organic chemistry. Two major challenges relate to this transformation: (1) ***reactivity*** – aryl C(sp^2)–H bonds are inherently inert and any phenol products, being in general more electron rich, are susceptible to over-reaction with electrophilic sources of OH, and (2) ***selectivity*** – oxidation of more reactive positions, including C(sp^3)–H bonds with lower bond dissociation energies, in diverse and complex substrates.

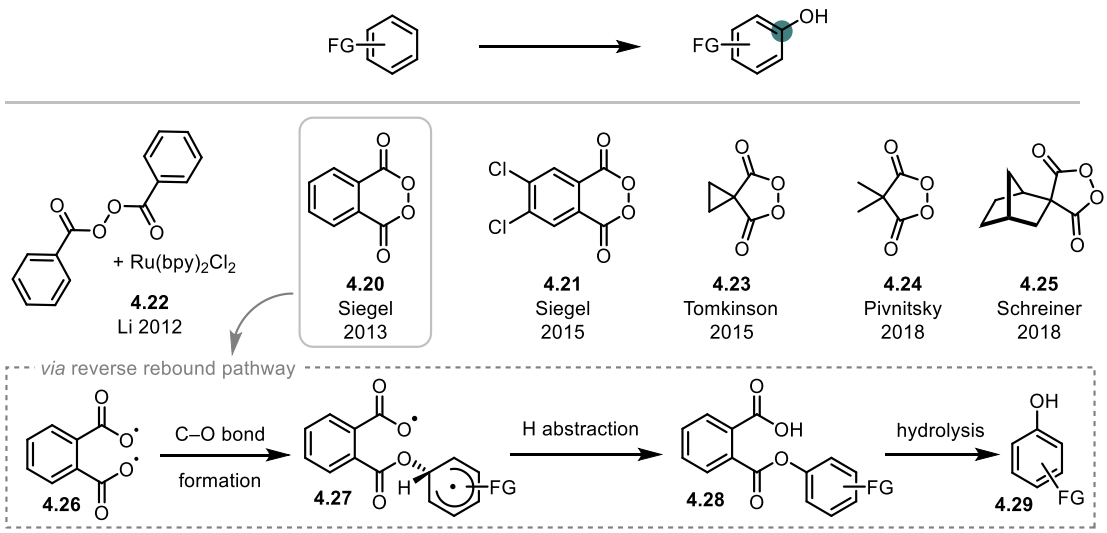
Early examples of this reaction include electrophilic aromatic substitutions involving strong Lewis acids and stoichiometric amounts of oxidant,[14] or transition metal-catalysed oxidative reactions.[15] Directed C–H functionalisation often uses metals such as palladium, which react *via* metallocycles to form a C–O bond at a specific neighbouring site. Directing groups are often nitrogen-based;[16] however, Rao reported the *ortho*-hydroxylation of aryl ketones **4.15** and 4.**16** under mild conditions, as described in *Scheme 3.A*, without the need for exclusion of air or water.[17] Such methods traditionally use expensive novel metal catalysts, based on Pd, Rh, Ru and Ir; however, Shi used a borylation/oxidation strategy to overcome this limitation (*Scheme 3.B*).[18]



Scheme 3 – Selected examples of directed *ortho*-hydroxylation of arenes.

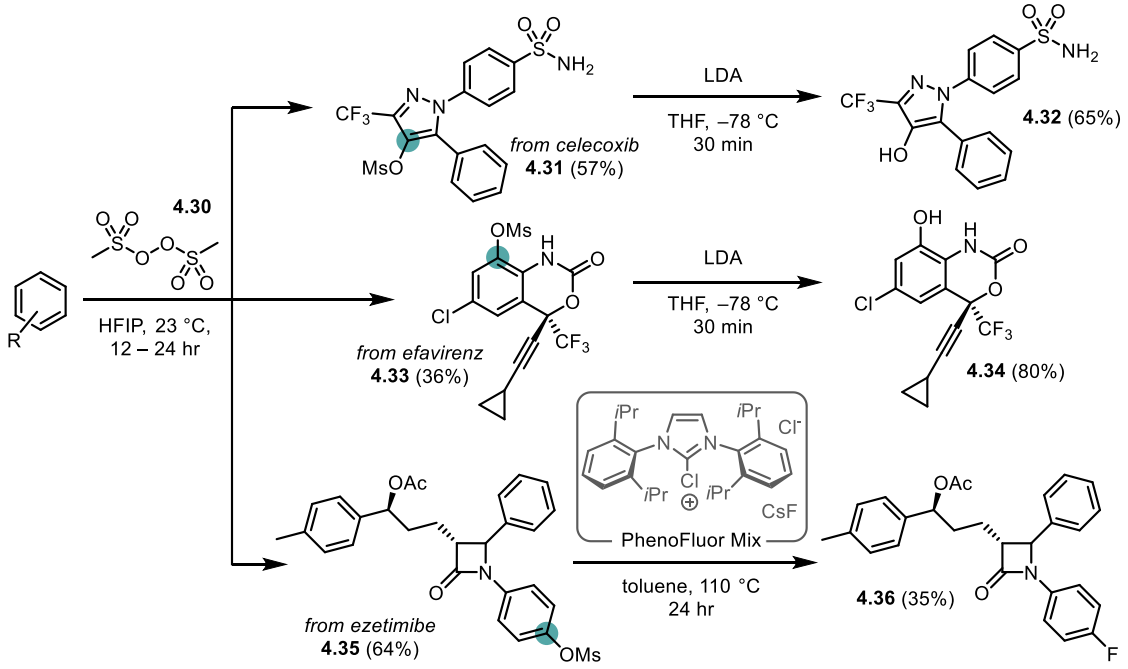
Seminal work by Siegel bypassed previous issues such as over-oxidation and harsh reaction conditions, by using phthaloyl peroxide **4.20** to achieve this overall transformation *via* a reverse-rebound mechanism (S*cheme 4*).[19] The mechanism was proposed to proceed through the diradical 4.**26** reacting with the arene to form the C–O bond in cyclohexadienyl radical **4.27**; H-atom abstraction by the remaining benzoyloxy radical produces *O*-acylphenol **4.28** which releases the phenolic product **4.29** upon hydrolysis.

The main drawback of this method is that it is limited to electron-rich arenes; however, a subsequent report from the same group showed that dichlorophthaloyl peroxide **4.21** was able to oxidise more electron deficient aromatic systems, thus expanding the scope of this methodology.[20] Many groups, including those of Li,[21] Tomkinson[22] and Pivnitsky[23] and have also reported the use of various organic peroxides (**4.22 – 4.24**) for aromatic hydroxylation. Following on from Siegel's report, Schreiner developed a sterically demanding peroxide **4.25** which was easy to synthesise, to achieve highly regioselective aryl oxidation.[24]



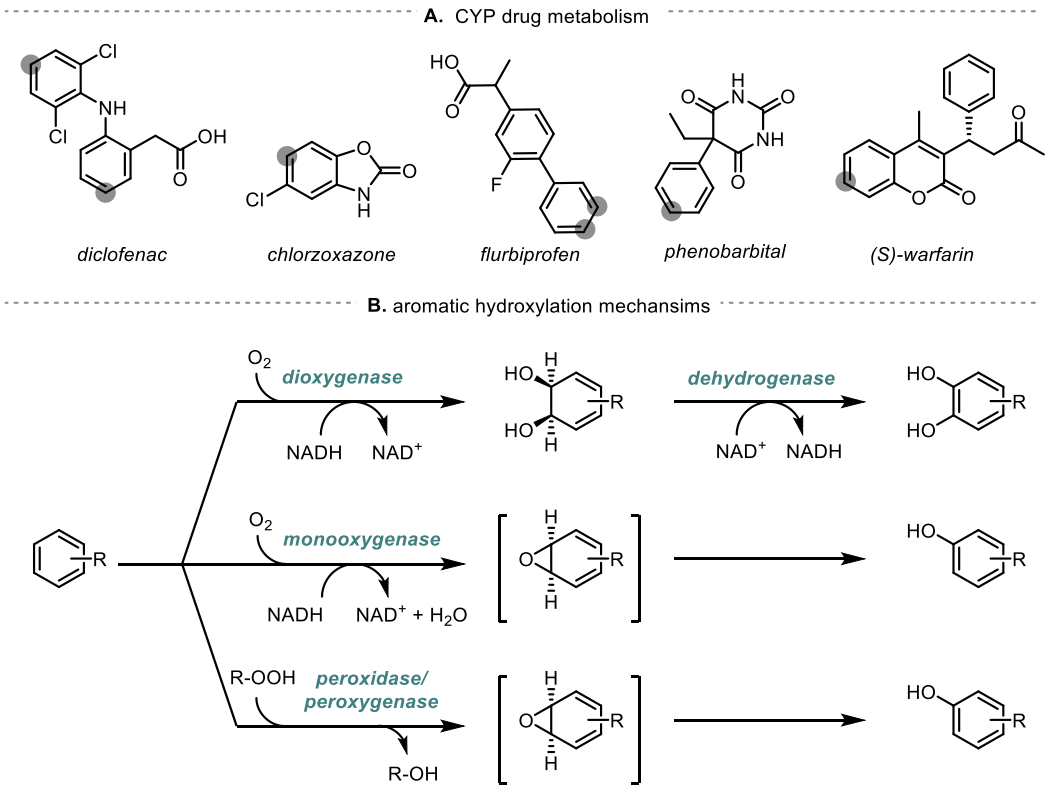
Scheme 4 – The use of organic peroxides for the direct hydroxylation of arenes.

Following on from this work, Ritter reported the use of bis(methanesulfonyl) peroxide **4.30**, which shows a wider substrate tolerance than previous cyclic peroxides and was able to oxidise both electron-rich and electron-poor arenes, including a range of complex pharmaceutical compounds (*Scheme 5*).[25] In comparison to the mechanism proposed by Siegel, the high functional group tolerance with this system is suggested to be due to the formation of a charge-transfer complex which favours arene functionalisation rather than H-abstraction chemistry. Deprotection of selected aryl mesylates was demonstrated, yielding the free phenols **4.32** and **4.34**, and fluorination using PhenoFluor mix[26] was also possible to yield compound **4.36**.



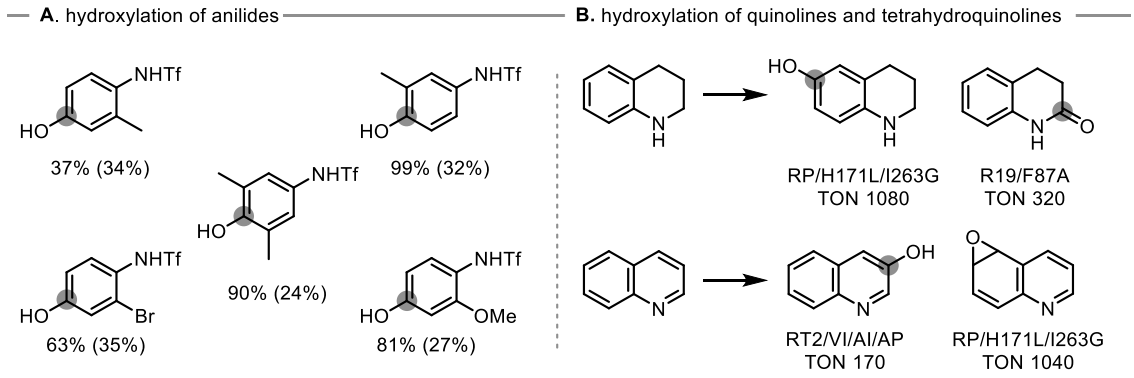
Scheme 5 – Selected examples of drug functionalisation reported by Ritter.

Enzymes are capable of undirected, yet highly selective, aromatic oxidations in a range of functionalised structures. The catabolism of many drug compounds occurs through cytochrome P450 (CYP) pathways,[27] some of which are shown in *Scheme 6.A* with the sites of CYP oxidation highlighted. The generally-accepted mechanism of how CYP catalyses aromatic hydroxylation is described in *Scheme 6.B* (monooxygenase), along with dioxygenases which also use O_2 as the oxygen source, and peroxygenases which use peroxides.[28]



Scheme 6 – A) CYP metabolism of selected drugs with grey dots indicating sites of aromatic hydroxylation;[29] B) mechanistic pathways of enzymatic aryl hydroxylation.

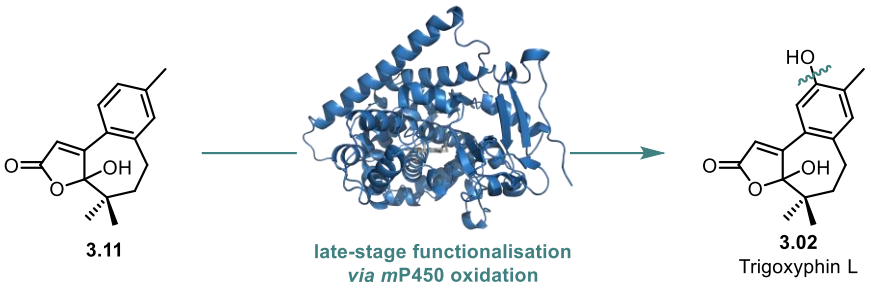
Reports from within the group show that the Wong group library of $P450_{BM3}$ mutants is capable of selective aromatic hydroxylation. The direct hydroxylation of a range of anilides was achieved in excellent conversion and moderate isolated yields; notably, selective oxidation of C(sp^2)–H bonds could be achieved in the presence of C(sp^3)–H bonds (*Scheme 7.A*).[30] Furthermore, aromatic hydroxylation of quinolines and tetrahydroquinolines could be achieved with high TON, as can be seen *Scheme 7.B*.[31]



Scheme 7 – Examples of aromatic hydroxylation of (A) anilides and (B) (tetrahydro)quinolines using the Wong library of $P450_{BM3}$ mutants. Substrate conversion percentages were measured by GC analysis, with isolated yield in parentheses.

4.1.3. Aims of this project

Natural products trigoxyphin K **3.01** and L **3.02** were considered to be ideal targets to test a late-stage functionalisation approach, as both contain an aromatic hydroxy functionality which we envisaged could be installed using our current library of $P450_{BM3}$ enzymes.



Scheme 8 – Proposed key transformation, installing hydroxy functionality in the final synthetic step.

4.2. Screening of trigoxyphin model systems with $P450_{BM3}$

3-(*p*-Tolyl)furan **4.37** was employed as a model substrate, to investigate aromatic hydroxylation on the relevant part of the trigoxyphin core. There was minimal activity with most mutants in the initial screening library, with only K19/F87V giving significant conversion (*Figure 1*); however, when preparative scale reactions were attempted with this mutant no products were isolated even though full conversion was achieved. This suggests either oxidation to polar or water-soluble products, unstable metabolites or oligomers which could not be detected.

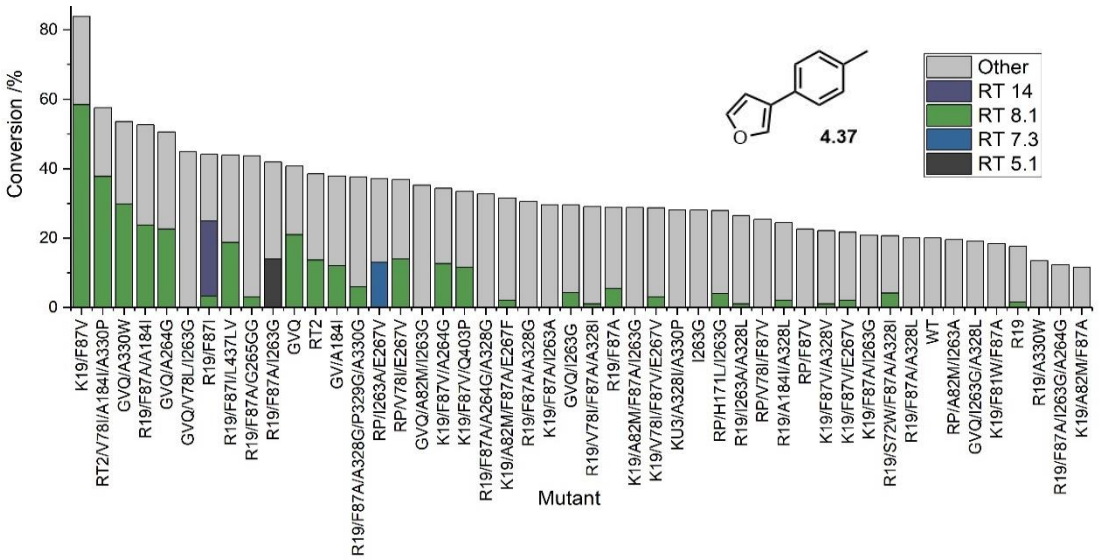


Figure 1 – Screening data for substrate **4.37**, ordered by conversion as measured by GC integration.

Substrate **3.63** was tested as a further model compound, differing from the trigoxyphin cores by replacement of the *gem*-dimethyl functionality with a carbonyl group, and containing no aromatic methyl substituent. High conversion was observed with multiple mutants; however, a lack of product peaks detected by GC analysis suggested either product degradation or the production of metabolites undetectable by this chromatographic method. Mutant R19/F87A/A264G/A328G showed high conversion to metabolite **4.38**, and a preparative scale reaction (0.1 mmol) resulted in a 14% isolated yield of compound **4.38** (*Figure 2*).

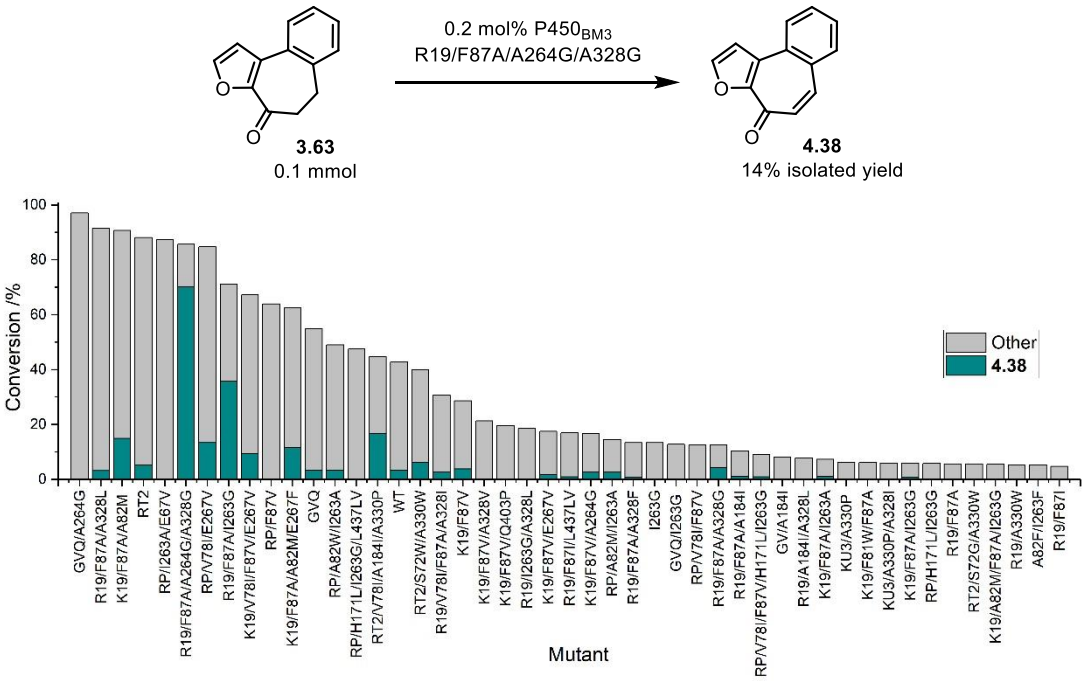
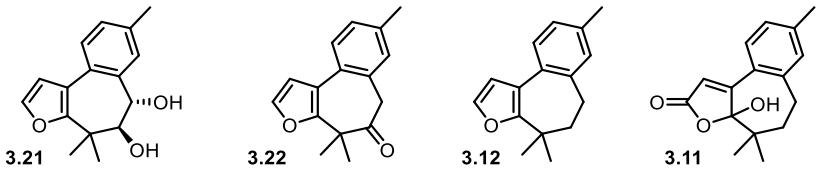


Figure 2 – Screening data and preparative scale reaction using R19/F87A/A263G/A328G for model compound **3.63**.

4.3. Screening of trigoxyphin intermediates with $P450_{BM3}$

With sufficient material of trigoxyphin tricyclic core structures **3.21**, **3.22**, **3.12** and **3.11** in hand, all four compounds were screened against selected P450 mutant libraries to allow the reactivity patterns to be tracked through the related structures.



Scheme 9 – Trigoxyphin core structures that were investigated in this project.

4.3.1. Diol 3.21

WT $P450_{BM3}$ was almost completely inactive towards diol **3.21** and showed only a 4% conversion to product **4.40**; however, the majority of mutants screened gave very high conversion (>80%). The data in *Figure 3* shows that out of the 45 mutants tested: 15 mutants gave 100% conversion, a further 14 giving 90 – 100%, with only 11 giving <60% conversion. Even in examples in which conversion was low, the selectivity was consistently extremely high.

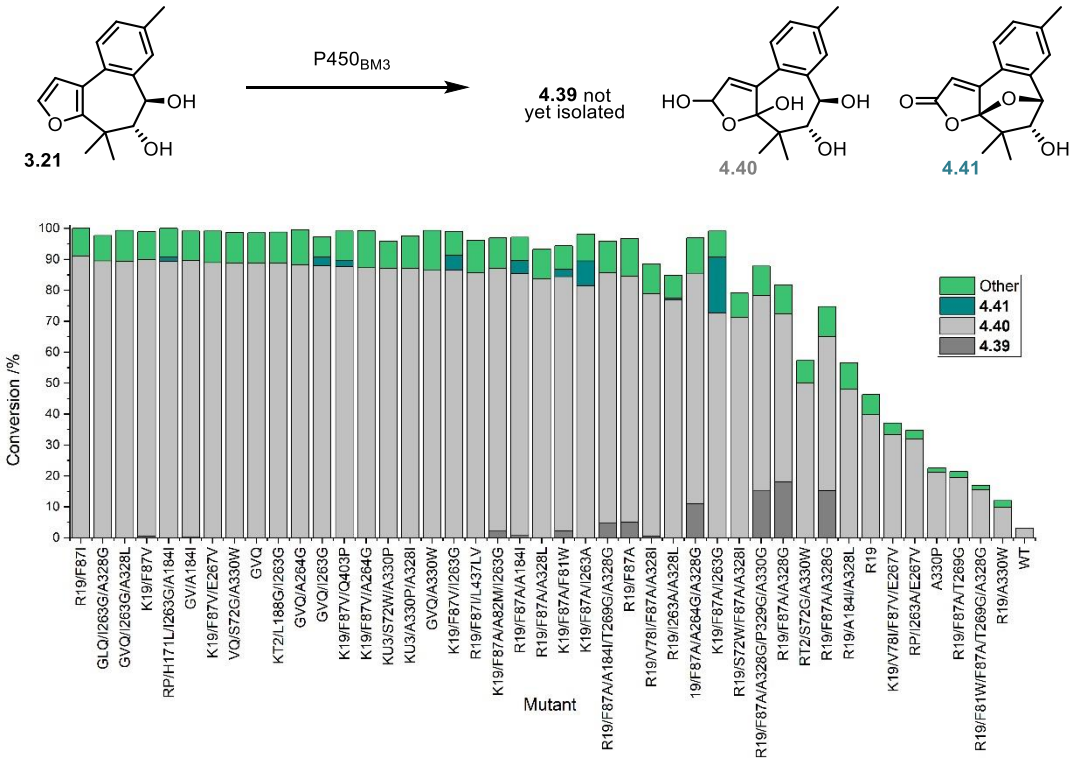
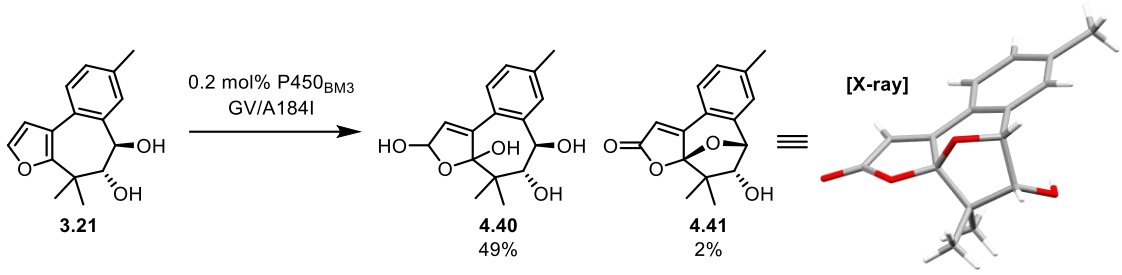


Figure 3 – Screening data for diol **3.21**, ordered by conversion to major metabolite **4.40**.

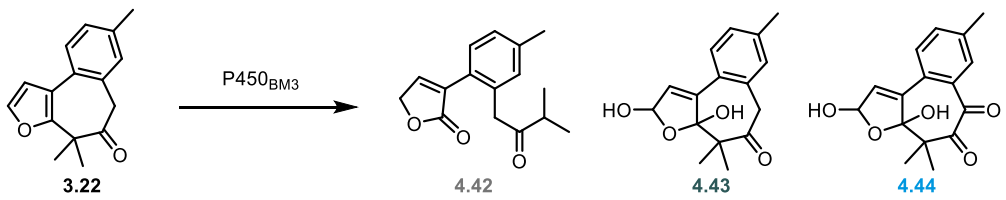
Full substrate conversion was achieved with mutant GV/A184I, and a preparative scale reaction (50 mg, 0.19 mmol) was conducted to isolate metabolites **4.40** and **4.41** (*Scheme 10*). Crystallisation of compound **4.41** was achieved by vapour diffusion (CH_2Cl_2/hexane/pentane) to support the structure assignment by single crystal X-ray crystallography.



Scheme 10 – Isolated metabolites from reaction of substrate **3.21** with GV/A184I.

4.3.2. Ketone 3.22

Our initial panel of 48 $P450_{BM3}$ mutants proved to be considerably less active towards ketone substrate **3.22**, compared to diol **3.21**, with more than half achieving <50% conversion (*Figure 4*). Multiple mutants including R19/F98I, R19/F87I/A328G, GVQ/A328G and GVQ were >90% selective for metabolite **4.45**, which has yet to be isolated. Mutant R19/F87A/A264G/A328G achieved ~20% conversion toward ketone product **4.42**, *via* oxidative cleavage of the seven-membered ring, and identified from a characteristic isopropyl proton in the ^{1}H NMR spectra appearing as a septet. Mutants GLQ/I263G/A328G and RP/A82M/I263A provided >90% conversion and selectivity for tentatively assigned product **4.43**, which was further oxidised to diketone product **4.44** in small quantities with mutants R19/F87A/A328L and KT2/L188G/A263G.



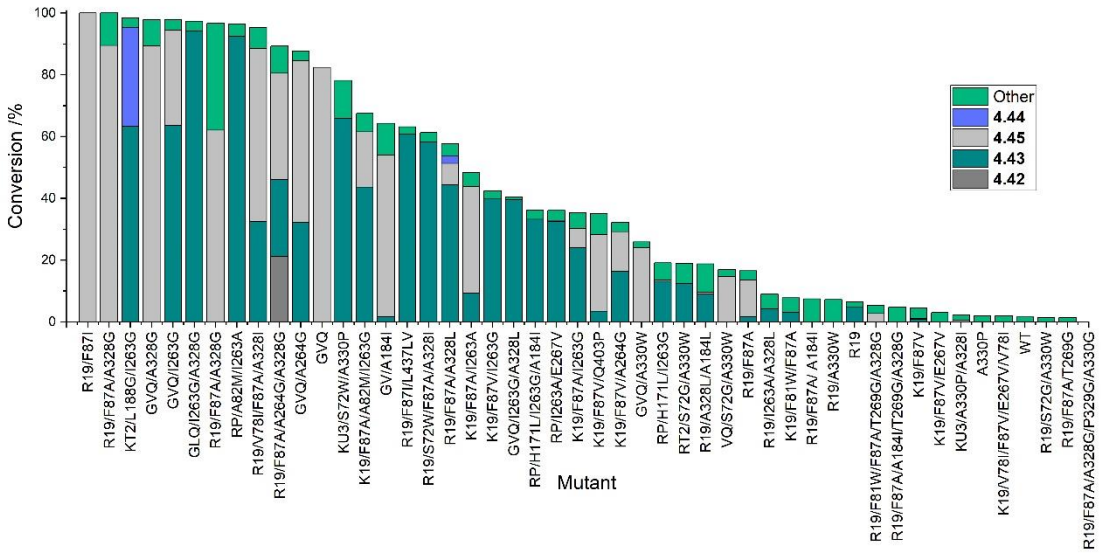


Figure 4 – Screening data for substrate **3.22**, ordered by overall conversion as measured by GC.

4.3.3. Furan 3.12

Out of the 48 P450$_{BM3}$ mutants screened, only 23 showed activity towards furan substrate **3.12** and the metabolites **4.46** and **4.47** are also products of furan oxidation (*Figure 5*). Mutants GVQ and K19/F87V show >70% selectivity, but moderate conversion, towards metabolite **4.47**; however, further isolation of products is required to evaluate the full reactivity profile of this substrate.

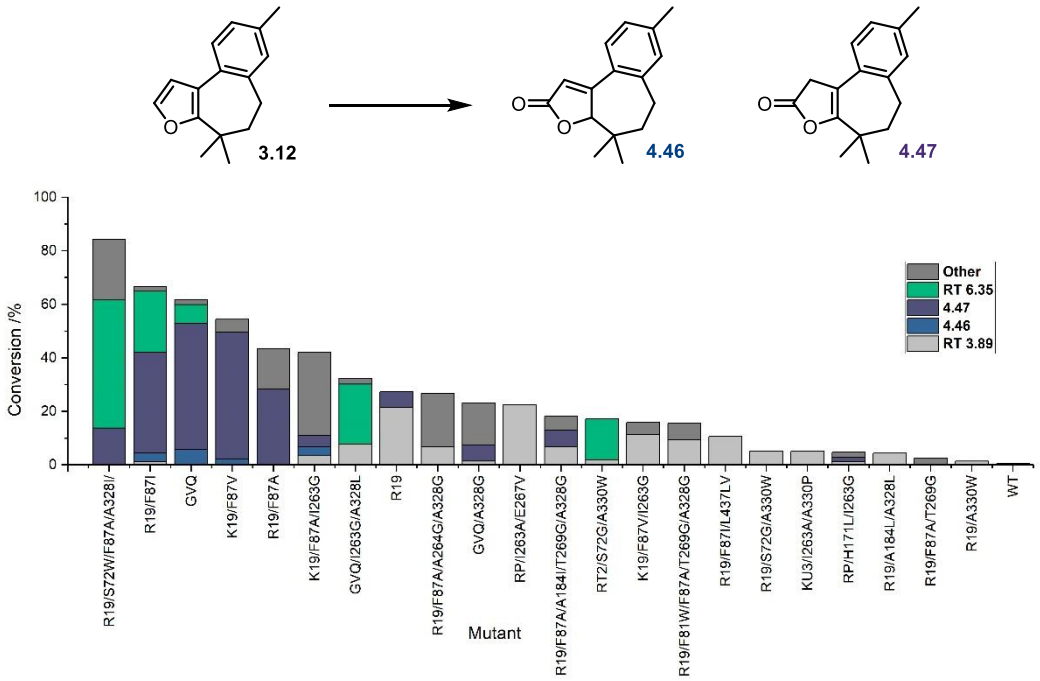


Figure 5 – Mutants which showed conversion of furan **3.12**, ordered by conversion as measured by GC.

4.3.4. Hydroxy-butenolide 3.11

When using hydroxy-butenolide **3.11** as substrate, the main product observed was that derived from hydroxylation of the aromatic methyl group, of which a graphical representation of the selectivity to **4.48** and overall conversion is shown in *Figure 6* (full data in *Chapter 5: Section 5.3.6.1.*). Mutant A3 (R47L/Y51F/I263R) was chosen to scale up because of its high conversion and high selectivity, and **4.48** was isolated in 94% yield.

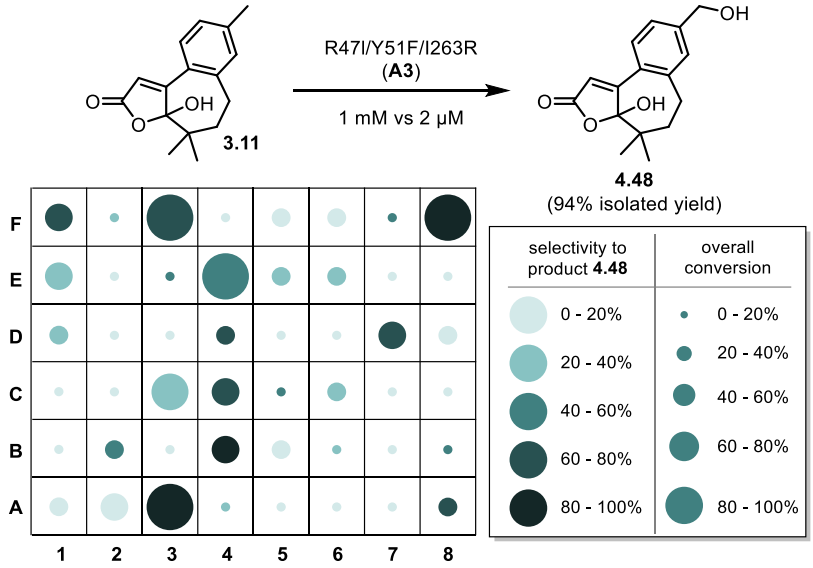
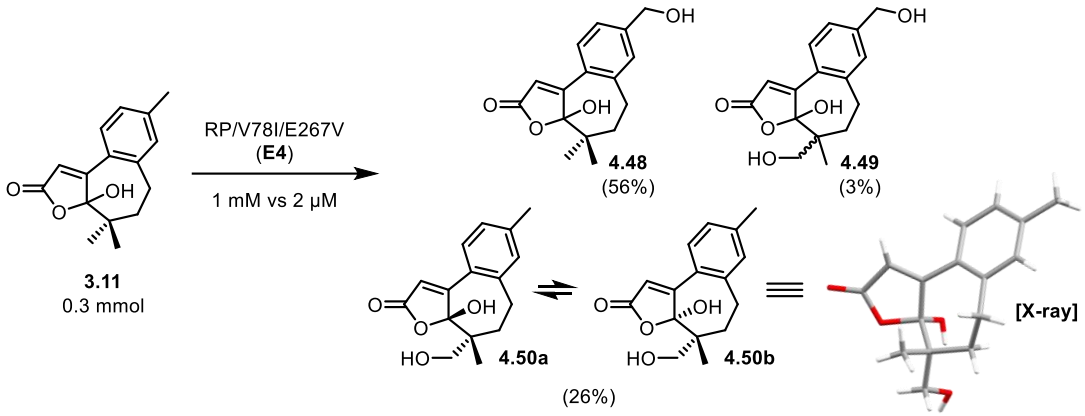


Figure 6 – Graphical representation of the initial screening data over 48 mutants with substrate **3.11**, and preparative scale reaction (0.05 mmol) with R47L/Y51F/I263R. Colour depicts % selectivity to product **4.48** (calculated by peak area ((benzylic product **4.48**/overall conversion)*100)), and size depicts overall % conversion as measured by GC.

Mutant RP/V78I/E267V (**E4**) achieved high conversion (83%) but low selectivity (58%), which is advantageous for isolating a diverse range of metabolites, and so a preparative scale reaction was carried out using this mutant (*Scheme 11*). Hydroxylation on both -CH_3 groups of the *gem*-dimethyl was observed, and recrystallisation of diastereomer **4.50b** by vapour diffusion (CH_2Cl_2/hexane/pentane) allowed for the relative configuration to be determined as that shown by single crystal X-ray crystallography. These compounds were isolated as a mixture, leading to the possibility that only one methyl group is hydroxylated but that the hemiacetal is unstable, in

equilibrium with the keto-acid, resulting in both diastereomers. A small amount of di-hydroxylated compound **4.49** was also obtained, along with 56% of major metabolite **4.48**.



Scheme 11 – Isolated yields of metabolites from preparative scale reaction of **3.11** with RP/V78I/E267V.

X-ray crystal structure of metabolite **4.50b,** which crystalised as a single enantiomer.

Benzylic alcohol **4.48** was the major product observed in all screening data, and RP/H171L/I263G-based mutants generally achieved the highest selectivity (*Table 1*).

Entry	Mutant	Conversion /%	4.48 /%	TTN	Selectivity /%
1	R47L/Y51F/I263R	81	70	406	87
2	RP/H171L/I263G	99	83	495	84
3	RP/H17L/I263G/A184I	42	34	209	81
4	RP/H17L/I263G/F87V/V78I	31	24	155	78
5	RP/H17L/I263G/A330W	43	31	213	73

Table 1 – Mutants with the highest conversion to product **4.48**, ordered by selectivity.

A further set of 19 RP/H171L/I263G-related mutants were screened (full data in *Chapter 5, Section 5.3.6.2*); however, GC traces showed low concentration, suggesting either issues with extraction or oxidation products which aren't detected using GC method (*Figure 7*). Aromatic hydroxylation products, such as desired trigoxyphin phenol **3.02**, possibly have too high BP to be detected using this analytical method and so a lack of peaks could indicate high conversion of substrate to phenolic metabolites. As such, preparative scale reaction using RP/I263G was conducted as it showed full conversion of starting material **3.11**; however, poor mass recovery was observed and only product **4.48** was isolated in <10% isolated yield.

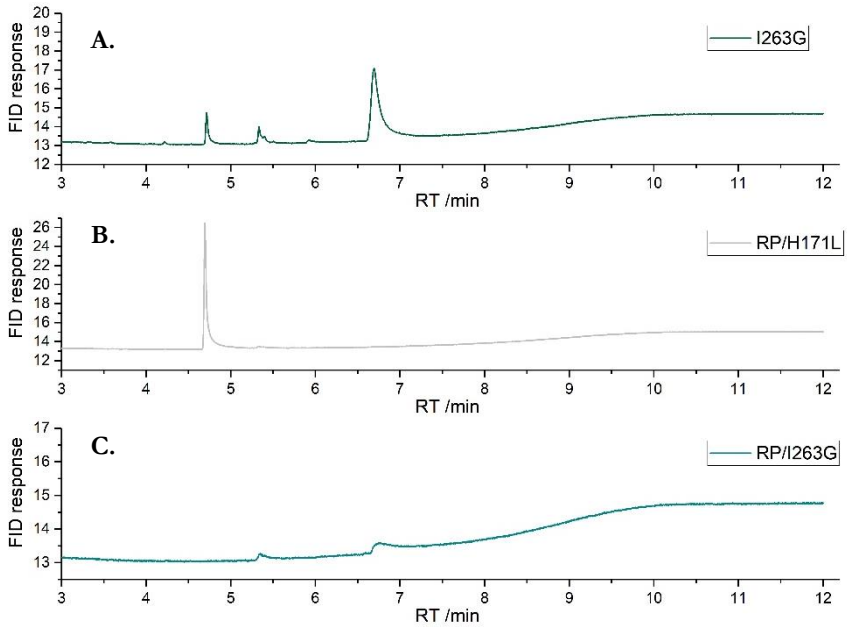


Figure 7 – GC traces highlighting high conversion of substrate **3.11**, but low mass recovery indicated by low concentration of the GC sample after extraction.

To further explore this issue, 13 new RP/H171L/I263G-based mutants[32] were screened to determine if extraction was the cause of the low product recovery (full data in *Chapter 5, Section 5.3.6.2*). Samples of each reaction were taken before extraction and ran directly on the LCMS as a solution in water, and the product profile of these matched the traces observed using GC. The data displayed in *Figure 8* shows the results after extraction using EtOAc and analysis using GC. High selectivity, and full conversion, was achieved with RP/H171L/I263G/L437LV/L188F and /L75M; however, the sample concetration was still low. The remaining reaction volume was acidified using conc. HCl, and re-extracted using EtOAc, to identify if any deprotonated metabolites were remaining in the basic reaction buffer. GC analysis of these samples revealed identical reacitivty profiles of the non-acidified samples, suggesting that one extraction was not fully recovering all material, but was recovering all products in a representative manner. This indicates that phenolic products are not being produced using these RP/H171L/I263G/L437LV-based mutants, or are produced in quantities too low for detection using current methods.

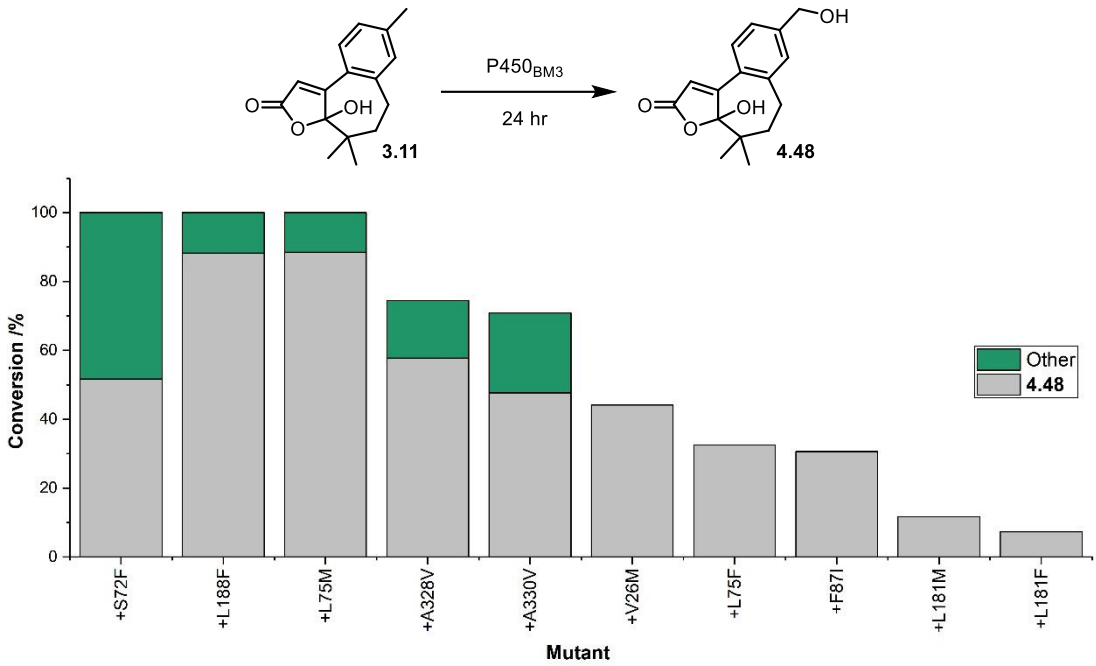
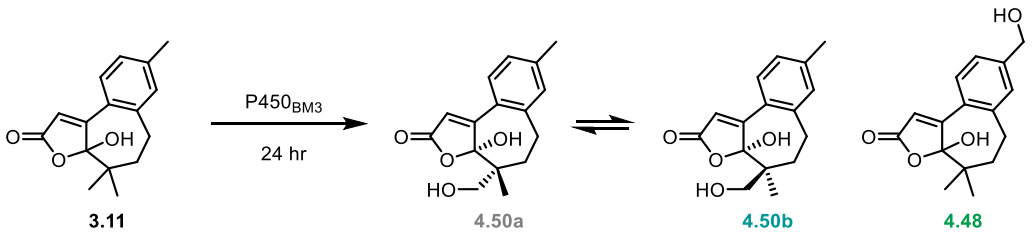


Figure 8 – Chart to show RP/H171L/I263G/L437LV-based mutants for conversion to **4.48**.

Substrate **3.11**, originally screened in 2017, was re-screened using more recently devloped mutants using LCMS to analyse the samples ensuring that phenolic products, or any new metabolites, are not produced, as opposed to simply not detected using GC. Considerably higher conversions were observed across the 2021 $P450_{BM3}$ mutant libray, than were achieved from the 2017 library; with higher yield to products other than the predominant metabolite **4.48** as previous (*Figure 9*). Notably, analysis using LCMS did not reveal any further products when compared with the traces obtained using GC. These results demonstrate how in a few generations of enzymes, the evolution of new P450 mutants within our library have lead to considerably higher activities with non-natural substrates, achieving high levels of conversion and selectivity for the oxidation of complex structures.



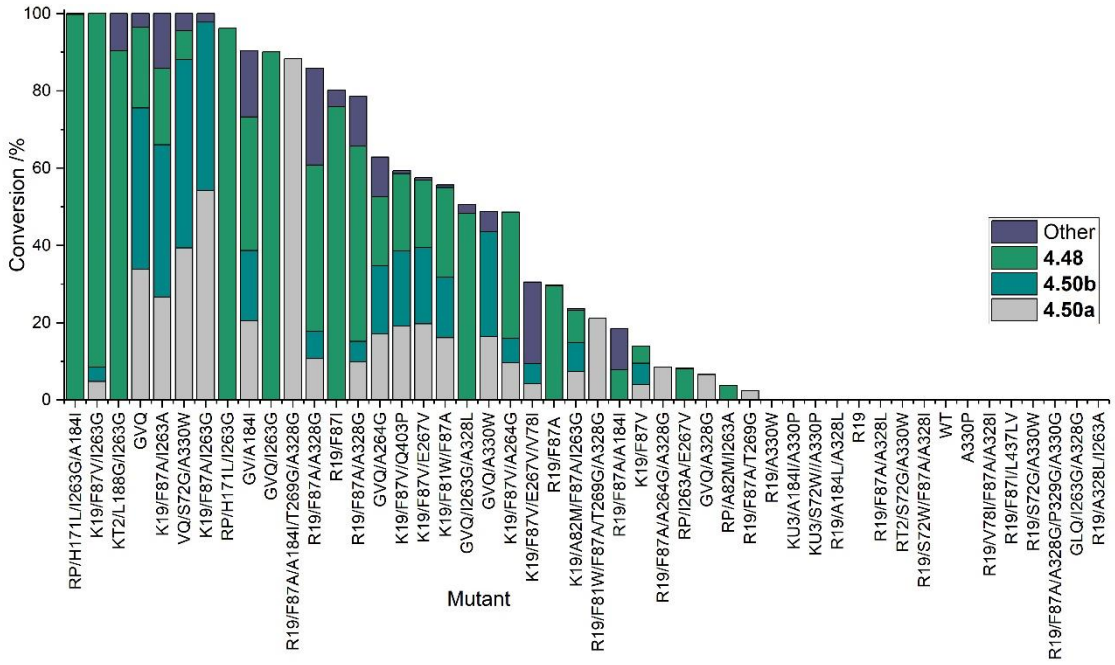


Figure 9 – Graph to show new screening data for substrate **3.11**, overed by conversion and measured by GC.

Although aromatic hydroxylation to afford trigoxyphin **3.02** was not observed, the consistent production of benzylic alcohol **4.48** suggested that substrate **3.11** was positioned in the desired orientation in the active site. As previously discussed in *Chapter 2.5.* docking into MD-simulated protein structures provided a tool for visualisation and a potential guide for mutagenesis. From replica1/cluster1 (R1/C1) there was only one productive pose but this did correctly predict the experimentally observed product (*Figure 10*). Residues within 4 Å of unproductive poses are shown in *Figure 10*, as these could be potential sites for mutagenesis during future work.

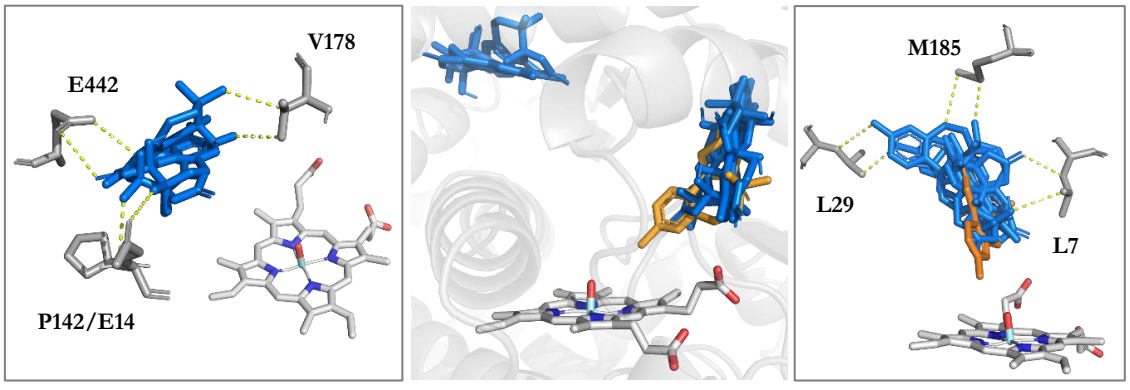
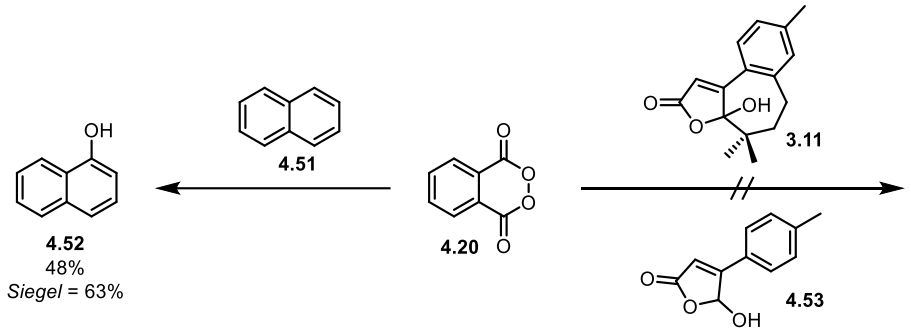


Figure 10 – R1/C1 poses docked into the MD simulated protein structure of R47L/Y51F/I263G (from PDB ID: 1JPZ); unproductive poses are shown in blue, with potentially interacting residues highlighted, and the productive pose is shown in orange.

4.4. Chemical late-stage functionalisation

Late-stage hydroxylation by chemical means was also explored, both as a comparison to the enzymatic method, and as an alternative route to achieve the synthesis of trigoxyphin L **3.02** *via* late-stage functionalisation. As previously discussed, pioneering work by Siegel and co-workers had shown phthaloyl peroxide **4.20** to be a suitable reagent for direct aryl hydroxylation. The reported results were reproducible when using electron-rich substrate naphthalene **4.51** to afford 1-naphtol **4.52**; however, electron-poor hydroxy-butenolides **3.11** and **4.53** relevant to this study were found to be completely unreactive and only returned starting material was observed (*Scheme 12*).



Scheme 12 – Unsuccessful attempts to achieve direct aryl hydroxylation of trigoxyphin structures using phthaloyl peroxide **4.20**.

4.5. Conclusions and future work

Interestingly, $P450_{BM3}$ WT was inactive towards all the furan-containing substrates tested, suggesting that it may be possible for aromatic hydroxylation to occur before furan oxidation in the natural product biosynthesis. However, our library of mutants which are evolved to give higher activity and selectivity in comparison to WT, produced only furan oxidation metabolites. Possibly oxidation at other positions occurred, and future work should include isolation of all metabolites which were produced in smaller quantities.

Although aromatic hydroxylation leading to the natural product trigoxyphin **3.02** was not observed, a plethora of related analogues were synthesised. Generating a range of structures similar to a compound of known biological activity, especially at a late-stage in the synthetic route, can be

highly advantageous for pharmacological studies. Through this work we have shown that the mutant $P450_{BM3}$ collection can be used as an excellent tool for diversity-oriented C–H hydroxylation of complex chemical scaffolds (*Figure 11*).

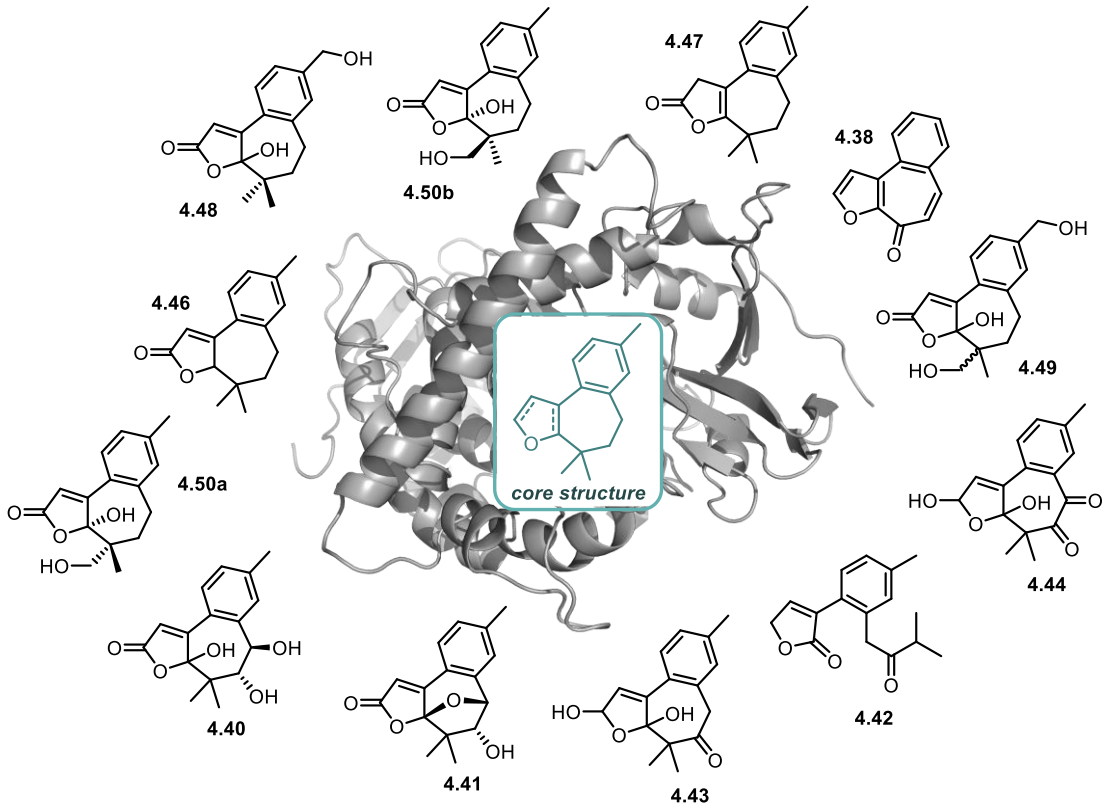


Figure 11 – Diversity-oriented synthesis of trigoxyphin-type scaffolds.

4.6. References for Chapter 4

(1) a) T. Cernak, K. D. Dykstra, S. Tyagarajan, P. Vachel and S. W. Krska, *Chem. Soc. Rev.*, **2016**, *45*, p546-576; b) L. Guillemard, N. Kaplaneris, L. Ackermann and M. J. Johansson, *Nat. Rev. Chem.*, **2021**, *5*, p522-545.

(2) Z. Wang, L. Yang, X. Yang and X. Zhang, *Synth. Commun.*, **2014**, *44*, p1987-3003.

(3) K. Zhang, B. M. Shafer, M. D. Demars II, H. A. Stern and R. Fasan, *J. Am. Chem. Soc.*, **2012**, *134*, p18695-18704.

(4) M. S. Chen, and M. C. White, *Science,* **2007**, *318*, p783-787.

(5) P. E. Gormisky and M. C. White, *J. Am. Chem. Soc.*, **2013**, *135*, p14052-14055.

(6) X. Huang, T. M. Bergsten and J. T. Groves, *J. Am. Chem. Soc.*, **2015**, *137*, p5300-5303.

(7) a) J. Li, F. Li, E. King-Smith and H. Renata, *Nat. Chem.*, **2020**, *12*, p173-179; b) E. A. Hall, R. Sarkar, J. H. Z. Lee, S. D. Munday and S. Bell, *ACS Catal.,* **2016**, *6(9)*, p6306-6317

(8) a) K. Chen, A. Eschenmoser, and P. Baran, *Angew. Chem. Int. Ed.*, **2009**, 48, p9705-9708; b) N. D. Chiappini, J. B. C. Mack and J. Du Bois, *Angew. Chem. Int. Ed.*, **2018**, *57*, p4956-4959.

(9) R. K. Quinn, Z. A. Kӧnst, S. E. Michalak, Y. Schmidt, A. R. Szklarski, A. R. Flores, S. Nam, D. A. Horne, C. D. Vanderwal, E. J. Alexanian, *J. Am. Chem. Soc.*, **2016**, *138*, p696-702.

(10) V. A. Schmidt, R. K. Quinn, A. T. Brusoe, E. J. Alexanian, *J. Am. Chem. Soc.*, **2014**, *136*, p14389-14392.

(11) W. L. Czaplyski, C. G. Na, E. J. Alexanian, *J. Am. Chem. Soc.*, **2016**, *138*, p13854-13857.

(12) M. S. Chen, M. C. White, *Science*, **2010**, *327*, p566-571.

(13) Y. Kawamata, M. Yan, Z. Liu, D. H. Bao, J. Chen, J. T. Starr, P. S. Baran, *J. Am. Chem. Soc.*, **2017**, *139*, p7448-7451.

(14) Z. Rappoport, The Chemistry of Phenols Vols 1 and 2, p395-490 (Wiley-VCH, 2003).

(15) Selected examples include; a) S. R. Neufeldt, M. S. Sanford, *Acc. Chem. Res.*, **2012**, *45*, p936-946; b) M. H. Emmert, A.K. Cook, Y. J. Xie, M. S. Sanford, *Angew. Chem. Int. Ed.*, **2011**, *50*, p9409-9412; c) D. C. Powers, D. Y. Xiao, M. A. Geibel, T. Ritter, *J. Am. Chem. Soc.*, **2010**, *132*, p14530-14536.

(16) Z. Iqbal, A. Joshi and S. R. De, *Adv. Synth. Catal.*, **2020**, *362*, p5301-5351.

(17) G. Shan, X. Yang, L. Ma and Y. Rao, *Angew. Chem. Int. Ed.*, **2012**, *51*, p13070-13074.

(18) J. Lv, B. Zhao, Y. Yuan, Y. Han and Z. Shi, *Nat. Commun.*, **2020**, *11*, p1316.

(19) C. Yuan, Y. Liang, T. Hernandez, A. Berriochoa, K. N. Houk and D. Siegel, *Nature*, **2013**, *499*, p192- 196.

(20) A. M. Camelio, Y. Liang, A. M. Eliasen, T. C. Johnson, C. Yuan, A. W. Schuppe, K. N. Houk and D. Siegel, *J. Org. Chem.*, **2015**, *80*, p8084-8095.

(21) H. Rao, P. Wang and C.-J. Li, *Eur. J. Org. Chem.*, **2012**, p6503-6507.

(22) A. Dragan, T. M. Kubczyk, J. H. Rowley, S. Sproule, and N. C. O. Tomkinson, *Org. Lett.,* **2015**, *17(11)*, p2618-2621.

(23) M. A. Lapitskaya, V. A. Vil', E. D. Daeva, A. O. Terent'ev, K. K. Pivnitsky, *Mendeleev Commun.*, **2018**, *28*, p505-507.

(24) A. Pilevar, A. Hosseini, M. Šekutor, H. Hausmann, J. Becker, K. Turke and P. R. Schreiner, *J. Org. Chem.,* **2018**, *83(17)*, p10070-10079.

(25) J. Börgel, L. Tanwar, F. Berger and T. Ritter, *J. Am. Chem. Soc.*, **2018**, *140*, p16026-16031.

(26) T. Fujimoto and T. Ritter, *Org. Lett.*, **2015**, *17(3)*, p544-547.

(27) T. Lynch and A. Price, *Am. Fam. Physician*, **2007**, *76(3)*, p391-396.

(28) R. Ullrich and M. Hofrichter, *Cell. Mol. Life Sci.*, **2007**, *64*, p271-293.

(29) B. M. El-Haj, S. B. M. Ahmed, M. A. Garawi and H. S. Ali, *Molecules*, **2018**, *23*, 2119.

(30) J. A. O'Hanlon, X. Ren, M. Morris, L.-L. Wong and J. Robertson, *Org. Biomol. Chem.*, **2017**, *15*, p8780-8787.

(31) Y. Li and L.-L. Wong, *Angew. Chem. Int. Ed.*, **2019**, *58*, p9551-9555.

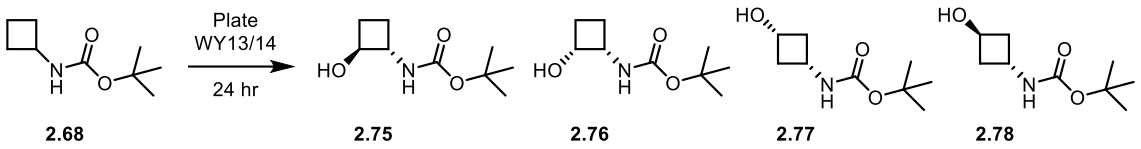
(32) Developed by amazing and brilliant DPhil student V. Barros-Metlova.

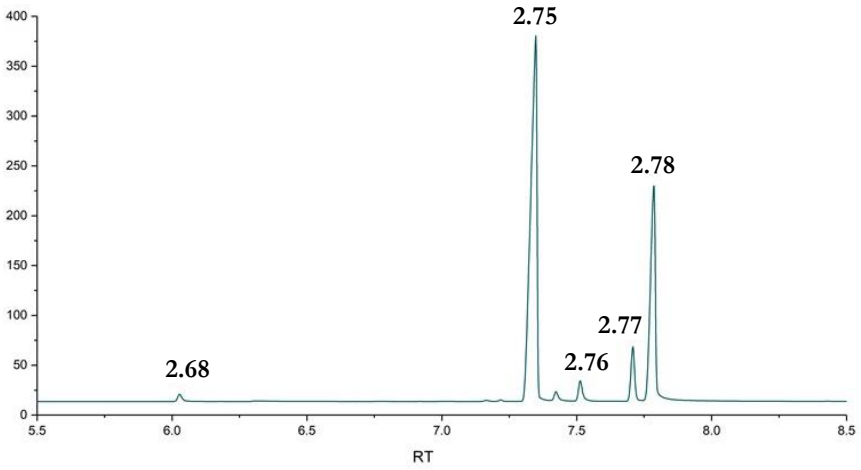
Chapter 5: Appendices

5.1. Appendices for Chapter 2

5.1.1. Screening data for substrate 2.68

5.1.1.1. Initial screening data





Mutant	Conversion /%	2.75 /%	2.76 /%	2.77 /%	2.78 /%	Other /%	TTN
RP/H171L/I263G/A184I	100	68	-	4	20	8	500
GV/A184I	99	9	6	3	71	10	495
RP/H171L/I263G	99	70	2	4	20	3	495
K19/F87V/E267V	98	33	5	4	47	9	490
KU3/A330P/S72W	98	61	28	1	5	3	490
KT2/L188G/I263G	97	79	1	4	12	1	485
K19/F87V/Q403P	97	16	1	4	62	14	485
R19/F87I/L437LV	96	54	1	5	26	10	480
VQ/S72G/A330W	93	26	7	5	51	4	465
GQ/I263G/A328L	91	3	2	33	49	4	455
R47L/Y51F/KSK19	90	63	-	-	13	14	450
K19/F87V/I263G	89	31	1	4	45	8	445
GVQ/A330W	86	22	4	5	43	12	430
GVQ/I263G	85	35	2	5	31	12	425

K19/F87A/I263G	83	42	2	5	28	6	415
R19/F87I	81	45	9	2	23	2	405
GVQ	78	24	3	3	39	9	390
GVQ/I263G/A328L	78	2	-	6	60	10	390
K19/F87V	71	19	7	2	36	7	355
R19/F87A/A328G	71	71	-	-	-	-	355
RT2/S72G/A330W	69	41	11	1	2	14	345
R47L/Y51F/KSK19/A184I	68	34	3	4	22	5	340
RP/A82M/I263A	64	5	8	8	42	1	320
K19/F87A/F81W	62	27	-	4	6	25	310
K19/F87A/I263A	54	13	4	2	29	6	270
R19/F87A/A328I/S72W	51	16	3	9	10	13	255
R19/F87A/A328L	50	8	22	2	10	8	250
GV/A184I/I263G/A328G	48	21	7	2	15	3	240
R19/F87A/A328G/P329G/A330G	43	37	1	-	2	3	215
R19/F87A/F81W/T26G/A328G	41	11	1	-	-	29	205
RP/I263A/E267V	39	17	5	1	12	4	195
K19/F87V/E267V/V78I	36	22	6	1	7	-	180
GVQ/A328G	34	22	6	1	4	1	170
R19/A330W	32	19	6	-	-	7	160
R19/S72G/A330W	31	21	5	-	-	5	155
K19/F87V/A264G	30	3	6	6	15	-	150
R47L/Y51F/K19	25	13	8	-	2	2	125
GVQ/A264G	16	2	2	4	7	1	80
GLQ/I263G/A328G	15	-	-	-	11	4	75
R19/A328L/I263A	12	-	7	-	3	2	60
R19/F87A/A328I/V78I	11	3	1	3	2	2	55
R19/F87A/A328G/A264G	8	5	1	-	-	2	40
K19/F87A/A82M/I263G	4	-	2	-	-	2	20
R19/F87A/A184I/T269G/A328G	4	2	1	-	-	1	20
R19/F87A/T260G	4	2	-	-	-	2	20
A330P	3	1	-	-	1	1	15
KU3/A330P/I263A	1	-	-	-	-	1	5
WT	-	-	-	-	-	-	-

5.1.1.2. Screening of RL/YF/HL/IG- and RP/HL/IG-based mutants for 2.75

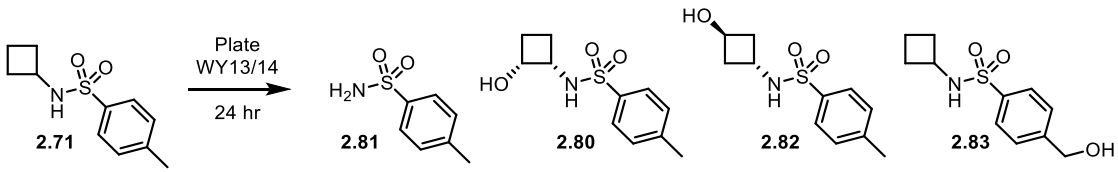
Mutant	Conversion /%	2.75 /%	Other /%	TTN	TON
R47L/Y51F/H171L/I263G/V78I/L437VL	70	59	12	1409	1171
RP/H171L/I263G/L437LV	67	56	11	1343	1126
R47L/Y51F/H171L/I263G/L437VL	64	49	15	1288	989
R47L/Y51F/H171L/I263G	64	31	33	1286	627
R47L/Y51F/H171L/I263G/L437LV	64	51	13	1283	1020
RP/H171L/I263G/A184I	62	44	19	1244	872
R47L/Y51F/H171L/I263G/F81W	58	23	35	1168	462
R47L/Y51F/H171L/I263G/V78I/L47LV	57	45	12	1147	903
R47L/Y51F/H171L/I263G/R398H	44	20	25	889	394
R47L/Y51F/H171L/I263G/K202KPG	43	22	21	863	438
R47L/Y51F/H171L/I263G/L437LA	42	32	11	848	632
R47L/Y51F/H171L/I263G/V78L	41	27	14	815	539
R47L/Y51F/H171L/I263G/V78I/L437LI	41	30	10	812	604
R47L/Y51F/H171L/I263G/V78I/L437LA	39	26	13	785	519
R47L/Y51F/H171L/I263G/L437LF	37	28	10	748	556
RP HL IG	37	27	11	743	530
R47L/Y51F/H171L/I263G/L437LH	35	27	8	700	532
I263G	32	17	15	635	743
H171L/I263G	31	15	16	615	293
RP/H171L/I263G/A330P	31	19	11	611	390
R47L/Y51F/H171L/I263G/A330P	30	17	13	607	347
R47L/Y51F/H171L/I263G/V78I/L327LH	27	17	10	534	344
R47L/Y51F/H171L/I263G/L437LM	23	14	10	469	273
R47L/Y51F/H171L/I263G/V78I/L437LS	21	13	8	427	257
I263S	21	1	20	416	10
R47L/Y51F/H171L/I623S	16	4	13	326	70
R47L/Y51F/H171L/I263G/L437LS	16	10	5	316	208
R47L/Y51F/H171L/I263G/L437S	15	4	11	308	86
R47L/Y51F/H171L/I263G/V78I/L437LM	14	9	5	275	178
R47L/Y51F/H171L/I263G/A82M	9	1	7	173	27
R47L/Y51F/V78L/H171L/I263R	7	5	1	130	109
R47L/Y51F/H171L/I263R	6	5	1	117	98
R47L/Y51F/H171L/I263V	2	1	1	48	18
R47L/Y51F/H171L/I263W	2	1	1	39	25
R47L/Y51F/V78L/H171L/I263V	2	1	1	37	23
I263R	2	1	-	31	26
R47L/Y51F/V78L/H171L/I263W	1	1	-	22	15
RP/H171L/I263R	-	-	1	15	-
I263W	-	-	-	6	8

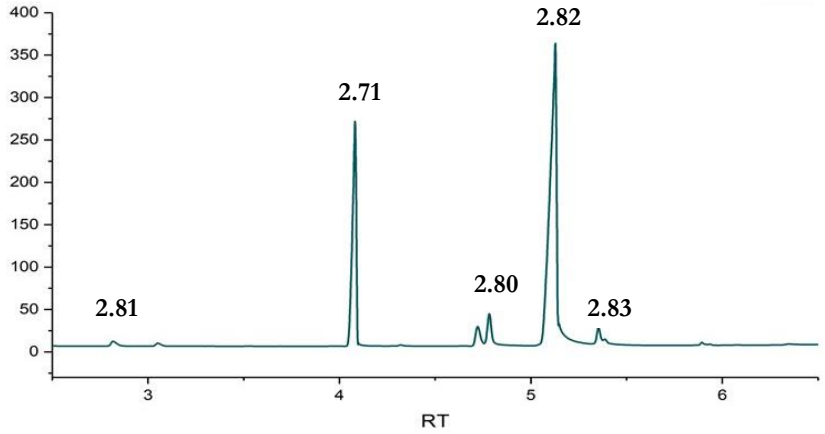
5.1.1.3. Screening of GV/A184I-based mutants for 2.78

Mutant	Conversion /%	2.75 /%	2.76 /%	2.77 /%	2.78 /%	Selectivity /%	TON
GV/A184I/H171L/L188Q	97	6	5	3	81	83	405
GV/A184I/V26M	94	4	8	3	78	84	391
GV/A184I/L188Q	92	6	5	3	77	83	383
GV/A184I/A330W	95	6	7	4	76	80	380
GV/A184I/L188M	94	5	11	3	74	79	371
GV/A184I/V26F	87	4	7	2	72	84	362
GV/A184I/L437M	95	6	10	4	72	75	359
GV/A184M	94	11	2	5	72	76	359
GV/A184I	86	4	12	2	67	78	334
GV/A184I/V26L	88	4	14	2	66	75	331
GV/A184I/A330I	79	3	8	3	64	81	322
GV/A184I/L437F	86	11	7	6	60	70	301
GV/A184I/L437LH	87	21	4	3	57	65	285
GL/A184I	52	2	7	1	42	80	209
S72W/F87V/A184I	60	7	7	4	41	68	205
GV/A184I/L437LM	95	44	4	6	39	41	195
GV/A184I/S72M	44	3	4	1	35	80	175
GV/A184I/L75F	58	11	14	4	28	48	138
GV/A184F	33	3	5	1	24	72	118
GV/A184I/A328L	51	5	27	1	16	32	80
GA/A184I	40	10	9	3	15	37	75
GV/A184I/L437LF	98	65	3	4	13	13	63
GV/A184I/I263W	27	5	3	4	9	33	45
GG/A184I	13	1	1	10	-	1	1

5.1.2. Screening data for substrate 2.71

5.1.2.1. Initial screening data





Mutant	Conversion /%	2.81 /%	2.80 /%	2.82 /%	2.83 /%	Other /%	TTN
VQ/S72G/A330W	100	9	2	75	7	8	500
K19/F87V/I263G	100	3	-	40	31	27	500
RP/H171L/I263G/A184I	100	-	-	57	31	13	500
GV/A184I	100	28	-	50	-	22	499
KT2/L188G/I263G	99	-	-	47	39	14	497
RP/H171L/I263G	99	-	-	37	51	11	496
GVQ/I263G	98	2	-	54	19	23	491
GVQ/A330W	98	7	-	68	11	11	489
K19/F87V/Q403P	97	11	5	52	2	26	484
GVQ	86	5	4	61	7	10	430
R19/F87I/L437LV	75	6	7	6	51	5	374
GLQ/I263G/A328G	72	-	-	24	20	28	358
R19/S72G/A330W	71	-	6	52	3	10	357
R47L/Y51F/K19	71	-	4	55	9	4	356
GVQ/I263G/A328L	69	1	1	54	8	6	345
R19/A330W	66	-	6	44	-	17	332
R19/F87I	66	15	4	26	4	17	331
KU3/A330P/S72W	62	6	12	12	14	18	311
RT2/S72G/A330W	55	-	-	37	-	18	276

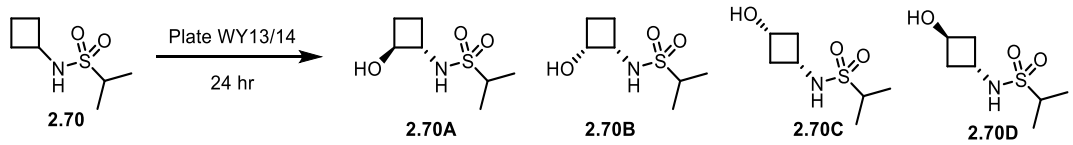
K19/F87V/E267V	43	1	1	31	8	3	215
K19/F87A/I263G	41	-	1	13	18	10	205
GVQ/A328G	38	-	-	25	-	12	188
K19/F87A/F81W	33	2	4	13	1	14	165
RP/A82M/I263A	29	-	-	-	13	16	146
K19/F87V	22	-	1	14	1	5	108
R47L/Y51F/KSK19/A184I	22	-	-	15	2	5	108
KSK19/I263A	21	1	-	16	3	1	105
GVQ/A264G	18	-	5	9	-	4	92
R47L/Y51F/KSK19	12	-	-	-	-	12	62
R19/F87A/A328I/S72W	12	-	-	-	-	12	59
A330P	10	-	-	-	-	10	49
K19/F87V/A264G	8	-	-	-	-	8	39
R19/A328L/I263A	8	-	-	-	-	8	38
R19/F87A/F81W/T269G/A328G	7	-	-	-	-	7	35
WT	6	-	-	-	-	6	30
R19/F87A/A328G	6	4	-	-	-	2	30
R19/F87A/A328L	3	-	-	-	-	3	16
R19/F87A/A328G/P329G/A330G	3	-	-	-	-	3	14
KU3/A330P/I263A	3	-	-	-	-	3	14
RP/I263A/E267V	2	-	-	-	2	1	12
K19/F87A/A82M/I263G	2	-	-	-	-	2	11
R19/A328L/A184L	2	-	-	-	-	2	10
R19/F87A/A328I/V78I	2	-	-	-	-	2	9
R19/F87A/A184I/T269G/A328G	2	-	-	-	-	2	8
K19/F87V/E267V/V78I	1	-	-	-	-	1	7
R19/F87A/T269G	1	-	-	-	-	1	5
R19/F87A/A328G	1	-	-	-	-	1	5
R19/F87A/A328G/A264G	1	-	-	-	-	1	5

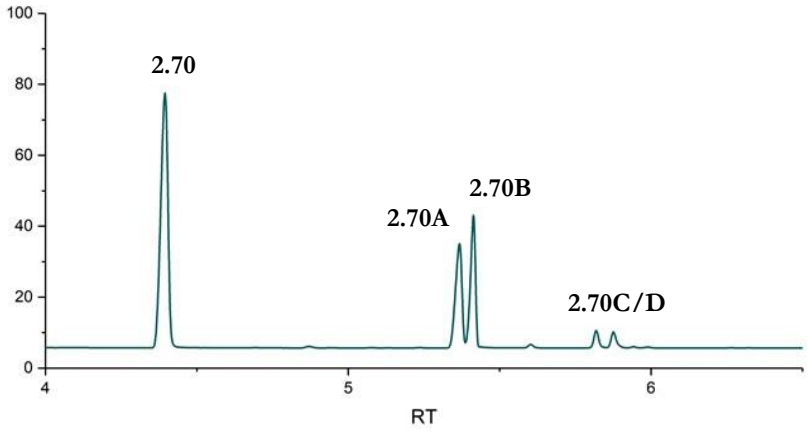
5.1.2.2. Further screening for 2.82

Mutant	Conversion /%	2.80 /%	2.82 /%	Other /%	Selectivity /%	TON
RT2/F81W	95	3	83	8	88	830
K19/F87A/A328I/I263A	99	1	79	19	79	789
RT2/A330W	82	6	67	10	81	665
GVQ/S72W	61	4	36	21	60	363
KU3/A330S/L437LA	68	24	23	22	33	226
R19/A330W	30	4	21	4	72	214
K19/F87V/A328L	54	1	17	36	32	174
R19/F87I/A330W	46	4	16	26	36	165
RP/E267V	22	1	14	7	64	143
RT2/A330P/V78I	16	1	10	5	62	98
RT2/A330P/A82M	16	1	9	6	58	91
RT2/I401P	14	1	8	5	55	76
K19/F87A/A82M	13	1	7	5	55	74
RT2/A330P/A184I	13	1	7	5	55	74
RP/F87V/E267V	14	-	7	6	52	73
K19/F87A/A184I	13	1	7	5	54	72
RT2/S72G/A330W/L437LA	17	5	4	8	26	44
R19/F87I/A330P	12	1	4	8	32	40
RT2	3	-	1	2	37	9
RP/E267G	1	-	-	1	-	-
RT2/S72G/A330P/L437LA	6	-	-	5	-	-
RT2/A330P/L437LA	6	1	-	6	-	-

5.1.3. Screening data for substrate 2.70

5.1.3.1. Initial screening data



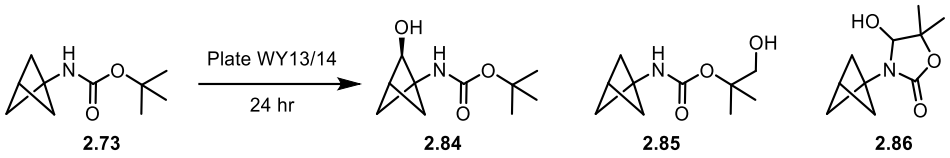


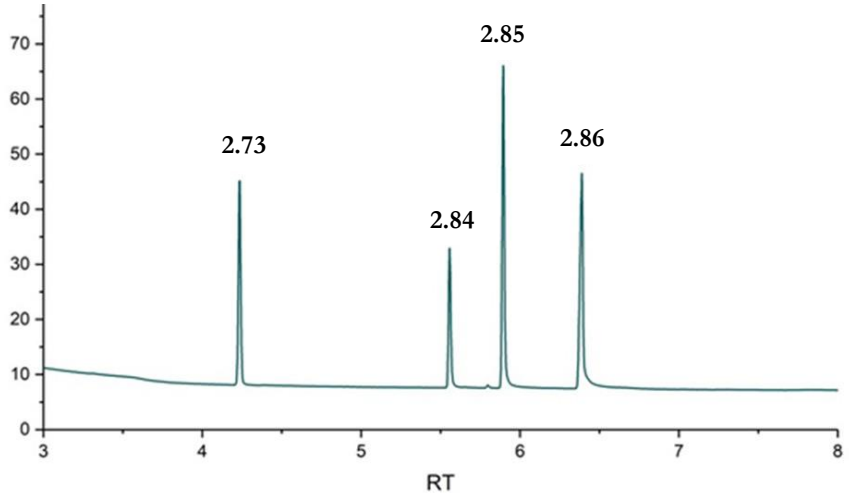
Mutant	Conversion /%	2.70A /%	2.70B /%	Other /%	TTN
KU3/A330P/S72W	91	27	53	11	910
R19/F87A/T269G	43	-	-	43	432
GV/A184I	38	-	-	38	379
RP/H171L/I263G/A184I	23	-	-	23	233
VQ/S72G/A330W	17	-	-	17	168
K19/F87A/I263G	12	-	-	12	117
K19/F87V/E267V	10	-	-	10	101
R19/F87A/A328I/S72W	9	-	-	9	93
R19/F87A/F81W	8	-	-	8	81
K19/F87V/Q403P	6	-	-	6	63
R19	6	-	-	6	62
RT2/S72G/A330W	6	-	-	6	57
R19/F87A/A328G	6	-	-	6	56
GVQ/A328G	6	-	-	6	55
R19/F87A/A184I/T269G/A328G	5	-	-	5	52
GLQ/I263G/A328G	5	-	-	5	51
GVQ/I263G/A328L	5	-	-	5	47
GVQ/A330W	5	-	-	5	45
R19/F87A/A328G/P329G/A330G	5	-	-	5	45
GVQ	4	-	-	4	44

A330P	4	-	-	4	41
R19/F87A/F81W/T269G/A328G	4	-	-	4	39
R19/S72G/A330W	4	-	-	4	38
K19/F87V/I263G	4	-	-	4	38
R19/F87I/L437LV	4	-	-	4	38
WT	4	-	-	4	37
RP/I263A/E267V	4	-	-	4	37
K19/F87V/E267V/V78I	4	-	-	4	36
KT2/L188G/I263G	3	-	-	3	33
R19/F87A/A328L	3	-	-	3	33
KU3/A330P/I263A	3	-	-	3	33
K19/F87A/I263A	3	-	-	3	32
R19/F87A/A328I/V78I	3	-	-	3	32
GVQ/I263G	3	-	-	3	32
R19	3	-	-	3	32
R19/F87A/A328G/A264G	3	-	-	3	32
GVQ/A264G	3	-	-	3	31
R19/F87A/A328G	3	-	-	3	31
R19/A328L/I263A	3	-	-	3	29
K19/F87V/A264G	3	-	-	3	29
R19/F87I	3	-	-	3	28
R19/A328L/A184L	3	-	-	3	27
K19/F87V	3	-	-	3	27
R19/F87A A184I	3	-	-	3	26
K19/F87A/A82M/I263G	2	-	-	2	23
RP/H171L/I263G	2	-	-	2	23
R19/A330W	1	-	-	1	5

5.1.4. Screening data for substrate 2.73

5.1.4.1. Initial screening data





Mutant	Conversion /%	2.84 /%	2.85 /%	Other /%	TON	2.84 % *ee*
GV/A184I	58	40	5	13	397	66
K19/F87V/E267V	35	27	-	8	267	20
R19/F87I/L437LV	30	19	-	11	187	-21
K19/F87A/F81W	29	20	4	5	204	76
R19/F87A/A328G	27	15	3	9	147	10
R19/F87A/A184I	27	14	2	10	141	77
K19/F87V/I263G	26	14	-	12	144	-47
R19/F87A	24	10	3	11	98	63
VQ/S72G/A330W	23	7	6	9	73	16
R19/F87A/A328G/P329G/A330G	22	13	-	10	127	-
K19/F87V/Q403P	20	7	2	11	65	50
GVQ/I263G	18	8	-	10	75	-58
K19/F87V/A264G	17	2	-	15	20	-50
R19/F87A/A328I/S72W	17	4	3	10	37	82
R19/F87A/A328I/V78I	16	2	-	14	24	82
K19/F87V/E267V/V78I	16	-	-	16	-	-
GVQ/A330W	13	3	2	8	33	11

K19/F87A/I263G	13	7	-	6	75	16
K19/F87A/I263A	13	8	1	4	76	50
GVQ/A328G	13	2	-	11	19	2
R19/F87A/A328L	12	3	1	8	33	82
RP/H171L/I263G/A184I	12	-	-	12	-	-
GVQ/A264G	11	-	-	11	-	-
WT	11	-	-	11	-	-
R19/F87A/A184I/T269G/A328G	11	-	-	11	-	-
GVQ/I263G/A328L	10	-	-	10	-	-
KT2/L188G/I263G	10	-	-	10	-	-
R19/S72G/A330W	9	-	-	9	-	-
R19/F87A/F81W/T269G/A328G	9	-	-	9	-	-
GLQ/I263G/A328G	9	-	-	9	-	-
KU3/A330P/S72W	9	-	2	6	-	-
RP/I263A/E267V	8	-	-	8	-	-
R19/F87A/A328G/A264G	8	-	-	8	-	-
R19/A328L/I263A	8	-	-	8	-	-
R19/F87A/T269G	8	-	-	8	-	-
K19/F87V	8	4	-	3	43	37
RP/A82M/I263A	7	-	-	7	-	-
A330P	7	-	-	7	-	-
R19	7	-	-	7	-	-
RT2/S72G/A330W	7	-	-	7	-	-
R19/A328L/A184L	7	-	-	7	-	-
RP/H171L/I263G	6	-	-	6	-	-
GVQ	4	4	-	-	40	17
R19/F87I	3	3	-	-	31	36
R19/A330W	-	-	-	-	-	-

5.1.4.2. Screening of GV/A184I/I263G-based mutants for 2.84

Mutant	Conversion /%	2.84 /%	% *ee*
GV/A184I/I263G/A328G/S72F/L188F	53	1	-61
GV/A184I/I263G/P329F	42	9	-40
GV/A184I/I263GS332F	39	5	-35
GL/A184I/I263G/A328G/L75M/V26M	37	2	ND
GV/A184I/I263G/A328G/L75F	33	7	-61
GL/A184I/I263G/A328G/S72F/L188F	33	1	-53
GL/A184I/I263G/A328G/S72F	33	1	-57
GL/A184I/I263G/A328G/A330F/S72F	32	2	-74
GL/A184I/I263G/A328G/S72F/V26L	32	1	-52
GV/A184I/I263G/A328G/A330F	31	5	-65
GI/A184I/I263G/A328G/L75F	29	6	-50
GL/A184I/I263G/A328G/A330F	28	1	-78
GV/A184I/I263G/A328G/S72F	28	2	-54
GI/A184I/I263GA328G/S72F	27	2	-31
GV/A184I/I263G/A328G/L437S	25	1	-73
GL/A184I/I263G/A328G/L75M	23	2	-77
GL/A184I/I263G/A328G	22	1	-74
GI/A184I/I263G/A328G	18	3	-43
GV/A184I/I263G/A328G	17	5	-56

5.1.4.3. Screening of A330P-based mutants for 2.85

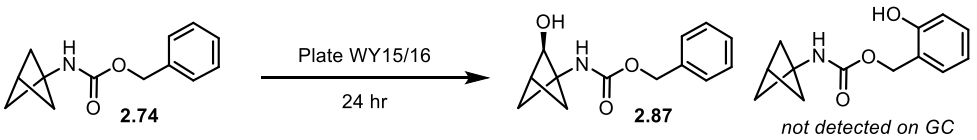
Mutant	Conversion /%	2.84 /%	2.85 /%
A330P	19	-	-
A330P/I263A	-	-	-
KU3/A330P	-	-	-
KU3/A330P/A184I	-	-	-
KU3/A330P/V78I	-	-	-
KU3/A330P/F81W	19	-	-
KU3/A330P/A82M	-	-	-
KU3/A330P/F87A	-	5	3
KU3/A330P/F87V	32	9	9
GVQ/A330P/A264G	12	-	-
GVQ/A330P/A264G/P329G	4	3	-
R19/F87A/A330P/A184I	19	7	-
R19/F87A/A330P/P329G	12	9	2
R19/F87A/A330P/P329G/I263G	14	7	-
RP/A330P	-	-	-
RT2/A330P	-	-	-
RT2/A330P/L437LA	-	-	-
RT2/A330P/V78I	-	-	-
RT2/A330P/A82M	-	-	-
RT2/A330P/S72G/L437LA	-	-	-

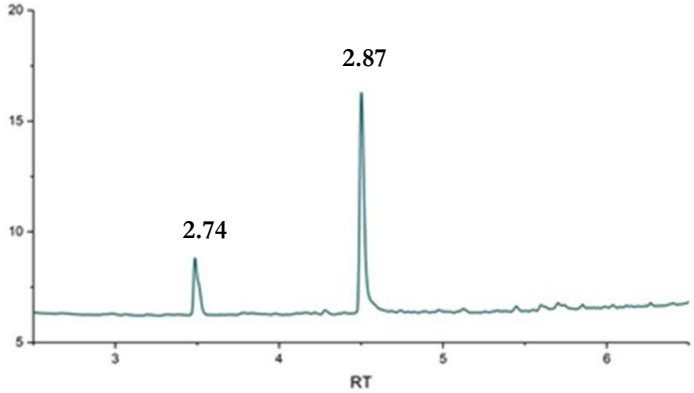
5.1.4.4. Screening of R19/F87I-based mutants for 2.86

Mutant	Conversion /%	2.84 /%	2.85 /%	2.86 /%	TTN
R19/F87I/A330P	79	14	32	33	794
R19/F87I/A330V/A184I	18	15	3	-	177
R19/F87I/A330I/A184I	17	15	2	-	175
R19/F87I/A82M/A184I	16	16	-	-	160
R19/F87I/A330V/A82M	12	9	3	-	124
R19/F87I/A330W/I263G	12	11	-	-	121
R19/F87I/L437F	11	8	3	-	112
R19/F87I/A330I/A82M	10	8	2	-	104
R19/F87I/A184F	9	7	2	-	90
R19/F87I/L75F	9	8	-	-	88
R19/F87I/A330W	8	7	1	-	83
R19/F87I/A330F	7	6	2	-	73
R19/F87I/A330W/A82M	7	7	1	-	71
R19/F87I/A330W/A82M/I263G	7	7	-	-	66
R19/F87I/L71M	6	4	2	-	64
R19/F87I/A330V	6	4	2	-	58
R19/F87I/L75M	6	5	1	-	58
R19/F87I/A330I	4	3	1	-	43
R19/F87I/S72I	4	2	-	-	39
R19/F87I/I263G/A82M	3	3	-	-	32
R19/F87I/S332I	3	2	1	-	28
R19/F87I/S332L	2	2	-	-	16
R19/F87I/T438V	1	1	-	-	12
R19/F87I/S72L	1	1	-	-	9

5.1.5. Screening data for substrate 2.74

5.1.5.1. Initial screening data



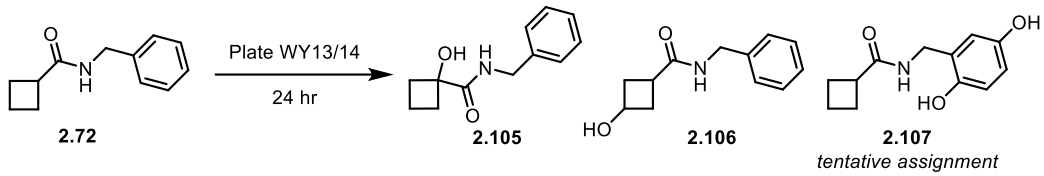


Mutant	Conversion /%	2.87 /%	Other /%	TTN	TON	2.87 % *ee*
R19/F87A	95	72	23	476	359	83
K19/F87V/Q403P	100	66	34	500	329	93
R19/F87A/A184I	88	64	23	439	322	51
K19/F87V	84	64	20	418	318	96
K19/F87A/I263G	100	61	39	500	306	12
K19/F87A/F81W	100	61	39	500	304	43
GVQ	78	55	23	392	276	95
K19/F87A/I263A	100	49	51	500	243	49
R19/F87A/A328G/P329G/A330G	82	47	36	411	233	69
KU3/A330P/S72W	94	44	50	469	221	96
K19/F87V/A264G	54	38	17	271	188	92
K19/F87V/E267V	39	33	6	194	165	98
GVQ/I263G	38	29	9	191	144	72
K19/F87V/I263G	34	28	6	170	142	88
R19	92	27	64	458	137	0
GVQ/A330W	94	24	70	470	120	0
R19/F87I/L437LV	26	23	3	130	114	98
GV/A184I	100	23	77	500	114	-
GVQ/A328G	77	19	58	387	96	24
RT2/S72G/A330W	86	17	69	430	84	-
GVQ/A264G	19	15	4	94	75	93

R19/F87I	17	14	3	87	72	>99
GV/A184I/I263G/A328G	18	14	4	89	68	77
RP/H171L/I263G/A184I	95	12	84	477	58	-
VQ/S72G/A330W	100	11	89	500	54	-
R19/F87A /T260G	24	8	16	121	41	-
KT2/L188G/I263G	69	8	61	344	41	-
RP/A82M/I263A	91	7	84	457	37	-
R19/A330W	49	6	44	247	28	-
RKA/S72W	8	4	5	42	18	-
K19/F87V/E267V/V78I	14	4	10	69	18	-
R19/F87A/A328L	3	2	1	16	12	-
RP/H171L/I263G	9	2	7	47	12	-
GQ/I263G/A328L	21	2	19	107	10	-
RKA/V78I	4	2	2	18	8	-
RP/I263A/E267V	4	1	3	22	7	-
R19/S72G/A330W	9	1	7	43	7	-
GVQ/I263G/A328L	3	1	2	13	3	-
A330P	3	-	2	13	2	-
K19/F87A/A82M/I263G	2	-	2	11	1	-
R19/A328L/I263A	1	-	1	6	1	-
WT	2	-	2	10	1	-
R19/F87A/A328G	100	-	100	500	-	-
R19/F87A/F81W/T269G/A328G	91	-	91	457	-	-
R19/F87A/A184I/T269G/A328G	45	-	45	227	-	-
KU3/A330P/I263A	26	-	26	128	-	-
R19/F87A/A328G/A264G	6	-	6	28	-	-
GLQ/I263G/A328G	3	-	3	16	-	-

5.1.6. Screening data for substrate 2.72

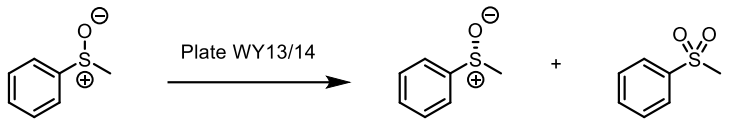
5.1.6.1. Initial screening data



Mutant	Conversion /%	2.105 /%	2.106 /%	2.107 /%	Other	TTN
KU3/A330P/S72W	97	4	57	20	15	969
R19/F87I/L437LV	68	4	40	-	19	682
R19/F87I	66	9	51	-	4	655
GV/A184I	62	7	42	2	8	617
K19/F87V/I263G	60	1	43	-	14	602
RP/H171L/I263G/A184I	58	8	31	-	17	582
VQ/S72G/A330W	52	17	9	5	14	517
K19/F87V/Q403P	51	25	20	-	5	509
RP/H171L/I263G	41	3	15	-	18	413
GVQ/A328G	35	29	-	-	4	353
KT2/L188G/I263G	34	2	13	-	18	339
GVQ/A330W	34	16	6	1	8	338
GVQ/I263G	33	1	24	-	7	330
RT2/S72G/A330W	30	-	1	5	21	304
R19/S72G/A330W	29	2	1	3	21	290
GVQ	28	16	7	1	4	284
R19/A330W	24	2	1	2	18	240
K19/F87A/I263G	23	-	13	-	7	233
GVQ/I263G/A328L	19	1	12	-	4	193
K19/F87V	18	11	5	-	2	185
R19/F87A/A328G	15	12	-	-	2	153
GLQ/I263G/A328G	14	1	2	-	10	140
R19	14	1	-	2	10	139
K19/F87V/A264G	13	6	4	-	3	128
K19/F87A/I263A	12	1	7	-	4	120
R19/F87A/A328G	11	11	-	-	2	106
K19/F87V/E267V	10	6	2	-	1	96
K19/F87A/F81W	8	2	2	-	2	76
GVQ/A264G	7	3	3	-	1	69
RP/A82M/I263A	7		3	1	-	67
R19/F87A/A184I	7	2	3	-	2	65
R19/F87A	5	2	1	-	2	55
RP/I263A/E267V	4	-	2	-	1	40
R19/F87A/A328I/S72W	3	-	-	-	1	31
R19/F87A/A328G/P329G/A330G	2	1	-	-	-	16
K19/F87A/A82M I263G	2	-	-	-	-	15

R19/F87A/A328L	1	-	-	-	-	13
K19/F87V/E267V/V78I	1	-	-	-	-	13
R19/F87A/A184I/T269G/A328G	1	-	-	-	-	13
R19/A328L/A184L	1	-	-	-	-	11
KU3/A330P/I263A	1	-	-	-	-	9
A330P	1	-	-	-	-	9
R19/F87A/A328G/A264G	1	-	-	-	-	9
R19/F87A/F81W/T269G/A328G	1	-	-	-	-	8
R19/F87A/A328I/V78I	1	-	-	-	-	6
R19/A328L/I263A	1	-	-	-	-	6
WT	1	-	-	-	-	5
R19/F87A/T269G	-	-	-	-	-	-

5.1.7. Screening data for substrate 2.108



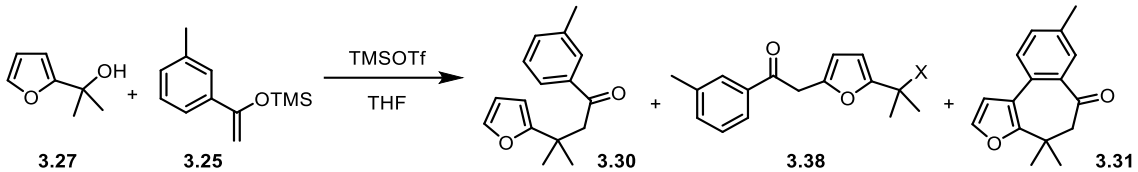
rac. **2.108** | *enantioenriched* **2.108** | **2.109**

	6 hr		24 hr	
Mutant	**Conversion /%**	**2.108 *ee* /%**	**Conversion /%**	**2.108 *ee* /%**
GV/A184I	93	-21	98	4
RP/H171L/I263G/A184I	91	80	94	86
K19/F87V/Q403P	83	-34	85	-34
GVQ/A328G	80	6	92	17
K19/F87A/F81W	76	4	98	-10
RP/A82M/I263A	73	-12	83	-17
KU3/A33OP/S72W	67	-38	81	-63
R19/F87A/A328L	64	-15	78	-23
R19/F87A/A328G	58	7	99	37
R19/F87A/A328G	57	7	99	39
R19/F87I	57	-17	90	-27
GVQ	55	-21	84	-33
KT2/L188G/I263G	49	-4	76	5

R19/A328L/A184L	46	4	55	5
RP/H171L/I263G	41	3	62	18
R19/A328L/I263A	31	1	53	6
K19/F87V/A264G	30	-2	39	-3
GVQ/I263G	27	1	51	4
K19/F87V/E267V	27	-2	83	-17
GVQ/A264G	26	1	38	1
GVQ/I263G/A328L	25	-1	40	-3
R19/F87A/A184I	25	4	41	6
R19/F87I/L437LV	24	-4	34	-5
RP/I263A/E267V	23	-3	38	-7
GVQ/A330W	22	-5	33	-9
K19/F87V/I263G	21	-1	42	0
GLQ/I263G/A328G	21	-2	34	-4
R19	20	0	40	0
R19/A330W	20	1	35	2
K19/F87V	19	0	33	-11
A330P	18	-4	23	-6
RT2/S72G/A330W	15	1	27	1
R19/F87A/A328I/V78I	14	0	29	-1
R19/F87A/A328I/S72W	14	0	27	0
K19/F87A/I263G	8	0	10	0
K19/F87A/A82M/I263G	7	2	17	4
R19/F87A	7	1	16	3
VQ/S72G/A330W	7	-1	10	-2
R19/F87A/A328G/A264G	6	2	11	5
KU3/A330P/I263A	4	-1	6	1
R19/S72G/A330W	4	0	5	0
R19/F87A/A184I/T269G/A328G	4	0	7	0
R19/F87A/F81W/T269G/A328G	4	0	5	0
WT	3	0	4	0
K19/F87A/I263A	3	0	5	0
K19/F87V/E267V/V78I	3	0	3	0
R19/F87A/A328G/P329G/A330G	2	0	4	0
R19/F87A/T269G	2	0	3	0

5.2. Appendices for Chapter 3

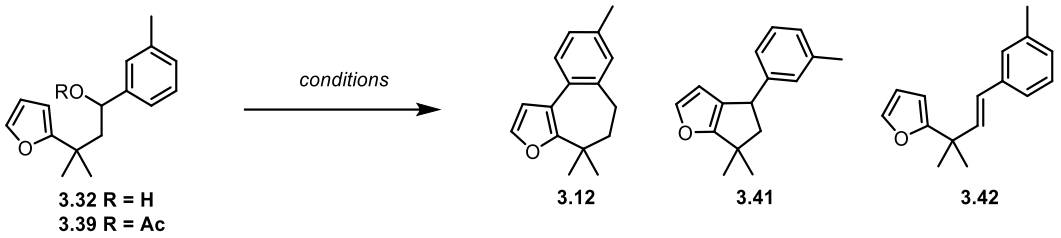
5.2.1. Conditions screened for Lewis acid coupling of 3.27 with 3.25



3.27 3.25 3.30 3.38 3.31

Entry	Catalyst	Temp. /°C	Time /min	3.30	3.38	3.31
1	TFA	–78	90	<5	-	-
2		0	90	<5	trace	-
3		rt	90	-	trace	-
4		reflux	90	-	trace	-
5	$Gd(OTf)_3$	–78	240	trace	-	-
6	$TiCl_4$	–78 to –10	90	-	-	-
7		0	90	-	-	-
8		rt	90	-	-	-
9		reflux	90	-	-	-
10	TMSOTf	–78	90	36	15	-
11*		–40	900	<10	26	-
12		0	90	5	11	-
13		rt	90	trace	-	-
14		reflux	90	trace	-	-
15		–78	35	38	<5	-
16		–78	10	61	<10	-
17		–78	5	59	trace	-
18		–92	5	57	trace	-

5.2.2. Conditions screened for cationic cyclisation of 3.32 and 3.39

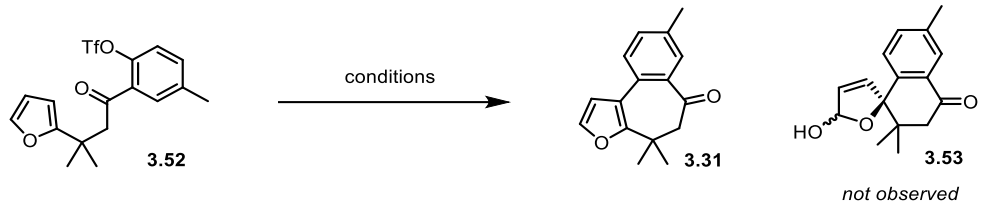


3.32 R = H
3.39 R = Ac

3.12 **3.41** **3.42**

Entry	R =	Conditions (based on 1 eq. starting material)	Outcome
1	H	0.3 eq. $PTSA.H_2O$, C_6H_6 [0.15]	a
2	H	1.05 eq. $BF_3.OEt_2$, CH_2Cl_2 [0.1], 1 hr	a
3	H	1.05 eq. Tf_2O, 1.5 eq. py, CH_2Cl_2 [0.2], 15 min	a
4	H	3.5 eq. BBr_3, CH_2Cl_2 [0.04], 3 hr	a
5	H	1 eq. PIDA, MeCN [0.01], 21 hr[1]	a
6	H	5 mol% $AlCl_3$, 5 mol% PPh_3, MeCN, 80 °C[2]	a
7	H	5 mol% $RuCl_3.H_2O$, 10 mol% AgOTf, DCM [0.2], 2 hr[3]	a
8	H	4 eq. $TiCl_4$, DCM [0.1], −78 °C, 3 min[4]	b
9	H	4 eq. $TiCl_4$, DCM [0.1], 3 min	b
10	H	TFA [0.1][5]	b
11	H	10 mol% I_2, $MeNO_2$ [0.25] 80 °C, 30 min[6]	b
12	H	1.3 eq. HBF_4, DCM [0.05], −78 °C to 0 °C over 15 min[7]	a
13	Ac	10 mol% $AuCl_3$, MeCN [0.5], 18 hr[8]	*trace* **3.41** and **3.42**
14	Ac	10 mol% $FeCl_3$, DCM [0.1], 16 hr[9]	c
15	Ac	10 mol% $Yb(OTf)_3.H_2O$, $MeNO_2$ [0.25], 18 hr[10]	*trace* **3.41**

5.2.3. Heck conditions screened by Syngenta for substrate 3.52



	$Pd_2(dba)_3$			$Pd(allyl)Cl_2$			$Pd(OAc)_2$		
	(1)	(2)	(3)	(1)	(2)	(3)	(1)	(2)	(3)
Sphos	-	-	-	-	-	-	<10%	<10%	<10%
Xphos	-	-	-	-	-	-	-	-	-
Qphos	-	-	-	-	-	-	-	-	-
TrixiePhos	-	-	-	-	-	-	-	-	-
XantPhos	-	-	-	-	-	-	-	-	-
tBuJohnPhos	-	-	-	-	-	-	-	-	-
$PCy_3.HBF_4$	-	-	-	-	-	-	-	-	-
Catacxium A	-	-	-	-	-	-	-	-	-

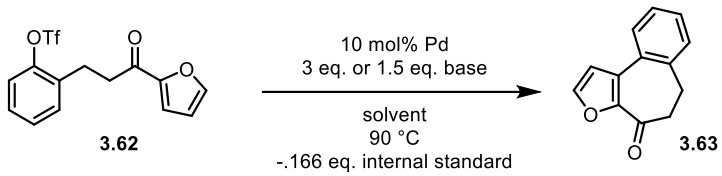
Bases; (1) K_2CO_3 (2) KOAc (3) Cs_2CO_3.

	DMA				Toluene			
	no PivOH		PivOH		no PivOH		PivOH	
	(1)	(2)	(1)	(2)	(1)	(2)	(1)	(2)
Sphos	<10%	<10%	<10%	-	-	-	-	<10%
RuPhos	<10%	<10%	<10%	<10%	-	-	-	-
BrettPhos	-	<10%	<10%	<10%	-	-	-	-
Cphos	<10%	<10%	<10%	<10%	-	-	-	-
DavePhos	-	-	-	-	-	-	-	-

Pd sources; (1) $Pd(OAc)_2$, (2) $PdCl_2$

5.2.4. Heck conditions screened by Syngenta for substrate 3.62

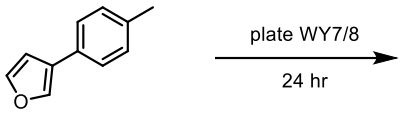
Shows % remaining starting material **3.62** as determined by LCMS.



		DMA				DMA:H_2O (10:1)			
		$Pd(PPh_3)_4$	PPh_3 Pd G2	DPPF Pd G3	SPhos Pd G4	$Pd(PPh_3)_4$	PPh_3 Pd G2	DPPF Pd G3	SPhos Pd G4
2 hr	**Hunig's**	93	98	93	77	87	92	95	79
	Cs_2CO_3	-	-	-	-	-	7	-	9
	K_3PO_4	-	-	-	-	-	-	11	14
	NaO^tAm	-	-	-	-	-	-	-	-
17.5 hr	**Hunig's**	86	95	93	79	80	90	90	79
	Cs_2CO_3	-	-	-	-	-	-	-	-
	K_3PO_4	-	-	-	-	-	-	-	-
	NaO^tAm	-	-	-	-	-	-	-	-
42 hr	**Hunig's**	82	93	88	72	74	87	83	73
	Cs_2CO_3	-	-	-	-	-	-	-	-
	K_3PO_4	-	-	-	-	-	-	-	-
	NaO^tAm	-	-	-	-	-	-	-	-

5.3. Appendics for Chapter 4

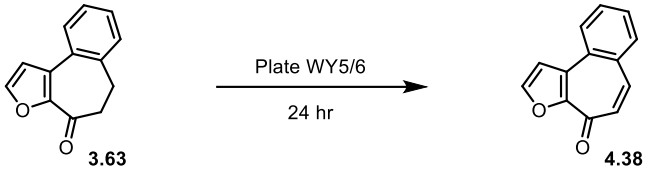
5.3.1. Screening data for substrate 4.37



Mutant	Conversion /%	RT 5.1 /%	RT 7.3 /%	RT 8.1 /%	RT 14 /%	TTN
K19/F87V	84	-	-	58	-	420
RT2/V78I/A184I/A330P	58	-	-	38	-	288
GVQ/A330W	54	-	-	30	-	268
R19/F87A/A184I	53	-	-	24	-	263
GVQ/A264G	51	-	-	23	-	253
GVQ/V78L/I263G	45	-	-	-	-	225
R19/F87I	44	-	-	3	22	221
R19/F87I/L437LV	44	-	-	19	-	220
R19/F87A/G265GG	44	-	-	3	-	218
R19/F87A/I263G	42	14	-	-	-	210
GVQ	41	-	-	21	-	204
RT2	39	-	-	14	-	193
GV/A184I	38	-	-	12	-	190
R19/F87A/A328G/P329G/A330G	38	-	-	6	-	188
RP/I263A/E267V	37	-	13	-	-	186
RP/V78I/E267V	37	-	-	14	-	184
GVQ/A82M/I263G	35	-	-	-	-	177
K19/F87V/A264G	34	-	-	13	-	172
K19/F87V/Q403P	34	-	-	12	-	168
R19/F87A/A264G/A328G	33	-	-	-	-	164
K19/A82M/F87A/E267F	32	-	-	2	-	158
R19/F87A/A328G	31	-	-	-	-	153
K19/F87A/I263A	30	-	-	-	-	148
GVQ/I263G	30	-	-	4	-	148
R19/V78I/F87A/A328I	29	-	-	1	-	145
R19/F87A	29	-	-	6	-	145
K19/A82M/F87A/I263G	29	-	-	-	-	144
K19/V78I/F87V/E267V	29	-	-	3	-	144
KU3/A328I/A330P	28	-	-	-	-	141
I263G	28	-	-	-	-	140
RP/H171L/I263G	28	-	-	4	-	140
R19/I263A/A328L	27	-	-	1	-	133
RP/V78I/F87V	25	-	-	-	-	127
R19/A184I/A328L	24	-	-	2	-	122
RP/F87V	23	-	-	-	-	113
K19/F87V/A328V	22	-	-	1	-	111
K19/F87V/E267V	22	-	-	2	-	108
K19/F87A/I263G	21	-	-	-	-	104

R19/S72W/F87A/A328I	21	-	-	4	-	103
R19/F87A/A328L	20	-	-	-	-	100
WT	20	-	-	-	-	100
RP/A82M/I263A	20	-	-	-	-	98
GVQ/I263G/A328L	19	-	-	-	-	96
K19/F81W/F87A	18	-	-	-	-	92
R19	18	-	-	2	-	88
R19/A330W	13	-	-	-	-	67
R19/F87A/I263G/A264G	12	-	-	-	-	62
K19/A82M/F87A	12	-	-	-	-	58

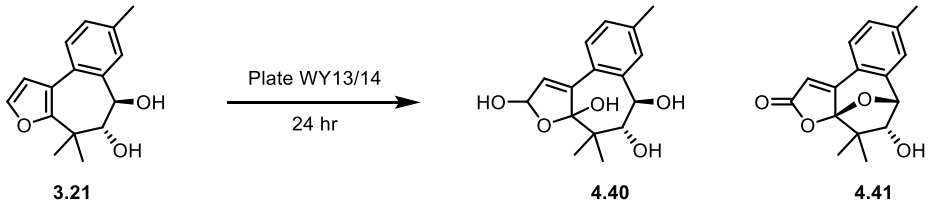
5.3.2. Screening data for substrate 3.63



Mutant	Conversion /%	4.38 /%	Other /%	TTN
GVQ/A264G	97	-	97	485
R19/F87A/A328L	92	3	88	458
K19/F87A/A82M	91	15	76	453
RT2	88	5	83	441
RP/I263A/E67V	87	-	87	437
R19/F87A/A264G/A328G	86	70	15	428
RP/V78I/E267V	85	13	71	424
R19/F87A/I263G	71	36	35	355
K19/V78I/F87V/E267V	67	9	58	336
RP/F87V	64	-	64	320
K19/F87A/A82M/E267F	62	12	51	312
GVQ	55	3	51	274
RP/A82W/I263A	49	3	46	245
RP/H171L/I263G/L437LV	47	-	47	237
RT2/V78I/A184I/A330P	45	17	28	223
WT	43	3	40	214
RT2/S72W/A330W	40	6	34	200
R19/V78I/F87A/A328I	31	3	28	153
K19/F87V	29	4	25	143
K19/F87V/A328V	21	-	21	106
K19/F87V/Q403P	20	-	20	98
R19/I263G/A328L	19	-	19	93
K19/F87V/E267V	18	2	16	88
R19/F87I/L437LV	17	1	16	85

K19/F87V/A264G	17	3	14	83
RP/A82M/I263A	14	3	12	72
R19/F87A/A328F	13	1	13	67
I263G	13	-	13	67
GVQ/I263G	13	-	13	64
RP/V78I/F87V	13	-	13	63
R19/F87A/A328G	13	4	8	63
R19/F87A/A184I	10	1	9	52
RP/V78I/F87V/H171L/I263G	9	1	8	45
GV/A184I	8	-	8	40
R19/A184I/A328L	8	-	8	39
K19/F87A/I263A	7	1	6	37
KU3/A330P	6	-	6	31
K19/F81W/F87A	6	-	6	31
KU3/A330P/A328I	6	-	6	30
K19/F87A/I263G	6	1	5	30
RP/H171L/I263G	6	-	6	29
R19/F87A	6	-	6	28
RT2/S72G/A330W	6	-	6	28
K19/A82M/F87A/I263G	6	-	6	28
R19/A330W	5	-	5	26
A82F/I263F	5	-	5	26
R19/F87I	5	-	5	24

5.3.3. Screening data for substrate 3.21

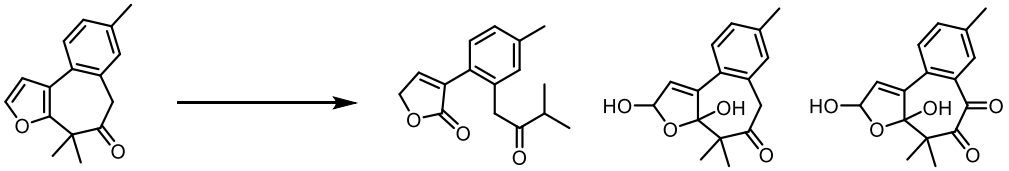


3.21 4.40 4.41

Mutant	Conversion /%	RT 3.8 /%	4.40 /%	4.41 /%	TTN
R19/F87I	100	-	91	-	500
GLQ/I263G/A328G	99	-	90	-	495
GVQ/I263G/A328L	100	-	89	-	500
K19/F87V	100	1	89	-	500
RP/H171L/I263G/A184I	100	-	89	1	500
GV/A184I	100	-	89	-	500
K19/F87V/E267V	100	-	89	-	500
VQ/S72G/A330W	100	-	89	-	500
GVQ	100	-	89	-	500
KT2/L188G/I263G	100	-	89	-	500
GVQ/A264G	100	-	88	-	500
GVQ/I263G	100	-	88	3	500
K19/F87VQ403P	100	-	88	2	500
K19/F87V /A264G	100	-	87	-	500
KU3/S72W/A330P	99	-	87	-	495
KU3/A328I/A330P	99	-	87	-	493
GVQ/A330W	100	-	87	-	500
K19/F87V/I263G	100	-	86	-	500
R19/F87I/L437LV	97	-	86	-	483
K19/A82M/F87A/I263G	99	2	85	-	497
R19/F87A/A184I	97	1	84	4	486
R19/F87A/A328L	94	-	84	-	472
K19/F81W/F87A	96	2	82	2	482
K19/F87A/I263A	99	-	81	8	495
R19/F87A/A184I/T269G/A328G	97	5	81	-	485
R19/F87A	97	5	80	-	484
R19/V78I/F87A/A328I	90	1	78	-	450
R19 A328L I263A	87	-	77	1	434
RK/A264G/A328G	98	11	75	-	491
K19/F87A/I263G	99	-	73	18	496
R19/S72W/F87A/A328I	80	-	71	-	400
R19/F87A/A328G/P329G/A330G	88	15	63	-	442
R19/F87A/A328G	82	18	54	-	409
RT2/S72G/A330W	59	-	50	-	294
R19/F87A/A328G	77	15	50	-	385
R19/A184L/A328L	60	-	48	-	299
R19	47	-	40	-	236

K19/V78I/F87V/E267V	39	-	33	-	193
RP/I263A/E267V	39	-	32	-	195
A330P	23	-	21	-	113
R19/F87A /269G	23	-	20	-	115
R19/F81W/F87A/T269G/A328G	19	-	16	-	94
R19/A330W	12	-	10	-	60
WT	4	-	3	-	20

5.3.4. Screening data for substrate 3.22

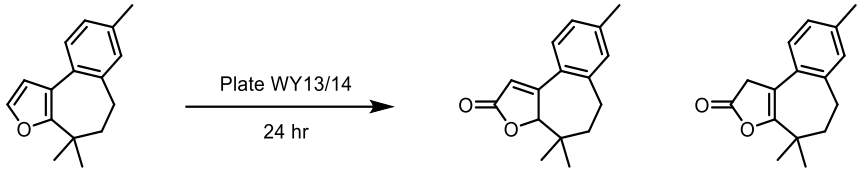


3.22 4.42 4.43 4.44

Mutant	Conversion /%	4.42 /%	4.43 /%	4.44 /%	Other /%	TTN
R19/F87I	100	-	-	100	-	500
R19/F87A/A328G	100	-	-	90	10	500
KT2/L188G/I263G	98	-	63	-	35	492
GVQ/A328G	98	-	-	89	8	490
GVQ/I263G	98	-	64	31	3	489
GLQ/I263G/A328G	97	-	94	-	3	487
R19/F87A/A328G	97	-	-	62	35	484
RP/A82M/I263A	96	-	92	-	4	482
R19/V78I/F87A/A328I	95	-	33	56	7	477
R19/F87A/A264G/A328G	89	21	25	34	9	447
GVQ/A264G	88	-	32	52	3	438
GVQ	82	-	-	82	-	412
KU3/S72W/A330P	78	-	66	-	12	391
K19/F87A/A82M/I263G	68	-	44	18	6	338
GV/A184I	64	-	2	52	10	322
R19/F87I/L437LV	63	-	61	-	2	316
R19/S72W/F87A/A328I	61	-	58	-	3	306
R19/F87A/A328L	58	-	44	7	6	289
K19/F87A/I263A	48	-	9	34	5	242
K19/F87V/I263G	42	-	40	-	3	212
GVQ/I263G/A328L	40	-	40	-	1	202
RP/H171L/I263G/A184I	36	-	33	-	3	181
RP/I263A/E267V	36	-	33	-	3	180

K19/F87A/I263G	35	-	24	6	5	177
K19/F87V/Q403P	35	-	3	25	7	176
K19/F87V/A264G	32	-	16	13	3	161
GVQ/A330W	26	-	-	24	2	129
RP/H171L/I263G	19	-	13	-	6	95
RT2/S72G/A330W	19	-	12	-	7	95
R19/A328L/A184L	19	-	9	-	9	94
VQ/S72G/A330W	17	-	-	15	2	85
R19/F87A	17	-	2	12	3	83
R19/I263A/A328L	9	-	4	-	5	45
K19/F81W/F87A	8	-	3	-	5	39
R19/F87A/ A184I	7	-	-	-	7	37
R19/A330W	7	-	-	-	7	36
R19	7	-	5	-	2	33
R19/F81W/F87A/T269G/A328G	5	-	-	3	3	27
R19/F87A/A184I/T269G/A328G	5	-	-	-	5	24
K19/F87V	5	-	1	-	3	23
K19/F87V/E267V	3	-	-	-	3	15
KU3/A330P/A328I	2	-	-	-	2	11
A330P	2	-	-	-	2	10
K19/V78I/F87V/E267V/V78I	2	-	-	-	2	10
WT	2	-	-	-	2	8
R19/S72G/A330W	1	-	-	-	1	7
R19/F87A/T269G	1	-	-	-	1	7
R19/F87A/A328G/P329G/A330G	-	-	-	-	-	-

5.3.5. Screening data for substrate 3.12



3.12 **4.46** tentative assignment **4.47** tentative assignment

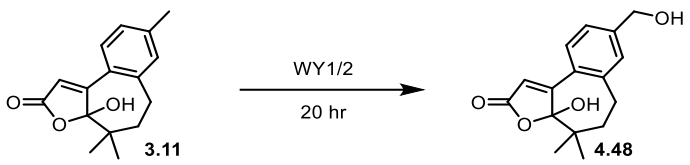
Mutant	Conversion /%	RT 3.89 /%	4.46 /%	4.47 /%	RT 6.35 /%
KT2/L188G/ I263G	87		* sample too weak		
R19/F87A/A328G	86		* sample too weak		
GLQ/I263G/A328G	86		* sample too weak		
R19/S72W/F87A/A328I	84	-	-	14	48
R19/F87A/A328G	77		* sample too weak		
K19/F81W/F87A	71		* sample too weak		
GVQ/A330W	68		* sample too weak		
R19/F87A/A184I	67		* sample too weak		
R19/F87I	67	1	3	38	23
R19/I263A/A328L	63		* sample too weak		
R19/F87A/A328L	63		* sample too weak		
GVQ	62	-	6	47	7
VQ/S72G/A330W	62		* sample too weak		
GV/A184I	59		* sample too weak		
RP/A82M/I263A	57		* sample too weak		
GVQ/A264G	56		* sample too weak		
K19/F87V	54	-	2	47	-
K19/F87V/Q403P	53		* sample too weak		
GVQ/I263G	49		* sample too weak		
KU3/S72W/A330P	49		* sample too weak		
K19/F87A/I263A	47		* sample too weak		
K19/F87V/A264G	6		* sample too weak		
K19/F87A	43	-	-	28	-
K10/F87A/I263G	42	4	3	4	-
GVQ/I263G/A328L	32	8	-	-	22
R19/V78I/F87A/A328I	29		* sample too weak		
R19	27	21	-	6	-
R19/F87A/A264G/A328G	27	7	-	-	-
R19/F87A/A328G/P329G/A330G	24		* sample too weak		
GVQ/A328G	23	1	-	6	-
RP/I263A/E267V	23	23	-	-	-
R19/F87A/A187I/T269G/A328G	18	7	-	6	-
RT2/S72G/A330W	17	2	-	-	15
K19/F87V/I263G	16	11	-	-	-
R19/F81W/F87A/T269G/A328G	16	9	-	-	-

R19/F87I/L437LV	11	11	-	-	-
R19/S72G/A330W	5	5	-	-	-
KU3/I263A/A330P	5	5	-	-	-
RP/H171L/I263G	5	1	-	2	-
R19/A184L/A328L	4	4	-	-	-
R19/F87A/T269G	3		-	-	-
R19/A330W	1	1	-	-	-
WT	1	-	-	-	-
K19/F87V/E267V	0	-	-	-	-
K19/A82M/F87A/I263G	0	-	-	-	-
K19/V78I/F87V/E267V	0	-	-	-	-
A330P	0	-	-	-	-
RP/H171L/I263G/A184I	0		too weak		

***sample too weak** – describes GC samples which showed conversion but few products, meaning the compound concentration was low. This could indicate poor extraction/ water-soluble metabolites/ product degradation etc.

5.3.6. Screening data for substrate 3.11

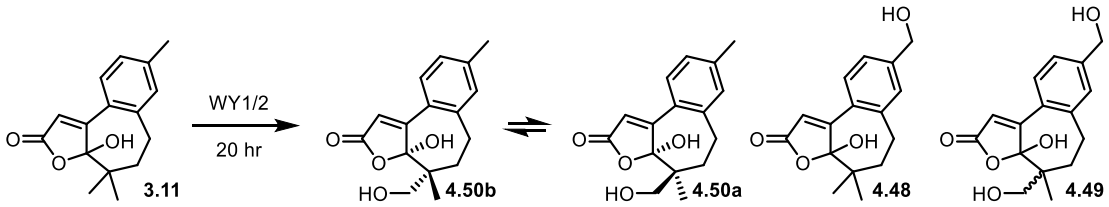
5.3.6.1. 2017 initial screening data



	Mutant	Conversion /%	4.48 /%	Other /%	Selectivity /%	TTN
A1	A82M/A330P	29	6	23	20	144
B1	I263A/A330P	18	0	18	0	88
C1	F81W/T260A	9	2	7	19	45
D1	GV/A184I	27	9	18	32	133
E1	GVQ/A264G	48	10	37	21	238
F1	K19/F87V/A264G	41	25	16	60	204
A2	K19/F87V/E267V/V78I	40	3	38	7	202
B2	KSK19/A82M/E267F	23	10	13	44	114
C2	RKA/E267F	3	0	3	0	15
D2	RK/A328L	7	0	7	0	36
E2	RKA/S72W	13	0	13	0	64
F2	RP/A82M/I263A	10	4	6	42	49
A3	RL/YF/IR	81	70	11	87	406
B3	RLYF/KSK19/A328F	8	0	8	0	41
C3	RLYF/KSK19/I263G	69	20	49	29	346

D3	RP/A82W/I263A	12	0	12	0	62
E3	RKA/V78I	10	3	7	32	49
F3	RP/F87V	81	56	25	69	403
A4	RP/F87V/V78I	18	6	12	31	88
B4	RP/H17L/I263G/A184I	42	34	8	81	209
C4	RP/H17L/I263G/A330W	43	31	12	73	213
D4	RP/H17L/I263G/F87V/V78I	31	24	7	78	155
E4	RP/V78I/E267V	82	47	35	58	411
F4	RT2/S72W/A330W	11	0	11	0	57
A5	A330P	7	0	7	0	33
B5	A82T/I263R	24	2	22	9	118
C5	GVQ	20	8	12	41	98
D5	K19	9	0	9	0	47
E5	K19/F87V	31	12	19	39	154
F5	K19/F87V/E267V	31	6	25	19	153
A6	KSK19/A82M/I263G	20	3	17	15	100
B6	K19/F87V/A328I	16	6	10	40	80
C6	KSK19/F81W	32	10	22	32	161
D6	KSK19/I263A	15	0	15	0	77
E6	K19/F87V/Q403P	26	7	19	25	129
F6	KU3/A330P/A328I	21	0	21	0	103
A7	KU3/A330P/S72W	13	0	13	0	63
B7	KU3/A330P/V78I	8	0	8	0	41
C7	RLYF/K19	4	0	4	0	18
D7	RLYF/KSK19/A184I	43	30	13	69	216
E7	RLYF/KSK19/A328I	8	1	7	11	41
F7	RLYF/KSK19	16	10	7	60	82
A8	RP/H171L	29	18	11	62	144
B8	RT2	12	7	5	58	59
C8	RT2/S72G/A330W	7	0	7	0	33
D8	RT2/A330P/V78I/A184I	22	0	22	0	111
E8	KU3/A330P	13	0	13	0	66
F8	RP/H171L/I263G	99	83	16	84	495

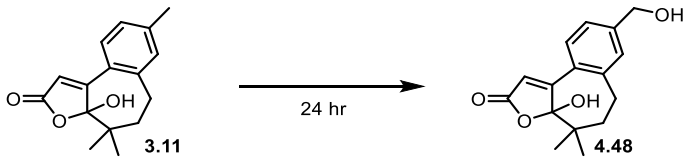
5.3.6.2. 2021 initial screening data



Mutant	Conversion /%	4.50b /%	4.50a /%	4.48 /%	Other /%	TTN
RP/H171L/I263G/A184I	100	-	-	100	-	500
K19/F87V/I263G	100	5	4	92	-	500
KT2/L188G/I263G	100	-	-	90	10	500
GVQ	100	34	42	21	3	500
K19/F87A/I263A	100	27	39	20	14	500
VQ/S72G/A330W	100	39	49	8	4	500
K19/F87A/I263G	100	54	44	-	2	500
RP/H171L/I263G	96	-	-	96	-	481
GV/A184I	90	21	18	35	17	452
GVQ/I263G	90	-	-	90	-	450
R19/F87A/A184I/T269G/A328G	88	88	-	-	-	441
R19/F87A/A328G	86	11	7	43	25	430
R19/F87I	80	-	-	76	4	401
R19/F87A/A328G	79	10	5	51	13	393
GVQ/A264G	63	17	18	18	10	314
K19/F87V/Q403P	59	19	20	20	1	297
K19/F87V/E267V	58	20	20	17	1	288
K19/F81W/F87A	56	16	16	23	1	278
GVQ/I263G/A328L	51	-	-	48	2	253
GVQ/A330W	49	17	27	-	5	244
K19/F87V/A264G	49	10	6	33	-	243
K19/F87V/E267V/V78I	31	4	5		21	153
R19/F87A	30	-	-	30	-	149
K19/A82M/F87A/I263G	24	7	8	8	-	118
R19/F81W/F87A/T269G/A328G	21	21	-	-	-	106
R19/F87A/A184I	19			8	11	93
K19/F87V	14	4	6	4	-	70
R19/F87A/A264G/A328G	9	9	-	-	-	43
RP/I263A/E267V	8	-	-	8	-	41
GVQ/A328G	7	7	-	-	-	33
RP/A82M/I263A	4	-	-	4	-	19
R19/F87A/T269G	2	2	-	-	-	12
R19/A330W	-	-	-	-	-	-
KU3/A184I/A330P	-	-	-	-	-	-
KU3/S72W//A330P	-	-	-	-	-	-

R19/A184L/A328L	-	-	-	-	-	-
R19	-	-	-	-	-	-
R19/F87A/A328L	-	-	-	-	-	-
RT2/S72G/A330W	-	-	-	-	-	-
R19/S72W/F87A/A328I	-	-	-	-	-	-
WT	-	-	-	-	-	-
A330P	-	-	-	-	-	-
R19/V78I/F87A/A328I	-	-	-	-	-	-
R19/F87I/L437LV	-	-	-	-	-	-
R19/S72G/A330W	-	-	-	-	-	-
R19/F87A/A328G/P329G/A330G	-	-	-	-	-	-
GLQ/I263G/A328G	-	-	-	-	-	-
R19/A328L/I263A	-	-	-	-	-	-

5.3.6.3. Further screening of RP/H171L/I263G-based mutants



Mutant	Conversion /%	4.48 /%	Selectivity /%	TTN
R47L/Y51F/H171L/I263G/L437LV	100	91	91	500
R47L/Y51F/H171L/I263G/K202KPG	90	79	88	451
R47L/Y51F/H171L/I263G	90	79	88	450
I263G	90	81	90	448
RP/H171L/I263G/L437LV	75	75	100	376
RP/H171L/I263G/S72W	72	63	88	358
R47L/Y51F/H171L/I263G/L437VL	67	59	89	334
RP/I263G	63	63	100	316
R47L/Y51F/H171L/I263G/L437LS	12	8	68	60
R47L/Y51F/H171L/I263G/R398H	11	8	74	55
H171L/I263G	5	-	-	25
R47L/Y51F/H171L/I263G/L437LH	5	-	-	24
R47L/Y51F/H171L/I263G/L437S	2	-	-	12
RP/H171L	2	-	-	9
RP/H171L/I263G/V78F	1	-	-	3
R47L/Y51F/H171L/I263G/L437LF	-	-	-	-
RP/H171L/I263G/V78I	-	-	-	-
RP/H171L/I263G/A184I	-	-	-	-
RP/H171L/I263G/P329G	-	-	-	-

Mutant	Conversion /%	4.48 /%	Selectivity /%	TTN
RP/H171L/I263G/L437LV/S72F	100	52	52	500
RP/H171L/I263G/L437LV/L188F	100	88	88	500
RP/H171L/I263G/L437LV/L75M	100	89	89	500
RP/H171L/I263G/L437LV/A328V	74	58	78	372
RP/H171L/I263G/L437LV/A330V	71	48	67	354
RP/H171L/I263G/L437LV/V26M	44	44	100	221
RP/H171L/I263G/L437LV/L75F	32	32	100	162
RP/H171L/I263G/L437LV/F87I	31	31	100	153
RP/H171L/I263G/L437LV/L181M	12	12	100	58
RP/H171L/I263G/L437LV/L181F	7	7	100	36
RP/H171L/I263G/L437LV/A74L	-	-	-	-
RP/H171L/I263G/L437LV/A330I	-	-	-	-
RP/H171L/I263G/L437LM	-	-	-	-

5.4. Tables of mutations

5.4.1. Initial screening plates

	Name: WY1	
	Variant	**Mutations**
1	A82M/A330P	A82M/A330P
2	I263A/A330P	I263A/A330P
3	F81W/T260A	F81W/T260A
4	GV/A184I	A74G/F87V/A184I
5	GVQ/A264G	A74G/F87V/L188Q/A264G
6	K19/F87V/A264G	F87V/H171L/A264G/Q307H/N319Y
7	K19/F87V/E267V/V78I	V78I/F87V/H171L/E267V/Q307H/N319Y
8	K19/A82M/F87A/E267F	A82M/F87A/H171L/E267F/Q307H/N319Y
9	R19/F87A/E267F/A328I	R47L/Y51F/F87A/H171L/E267F/Q307H/N319Y/A328I
10	R19/F87A/A328L	R47L/Y51F/F87A/H171L/Q307H/N319Y/A328L
11	R19/S72W/F87A/A328I	R47L/Y51F/S72W/F87A/H171L/Q307H/N319Y/A328I
12	R19/V78I/F87A/A328I	R47L/Y51F/V78I/F87A/H171L/Q307H/N319Y/A328I
13	RL/YF/IR	R47L/Y51F/I263R
14	R19/F87A/A328F	R47L/Y51F/F87A/H171L/Q307H/N319Y/A328F
15	R19/F87A/I263G	R47L/Y51F/F87A/H171L/I263G/Q307H/N319Y
16	RP/A82W/I263A	R47L/Y51F/A82W/I263A/I401P
17	RP/A82M/I263A	R47L/Y51F/A82M/I263A/I401P
18	RP/F87V	R47L/Y51F/F87V/I401P
19	RP/F87V/V78I	R47L/Y51F/V78I/F87V/I401P
20	RP/H171L/I263G/A184I	R47L/Y51F/H17L/I263G/A184I/I401P
21	RP/H171L/I263G/A330W	R47L/Y51F/H17L/I263G/A330W/I401P
22	RP/H171L/I263G/F87V/V78I	R47L/Y51F/V78I/F87V/H171L/I263G/I401P
23	RP/V78I/E267V	R47L/Y51F/V78I/E267V/I401P
24	RT2/S72W/A330W	R47L/Y51F/S72W/A191T/N239H/I259V/A276T/A330W /L353I

	Name: WY2	
	Variant	**Mutations**
1	A330P	A330P
2	A82T/I263R	A82T/I263R
3	GVQ	A74G/F87V/L188Q
4	K19	H171L/Q307H/N319Y
5	K19/F87V	F87V/H171L/Q307H/N319Y
6	K19/F87V/E267V	F87V/H171L/E267V/Q307H/N319Y
7	K19/F87A/A82M/I263G	A82M/F87A/H171L/I263G/Q307H/N319Y
8	K19/F87V/A328I	F87V/H171L/Q307H/N319Y/A328I
9	K19/F87A/F81W	F81W/F87A/H171L/Q307H/N319Y
10	K19/F87A/I263A	F87A/H171L/I263A/Q307H/N319Y
11	K19/F87V/Q403P	F87V/H171L/Q307H/N319Y/Q403P
12	KU3/A330P/A328I	N239H/I259V/A276T/A330P/A328I
13	KU3/A330P/S72W	S72W/N239H/I259V/A276T/A330P
14	KU3/A330P/V78I	V78I/N239H/I259V/A276T/A330P
15	R19	R47L/Y51F/H171L/Q307H/N319Y
16	R19/F87A/A184I	R47L/Y51F/F87A/H171L/A184I/Q307H/N319Y
17	R19/F87A/A328I	R47L/Y51F/F87A/H171L/Q307H/N319Y/A328I
18	R19/F87A	R47L/Y51F/F87A/H171L/Q307H/N319Y
19	RP/H171L	R47L/Y51F/H171L/I401P
20	RT2	R47L/Y51F/A191T/N239H/I259V/A276T/L353I
21	RT2/S72G/A330W	R47L/Y51F/S72G/A191T/N239H/I259V/A276T/A330W/L353I
22	RT2/A330P/V78I/A184I	R47L/Y51F/V78I/A184I/A191T/N239H/I259V/A276T/A330P /L353I
23	KU3/A330P	N239H/I259V/A276T/A330P
24	RP/H171L/I263G	R47L/Y51F/H171L/I263G/I401P

	Name: WY5	
	Variant	**Mutations**
1	R19/A330W	R47L/Y51F/H171L/Q307H/N319Y/A330W
2	K19/F87A/I263G	F87A/H171L/I263G/Q307H/N319Y
3	GVQ	A74G/F87V/L188Q
4	R19/F87I	R47L/Y51F/F87I/H171L/Q307H/N319Y
5	K19/F87V	F87V/H171L/Q307H/N319Y
6	K19/F87V/E267V	F87V/H171L/E267V/Q307H/N319Y
7	K19/A82M/F87A/I263G	A82M/F87A/H171L/I263G/Q307H/N319Y
8	K19/F87V/A328V	F87V/H171L/Q307H/N319Y/A328V
9	K19/F81W/F87A	F81W/F87A/H171L/Q307H/N319Y
10	K19/F87A/I263A	F87A/H171L/I263A/Q307H/N319Y
11	K19/F87V/Q403P	F87V/H171L/Q307H/N319Y/Q403P
12	KU3/A328I/A330P	N239H/I259V/A276T/A328I/A330P
13	R19/A184I/A328L	R47L/Y51F/H171L/A184I/Q307H/N319Y/A328I
14	R19/F87A/A328G	R47L/Y51F/F87A/H171L/Q307H/N319Y/A328G
15	R19	R47L/Y51F/H171L/Q307H/N319Y
16	R19/F87A/A184I	R47L/Y51F/F87A/H171L/A184I/Q307H/N319Y
17	A82F/I263F	A82F/I263F
18	R19/F87A	R47L/Y51F/F87A/H171L/Q307H/N319Y
19	GV/A184I	A74G/F87V/A184I
20	RT2	R47L/Y51F/A191T/N239H/I259V/A276T/L353I
21	RT2/S72G/A330W	R47L/Y51F/S72G/A191T/N239H/I259V/A276T/ A330W/L353I
22	RT2/V78I/A330P/A184I	R47L/Y51F/V78I/A184I/A191T/N239H/I259V/A276T/ A330P/L353I
23	KU3/A330P	N239H/I259V/A276T/A330P
24	RP/H171L/I263G	R47L/Y51F/H171L/I263G/I401P

	Name: WY6	
	Variant	**Mutations**
1	RP/I263A/E267V	R47L/Y51F/I263A/E267V/I401P
2	RP/H171L/I263G/L437V	R47L/Y51F/I401P/H171L/I263G/L437V
3	WT	WT
4	GVQ/I263G	A74G/F87V/L188Q/I263G
5	GVQ/A264G	A74G/F87V/L188Q/A264G
6	K19/F87V/A264G	F87V/H171L/A264G/Q307H/N319Y
7	K19/V78I/F87V/E267V	V78I/F87V/H171L/E267V/Q307H/N319Y
8	K19/A82M/F87A/E267F	A82M/F87A/H171L/E267F/Q307H/N319Y
9	K19/A82M/F87A	A82M/F87A/H171L/Q307H/N319Y
10	R19/F87A/A328L	R47L/Y51F/F87A/H171L/Q307H/N319Y/A328L
11	R19/F87A/A264G/A328G	R47L/Y51F/F87A/H171L/A264G/Q307H/N319Y/ A328G
12	R19/V78I/F87A/A328I	R47L/Y51F/V78I/F87A/H171L/Q307H/N319Y/A328I
13	R19/F87I/L437LV	R47L/Y51F/F87I/H171L/Q307H/N319Y/L437LV
14	R19/F87A/A328F	R47L/Y51F/F87A/H171L/Q307H/N319Y/A328F
15	R19/F87A/I263G	R47L/Y51F/F87A/H171L/I263G/Q307H/N319Y
16	RP/A82W/I263A	R47L/Y51F/A82W/I263A/I401P
17	RP/A82M/I263A	R47L/Y51F/A82M/I263A/I401P
18	RP/F87V	R47L/Y51F/F87V/I401P
19	RP/V78I/F87V	R47L/Y51F/V78I/F87V/I401P
20	I263G	I263G
21	R19/I263G/A328L	R47L/Y51F/H171L/I263G/Q307H/N319Y/A328I
22	RP/V78I/F87V/H171L/I263G	R47L/Y51F/V78I/F87V/H171L/I263G/I401P
23	RP/V78I/E267V	R47L/Y51F/V78I/E267V/I401P
24	RT2/S72W/A330W	R47L/Y51F/S72W/A191T/N239H/I259V/A276T/ A330W/L353I

	Name: WY7	
	Variant	**Mutations**
1	R19/A330W	R47L/Y51F/H171L/Q307H/N319Y/A330W
2	K19/F87A/I263G	F87A/H171L/I263G/Q307H/N319Y
3	GVQ	A74G/F87V/L188Q
4	R19/F87I	R47L/Y51F/F87I/H171L/Q307H/N319Y
5	K19/F87V	F87V/H171L/Q307H/N319Y
6	K19/F87V/E267V	F87V/H171L/E267V/Q307H/N319Y
7	K19/A82M/F87A/I263G	A82M/F87A/H171L/I263G/Q307H/N319Y
8	K19/F87V/A328V	F87V/H171L/Q307H/N319Y/A328V
9	K19/F81W/F87A	F81W/F87A/H171L/Q307H/N319Y
10	K19/F87A/I263A	F87A/H171L/I263A/Q307H/N319Y
11	K19/F87V/Q403P	F87V/H171L/Q307H/N319Y/Q403P
12	KU3/A328I/A330P	N239H/I259V/A276T/A328I/A330P
13	R19/A184I/A328L	R47L/Y51F/H171L/A184I/Q307H/N319Y/A328I
14	R19/F87A/A328G	R47L/Y51F/F87A/H171L/Q307H/N319Y/A328G
15	R19	R47L/Y51F/H171L/Q307H/N319Y
16	R19/F87A/A184I	R47L/Y51F/F87A/H171L/A184I/Q307H/N319Y
17	GVQ/V78L/I263G	A74G/V78L/F87V/L188Q/I263G
18	R19/F87A	R47L/Y51F/F87A/H171L/Q307H/N319Y
19	GV/A184I	A74G/F87V/A184I
20	RT2	R47L/Y51F/A191T/N239H/I259V/A276T/L353I
21	R19/F87A/I263G/A264G	R47L/Y51F/F87A/H171L/I263G/A264G/Q307H/N319Y
22	RT2/V78I/A184I/A330P	R47L/Y51F/V78I/A184I/A191T/N239H/I259V/A276T/ A330P/L353I
23	R19/F87A/G265GG	R47L/Y51F/F87A/H171L/G265GG/Q307H/N319Y
24	RP/H171L/I263G	R47L/Y51F/H171L/I263G/I401P

	Name: WY8	
	Variant	**Mutations**
1	RP/I263A/E267V	R47L/Y51F/I263A/E267V/I401P
2	R19/S72W/F87A/A328I	R47L/Y51F/S72W/F87A/H171L/Q307H/N319Y/A328I
3	WT	WT
4	GVQ/I263G	A74G/F87V/L188Q/I263G
5	GVQ/A264G	A74G/F87V/L188Q/A264G
6	K19/F87V/A264G	F87V/H171L/A264G/Q307H/N319Y
7	K19/V78I/F87V/E267V	V78I/F87V/H171L/E267V/Q307H/N319Y
8	K19/A82M/F87A/E267F	A82M/F87A/H171L/E267F/Q307H/N319Y
9	K19/A82M/F87A	A82M/F87A/H171L/Q307H/N319Y
10	R19/F87A/A328L	R47L/Y51F/F87A/H171L/Q307H/N319Y/A328L
11	R19/F87A/A264G/A328G	R47L/Y51F/F87A/H171L/A264G/Q307H/N319Y/A328G
12	R19/V78I/F87A/A328I	R47L/Y51F/V78I/F87A/H171L/Q307H/N319Y/A328I
13	R19/F87I/L437LV	R47L/Y51F/F87I/H171L/Q307H/N319Y/L437LV
14	GVQ/A330W	A74G/F87V/L188Q/A330W
15	R19/F87A/I263G	R47L/Y51F/F87A/H171L/I263G/Q307H/N319Y
16	GVQ/A82M/I263G	A74G/A82M/F87V/L188Q/I263G
17	RP/A82M/I263A	R47L/Y51F/A82M/I263A/I401P
18	RP/F87V	R47L/Y51F/F87V/I401P
19	RP/V78I/F87V	R47L/Y51F/V78I/F87V/I401P
20	I263G	I263G
21	GVQ/I263G/A328L	A74G/F87V/L188Q/I263G/A328L
22	R19/F87A/A328G/P329G/A330G	R47L/Y51F/F87A/H171L/Q307H/N319Y/A328G/P329G/A330G
23	RP/V78I/E267V	R47L/Y51F/V78I/E267V/I401P
24	R19/I263A/A328L	R47L/Y51F/H171L/I263A/Q307H/N319Y/A328L

	Name: WY13	
	Variant	**Mutations**
1	R19/A330W	R47L/Y51F/H171L/Q307H/N319Y/A330W
2	K19/F87A/I263G	F87A/H171L/I263G/Q307H/N319Y
3	GVQ	A74G/F87V/L188Q
4	R19/F87I	R47L/Y51F/F87I/H171L/Q307H/N319Y
5	K19/F87V	F87V/H171L/Q307H/N319Y
6	K19/F87V/E267V	F87V/H171L/E267V/Q307H/N319Y
7	K19/A82M/F87A/I263G	A82M/F87A/H171L/I263G/Q307H/N319Y
8	R19/F87A/A328G	R47L/Y51F/F87A/H171L/Q307H/N319Y/A328G
9	K19/F81W/F87A	F81W/F87A/H171L/Q307H/N319Y
10	K19/F87A/I263A	F87A/H171L/I263A/Q307H/N319Y
11	KU3/A184I/A330P	N239H/I259V/A276T/A330P/A328I
12	KU3/S72W//A330P	S72W/N239H/I259V/A276T/A330P
13	R19/A184L/A328L	R47L/Y51F/H171L/A184L/Q307H/N319Y/A328L
14	R19/F87A/A328G	R47L/Y51F/F87A/H171L/Q307H/N319Y/A328G
15	R19	R47L/Y51F/F87V/H171L/Q307H/N319Y
16	R19/F87A/A184I	R47L/Y51F/H171L/Q307H/N319Y
17	KT2/L188G/I263G	R47L/Y51F/L188G/A191T/N239H/I259V/I263G/ A276T/L353I
18	R19/F87A	R47lL/Y51F/F87A/H171L/Q307H/N319Y
19	GV/A184I	A74G/F87V/A184I
20	K19/F87V/Q403P	F87V/H171L/Q307H/N319Y/Q403P
21	R19/F87A/A184I/T269G/A328G	R47L/Y51F/F87A/H171L/A184I/T269G/Q307H/ N319Y/A328G
22	R19/F87A/A328L	R47L/Y51F/F87A/H171L/Q307H/N319Y/A328L
23	RT2/S72G/A330W	R47L/Y51F/A191T/N239H/I259V/A276T/L353I
24	RP/H171L/I263G	R47L/Y51F/H171L/I263G/I401P

	Name: WY14	
	Variant	**Mutations**
1	RP/I263A/E267V	R47L/Y51F/I263A/E267V/I401P
2	R19/S72W/F87A/A328I	R47L/Y51F/S72W/F87A/H171L/Q307H/ N319Y/A328I
3	WT	WT
4	GVQ/I263G	A74G/F87V/L188Q/I263G
5	GVQ/A264G	A74G/F87V/L188Q/A264G
6	K19/F87V/A264G	F87V/H171L/A264G/Q307H/N319Y
7	K19/F87V/E267V/V78I	V78I/F87V/H171L/E267V/Q307H/N319Y
8	A330P	A330P
9	K19/F87V/I263G	F87V/H171L/I263G/Q307H/N319Y
10	R19/F81W/F87A/T269G/A328G	R47L/Y51F/F81W/F87A/H171L/T269G/Q307H/ N319Y/A328G
11	R19/F87A/A264G/A328G	R47L/Y51F/F87A/H171L/A264G/Q307H/ N319Y/A328G
12	R19/V78I/F87A/A328I	R47L/Y51F/V78I/F87A/H171L/Q307H/ N319Y/A328I
13	R19/F87I/L437LV	R47L/Y51F/F87I/H171L/Q307H/N319Y/L437LV
14	GVQ/A330W	A74G/F87V/L188Q/A330W
15	R19/S72G/A330W	R47L/Y51F/S72G/H171L/Q307H/N319Y/A330W
16	GVQ/A328G	A74G/F87V/L188Q/A328G
17	RP/A82M/I263A	R47L/Y51F/A82M/I263A/I401P
18	R19/F87A/T269G	R47L/Y51F/F87A/H171L/T269G/Q307H/N319Y
19	RP/H171L/I263G/A184I	R47L/Y51F/H171L/I263G/A328I/I401P
20	VQ/S72G/A330W	S72G/F87V/L188Q/A330W
21	GVQ/I263G/A328L	A74G/F87V/L188Q/I263G/A328L
22	R19/F87A/A328G/P329G/A330G	R47L/Y51F/F87A/H171L/Q307H/N319Y/A328G/ P329G/A330G
23	GLQ/I263G/A328G	A74G/F87V/L188Q/I263G/A328G
24	R19/A328L/I263A	R47L/Y51F/H171L/I263A/Q307H/N319Y/A328L

	Name: WY15	
	Variant	**Mutations**
1	R19/A330W	R47L/Y51F/H171L/Q307H/N319Y/A330W
2	KSK19/I263G	F87A/H171L/I263G/Q307H/N319Y
3	GVQ	A74G/F87V/L188Q
4	R19/F87I	R47L/Y51F/F87I/H171L/Q307H/N319Y
5	K19/F87V	F87V/H171L/Q307H/N319Y
6	K19/F87V/E267V	F87V/H171L/E267V/Q307H/N319Y
7	K19/A82M/F87A/I263G	A82M/F87A/H171L/I263G/Q307H/N319Y
8	GV/A184I/I263G/A328G	A74G/F87V/A184I/I263G/A328G
9	K19/F81W/F87A	F81W/F87A/H171L/Q307H/N319Y
10	K19/F87A/I263A	F87A/H171L/I263A/Q307H/N319Y
11	KU3/A184I/A330P	N239H/I259V/A276T/A328I/A330P/A328I
12	KU3/S72W/A330P	S72W/N239H/I259V/A276T/A330P
13	GQ/I263G/A328L	A74G/L188Q/I263G/A328L
14	R19/F87A/A328G	R47L/Y51F/F87A/H171L/Q307H/N319Y/A328G
15	R19	R47L/Y51F/F87V/H171L/Q307H/N319Y
16	R19/F87A/A184I	R47L/Y51F/H171L/Q307H/N319Y
17	KT2/L188G/I263G	R47L/Y51F/L188G/A191T/N239H/I259V/I263G/ A276T/L353I
18	R19/F78A	R47lL/Y51F/F87A/H171L/Q307H/N319Y
19	GV/A184I	A74G/F87V/A184I
20	K19/F87V/Q403P	F87V/H171L/Q307H/N319Y/Q403P
21	R19/F87A/A184I/T269G/A328G	R47L/Y51F/F87A/H171L/A184I/T269G/Q307H/ N319Y/A32G
22	R19/F87A/A328L	R47L/Y51F/F87A/H171L/Q307H/N319Y/A328L
23	RT2/S72G/A330W	R47L/Y51F/A191T/N239H/I259V/A276T/L353I
24	RP/H171L/I263G	R47L/Y51F/H171L/I263G/I401P

	Name: WY16	
	Variant	**Mutations**
1	RP/I263A/E267V	R47L/Y51F/I263A/E267V/I401P
2	R19/S72W/F87A/A328I	R47L/Y51F/S72W/F87A/H171L/Q307H /N319Y/A328I
3	WT	WT
4	GVQ/I263G	A74G/F87V/L188Q/I263G
5	GVQ/A264G	A74G/F87V/L188Q/A264G
6	K19/F87V/A264G	F87V/H171L/A264G/Q307H/N319Y
7	K19/F87V/E267V/V78I	V78I/F87V/H171L/E267V/Q307H/N319Y
8	A330P	A330P
9	K19/F87V/I263G	F87V/H171L/I263G/Q307H/N319Y
10	RK/F81W/T269G/A328G	R47L/Y51F/F81W/F87A/H171L/T269G /Q307H/ N319Y/A328G
11	RK/A328G/A264G	R47L/Y51F/F87A/H171L/A264G/Q307H /N319Y/A328G
12	RKA/V78I	R47L/Y51F/V78I/F87A/H171L/Q307H /N319Y/A328I
13	R19/F87I/L437LV	R47L/Y51F/F87I/H171L/Q307H/N319Y /L437LV
14	GVQ/A330W	A74G/F87V/L188Q/A330W
15	R19/S72G/A330W	R47L/Y51F/S72G/H171L/Q307H/N319Y /A330W
16	GVQ/A328G	A74G/F87V/L188Q/A328G
17	RP/A82M/I263A	R47L/Y51F/A82M/I263A/I401P
18	RK/T260G	R47L/Y51F/F87A/H171L/T260G/Q307H /N319Y
19	RP/H171L/I263G/A184I	R47L/Y51F/H171L/I263G/A328I/I401P
20	VQ/S72G/A330W	S72G/F87V/L188Q/A330W
21	GVQ/I263G/A328L	A74G/F87V/L188Q/I263G/A328L
22	RK/A328G/P329G/A330G	R47L/Y51F/F87A/H171L/Q307H/N319Y/ A328G/P329G/A330G
23	GLQ/I263G/A328G	A74G/F87V/L188Q/I263G/A328G
24	R19/A328L/I263A	R47L/Y51F/H171L/I263A/Q307H/N319Y /A328L

5.4.2. Focused second generation libraries

	Name: V1/V2	
	Variant	**Mutations**
1	I263G	I263G
2	I263S	I263S
3	I263V	I263V
4	I263W	I263W
5	I263R	I263R
6	H171L/I263G	H171L/I263G
7	RP/H171L/I263G	R47L/Y51F/H171L/I263G/I401P
8	RP/H171L/I263R	R47L/Y51F/H171L/I263R/I401P
9	RP/H171L/I263G/A184I	R47L/Y51F/H171L/A184I/I263G/I401P
10	RP/H171L/I263G/A330P	R47L/Y51F/H171L/I263G/A330P/I401P
11	RP/H171L/I263G/L437LV	R47L/Y51F/H171L/I263G/I401P/L437LV
12	R47L/Y51F/H171L/I263G	R47L/Y51F/H171L/I263G
13	R47L/Y51F/H171L/I263S	R47L/Y51F/H171L/I263S
14	R47L/Y51F/H171L/I263V	R47L/Y51F/H171L/I263V
15	R47L/Y51F/H171L/I263W	R47L/Y51F/H171L/I263W
16	R47L/Y51F/H171L/I263R	R47L/Y51F/H171L/I263R
17	R47L/Y51F/H171L/I263G/L437S	R47L/Y51F/H171L/I263G/L437S
18	R47L/Y51F/H171L/I263G/L437LV	R47L/Y51F/H171L/I263G/L437LV
19	R47L/Y51F/H171L/I263G/L437LA	R47L/Y51F/H171L/I263G/L437LA
20	R47L/Y51F/H171L/I263G/L437LH	R47L/Y51F/H171L/I263G/L437LH
21	R47L/Y51F/H171L/I263G/L437LM	R47L/Y51F/H171L/I263G/L437LM
22	R47L/Y51F/H171L/I263G/L437LF	R47L/Y51F/H171L/I263G/L437LF
23	R47L/Y51F/H171L/I263G/L437VL	R47L/Y51F/H171L/I263G/L437VL
24	R47L/Y51F/H171L/I263G/L437LS	R47L/Y51F/H171L/I263G/L437LS
25	R47L/Y51F/H171L/I263G/V78I/L437LH	R47L/Y51F/V78I/H171L/I263G/L437LH
26	R47L/Y51F/H171L/I263G/V78I/L437LS	R47L/Y51F/V78I/H171L/I263G/L437LS
27	R47L/Y51F/H171L/I263G/V78I/L437VL	R47L/Y51F/V78I/H171L/I263G/L437VL
28	R47L/Y51F/H171L/I263G/V78I/L437LA	R47L/Y51F/V78I/H171L/I263G/L437LA
29	R47L/Y51F/H171L/I263G/V78I/L437LI	R47L/Y51F/V78I/H171L/I263G/L437LI
30	R47L/Y51F/H171L/I263G/V78I/L437LV	R47L/Y51F/V78I/H171L/I263G/L437LV
31	R47L/Y51F/H171L/I263G/V78I/L437LM	R47L/Y51F/V78I/H171L/I263G/L437LM
32	R47L/Y51F/V78L/H171L/I263R	R47L/Y51F/V78L/H171L/I263R
33	R47L/Y51F/V78L/H171L/I263W	R47L/Y51F/V78L/H171L/I263W
34	R47L/Y51F/H171L/I263G/V78L	R47L/Y51F/V78L/H171L/I263G
35	R47L/Y51F/V78L/H171L/I263S	R47L/Y51F/V78L/H171L/I263S
36	R47L/Y51F/V78L/H171L/I263V	R47L/Y51F/V78L/H171L/I263V
37	R47L/Y51F/H171L/I263G/F81W	R47L/Y51F/F81W/H171L/I263G

38	R47L/Y51F/H171L/I263G/A82M	R47L/Y51F/A82M/H171L/I263G
39	R47L/Y51F/H171L/I263G/K202KPG	R47L/Y51F/H171L/I263G/K202KPG
40	R47L/Y51F/H171L/I263G/A330P	R47L/Y51F/H171L/I263G/A330P
41	R47L/Y51F/H171L/I263G/R398H	R47L/Y51F/H171L/I263G/R398H

	Name: LAH1	
	Variant	**Mutations**
1	GV/A184I	A74G/F87V/A184I
2	GV/A184F	A74G/F87V/A184F
3	GV/A184M	A74G/F87V/A184M
4	GL/A184I	A74G/F87L/A184I
5	GG/A184I	A74G/F87G/A184I
6	GA/A184I	A74G/F87A/A184I
7	GV/A184I/V26L	V26L/A74G/F87V/A184I
8	GV/A184I/V26M	V26M/A74G/F87V/A184I
9	GV/A184I/V26F	V26F/A74G/F87V/A184I
10	GV/A184I/S72M	S72M/A74G/F87V/A184I
11	S72W/F87V/A184I	S72W/F87V/A184I
12	GV/A184I/L75F	A74G/L75F/F87V/A184I
13	GV/A184I/L188M	A74G/F87V/A184I/L188M
14	GV/A184I/L188Q	A74G/F87V/A184I/L188Q
15	GV/A184I/A328L	A74G/F87V/A184I/A328L
16	GV/A184I/I263W	A74G/F87V/A184I/I263W
17	GV/A184I/A330I	A74G/F87V/A184I/A330I
18	GV/A184I/A330W	A74G/F87V/A184I/A330W
19	GV/A184I/L437M	A74G/F87V/A184I/L437M
20	GV/A184I/L437F	A74G/F87V/A184I/L437F
21	GV/A184I/L437LM	A74G/F87V/A184I/L437LM
22	GV/A184I/L437LF	A74G/F87V/A184I/L437LF
23	GV/A184I/L437LH	A74G/F87V/A184I/L437LH
24	GV/A184I/H171L/L188Q	A74G/F87V/H171L/A184I/L188Q

	Name: SES3	
	Variant	**Mutations**
1	RP/F87V/E267V	R47L/Y51F/F87V/E267V/I401P
2	RT2/A328N	R47L/Y51F/A191T/N239H/I259V/A276T/A328N/L353I
3	R19/F87I/A330W	R47L/Y51F/F87I/H171L/Q307H/N319Y/A330W
4	RT2/A330P/V78I	R47L/Y51F/V78I/A191T/N239H/I259V/A276T/A330P /L353I
5	RT2/A330P/A82M	R47L/Y51F/A82M/A191T/N239H/I259V/A276T/A330P /L353I
6	RP/E267V	R47L/Y51F/E267V/I401P
7	K19/A82M/F87A	A82M/F87A/H171L/Q307H/N319Y
8	RP/E267G	R47L/Y51F/E267G/I401P
9	RT2/I401P	R47L/Y51F/A191T/N239H/I259V/A276T/L353I/I401P
10	RT2	R47L/Y51F/A191T/N239H/I259V/A276T/L353I
11	RT2/A330P/A184I	R47L/Y51F/A184I/A191T/N239H/I259V/A276T/A330P /L353I
12	RT2/F81W	R47L/Y51F/F81W/A191T/N239H/I259V/A276T/L353I
13	KSK19/A328I/I263A	F87A/H171L/I263A/Q307H/N319Y/A328I
14	KSK19/A328I	F87A/H171L/Q307H/N319Y/A328I
15	RT2/S72G/A330P/L437LA	R47L/Y51F/S72G/A191T/N239H/I259V/A276T/A330P /L353I/L437LA
16	RT2/A330P/L437LA	R47L/Y51F/A191T/N239H/I259V/A276T/A330P/L353I /L437LA
17	KU3/A330S/L437LA	N239H/I259V/A276T/A330S/L437LA
18	R19/A330W	R47L/Y51F/H171L/Q307H/N319Y/A330W
19	RT2/S72G/A330W/L437LA	R47L/Y51F/S72G/A191T/N239H/I259V/A276T/A330W /L353I/L437LA
20	RP/H171L/I263G	R47L/Y51F/H171L/I263G/I401P
21	K19/F87V/A328L	F87V/H171L/Q307H/N319Y/A328L
22	GVQ/S72W	S72W/A74G/F87V/L188Q
23	R19/F87I/A330P	R47L/Y51F/F87I/H171L/Q307H/N319Y/A330P
24	RT2/A330P	R47L/Y51F/A191T/N239H/I259V/A276T/A330P/L353I

5.5. References for Chapter 5

(1) M. Odagi, Y. Yamamoto and K. Nagasawa, *Angew. Chem. Int. Ed.,* **2018**, *57*, p2229-2232.

(2) C. Liu, B. Pan and Y. Gu, *Chinese Journal of Catalysis*, **2016**, *37*, p979-986.

(3) S. W. Youn, S. J. Pastine and D. Sames, *Org. Lett.,* **2004**, **6**, p581-584.

(4) S. R. Angle and M. S. Louie, *Tet. Lett.,* **1989**, *30(42)*, p5741-5744.

(5) C. S. Schneider and K. H. Pook, *J. Chem. Soc. Perkin Trans. I,* **1986**, p877-883.

(6) Z. Li, Z. Duan, H. Wang, R. Tian, Q. Zhu and Y. Wu, *Synlett,* **2008,** *16*, p2535-2539.

(7) F. Muhlthau, D. Stadler, A. Goeppert, G. A. Olah, G. K. S. Prakash and T. Bach, *J. Am. Chem. Soc.,* **2006**, *128*, p9668-9675.

(8) K. Mertins, I. Iovel, J. Kischel, A. Zapf and M. Beller, *Adv. Synth. Catal.,* **2006**, *348*, p691-695.

(9) I. Iovel, K. Mertins, J. Kischel, A. Zapf and M. Beller, *Angew. Chem. Int. Ed.,* **2005**, *44*, p3913-3917.

(10) M. Noji, T. Ohno, K. Fuji, N. Futaba, H. Tajima and K. Ishii, *J. Org. Chem.,* **2003**, *68*, p9340-9347.

Chapter 6: Experimental Details

6.1. Materials and Methods

6.1.1. General considerations

Atom numbering illustrates peak assignments and do not necessarily correspond to IUPAC nomenclature. Solvents and reagents were used as commercially supplied or purified by standard techniques. Acetonitrile, ether, CH_2Cl_2 and benzene were obtained in Grubbs canisters, with the solvent passing through an activated alumina column under argon. THF was freshly distilled over Na/ benzophenone. Hünig's base and triethylamine were distilled over KOH and stored under Ar. Trimethylsilyl trifluoromethanesulfonate was freshly distilled before use, and stored under Ar. All glassware flame dried before use. N_2 or Ar atmosphere was used for all reactions unless otherwise stated.

Media components, kanamycin and IPTG were supplied by Melford Laboratories, UK; Lysozyme was from Sigma-Aldrich, $NADP^+$ was from Prozomix and glucose dehydrogenase (GDH) was from Codexis, USA. Oligonucleotides were supplied by Eurofins Genetic Service, UK. Standard phosphate buffer used as reaction media in biotransformations (2.4 g KH_2PO_4 and 31.7 g K_2HPO_4 dissolved in 1 L deionised H_2O, adjusted to pH 7.9 before use).

Merck aluminium backed DC60 F254 plates (0.2 mm) were used for TLC analysis and were visualised with long wave ultra-violet light before staining with potassium permanganate, anisaldehyde or vanillin and developed with heat. Merck silicagel 60 (43- 60 μm) was used for column chromatography and the solvent system used and retention factors are recorded with experimental data.

Proton ^1H, carbon ^{13}C, ^{31}P ^{19}F NMR spectra were recorded on a Bruker AVIII400 MHz or 500 MHz spectrometer as specified. δ_H and δ_C are recorded to the nearest 0.01 ppm and 0.1 ppm respectively; coupling constants have been rounded to the nearest 0.1 Hz. Peak multiplicities are described as apparent (app.), broad (br.), singlet (s), doublet (d), triplet (t), quartet (q) etc..., or as combinations or multiplets (m). Solvents are referenced as C_6D_6: δ_H 7.16, δC 128.06 ppm; $CDCl_3$ δ_H 7.26, 77.16 ppm.

Peak assignments were made based on chemical shift, integration, coupling constants, COSY and HSQC spectra. HMBC spectra were obtained if required. Infra-red spectra were recorded using a Bruker Tensor 27 FT-IR spectrometer. Absorption maxima are reported in wavenumbers/cm^{-1} and described as strong (s), medium (m), weak (w) and broad (br.) relative to the most intense peak. Low resolution mass spectra were recorded using a Micromass LCT Premier spectrometer (ESI±). High resolution mass spectra were obtained for novel compounds on a Bruker Daltronics MicroTOF spectrometer (ESI/FI). Mass to charge ratios (m/z) are reported in Daltons and intensities are recorded as a percentage relative to the most intense peak. The injector temperature was 280 °C and the FID was at 250 °C. Melting points are recorded in degree Celsius using a Griffin melting point apparatus, where relevant a range may be specified.

6.1.2. Gas chromatographic analysis

Gas chromatographic (GC) analyses were carried out with a ThermoFisher Scientific Trace 1300 instrument equipped with a flame ionisation detector (FID) and an AI1310 autosampler using a J&W DB-1MS fused silica column (30 m × 0.25 mm × 0.25 μm, Agilent Technology, UK) with He as carrier gas at a flow rate of 1.5 mL min^{-1}. The injector was held at 280 °C and the FID temperature was 250 °C. GC methods were optimised for each substrate/product combination.

6.1.3. Enzymes and molecular biology

Genes encoding CYP102A1 enzymes were cloned in the pET28+ vector by NcoI and BamHI restriction sites.[1] Site-directed mutagenesis was carried out by standard PCR-based protocols using a KOD Hot Start DNA Polymerase kit from Sigma-Aldrich, UK. The presence of the target mutation(s) was confirmed by DNA sequencing. The relevant plasmid was transformed into chemically competent *E. coli* BL21 (DE3) cells for enzyme production and subsequent purification as described previously.[2] P450 content was quantified using the CO-difference method, using UV-vis spectra acquired on a Varian CARY50 spectrophotometer at 30 °C using 1 cm pathlength quartz cuvettes.[3]

6.2. Experimental procedures for Chapter 2

6.2.1. $P450_{BM3}$ screening conditions

24-well screening plates were prepared by diluting enzymes to 10 mM stock solutions and pipetting 100 μL into each well. 400 μL of the screening mixture detailed below was added to make the final reaction volume up to 500 μL. Substrates were dissolved in DMSO, MeOH or EtOH to give 100 mM stock solutions. The below describes 1 mM substrate : 2 μM enzyme (500:1); where higher substrate concentration are used, buffer is adjusted to keep final reaction volume at 500 μL.

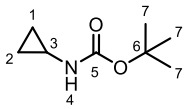
Reagent	Stock Concentration	Final Concentration	Volume (μL)
Phosphate Buffer	200 mM	-	325
Glucose	1 M	100 mM	50
GDH	200 U mL^{-1}	4 U mL^{-1}	10
$NADP^+$	4 mM	80 μM	10
Substrate	100 mM	1 mM	5

Table 1 - Composition of initial screening mixture.

Plates were left to shake at ambient temperature, 150 rpm. After 24 hours, the contents of each well was transferred to a 1.5 mL microcentrifuge tube and 300 mL ethyl acetate was added to extract the organics. The mixture was vortexed for 15 s then centrifuged at 13,300 rpm for 2 min to separate the aqueous and organic layers. 100 μL of the organic layer was removed for GC analysis.

6.2.2. Synthesis of starting materials

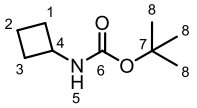
tert-Butyl cyclopropylcarbamate **2.64**



Chemical Formula: $C_8H_{15}NO_2$
Exact Mass: 157.1103
Molecular Weight: 157.2130

To a stirred solution of aminocyclopropane (602 µL, 8.76 mmol, 1 eq.) in CH_2Cl_2 (17.5 mL) at 0 °C, di-*tert*-butyl decarbonate (2.1 g, 9.6 mmol, 1.1 eq.) in CH_2Cl_2 (9 mL) was slowly added. The reaction was then warmed to RT and stirred for 1 hr. Upon completion, the reaction was washed with H_2O (2 x 30 mL), brine (50 mL), dried over $MgSO_4$ and filtered. The solvent was removed *in vacuo* yielding the title compound as a white crystalline solid (1.24 g, 7.9 mmol, 90%) which was used without further purification. $\mathbf{R_f}$ 0.13 (5% EtOAc in pentane). **^{1}H NMR** (400 MHz, $CDCl_3$) δ 0.43 – 0.53 (m, 2H), 0.63 – 0.74 (m, 2H), 1.43 (s, 9H), 2.47 – 2.57 (m, 1H), 4.71 (br. s, 1H). **^{13}C NMR** (101 MHz, $CDCl_3$) δ 6.9, 23.0, 28.5, 79.5, 157.8. **MP** 58 – 60 °C. Matches literature data.[4]

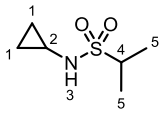
tert-Butyl cyclobutylcarbamate **2.68**



Chemical Formula: $C_9H_{17}NO_2$
Exact Mass: 171.1259
Molecular Weight: 171.2400

To a stirred solution of aminocyclobutane (119 µL, 1.41 mmol, 1 eq.) in CH_2Cl_2 (3 mL) at 0 °C, di-*tert*-butyl decarbonate (337 g, 1.55 mmol, 1.1 eq.) in CH_2Cl_2 (2 mL) was slowly added. The reaction was then warmed to RT and stirred for 1 hr. Upon completion, the reaction was washed with H_2O (2 x 10 mL), brine (10 mL), dried over $MgSO_4$ and filtered. The solvent was removed *in vacuo* yielding the title compound as a white crystalline solid (191 mg, 1.1 mmol, 79%) which was used without further purification. $\mathbf{R_f}$ 0.23 (5% EtOAc in pentane). **^{1}H NMR** (400 MHz, $CDCl_3$) δ 1.42 (s, 9H), 1.69 – 1.55 (m, 2H), 1.80 (m, 2H), 2.28 (m, 2H), 4.15 – 4.00 (m, 1H), 4.69 (s, 1H). **^{13}C NMR** (101 MHz, $CDCl_3$) δ 14.9, 28.5, 31.6, 47.9, 80.0, 153.6. **HRMS** (ESI+) Found: 194.1154, $C_9H_{17}O_2NNa$ $[M+Na]^+$ requires: 194.1152. **MP** 72 – 74 °C. Matches literature data.[5]

N-cyclopropylpropane-2-sulfonamide **2.66**

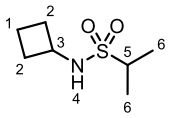


Chemical Formula: $C_6H_{13}NO_2S$
Exact Mass: 163.0667
Molecular Weight: 163.2350

To a stirred solution of aminocyclopropane (500mg, 8.76 mmol, 1 eq.) in CH_2Cl_2 (58 mL) at 0 °C under argon, was added triethylamine (6.1 mL, 43.8 mmol, 5 eq.) and 2-propanesulfonyl chloride (1.08 mL, 9.64 mmol, 1.1 eq.) and the reaction was left to return to RT and stirred overnight. When complete, the reaction was quenched with aq. sat. $NaHCO_3$ (50 mL), extracted with CH_2Cl_2 (3 x 50 mL), dried over $MgSO_4$, filtered and concentrated *in vacuo*. The crude product was purified by column chromatography (10 – 30% EtOAc in pentane) to yield the product as a yellow crystalline solid (1.18 g, 83%).

R_f 0.47 (50% EtOAc in pentane). **^{1}H NMR** (400 MHz, $CDCl_3$) δ 0.76 – 0.62 (m, 4H, H1), 1.37 (d, *J* = 7.0 Hz, 6H, H5), 2.56 (m, 1H, H2), 3.26 (sept, *J* = 7.0 Hz, 1H, H4), 4.82 (br. s, 1H, NH). **^{13}C NMR** (101 MHz, CDCl3) δ 6.8 (C1), 16.5 (C5), 24.5 (C2), 52.3 (C4). **HRMS** (ESI+) Found: 186.0561, $C_9H_{17}O_3NNa$ $[M+Na]^+$ requires: 186.0559. **MP** 61 – 63 °C.

N-cyclobutylpropane-2-sulfonamide **2.70**

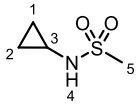


Chemical Formula: $C_7H_{15}NO_2S$
Exact Mass: 177.0823
Molecular Weight: 177.2620

To a stirred solution of aminocyclobutane (100mg, 1.41 mmol, 1 eq.) in CH_2Cl_2 (9.5 mL) at 0 °C under argon, was added triethylamine (983 µL, 7.05 mmol, 5 eq.) and 2-propanesulfonyl chloride (174 µL, 1.55 mmol, 1.1 eq.) and the reaction was left to return to RT and stirred overnight. When complete, the reaction was quenched with aq. sat. $NaHCO_3$ (10 mL), extracted with CH_2Cl_2 (3 x 20 mL), dried over $MgSO_4$, filtered and concentrated *in vacuo*. The crude product was purified by column chromatography (10 – 30% EtOAc in pentane) to yield the product as a yellow crystalline solid (111 mg, 45%).

R_f 0.6 (50% EtOAc in pentane). **^{1}H NMR** (400 MHz, CDCl3) δ 1.35 (d, *J* = 6.8 Hz, H6), 1.71 – 1.55 (2H, m, H1), 2.02 – 1.86 (2H, m, H2'), 2.41 – 2.29 (2H, m, H2), 3.08 (1H, sept, *J* = 6.8 Hz, H5), 3.91 (1H, app. qtd, *J* = 9.0, 7.5, 1.0 Hz, H3), 4.44 (1H, d, *J* = 9.3 Hz, NH). **^{13}C NMR** (101 MHz, $CDCl_3$) δ 14.5, 16.8, 32.9, 48.7, 53.9. **HRMS** (ESI+) Found: 200.0718, $C_9H_{17}O_3NNa$ $[M+Na]^+$ requires: 200.0716. **MP** 74 – 76 °C.

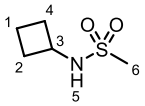
N-cyclopropylmethanesulfonamide **2.65**



Chemical Formula: $C_4H_9NO_2S$
Exact Mass: 135.0354
Molecular Weight: 135.1810

To a stirred solution of aminocyclopropane (500mg, 8.76 mmol, 1 eq.) in CH_2Cl_2 (58 mL) at 0 °C under argon, was added triethylamine (6.1 mL, 43.8 mmol, 5 eq.) and methanesulfonyl chloride (1.36 mL, 17.5 mmol, 2 eq.) and the reaction was left to return to RT and stirred overnight. When complete, the reaction was quenched with aq. sat. $NaHCO_3$ (50 mL), extracted with CH_2Cl_2 (3 x 50 mL), dried over $MgSO_4$, filtered and concentrated *in vacuo*. The crude product was purified by column chromatography (50% EtOAc in pentane) to yield the product as a yellow crystalline solid (368 mg, 31%). $\mathbf{R_f}$ 0.26 (50% EtOAc in pentane). **^{1}H NMR** (400 MHz, $CDCl_3$) δ 4.92 (s, 1H), 2.99 (s, 3H), 2.57 m, 1H), 0.79 – 0.64 (m, 4H). **^{13}C NMR** (101 MHz, $CDCl_3$) δ 6.5, 6.6, 24.5, 31.7, 40.1.

N-cyclobutylmethanesulfonamide **2.69**

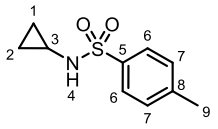


Chemical Formula: $C_5H_{11}NO_2S$
Exact Mass: 149.0510
Molecular Weight: 149.2080

To a stirred solution of aminocyclobutane (100mg, 1.41 mmol, 1 eq.) in CH_2Cl_2 (9.5 mL) at 0 °C under argon, was added triethylamine (983 µL, 7.05 mmol, 5 eq.) and methanesulfonyl chloride (218 µL, 2.82 mmol, 2 eq.) and the reaction was left to return to rt and stirred overnight. When complete, the reaction was quenched with aq. sat. $NaHCO_3$ (10 mL), extracted with CH_2Cl_2 (3 x 20 mL), dried over $MgSO_4$, filtered and concentrated *in vacuo*. The crude product was purified by column chromatography (40 – 50% EtOAc in pentane) to yield the product as a yellow oil (204 mg, 97%).

$\mathbf{R_f}$ 0.36 (50% EtOAc in pentane). **^{1}H NMR** (400 MHz, $CDCl_3$) δ 4.50 (s, 1H), 3.94 (h, J = 8.3 Hz, 1H), 2.92 (s, 3H), 2.46 – 2.33 (m, 2H), 2.02 – 1.87 (m, 2H), 1.79 – 1.61 (m, 2H). **^{13}C NMR** (101 MHz, $CDCl_3$) δ 48.3 (C3), 41.5 (C6), 32.4 (C2/4), 14.9 (C1). **HRMS** (ESI+) Found: 172.0404, $C_5H_{11}O_2NNaS$ $[M+Na]^+$ requires: 172.0403.

N-cyclopropyl-4-methylbenzenesulfonamide **2.67**

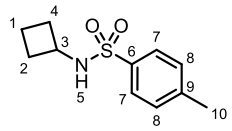


Chemical Formula: $C_{10}H_{13}NO_2S$
Exact Mass: 211.0667
Molecular Weight: 211.2790

To a stirred solution of aminocyclopropane (500mg, 8.76 mmol, 1 eq.) in CH_2Cl_2 (58 mL) at 0 °C under argon, was added triethylamine (6.1 mL, 43.8 mmol, 5 eq.) and *p*-toluenesulfonyl chloride (1.67 g, 17.5 mmol, 2 eq.) and the reaction was left to return to RT and stirred overnight. When complete, the reaction was quenched with aq. sat. $NaHCO_3$ (50 mL), extracted with CH_2Cl_2 (3 x 50 mL), dried over $MgSO_4$, filtered and concentrated *in vacuo*. The crude product was purified by column chromatography (10 – 40% EtOAc in pentane) to yield the product as a white crystalline solid (890.3 mg, 48%).

R_f 0.57 (50% EtOAc in pentane). **^{1}H NMR** (400 MHz, $CDCl_3$) δ 7.79 (d, *J* = 8.0 Hz, 2H), 7.31 (d, *J* = 8.0 Hz, 2H), 5.00 (s, 1H), 2.43 (s, 3H), 2.27 – 2.19 (m, 1H), 0.62 – 0.53 (m, 4H). **^{13}C NMR** (101 MHz, $CDCl_3$) δ 6.2, 21.7, 24.4, 127.6, 129.8, 136.8, 143.7. Matches literature data.[6]

N-cyclobutyl-4-methylbenzenesulfonamide **2.71**

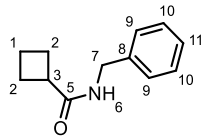


Chemical Formula: $C_{11}H_{15}NO_2S$
Exact Mass: 225.0823
Molecular Weight: 225.3060

To a stirred solution of aminocyclobutane (100mg, 1.41 mmol, 1 eq.) in CH_2Cl_2 (9.5 mL) at 0 °C under argon, was added triethylamine (983 µL, 7.05 mmol, 5 eq.) and *p*-toluenesulfonyl chloride (538 µL, 2.82 mmol, 2 eq.) and the reaction was left to return to RT and stirred overnight. When complete, the reaction was quenched with aq. sat. $NaHCO_3$ (10 mL), extracted with CH_2Cl_2 (3 x 20 mL), dried over $MgSO_4$, filtered and concentrated *in vacuo*. The crude product was purified by column chromatography (30% EtOAc in pentane) to yield the product as a yellow oil (251 mg, 79%).

R_f 0.54 (50% EtOAc in pentane). **^{1}H NMR** (400 MHz, $CDCl_3$) δ 7.74 (d, *J* = 8.0 Hz, 2H), 7.28 (d, *J* = 8.0 Hz, 2H), 4.87 (d, *J* = 8.9 Hz, 1H), 3.85 – 3.70 (m, 1H), 2.42 (s, 3H), 2.20 – 2.02 (m, 2H), 1.84 – 1.68 (m, 2H), 1.65 – 1.49 (m, 2H). **^{13}C NMR** (101 MHz, $CDCl_3$) δ 15.1, 21.6, 31.8, 48.3, 127.1, 127.2, 129.8, 138.1, 143.5. **HRMS** (ESI+) Found: 226.0897, $C_{11}H_{16}O_2NS$ $[M+H]^+$ requires: 226.0896.

N-benzylcyclobutanecarboxamide **2.72**

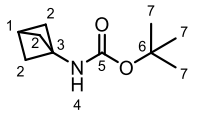


Chemical Formula: $C_{12}H_{15}NO$
Exact Mass: 189.1154
Molecular Weight: 189.2580

To a stirred solution of cyclobutanecarboxylic acid (110 µL, 1.05 mmol, 1.15 eq.) in acetonitrile (5 mL), DIPEA (500 µL, 4 mmol, 4.4 eq.) and then HATU (400 mg, 1.1 mmol, 1.2 eq.) was added. The reaction was stirred at RT for 10 mins and then benzylamine (100 µL, 0.9 mmol, 1 eq.) was then added, and stirred for a further 2 hr. The reaction was then quenched with 1N aq. HCl (5 mL), extracted with EtOAc (3 x 10mL), dried over $MgSO_4$, filtered and concentrated *in vacuo*. The crude reaction mixture was purified by column chromatography (30% EtOAc in pentane) yielding the title compound as a white solid (159.1 mg, 0.84 mmol, 93%).

R_f 0.24 (40% EtOAc in pentane). **^{1}H NMR** (400 MHz, $CDCl_3$) δ 7.37 – 7.23 (m, 5H), 5.67 (br. s, 1H), 4.43 (d, *J* = 5.7 Hz, 2H), 3.02 (pd, *J* = 8.6, 1.1 Hz, 1H), 2.36 – 2.25 (m, 2H), 2.20 – 2.11 (m, 2H), 2.01 – 1.84 (m, 2H). **^{13}C NMR** (101 MHz, $CDCl_3$) δ 18.3, 25.5, 40.1, 43.6, 127.6, 127.9, 128.8, 138.6, 174.9. **MP** 74 – 75 °C. Matches literature data.[7]

tert-Butyl bicyclo[1.1.1]pentan-1-ylcarbamate **2.73**

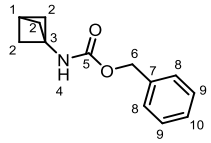


Chemical Formula: $C_{10}H_{17}NO_2$
Exact Mass: 183.1259
Molecular Weight: 183.2510

To a stirred suspension of 1-bicyclo[1.1.1]pentylamine hydrochloride (50 mg, 0.42 mmol, 1eq.) and NaH (42 mg, 1.05 mmol, 2.5 eq., 60% in mineral oil) in dry THF (2.1 mL) under Ar at 0 °C, di-*tert*-butyl decarbonate (137 mg, 0.63 mmol, 1.5 eq.) was added. The reaction was left stirring to return to RT and stirred for 21 hr. When complete, the reaction was cooled to 0 °C and quenched slowly with H_2O (2 mL). The reaction was then extracted with EtOAc (10 mL x 2), dried over MgSO4, filtered and concentrated *in vacuo*. The crude reaction mixture was purified by column chromatography (5 – 15% EtOAc in pentane) yielding the title compound as a white solid (54.5 mg, 0.297 mmol, 71%).

R_f 0.52 (20% EtOAc in pentane). **^{1}H NMR** (400 MHz, $CDCl_3$) δ 1.44 (s, 9H, H6), 2.00 (s, 6H, H2), 2.38 (s, 1H, H3). **^{13}C NMR** (126 MHz, $CDCl_3$) δ 24.2 (C3), 28.6 (C6), 48.7 (C1), 52.6 (C2), 79.5 (C5), 155.1 (C4). **HRMS** (ESI+) Found: 206.1155, $C_{10}H_{17}O_2NNa$ $[M+Na]^+$ requires: 206.1152. **IR** ν_{max} (thin film)/cm^{-1} 3340m, 2876w, 1690s, 1514s, 1367m, 1146m. **MP** 98–99 °C.

Benzyl bicyclo[1.1.1]pentan-1-ylcarbamate **2.74**



Chemical Formula: $C_{13}H_{15}NO_2$
Exact Mass: 217.1103
Molecular Weight: 217.2680

To a stirred suspension of 1-bicyclo[1.1.1]pentylamine hydrochloride (50 mg, 0.42 mmol, 1 eq.) in CH_2Cl_2 (2 mL) under argon at 0 °C, was added dropwise benzyl chloroformate (55 uL, 0.55 mmol, 1.3 eq.) and triethylamine (129 μL, 0.92 mmol, 2.2 eq.). The reaction was left stirring to return to RT and stirred for 24 hr. When complete, the reaction was washed with $NaHCO_3$ (5 mL), and then extracted with EtOAc (10 mL x 2), dried over $MgSO_4$, filtered and concentrated *in vacuo*. The crude reaction mixture was purified by column chromatography (0 – 40% EtOAc in pentane) yielding the title compound as a white solid (34.9 mg, 0.16 mmol, 38%).

R_f 0.36 (50% EtOAc in pentane). **^{1}H NMR** (400 MHz, $CDCl_3$) δ 2.04 (s, 6H, H2), 2.41 (s, 1H, H3), 5.08 (s, 2H, H5), 5.22 (s, 1H, NH), 7.30–7.37 (m, 5H, H7,8,9). **^{13}C NMR** (101 MHz, $CDCl_3$) δ 24.1 (C3), 48.7 (C1), 51.9 (C2), 66.5 (C5), 128.2, 128.6 and 136.6 (C7,8,9) C4 and C6 resonances not observed. **HRMS** (ESI+) Found: 240.0996, $C_{13}H_{15}NO_2Na$ $[M+Na]^+$ requires: 240.0995. **IR** ν_{max} (thin film)/cm^{-1} 3320w, 2877w, 1699s, 1518m, 1454m, 1244s, 1202s, 1057s, 731s, 696s.

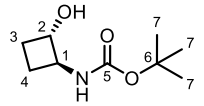
6.2.3. Preparative scale $P450_{BM3}$ reactions

6.2.3.1. General procedure I (GP-I)

The substrate (as a solution in the solvent specified) was added to a solution of the $P450_{BM3}$ mutant (stored in phosphate buffer at the specified concentration), glucose (1.0 M solution in phosphate buffer), GDH (2.0 U/μL solution in phosphate buffer), and $NADP^+$ monosodium salt (4.0 mM solution in buffer) in phosphate buffer. After shaking at 120 rpm at 20 °C for the specified reaction time, ethyl acetate (4 x reaction volume) was added; the biphasic mixture was transferred into 50 mL centrifuge tubes (Falcon), shaken for 30 seconds and then centrifuged at 9,500 rpm for 4 min after which the organic layer was removed. The extraction process was repeated (×3). The organic layer was dried ($MgSO_4$), filtered, and concentrated in vacuo to give the crude product that was then purified by column chromatography.

6.2.3.2. Isolation of amine metabolites

tert-Butyl [(1*S*,2*S*)-2-hydroxycyclobutyl]carbamate **2.75**

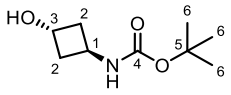


Chemical Formula: $C_9H_{17}NO_3$
Exact Mass: 187.1208
Molecular Weight: 187.2390

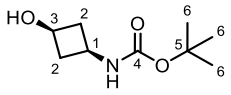
Prepared according to **GP-I**, using mutant RP/H171L/I263G (4.0 mL of 75 μM concentration in phosphate buffer, overall concentration of 2.0 μM), glucose (15 mL of 1.0 M stock in phosphate buffer), GDH (3.0 mL of 2.0 U/μL stock in phosphate buffer), $NADP^+$ monosodium salt (3.0 mL of 4.0 mM stock in phosphate buffer) in phosphate buffer (122 mL) and substrate **2.68** (3.0 mL of 0.2 M stock in DMSO, 0.6 mmol, overall concentration of 4.0 mM) stirring for 48 h. Purification by column chromatography (20–60% EtOAc in pentane) yielded the *title comopund* as a colourless crystalline solid (42.8 mg, 38%).

R_f 0.34 (50% EtOAc in pentane). **^{1}H NMR** (400 MHz, $CDCl_3$) δ 1.22–1.34 (m, 1H, H4), 1.44 (s, 9H, H7), 1.54–1.68 (m, 1H, H3), 1.98–2.15 (m, 1H, H4), 3.18 (s, 1H, H3), 3.63–3.76 (m, 1H, H1), 3.90–4.01 (m, 1H, H2), 4.80 (s, 1H, NH). **^{13}C NMR** (101 MHz, $CDCl_3$) δ 19.4 (C4), 25.0 (C3), 28.5 (C7), 55.5 (C1), 73.6 (C2), 79.8 (C6), 156.0 (C5). **HRMS** (ESI+) Found: 210.1102, $C_9H_{17}NO_3Na$ $[M+Na]^+$ requires: 210.1101. **IR** ν_{max} (thin film)/cm^{-1} 3235br.w, 2988w, 1681s, 1531s, 1365m, 1277m, 1165s, 1106m, 1020m. **$[\alpha]_D$** –11.3 (c = 1.0, $CHCl_3$, 25 °C). **MP** 101–103 °C.

trans- and *cis*- *tert*-Butyl (3-hydroxycyclobutyl)carbamate **2.78 and 2.77**



Chemical Formula: $C_9H_{17}NO_3$
Exact Mass: 187.1208
Molecular Weight: 187.2390

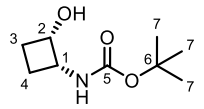


Chemical Formula: $C_9H_{17}NO_3$
Exact Mass: 187.1208
Molecular Weight: 187.2390

Prepared according to **GP-I**, using mutant RP/H171L/I263G (4.0 mL of 75 μM concentration in phosphate buffer, overall concentration of 2.0 μM), glucose (15 mL of 1.0 M stock in phosphate buffer), GDH (3.0 mL of 2.0 U/μL stock in phosphate buffer), $NADP^+$ monosodium salt (3.0 mL of 4.0 mM stock in phosphate buffer) in phosphate buffer (122 mL) and substrate **2.68** (3.0 mL of 0.2 M stock in DMSO, 0.6 mmol, overall concentration of 4.0 mM) stirring for 48 h. Purification by column chromatography (20–60% EtOAc in pentane) yielded the *title comopund* as a colourless crystalline solid (42.8 mg, 38%).

R_f 0.29 (50% EtOAc in pentane). ***Trans*- diastereomer**: **^{1}H NMR** (500 MHz, $CDCl_3$) δ 1.43 (s, 9H, H6), 2.17–2.25 (m, 2H, H2), 2.27–2.34 (m, 2H, H2), 4.21 (br. s, 1H, H1), 4.42–4.50 (m, 1H, H3), 4.71 (br. s, 1H, NH). **^{13}C NMR** (126 MHz, $CDCl_3$) δ 28.5 (C6), 40.3 (C2), 42.2 (C1), 65.0 (C3), 77.4 (C5), 155.4 (C4). ***Cis*- diastereomer**: **^{1}H NMR** (400 MHz, $CDCl_3$) δ 1.43 (s, 9H, H6), 1.75–1.84 (m, 2H, H2), 2.69–2.81 (m, 2H, H2), 3.63 (m, 1H, H1), 3.95–4.06 (m, 1H, H3). **^{13}C NMR** (126 MHz, $CDCl_3$) δ 28.5 (C6), 37.3 (C1), 41.9 (C2), 61.0 (C3), 79.6 (C5), 155.2 (C4). **HRMS** (ESI+) Found: 210.1103, $C_9H_{17}NO_3Na$ $[M+Na]^+$ requires: 210.1101.

tert-Butyl [(1*R*,2*S*)-2-hydroxycyclobutyl]carbamate **2.76**

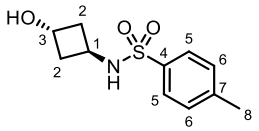


Chemical Formula: $C_9H_{17}NO_3$
Exact Mass: 187.1208
Molecular Weight: 187.2390

Prepared according to **GP-I**, using mutant RL/YF/HL/IG/LLV (3.0 mL of 65 μM concentration in phosphate buffer, overall concentration of 2.0 μM), glucose (9.0 g), GDH (80 mg), $NADP^+$ monosodium salt (30 mg) in phosphate buffer (95 mL) and substrate **2.68** (171 mg neat solid, 1.0 mmol, overall concentration of 10 mM) stirring for 24 h. Purification by column chromatography (30% EtOAc in pentane) yielded the title compound as a colourless oil (10.3 mg, 6%).

R_f 0.41 (50% EtOAc in pentane). **^{1}H NMR** (500 MHz, $CDCl_3$) δ 1.43 (s, 9H, H7), 1.80–1.87 (m, 1H, H3), 1.89–1.98 (m, 1H, H4), 2.04–2.19 (m, 2H, H3 and H4), 2.67 (s, 1H, OH), 4.07–4.15 (m, 1H, H1), 4.42 (s, 1H, H2), 5.18 (br.s, 1H, NH). **^{13}C NMR** (126 MHz, $CDCl_3$) δ 25.6 (C4), 27.3 (C3), 28.5 (C7), 50.0 (C1), 69.8 (C2), 79.7 (C6), 156.1 (C5). **HRMS** (ESI+) Found: 210.1104, $C_9H_{17}NO_3Na$ $[M+Na]^+$ requires: 210.1101. **IR** ν_{max} (thin film)/cm^{-1} 3421br.w, 2926w, 1686s, 1504m, 1391m, 1252m, 1168s. **$[\alpha]_D$** +16.9 (*c* = 1.08, $CHCl_3$, 25 °C).

N-[(*trans*)-3-hydroxycyclobutyl]-4-methylbenzenesulfonamide **2.82**

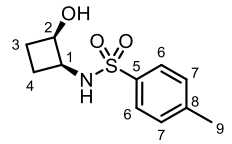


Chemical Formula: $C_{11}H_{15}NO_3S$
Exact Mass: 241.0773
Molecular Weight: 241.3050

Prepared according to **GP-I**, using mutant RT2/A330W (0.9 mL of 110 μM concentration in phosphate buffer, overall concentration of 2.0 μM), glucose (5.0 mL of 1.0 M stock in phosphate buffer), GDH (1.0 mL of 2.0 U/μL stock in phosphate buffer), $NADP^+$ monosodium salt (1.0 ml of 4.0 mM stock in phosphate buffer) in phosphate buffer (41 mL) and substrate **2.71** (1.0 mL of 0.2 M stock in DMSO, 0.2 mmol, overall concentration of 4.0 mM) stirring for 48 h. Purification by column chromatography (20–70% EtOAc in pentane) yielded the title compound as a colourless crystalline solid (31.2 mg, 65%).

R_f 0.18 (50% EtOAc in pentane). **^{1}H NMR** (400 MHz, DMSO-d_6) δ 1.79–1.95 (m, 2H, H2), 1.92–2.01 (m, 2H, H2), 2.39 (s, 3H, H8), 3.70 (m, 1H, H1), 4.12 (m, 1H, H3), 4.90 (d, J = 4.5 Hz, 1H, OH), 7.39 (d, J = 8.0 Hz, 2H, H6), 7.65 (d, J = 8.0 Hz, 2H, H5), 7.80 (d, J = 7.5 Hz, 1H, NH). **^{13}C NMR** (101 MHz, DMSO-d_6) δ 20.9 (C8), 39.4 (C2), 44.4 (C1), 62.6 (C3), 126.5 (C6), 129.5 (C5), 138.3 (C7), 142.5 (C4). **HRMS** (ESI+) Found: 242.0842, $C_{11}H_{16}NO_3S$ $[M+H]^+$ requires: 242.0845. **IR** ν_{max} (thin film)/cm^{-1} 3267br.w, 2936w, 1305m, 1157s, 1092s, 988m, 815m, 665m. **MP** 124–126 °C.

N-[(1*S*,2*R*)-2-hydroxycyclobutyl]-4-methylbenzenesulfonamide **2.80**

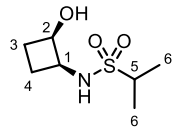


Chemical Formula: $C_{11}H_{15}NO_3S$
Exact Mass: 241.0773
Molecular Weight: 241.3050

Prepared according to **GP-I**, using mutant RT2/A330W (2.7 mL of 110 μM concentration in phosphate buffer, overall concentration of 2.0 μM), glucose (15.0 mL of 1.0 M stock in phosphate buffer), GDH (3.0 mL of 2.0 U/μL stock in phosphate buffer), $NADP^+$ monosodium salt (3.0 ml of 4.0 mM stock in phosphate buffer) in phosphate buffer (124 mL) and substrate **2.71** (3.0 mL of 0.2 M stock in DMSO, 0.2 mmol, overall concentration of 4.0 mM) stirring for 48 h. Purification by column chromatography (20–100% EtOAc in pentane) yielded the title compound as a colourless crystalline solid (1.2 mg, 1%).

R_f 0.19 (50% EtOAc in pentane). **^{1}H NMR** (500 MHz, $CDCl_3$) δ 1.71–1.82 (m, 1H, H3) and 1.93–2.15 (m, 3H, H3 and H4), 2.43 (s, 3H, H9), 3.78 (s, 1H, H1), 4.26–4.32 (m, 1H, H2), 5.12 (s, 1H, NH), 7.31 (d, *J* = 8.0 Hz, 2H, H7), 7.76 (d, *J* = 8.0 Hz, 2H, H6). **^{13}C NMR** (126 MHz, $CDCl_3$) δ 21.7 (C9), 26.5 (C3), 26.9 (C4), 51.2 (C1), 70.3 (C2), 127.3 (C6), 129.9 (C7), 137.4 (C8), 143.8 (C5). **HRMS** (ESI+) Found: 264.0666, $C_{11}H_{15}NO_3SNa$ $[M+Na]^+$ requires: 264.0665. **IR** ν_{max} (thin film)/cm^{-1} 3499br.w, 3279br.w, 1332m, 1159s, 1093m, 668m. **$[\alpha]_D$** +1.96 (*c* = 0.51, $CHCl_3$, 25 °C). **MP** 101–103 °C.

N-[(1*S*,2*R*)-2-hydroxycyclobutyl]propane-2-sulfonamide **2.70B**

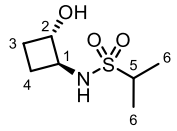


Chemical Formula: $C_7H_{15}NO_3S$
Exact Mass: 193.0773
Molecular Weight: 193.2610

Prepared according to **GP-I**, using mutant KU3/S72W/A330P (0.8 mL of 123 μM concentration in phosphate buffer, overall concentration of 2.0 μM), glucose (10 mL of 1.0 M stock in phosphate buffer), GDH (2.0 ml of 2.0 U/μL stock in phosphate buffer), $NADP^+$ monosodium salt (2.0 ml of 4.0 mM stock in phosphate buffer) in phosphate buffer (35 mL) and substrate **2.70** (17.7 mg neat, 0.0999 mmol, overall concentration of 4.0 mM) stirring for 48 h. Purification by column chromatography (10–50% EtOAc in pentane) afforded the *title compound* as a colourless oil (4.2 mg, 22%).

R_f 0.12 (40% EtOAc in pentane). **^{1}H NMR** (400 MHz, $CDCl_3$) δ 1.37 (d, *J* = 2.4 Hz, 3H, H6), 1.39 (d, *J* = 2.4 Hz, 3H, H6), 1.74–1.85 (m, 1H, H3), 2.03–2.19 (m, 2H, H3 and H4) and 2.24–2.34 (m, 1H, H4), 3.14 (sept, *J* = 6.5 Hz, 1H, H5), 3.91–4.02 (m, 1H, H1), 4.40–4.50 (m, 1H, H2), 4.84 (d, *J* = 9.3 Hz, 1H, NH). **^{13}C NMR** (101 MHz, $CDCl_3$) δ 16.6 and 16.8 (C5), 26.2 (C3), 28.0 (C4), 51.7 (C1), 54.0 (C5), 71.1 (C2). **HRMS** (ESI+) Found: 216.0666, $C_7H_{15}NO_3SNa$ $[M+Na]^+$ requires: 216.0665. **IR** ν_{max} (thin film)/cm^{-1} 3282br.w, 2981w, 2946w, 1269m, 1132s, 695m. **$[\alpha]_D$** –12.7 (*c* = 0.4, $CHCl_3$, 25 °C).

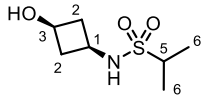
N-[(*trans*)-2-hydroxycyclobutyl]propane-2-sulfonamide **2.70A**



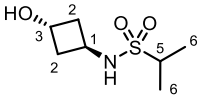
Chemical Formula: $C_7H_{15}NO_3S$
Exact Mass: 193.0773
Molecular Weight: 193.2610

Also isolated from the previous reaction of **2.70** with KU3/S72W/A330P was the *trans*-1,2-diastereomer as a colourless oil (5.1 mg, 26% yield). $\mathbf{R}_f$0.08 (40% EtOAc in pentane). **^{1}H NMR** (400 MHz, $CDCl_3$) δ 1.37 (m, 1H, H4), 1.38 (d, *J* = 6.5 Hz, 3H, H6), 1.39 (d, *J* = 6.5 Hz, 3H, H6), 1.49–1.64 (m, 1H, H3), 2.08–2.17 (m, 2H, H3 and H4), 3.22 (sept, *J* = 6.5 Hz, 1H, H5), 3.56 (m, 1H, H1), 3.99–4.07 (m, 1H, H2), 4.61 (d, *J* = 7.5 Hz, 1H, NH). **^{13}C NMR** (101 MHz, $CDCl_3$) δ 16.6 and 16.8 (C6), 21.0 (C4), 24.8 (C3), 53.9 (C5), 57.7 (C1), 74.4 (C2). **HRMS** (ESI+) Found: 216.0666, $C_7H_{15}NO_3SNa$ $[M+Na]^+$ requires: 216.0665. **IR** ν_{max} (thin film)/cm^{-1} 3278br.w, 2921m, 2851w, 1307m, 1135s, 1095m, 1060m, 694m. **$[\alpha]_D$** +8.16 (*c* = 0.49, $CHCl_3$, 25 °C).

cis- and *trans N*-(3-hydroxycyclobutyl)propane-2-sulfonamide **2.70C and 2.70D**



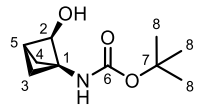
Chemical Formula: $C_7H_{15}NO_3S$
Exact Mass: 193.0773
Molecular Weight: 193.2610



Chemical Formula: $C_7H_{15}NO_3S$
Exact Mass: 193.0773
Molecular Weight: 193.2610

Also isolated from the same reaction of **2.70** with KU3/S72W/A330P was a mixture of the 3-hydroxylated metabolites as a colourless oil (1.6 mg, 8.5%, 1.5:1, *cis*-/*trans*-). $\mathbf{R}_f$0.05 (50% EtOAc in pentane). ***Trans* diastereomer; ^{1}H NMR** (500 MHz, $CDCl_3$) δ 1.36 (d, *J* = 7.0 Hz, 6H, H6) 2.23–2.30 (m, 1H, H2), 2.36–2.42 (m, 1H, H2), 3.10 (sept, *J* = 7.0 Hz, 1H, H5), 4.20–4.29 (m, 1H, H1), 4.48 (m, 1H, H3). **^{13}C NMR** (126 MHz, $CDCl_3$) δ 16.7 (C5), 41.4 (C2), 46.0 (C1), 53.8 (C4), 64.4 (C3). ***Cis* diastereomer; ^{1}H NMR** (500 MHz, $CDCl_3$) δ 1.36 (d, *J* = 7.0 Hz, 6H, H6), 1.86–1.94 (m, 2H, H2), 2.79–2.86 (m, 2H, H2), 3.10 (sept, *J* = 7.0 Hz, 1H, H5), 3.46–3.57 (m, 1H, H1), 3.99–4.05 (m, 1H, H3), 4.29 (br.s, 1H, OH). **^{13}C NMR** (126 MHz, $CDCl_3$) δ 16.7 (C6), 40.3 (C1), 43.0 (C2), 54.0 (C5), 60.5 (C3). **HRMS** (ESI–) Found: 192.0690, $C_7H_{14}NO_3S$ $[M–H]^-$ requires: 192.0700. **IR** ν_{max} (thin film)/cm^{-1} 3458br.w, 3272br.w, 2983w, 2936w, 1307m, 1133s, 1056m.

tert-Butyl (*R*-2-hydroxybicyclo[1.1.1]pent-1-yl)carbamate **2.84**

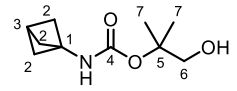


Chemical Formula: $C_{10}H_{17}NO_3$
Exact Mass: 199.1208
Molecular Weight: 199.2500

Prepared according to **GP-I**, using mutant GV/A184I (9.0 mL of 50 μM concentration in phosphate buffer, overall concentration of 9.0 μM), glucose (30 mL of 1.0 M stock in phosphate buffer), GDH (6.0 mL of 2.0 U/μL stock in phosphate buffer), $NADP^+$ monosodium salt (6.0 ml of 4.0 mM stock in phosphate buffer) in phosphate buffer (122 mL) and substrate **2.73** (1.5 mL of 0.1 M stock in EtOH, 0.15 mmol, overall concentration of 1.0 mM) stirring for 42 h. Purification by column chromatography (0–35% EtOAc in pentane) afforded the title compound as a colourless solid (7.6 mg, 25%).

R_f 0.16 (30% EtOAc in pentane). **^{1}H NMR** (400 MHz, $CDCl_3$) δ 1.40 (dd, *J* = 9.5, 2.5 Hz, 1H, H3 or H4), 1.43 (s, 9H, H8), 1.74 (d, *J* = 2.5 Hz, 1H, H3 or H4), 1.88 (dd, *J* = 6.0, 2.0 Hz, 1H, H3 or H4), 2.43 (s, 1H, H5), 3.01 (d, *J* = 9.5 Hz, 1H, H3 or H4), 4.19 (d, *J* = 6.0 Hz, 1H, H2), 4.92 (br.s, 1H) and 5.12 (br.s, 1H, OH/NH). **^{13}C NMR** (101 MHz, $CDCl_3$) δ 28.4 (C8), 29.8 (C5), 41.6 (C3 or C4), 47.5 (C3 or C4), 53.3 (C1), 80.5 (C7), 84.6 (C2), 156.6 (C6). **HRMS** (ESI+) Found: 222.1103, $C_{10}H_{17}NO_3Na$ $[M+Na]^+$ requires: 222.1101. **IR** ν_{max} (thin film)/cm^{-1} 3317br.w, 2978w, 1683s, 1515m, 1367m, 1281m, 1168s, 1122m, 1064m. **MP** 87–90 °C. **$[\alpha]_D$** −6.16 (*c* = 0.76, $CHCl_3$, 25 °C).

1-Hydroxy-2-methylprop-2-yl bicyclo[1.1.1]pent-1-ylcarbamate **2.85**

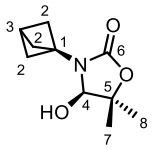


Chemical Formula: $C_{10}H_{17}NO_3$
Exact Mass: 199.1208
Molecular Weight: 199.2500

Prepared according to **GP-I**, using mutant R19/F87I/A330P (4.0 mL of 50 μM concentration in phosphate buffer, overall concentration of 2.0 μM), glucose (10 mL of 1.0 M stock in phosphate buffer), GDH (2.0 ml of 2.0 U/μL stock in phosphate buffer), $NADP^+$ monosodium salt (2.0 ml of 4.0 mM stock in phosphate buffer) in phosphate buffer (81 mL) and substrate **2.73** (1.0 mL of 0.1 M stock in DMSO, 0.1 mmol, overall concentration of 1.0 mM) stirring for 48 h. Purification by column chromatography (0–50% EtOAc in pentane) afforded the *title compound* as a colourless oil (4.1 mg, 21%).

R_f 0.08 (30% EtOAc in pentane). **^{1}H NMR** (400 MHz, $CDCl_3$) δ 1.38 (s, 6H, H7), 2.02 (s, 6H, H2), 2.41 (s, 1H, H3), 3.63 (d, J = 3.0 Hz, 2H, H6), 4.26 (br.s, 1H, OH). **^{13}C NMR** (101 MHz, $CDCl_3$) δ 23.9 (C7), 24.2 (C3), 49.0 (C1), 53.1 (C2), 70.1 (C6), 156.2 (C4) (C5 not visible). **HRMS** (ESI+) Found: 222.1102, $C_{10}H_{17}NO_3Na$ [M+Na]+ requires: 222.1101. **IR** ν_{max} (thin film)/cm^{-1} 3317br.w, 2977m, 2916w, 2878w, 1688s, 1520m, 1285m, 1204m, 1144m, 1056m.

(±)-3-(Bicyclo[1.1.1]pent-1-yl)-4-hydroxy-5,5-dimethyloxazolidin-2-one **2.86**

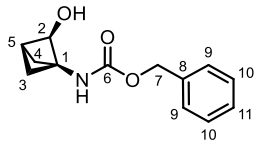


Chemical Formula: $C_{10}H_{15}NO_3$
Exact Mass: 197.1052
Molecular Weight: 197.2340

Also isolated from the same experiment of **2.73** with R19/F87I/A330P was the *title compound* as a colourless crystalline solid (1.7 mg, 9%).

$\mathbf{R}_f$ 0.3 (60% EtOAc in pentane). **^{1}H NMR** (400 MHz, $CDCl_3$) δ 1.37 (s, 3H, H7 or H8), 1.40 (s, 3H, H7 or H8), 2.15 (dd, *J* = 9.5, 1.5 Hz, 3H, H2), 2.21 (dd, *J* = 9.5, 1.5 Hz, 3H, H2), 2.29 (d, *J* = 9.0 Hz, 1H, OH), 2.51 (s, 1H, H3), 4.79 (d, *J* = 9.0 Hz, 1H, H4). **^{13}C NMR** (151 MHz, $CDCl_3$) δ 20.9 (C7 or C8), 24.7 (C3), 26.5 (C7 or C8), 49.3 (C1), 52.6 (C2), 81.5 (C5), 86.4 (C4), 155.1 (C6). **HRMS** (APCI+) Found 198.1128, $C_{10}H_{16}O_3N$ $[M+H]^+$ requires: 198.1125. **IR** ν_{max} (thin film)/cm^{-1} 3343br.w, 2920s, 2851m, 1725s, 1419m, 1284w. **MP** 93–96 °C.

Benzyl (2-hydroxybicyclo[1.1.1]pent-1-yl)carbamate **2.87**



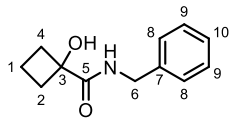
Chemical Formula: $C_{13}H_{15}NO_3$
Exact Mass: 233.1052
Molecular Weight: 233.2670

Prepared according to **GP-I**, using mutant K19/F87V/Q403P (1.2 mL of 164 μM concentration in phosphate buffer, overall concentration of 2.0 μM), glucose (10 mL of 1.0 M stock in phosphate buffer), GDH (2.0 ml of 2.0 U/μL stock in phosphate buffer), $NADP^+$ monosodium salt (2.0 ml of 4.0 mM stock in phosphate buffer) in phosphate buffer (84 mL) and substrate **2.74** (1.0 mL of 0.1 M stock in DMSO, 0.1 mmol, overall concentration of 1.0 mM) stirring for 40 h. Purification by column chromatography (10–20% EtOAc in pentane) afforded the title compound as a yellow oil (4.8 mg, 21%).

R_f 0.59 (80% EtOAc in pentane). **^{1}H NMR** (400 MHz, $CDCl_3$) δ 1.44 (dd, *J* = 9.5, 2.5 Hz, 1H, H3 or H4), 1.78 (d, *J* = 2.5 Hz, 1H, H3 or H4), 1.92 (dd, *J* = 6.0, 2.0 Hz, 1H, H3 or H4), 2.45 (s, 1H, H5), 3.02 (d, *J* = 9.5 Hz, 1H, H3 or H4), 4.23 (d, *J* = 6.0 Hz, 1H, H2), 5.08 (m, 2H, H7), 7.32–7.38 (m, 5H, H9/10/11). **^{13}C NMR** (151 MHz, $CDCl_3$) δ 29.7 (C5), 41.5 (C3 or C4), 47.4 (C3 or C4), 53.1 (C1), 67.1 (C7), 84.5 (C2), 128.2 (C9/C11), 128.6 (C10), 135.9 (C8), 156.7 (C6). **HRMS** (ESI+) Found: 256.0945, $C_{13}H_{15}NO_3Na$ $[M+Na]^+$ requires: 256.0944. **IR** ν_{max} (thin film)/cm^{-1} 3336br.w, 2924w, 1700s, 1521m, 1456m, 1402m, 1339m, 1261m, 1207m, 1061m, 697m. **$[\alpha]_D$** −5.29 (*c* = 1.53, $CHCl_3$, 25 °C).

6.2.3.3. Isolation of carboxamide metabolites

N-benzyl-1-hydroxycyclobutane-1-carboxamide **2.105**

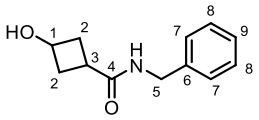


Chemical Formula: $C_{12}H_{15}NO_2$
Exact Mass: 205.1103
Molecular Weight: 205.2570

Prepared according to **GP-I**, using mutant GVQ/A328G (1.25 mL of 80 μM concentration in phosphate buffer, overall concentration of 2.0 μM), glucose (5 mL of 1.0 M stock in phosphate buffer), GDH (1.0 ml of 2.0 U/μL stock in phosphate buffer), $NADP^+$ monosodium salt (1.0 ml of 4.0 mM stock in phosphate buffer) in phosphate buffer (41.25 mL) and substrate **2.72** (0.5 mL of 0.1 M stock in DMSO, 0.1 mmol, overall concentration of 1.0 mM) stirring for 40 h. Purification by column chromatography (20–50% EtOAc in pentane) afforded the title compound as a clear, colourless oil (1.0 mg, 10%).

R_f 0.23 (50% EtOAc in pentane). **^{1}H NMR** (400 MHz, $CDCl_3$) δ 2.08 – 1.89 (m, 2H), 2.25 – 2.08 (m, 2H), 2.73 – 2.63 (m, 2H), 4.48 (d, *J* = 6.0 Hz, 2H, H6), 6.83 (br.s, 1H, NH), 7.39 – 7.26 (m, 5H, H8/9/10). **^{13}C NMR** (151 MHz, $CDCl_3$) δ 13.5 (C1), 35.8 (C2/4), 43.5 (C6), 76.2 (C3), 127.7 (C10), 127.9 (C8), 128.9 (C9), 138.4 (C7), 174.8 (C5). **IR** ν_{max} (thin film)/cm^{-1} 3336 br.w, 2853w, 1648m, 1532m, 1455w, 1231w, 1179w, 989w, 727w, 656w, 632w. **HRMS** Not found.

N-benzyl-3-hydroxycyclobutane-1-carboxamide **2.106**

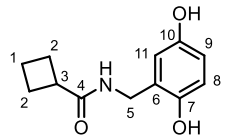


Chemical Formula: $C_{12}H_{15}NO_2$
Exact Mass: 205.1103
Molecular Weight: 205.2570

Prepared according to **GP-I**, using mutant KU3/S72W/A330P (1.2 mL of 123 μM concentration in phosphate buffer, overall concentration of 2.0 μM), glucose (15 mL of 1.0 M stock in phosphate buffer), GDH (3.0 ml of 2.0 U/μL stock in phosphate buffer), $NADP^+$ monosodium salt (3.0 ml of 4.0 mM stock in phosphate buffer) in phosphate buffer (51.3 mL) and substrate **2.72** (1.5 mL of 0.1 M stock in MeOH, 0.1 mmol, overall concentration of 2.0 mM) stirring for 48 h. Purification by column chromatography (20–50% EtOAc in pentane) afforded the title compound as a white solid (10.5 mg, 35%).

$\mathbf{R_f}$ 0.23 (80% EtOAc in pentane). **^{1}H NMR** (400 MHz, $CDCl_3$) δ 2.24 – 2.11 (m, 2H, H2), 2.66 – 2.54 (m, 2H, H2'), 2.89 (ttd, *J* = 9.5, 4.0, 1.0 Hz, 1H, H3), 4.44 (d, *J* = 5.5 Hz, 2H, H5), 4.64 (p, *J* = 6.5 Hz, 1H, H1), 5.71 (br.s, OH) 7.36 – 7.24 (m, 5H, H7/8/9). **^{13}C NMR** (101 MHz, $CDCl_3$) δ 33.1 (C3), 36.4 (C2), 43.1 (C5), 66.0 (C1), 127.2 (C9), 127.4 (C7), 128.9 (C8), 138.3 (C6), 175.2 (C4). **HRMS** (ESI+) Found: 206.1178, $C_{12}H_{16}NO_2$ $[M+H]^+$ requires: 206.1176. **MP** 145 – 147 °C.

N-(2,5-dihydroxybenzyl)cyclobutanecarboxamide **2.107**

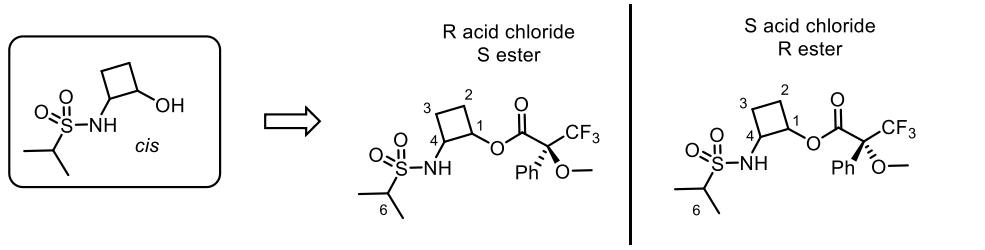


Chemical Formula: $C_{12}H_{15}NO_3$
Exact Mass: 221.1052
Molecular Weight: 221.2560

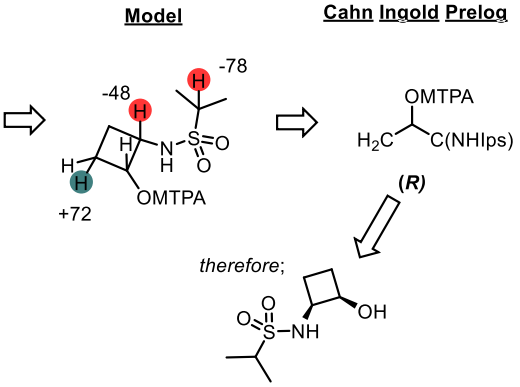
Also isolated from the previous reaction for **2.106**. Purification by column chromatography (20–50% EtOAc in pentane) afforded the title compound as a clear, colourless oil (2.9 mg, 9%).

R_f 0.38 (80% EtOAc in pentane). **^{1}H NMR** (600 MHz, $CDCl_3$) δ 1.90 – 1.83 (m, 1H, H1), 2.02 – 1.92 (m, 1H, H1'), 2.19 – 2.10 (m, 2H, H2), 2.33 – 2.22 (m, 2H, H2'), 3.01 (p, *J* = 8.5 Hz, 1H, H3), 4.26 (d, *J* = 6.5 Hz, 2H, H5), 4.55 (br.s, OH), 6.15 (br.s, NH), 6.58 (d, *J* = 3.0 Hz, 1H, H11), 6.69 (dd, *J* = 8.5, 3.0 Hz, 1H, H9), 6.82 (d, *J* = 8.5 Hz, 1H, H8), 8.99 (s, 1H, OH). **^{13}C NMR** (151 MHz, $CDCl_3$) δ 18.2 (C1), 25.5 (C2), 39.6 (C3), 40.6 (C5), 116.9 (C9), 117.1 (C11), 119.0 (C8), 125.2 (C6), 148.7 (C7), 149.8 (C10), 177.5 (C4). **IR** ν_{max} (thin film)/cm^{-1} 3284 br.w, 2922m, 1541w, 1295m, 1206m, 1105m, 1009m, 654w.

6.2.4. Moshers ester analysis for determination of absolute configuration of 2.70A



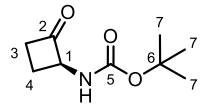
	S ester (ppm)	R ester (ppm)	S-R	x600 (MHz)
H2	2.01	1.89	+0.12	+72
H3	2.37	2.34	+0.03	+18
H4	4.24	4.32	-0.08	-48
H6	2.94	3.07	-0.13	-78



N-((1*S*,2*R*)-2-hydroxycyclobutyl)propane-2-sulfonamide

6.2.5. Derivatisation of metabolites

tert-Butyl (*S*)-(2-oxocyclobutyl)carbamate **2.79**

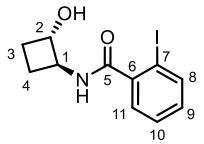


Chemical Formula: $C_9H_{15}NO_3$
Exact Mass: 185.1052
Molecular Weight: 185.2230

Dess–Martin periodinane (136 mg, 0.321 mmol) was added to a stirred solution of *tert*-butyl [(1*S*,2*S*)-2-hydroxycyclobutyl]carbamate **2.75** (40.0 mg, 0.214 mmol) in dichloromethane (2 mL). The mixture was stirred at RT for 20 h, quenched with sat. aq. $NaHCO_3$ solution (5 mL) and extracted with ethyl acetate (3 × 10 mL). The combined organic extracts were dried ($MgSO_4$), filtered, and concentrated *in vacuo* to give a residue that was purified by column chromatography (20–40% EtOAc in pentane), affording the title compound as a white powder (31.5 mg, 81%).

R_f 0.53 (50% EtOAc in pentane). **^{1}H NMR** (400 MHz, $CDCl_3$) δ 1.42 (s, 9H, H7), 1.89–2.06 (m, 1H, H4), 2.35–2.48 (m, 1H, H4), 2.72–2.95 (m, 2H, H3), 4.82 (dd, *J* = 8.5 Hz, 1H, H1), 5.10 (br. s, 1H, NH). **^{13}C NMR** (101 MHz, $CDCl_3$) δ 20.1 (C4), 28.4 (C7), 41.6 (C3), 65.2 (C1), 80.4 (C6), 154.8 (C5), 205.9 (C2). **IR** ν_{max} (thin film)/cm^{-1} 3349br.w, 2978w, 2935w, 1791s, 1693s, 1515m, 1330m, 1254m, 1162s, 992m. **HRMS** (ESI+) Found: 208.0947, $C_9H_{15}NO_3Na$ $[M+Na]^+$ requires: 208.0944. **MP** 72–75 °C. **$[\alpha]_D$** –1.98 (*c* = 1.02, $CHCl_3$, 25 °C).

N-[(*1S*,*2S*)-2-Hydroxycyclobutyl]-2-iodobenzamide **2.90**

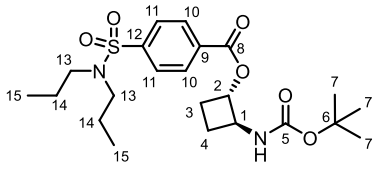


Chemical Formula: $C_{11}H_{12}INO_2$
Exact Mass: 316.9913
Molecular Weight: 317.1265

Hydrochloric acid (100 μL, conc.) was added to a stirred solution of *tert*-butyl [(1*S*,2*S*)-2-hydroxycyclobutyl]carbamate **2.75** (20.0 mg, 0.107 mmol) in methanol (500 μL) and the mixture was stirred at RT for 2 h. Methanol was removed *in vacuo* and the crude material was redissolved in acetonitrile (1 mL). To this solution was added DIPEA (61 μL, 0.35 mmol), HATU (49.0 mg, 0.129 mmol) and 2-iodobenzoic acid (32 mg, 0.129 mmol) and the mixture was stirred for 16 h. After this time, the reaction was quenched with hydrochloric acid (1.0 mL, 1.0 M) and extracted with ethyl acetate (3 × 2 mL); the combined extracts were dried ($MgSO_4$), filtered, and concentrated *in vacuo*. The residue was purified by column chromatography (40–50% EtOAc in pentane) to yield the title compound as a yellow oil (31.2 mg, 92%).

R_f 0.22 (60% EtOAc in pentane). **^{1}H NMR** (400 MHz, $CDCl_3$) δ 1.40–1.56 (m, 1H, H3 or H4), 1.78 (m, 1H, H3 or H4), 2.10–2.29 (m, 2H, H3 and H4), 3.43 (br. s, 1H, NH), 3.98–4.10 (m, 1H, H1), 4.20 (app. q, *J* = 8.0 Hz, 1H, H2), 6.05 (br. s, 1H, OH), 7.11 (ddd, *J* = 8.0, 7.0, 2.0 Hz, 1H, H9), 7.36–7.44 (m, 2H, H10 and H11), 7.87 (ddd, *J* = 8.0, 1.0, 0.5 Hz, 1H, H8). **^{13}C NMR** (126 MHz, $CDCl_3$) δ 18.8 (C4), 25.1 (C3), 55.8 (C1), 73.2 (C2), 92.6 (C7), 128.4 (C10 or C11), 128.5 (C10 or C11), 131.5 (C9), 140.1 (C8), 141.6 (C6), 170.2 (C5). **IR** ν_{max} (thin film)/cm^{-1} 3265 br.w, 2917w, 1646m, 1540m, 846m. **HRMS** (ESI+) Found: 317.9987, $C_{11}H_{13}INO_2$ $[M+H]^+$ requires: 317.9984. **$[\alpha]_D$** +0.61 (*c* = 1.20, $CHCl_3$, 25 °C).

(1*S*,2*S*)-[2-(*tert*-Butoxycarbonyl)amino]cyclobutyl 4-(*N*,*N*-dipropylsulfamoyl)benzoate **2.91**

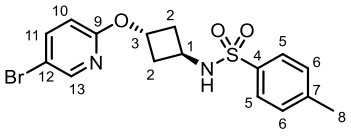


Chemical Formula: $C_{22}H_{34}N_2O_6S$
Exact Mass: 454.2138
Molecular Weight: 454.5820

N,*N*'-Dicyclohexylcarbodiimide (18.0 mg, 0.0872 mmol) was added to a stirred solution of *tert*-butyl [(1*S*,2*S*)-2-hydroxycyclobutyl]carbamate **2.75** (11.0 mg, 0.0587 mmol), probenecid (25.0 mg, 0.0876 mmol) and DMAP (2.10 mg, 0.017 mmol) in dry dichloromethane (0.5 mL) at 0 °C under argon. The mixture was stirred at 0 °C for 30 min and then at RT for 14 h. The mixture was then filtered through Celite, washed with sat. aq. $NaHCO_3$ solution (1 mL), and the aqueous extracted with ethyl acetate (3 × 2 mL); the combined extracts were dried ($MgSO_4$), filtered, and concentrated *in vacuo*. The crude product was purified by column chromatography (0–30% EtOAc in pentane) to yield the title compound as a white powder (19.9 mg, 75%).

R_f 0.63 (50% EtOAc in pentane). **^{1}H NMR** (600 MHz, $CDCl_3$) δ 0.86 (t, *J* = 7.4 Hz, 6H, H15), 1.43 (s, 9H, H7), 1.51–1.56 (m, 4H, H14), 1.56–1.61 (m, 1H, H4), 1.79–1.89 (m, 1H, H3), 2.25–2.36 (m, 2H, H3 and H4), 3.08–3.11 (m, 4H, H13), 4.16 (br.s, 1H, H1), 5.04 (app. q, *J* = 7.5 Hz, 1H, H2), 5.11 (br. s, 1H, NH), 7.87 (d, *J* = 8.5 Hz, 2H, H11), 8.15 (d, *J* = 8.5 Hz, 2H, H10). **^{13}C NMR** (101 MHz, $CDCl_3$) δ 11.3 (C15), 22.0 (C14), 28.5 (C7), 29.9 (C3/4), 50.0 (C13), 52.8 (C1), 74.4 (C2), 79.8 (C6), 127.1 (C11), 130.5 (C10), 133.3 (C9), 144.6 (C12), 155.0 (C5), 165.0 (C8). **IR** ν_{max} (thin film)/cm^{-1} 3381w, 2924m, 1718s, 1343m, 1276s, 1162s, 1106m, 996m. **MP** 92–94 °C. **HRMS** (ESI+) Found: 477.2029, $C_{22}H_{34}NO_6SNa$ $[M+Na]^+$ requires: 477.2030. **$[\alpha]_D$** +40.6 (*c* = 1.22, $CHCl_3$, 25 °C).

N-{(*trans*)-3-[(5-bromopyridin-2-yl)oxy]cyclobutyl}-4-methylbenzenesulfonamide **2.97**

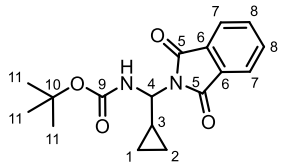


Chemical Formula: $C_{16}H_{17}BrN_2O_3S$
Exact Mass: 396.0143
Molecular Weight: 397.2870

NaH (6.5 mg, 0.16 mmol, 60% in mineral oil) was added to a stirred solution of *N*-[(*trans*)-3-hydroxycyclobutyl]-4-methylbenzenesulfonamide (20.0 mg, 0.0829 mmol) in DMF (0.5 mL) at RT. After 10 min, 5-bromo-2-fluoropyridine (8.5 μL, 0.083 mmol) was added and the mixture was stirred at RT for a further 6 h and then at 90 °C for 18 h. The mixture was then cooled to RT, diluted with water (1 mL), extracted with ethyl acetate (3 x 1 mL), and the combined extracts were dried ($MgSO_4$), filtered, and concentrated *in vacuo*. The crude product was purified by preparative TLC (50% EtOAc in pentane) to yield the title compound as a yellow oil (15.9 mg, 48%, 61% b.r.s.m.).

R_f 0.7 (50% EtOAc in pentane). **^{1}H NMR** (600 MHz, $CDCl_3$) δ 2.28–2.34 (m, 2H, H2), 2.35–2.40 (m, 2H, m, H2), 2.42 (s, 3H, s, H8), 4.04 (m, *J* = 8.0 Hz, 1H, H1), 4.93 (d, *J* = 7.5 Hz, 1H, NH), 5.15 (tt, *J* = 7.0, 3.5 Hz, 1H, H3), 6.59 (d, *J* = 9.0 Hz, 1H, H10), 7.30 (d, *J* = 8.0 Hz, 2H, H6), 7.62 (dd, *J* = 9.0, 2.5 Hz, 1H, H11), 7.75 (d, *J* = 8.0 Hz, 2H, H5), 8.10 (d, *J* = 2.5 Hz, 1H, H13). **^{13}C NMR** (151 MHz, $CDCl_3$) δ 21.7 (C8), 38.0 (C2), 45.5 (C1), 68.5 (C3), 112.1 (C12), 112.9 (C10), 127.2 (C5), 129.9 (C6), 137.4 (C7), 141.4 (C11), 143.8 (C4), 147.8 (C13), 161.8 (C9). **IR** ν_{max} (thin film)/cm^{-1} 3267w, 1483s, 1341m, 1280s, 1160s,1139m, 1091m, 666m. **HRMS** (ESI+) Found: 399.0202, $C_{16}H_{18}O_3N_2BrS$ $[M+H]^+$ requires 399.0195**.**

tert-Butyl (cyclopropyl(1,3-dioxoisoindolin-2-yl)methyl)carbamate **2.93**



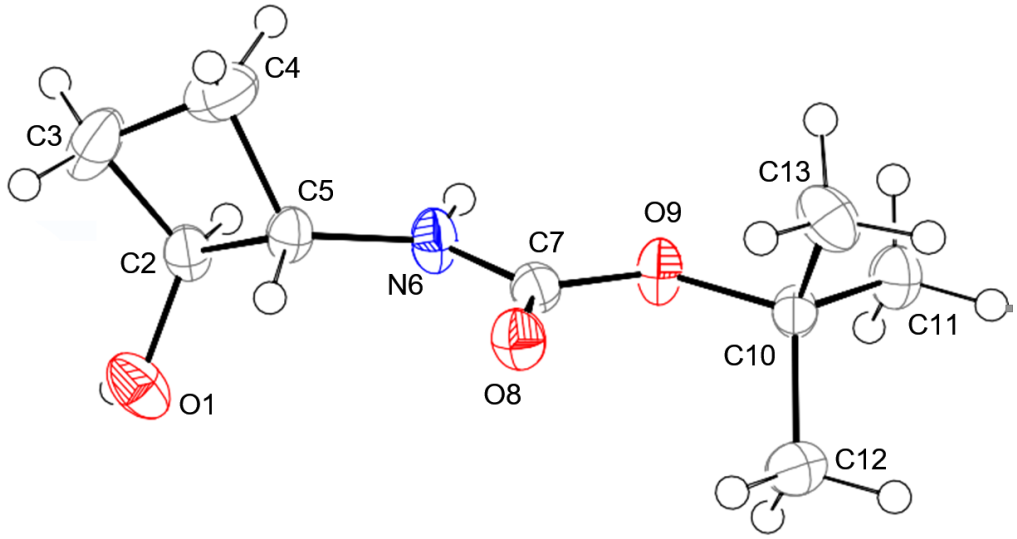
Chemical Formula: $C_{17}H_{20}N_2O_4$
Exact Mass: 316.1423
Molecular Weight: 316.3570

Adapted from modified literature procedure.[8] To a solution of *tert*-butyl ((1*S*,2*S*)-2-hydroxycyclobutyl)carbamate **2.75** (100 mg, 0.53 mmo, 1 eq.), phthalimide (79 mg, 0.53 mmol, 1 eq.) and triphenylphosphine (140 mg, 0.53 mmol, 1 eq.) in anhydrous THF (3.5 mL) at 0 °C was added dropwise DIAD (116 μL, 0.59 mmol, 1.1 eq.). The reaction mixture was warmed to RT and left stirring for 24 hr. When complete, the solvent was removed *in vacuo* and the crude material was purified by column chromatography (10–50% EtOAc in pentane) to yield the title compound as a white solid (96.6 mg, 0.305 mmol, **58%**).

R_f 0.61 (50% EtOAc in pentane). **^{1}H NMR** (400 MHz, $CDCl_3$) δ 0.54 – 0.43 (m, 2H, H1/2), 0.62 – 0.52 (m, 1H, H1/2), 0.70 – 0.60 (m, 1H, H3), 1.39 (s, 9H, H11), 5.13 (s, 1H, H4), 5.88 (s, 1H, NH), 7.71 (dd, *J* = 5.5, 3.0 Hz, 2H, H7/8), 7.84 (dd, *J* = 5.5, 3.0 Hz, 2H, H7/8). **^{13}C NMR** (101 MHz, $CDCl_3$) δ 3.4 (C1/2), 15.1 (C3), 28.4 (C11), 62.8 (C10), 77.4 (C4), 123.6 (C7), 132.0 (C8), 134.2 (C6), 154.1 (C9), 167.7 (C5). **IR** ν_{max} (thin film)/cm^{-1} 3371w, 2976w, 1776w, 1710s, 1500w, 1382m, 1157w, 1047w, 980w, 720m, 636w. **MP** 112 – 114 °C. **$[\alpha]_D$** +1.98 (*c* = 1.01 in $CHCl_3$, 25 °C).

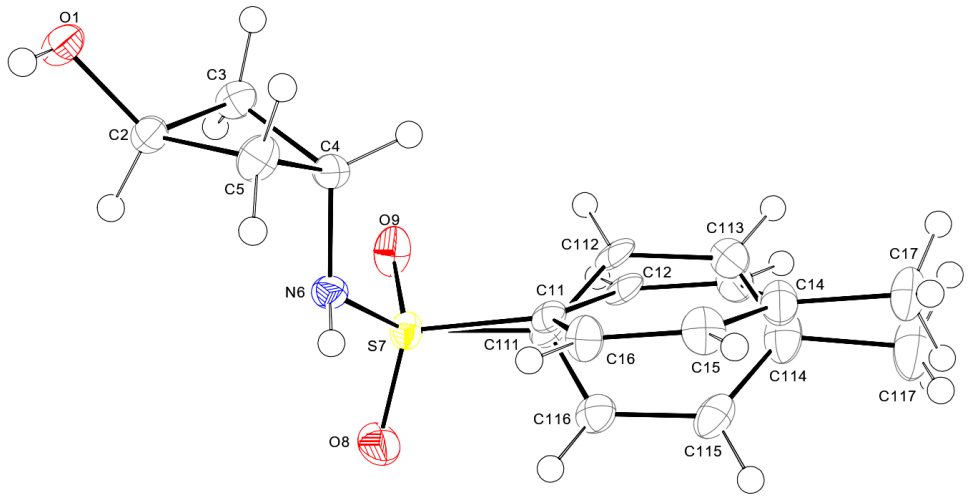
6.2.6. Single crystal X-ray data for compounds in Chapter 2

6.2.6.1. Crystal data and structure refinement for 2.75.



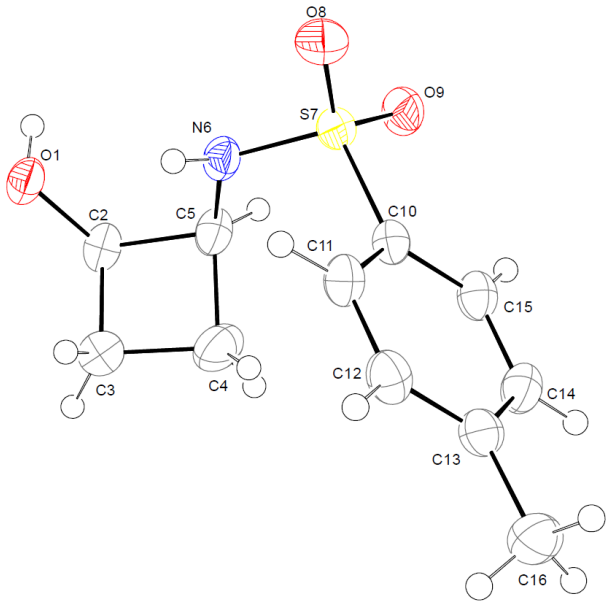
Empirical formula	C9H17N1O3	
Formula weight	187.24	
Temperature	150 K	
Wavelength	1.54184 Å	
Crystal system	Orthorhombic	
Space group	P 21 21 21	
Unit cell dimensions	a = 10.15030(10) Å	α= 90°.
	b = 10.5070(2) Å	β= 90°.
	c = 29.2042(4) Å	γ = 90°.
Volume	3114.61(8) $Å^3$	
Z	12	
Density (calculated)	1.198 Mg/m^3	
Absorption coefficient	0.734 mm^{-1}	
F(000)	1224	
Crystal size	0.38 x 0.17 x 0.01 mm^3	
Theta range for data collection	4.472 to 76.877°.	
Index ranges	-12<=h<=7, -13<=k<=11, -36<=l<=36	
Reflections collected	16862	
Independent reflections	6496 [R(int) = 0.043]	
Completeness to theta = 75.340°	99.6 %	
Absorption correction	Semi-empirical from equivalents	
Max. and min. transmission	0.99 and 0.61	
Refinement method	Full-matrix least-squares on F^2	
Data / restraints / parameters	6496 / 0 / 353	
Goodness-of-fit on F^2	1.0029	
Final R indices [I>2sigma(I)]	R1 = 0.0434, wR2 = 0.1003	
R indices (all data)	R1 = 0.0516, wR2 = 0.1076	
Absolute structure parameter	-0.09(11)	
Largest diff. peak and hole	0.25 and -0.23 $e.Å^{-3}$	

6.2.6.2. Crystal data and structure refinement for 2.82.



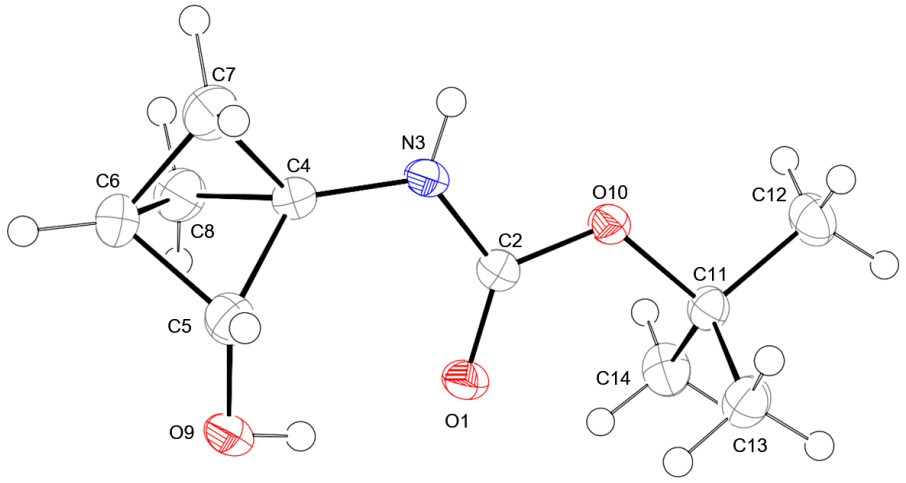
Empirical formula	C11 H15 N O3 S	
Formula weight	241.31	
Temperature	150 K	
Wavelength	1.54184 Å	
Crystal system	Monoclinic	
Space group	P 21/n	
Unit cell dimensions	a = 6.62580(10) Å	α= 90°.
	b = 24.4743(3) Å	β= 90.2022(11)°.
	c = 7.09120(10) Å	γ = 90°.
Volume	1149.91(3) Å^3	
Z	4	
Density (calculated)	1.394 Mg/m^3	
Absorption coefficient	2.454 mm^{-1}	
F(000)	512.000	
Crystal size	0.27 x 0.24 x 0.22 mm^3	
Theta range for data collection	3.612 to 76.800°.	
Index ranges	-8<=h<=8, -27<=k<=30, -8<=l<=8	
Reflections collected	9632	
Independent reflections	2408 [R(int) = 0.019]	
Completeness to theta = 76.800°	99.6 %	
Absorption correction	Semi-empirical from equivalents	
Max. and min. transmission	0.58 and 0.48	
Refinement method	Full-matrix least-squares on F^2	
Data / restraints / parameters	2403 / 152 / 209	
Goodness-of-fit on F^2	0.9818	
Final R indices [I>2sigma(I)]	R1 = 0.0825, wR2 = 0.0245	
R indices (all data)	R1 = 0.0826, wR2 = 0.0245	
Largest diff. peak and hole	0.55 and -0.59 e.Å^{-3}	

6.2.6.3. Crystal data and structure refinement for 2.80.



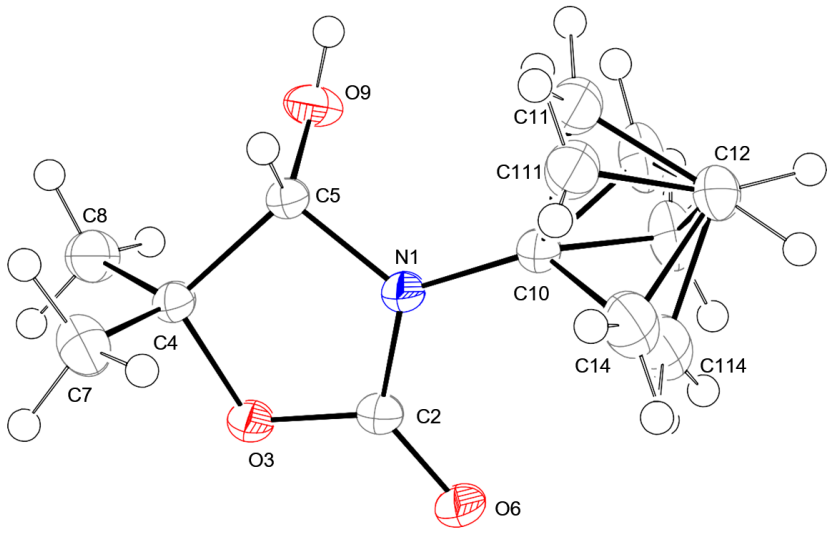
Empirical formula	C11 H15 N O3 S	
Formula weight	241.31	
Temperature	150 K	
Wavelength	1.54184 Å	
Crystal system	Monoclinic	
Space group	P 21/n	
Unit cell dimensions	a = 6.53200(10) Å	α= 90°.
	b = 7.39220(10) Å	β= 94.7894(11)°.
	c = 24.2354(3) Å	γ = 90°.
Volume	1166.14(3) Å^3	
Z	4	
Density (calculated)	1.374 Mg/m^3	
Absorption coefficient	2.420 mm^{-1}	
F(000)	512.000	
Crystal size	0.26 x 0.20 x 0.07 mm^3	
Theta range for data collection	3.660 to 76.205°.	
Index ranges	-8<=h<=8, -9<=k<=9, -29<=l<=30	
Reflections collected	21100	
Independent reflections	2428 [R(int) = 0.028]	
Completeness to theta = 76.800°	99.5 %	
Absorption correction	Semi-empirical from equivalents	
Max. and min. transmission	0.84 and 0.61	
Refinement method	Full-matrix least-squares on F^2	
Data / restraints / parameters	2428 / 0 / 145	
Goodness-of-fit on F^2	1.0088	
Final R indices [I>2sigma(I)]	R1 = 0.0327, wR2 = 0.0934	
R indices (all data)	R1 = 0.0336, wR2 = 0.0944	
Largest diff. peak and hole	0.34 and -0.34 e.Å^{-3}	

6.2.6.4. Crystal data and structure refinement for 2.84.



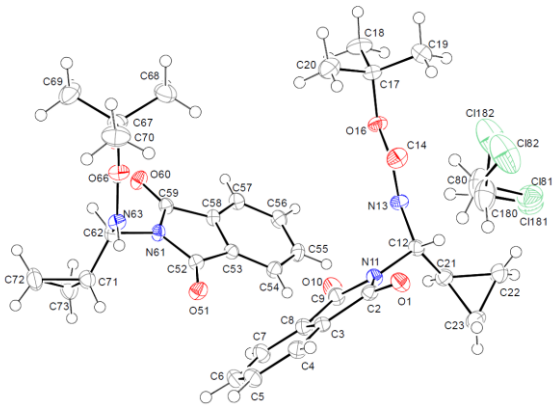
Empirical formula	C10 H17 N O3	
Formula weight	199.25	
Temperature	150 K	
Wavelength	1.54184 Å	
Crystal system	Orthorhombic	
Space group	P 21 21 21	
Unit cell dimensions	a = 6.06410(10) Å	α= 90°.
	b = 9.73480(10) Å	β= 90°.
	c = 18.3114(2) Å	γ = 90°.
Volume	1080.97(2) $Å^3$	
Z	4	
Density (calculated)	1.224 Mg/m^3	
Absorption coefficient	0.738 mm^{-1}	
F(000)	432	
Crystal size	0.24 x 0.21 x 0.08 mm^3	
Theta range for data collection	4.830 to 76.169°.	
Index ranges	-7<=h<=7, -12<=k<=12, -22<=l<=22	
Reflections collected	22828	
Independent reflections	2260 [R(int) = 0.032]	
Completeness to theta = 76.169°	99.9 %	
Absorption correction	Semi-empirical from equivalents	
Max. and min. transmission	0.94 and 0.77	
Refinement method	Full-matrix least-squares on F^2	
Data / restraints / parameters	2260 / 0 / 129	
Goodness-of-fit on F^2	1.0043	
Final R indices [I>2sigma(I)]	R1 = 0.0306, wR2 = 0.0855	
R indices (all data)	R1 = 0.0313, wR2 = 0.0866	
Absolute structure parameter	-0.05(4)	
Extinction coefficient	22(5)	
Largest diff. peak and hole	0.23 and -0.13 $e.Å^{-3}$	

6.2.6.5. Crystal data and structure refinement for 2.86.



Empirical formula	C10 H15 N O3	
Formula weight	197.23	
Temperature	150 K	
Wavelength	1.54184 Å	
Crystal system	Orthorhombic	
Space group	P n a 21	
Unit cell dimensions	a = 9.5843(3) Å	α= 90°.
	b = 6.42090(10) Å	β= 90°.
	c = 16.9036(4) Å	γ = 90°.
Volume	1040.24(4) $Å^3$	
Z	4	
Density (calculated)	1.259 Mg/m^3	
Absorption coefficient	0.767 mm^{-1}	
F(000)	424	
Crystal size	0.25 x 0.12 x 0.05 mm^3	
Theta range for data collection	5.233 to 76.185°.	
Index ranges	-11<=h<=11, -8<=k<=6, -21<=l<=16	
Reflections collected	6287	
Independent reflections	1862 [R(int) = 0.032]	
Completeness to theta = 74.661°	99.6 %	
Absorption correction	Semi-empirical from equivalents	
Max. and min. transmission	0.96 and 0.85	
Refinement method	Full-matrix least-squares on F^2	
Data / restraints / parameters	1862 / 13 / 138	
Goodness-of-fit on F^2	1.0007	
Final R indices [I>2sigma(I)]	R1 = 0.0340, wR2 = 0.0912	
R indices (all data)	R1 = 0.0346, wR2 = 0.0925	
Absolute structure parameter	0.21(10)	
Largest diff. peak and hole	0.17 and -0.17 $e.Å^{-3}$	

6.2.6.6. Crystal data and structure refinement for 2.93.

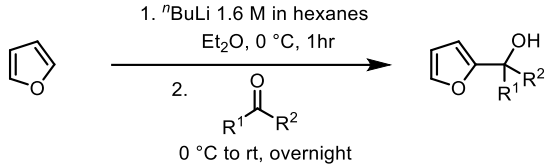


Empirical formula	C35 H42 Cl2 N4 O8	
Formula weight	717.65	
Temperature	150 K	
Wavelength	1.54180 Å	
Crystal system	Triclinic	
Space group	P -1	
Unit cell dimensions	a = 9.7434(3) Å	α= 115.713(2)°.
	b = 13.5596(3) Å	β= 92.231(2)°.
	c = 15.1971(3) Å	γ = 95.383(2)°.
Volume	1793.89(8) Å3	
Z	2	
Density (calculated)	1.2329 Mg/m^3	
Absorption coefficient	2.094 mm^{-1}	
F(000)	756	
Crystal size	0.26 x 0.09 x 0.04 mm^3	
Theta range for data collection	3.240 to 76.045°.	
Index ranges	-12<=h<=12, -17<=k<=16, -19<=l<=18	
Reflections collected	38062	
Independent reflections	7416 [R(int) = 0.043]	
Completeness to theta = 74.661°	99.6 %	
Absorption correction	Semi-empirical from equivalents	
Max. and min. transmission	0.92 and 0.76	
Refinement method	Full-matrix least-squares on F^2	
Data / restraints / parameters	7411 / 4 / 453	
Goodness-of-fit on F^2	1.0118	
Final R indices [I>2sigma(I)]	R1 = 0.0520, wR2 = 0.1588	
R indices (all data)	R1 = 0.0590, wR2 = 0.1648	
Largest diff. peak and hole	0.51 and -0.71 $e.Å^{-3}$	

6.3. Experimental procedures for Chapter 3

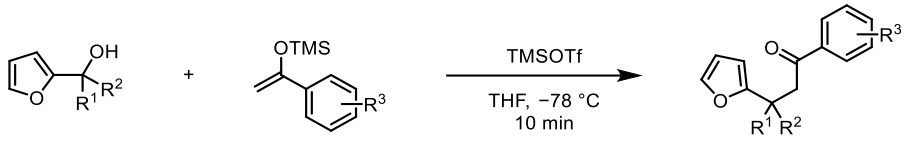
6.3.1. General procedures

General procedure for the synthesis of furfuryl alcohols (**GP-II**)



Adapted from a literature procedure.[9] To a stirred solution of furan (1.6 eq.) in ether (0.32 M w.r.t. furan), at 0 °C under argon, *n*BuLi (1.6 M solution in hexanes, 1.2 eq.) was slowly added and the reaction was stirred for 1 hr. The reaction mixture was then cooled to −78 °C and acetone (1 eq.) was added dropwise and the reaction mixture was allowed to warm to RT and stirred for 12 − 18 hr (overnight). The resulting reaction mixture was quenched under inert atmosphere *via* slow addition of sat. NH_4Cl (50% reaction volume) followed by brine (50% reaction volume). The aqueous phase was extracted with EtOAc (x3 reaction volume), and the combined organic phase was dried over $MgSO_4$ and concentrated *in vacuo*. Purification by column chromatography when required.

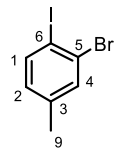
General procedure for the Lewis acid mediated coupling of furfuryl alcohols with silyl enol ethers (**GP-III**)



To a stirred solution of alcohol (1 eq.) and silyl enol ether (1.8 eq.) in anhydrous THF (0.3 M w.r.t. alcohol), under argon at −78 °C, freshly distilled TMSOTf (1 eq.) was slowly added dropwise. The reaction was stirred vigorously for 10 min, and then aq. $NaHCO_3$ (50% vol. w.r.t. THF) was slowly added and stirred for a further 5 min. The reaction was extracted with EtOAc (3 x reaction volume) and then washed with 1M aq. HCl. The combined organic layers were dried over $MgSO_4$, filtered and concentrated. The compound was purified by column chromatography.

6.3.2. Experimental details for first-generation route to trigoxyphin

2-Bromo-1-iodo-4-methylbenzene **3.15**

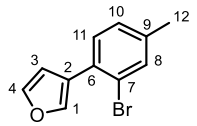


Chemical Formula: C_7H_6BrI
Exact Mass: 295.8698
Molecular Weight: 296.9335

Adapted from literature procedure.[10] A solution of conc. HCl (42 mL) in water (100 mL) was added to a solution of 2-bromo-4-methylaniline (10.0 mL, 80.6 mmol, 1 eq.) in acetonitrile (150 mL). $NaNO_2$ (6.68 g, 96.8 mmol, 1.2 eq) in water (100 mL) was added. The solution was stirred for 30 mins and a solution of KI (20.0 g, 120 mmol, 1.5 eq.) in water (100 mL) was added. The solution was stirred at RT for 15 hr then poured into water and extracted with CH_2Cl_2. The combined organic layers were washed with saturated aqueous $Na_2S_2O_3$ and brine, dried over $MgSO_4$, filtered, and concentrated in vacuo to a brown oil (21.4 g, 91%). The *title compound* was used without further purification (<98% pure).

R_f 0.7 (pentane). **^{1}H NMR** (400 MHz, $CDCl_3$) δ 2.28 (s, 3H, H9), 6.81 (ddq, *J* = 8.0, 2.0, 0.5 Hz, 1H, H2), 7.46 (dq, *J* = 2.0, 0.5 Hz, 1H, H4), 7.70 (d, *J* = 8.0 Hz, 1H, H1). **^{13}C NMR** (101 MHz, $CDCl_3$) δ 20.8 (C9), 97.0 (C6), 129.5 (C5), 129.6 (C2), 133.5 (C4), 140.0 (C1), 140.0 (C3). **IR** ν_{max} (thin film)/cm^{-1} 2918w, 2360w, 2342w, 1457m, 1005m, 805s, 667m. **HRMS** (EI) Found: 295.8698, C_7H_6BrI [$M^{\bullet+}$] requires: 295.8692.

3-(2-Bromo-4-methylphenyl)furan **3.17**

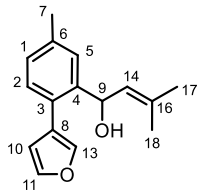


Chemical Formula: $C_{11}H_9BrO$
Exact Mass: 235.9837
Molecular Weight: 237.0960

Ar was bubbled through a solution of water (0.17 mL) and dimethoxyethane (1.1 mL) for 5 min. 2-Bromo-1-iodo-4-methylbenzene **3.15** (50.1 mg, 0.17 mmol), furan-3-ylboronic acid (22.7 mg, 0.2 mmol), and K_2CO_3 (58.5 mg, 0.42 mmol) were added sequentially, then Ar was bubbled through the solution for a further 5 min. $(Ph_3P)_2PdCl_2$ (5.91 mg, 8.4 μmol, 5 mol%) was added and the solution was heated at 80 °C for 18 h. The solution was cooled to RT, when water (2 mL) was added and then extracted with ether (3 × 2 mL). The combined organic phases were washed with brine (4 mL), dried over anhydrous Mg_2SO_4, filtered, and concentrated *in vacuo* to produce a brown oil. The crude product was purified by column chromatography (1% EtOAc in pet. $ether_{30\text{-}40}$) to afford the title compound as a colourless oil (21.3 mg, 53%).

R_f 0.45 (pentane). **^{1}H NMR** (400 MHz, $CDCl_3$) δ 2.35 (s, 3H, H12), 6.69 (dd, *J* = 2.0, 1.0 Hz, 1H, H3), 7.13 (ddd, *J* = 8.0, 2.0, 1.0 Hz, 1H, H10), 7.27 (d, *J* = 8.0 Hz, 1H, H11), 7.48 (t, *J* = 1.5 Hz, 1H, H4), 7.49 (d, *J* = 1.0 Hz, 1H, H8), 7.75 (dd, *J* = 1.5, 1.0 Hz, 1H, H1). **^{13}C NMR** (101 MHz, $CDCl_3$) δ 20.8 (C12), 111.6 (C3), 122.3 (C7), 125.1 (C2), 128.4 (C10), 130.6 (C11), 130.7 (C6), 134.2 (C8), 138.8 (C9), 140.8 (C1), 142.5 (C4). **IR** ν_{max} (thin film)/cm^{-1} 3149w, 2921w, 2865w, 1063s, 1511w, 1163m, 1107m, 1063m, 1035m, 873s, 787s, 728m. **HRMS** (CI) Found: 236.9910, $C_{11}H_{10}BrI$ $[M+H]^+$ requires: 236.9910.

1-(2-(Furan-3-yl)-5-methylphenyl)-3-methylbut-2-en-1-ol **3.19**

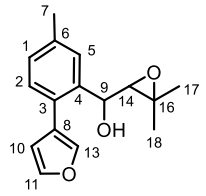


Chemical Formula: $C_{16}H_{18}O_2$
Exact Mass: 242.1307
Molecular Weight: 242.3180

A solution of 3-(2-bromo-4-methylphenyl)furan **3.17** (610 μL, 4.22 mmol, 1 eq.) in anhydrous THF (55 mL) was cooled to −78 °C, then *n*-BuLi [2.5 M solution in hexanes] (2.2 mL, 5.48 mmol, 1.3 eq.) was added dropwise over 10 min and left to stir for 10 min. 3-Methylcrotonaldehyde (524 μL, 5.48 mmol, 1.3 eq.) was then added and left to return to RT over 75 min. The reaction was then quenched with NH_4Cl (60 mL), extracted with ethyl acetate (3 x 50 mL), washed with brine, dried over $MgSO_4$ and concentrated *in vacuo*. The resulting oil was purified quickly by column chromatography (10 – 20% ether in pet. $ether_{30\text{-}40}$) yielding the *title compound* as a clear colourless oil (398 mg, 39% (51% brsm)).

R_f 0.36 (5% EtOAc in pet. $ether_{30\text{-}40}$). **^{1}H NMR (**400 MHz, C_6D_6) δ 1.37 (d, *J* = 1.0 Hz, 3H, H18), 1.48 (d, *J* = 1.0 Hz, 3H, H17), 2.19 (s, 3H, H7), 5.46 (app. dp, *J* = 8.5, 1.5 Hz, 1H, H14), 5.62 (d, *J* = 8.5 Hz, 1H, H9), 6.39 (dd, *J* = 1.5, 1.0 Hz, 1H, H10), 6.91 (dd, *J* = 7.5, 1.0 Hz, 1H, H1), 7.11 (d, *J* = 7.5 Hz, 1H, H2), 7.15 (t, *J* = 1.5 Hz, 1H, H11), 7.38 (dd, *J* = 1.5, 1.0 Hz, 1H, H13), 7.61 (d, *J* = 1.0 Hz, 1H, H5). **^{13}C NMR** (101 MHz, C_6D_6) δ 18.0 (C18), 21.3 (C7), 25.7 (C17), 67.9 (C9), 112.6 (C10), 125.3 (C8), 127.8 (C5), 128.1 (C1), 128.8 (C3), 129.4 (C14), 130.3 (C2), 134.6 (C16), 137.6 (C6), 140.6 (C11), 142.8 (C13), 143.2 (C4). **IR** ν_{max} (thin film)/cm^{-1} 3327br.m, 2966m, 2927m, 2871m, 2859, 1510w, 1447w, 1376w, 1160m, 1013s, 873s, 790s, 729w. **HRMS** Not found.

(*S*)-((*R*)-3,3-Dimethyloxiran-2-yl)(2-(furan-3-yl)-5-methylphenyl)methanol **3.20**

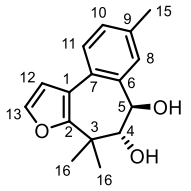


Chemical Formula: $C_{16}H_{18}O_3$
Exact Mass: 258.1256
Molecular Weight: 258.3170

To a solution of 1-[2-(furan-3-yl)-5-methylphenyl]-3-methylbut-2-en-1-ol **3.19** (201 mg, 0.83 mmol, 1 eq.) in anhydrous CH_2Cl_2 (8.3 mL) cooled to 0 °C, 3-chloroperbenzoic acid (203 mg, 0.91 mmol, 1.1 eq.) was added. The mixture was stirred for 90 min and then quenched with aq. K_2CO_3 (0.72 M) and extracted with CH_2Cl_2 (x3). The combined organic phases were washed with brine, dried over Na_2SO_4, filtered, and concentrated *in vacuo* to a yellow oil. The crude product was purified by column chromatography (quickly) to afford the *title compound* as a yellow oil (194 mg, 91%).

R_f 0.21 (5% EtOAc in pet. ether$_{30\text{-}40}$). **^{1}H NMR** (400 MHz, $CDCl_3$) δ 1.03 (s, 3H, H18). 1.25 (s, 3H, H17), 2.41 (s, 3H, H11), 3.07 (d, *J* = 7.0 Hz, 1H, H14), 4.77 (dd, *J* = 7.10, 1.5 Hz, 1H, H9), 6.50 (dd, *J* = 1.5, 1.0 Hz, 1H, H10), 7.15 (dd, *J* = 8.0, 1.5 Hz, 1H, H11), 7.19 (t, *J* = 8.0 Hz, 1H, H1), 7.49 – 7.46 (m, 3H, H2/5/13). **^{13}C NMR** (101 MHz, $CDCl_3$) δ 18.9 (C18), 21.4 (C7), 24.8 (C17), 60.6 (C16), 67.9 (C14), 68.9 (C9), 112.2 (C10), 124.6 (C8), 127.6 (C5), 129.0 (C1), 129.0 (C3), 130.5 (C2), 138.1 (C4), 138.8 (C6), 140.1 (C13), 143.0 (C11). **IR** ν_{max} (thin film)/cm^{-1} 3412br.m (OH), 3142w, 2961m, 2927m, 2873w, 2353w, 1511m, 1456m, 1379m, 1014s, 1096s, 873s, 818s, 793s, 642m. **HRMS** (ESI+) Found: 281.1148, $C_{16}H_{18}NaO_3$ $[M+Na]^+$ requires: 281.1148.

4,4,8-Trimethyl-5,6-dihydro-4*H*-benzo[3,4]cyclohepta[1,2-*b*]furan-5,6-diol **3.21**

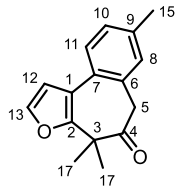


Chemical Formula: $C_{16}H_{18}O_3$
Exact Mass: 258.1256
Molecular Weight: 258.3170

Chlorotriisopropoxytitanium (IV) (2.64 mL, 1.0 M in hexanes, 2.64 mmol, 5.5 eq.) was added to a stirred solution of 1-(2-(furan-3-yl)-5-methylphenyl)-3-methylbut-2-en-1-ol **3.20** (125.0 mg, 0.484 mmol, 1 eq.) in anhydrous CH_2Cl_2 (8.97 mL). The mixture was stirred for 1 hr and then quenched with aq. 1M HCl (8.97 mL) and allowed to stir for 10 min before extracting with ethyl acetate (x3). The combined organic phases were washed with brine, dried over anhydrous $MgSO_4$, filtered, and concentrated *in vacuo* to a brown oil. The crude product was purified by column chromatography (10% EtOAc in pentane) to afford *title compound* as an off-white solid (97.0 mg, 78%).

R_f 0.39 (10% EtOAc in pentane). **^{1}H NMR** (400 MHz, $CDCl_3$) δ 1.38 (s, 3H, H16'), 1.46 (s, 3H, H16), 2.39 (s, 3H, H15), 3.58 (d, *J* = 8.5 Hz, 1H, H4), 4.63 (d, *J* = 8.5 Hz, 1H, H5), 6.55 (d, *J* = 2.0 Hz, 1H, H12), 7.11 (d, *J* = 8.0 Hz, 1H, H10), 7.37 (d, *J* = 8.0 Hz, 1H, H11), 7.40 (d, *J* = 2.0 Hz, 1H, H13), 7.53 (s, 1H, H8). **^{13}C NMR** (101 MHz, $CDCl_3$) δ 20.8 (C16), 21.5 (C15), 27.8 (C5), 42.4 (C4), 69.2 (C5), 78.1 (C4), 110.2 (C12), 117.2 (C1), 123.6 (C7), 125.8 (C8), 126.0 (C10), 127.8 (C11), 136.5 (C6), 140.0 (C9), 141.6 (C13), 154.6 (C2). **IR** ν_{max} (thin film)/cm^{-1} 3372br.m (OH), 2975m, 2934w, 2877w, 2360m, 2342m, 1704w, 1601w, 1524m, 1167m, 1094m, 1071s, 822m, 750m, 625m. **HRMS** (ESI+) calc. for $C_{16}H_{18}NaO_3$ $[M+Na]^+$ Requires: 281.1148, Found: 281.1149. **MP** 132 – 135 °C.

4,4,8-Trimethyl-4,6-dihydro-5*H*-benzo[3,4]cyclohepta[1,2-*b*]furan-5-one **3.22**

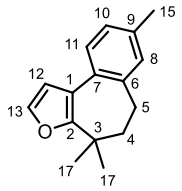


Chemical Formula: $C_{16}H_{16}O_2$
Exact Mass: 240.1150
Molecular Weight: 240.3020

To a solution of (5*S*,6*S*)-4,4,8-trimethyl-5,6-dihydro-4*H*-benzo[3,4]cyclohepta[1,2-*b*]furan-5,6-diol **3.21** (80.0 mg, 0.31 mmol, 3.1 eq.) in benzene (2.4 mL) *p*-toluenesulfonic acid (19.6 mg, 0.10 mmol, 1 eq.) was added, the mixture was then heated to 60 °C for 16 hr. The mixture was cooled to RT, diluted with Et_2O and washed with sat. aq. $NaHCO_3$ then H_2O. The organic layer was dried over anhydrous $MgSO_4$, filtered and concentrated *in vacuo* to afford the *title compound* as a brown solid without further purification (60.2 mg, 81%).

R_f 0.82 (10% EtOAc in pentane). **^{1}H NMR** (400 MHz, $CDCl_3$) δ 1.45 (s, 6H, H17), 2.36 (s, 3H, H15), 3.80 (s, 2H, H5), 6.62 (d, *J* = 2.0 Hz, 1H, H12), 7.12 (s, 1H, H8), 7.15 (d, *J* = 8.0 Hz, 1H, H10), 7.36 (d, *J* = 8.0 Hz, 1H, H11), 7.47 (d, *J* = 2.0 Hz, 1H, H13). **^{13}C NMR** (101 MHz, $CDCl_3$) δ 21.2 (C15), 25.0 (C17), 48.1 (C5), 50.4 (C3), 110.5 (C12), 119.1 (C1), 126.8 (C11), 128.4 (C9), 128.5 (C10), 130.4 (C7), 130.5 (C8), 137.7 (C6), 141.9 (C13), 152.8 (C2), 207.0 (C4). **IR** ν_{max} (thin film)/cm^{-1} 2978w, 2932w, 2871w, 2360s, 2342s, 1716s, 1376w, 1359w, 821m, 754m. **HRMS** (ESI+) Found: 241.1225, $C_{16}H_{17}O_2$ $[M+H]^+$ requires: 241.1223. **MP** 106 – 109 °C.

4,4,8-Trimethyl-5,6-dihydro-4*H*-benzo[3,4]cyclohepta[1,2-*b*]furan **3.12**

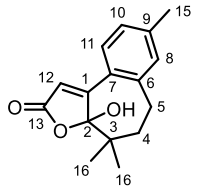


Chemical Formula: $C_{16}H_{18}O$
Exact Mass: 226.1358
Molecular Weight: 226.3190

Hydrazine monohydrate (190 μL, 3.87 mmol, 9.3 eq.) and KOH (70.0 mg, 1.25 mmol, 3 eq.) were added consecutively to a stirred solution of 4,4,8-trimethyl-4,6-dihydro-5*H*-benzo[3,4]cyclohepta[1,2-*b*]furan-5-one **3.22** (99.8 mg, 0.416 mmol, 1 eq.) in ethylene glycol (0.64 mL). The mixture was heated to 130 °C for 2 hr, then at 180 °C for a further 20 hr. The mixture was poured into H_2O, extracted with ether and washed with brine. Then dried over anhydrous Mg_2SO_4, filtered and concentrated *in vacuo* to achieve the *title compound* as a white solid (48.5 mg, 63%).

R_f 0.38 (Pentane). **^{1}H NMR** (400 MHz, $CDCl_3$) δ 1.36 (s, 6H, H17), 1.85 – 1.80 (m, 2H, H4), 2.33 (s, 3H, H15), 2.81 – 2.74 (m, 2H, H5), 6.59 (d, *J* = 2.0 Hz, 1H, H12), 6.97 (s, 1H, H8), 7.04 (d, *J* = 8.0 Hz, 1H, H10), 7.36 (d, *J* = 2.0 Hz, 1H, H13), 7.39 (d, *J* = 8.0 Hz, 1H, H11). **^{13}C NMR** (101 MHz, $CDCl_3$) δ 21.1 (C15), 29.6 (C17), 31.4 (C5), 38.1 (C3), 40.8 (C4), 110.2 (C12), 117.9 (C1), 127.0 (C8), 127.1 (C7), 129.1 (C10), 129.8 (C11), 135.7 (C6), 140.6 (C9), 141.6 (C13), 157.8 (C2). **IR** ν_{max} (thin film)/cm^{-1} 2962w, 2923w, 2865w, 2361s, 2342m, 1362w. **HRMS** (ESI+) Found: 227.1433, $C_{16}H_{19}O$ $[M+H]^+$ requires: 227.1430.

3a-Hydroxy-4,4,8-trimethyl-3a,4,5,6-tetrahydro-2*H*-benzo[3,4]cyclohepta[1,2-*b*]furan-2-one **3.11**



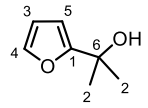
Chemical Formula: $C_{16}H_{18}O_3$
Exact Mass: 258.1256
Molecular Weight: 258.3170

To a solution of 4,4,8-trimethyl-5,6-dihydro-4*H*-benzo[3,4]cyclohepta[1,2-*b*]furan **3.12** (28.2 mg, 0.12 mmol, 1 eq.) in DCM (11.7 mL), DIPEA (102 μL, 0.59 mmol, 5 eq.) and Rose Bengal (spatula tip) were added. O_2 was bubbled through the mixture for 10 min and then cooled to 0 °C and irradiated for 5 min. Bubbling was stopped and the reaction was irradiated under O_2 atmosphere for a further 150 min. The mixture was washed with sat. aq. NH_4Cl and extracted with CH_2Cl_2 (x3). The combined organic phases were washed with brine and dried over anhydrous Na_2SO_4, filtered and concentrated *in vacuo*. Purification by column chromatography (5 – 50% EtOAc in pentane) afforded the *title compound* as a white solid (14.0 mg, 47%).

R_f 0.09 (5% EtOAc in pentane) **^{1}H NMR** (400 MHz, $CDCl_3$) δ 1.10 (s, 3H, H16'), 1.28 (s, 3H, H16), 1.58 (ddd, *J* = 14.5, 7.0, 2.0 Hz, 1H, H4'), 2.25 (t, *J* = 13.5 Hz, 1H, H4), 2.35 (s, 3H, H15), 2.67 (ddd, *J* = 15.9, 7.0, 1.5 Hz, 2H, H5'), 3.00 (t, *J* = 14.5 Hz, 1H, H5), 3.34 (br.s, 1H, OH), 6.06 (s, 1H, H12), 7.01 (s, 1H, H8), 7.07 (d, *J* = 7.5 Hz, 1H, H11), 7.24 (d, *J* = 7.5 Hz, 1H, H10). **^{13}C NMR** (101 MHz, $CDCl_3$) δ 21.3 (C16'), 21.4 (C15), 24.9 (C16), 31.6 (C5), 38.2 (C4), 41.4 (C3), 110.4 (C2), 117.1 (C12), 127.6 (C7), 127.6 (C10), 130.9 (C11), 131.5 (C8), 141.1 (C9), 141.5 (C6), 169.6 (C1), 170.6 (C13). **IR** **ν_{max}** (thin film)/cm^{-1} 3370br.m, 2971m, 2928m, 2361s, 2341m, 1758s, 1739s, 1363w. **HRMS** (ESI+) Found: 259.1330, $C_{16}H_{19}O_3$ $[M+H]^+$ requires: 259.1329.

6.3.3. Experimental details for second-generation route to trigoxyphin

2-(Furan-2-yl)propan-2-ol **3.27**



Chemical Formula: $C_7H_{10}O_2$
Exact Mass: 126.0681
Molecular Weight: 126.1550

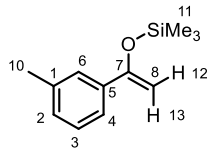
Adapted from a literature procedure.[11] To a stirred solution of acetylfuran (4.00 g, 36.33 mmol, 1 eq.) in anhydrous THF 160 mL), MeMgBr [3 M in ether] (18.6 mL, 55.8 mmol, 1.5 eq.) was added at 0 °C under argon. The mixture was then warmed to RT. After 4 hr, the reaction was quenched with sat. NH_4Cl and extracted with CH_2Cl_2 (x3). The organic phase was dried over Na_2SO_4 and concentrated *in vacuo*. The product was purified by column chromatography (5% EtOAc in pentane), yielding a clear colourless oil (3.27 g, 71%).

OR,

Prepared according to **GP-II**; using acetone (1.5 mL, 20 mmol), stirring for 16 hours. The resulting yellow oil was used without further purification (2.51 g, 99%).

R_f 0.42 (5% EtOAc in pet. ether$_{30\text{-}40}$). **^{1}H NMR** (400 MHz, $CDCl_3$) δ 1.54 (s, 6H, H2), 2.50 (s, 1H, OH), 6.15 (dd, *J* = 3.0, 1.0 Hz, 1H, H3), 6.27 (dd, *J* = 3.0, 2.0 Hz, 1H, H5), 7.31 (dd, *J* = 2.0, 1.0 Hz, 1H, H4). **^{13}C NMR** (101 MHz, $CDCl_3$) δ 28.6 (C2), 68.8 (C6), 103.6 (C5), 110.0 (C3), 141.4 (C4), 160.3 (C1). **IR** ν_{max} (thin film)/cm^{-1} 3377br.m, 2981m, 2934w, 1364w, 1264w, 1157s, 1015m, 952m, 924m, 841m, 807m, 732s. **HRMS** (EI) Found: 126.0673, $C_7H_{10}O_2$ [$M^{\bullet+}$] requires: 126.0675. Data consistent with literature values.[ii]

Trimethyl((1-(*m*-tolyl)vinyl)oxy)silane **3.25**

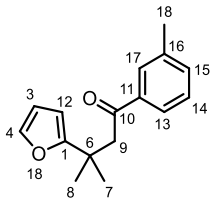


Chemical Formula: $C_{12}H_{18}OSi$
Exact Mass: 206.1127
Molecular Weight: 206.3600

To a stirred solution of diisopropylamine (175 μL, 1.25 mmol, 1.25 eq.) in anhydrous THF (1 mL), *n*-Buli [1.6 M solution in hexanes] (0.78 mL, 1.25 mmol, 1.25 eq.) was added dropwise over 5 min at 0 °C under argon. The reaction was left to stir for 20 min, then the ice bath removed and replaced with a dry ice/ acetone bath at −78 °C. 3-Methylacetophenone (136 μL, 1 mmol, 1 eq.) in anhydrous THF (0.5 mL) was added slowly over 5 min, and the reaction was left stirring at −78 °C for 20 min. Chlorotrimethylsilane (127 μL, 1 mmol, 1 eq.) was then added and the reaction was allowed to return to RT, then stirred for a further 2 hr. The solvent was then removed *in vacuo*, and re-dissolved in hexane. The reaction was filtered through Celite, washed again with hexane and filtered for a second time, then dried over $MgSO_4$ and concentrated to give a yellow oil with was used without further purification (200 mg, 97%).

R_f 0.83 (5% EtOAc in pet. ether$_{30\text{-}40}$). **^{1}H NMR** (400 MHz, C_6D_6) δ 0.00 (s, 9H, H11), 1.92 (s, 3H, H10), 4.27 (d, *J* = 1.5 Hz, 1H, H12), 4.74 (d, *J* = 1.5 Hz, 1H, H13), 6.75 (d, *J* = 7.5 Hz, 1H, H2), 6.92 (t, *J* = 8.5 Hz, 1H, H3), 7.34 (s, 1H, H6), 7.36 – 7.34 (m, 1H, H4). **^{13}C NMR** (101 MHz, C_6D_6) δ 0.1 (C11), 21.5 (C10), 91.1 (C8), 123.0 (C4), 126.4 (C6), 128.4 (C2), 129.4 (C3), 137.7 (C5), 138.1 (C1), 156.5 (C7). **IR** ν_{max} (thin film)/cm^{-1} 2960w, 1585w, 1275m, 1252m, 1012m, 843s, 681m. Data consistent with literature values.[12]

3-(Furan-2-yl)-3-methyl-1-(*m*-tolyl)butan-1-one **3.24**

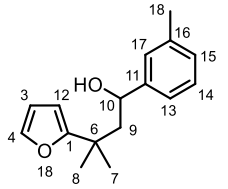


Chemical Formula: $C_{16}H_{18}O_2$
Exact Mass: 242.1307
Molecular Weight: 242.3180

Prepared according to **GP-III**; using 2-(furan-2-yl)propan-2-ol **3.27** (2.09 g, 16.6 mmol), trimethyl((1-(*m*-tolyl)vinyl)oxy)silane **3.25** (6.15 g, 29.8 mmol) and TMSOTf (3 mL, 16.6 mmol) in THF (55 mL). The product was purified *via* column chromatography (1% EtOAc in pentane) to yield a clear colourless oil (2.95 g, 74%).

R_f 0.66 (5% EtOAc in pet. $ether_{30\text{-}40}$). **^{1}H NMR** (400 MHz, $CDCl_3$) δ 1.36 (s, 6H, H7/8), 2.29 (s, 3H, H18), 3.16 (s, 2H, H9), 5.87 (dd, *J* = 3.0, 1.0 Hz, 1H, H12), 6.11 (dd, *J* = 3.0, 2.0 Hz, 1H, H3), 7.16 (dd, *J* = 2.0, 1.0 Hz, 1H, H4), 7.24 – 7.18 (m, 2H, H14/15), 7.55 – 7.50 (m, 2H, H13/17). **^{13}C NMR** (101 MHz, $CDCl_3$) δ 21.4 (C18), 27.1 (C7/8), 35.5 (C6), 48.6 (C9), 103.4 (C12), 110.0 (C3), 125.3 (C13), 128.2 (C17), 128.7 (C14), 133.4 (C15), 138.0 (C11), 138.1 (C16), 140.6 (C4), 161.6 (C1), 199.3 (C10). **IR** ν_{max} (thin film)/cm^{-1} 2968w, 2929w, 2874w, 1672s, 1586m, 1102m, 1020m, 729s, 691m. **HRMS** (ESI+) Found: 265.1199, $C_{16}H_{18}O_2Na$ $[M+Na]^+$ requires: 265.1199.

3-(Furan-2-yl)-3-methyl-1-(*m*-tolyl)butan-1-ol **3.32**

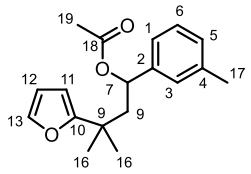


Chemical Formula: $C_{16}H_{20}O_2$
Exact Mass: 244.1463
Molecular Weight: 244.3340

To a stirred solution of 3-(furan-2-yl)-3-methyl-1-(*m*-tolyl)butan-1-one **3.24** (22.8 mg, 0.094 mmol) in anhydrous ethanol (1 mL), $NaBH_4$ (4.00 mg, 0.106 mmol) was added and the reaction was left to stir for 5 hr. When complete, the reaction was concentrated, re-dissolved in CH_2Cl_2 and washed with water. The organic layer was dried over $MgSO_4$ and concentrated. The product was purified by column chromatography (2-5% EtOAc in pentane) yielding a clear, colourless oil (13.0 mg, 57%).

R_f 0.31 (5% EtOAc in pentane). **^{1}H NMR** (400 MHz, $CDCl_3$) δ 1.35 (s, 3H, H7), 1.39 (s, 3H, H8), 1.96 (dd, *J* = 14.5, 3.0 Hz, 1H, H9'), 2.13 (dd, *J* = 14.5, 9.0 Hz, 1H, H9), 2.34 (s, 3H, H18), 4.61 (d, *J* = 9.0 Hz, 1H, H10), 6.08 (dd, *J* = 3.0, 1.0 Hz, 1H, H12), 6.30 (dd, *J* = 3.0, 2.0 Hz, 1H, H3), 7.04 (s, 1H, H15), 7.06 (s, 1H, H17), 7.09 (s, 1H, H13), 7.20 (t, *J* = 7.5 Hz, 1H, H14), 7.36 (dd, *J* = 1.9, 0.8 Hz, 1H, H4). **^{13}C NMR** (101 MHz, $CDCl_3$) δ 21.6 (C18), 27.3 (C7), 28.0 (C8), 35.5 (C6), 51.6 (C9), 72.3 (C10), 104.0 (C12), 110.1 (C3), 122.8 (C13), 126.4 (C15), 128.1 (C14), 128.4 (C17), 138.2 (C16), 141.2 (C11), 145.7 (C4), 162.4 (C1). **IR** ν_{max} (thin film)/cm^{-1} 3406br.w, 2965m, 2925m, 2872w, 1507w, 1157m, 1006m, 785m, 730s. **HRMS** (ESI+) Found: 267.1357, $C_{16}H_{20}O_2Na$ $[M+Na]^+$ requires: 267.1356.

3-(Furan-2-yl)-3-methyl-1-(*m*-tolyl)butyl acetate **3.39**

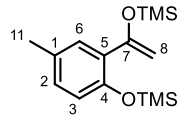


Chemical Formula: $C_{18}H_{22}O_3$
Exact Mass: 286.1569
Molecular Weight: 286.3710

Triethylamine (57.0 μL, 0.409 mmol, 1 eq.), acetic anhydride (58.0 μL, 0.614 mmol, 1.5 eq.) and 4-dimethylaminopyridine (5.00 mg, 0.041 mmol, 0.1 eq.) were added to a stirred solution of 3-(furan-2-yl)-3-methyl-1-(*m*-tolyl)butan-1-ol **3.32** (100 mg, 0.409 mmol) in DCM (2 mL). Reaction left stirring at RT for 3 hr. Upon completion, water was added and the reaction was extracted with CH_2Cl_2 (x3). The organic layer was washed with brine, dried over $MgSO_4$, and concentrated *in vacuo*. Yielded the *title compound* without further purification as an orange oil (115.7 mg, 99%).

R_f 0.41 (5% EtOAc in pentane). **^{1}H NMR** (400 MHz, $CDCl_3$) δ 1.33 (s, 3H, H16'), 1.34 (s, 3H, H16), 1.86 (s, 3H, H19), 1.92 (dd, *J* = 15.0, 2.5 Hz, 1H, H8'), 2.33 (s, 3H, H17), 2.40 (dd, *J* = 15.0, 9.5 Hz, 1H, H8), 5.70 (dd, *J* = 9.5, 2.5 Hz, 1H, H7), 5.99 (dd, *J* = 3.0, 1.0 Hz, 1H, H11), 6.26 (dd, *J* = 3.0, 2.0 Hz, 1H, H12), 7.04 (s, 2H, H1/5), 7.06 (s, 1H, H3), 7.19 (t, *J* = 8.0 Hz, 1H, H6), 7.33 (dd, *J* = 2.0, 1.0 Hz, 1H, H13). **^{13}C NMR** (101 MHz, $CDCl_3$) δ 21.3 (C19), 21.5 (C17), 26.8 (C16'), 28.0 (C16), 35.2 (C9), 48.4 (C8), 73.5 (C7), 103.7 (C11), 110.1 (C12), 123.3 (C1), 127.0 (C5), 128.5 (C6), 128.5 (C3), 138.1 (C4), 141.0 (C2), 142.0 (C13), 161.9 (C10), 170.2 (C18). **IR** ν_{max} (thin film)/cm^{-1} 2968w, 2361w, 1737s, 1311m, 1231s, 1160m, 960w, 785m, 731m. **HRMS** (ESI+) calc. for $C_{18}H_{22}O_3Na$ $[M+Na]^+$ Requires: 309.1461, found: 309.1461.

Trimethyl((1-(5-methyl-2-((trimethylsilyl)oxy)phenyl)vinyl)oxy)silane **3.44**

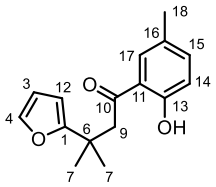


Chemical Formula: $C_{15}H_{26}O_2Si_2$
Exact Mass: 294.1471
Molecular Weight: 294.5410

To a stirred solution of 1-(2-hydroxy-5-methylphenyl)ethan-1-one (1.00g, 6.66 mmol, 1 eq.), triethylamine (2.30 mL, 16.6 mmol, 2.5 eq.) and TMSCl (2.10 mL, 16.6 mmol, 2.5 eq.) in 34 mL acetonitrile under argon at 0 °C, was added NaI (2.50 g, 16.6 mmol, 2.5 eq.) in 60 mL acetonitrile via cannula. The reaction was stirred at 0 °C for 2 hr. Solvent was removed *in vacuo*, and then re-dissolved in hexane. The resulting precipitate was filtered off through Celite, and the filtrate was concentrated *in vacuo* yielding a yellow oil which was used without further purification. Characterised as a 3:1 mixture with the starting material.

R_f 0.75 (5% EtOAc in pentane). **^{1}H NMR** (400 MHz, C_6D_6) δ 0.21 (s, 9H, TMS), 0.22 (s, 9H, TMS), 2.13 (s, 3H, H11), 4.75 (d, *J* = 0.5 Hz, 1H, H8), 5.29 (d, *J* = 0.5 Hz, 1H, H8'), 6.73 (d, *J* = 8.0 Hz, 1H, H3), 6.84 (ddq, *J* = 8.0, 2.5, 0.5 Hz, 1H, H2), 7.54 (d, *J* = 2.5 Hz, 1H, H6). **^{13}C NMR** (101 MHz, C_6D_6) δ 0.3 (Si(**C**H_3)$_3$), 0.5 (Si(**C**H_3)$_3$), 20.8 (C11), 96.4 (C8), 120.4 (Ar**C**H), 129.7 (Ar**C**H), 130.0 (Ar**C**H), 130.4 (Ar**C**), 151.2 (Ar**C**), 153.9 (Ar**C**), 198.2 (C7). **HRMS** (APCI) Found: 295.1548, $C_{15}H_{26}O_2Si_2$ $[M+H]^+$ requires: 295.1544.

3-(Furan-2-yl)-1-(2-hydroxy-5-methylphenyl)-3-methylbutan-1-one **3.45**

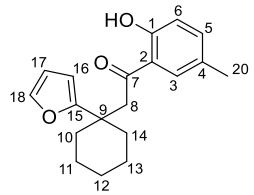


Chemical Formula: $C_{16}H_{18}O_3$
Exact Mass: 258.1256
Molecular Weight: 258.3170

Prepared according to **GP-III**; trimethyl((1-(5-methyl-2-((trimethylsilyl)oxy)phenyl)vinyl)oxy)silane **3.44** (200 mg, 0.68 mmol), 2-(furan-2-yl)propan-2-ol **3.27** (48 mg, 0.38 mmol) and TMSOTf (68 μL, 0.38 mmol) in THF (1.1 mL). The product was purified *via* column chromatography (1% EtOAc in pentane) yielding the *title compound* as a yellow oil (66 mg, 68%).

R_f 0.56 (5% EtOAc in pentane). **^{1}H NMR** (400 MHz, $CDCl_3$) δ 1.37 (s, 6H, H7), 2.15 (s, 3H, H18), 3.15 (s, 2H, H9), 5.88 (d, *J* = 3.0 Hz, 1H, H12), 6.12 (dd, *J* = 3.0, 2.0 Hz, 1H, H3), 6.74 (d, *J* = 8.5 Hz, 1H, H14), 7.12 (dd, *J* = 8.5, 2.0 Hz, 1H, H15), 7.18 – 7.17 (m, 2H, H4/17), 12.14 (s, 1H, OH). **^{13}C NMR** (101 MHz, $CDCl_3$) δ 20.6 (C18), 27.4 (C7), 35.9 (C6), 48.6 (C9), 103.8 (C12), 110.2 (C3), 118.1 (C14), 120.0 (C11), 127.7 (C17), 130.4 (C16), 137.3 (C15), 140.8 (C4), 160.6 (C13), 161.1 (C1), 205.4 (C10). **IR** ν_{max} (thin film)/cm^{-1} 2969m, 2924m, 1636s, 1486s, 1281s, 1009m, 919w, 732m. **HRMS** (APCI) Found: 257.1184, $C_{16}H_{17}O_3$ $[M-H]^-$ requires: 257.1183.

2-(1-(Furan-2-yl)cyclohexyl)-1-(2-hydroxy-5-methylphenyl)ethan-1-one **3.47**

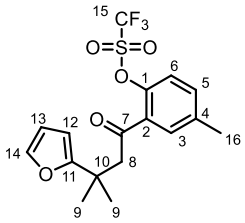


Chemical Formula: $C_{19}H_{22}O_3$
Exact Mass: 298.1569
Molecular Weight: 298.3820

Prepared according to **GP-III**; using trimethyl((1-(5-methyl-2-((trimethylsilyl)oxy)phenyl)vinyl)oxy)silane (1.8 mmol), 1-(furan-2-yl)cyclohexan-1-ol (166 mg, 1 mmol) and TMSOTf (181 μL, 1 mmol) in anhydrous THF (3.4 mL). The compound was purified by column chromatography (1% EtOAc in pentane) yielding the *title compound* as a yellow oil (86.9 mg, 0.291 mmol, 29%).

R_f 0.56 (5% EtOAc in pentane). **^{1}H NMR** (400 MHz, $CDCl_3$) δ 1.46 – 1.66 (m, 10H, H10/11/12/13/14), 2.19 (s, 3H, H20), 3.11 (s, 2H, H8), 5.95 (dd, *J* = 3.0, 1.0 Hz, 1H, H16), 6.14 (dd, *J* = 3.0, 2.0 Hz, 1H, H17), 6.78 (d, *J* = 8.5 Hz, 1H, H6), 7.04 – 6.99 (m, 1H, H3), 7.16 (dd, *J* = 8.5, 2.0 Hz, 1H, H5), 7.20 (dd, *J* = 2.0, 0.5 Hz, 1H, H18), 12.26 (s, 1H, OH). **^{13}C NMR** (101 MHz, $CDCl_3$) δ 20.6 (C20), 22.5 (C11/12), 26.0 (C12), 35.6(C10/C14), 40.6 (C8), 49.4 (C9), 106.5 (C16), 110.2 (C17), 117.8 (C6), 120.3 (C2), 127.5 (C3), 130.6 (C4), 137.1 (C5), 140.5 (C18), 158.4 (C15), 160.5 (C1), 205.8 (C7). **HRMS** (ESI+) Found: 299.1643, $C_{19}H_{23}O_3$ $[M+H]^+$ requires: 299.1642. **IR** ν_{max} (thin film)/cm^{-1} 2931m, 1635s, 1610m, 1487s, 1451w, 1341w, 1272m, 1249s, 1162m, 822m, 781w, 731s, 648m.

2-(3-(Furan-2-yl)-3-methylbutanoyl)-4-methylphenyl trifluoromethanesulfonate **3.52**

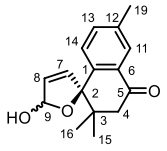


Chemical Formula: $C_{17}H_{17}F_3O_5S$
Exact Mass: 390.0749
Molecular Weight: 390.3732

To a stirred solution of 3-(furan-2-yl)-1-(2-hydroxy-5-methylphenyl)-3-methylbutan-1-one **3.45** (123 mg, 0.478 mmol, 1 eq.) in pyridine (480 μL) under argon at 0 °C was added Tf_2O (96.0 μL, 0.57 mmol, 1.2 eq.). The mixture was allowed to warm to RT and left to stir overnight. When complete, the reaction was diluted with ethyl acetate, sat. aq. Cu_2SO_4 was added and the mixture was extracted into EtOAc (x3). The combined organic layers were washed with brine, dried over $MgSO_4$, filtered and concentrated *in vacuo*. Purification by column chromatography (5% EtOAc in pentane) yielded the *title compound* as a yellow oil (141 mg, 76%).

R_f 0.42 (5% EtOAc in pentane). **^{1}H NMR** (400 MHz, $CDCl_3$) δ 1.43 (s, 6H, H9), 2.34 (s, 3H, H16), 3.21 (s, 2H, H8), 5.93 (dd, *J* = 3.0, 1.0 Hz, 1H, H12), 6.13 (dd, *J* = 3.0, 2.0 Hz, 1H, H13), 7.12 (d, *J* = 8.5 Hz, 1H, H6), 7.15 (dd, *J* = 2.0, 1.0 Hz, 1H, H14), 7.18 (d, *J* = 2.0 Hz, 1H, H5), 7.27 – 7.23 (m, 1H, H3). **^{13}C NMR** (101 MHz, $CDCl_3$) δ 20.9 (C16). 27.1 (C9), 35.9 (C10), 52.3 (C8), 103.9 (C12), 110.0 (C13), 118.7 (q, *J* = 320.5 Hz, C15), 122.1 (C6), 130.7 (C5), 133.1 (C2), 133.3 (C3), 138.6 (C4), 140.8 (C14), 144.3 (C1), 160.8 (C11), 198.6 (C7). **^{19}F NMR** (376 MHz, $CDCl_3$) δ -73.42. **IR** ν_{max} (thin film)/cm^{-1} 2971w, 1689m, 1423s, 1204s, 1139s, 1009w, 866s, 732s, 611s. **HRMS** (ESI+) Found: 309.1461, $C_{17}H_{17}O_5F_3Na$ $[M+Na]^+$ requires: 390.0749.

(2*R*)-5-Hydroxy-2',2',6'-trimethyl-2',3'-dihydro-4'*H*,5*H*-spiro[furan-2,1'-naphthalen]-4'-one **3.53**

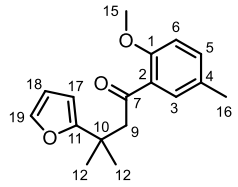


Chemical Formula: $C_{16}H_{18}O_3$
Exact Mass: 258.1256
Molecular Weight: 258.3170

A solution of 2-(3-(furan-2-yl)-3-methylbutanoyl)-4-methylphenyl trifluoromethanesulfonate **3.52** (20.0 mg, 51.2 μmol, 1 eq.) and Hünig's base (37 μL, 0.216 mmol, 4.2 eq.) in aq. DMA (5 mL (1:9 H_2O:DMA)), was degassed with argon for 10 min before $Pd(PPh_3)_4$ (6.00 mg, 5.19 μmol, 10 mol%) was added. The mixture was degassed for a further 5 min before heating to 90 °C, before a second portion of $Pd(PPh_3)_4$ (6.00 mg, 5.19 μmol, 10 mol%) was added and the reaction was stirred for 19 hr. The mixture was cooled to RT and quenched with sat. aq. $NaHCO_3$ (10 mL) and extracted into ether (3 × 10 mL). The combined organic layers were washed with brine (10 mL), dried over $MgSO_4$, filtered and concentrated *in vacuo*. The crude product was purified by column chromatography (5 – 30% EtOAc in pentane) to yield the *title compound* as a yellow oil (10.7 mg, 77%). Characterised as a mixture of diastereomers (2:3).

R_f 0.62 and 0.69 (50% EtOAc in pentane). **^{1}H NMR** (400 MHz, $CDCl_3$) δ 0.98 (s, 2H, H16), 1.02 (s, 2H, H15), 1.06 (s, 1H, H16'), 1.09 (s, 1H, H15'), 2.38 (s, 3H, H19), 2.53 (d, *J* = 17.5 Hz, 1H, H4), 2.61 (t, *J* = 17.5 Hz, 0.6H, H4), 2.75 (d, *J* = 17.5 Hz, 0.6H, H4'), 5.95 (, dd, *J* = 6.0, 1.0 Hz, 0.4H H8'), 6.01 (d, *J* = 6.0 Hz, 0.6H, H8), 6.21 (dd, *J* = 6.0, 1.0 Hz, 0.4H, H7'), 6.24 (dd, *J* = 6.0, 1.0 Hz, 0.6H, H7), 6.26 (d, *J* = 6.0 Hz, 0.6H, H9), 6.40 (s, 0.4H, H9'), 7.22 (d, *J* = 8.0 Hz, 0.4H, H14'), 7.37 (app. ddd, *J* = 8.0, 1.5, 0.5 Hz, 0.4H, H13'), 7.40 (app. ddd, *J* = 8.0, 1.5, 0.5 Hz, 0.6H, H13), 7.55 (d, *J* = 8.0 Hz, 0.6H, H14), 7.82 (s, 0.4H, H11), 7.90 (s, 0.4H, H11'). **^{13}C NMR** (101 MHz, $CDCl_3$) δ 21.1 (C19), 23.7 (C15), 23.9 (C16'), 24.7 (C16), 25.4 (C15'), 39.3 (C3'), 40.5 (C3), 50.1 (C4'), 50.6 (C4), 103.6 (C9), 103.6 (C9'), 126.5 (C14), 126.9 (C11), 127.0 (C11'), 127.9 (C14'), 127.9 (C8), 128.6 (C8'), 130.7 (C12), 131.0 (C12'), 135.5 (C13), 135.6 (C7), 136.3 (C7'), 138.1 (C1'), 138.3 (C1), 141.5 (C6), 142.1 (C6'), 197.5 (C5). **IR** ν_{max} (thin film)/cm^{-1} 3408 br.w, 2964w, 2926w, 1682s, 1610m, 1410s, 1249m, 1031s, 820w, 729w. **HRMS** (ESI+) Found: 281.1150, $C_{16}H_{18}O_3Na$ $[M+Na]^+$ requires: 281.1150.

3-(Furan-2-yl)-1-(2-methoxy-5-methylphenyl)-3-methylbutan-1-one **3.46**

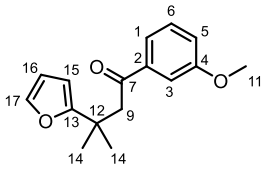


Chemical Formula: $C_{17}H_{20}O_3$
Exact Mass: 272.1412
Molecular Weight: 272.3440

Prepared according to **GP-III**; using 2-(furan-2-yl)propan-2-ol **3.27** (86 mg, .067 mmol, 1 eq.), ((1-(2-methoxy-5-methylphenyl)vinyl)oxy)trimethylsilane (1.22 mmol, 1.8 eq.) and TMSOTf (121 μL, 0.67 mmol) in THF (2.5 mL). The product was purified *via* column chromatography (0 – 3% EtOAc in pentane) to yield a clear colourless oil (108 mg, 59%).

R_f 0.49 (10% EtOAc in pentane). **^{1}H NMR** (400 MHz, $CDCl_3$) δ 7.21 – 7.12 (m, 3H, H3/5/19), 6.77 (d, *J* = 8.5 Hz, 1H, H6), 6.18 (dd, *J* = 3.0, 2.0 Hz, 1H, H18), 5.92 (dd, *J* = 3.0, 1.0 Hz, 1H, H17), 3.83 (s, 3H, H15), 3.31 (s, 2H, H9), 2.25 (s, 3H, H16), 1.39 (s, 6H, H12). **^{13}C NMR** (101 MHz, $CDCl_3$) δ 20.3 (C16), 27.3 (C12), 35.7 (C3), 53.4 (C9), 55.7 (C15), 103.1 (C17), 109.9 (C18), 111.5 (C3), 129.9 (C6), 130.0 (C2), 130.2 (C4), 133.2 (C5), 140.5 (C19), 156.0 (C1), 162.3 (C11), 202.3 (C7). **IR** ν_{max} (thin film)/cm^{-1} 2965w, 1678m, 1608m, 1496s, 1464w, 1284m, 1249s, 1178m, 1076w, 1024w, 1010m, 920w, 884w, 809m, 730s. **HRMS** (ESI+) Found: 295.1303, $C_{17}H_{20}O_3Na$ $[M+Na]^+$ requires: 295.1305.

3-(Furan-2-yl)-1-(3-methoxyphenyl)-3-methylbutan-1-one **3.51**



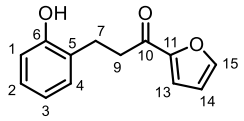
Chemical Formula: $C_{16}H_{18}O_3$
Exact Mass: 258.1256
Molecular Weight: 258.3170

To a stirred solution of 2-(furan-2-yl)propan-2-ol **3.27** (47 mg, 0.37, 1 eq.) and ((1-(3-methoxyphenyl)vinyl)oxy)trimethylsilane (0.67 mmol, 1.8 eq.) in anhydrous THF (1.5 mL), under argon at −78 °C, Zn(OTf)2 (135 mg, 0.37 mmol, 1 eq.) was added. The reaction was stirred for 21 hr, and then aq. $NaHCO_3$ was slowly added and stirred for a further 5 min. The reaction was extracted with EtOAc (3 x 5 mL) and then washed with 1M aq. HCl. The combined organic layers were dried over $MgSO_4$, filtered and concentrated. The crude product was purified by column chromatography (1 – 5% EtOAc in pentane) to yield the *title compound* (40.4 mg, 29%).

R_f 0.59 (10% EtOAc in pentane). **^{1}H NMR** (400 MHz, $CDCl_3$) δ 1.44 (s, 6H, H14), 3.24 (s, 2H, H9), 3.82 (s, 3H, H11), 5.96 (dd, *J* = 3.0, 1.0 Hz, 1H, H15), 6.20 (dd, *J* = 3.0, 2.0 Hz, 1H, H16), 7.04 (ddd, *J* = 8.0, 3.0, 1.0 Hz, 1H, H5), 7.24 (dd, *J* = 2.0, 1.0 Hz, 1H, H17), 7.28 (t, *J* = 8.0 Hz, 1H, H3), 7.41 – 7.36 (m, 2H, H1/6), **^{13}C NMR** (101 MHz, $CDCl_3$) δ 27.1, 35.5, 48.6, 55.4, 103.3, 110.0, 112.1, 119.3, 120.8, 129.3, 139.3, 140.6, 159.7, 161.6, 198.8. **IR** ν_{max} (thin film)/cm^{-1} 2967w, 1673m, 1596m, 1582m, 1463m, 1259s, 1155m, 1031m, 919m, 787m, 732s, 687m. **HRMS** (ESI+) Found: 259.1331, $C_{16}H_{19}O_3$ $[M+H]^+$ requires: 259.1329.

6.3.4. Experimental details for third-generation route to trigoxyphin

1-(Furan-2-yl)-3-(2-hydroxyphenyl)propan-1-one **3.61**

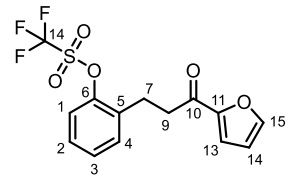


Chemical Formula: $C_{13}H_{12}O_3$
Exact Mass: 216.0786
Molecular Weight: 216.2360

To a solution of furan (3.5 mL, 48.1 mmol, 1.2 eq.) in THF (40 mL) at −78 °C under argon was added *n*-BuLi [2.5 M solution in hexanes] (16.0 mL, 40 mmol). The reaction mixture was allowed to reach 0 °C and left to stir for 2 hr before being cooled to −78 °C. The reaction mixture was then added dropwise to a pre-mixed solution of dihydrocoumarin (5.00 mL, 39.5 mmol, 1 eq.) and TMSCl (10.5 mL, 80 mmol, 2 eq.) in THF (4 mL) under argon at −78 °C and was left to stir and naturally rise to RT for 18 hr. The reaction was quenched with sat. aq. NH_4Cl, concentrated *in vacuo*, extracted with ether (x3) and washed with brine. The combined organic layers were dried over $MgSO_4$, filtered and concentrated *in vacuo*. The crude product was purified by column chromatography (1 – 5% EtOAc in pentane) to yield the *title compound* (2.54 g, 29%).

R_f 0.22 (5% EtOAc in pentane). **^{1}H NMR** (400 MHz, $CDCl_3$) δ 3.01 (t, *J* = 6.0 Hz, 2H, H7), 3.30 (app. q, *J* = 6.0 Hz, 2H, H9), 6.53 (dd, *J* = 3.5, 1.5 Hz, 1H, H14), 6.91 – 6.83 (m, 2H, Ar-H), 7.14 – 7.08 (m, 2H, Ar-H), 7.24 (dd, *J* = 3.5, 0.5 Hz, 1H, H13), 7.57 (dd, *J* = 1.5, 0.5 Hz, 1H, H15). **^{13}C NMR** (101 MHz, $CDCl_3$) δ 23.3 (C), 40.0 (C9), 112.6 (C14), 117.5 (Ar-C), 118.2 (C13), 120.8 (Ar-C), 127. 7 (C5), 128.1 (Ar-C), 130.7 (Ar-C), 147.0 (C15), 152.4 (C11), 154.5 (C6), 190.8 (C10). **IR** ν_{max} (thin film)/cm^{-1} 3338br.w, 2918w, 1655m, 1459s, 1396m, 883w, 753s. **HRMS** (ESI+) Found: 217.0861, $C_{13}H_{13}O_3$ $[M+H]^+$ requires: 217.0859. Data consistent with literature values.[13]

2-(3-(Furan-2-yl)-3-oxopropyl)phenyl trifluoromethanesulfonate **3.62**

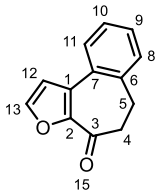


Chemical Formula: $C_{14}H_{11}F_3O_5S$
Exact Mass: 348.0279
Molecular Weight: 348.2922

To a solution of 1-(furan-2-yl)-3-(2-hydroxyphenyl)propan-1-one (442 mg, 2.04 mmol, 1 eq.) in pyridine (2.1 mL) under Ar at 0 °C was added Tf_2O (412 μL, 2.45 mmol, 1.2 eq.). The mixture was allowed to warm to RT and left to stir overnight. Pyridine was then removed *in vacuo* and the reaction was redissolved in EtOAc. The reaction mixture was then washed with 1M HCl, followed by sat. aq $NaHCO_3$, water, brine and then dried over $MgSO_4$, before being filtered and concentrated *in vacuo.* Purification by column chromatography (5% EtOAc in pentane) yielded the *title compound* as a colourless oil (447 mg, 63%).

R_f 0.44 (5% EtOAc in pentane). **^{1}H NMR** (400 MHz, $CDCl_3$) δ 3.17 (app.qt, *J* = 11.5, 4.5 Hz, 4H, H7/8), 6.52 (dd, *J* = 3.5, 2.0 Hz, 1H, H12), 7.19 (dd, *J* = 3.5, 1.0 Hz, 1H, H13), 7.32 – 7.25 (m, 3H, Ar-H), 7.41 – 7.37 (m, 1H, Ar-H), 7.57 (dd, *J* = 1.5, 1.0 Hz, 1H, H11). **^{13}C NMR** (101 MHz, $CDCl_3$) δ 24.4 (C7), 38.4 (C8), 112.4 (C12), 117.4 (C13), 118.7 (q, *J* = 320.1 Hz, C14), 121.5 (Ar-C), 128.4 (Ar-C), 128. 7 (Ar-C), 131.8 (Ar-C), 133.8 (C5), 146.6 (C11), 148.1 (C6), 152.6 (C10), 187.6 (C9).**^{19}F NMR** (377 MHz, $CDCl_3$) δ -73.82. **IR** ν_{max} (thin film)/cm^{-1} 1676m, 1569w, 1469m, 1416m, 1209s, 1136s, 1079m, 892s, 760s. **HRMS** (ESI+) Found: 349.0351, $C_{14}H_{12}F_3O_5S$ $[M+H]^+$ requires: 349.0352.

5,6-Dihydro-4*H*-benzo[3,4]cyclohepta[1,2-*b*]furan-4-one **3.63**

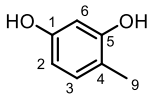


Chemical Formula: $C_{13}H_{10}O_2$
Exact Mass: 198.0681
Molecular Weight: 198.2210

To a solution of 2-(3-(furan-2-yl)-3-oxopropyl)phenyl trifluoromethanesulfonate (500 mg, 1.44 mmol, 1 eq.) in aq. DMA (144 mL (1:9 H_2O:DMA)), DIPEA (934 μL, 5.46 mmol, 3.8 eq.) was added. The reaction was then degassed using freeze-pump-thaw three times. $Pd(PPh_3)_4$ (83 mg, 72 μmol, 5 mol%) was added, and the reaction was heated to 80 °C when a second portion of $Pd(PPh_3)_4$ (83 mg, 72 μmol, 5 mol%) was added. The reaction was left stirring at 80 °C for 15 hr. When complete, the reaction was cooled to RT and quenched with sat. aq. $NaHCO_3$, extracted with ether (x3). The combined organic layers were washed with brine, dried over $MgSO_4$, filtered and concentrated *in vacuo*. The crude product was purified by column chromatography (2 – 10% EtOAc in pentane) to afford the *title compound* as a yellow oil (47.6 mg, 17% (24% brsm)).

R_f 0.42 (20% EtOAc in pentane). **^{1}H NMR** (400 MHz, $CDCl_3$) δ 2.82 – 2.76 (m, 2H, H5), 3.05 – 3.00 (m, 2H, H4), 6.84 (d, *J* = 2.0 Hz, 1H, H12), 7.32 – 7.29 (m, 2H, Ar-H), 7.38 – 7.32 (m, 1H, Ar-H), 7.60 (d, *J* = 7.5 Hz, 1H, Ar-H), 7.68 (d, *J* = 2.0 Hz, 1H, H13). **^{13}C NMR** (101 MHz, $CDCl_3$) δ 29.9 (C5), 40.5 (C4), 111.5 (C12), 127.5 (Ar-C), 128.2 (Ar-C), 129.1 (Ar-C), 129.7 (Ar-C), 130.1 (C7), 133.2 (C2), 134.1(C6), 139.9 (C1), 147.1 (C13), 188.8 (C3). **IR** ν_{max} (thin film)/cm^{-1} 3118w, 2924w, 1656s, 1480m, 1402m, 1214m, 1067m, 892m, 874m, 759s, 665w. **HRMS** (ESI+) Found: 199.0755, $C_{13}H_{11}O_2$ $[M+H]^+$ requires: 199.0754.

4-Methylbenzene-1,3-diol **3.79**

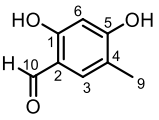


Chemical Formula: $C_7H_8O_2$
Exact Mass: 124.0524
Molecular Weight: 124.1390

Synthesis from literature procedure.[14] To a solution of 2,4-dihydroxybenzaldehyde (100 mg, 0.724 mmol) and sodium cyanoborohydride (145 mg) in 4.4 mL of THF was added methyl orange as an indicator, giving the solution a yellow colour. 1N aq. HCl solution (2.2 mL) was slowly added to the reaction, keeping the solution orange. The mixture was stirred for 3 hours at room temperature. Water was added, and the mixture was extracted with Et_2O three times. The organic layer was washed with saturated $NaHCO_3$, brine and dried over $MgSO_4$ and concentrated *in vacuo*. The crude mixture was purified by silica gel column chromatography (20-50% EtOAc in pentane) to afford the title compound as a white solid (82.1 mg, 91%).

R_f 0.11 (20% EtOAc in pentane). **^{1}H NMR** (400 MHz, DMSO-d_6) δ 1.98 (s, 3H, H9), 6.09 (dd, J = 8.0, 2.5 Hz, 1H, H2), 6.25 (d, J = 2.5 Hz, 1H, H6), 6.77 (d, J = 8.0 Hz, 1H, H3), 8.88 (s, 1H, H7), 9.02 (s, 1H, H8). **^{13}C NMR** (101 MHz, DMSO-d_6) δ 15.2 (C9), 102.2 (C6), 105.8 (C2), 113.9 (C4), 130.6 (C3), 155.9 (C1), 156.1 (C5). **MP** 103 – 104 °C.

2,4-Dihydroxy-5-methylbenzaldehyde **3.80**

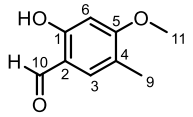


Chemical Formula: $C_8H_8O_3$
Exact Mass: 152.0473
Molecular Weight: 152.1490

To a stirred solution of 4-methylbenzene-1,3-diol (1 g, 8.06 mmol, 1 eq.) and *N,N*-dimethylformamide (1.26 mL, 16.1 mmol, 2 eq.) in dry acetonitrile (14 mL) was added phosphorus oxychloride (910 μL, 9.5 mmol, 1.2eq.) dropwise over a period of 5 min at 0 °C. The reaction was then stirred at RT for 1 hr, after which the resulting yellow precipitate was filtered. The remaining liquid was concentrated until further yellow precipitate was formed. The yellow solid was then filtered, and the procedure repeated until no further solid precipitates. The combined yellow solids were washed with cold acetonitrile (3 x 5 mL), and then recrystallised from the minimal amount of hot water yielding the title compound as a white crystalline solid (832.8 mg, **68%**).

R_f 0.21 (10% EtOAc in pentane). **^{1}H NMR** (400 MHz, $CDCl_3$) δ 2.21 (s, 3H, H9), 5.65 (s, 1H, OH), 6.35 (s, 1H, H6), 7.27 (s, 1H, H3), 9.68 (s, 1H, H10), 11.26 (1H, s, OH). **^{13}C NMR** (101 MHz, $CDCl_3$) δ 14.9, 102.9, 115.5, 117.0, 136.1, 161.8, 162.8, 194.6. **MP** 143–144 °C. Matches literature data.[15]

2-Hydroxy-4-methoxy-5-methylbenzaldehyde **3.81**

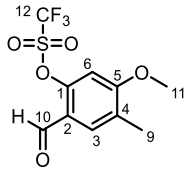


Chemical Formula: $C_9H_{10}O_3$
Exact Mass: 166.0630
Molecular Weight: 166.1760

To a stirred suspension of 2,4-dihydroxy-5-methylbenzaldehyde (1.82 g, 11.96 mmol, 1 eq.) and K_2CO_3 (1.65 g, 11.96 mmol, 1 eq.) in acetonitrile (36 mL), dimethyl sulfate (1.13 mL, 11.96 mmol, 1 eq.) was added and then reaction was stirred for 21hr at RT. The reaction was then quenched with 2M HCl (20 mL) and extracted with ethyl acetate (2 x 50 mL). The combined organic layers were dried over MgSO4, filtered and concentrate *in vacuo*. The reaction was purified by column chromatography (8% EtOAc in pentane) to yield the title compound as a white solid (1.65 g, 83%).

R_f 0.54 (10% EtOAc in pentane). **^{1}H NMR** (400 MHz, $CDCl_3$) δ 2.15 (d, *J* = 0.5 Hz, 3H, H9), 3.87 (s, 3H, H11), 6.39 (s, 1H, H6), 7.22 (d, *J* = 0.5 Hz, 1H, H3), 9.68 (s, 1H, H10), 11.43 (s, 1H, OH). **^{13}C NMR** (101 MHz, $CDCl_3$) δ 15.5 (C9), 56.0 (C11), 98.6 (C6), 114.4 (C4), 119.4 (C2), 134.5 (C3), 163.4 (C1), 165.3 (C5), 194.5 (C10). **MP** 72 – 73 °C. Matches literature data.[15]

2-Formyl-5-methoxy-4-methylphenyl trifluoromethanesulfonate **3.75**

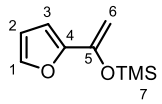


Chemical Formula: $C_{10}H_9F_3O_5S$
Exact Mass: 298.0123
Molecular Weight: 298.2322

To a solution of 2-hydroxy-4-methoxy-5-methylbenzaldehyde (256 mg, 1.5 mmol, 1 eq.) in dry pyridine (1.5 mL) at 0 °C, trifluoromethanesulfonic anhydride (310 µL, 1.85 mmol, 1.2 eq.) was added dropwise. The reaction was stirred at 0 °C for 2hr. After completion, the reaction was diluted with ethyl acetate (30 mL) and washed with 1M $CuSO_4$ (2 x 30 mL). The organic layer was dried over $MgSO_4$, filtered and concentrated *in vacuo* to yield a brown oil. The reaction was purified by column chromatography (10% EtOAc in pentane) to yield a white solid (362 mg, **81%**).

R_f 0.61 (10% EtOAc in pentane). **^{1}H NMR** (400 MHz, $CDCl_3$) δ 2.25 (s, 3H, H9), 3.93 (s, 3H, H11), 6.76 (s, 1H, H6), 7.74 (s, 1H, H3), 10.11 (s, 1H, H10). **^{13}C NMR** (101 MHz, $CDCl_3$) δ 15.9, 56.4, 103.9, 118.8 (d, J = 320.6 Hz), 121.2, 128.3, 131.5, 150.0, 163.4, 185.7. **^{19}F NMR** (377 MHz, $CDCl_3$) δ -72.86. **IR** ν_{max} (thin film)/cm^{-1} 1692m, 1612s, 1504m, 1427s, 1333m, 1279m, 1244s, 1211s, 1139m, 1067s, 1005w, 889m, 813w, 607m. **HRMS** (ESI+) Found: 299.0196, $C_{10}H_{10}O_5F_3S$ $[M+H]^+$ requires: 299.0196. **MP** 51 – 53 °C.

((1-(Furan-2-yl)vinyl)oxy)trimethylsilane **3.83**



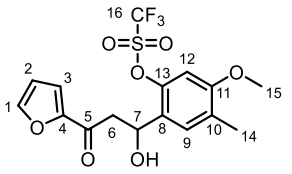
Chemical Formula: $C_9H_{14}O_2Si$
Exact Mass: 182.0763
Molecular Weight: 182.2940

Prepared according to literature procedure.[16] To a solution of 2-acetylfuran (220mg, 2 mmol, 1 eq.) and NEt_3 (670 µL, 4.8 mmol, 2.4 eq.) in dry CH_2Cl_2 (5 mL) at 0 °C, TMSOTf (400 µL, 2.2 mmol, 1.1 eq.) was added dropwise. Reaction was stirred at 0 °C for 20 mins, and then warmed to RT and stirred for a further 20 mins. The reaction was then diluted with hexane (20 mL) and washed with sat. aq. $NaHCO_3$ (20 mL). The organic layer was dried over $MgSO_4$, filtered and concentrated *in vacuo*. The crude material (295.1 mg) was used without further purification.

R_f 0.67 (5% EtOAc in pentane). **^{1}H NMR** (400 MHz, C_6D_6) δ 0.15 (s, 9H, H7), 4.41 (d, *J* = 1.5 Hz, 1H, H6), 5.11 (d, *J* = 1.5 Hz, 1H, H6'), 6.07 (dd, *J* = 3.5, 2.0 Hz, 1H, H2), 6.43 (d, *J* = 3.5 Hz, 1H, H3), 6.99 (dd, *J* = 2.0, 0.5 Hz, 1H, H1). **^{13}C NMR** (101 MHz, C_6D_6) δ 0.0 (C7), 90.5 (C6), 107.5 (C3), 111.4 (C2), 142.6 (C1), 148.3 (C4), 152.9 (C5). Matches literature data.[16]

2-(3-(Furan-2-yl)-1-hydroxy-3-oxopropyl)-5-methoxy-4-methylphenyl trifluoromethanesulfonate

3.82

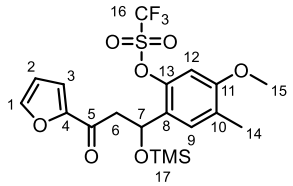


Chemical Formula: $C_{16}H_{15}F_3O_7S$
Exact Mass: 408.0491
Molecular Weight: 408.3442

To a solution of ((1-(furan-2-yl)vinyl)oxy)trimethylsilane (458 mg, 2.5 mmol, 1.5 eq.) and 2-formyl-5-methoxy-4-methylphenyl trifluoromethanesulfonate (500 mg, 1.68 mmol, 1 eq.) in dry CH_2Cl_2 (17 mL) at 0 °C, was added 1.0 M $TiCl_4$ (588 µL, 0.59 mmol, 0.35 eq.). The reaction was stirred at 0 °C for 15 mins, after which it was quenched with $NaHCO_3$ (20 mL) and extracted with ethyl acetate (3 x 30 mL). The combined organic layers were dried over $MgSO_4$, filtered and concentrated *in vacuo*. The reaction was purified by column chromatography (10 – 40% EtOAc in pentane) to yield a yellow solid (491 mg, **72%**).

R_f 0.13 (10% EtOAc in pentane). **^{1}H NMR** (400 MHz, $CDCl_3$) δ 2.23 (s, 3H, H14), 3.18 (dd, *J* = 17.0, 9.5 Hz, 1H, H6), 3.28 (dd, *J* = 17.0, 3.0 Hz, 1H, H6'), 3.62 (d, *J* = 3.0 Hz, 1H, OH), 3.83 (s, 3H, H15), 5.51 (dt, *J* = 9.5, 2.5 Hz, 1H, H7), 6.55 (dd, *J* = 3.5, 1.5 Hz, 1H, H2), 6.69 (s, 1H, H12), 7.24 (dd, *J* = 3.5, 0.5 Hz, 1H, H3), 7.45 (s, 1H, H9), 7.60 (dd, *J* = 1.5, 0.5 Hz, 1H, H1). **^{13}C NMR** (101 MHz, $CDCl_3$) δ 16.1 (C14), 45.7 (C6), 55.9 (C15), 64.1 (C7), 103.3 (C12), 112.7 (C2), 118.4 (C3), 118.7 (q, $J_{C\text{-}F}$ = 320.2 Hz, C16), 126.5 (C10), 128.1 (C8), 129.7 (C9), 144.1 (C1), 147.2 (C13), 152.4 (C4), 158.1 (C11), 188.3 (C5). **^{19}F NMR** (377 MHz, $CDCl_3$) δ -73.63. **IR** ν_{max} (thin film)/cm^{-1} 3441 br.w, 1668w, 1623w, 1569w, 1503w, 1467m, 1418m, 1206s, 1138s, 1058m, 883s, 765m, 610m. **HRMS** (ESI+) Found: 431.0384, $C_{16}H_{15}O_7F_3NaS$ $[M+Na]^+$ requires: 431.0383. **MP** 67 – 70 °C.

2-(3-(Furan-2-yl)-3-oxo-1-((trimethylsilyl)oxy)propyl)-5-methoxy-4-methylphenyl trifluoromethanesulfonate **3.84**



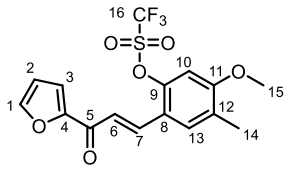
Chemical Formula: $C_{19}H_{23}F_3O_7SSi$
Exact Mass: 480.0886
Molecular Weight: 480.5262

Also isolated from previous procedure (**3.82**) as a yellow oil (189 mg, **23%**).

R_f 0.46 (10% EtOAc in pentane). **^{1}H NMR** (400 MHz, $CDCl_3$) δ -0.04 (s, 9H, H17), 2.23 (s, 3H, H14), 2.96 (dd, *J* = 15.0, 3.0 Hz, 1H, H6), 3.28 (dd, *J* = 15.0, 9.5 Hz, 1H, H6'), 3.83 (s, 3H, H15), 5.55 (dd, *J* = 9.5, 3.0 Hz, 1H, H7), 6.53 (dd, *J* = 3.5, 1.5 Hz, 1H, H2), 6.67 (s, 1H, H12), 7.23 (dd, *J* = 3.5, 0.5 Hz, 1H, H3), 7.40 (s, 1H, H9), 7.59 (dd, *J* = 1.5, 0.5 Hz, 1H, H1). **^{13}C NMR** (101 MHz, $CDCl_3$) δ -0.3 (C17), 16.1 (C14), 48.5 (C6), 55.8 (C15), 65.9 (C7), 103.2 (C12), 112.4 (C2), 117.6 (C3), 118.7 (q, *J* = 320.2 Hz, C16), 127.7 (C10), 128.2 (C8), 130.0 (C9), 143.8 (C1), 146.6 (C13), 153.2 (C4), 157.9 (C11), 186.1 (C5). **^{19}F NMR** (376 MHz, $CDCl_3$) δ -73.81. **HRMS** (ESI+) Found: 503.0780, $C_{19}H_{23}O_7F_3NaSSi$ $[M+Na]^+$ requires: 503.0778. **IR** ν_{max} (thin film)/cm^{-1} 2981m, 1676w, 1622w, 1569w, 1503m, 1468m, 1421m, 1245m, 1212s, 1140s, 1063m, 999m, 945m, 885m, 844m, 764w, 612w.

(*E*)-2-(3-(Furan-2-yl)-3-oxoprop-1-en-1-yl)-5-methoxy-4-methylphenyl trifluoromethanesulfonate

3.85

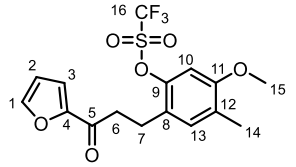


Chemical Formula: $C_{16}H_{13}F_3O_6S$
Exact Mass: 390.0385
Molecular Weight: 390.3292

To a stirred solution of ((1-(furan-2-yl)vinyl)oxy)trimethylsilane (91 mg, 0.5 mmol, 1.5 eq.) and 2-formyl-5-methoxy-4-methylphenyl trifluoromethanesulfonate (100 mg, 0.34 mmol, 1 eq.) in dry CH_2Cl_2 (5 mL) under at Ar at 0 °C, was added 1M $TiCl_4$ (47 μL, 0.047 mmol, 0.15 eq.). The reaction was then stirred at 0 °C for 10 mins, before adding dry pyridine (135 μL, 1.68 mmol, 5 eq.) and warming to RT. After 1 hour, H_2O (5 mL) was added and the reaction was extracted with EtOAc (3 x 10 mL), dried over $MgSO_4$, filtered and concentrated *in vacuo*. The resulting yellow solid (94 mg, 0.24 mmol, 72%) was used without further purification.

R_f 0.21 (5% EtOAc in pentane). **^{1}H NMR** (400 MHz, $CDCl_3$) δ 2.26 (s, 3H, H15), 3.89 (s, 3H, H14), 6.59 (dd, *J* = 3.5, 1.5 Hz, 1H, H2), 6.79 (s, 1H, 1H), 7.33 (dd, *J* = 3.5, 1.0 Hz, 1H, H3), 7.38 (d, *J* = 15.8 Hz, 1H), 7.57 (s, 1H), 7.65 (dd, *J* = 1.5, 1.0 Hz, 1H, H1), 7.97 (d, *J* = 15.8 Hz, 1H). **^{13}C NMR** (101 MHz, $CDCl_3$) δ 16.1, 56.1, 104.3, 112.7, 117.8, 118.8 (d, $J_{C\text{-}F}$ = 320.7 Hz), 119.8, 122.7, 128.0, 129.7, 135.5, 146.7, 147.3, 153.7, 160.4, 177.7. **^{19}F NMR** (377 MHz, $CDCl_3$) δ -73.06. **IR** ν_{max} (thin film)/cm^{-1} 1661m, 1605m, 1501m, 1463m, 1415m, 1303m, 1210s, 1138m, 1047m, 1003m, 895m, 846m, 769w, 647m, 620m. **HRMS** (ESI+) Found: 391.0463, $C_{16}H_{14}O_6F_3S$ $[M+H]^+$ requires: 391.0458.

2-(3-(Furan-2-yl)-3-oxopropyl)-5-methoxy-4-methylphenyl trifluoromethanesulfonate **3.74**

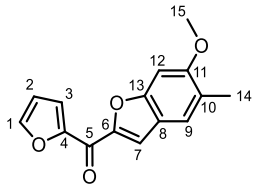


Chemical Formula: $C_{16}H_{15}F_3O_6S$
Exact Mass: 392.0541
Molecular Weight: 392.3452

To a solution of (E)-2-(3-(furan-2-yl)-3-oxoprop-1-en-1-yl)-5-methoxy-4-methylphenyl trifluoromethanesulfonate (155 mg, 0.397 mmol, 1 eq.) and 2,4,6-triisopropylbenzenesulfonohydrazide (178 mg, 0.596 mmol, 1.5 eq.) stirring under Ar in THF (10 mL) at RT, was added triethylamine (166 μL, 1.19 mmol, 3 eq.) dropwise *via* syringe. The reaction mixture was then refluxed for 3 hrs. After the reaction was complete, it was left to cool to RT upon which the solvent was removed *in vacuo*. The reaction was purified by column chromatography (0 – 40% EtOAc in pentane) to yield a yellow solid (68.0 mg, 0.173 mmol, 44%).

R_f 0.20 (10% EtOAc in pentane). **^{1}H NMR** (400 MHz, $CDCl_3$) δ 2.17 (s, 3H, H15), 3.06 – 3.01 (m, 2H, H7), 3.16 – 3.10 (m, 2H, H6), 3.81 (s, 3H, H14), 6.52 (dd, *J* = 3.5, 1.5 Hz, 1H, H2), 6.69 (s, 1H, H10), 7.11 (s, 1H, H13), 7.19 (dd, *J* = 3.5, 0.5 Hz, 1H, H3), 7.57 (dd, *J* = 1.5, 0.5 Hz, 1H, H1). **^{13}C NMR** (126 MHz, $CDCl_3$) δ 16.0 (C15), 23.8 (C7), 38.9 (C6), 55.8 (C14), 103.6 (C10), 112.4 (C2), 117.4 (C3), 118.8 ($J_{C\text{-}F}$, q, *J* = 320.1 Hz, C16), 124.5 (C3), 127.5 (C12), 132.7 (C13), 146.0 (C9), 146.6 (C1), 152.6 (C4), 157.1 (C11), 187.9 (C5). **^{19}F NMR** (377 MHz, $CDCl_3$) δ -73.79. **IR** ν_{max} (thin film)/cm^{-1} 1631s, 1505w, 1400w, 1266m, 1190w, 1015, 751m, 751s, 665w. **HRMS** Not found.

Benzofuran-2-yl(furan-2-yl)methanone **3.94**



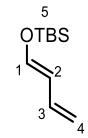
Chemical Formula: $C_{15}H_{12}O_4$
Exact Mass: 256.0736
Molecular Weight: 256.2570

A solution of 2-(3-(furan-2-yl)-3-oxopropyl)-5-methoxy-4-methylphenyl trifluoromethanesulfonate (38 mg, 0.065 mmol, 1 eq.) in dry DMA (1.3 mL) was degassed for 10 mins, after which Cs_2CO_3 (50.7 mg, 0.156 mmol, 2.4 eq.) was added and the reaction mixture was degassed for a further 10 mins. [1,3-Bis(2,6-diisopropylphenyl)imidazol-2-ylidene](3-chloropyridyl)palladium(II) dichloride (8.8 mg, 0.013 mmol, 0.2 eq.) was then added and the reaction was flushed with Ar, before being heated to 80 °C for 18 hours. When complete, the reaction was cooled to RT and quenched with sat. aq. $NaHCO_3$ (10mL) and then extracted with EtOAc (3 x 10mL). The combined organic layers were washed with brine, dried over $MgSO_4$, filtered and concentrated *in vacuo*. The crude product was purified by column chromatography (0 – 80% EtOAc in pentane) to afford the *title compound* as a clear colourless oil (5.3 mg, 0.021 mmol, 32%).

R_f 0.36 (10% EtOAc in pentane). **^{1}H NMR** (400 MHz, $CDCl_3$) δ 2.30 (s, 3H, H14), 3.92 (s, 3H, H15), 6.64 (dd, *J* = 3.5, 1.5 Hz, 1H, H2), 7.82 (d, *J* = 1.0 Hz, 1H, H7), 7.71 (dd, *J* = 1.5, 1.0 Hz, 1H, H1), 7.04 (s, 1H, H12), 7.44 (d, *J* = 1.0 Hz, 1H, H9), 7.62 (dd, *J* = 3.5, 1.0 Hz, 1H, H3). **^{13}C NMR** (101 MHz, $CDCl_3$) δ 169.8 (C5), 159.9 (C11), 156.4 (C13), 152.0 (C4), 150.9 (C6), 146.8 (C1), 125.2 (C10), 123.5 (C9), 119.9 (C8), 119.6 (C3), 116.3 (C7), 112.6 (C2), 93.7 (C12), 55.9 (C15), 16.9 (C14).

6.3.5. Experimental details for fourth-generation route to trigoxyphin

(*E*)-(Buta-1,3-dien-1-yloxy)(tert-butyl)dimethylsilane **3.100**

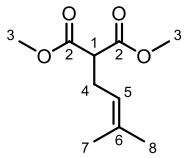


Chemical Formula: $C_{10}H_{20}OSi$
Exact Mass: 184.1283
Molecular Weight: 184.3540

To a solution of crotonaldehyde (333 µL, 4.02 mmol, 1 eq.) in dry CH_2Cl_2 (4.6 mL) under argon at –10 °C, triethylamine (780 µL, 5.63 mmol, 1.4 eq.) was added and the reaction was stirred for 5 mins. *tert*-Butyldimethylsilyl trifluoromethanesulfonate (1.0 mL, 4.42 mmol, 1.1 eq.) was slowly added dropwise and the reaction was warmed to RT over 2 hours, and then left to stir for 16 hr. When complete, the reaction was washed with $NaHCO_3$ (10 mL), brine (10 mL), dried over $MgSO_4$, filtered and concentrated *in vacuo*. The crude product was purified by column chromatography (pentane) to afford the *title compound* as a clear, colourless oil (559 mg, 3.03 mmol, 75%).

R_f 0.72 (5% EtOAc in pentane). **^{1}H NMR** (400 MHz, $CDCl_3$) δ 0.16 (s6H,), 0.92 (s9H,), 4.81 (ddt, *J* = 10.5, 2.0, 1.0 Hz, 1H), 4.98 (ddt, *J* = 17.0, 2.0, 1.0 Hz, 1H), 5.73 (ddt, *J* = 12.0, 11.0, 1.0 Hz, 1H), 6.22 (dddd, *J* = 17.0, 11.0, 10.5, 1.0 Hz, 1H), 6.57 (dq, *J* = 12.0, 1.0 Hz, 1H). **^{13}C NMR** (101 MHz, $CDCl_3$) δ -5.1, 18.4, 25.7, 112.0, 114.3, 133.5, 145.5. Matches literature data.[17]

Dimethyl 2-(3-methylbut-2-en-1-yl)malonate **3.108**

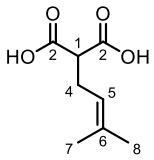


Chemical Formula: $C_{10}H_{16}O_4$
Exact Mass: 200.1049
Molecular Weight: 200.2340

To a solution of dimethyl malonate (6.8 mL, 60 mmol, 1.2 eq.) in THF (130 mL) at 0 °C under Ar, was added NaH (2.5 g, 60% in mineral oil) portionwise. The reaction was stirred for 30 mins and then 1-bromo-3-methylbut-2-ene (5.8 mL, 50 mmol, 1 eq.) was added dropwise. The reaction was left to return to RT stirring overnight. When complete, the crude mixture was extracted with EtOAc (3 x 150 mL), dried over $MgSO_4$, filtered and concentrated *in vacuo*. The product was purified by column chromatograph (0–10% EtOAc in pentane) yielding the title compound as a white solid (7.3 g, 73%).

R_f 0.4 (10% EtOAc in pentane). **^{1}H NMR** (400 MHz, $CDCl_3$) δ 1.60 (s, H83H,), 1.65 (s, 3H, H7), 2.57 (ddd, *J* = 8.5, 6.0, 1.0 Hz, 2H, H4), 3.34 (td, *J* = 7.5, 1.0 Hz, 1H, H1), 3.70 (s, 6H, H3), 5.02 (dddd, *J* = 8.5, 6.0, 2.5, 1.0 Hz, 1H, H5). **^{13}C NMR** (101 MHz, $CDCl_3$) δ 17.8 (C8), 25.8 (C7), 27.7 (C4), 52.0 (H1), 52.5 (C3), 119.6 (C5), 135.2 (C6), 169.7 (C2). Matches literature data.[18]

2-(3-Methylbut-2-en-1-yl)malonic acid **3.109**

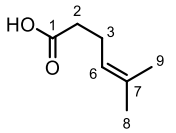


Chemical Formula: $C_8H_{12}O_4$
Exact Mass: 172.0736
Molecular Weight: 172.1800

To a stirred solution of dimethyl 2-(3-methylbut-2-en-1-yl)malonate (7.3g, 36 mmol) in MeOH:H_2O (287 mL:143 mL), NaOH (5.85 g, 146 mmol) was added and the reaction mixture was heated to reflux and left stirring overnight. When complete, the reaction was cooled to RT and MeOH was removed *in vacuo*. The crude reaction mixture was extracted using EtOAc (3 x 300 mL), and the combined organic layers were dried over $MgSO_4$, filtered and concentrated *in vacuo*. The crude material was purified by column chromatography (20–50% EtOAc in pentane) to yield the title compound as a white solid (4.73 g, 75%).

R_f 0.4 (10% EtOAc in pentane). **^{1}H NMR** (400 MHz, $CDCl_3$) δ 1.65 (s, 3H, H8), 1.71 (s, 3H, H7), 2.70 – 2.61 (m, 2H, H4), 3.45 (t, *J* = 7.5 Hz, 1H, H1), 5.10 (tdd, *J* = 6.0, 3.0, 1.5 Hz, 1H, H5). Matches literature data.[20]

5-Methylhex-4-enoic acid **3.103**

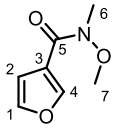


Chemical Formula: $C_7H_{12}O_2$
Exact Mass: 128.0837
Molecular Weight: 128.1710

A solution of 2-(3-methylbut-2-en-1-yl)malonic acid (4.7 g, 27.4 mmol) in pyridine:H_2O (30 mL:5 mL) was heated to 80 °C and stirred for 2 hr. When complete, the reaction was diluted with H_2O (20 mL) and acidified using 2N aq. HCl. The crude reaction mixture was extracted with CH_2Cl_2 (3 x 100 mL), and the combined organic layers were dried over MgSO4, filtered and concentrated *in vacuo*. The crude product was sufficiently pure to use without further purification, yielding a white solid (3.29 g, 94%).

R_f 0.52 (20% EtOAc in pentane). **^{1}H NMR** (400 MHz, $CDCl_3$) δ 1.62 (d, *J* = 1.5 Hz, 3H, H8), 1.69 (d, *J* = 1.5 Hz, 3H, H9), 2.41 – 2.28 (m, 4H, H2/3), 5.10 (m, 1H, H6), 11.66 (s, 1H, COOH). **^{13}C NMR** (101 MHz, CDCl3) δ 17.8 (C9), 23.5 (C8), 25.8 (C3), 34.4 (C2), 122.2 (C6), 133.5 (C7), 180.3 (C1). Matches literature data.[20]

N-methoxy-*N*-methylfuran-3-carboxamide **3.104**



Chemical Formula: $C_7H_9NO_3$
Exact Mass: 155.0582
Molecular Weight: 155.1530

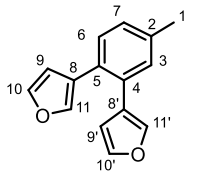
Method A: To a stirred solution of 3-furoic acid (200 mg) in DMF (0.5mL) : DCM (2mL), oxalyl chloride (167 μL) was added dropwise and the reaction was left to stir at RT for 1hr. When complete the solvent was removed *in vacuo* and the resulting residue was re-dissolved in DCM (2 mL). To this solution was added *N,O*-dimethylhydroxylamine (208 mg) and triethylamine (592 μL) at 0 dC under argon, and then the reaction was left to return to RT and stirred for 30 mins. When complete H2O (10 mL) was added and the reaction was extracted with CH_2Cl_2 (3 x 20 mL), dried over MgSO4, filtered and concentrated *in vacuo*. The crude product was purified by column chromatography (30% EtOAc in pentane) to yield the product as a yellow oil (91 mg, 46%).

Method B: To a stirred solution of 3-furoic acid (200 mg, 1.78 mmol, 1 eq.) in dry THF (10 mL), was added *N,O*-dimethylhydroxylamine (522 mg, 5.35 mmol, 3 eq.), HATU (2.034g, 5.35 mmol, 3 eq.) and DIPA (2.1 mL, 14.9 mmol, 8.4 eq.) and the reaction was left to stir at RT overnight. When complete H_2O (20 mL) was added and the reaction was extracted with CH_2Cl_2 (3 x 20 mL), dried over MgSO4, filtered and concentrated *in vacuo*. The crude product was purified by column chromatography (30 – 40% EtOAc in pentane) to yield the product as a yellow oil (170 mg, 62%).

R_f 0.35 (30% EtOAc in pentane). **^{1}H NMR** (400 MHz, $CDCl_3$) δ 8.01 (dd, *J* = 1.5, 1.0 Hz, 1H, H4), 7.40 (t, *J* = 1.5 Hz, 1H, H1), 6.85 (dd, *J* = 1.5, 1.0 Hz, 1H, H2), 3.70 (s, 3H, H7), 3.32 (s, 3H, H6). **^{13}C NMR** (101 MHz, $CDCl_3$) δ 163.3 (C5), 146.6 (C4), 142.7 (C1), 119.8 (C3), 111.4 (C2), 61.2 (C7), 32.9 (C6). Matches literature data.

6.3.6. Miscellaneous compounds

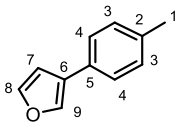
3,3'-(4-Methyl-1,2-phenylene)difuran



Chemical Formula: $C_{15}H_{12}O_2$
Exact Mass: 224.0837
Molecular Weight: 224.2590

Also isolated from reaction for synthesis of 3-(2-Bromo-4-methylphenyl)furan **3.17**. The crude product was purified by column chromatography (pentane) to afford the title compound as a yellow oil (5.6 mg, 15%). $\mathbf{R}_f$ 0.33 (pentane). **^{1}H NMR** (400 MHz, $CDCl_3$) δ 2.40 (s3H,), 6.33 (ddd, *J* = 6.0, 2.0, 1.0 Hz, 2H), 7.15 (ddq, *J* = 8.0, 2.0, 0.5 Hz, 1H), 7.23 (dd, *J* = 1.5, 0.5 Hz, 1H), 7.30 (d, *J* = 8.0 Hz, 1H), 7.35 (dd, *J* = 1.5, 1.0 Hz, 1H), 7.37 (dd, *J* = 1.5, 1.0 Hz, 1H), 7.39 (t, *J* = 3.5, 1.5 Hz, 1H), 7.38 (t, *J* = 3.5, 2.0 Hz, 1H). **^{13}C NMR** (101 MHz, $CDCl_3$) δ 21.1, 111.6, 111.6, 125.6, 125.7, 128.2, 128.6, 130.0, 130.8, 131.3, 137.2, 139.9, 140.0, 142.3, 142.4. **IR** ν_{max} (thin film)/cm^{-1} 3145w, 2921w, 1512m, 1199m, 10467m, 1015m, 872s, 786s, 664m. **HRMS** (ESI+) Found: 225.0912, $C_{15}H_{13}O_2$ $[M+H]^+$ requires: 225.0910.

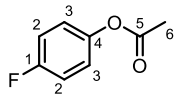
3-(*p*-Tolyl)furan **4.37**



Chemical Formula: $C_{11}H_{10}O$
Exact Mass: 158.0732
Molecular Weight: 158.2000

Also isolated from reaction for synthesis of 3-(2-Bromo-4-methylphenyl)furan **3.17**. Isolated as a white solid (7.3 mg, 27%) $\mathbf{R}_f$ 0.81 (5% EtOAc in pentane). **^{1}H NMR** (400 MHz, $CDCl_3$) δ 2.38 (s, 3H, H1), 6.70 (dd, *J* = 2.0, 1.0 Hz, 1H, H7).7.20 (d, *J* = 8.0 Hz, 2H, H3), 7.40 (d, *J* = 8.0 Hz, 2H, H4), 7.48 (app. t, *J* = 2.0 Hz, 1H, H8), 7.71 (app. dd, *J* = 1.5, 1.0 Hz, 1H, H9). **^{13}C NMR** (101 MHz, $CDCl_3$) δ 21.3 (C1), 109.0 (C7), 125.9 (C4), 126.5 (C6), 129.6 (C3), 129.7 (C2), 136.8 (C5), 138.3 (C9), 143.7 (C8). **MP** 57 °C. Data consistent with literature values.[21]

4-Fluorophenyl acetate

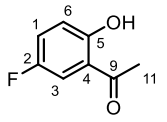


Chemical Formula: $C_8H_7FO_2$
Exact Mass: 154.0430
Molecular Weight: 154.1404

Triethylamine (124 μL, 0.89 mmol, 1 eq.), acetic anhydride (126 μL, 1.34 mmol, 1.5 eq.) and 4-dimethylaminopyridine (11 mg, 0.09 mmol, 0.1 eq.) were added to a stirred solution of 4-fluorophenol (100 mg, 0.89 mmol) in CH_2Cl_2 (4.5 mL). Reaction left stirring at room temperature for 2 hr. Upon completion, H_2O was added and the reaction was extracted with CH_2Cl_2 (x3). The organic layer was washed with brine, dried over $MgSO_4$, and concentrated. Afforded the title compound without further purification as a clear colourless oil (76.8 mg, 0.498 mmol, 56%).

R_f 0.55 (10% EtOAc in pentane). **^{1}H NMR** (400 MHz, $CDCl_3$) δ 2.28 (s, 3H, H6), 7.06 – 7.04 (m, 4H, H2/3). **^{13}C NMR** (101 MHz, $CDCl_3$) δ 21.0 (C6), 116.0 (d, J = 23.6 Hz, C2), 122.9 (d, J = 8.7 Hz, C3), 146.5 (C4), 160.2 (d, J = 244.5 Hz, C1), 169.4 (C5). **^{19}F NMR** (377 MHz, $CDCl_3$) δ -117.11. **IR** ν_{max} (thin film)/cm^{-1} 1760s, 1501s, 1370m, 1210s, 1178s, 1012m, 907m, 824m, 769m. Data consistent with literature values.[22]

1-(5-Fluoro-2-hydroxyphenyl)ethan-1-one

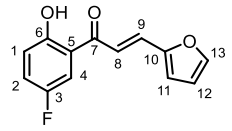


Chemical Formula: $C_8H_7FO_2$
Exact Mass: 154.0430
Molecular Weight: 154.1404

Adapted from literature procedure.[23] A mixture of 4-fluorophenol (1.0 g, 8.94 mmol) and acetyl chloride (955 μL, 13.4 mmol, 1.5 eq.) was stirred at r.t. for 30 min then $AlCl_3$ (2.14 g, 16.1 mmol, 1.8 eq.) was added. The mixture was stirred at 130 °C for 2 h then the reaction mixture was allowed to cool to ambient temperature. H_2O was then added and the mixture was filtered to give a solid, which was washed with cold H_2O (x3). Purification by column chromatography (3-5% EtOAc in pentane) yielded the title compound as a white crystalline solid (838 mg, 5.44 mmol, 61%).

R_f 0.62 (10% EtOAc in pentane). **^{1}H NMR** (400 MHz, $CDCl_3$) δ 2.60 – 2.59 (m, 3H, H11), 6.96 – 6.89 (m, 1H, H6), 7.23 – 7.16 (m, 1H, H1), 7.40 – 7.34 (m, 1H, H3), 11.95 (s, 1H, OH). **^{13}C NMR** (101 MHz, $CDCl_3$) δ ^{13}C NMR (101 MHz, $CDCl_3$) δ 26.6, 115.5 (d, J = 23.5 Hz), 119.1 (d, J = 6.2 Hz), 119.7 (d, J = 7.2 Hz), 124.0 (d, J = 23.5 Hz), 154.9 (d, J = 238.6 Hz), 158.6, 203.5. **^{19}F NMR** (376 MHz, $CDCl_3$) δ -124.05. **MP** 51 – 54 °C. Data consistent with literature values.[24]

(*E*)-1-(5-Fluoro-2-hydroxyphenyl)-3-(furan-2-yl)prop-2-en-1-one

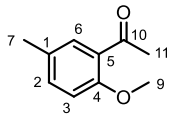


Chemical Formula: $C_{13}H_9FO_3$
Exact Mass: 232.0536
Molecular Weight: 232.2104

To a stirred solution of 1-(5-fluoro-2-hydroxyphenyl)ethan-1-one (300 mg, 1.95 mmol, 1 eq.) and furan-2-carbaldehyde (322 μL, 3.89, 2 eq.) in EtOH (0.3 mL), was added aq. NaOH (8% w/v) dropwise. The reaction was left to return to RT stirring for 24 hr. When complete, the crude material was extracted with Et_2O (3 x 5 mL), washed with brine, dried over $MgSO_4$, filtered and concentrated *in vacuo*. Purification by column chromatography (0–20% EtOAc in pentane) yielded the title compound as a yellow oil (154 mg, 34%).

R_f 0.32 (10% EtOAc in pentane). **^{1}H NMR** (400 MHz, $CDCl_3$) δ 6.55 (dd, *J* = 3.5, 2.0 Hz, 1H), 6.80 (d, *J* = 3.5 Hz, 1H), 6.98 (dd, *J* = 9.0, 4.5 Hz, 1H), 7.23 (ddd, *J* = 9.0, 8.0, 3.0 Hz, 1H), 7.43 (d, *J* = 15.0 Hz, 1H), 7.59 – 7.55 (m, 2H), 7.69 (d, *J* = 15.0 Hz, 1H), 12.60 (s, 1H). **^{13}C NMR** (101 MHz, $CDCl_3$) δ 113.2, 114.7 (d, *J* = 23.0 Hz), 117.2, 117.8, 119.9 (d, *J* = 7.2 Hz), 123.9 (d, *J* = 23.4 Hz), 131.9, 145.9, 151.5, 153.9, 156.2, 159.8, 192.60 (d, *J* = 2.4 Hz). **HRMS** (ESI+) Found: 233.0610, $C_{13}H_{10}O_3F$ $[M+H]^+$ requires: 233.0609. **IR** ν_{max} (thin film)/cm^{-1} 2919w, 1646m, 1583s, 1554m, 1478s, 1421w, 1346m, 1211s, 1170s, 1017m, 966w, 848w, 785m, 747m, 671m.

1-(2-Methoxy-5-methylphenyl)ethan-1-one

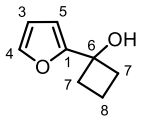


Chemical Formula: $C_{10}H_{12}O_2$
Exact Mass: 164.0837
Molecular Weight: 164.2040

To a solution of NaH (26 mg, 60% in mineral oil, 0.66 mmol, 2 eq.) in THF (2.5 mL), at 0 °C under argon, 1-(2-hydroxy-5-methylphenyl)ethan-1-one (50 mg, 0.33 mmol, 1 eq.) in THF (7.5 mL) was added. The reaction was stirred for 10 mins and then MeI (41 μL, 0.66 mmol, 2 eq.) was added dropwise. The reaction was then warmed to RT and refluxed for 16 hr until complete. After completion, the reaction was cooled to RT and quenched with NH_4Cl (10 mL) and extracted with EtOAc (3 x 15 mL). The combined organic layers were dried over MgSO4, filtered and concentrated *in vacuo*. Purification by column chromatography (5 – 20% EtOAc in pentane) yielded the *title compound* as a yellow oil (41.6 mg, 0.253 mmol, 77%).

R_f 0.24 (10% EtOAc in pentane). **^{1}H NMR** (400 MHz, $CDCl_3$) δ 2.24 (s, 3H, H7), 2.55 (s, 3H, H11), 3.89 (s, 3H, H9), 6.84 (d, *J* = 8.5 Hz, 1H, H3), 7.78 – 7.76 (m, 1H, H2), 7.82 (dd, *J* = 8.5, 2.2 Hz, 1H, H6). **^{13}C NMR** (101 MHz, $CDCl_3$) δ 16.4, 26.4, 55.7, 109.3, 126.9, 128.7, 129.9, 131.1, 162.0, 197.5. Data consistent with literature values.[25]

1-(Furan-2-yl)cyclobutan-1-ol

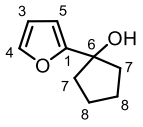


Chemical Formula: $C_7H_{10}O_2$
Exact Mass: 126.0681
Molecular Weight: 126.1550

Prepared according to **GP-II**, using 2 mmol of cyclobutanone. Yielded desired product as a clear, colourless oil (210 mg, 1.52 mmol, 76%).

R_f 0.26 (10% EtOAc in pentane). **^{1}H NMR** (400 MHz, $CDCl_3$) δ 1.65 (m, 1H), 1.86 (m, 1H), 2.38 – 2.25 (m, 2H), 2.54 – 2.45 (m, 2H), 6.28 (dd, *J* = 3.0, 1.0 Hz, 1H), 6.33 (dd, *J* = 3.0, 2.0 Hz, 1H), 7.38 (dd, J = 2.0, 1.0 Hz, 1H). **^{13}C NMR** (101 MHz, $CDCl_3$) δ 12.8, 35.8, 72.4, 105.0, 110.2, 142.2, 158.3. Matches literature data.[26]

1-(Furan-2-yl)cyclopentan-1-ol

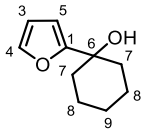


Chemical Formula: $C_7H_{10}O_2$
Exact Mass: 126.0681
Molecular Weight: 126.1550

Prepared according to **GP-II**, using 2 mmol of cyclopentanone. Yielded desired product as a clear, colourless oil (262 mg, 1.72 mmol, 86%).

R$_f$ 0.35 (10% EtOAc in pentane). **^{1}H NMR** (400 MHz, $CDCl_3$) δ 1.79 – 1.71 (m 2H), 1.98 – 1.91 (m, 4H), 2.07 – 2.02 (m, 1H), 6.20 (dd, *J* = 3.2, 0.9 Hz, 1H), 6.30 (dd, *J* = 3.2, 1.8 Hz, 1H), 7.35 (dd, *J* = 1.8, 0.9 Hz, 1H). **^{13}C NMR** (101 MHz, $CDCl_3$) δ 23.7, 39.7, 79.6, 104.2, 110.1, 141.7, 159.4. Matches literature data. [27]

1-(Furan-2-yl)cyclohexan-1-ol

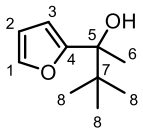


Chemical Formula: $C_7H_{10}O_2$
Exact Mass: 126.0681
Molecular Weight: 126.1550

Prepared according to **GP-II**, using 2 mmol of cyclohexanone. Yielded desired product as a clear, colourless oil (226 mg, 1.36 mmol, 68%).

R$_f$ 0.35 (10% EtOAc in pentane). **^{1}H NMR** (400 MHz, $CDCl_3$) δ 1.59 – 1.32 (m, 4H), 1.78 – 1.67 (m, 2H), 1.83 – 1.80 (m, 1H), 1.88 – 1.83 (m, 1H), 1.98 (app. ddd, *J* = 13.5, 9.5, 4.0 Hz, 2H), 6.21 (dd, *J* = 3.5, 1,0 Hz, 1H), 6.32 (dd, *J* = 3.5, 2.0 Hz, 1H), 7.35 (dd, *J* = 2.0, 1.0 Hz, 1H). **^{13}C NMR** (101 MHz, $CDCl_3$) δ 22.4, 25.6, 36.8, 70.2, 104.5, 110.2, 141.5, 160.1. **MP** 31 – 33 °C.

2-(Furan-2-yl)-3,3-dimethylbutan-2-ol

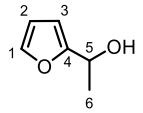


Chemical Formula: $C_{10}H_{16}O_2$
Exact Mass: 168.1150
Molecular Weight: 168.2360

Prepared according to **GP-II**, using 10 mmol of α,α,α-trimethylacetone. Yielded desired product as a clear, colourless oil (1.52g, 91%).

R_f 0.38 (10% EtOAc in pentane). **^{1}H NMR** (400 MHz, $CDCl_3$) δ 0.94 (s, 9H, H7), 1.50 (s, 3H, H6), 6.16 (dd, *J* = 3.0, 1.0 Hz, 1H, H3), 6.31 (dd, *J* = 3.0, 2.0 Hz, 1H, H2), 7.32 (dd, *J* = 2.0, 1.0 Hz, 1H, H1). **^{13}C NMR** (101 MHz, $CDCl_3$) δ 158.2, 140.9, 110.1, 106.0, 60.5, 25.7, 23.2. **HRMS** Not found.

1-(Furan-2-yl)ethan-1-ol

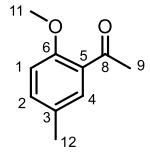


Chemical Formula: $C_6H_8O_2$
Exact Mass: 112.0524
Molecular Weight: 112.1280

Sodium borohydride (412 mg, 10.9 mmol, 1.2 eq.) was added to a stirred solution of 2-acetylfuran (1.0 g, 9.08 mmol, 1 eq.) in dry EtOH (91 mL). The reaction was stirred for 5 hr after which the solvent was removed *in vacuo* and the remaining residue was re-dissolved in CH_2Cl_2 (100 mL). The organic layer was then washed with H_2O (100 mL), dried over $MgSO_4$, filtered and concentrated. The product was purified via column chromatography (20% EtOAc in pentane) to yield a clear colourless oil (608 mg, 5.42 mmol, 60%).

R_f 0.39 (20% EtOAc in pentane). **^{1}H NMR** (400 MHz, $CDCl_3$) δ 1.51 (d, *J* = 6.5 Hz, 3H), 2.38 (s, 1H), 4.85 (q, *J* = 6.5 Hz, 1H), 6.21 (dt, *J* = 3.3, 1.0 Hz, 1H), 6.31 (dd, *J* = 3.2, 2.0 Hz, 1H), 7.35 (dd, J = 2.0, 1.0 Hz, 1H). **^{13}C NMR** (101 MHz, $CDCl_3$) δ 21.3, 63.7, 105.2, 110.2, 141.9, 156.7. Matches literature data.[28]

1-(2-Methoxy-5-methylphenyl)ethan-1-one

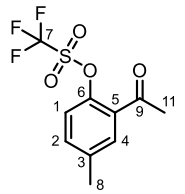


Chemical Formula: $C_{10}H_{12}O_2$
Exact Mass: 164.0837
Molecular Weight: 164.2040

To a suspension of NaH (26.0 mg, 0.66 mmol, 2 eq.) in THF (2 mL), a solution of 1-(2-hydroxy-5-methylphenyl)ethan-1-one (50.0 mg, 0.33 mmol, 1 eq.) in THF (7.5 mL) was added under argon at 0 °C. Methyl iodide (41.0 µL, 0.66 mmol, 2 eq.) was added dropwise. The reaction was left to warm to RT, and then refluxed for 20 hr. When complete, the reaction was quenched with sat. aq. NH_4Cl, and extracted with EtOAc (x3), before being dried over $MgSO_4$, filtered and concentrated *in vacuo*. The crude product was purified by column chromatography (5 – 20% EtOAc in pentane) to yield the title compound as a yellow oil (41.6 mg, 77%).

R_f 0.23 (5% EtOAc in pentane). **^{1}H NMR (**400 MHz, $CDCl_3$ δ 2.29 (s, 3H, H12), 2.60 (s, 3H, H9), 3.88 (s, 3H, H11), 6.86 (d, *J* = 8.5 Hz, 1H, H1), 7.25 (dd, *J* = 8.5, 2.0 Hz, 1H, H2) 7.53 (d, *J* = 2.0 Hz, 1H, H4). **^{13}C NMR** (101 MHz, $CDCl_3$) δ 20.4 (C12), 31.9 (C9), 55.7 (C11), 111.7 (C1), 128.1 (C4), 130.0 (C5), 130.7 (C3), 134.3 (C2), 157.1 (C6), 200.2 (C8). Data consistent with literature values.[25]

2-Acetyl-4-methylphenyl trifluoromethanesulfonate

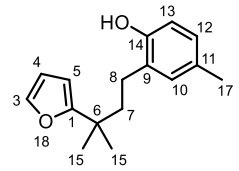


Chemical Formula: $C_{10}H_9F_3O_4S$
Exact Mass: 282.0174
Molecular Weight: 282.2332

To a solution of 2'-hydroxy-5'-methylacetophenone (500 mg, 3.33 mmol, 1 eq.) in pyridine (3.33 mL) at 0 °C, trifluroromethanesulfonic anhydride (671 μL, 3.99 mmol, 1.2 eq.) was slowly added dropwise. The reaction was stirred at room temperature for 15 hrs. On completion, the reaction was diluted with EtOAc, washed with 1.0 M aq. $CuSO_4$ (x4) then brine, and dried over $MgSO_4$. The solvent was removed *in vacuo* and the compound was purified by column chromatography (1% EtOAc in pet. $ether_{30\text{-}40}$) yielding a white crystalline solid (769.7 mg, 2.73 mmol, 82%).

R_f 0.38 (5% EtOAc in pet. $ether_{30\text{-}40}$). **^{1}H NMR** (400 MHz, $CDCl_3$) δ 2.41 (s, 3H, H8), 2.60 (s, 3H, H11), 7.19 (d, *J* = 8.5 Hz, 1H, H1), 7.37 (dd, *J* = 8.5, 2.0 Hz, 1H, H2), 7.58 (d, *J* = 2.0 Hz, 1H, H4). **^{13}C NMR** (101 MHz, $CDCl_3$) δ 20.8 (C8), 29.4 (C11), 118.6 (q, *J* = 320.7 Hz, C7), 122.4 (C1), 131.2 (C5), 131.7 (C4), 134.1 (C3), 138.9 (C2), 144.7 (C6), 196.9 (C9). **^{19}F NMR** (377 MHz, $CDCl_3$) δ -73.50. **MP** 43-45 °C. **IR** ν_{max} (thin film)/cm^{-1} 2930w, 1696m, 1422s, 1199s, 1137s, 1095m, 898s, 866s, 694m. Data consistent with literature values.[29]

2-(3-(Furan-2-yl)-3-methylbutyl)-4-methylphenol

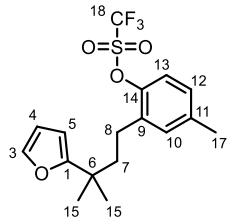


Chemical Formula: $C_{16}H_{20}O_2$
Exact Mass: 244.1463
Molecular Weight: 244.3340

Hydrazine monohydrate (254 μL, 5.02 mmol. 9.3 eq.) and KOH (91 mg, 1.62 mmol, 3 eq.) were added consecutively to a stirred solution of 3-(furan-2-yl)-1-(2-hydroxy-5-methylphenyl)-3-methylbutan-1-one (139.3 mg, 0.54 mmol, 1 eq.) in ethylene glycol (0.83 mL). The mixture was heated to 130 °C for 2 hr, then at 180 °C for a further 20 hr. The mixture was poured into H_2O, extracted with ether and washed with brine. Then dried over anhydrous $MgSO_4$, filtered and concentrated *in vacuo* to achieve the *title compound* as a yellow solid (46.8 mg, 0.19 mmol, 35%).

R_f 0.2 (10% EtOAc in pentane). **^{1}H NMR** (400 MHz, $CDCl_3$) δ 1.34 (s, 6H, H15), 1.90 – 1.85 (m, 2H, H7), 2.24 (s, 3H, H17), 2.37 – 2.32 (m, 2H, H8), 4.61 (s, 1H, OH), 6.08 (dd, *J* = 3.0, 0.5 Hz, 1H, H5), 6.32 (dd, *J* = 3.0, 2.0 Hz, 1H, H4), 6.68 – 6.65 (m, 1H, H13), 6.89 – 6.85 (m, 2H, H10/12), 7.37 (dd, *J* = 2.0, 0.5 Hz, 1H, H3). **^{13}C NMR** (101 MHz, $CDCl_3$) δ 20.6, 25.8, 27.1, 36.2, 42.2, 104.0, 110.1, 115.3, 127.7, 128.1, 130.0, 130.7, 141.0, 151.3, 162.7. **HRMS** (ESI+) Found: 245.1539, $C_{16}H_{21}O_2$ $[M+H]^+$ requires: 245.1536. **MP** 87 – 88 °C.

2-(3-(furan-2-yl)-3-methylbutyl)-4-methylphenyl trifluoromethanesulfonate

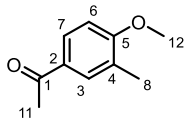


Chemical Formula: $C_{17}H_{19}F_3O_4S$
Exact Mass: 376.0956
Molecular Weight: 376.3902

To a stirred solution of 2-(3-(furan-2-yl)-3-methylbutyl)-4-methylphenol (21.1 mg, 0.086 mmol, 1 eq.) in dry pyridine (100 μL) at 0 ºC under argon, Tf_2O (17 μL. 0.104 mmol, 1.2 eq.) was added. The mixture was allowed to warm to RT and left to stir for 3 hr. 1M aq. Cu_2SO_4 was added and the mixture was extracted into EtOAc (x3). The combined organic layers were washed with brine, dried over $MgSO_4$, filtered and concentrated *in vacuo*. Purification by column chromatography (2–5% EtOAc in pentane) yielded the *title compound* as a yellow oil (26.5 mg, 0.704 mmol, 82%).

R_f 0.77 (5% EtOAc in pentane). **^{1}H NMR** (400 MHz, $CDCl_3$) δ 1.34 (s, 6H, H15), 1.90 – 1.85 (m, 2H, H7), 2.32 (s, 3H, H17), 2.49 – 2.44 (m, 2H, H8), 6.04 (dd, *J* = 3.0, 1.0 Hz, 1H, H5), 6.29 (dd, *J* = 3.0, 2.0 Hz, 1H, H4), 7.03 – 7.00 (m, 2H, H10/12), 7.11 – 7.07 (m, 1H, H13), 7.35 (dd, *J* = 2.0, 1.0 Hz, 1H, H3). **^{13}C NMR** (101 MHz, $CDCl_3$) δ 21.0, 25.8, 26.8, 36.0, 42.7, 103.9, 109.8, 118.7 (q, *J* = 320.0 Hz), 121.0, 128.3, 131.9, 135.2, 138.5, 141.1, 146.0, 162.1. **IR** ν_{max} (thin film)/cm^{-1} 2970w, 2928w, 2360w, 1420m, 1212s, 1142s, 1079w, 876m, 621w. **HRMS** (ESI+) Found: 377.1028, $C_{17}H_{19}F_3O_4S$ $[M+H]^+$ requires: 377.1029.

1-(4-Methoxy-3-methylphenyl)ethan-1-one

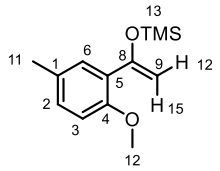


Chemical Formula: $C_{10}H_{12}O_2$
Exact Mass: 164.0837
Molecular Weight: 164.2040

To a solution of NaH (27 mg, 60% in mineral oil, 0.67 mmol, 2 eq.) in THF (2.5 mL), at 0 °C under argon, 1-(4-hydroxy-3-methylphenyl)ethan-1-one (50 mg, 0.33 mmol, 1 eq.) in THF (7.5 mL) was added. The reaction was stirred for 10 mins and then MeI (42 μL, 0.67 mmol, 2 eq.) was added dropwise. The reaction was then warmed to RT and refluxed for 6 hr until complete. After completion, the reaction was cooled to RT and quenched with NH_4Cl (10 mL) and extracted with EtOAc (3 x 15 mL). The combined organic layers were dried over MgSO4, filtered and concentrated *in vacuo*. Purification by column chromatography (5 – 10% EtOAc in pentane) yielded the *title compound* as a yellow oil (45.4 mg, 0.276 mmol, 83%).

R_f 0.49 (5% EtOAc in pentane). **^{1}H NMR** (400 MHz, CDCl3) δ 2.24 (s, 3H, H6), 2.55 (s, 3H, H11), 3.89 (s, 3H, H12), 6.84 (d, *J* = 8.5 Hz, 1H, H6), 7.78 – 7.76 (m, 1H, H3), 7.82 (dd, *J* = 8.5, 2.0 Hz, 1H, H7). **^{13}C NMR** (101 MHz, $CDCl_3$) δ 16.4 (C6), 26.4 (C11), 55.7 (C12), 109.3 (C6), 126.9 (C4), 128.7 (C7), 129.9 (C2), 131.1 (C3), 162.0 (C5), 197.5 (C1). Data consistent with literature values. [30]

((1-(2-Methoxy-5-methylphenyl)vinyl)oxy)trimethylsilane

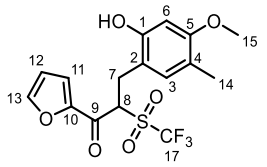


Chemical Formula: $C_{13}H_{20}O_2Si$
Exact Mass: 236.1233
Molecular Weight: 236.3860

To a stirred solution of 1-(2-methoxy-5-methylphenyl)ethan-1-one (500 mg, 3.05 mmol, 1 eq.), triethylamine (760 µL, 5.48 mmol, 1.8 eq.) and TMSCl (692 µL, 5.48 mmol, 1.8 eq.) in acetonitrile (21 mL) was added NaI (822 mg, 5.48 mmol, 1.8 eq.) in acetonitrile (10 mL) at 0 °C under Ar. The reaction was stirred for 3 hours, before the solvent was removed *in vacuo* and then redissolved in hexane. The suspension was then filtered through Celite to remove insoluble precipitates, and then concentrated *in vacuo* to yield a yellow oil (719 mg, 3.05 mmol, quant. yield) which was used without further purification.

R_f 0.78 (5% EtOAc in pentane). **^{1}H NMR** (400 MHz, C_6D_6) δ 0.24 (s, 9H, H13), 2.15 (s, 3H, H11), 3.33 (s, 3H, H12), 4.87 (s, 1H, H14), 5.35 (s, 1H, H15), 6.51 (d, *J* = 8.5 Hz, 1H, H3), 6.95 – 6.87 (m, 1H, H2), 7.61 (d, *J* = 2.0 Hz, 1H, H6). **^{13}C NMR** (101 MHz, C_6D_6) δ 0.4, 20.6, 55.1, 96.9, 111.6, 127.6, 129.4, 129.6, 130.2, 153.8, 155.8.

1-(Furan-2-yl)-3-(2-hydroxy-4-methoxy-5-methylphenyl)-2-((trifluoromethyl)sulfonyl)propan-1-one



Chemical Formula: $C_{16}H_{15}F_3O_6S$
Exact Mass: 392.0541
Molecular Weight: 392.3452

A solution of 2-(3-(furan-2-yl)-3-oxopropyl)-5-methoxy-4-methylphenyl trifluoromethanesulfonate (38 mg, 0.065 mmol, 1 eq.) in dry DMA (1.3 mL) was degassed for 10 mins, after which Cs_2CO_3 (50.7 mg, 0.156 mmol, 2.4 eq.) was added and the reaction mixture was degassed for a further 10 mins. [1,3-Bis(2,6-Diisopropylphenyl)imidazol-2-ylidene](3-chloropyridyl)palladium(II) dichloride (8.8 mg, 0.013 mmol, 0.2 eq.) was then added and the reaction was flushed with Ar, before being heated to 80 °C for 18 hours. When complete, the reaction was cooled to RT and quenched with sat. aq. $NaHCO_3$ (10mL) and then extracted with EtOAc (3 x 10mL). The combined organic layers were washed with brine, dried over $MgSO_4$, filtered and concentrated *in vacuo*. The crude product was purified by column chromatography (0 – 80% EtOAc in pentane) to afford the *title compound* (4.0 mg, 0.01mmol, 16%).

R_f 0.21 (20% EtOAc in pentane). **^{1}H NMR** (400 MHz, $CDCl_3$) δ 2.02 (s, 3H, H14), 3.45 (dd, *J* = 14.0, 3.5 Hz, 1H, H7'), 3.56 (dd, *J* = 14.0, 11.0 Hz, 1H, H7), 3.71 (s, 3H, H15), 5.35 (s, 1H, OH), 5.54 (dd, *J* = 11.0, 3.5 Hz, 1H, H8), 6.25 (s, 1H, H6), 6.55 (dd, *J* = 3.5, 1.5 Hz, 1H, H12), 6.79 (s, 1H, H3), 7.30 (dd, *J* = 3.5, 1.0 Hz, 1H, H11), 7.61 (dd, *J* = 1.5, 1.0 Hz, 1H, H13). **^{13}C NMR** (101 MHz, $CDCl_3$) δ 15.4 (C14), 27.2 (C7), 55.5 (C15), 65.7 (C8), 99.4 (C6), 111.5 (C2), 113.7 (C12), 119.5 (C4), 120.9 (C11), 132.9 (C3), 148.8 (C13), 152.1 (C10), 152.6 (C1), 158.2 (C5), 176.8 (C9). **^{19}F NMR** (376 MHz, $CDCl_3$) δ -75.17.

6.4. Experimental Procedures for Chapter 4

6.4.1. $P450_{BM3}$ screening conditions

24-well screening plates were prepared by diluting enzymes to 10 mM stock solutions and pipetting 100 μL into each well. 400 μL of the screening mixture detailed below was added to make the final reaction volume up to 500 μL. Substrates were dissolved in DMSO, MeOH or EtOH to give 100 mM stock solutions. The below describes 1 mM substrate : 2 μM enzyme (500:1) which all screening described during this chapter was conducted at.

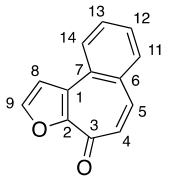
Reagent	Stock Concentration	Final Concentration	Volume (μL)
Phosphate Buffer	200 mM	-	325
Glucose	1 M	100 mM	50
GDH	200 U mL^{-1}	4 U mL^{-1}	10
$NADP^+$	4 mM	80 μM	10
Substrate	100 mM	1 mM	5

Table 2 - Composition of initial screening mixture.

Plates were left to shake at ambient temperature, 150 rpm. After 24 hours, the contents of each well were transferred to a 1.5 mL microcentrifuge tube and 300 mL EtOAc was added to extract the organics. The mixture was vortexed for 15 s then centrifuged at 13,300 rpm for 2 min to separate the aqueous and organic layers. 100 μL of the organic layer was removed for GC analysis.

6.4.2. Preparative scale $P450_{BM3}$ reactions and isolation of metabolites

4*H*-Benzo[3,4]cyclohepta[1,2-*b*]furan-4-one **4.38**



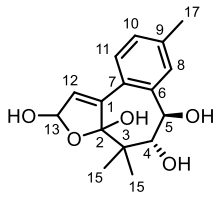
Chemical Formula: $C_{13}H_8O_2$
Exact Mass: 196.0524
Molecular Weight: 196.2050

Prepared according to **GP-I**, using $P450_{BM3}$ mutant R19/F87A/A264G/A328G (3.0 mL of 64 μM concentration in phosphate buffer, overall concentration of 2.0 μM), glucose (10 mL of 1.0 M stock in phosphate buffer), GDH (2.0 mL of 2.0 U/μL stock in phosphate buffer), $NADP^+$ monosodium salt (2.0 mL of 4.0 mM stock in phosphate buffer) in phosphate buffer (82 mL) and substrate **3.63** (1.0 mL of 0.1 M stock in DMSO, 0.1 mmol, overall concentration of 1.0 mM) stirring for 21 hr. Purification by preparative thin layer chromatography yielded a white solid (2.8 mg, 0.014 mmol, 14%).

R_f 0.34 (20% EtOAc in pentane). **^{1}H NMR** (500 MHz, CD_2Cl_2) δ 6.92 (d, *J* = 13.0 Hz, 1H), 7.37 (d, *J* = 2.0 Hz, 1H), 7.62 (ddd, *J* = 8.0, 7.5, 1.5 Hz, 1H), 7.66 (d, *J* = 13.0 Hz, 1H), 7.72 (ddd, *J* = 8.0, 7.5, 1.5 Hz, 1H), 7.81 (d, *J* = 7.8 Hz, 1H), 7.89 (d, *J* = 2.0 Hz, 1H), 8.18 (d, *J* = 8.1 Hz, 1H). **^{13}C NMR** (126 MHz, CD_2Cl_2) δ 110.5, 128.3, 129.4, 130.6, 131.3, 131.4, 132.3, 133.5, 136.0, 141.9, 147.5, 152.3, 176.4, 207.0. **HRMS** (ESI+) Found: 197.0598, $C_{13}H_9O_2$ $[M+H]^+$ requires: 197.0597. **IR** ν_{max} (thin film)/cm^{-1} 2981w, 2919w, 1742s, 1463m, 1382m, 1152w, 1071w, 967m, 880w, 785m, 659w.

(5R,6R)-4,4,8-Trimethyl-2,4,5,6-tetrahydro-3aH-benzo[3,4]cyclohepta[1,2-b]furan-2,3a,5,6-tetraol

4.40

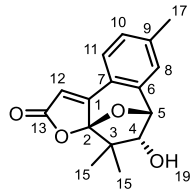


Chemical Formula: $C_{16}H_{18}O_4$
Exact Mass: 274.1205
Molecular Weight: 274.3160

Prepared according to **GP-I**, using $P450_{BM3}$ mutant GV/A184I (3.2 mL of 126 μM concentration in phosphate buffer, overall concentration of 2.0 μM), glucose (20 mL of 1.0 M stock in phosphate buffer), GDH (4.0 mL of 2.0 U/μL stock in phosphate buffer), $NADP^+$ monosodium salt (4.0 mL of 4.0 mM stock in phosphate buffer) in phosphate buffer (165 mL) and substrate **3.21** (2.2 mL of 0.1 M stock in MeOH, 0.22 mmol, overall concentration of 1.0 mM) stirring for 20 h. Purification by column chromatography (20–100% EtOAc in pentane) yielding the *title compound* as a clear, colourless oil (36.8 mg, 61%). Characterised as a mixture of diastereomers in 1.5:1 ratio.

R_f 0.19 (50% EtOAc in pentane). Diastereomer 1: **^{1}H NMR** (400 MHz, $CDCl_3$) δ 0.73 (s, 3H, H15), 1.19 (s, 3H, H15'), 2.35 (s, 3H, H17), 3.56 (br.d, *J* = 6.5 Hz, OH), 4.17 – 4.05 (m, 1H, H4), 5.04 (d, *J* = 6.5 Hz, 1H, H5), 5.95 (dd, *J* = 2.0, 1.0 Hz, 1H, H12), 6.27 (br.d, *J* = 4.0 Hz, 1H, H13), 6.95 (s, 1H, H8), 7.13 (dt, *J* = 8.0, 2.0 Hz, 1H, H11), 7.44 (d, *J* = 8.0 Hz, 1H, H10). **^{13}C NMR** (101 MHz, $CDCl_3$) δ 19.5 (C15), 21.6 (C15), 26.7 (C3), 42.8 (C17), 78.4 (C4), 79.0 (C5), 102.8 (C13), 116.9 (C12), 117.3 (C2), 125.7 (C10), 128.1 (C8), 129.8 (C11), 134.4 (C7), 139.5 (C9), 142.2 (C8), 142.7 (C1). Diastereomer 2: δ **^{1}H NMR** (400 MHz, $CDCl_3$) 0.62 (s, 3H, H15), 1.21 (s, 3H, H15'), 2.35 (s, 3H, H17), 3.67 (br.s, OH), 4.15 – 4.07 (m, 1H, H4), 5.01 (d, *J* = 7.0 Hz, 1H, H5), 5.93 (s, 1H, H12), 6.09 (br.s, 1H, H13), 6.93 (d, *J* = 1.5 Hz, 1H, H8), 7.13 (dt, *J* = 8.0, 2.0 Hz, 1H, H11), 7.41 (d, *J* = 8.0 Hz, 1H, H10). **^{13}C NMR** (101 MHz, $CDCl_3$) δ 19.5 (C15), 21.6 (C15), 26.7 (C3), 42.8 (C17), 78.4 (C4), 79.0 (C5), 103.5 (C13), 117.3 (C2), 118.9 (C12), 125.7 (C10), 128.1 (C8), 129.8 (C11), 134.4 (C7), 139.5 (C9), 142.2 (C8), 142.7 (C1). **IR** ν_{max} (thin film)/cm^{-1} 3390br.w, 1463w, 1382m, 1242m, 1153m, 1071w, 967w, 880m, 785w, 687w, 638w.

5-Hydroxy-4,4,8-trimethyl-5,6-dihydro-3a,6-epoxybenzo[3,4]cyclohepta[1,2-b]furan-2(4H)-one **4.41**

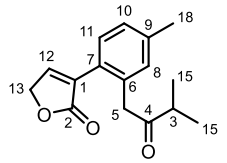


Chemical Formula: $C_{16}H_{16}O_4$
Exact Mass: 272.1049
Molecular Weight: 272.3000

Also isolated from previous reaction of substrate **3.21** with GV/A184I (**4.40**) . Purification by column chromatography (20–100% EtOAc in pentane) yielding the *title compound* as a colourless crystalline solid (2.3 mg, 4%).

R_f 0.43 (50% EtOAc in pentane). **^{1}H NMR** (600 MHz, $CDCl_3$) δ 0.72 (s, 3H, H15), 1.34 (s, 3H, H15), 2.43 (s, 3H, H17), 4.28 (dd, *J* = 9.0, 7.0 Hz, 1H, H4), 5.26 (d, *J* = 7.0 Hz, 1H, H5), 6.07 (s, 1H, H12), 7.09 (dd, *J* = 2.0, 1.0 Hz, 1H, H8), 7.28 – 7.27 (m, 1H, H11), 7.59 (d, *J* = 8.0 Hz, 1H, H10). **^{13}C NMR** (151 MHz, $CDCl_3$) δ 19.4 (C15), 22.0 (C17), 26.9 (C15), 43.3 (C3), 77.5 (C4), 79.5 (C5), 108.3 (C12), 111.9 (C2), 123.7 (C7), 127.1 (C10), 128.6 (C8), 130.4 (C11), 136.3 (C6), 142.9 (C9), 163.4 (C1), 170.5 (C13). **IR** ν_{max} (thin film)/cm^{-1} 3463br.w, 2922m, 2851w, 1766s, 1638m, 1614m, 1466w, 1334m, 1274w, 1241m, 1174w, 1120w, 1080m, 1021w, 905w, 823w. **LRMS** Found 273.1, $C_{16}H_{17}O_4$ $[M+H]^+$ requires 273.1.

3-(4-Methyl-2-(3-methyl-2-oxobutyl)phenyl)furan-2(5H)-one **4.42**

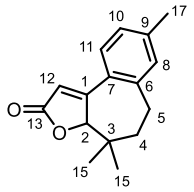


Chemical Formula: $C_{16}H_{18}O_3$
Exact Mass: 258.1256
Molecular Weight: 258.3170

Prepared according to **GP-I**, using $P450_{BM3}$ mutant GLQ/I263G/A328G (1.2 mL of 87 μM concentration in phosphate buffer, overall concentration of 2.0 μM), glucose (50 mL of 1.0 M stock in phosphate buffer), GDH (1.0 mL of 2.0 U/μL stock in phosphate buffer), $NADP^+$ monosodium salt (1.0 mL of 4.0 mM stock in phosphate buffer) in phosphate buffer (41.3 mL) and substrate **3.22** (0.5 mL of 0.2 M stock in DMSO, 0.1 mmol, overall concentration of 1.0 mM) stirring for 20 h. Purification by column chromatography (10–50% EtOAc in pentane) yielding the *title compound* as a clear, colourless oil (0.6 mg, 2%).

$\mathbf{R_f}$ 0.16 (20% EtOAc in pentane). **^{1}H NMR** (400 MHz, $CDCl_3$) δ 1.08 (s, 3H, H15), 1.09 (s, 3H, H15), 2.35 (s, 3H, H18), 2.69 (sept, J = 7.0 Hz, 1H, H3), 3.81 (s, 2H, H5), 4.92 (d, J = 2.0 Hz, 2H, H13), 7.02 (s, 1H, H8), 7.13 (d, J = 8.0 Hz, 1H, H10), 7.21 (d, J = 8.0 Hz, 1H, H11), 7.42 (t, J = 2.0 Hz, 1H, H12). **HRMS** (ESI+) Found: 259.1329, $C_{16}H_{18}O_3$ $[M+H]^+$ requires: 259.1329.

4,4,8-Trimethyl-3a,4,5,6-tetrahydro-2H-benzo[3,4]cyclohepta[1,2-b]furan-2-one **4.46**

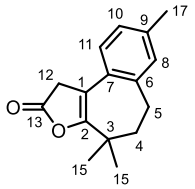


Chemical Formula: $C_{16}H_{18}O_2$
Exact Mass: 242.1307
Molecular Weight: 242.3180

Prepared according to **GP-1**, using $P450_{BM3}$ mutant R19/F87I (2.75 mL of 160 μM concentration in phosphate buffer, overall concentration of 2.0 μM), glucose (20 mL of 1.0 M stock in phosphate buffer), GDH (4.0 mL of 2.0 U/μL stock in phosphate buffer), $NADP^+$ monosodium salt (4.0 mL of 4.0 mM stock in phosphate buffer) in phosphate buffer (187 mL) and substrate **3.12** (2.2 mL of 0.1 M stock in MeOH, 0.22 mmol, overall concentration of 1.0 mM) stirring for 45 h. Purification by column chromatography (20–100% EtOAc in pentane) yielding the *title compound* as a clear, colourless oil (1.2 mg, 2%).

R_f 0.51 (20% EtOAc in pentane). **^{1}H NMR** (600 MHz, $CDCl_3$) δ 1.11 (s, 3H, H15), 1.28 (s, 3H, H15'), 1.58 (ddd, *J* = 14.5, 7.0, 2.0 Hz, 1H, H4), 2.31 – 2.20 (m, 1H, H4'), 2.35 (s, 3H, H17), 2.68 (ddd, *J* = 16.0, 7.0, 2.0 Hz, 1H, H5), 3.00 (t, *J* = 14.5 Hz, 1H, H5'), 6.08 (s, 1H, H12), 7.01 (s, 1H, H8), 7.07 (d, *J* = 8.0 Hz, 1H, H10), 7.22 (d, *J* = 8.0 Hz, 1H, H11). **^{13}C NMR** (151 MHz, $CDCl_3$) δ 21.3 (C17), 21.4 (C15), 24.8 (C15'), 31.6 (C5), 38.2 (C4), 41.4 (C3), 110.1 (C2), 117.2 (C12), 127.5 (C9), 127.7 (C10), 130.8 (C11), 131.6 (C8), 141.1 (C6), 141.6 (C7), 169.4 (C1), 170.2 (C13). **IR** ν_{max} (thin film)/cm^{-1} 3325br.s, 2922w, 1739s, 1610w, 1455w, 1265w, 1173w, 1116w, 1052w, 990w, 873w, 822w, 747w, 669w. **LRMS** Found: 243.1, $C_{16}H_{19}O_2$ $[M+H]^+$ requires: 243.1.

4,4,8-Trimethyl-1,4,5,6-tetrahydro-2H-benzo[3,4]cyclohepta[1,2-b]furan-2-one **4.47**

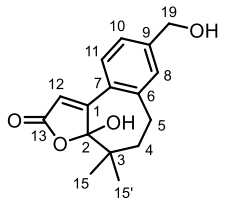


Chemical Formula: $C_{16}H_{18}O_2$
Exact Mass: 242.1307
Molecular Weight: 242.3180

Also isolated from previous reaction of substrate **3.12** with R19/F87I (**4.46**). Purification by column chromatography (20–100% EtOAc in pentane) yielding the *title compound* as a clear, colourless oil (4.6 mg, 9%).

R_f 0.29 (20% EtOAc in pentane). **^{1}H NMR** (400 MHz, $CDCl_3$) δ 1.28 (s, 6H, H15), 1.86 – 1.78 (m, 2H, H4), 2.30 (s, 3H, H17), 2.79 – 2.71 (m, 2H, H5), 3.46 (s, 2H, H12), 6.93 (s, 1H, H8), 7.02 – 6.97 (m, 2H, H10/11). **^{13}C NMR** (151 MHz, $CDCl_3$) δ 21.0 (C17), 28.6 (C15), 31.5 (C5), 37.5 (C3), 40.5 (C12), 41.0 (C4), 111.1 (C1) 126.4 (C10), 127.0 (C11), 129.7 (C8), 130.2 (C7), 135.6 (C6) 141.1 (C9),144.4 (C2), 178.2 (C13). **IR** ν_{max} (thin film)/cm^{-1} 3236br.s, 2951m, 1768s, 1541m, 1333w, 1256w, 1058w, 1023w, 954m, 752w, 734w, 650w. **LRMS** Found: 281.1, $C_{16}H_{18}KO_2$ $[M+K]^+$ requires: 281.1.

3a-Hydroxy-8-(hydroxymethyl)-4,4-dimethyl-3a,4,5,6-tetrahydro-2*H*-benzo[3,4]cyclohepta[1,2-*b*]furan-2-one **4.48**

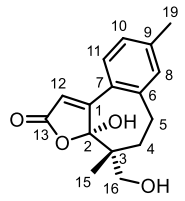


Chemical Formula: $C_{16}H_{18}O_4$
Exact Mass: 274.1205
Molecular Weight: 274.3160

Prepared according to **GP-1**, using $P450_{BM3}$ mutant R47L/Y51F/I263R (1.0 mL of 130 μM concentration in phosphate buffer, overall concentration of 2.0 μM), glucose (15 mL of 1.0 M stock in phosphate buffer), GDH (3.0 mL of 2.0 U/μL stock in phosphate buffer), $NADP^+$ monosodium salt (3.0 mL of 4.0 mM stock in phosphate buffer) in phosphate buffer (122 mL) and substrate **3.11** (0.5 mL of 0.1 M stock in DMSO, 0.05 mmol, overall concentration of 1.0 mM) stirring for 45 h. Purification by column chromatography (20–60% EtOAc in pentane) yielding the *title compound* as a white solid (13.5 mg, 98%).

R_f 0.13 (40% EtOAc in pentane). **^{1}H NMR** (600 MHz, d_6-acetone) δ 0.96 (s, 3H, H15), 1.12 (s, 3H, H15), 1.47 (ddd, *J* = 14.5, 7.0, 2.0 Hz, 1H, H4), 2.15 (ddd, *J* = 14.5, 13.0, 2.0 Hz, 1H, H4'), 2.63 (ddd, *J* = 16.0, 7.0, 2.0 Hz, 1H, H5), 2.95 – 2.87 (m, 1H, H5'), 4.52 (d, *J* = 6.0 Hz, 2H, H19), 6.04 (s, 1H, H12), 7.09 (s, 1H, H8), 7.13 (d, *J* = 7.8 Hz, 1H, H10), 7.21 (d, *J* = 7.8 Hz, 1H, H11). **^{13}C NMR** (151 MHz, d_6-acetone) δ 21.6 (C15), 25.6 (C15), 32.4 (C5), 39.0 (C4), 42.0 (C3), 64.3 (C19), 111.2 (C12), 118.4 (C10), 125.4 (C8), 129.2 (C11), 130.7 (C2), 132.0 (C7), 142.0 (C6), 146.1 (C9), 170.2 (C1) 170.6 (C13). **IR** ν_{max} (thin film)/cm^{-1} 3353w, 2918m, 2850m, 1736s, 1456w, 1261s, 1005s, 957w, 803m, 731m. **HRMS** (ESI+) Found: 297.1097, $C_{16}H_{18}O_4Na$ $[M+Na]^+$ requires: 297.1097. **MP** 165 – 168 °C.

3a-Hydroxy-4-(hydroxymethyl)-4,8-dimethyl-3a,4,5,6-tetrahydro-2H-benzo[3,4]cyclohepta[1,2-b]furan-2-one **4.50b**

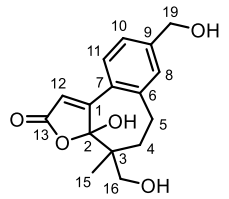


Chemical Formula: $C_{16}H_{18}O_4$
Exact Mass: 274.1205
Molecular Weight: 274.3160

Prepared according to **GP-I** using $P450_{BM3}$ mutant RP/V78I/E267V (5.0 mL of 97 μM concentration in phosphate buffer, overall concentration of 2.0 μM), glucose (26 mL of 1.0 M stock in phosphate buffer), GDH (5.2 mL of 2.0 U/μL stock in phosphate buffer), $NADP^+$ monosodium salt (5.2 mL of 4.0 mM stock in phosphate buffer) in phosphate buffer (170 mL) and substrate **3.11** (3 mL of 0.1 M stock in DMSO, 0.3 mmol, overall concentration of 1.0 mM) stirring for 45 h. Purification by column chromatography (20–60% EtOAc in pentane) yielding the *title compound* as a white solid (21.3 mg, 26%).

R_f 0.29 (20% EtOAc in pentane). **^{1}H NMR** (400 MHz, $CDCl_3$) δ 0.96 (s, 3H, H15), 1.62 (ddd, *J* = 14.0, 6.5, 2.0 Hz, 1H, H5), 2.34 (s, 3H, H19), 2.82 – 2.70 (m, 2H, H4'/5'), 3.08 (t, *J* = 14.0 Hz, 1H, H4), 3.26 (br.s, 1H, OH), 3.55 (d, *J* = 10.5 Hz, 1H, H16'), 4.39 (d, *J* = 10.5 Hz, 1H, H16), 6.08 (s, 1H, H12), 7.03 (s, 1H, H8), 7.07 (d, *J* = 8.0 Hz, 1H, H10), 7.24 (d, *J* = 8.0 Hz, 1H, H11). **^{13}C NMR** (101 MHz, $CDCl_3$) δ 17.1 (C15), 21.4 (C19), 31.0 (C4), 33.7 (C5), 43.7 (C3), 71.6 (C16), 112.4 (C2), 117.2 (C12), 127.8 (C10), 128.1 (C9), 130.9 (C11), 131.5 (C8), 140.1 (C7), 141.4 (C6), 168.7 (C1), 171.3 (C13). **MP** 163 – 164 °C.

3a-Hydroxy-4,8-bis(hydroxymethyl)-4-methyl-3a,4,5,6-tetrahydro-2*H*-benzo[3,4]cyclohepta[1,2-*b*]furan-2-one **4.49**



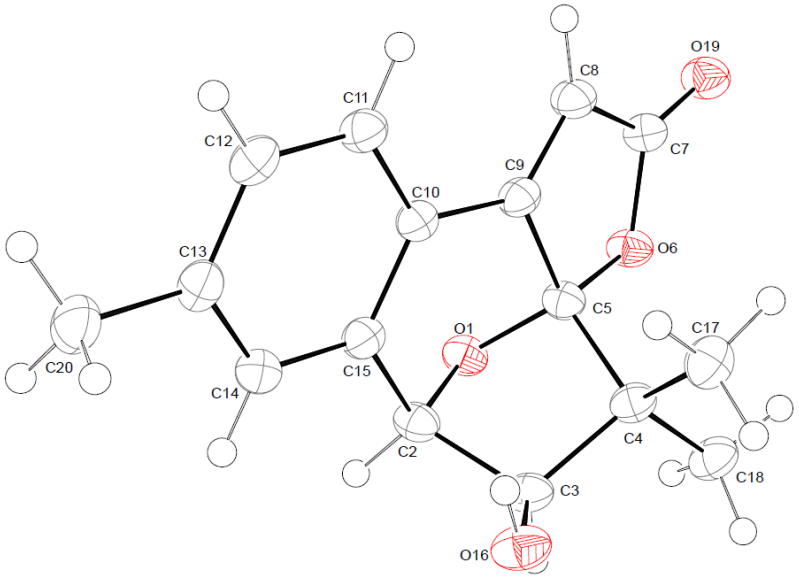
Chemical Formula: $C_{16}H_{18}O_5$
Exact Mass: 290.1154
Molecular Weight: 290.3150

Also isolated from previous reaction of substrate **3.11** with RP/V78I/E267V (**4.50b**). Purification by column chromatography (20–100% EtOAc in pentane) yielding the *title compound* as a yellow oil (2.5 mg, 3%).

R*f* 0.06 (50% EtOAc in pentane). **^{1}H NMR** (400 MHz, $CDCl_3$) δ 0.98 (s, 3H, H15), 1.13 (dd, *J* = 12.5, 6.0 Hz, 1H, H4), 1.68 – 1.60 (m, 1H, H4'), 2.83 – 2.73 (m, 1H, H5), 3.13 (app. t, *J* = 14.5 Hz, 1H, H5'), 3.58 (d, *J* = 10.5 Hz, 1H, H16), 4.40 (d, *J* = 10.5 Hz, 1H, H16), 4.71 (s, 2H, H19), 6.12 (s, 1H, H12), 7.28 – 7.23 (m, 2H, H9/10), 7.34 (d, *J* = 7.5 Hz, 1H, H11). **^{13}C NMR** (101 MHz, $CDCl_3$) δ 16.8 (C15), 30.6 (C4), 33.6 (C5), 43.9 (C3), 65.4 (C16), 70.3 (C19), 118.0 (C12), 120.7 (C2), 125.2 (C10), 128.9 (C8), 131.0 (C11), 135.5 (C7), 140.4 (C6), 142.67 (C9), 158.6 (C1), 173.5 (C13). **HRMS** (ESI+) Found: 313.1048, $C_{16}H_{18}O_5Na$ $[M+Na]^+$ requires: 313.1046.

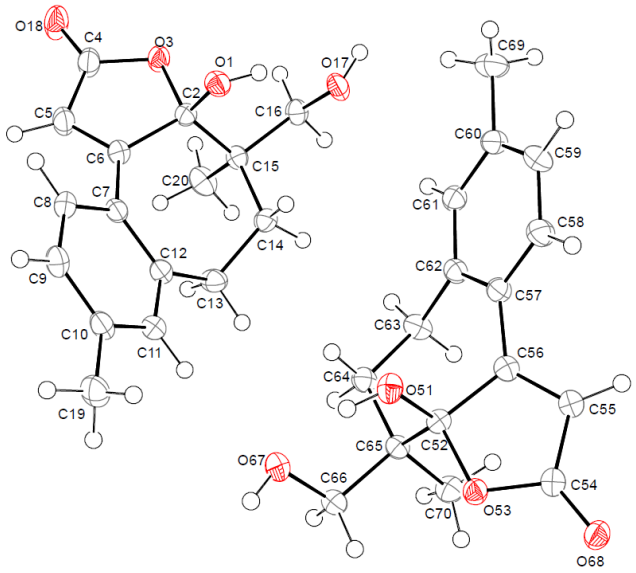
6.4.3. Single crystal X-ray data for compounds in Chapter 4

6.4.3.1. Crystal data and structure refinement for 4.41.



Empirical formula	C16 H16 O4
Formula weight	272.30
Temperature	150 K
Wavelength	1.54184 Å
Crystal system	Monoclinic
Space group	P21/c
Unit cell dimensions	a = 8.5178(2) Å α= 90°. b = 6.61970(10) Å β= 99.2397(18)°. c = 23.1669(4) Å γ = 90°.
Volume	1289.32(4) $Å^3$
Z	4
Density (calculated)	1.403 Mg/m^3
Absorption coefficient	0.827 mm^{-1}
F(000)	576
Crystal size	0.20 x 0.11 x 0.09 mm^3
Theta range for data collection	3.866 to 75.776°.
Index ranges	-8<=h<=10, -8<=k<=7, -28<=l<=29
Reflections collected	7544
Independent reflections	2667 [R(int) = 0.025]
Completeness to theta = 72.434°	99.9 %
Absorption correction	Semi-empirical from equivalents
Max. and min. transmission	0.93 and 0.86
Refinement method	Full-matrix least-squares on F^2
Data / restraints / parameters	2663 / 0 / 181
Goodness-of-fit on F^2	0.9993
Final R indices [I>2sigma(I)]	R1 = 0.0375, wR2 = 0.0954
R indices (all data)	R1 = 0.0449, wR2 = 0.1042
Largest diff. peak and hole	0.27 and -0.23 $e.Å^{-3}$

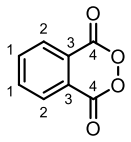
6.4.3.2. Crystal data and structure refinement for 4.50b.



Empirical formula	C16 H18 O4	
Formula weight	274.32	
Temperature	150 K	
Wavelength	1.54184 Å	
Crystal system	Monoclinic	
Space group	P 21	
Unit cell dimensions	a = 6.41110(10) Å	α= 90°.
	b = 20.5782(2) Å	β= 92.8361(7)°.
	c = 10.67850(10) Å	γ = 90°.
Volume	1407.08(3) $Å^3$	
Z	4	
Density (calculated)	1.295 Mg/m^3	
Absorption coefficient	0.758 mm^{-1}	
F(000)	584	
Crystal size	0.23 x 0.20 x 0.18 mm^3	
Theta range for data collection	4.145 to 76.111°.	
Index ranges	-6<=h<=8, -25<=k<=25, -13<=l<=13	
Reflections collected	15303	
Independent reflections	5776 [R(int) = 0.018]	
Completeness to theta = 73.356°	100.0 %	
Absorption correction	Semi-empirical from equivalents	
Max. and min. transmission	0.87 and 0.85	
Refinement method	Full-matrix least-squares on F^2	
Data / restraints / parameters	5775 / 1 / 363	
Goodness-of-fit on F^2	1.0083	
Final R indices [I>2sigma(I)]	R1 = 0.0257, wR2 = 0.0669	
R indices (all data)	R1 = 0.0259, wR2 = 0.0673	
Absolute structure parameter	-0.01(3)	
Extinction coefficient	35(4)	
Largest diff. peak and hole	0.15 and -0.13 $e.Å^{-3}$	

6.4.4. Experimental details for chemical LSF

Benzo[d][1,2]dioxine-1,4-dione **4.20**

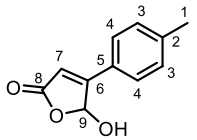


Chemical Formula: $C_8H_4O_4$
Exact Mass: 164.0110
Molecular Weight: 164.1160

Synthesis from literature procedure.[31] Perform reaction behind a blast shield if >1g. To a solution of solid sodium percarbonate (2.32 g, 14.8 mmol, 1.5 eq.) in 49 mL wet CH_2Cl_2, add neat phthaloyl chloride (1.4 mL, 9.9 mmol, 1 eq.) in one portion. Stir the reaction mixture (800 r.p.m.) at 23 °C for 3 hr. Filter through celite, and wash (x2) with CH_2Cl_2. Remove CH_2Cl_2*in vacuo*, with the rotary evaporator bath no greater than 23 °C to minimise the risk of explosions. Warm benzene to 70 °C, and re-dissolve crude reaction mixture in 5 mL warm benzene. Add solution to cold pentane to precipitate phthaloyl peroxide, filter and wash precipitate with cold pentane (2 x 10 mL). Title compound was isolated as a white solid (418.5 mg, 26%).

^{1}H NMR (400 MHz, $CDCl_3$) δ 8.03 (dd, *J* = 6.0, 3.5 Hz, 2H, H1), 8.30 (dd, *J* = 6.0, 3.5 Hz, 2H, H2). **^{13}C NMR** (101 MHz, $CDCl_3$) δ 123.8 (C2), 130.3 (C3), 136.6 (C1), 162.1 (C4). **IR** ν_{max} (thin film)/cm^{-1} 2361m, 2341m, 1753s, 1284s, 1094m, 1040m. Matches literature data. [31]

5-Hydroxy-4-(*p*-tolyl)furan-2(5*H*)-one **4.53**



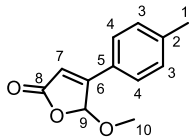
Chemical Formula: $C_{11}H_{10}O_3$
Exact Mass: 190.0630
Molecular Weight: 190.1980

Method A: Adapted from literature procedure.[32] To a solution of 3-(*p*-tolyl)furan (200 mg, 1.27 mmol) in CH_2Cl_2 (127 mL), DIPEA (1.11 mL, 6.33 mmol) and Rose Bengal (spatula tip) were added. O_2 was bubbled through the mixture for 10 min and then cooled to 0 °C and irradiated for 5 min. Bubbling was stopped and the reaction was irradiated under O_2 atmosphere for a further 90 min. The mixture was washed with sat. aq. NH_4Cl and extracted with CH_2Cl_2 (x3). The combined organic phases were washed with brine and dried over anhydrous Na_2SO4, filtered and concentrated *in vacuo*. Purification by column chromatography (5-50% EtOAc in pentane) afforded the *title compound* as an off-white solid (73.1 mg, 30% (62% b.r.s.m.)).

Method B: Adapted from literature procedure.[33] A solution of sodium chlorite (697 mg, 7.71 mmol) and potassium dihydrogen orthophosphate (688 mg, 5.06mmol) in water (6.8mL) was added to solution of furan 11 (20mg, 0.126 mmol) in EtOH (6.8mL) via syringe slowly over 10 min. The reaction was left to stir at RT for 15h with the flask open to the air, before being quenched with sat. aq. $Na_2S_2O_3$. Water was added, and the reaction was extracted with Et_2O (x2). The organic layer was washed with water and brine, dried over anhydrous $MgSO_4$, filtered and concentrated *in vacuo* to give the title compound as an off-white solid (10.1 mg, 42%).

R_f 0.12 (5% EtOAc in pentane). **^{1}H NMR** (400 MHz, $CDCl_3$) δ 2.41 (s, 3H, H1), 6.33 (s, 1H, H7), 6.51 (s, 1H, H10), 7.27 (d, *J* = 8.5 Hz, 2H, H4), 7.59 (d, *J* = 8.5 Hz, 2H, H3). **^{13}C NMR** (101 MHz, $CDCl_3$) δ 21.6 (C1), 97.8 (C9), 113.9 (C7), 126.2 (C4), 127.9 (C3), 129.9 (C5), 142.6 (C2), 162.8 (C6), 171.0 (C8). **IR** ν_{max} (thin film)/cm^{-1} 3230br.w, 1702s, 1626s, 1128m, 949m, 791m, 727m. **HRMS** (ESI+) Found: 191.0704, $C_{11}H_{11}O_3$ $[M+H]^+$ requires: 191.0702. **MP** 139 – 142 °C.

5-Methoxy-4-(*p*-tolyl)furan-2(5*H*)-one



Chemical Formula: $C_{12}H_{12}O_3$
Exact Mass: 204.0786
Molecular Weight: 204.2250

O_2 was bubbled through a solution of 3-(*p*-tolyl)furan (20 mg, 0.126 mmol, 1 eq.) and a catalytic amount of Rose Bengal in methanol (3.2 mL), for 5 mins. The reaction was then cooled to 0 °C, while under an atmosphere of O_2, and then irradiated for 10 mins. The solvent was removed *in vacuo* and redissolved in pyridine (1.6 mL) and acetic anhydride (12 μL, 0.126 mmol, 1 eq.). The reaction was left stirring for 15 mins at RT, and when complete water (5 mL) was added and the reaction was extracted with CH_2Cl_2 (3 x 5 mL). The combined organic layers were successively washed with $CuSO_4$ (2 x 5 mL), H_20 (10 mL), brine (10 mL) and then dried over $MgSO_4$, filtered and concentrated *in vacuo*. The compound was purified by preparative thin layer chromatography, yielding a clear colourless oil (11 mg, 43%).

R_f 0.21 (5% EtOAc in pentane). **^{1}H NMR** (400 MHz, $CDCl_3$) δ 2.38 (s, 3H, H1), 3.61 (s, 3H, H10), 5.86 (d, *J* = 1.5 Hz, 1H, H9), 7.21 (d, *J* = 1.5 Hz, 1H, H7), 7.23 (d, *J* = 8.5 Hz, 2H, H4), 7.75 (d, *J* = 8.5 Hz, 2H, H3). **^{13}C NMR** (101 MHz, $CDCl_3$) δ 21.6, 29.8, 57.0, 101.7, 126.1, 127.5, 129.6, 135.3, 140.2, 140.4, 169.8. **IR** ν_{max} (thin film)/cm^{-1} 2922w, 2849w, 1768s, 1514w, 1367m, 1201w, 1115s, 1040m, 935s, 824m, 710w. **HRMS** (ESI+) Found: 205.0861, $C_{12}H_{13}O_3$ $[M+H]^+$ requires: 205.0859.

6.5. References for Chapter 6

(1) C. J. C. Whitehouse, S. G. Bell, H. G. Tufton, R. J. Kenny, L. C. Ogilvie, and L. L. Wong, *Chem. Commun.* **2008**, *44*, p966-968.

(2) a) C. J. C. Whitehouse, W. Yang, J. A. Yorke, B. C. Rowlatt, A. J. Strong, C. F. Blanford, M. Bartlam, L. L. Wong, and Z. Rao, *Chembiochem*, **2010**, *11*, p2549-2556; b) C. J. C. Whitehouse, W. Yang, J. A. Yorke, H. G. Tufton, L. C. Ogilvie, S. G. Bell, W. Zhou, M. Bartlam, Z. Rao and L. L. Wong, *Dalton Trans.*, **2011**, *40*, p10383-10396; c) X. Ren, J. A. Yorke, E. Taylor, T. Zhang, W. Zhou and L. L. Wong, *Chem. Eur. J.*, **2015**, *21*, p15039-15047.

(3) T. Omura and R. Sato, *J. Biol. Chem*., **1964**, *239*, p2370-2378.

(4) G. Molander and I. Shin, *Org. Lett.*, **2012**, *14(17)*, p4458-4461.

(5) P. Li, N. Ma, Z. Wang, Q. Dai, C. Hu, *J. Org. Chem.*, **2018**, *83*, p8233-8240.

(6) S. O'Sullivan, E. Doni, T. Tuttle and J. A. Murphy, *Angew. Chem. Int. Ed.*, **2014**, *53*, p474-478.

(7) D. Lafrance, P. Bowles, K. Leeman, *Org. Lett.* **2011**, *13(9)*, p2322-2325.

(8) H. Liu and D-M. Du, *Adv. Synth. Catal.*, **2010**, *352*, p1113-1118.

(9) M. B. Plutschack, P. H. Seeberger and K. Gilmore, *Org. Lett.*, **2017**, *19*, p30-33.

(10) J. Lv, Q. Liu, J. Tang, F. Perdih and K. Kranjc, *Tetrahedron Lett.,* **2012**, *53*, p5248-5252.

(11) H-Y. Wang, K. Yang, S. R. Bennett, S-r. Guo and W. Tang, *Angew. Chem. Int. Ed.,* **2015**, *54*, p8756-59.

(12) T. Nagata, H. Matsubara, K. Kiyokawa and S. Minakata, Org. Lett., **2017**, *19*, p4672-4675.

(13) Orr, R.; Campeau, L. -C.; Chobanian, H.; McCabe Dunn, J.; Pio, B.; Plummer, C.; Nolting, A.; Ruck, R., *Synthesis*, **2016**, *49*, p657-666.

(14) W. Shi, W-J. Dan, J-J. Tang, Y. Zhang, T. Nandinsuren, A-L. Zhang and J-M. Gao, *Bioorg. Med. Chem. Lett.*, **2016**, *26*, p2156-2158.

(15) S. B. Bhorkade, K. B. Gavhane and V. S. Shinde, *Tetrahedron*, **2016**, *72 (16)*, p1954-1959.

(16) K. Yamamoto, F. Yakushiji, T. Matsumaru and S. Ichikawa*, Org. Lett.,* **2018**, *20 (1)*, p256-259.

(17) E. Tayama and S. Saito, *Synlett*, **2015**, *26(13)*, p1880-1884.

(18) N. D. C. Tappin, M. Gnägi-Lux and P. Renaud, *Chem. Eur. J.*, **2018**, *24*, p11498-11502.

(19) J. Davies, L. Angelini, M. A. Alkhalifah, L. M. Sanz, N. S. Sheikh and D. Leonori, *Synthesis*, **2018**, *50*, p821-830.

(20) J. Davies, L. Angelini, M. A. Alkhalifah, L. M. Sanz, N. S. Sheikh and D. Leonori, *Synthesis*, **2018**, *50*, p821-830.

(21) a) T. Taniguchi, H. Nagata, R. M. Kanada, K. Kadota, M. Takeuchi and K. Ogasawara, *Heterocycles*, **2000**, *52*, p67-71; b) P. Nanayakkara and H. Alper, *Adv. Synth. Catal.,* **2006**, *348*, p545-550.

(22) B. Kashyap, and P. Phukan, *RCS Advances*, **2013**, *3*, p15327-15336.

(23) N-X. Wang, A-G. Yu, G-X. Wang, X-H. Zhang, Q-S. Li and Z. Li, *Synthesis*, **2007**, *8*, p1154 – 1158.

(24) Z-T. Du, J. Lu, H-R. Yu, Y. Xu, A-P. Li, *Journal of Chemical Research*, **2010**, *4*, p222- 227.

(25) R. Hayashi, A. Shimizu and J-I. Yoshida, *J. Am. Chem. Soc.,* **2016**, *138*, p8400-8403.

(26) J. Guo, X. Xu, Q. Xing, Z. Gao, J. Gou and B. Yu, *Org. Lett.* **2018**, *20(23)*, p7410-7414.

(27) F. D. Ferrari, A. J. Ledgard and R. Marquez, *Tetrahedron*, **2011**, *67*, p4988-4994.

(28) *Angew.Chem. Int.Ed.*, **2018***, 57,* p11598-11602.

(29) Y. Tian, J. Qi, C. Sun, D. Yin, X. Wang, Q. Xiao, *Org. Biomol. Chem.,* **2013**, *11*, p7262-7266.

(30) L. K. Kinthada, K. N. Babu, D. Padhi and A. Bisai, *Eur. J. Org. Chem.,* **2017**, *21*, p3078-3091.

(31) C. Yuan, A. M. Eliasen, A. M. Camelio and D. Siegal., *Nat. Protoc.,* **2014**, *9*, p2624-2629.

(32) C. L. Hugelshofer and T. Magauer, J. Am. Chem. Soc., **2015**, *137*, p3807-3810.

(33) T. W. Fenlon, M. W. Jones, R. M. Adlington and V. Lee, *Synlett*, **2018**, *29*, p1020-1023.